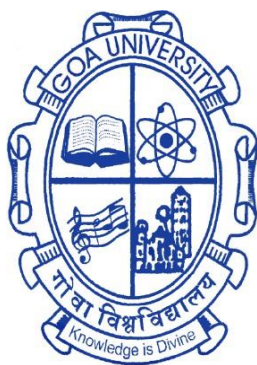


A THESIS ENTITLED

**SYNTHESIS, PROPERTIES AND APPLICATIONS
OF SOME POLYCARBONATE AND
POLYURETHANE POLYMERS**

SUBMITTED TO THE GOA UNIVERSITY FOR THE DEGREE OF

**DOCTOR OF PHILOSOPHY
IN CHEMISTRY**



BY

Mr. ABHIJIT DIGAMBER SHETGAONKAR

**SCHOOL OF CHEMICAL SCIENCES
GOA UNIVERSITY
TALEIGAO PLATEAU
GOA-INDIA**

June 2022

**SYNTHESIS, PROPERTIES AND APPLICATIONS
OF SOME POLYCARBONATE AND
POLYURETHANE POLYMERS**

A thesis submitted to Goa University for the Award of the Degree of

**DOCTOR OF PHILOSOPHY
in
CHEMISTRY**

By

**Mr. ABHIJIT DIGAMBER SHETGAONKAR
(M. Sc.)**

Research Guide

Prof. Vishnu. S. Nadkarni

School of Chemical Sciences

Goa University

Taleigao Plateau

Goa 403206

INDIA

June 2022

DECLARATION

I hereby declare that the work contained in the thesis entitled “**Synthesis, properties and applications of some polycarbonate and polyurethane polymers**” is the result of investigations carried out by me under the guidance of **Prof. V. S. Nadkarni** at School of Chemical Sciences, Goa University and that it has not previously formed the basis for the award of any degree or diploma or other similar titles.

In keeping with general practice of reporting scientific observations, due acknowledgement has been made wherever the work described is based on the findings of other investigators. I further state that the thesis has been prepared by me and it is my original work and is free of any plagiarism. This document has been duly checked through Plagiarism detection tool approved by the Goa University and confirms to the provisions of OA-29.

Mr. Abhijit D. Shetgaonkar
Ph.D Student
Goa University

Goa University
June 2022

SCHOOL OF CHEMICAL SCIENCES

CERTIFICATE

This is to certify that the thesis entitled “**Synthesis, properties and applications of some polycarbonate and polyurethane polymers**” submitted by **Mr. Abhijit D. Shetgaonkar**, is a record of research work carried out by her during the period of study under my supervision and that it has not previously formed the basis for the award of any degree or diploma or other similar titles. This document has been duly checked through Plagiarism detection tool approved by the Goa University and confirms to the provisions of OA-29.

Prof. V. S. Nadkarni,
Research Guide
School of Chemical Sciences,
Goa University

Goa University
June 2022

ACKNOWLEDGEMENT

The entire journey of the doctoral study was one of the biggest learning experiences of my life. The journey had its own challenges and difficulties, ups and downs, but it was one of the greatest opportunities, to work independently along with shouldering several responsibilities.

The journey began with my Ph.D. guide Prof. V.S. Nadkarni, who offered me the magnificent opportunity to work under his mentorship on the recent area of polymer research. The constant motivation, guidance and autonomy given by Professor helped me to construct myself as an independent researcher. Prof. Nadkarni is a very enthusiastic personality and receptive towards innovative ideas, which encouraged me to work with full potential as a hardcore researcher. During my difficult times he has always supported me and boosted my morals, which helped me to become a responsible individual. His valuable feedback was the key towards shaping my final research work and materialization of this doctoral thesis. I shall always be grateful towards him throughout my life.

I would sincerely like to thank my subject expert, Dr. Rashmi Chauhan, BITS Pilani, Goa for periodically examining my research work at FRC progress meetings. Her valuable suggestion and encouragement helped me to improve my research aptitude. Additionally, I thank her profoundly for providing LC-MS facilities at BITS Pilani, Goa.

I wish to offer my special thanks to Prof. Santosh Tilve, SCS, Goa University for his constant motivation and appreciating my research work along with thorough reviews especially during journal manuscript writing. I shall be always obliged to him for providing me all the valuable laboratory facilities whenever required and making my research journey easier.

I owe my deepest gratitude to Dr. Delicia Barretto (SCS, Goa University) for her consistent guidance and for investing her precious time on collaborative work pertaining to biological studies. Her dedicated efforts, systematic approach and critical thinking inspired me to learn various aspects of microbiology. I would like to heartily thank her for helping me in compiling my final research draft even in her difficult times. She is the humblest person I have ever met. I will always be indebted towards her.

I wish to express my sincere gratitude towards the School of Chemical Sciences (then Department of chemistry) and Prof. V.M.S. Verenkar (Dean, SCS, Goa University), Prof.

V.S. Nadkarni (former dean, SCS) and Prof. B. R. Srinivasan, Prof. S. G. Tilve (former heads then Dept. of chemistry) for providing me an excellent laboratory, research facilities and financial assistance to carry out my research work smoothly. I was fortunate enough to handle some sophisticated instruments such as NMR, GPC, LC-MS, etc. at SCS, Goa University, which facilitated me greatly in upgrading my analytical skills.

I would like to acknowledge the University Grants Commission, New Delhi, India for awarding me the UGC-BSR Fellowship that provided me financial stability and helped me in completing my thesis work. I am extremely grateful to my Ph.D. guide for providing me the research fellowship at the end of my Ph.D. tenure from his Research Incentive Fund (RIF).

I wish to thank Prof. H. B. Menon, (Vice chancellor, Goa University), Prof. V.S. Nadkarni, (Registrar, Goa University), Prof. V. Sahni, (former Vice chancellor, Goa University), Prof. Y. V. Reddy, (former Registrar, Goa University), Prof. S. Shetye (former Vice-Chancellor, Goa University) and Prof. V. P. Kamat (former Registrar, Goa University) for their valuable administrative and studentship support.

I extend my warm gratitude to all my teachers, Prof. B.R. Srinivasan, Prof. S.G. Tilve, Prof. V.S. Nadkarni, Prof. A.V. Salker, Prof. J.B. Fernandes, Prof. R.N. Shirsat, Prof. V.M.S. Verenkar, Prof. S.N. Dhuri, Prof. S. V. Bhosale, Mrs. S.V. Girkar, Dr. M. S. Majik, Dr. P.P. Morajkar, Dr. V.V. Gobre and Dr. R.K. Kunkalkar, SCS, Goa University for constant motivation, valuable advice, scientific discussions and their insightful comments. I am deeply benefited from all their precious inputs.

I am profoundly grateful to Prof. Vidya Desai, DMs College and Research Centre, Assagao for her constant motivation, support and encouragement to uptake doctoral studies as an advancement in my career.

I am profusely grateful to Dr. Salman Khan (Research Associate at I.I.T. Bombay) and Dr. Rupesh Kunkalkar (SCS, Goa University) for their timely support in analysing my research samples for HRMS studies, without any reluctances. This has helped me immensely in submitting the revised journal manuscript within a given time frame.

I wish to extend my gratitude to Dr. Aishwarya Rao, MALDI-TOF central facility, Department of Biosciences and Bioengineering, I.I.T. Bombay, for mass analysis trials, helpful suggestions and patiently addressing my queries during the analysis. I would like to

acknowledge the Sophisticated Test and Instrumentation Centre (STIC), Cochin, Kerala for DSC thermal analysis. I wish to thank Mr. G. Prabhu (CSIR NIO-Goa) for X-ray powder diffraction measurements.

I extend my kind gratitude to the administrative staff of Goa University, especially to Mrs. Sneha R. Haldankar, Mr. Agostinho Rodrigues, Mr. Kalpesh B. Dhuri for their timely help and cooperation. I wish to thank all the non-teaching staff of the School of Chemical Sciences, Goa University for their kind help and support especially Mr. Yoganand Kholkar, Mr. Kiran Dabolkar, Late. Rohidas Naik, Mr. Rayappa Harijan, Mr. Rudraunsh Mahale, Mr. Kirtesh Sawant, Mr. Deepak Chari, Mr. Nikhil Pednekar, Mr. Prajyot Chari, Mr. Deepak Kadam and Mr. Gaurav Kinlekar.

I profusely thank all my research group members Dr. Diptesh Naik, Dr. Vinod Mandrekar and Dr. Vishal Pawar for their helpful suggestions in tackling the research problems. A heartfelt thanks to all my past and present SCS research colleagues Dr. Hari Kadam, Dr. Chinmay Bhat, Dr. Mira Parmekar, Dr. Mithil Fal Desai, Dr. Madhavi Naik, Dr. Shambhu Parab, Dr. Satu Gawas, Dr. Daniel Coutinho, Dr. Dattaprasad Narulkar, Dr. Durga Kamat, Dr. Mayuri Naik, Dr. Savita Khandolkar, Dr. Rita Jyai, Dr. Celia Braganza, Dr. Madhavi Shete, Dr. Sudarshana Mardolkar, Dr. Prajyoti Gauns Desai, Dr. Chandan Naik, Dr. Johnross Albuquerque, Dr. Apurva Narvekar, Mr. Vishnu Chari, Dr. Kedar Narvekar, Dr. Rahul Kerkar, Dr. Pratik Asogekar, Dr. Sumit Kamble, Dr. Megha Deshpande, Mr. Sarvesh Harmalkar, Mr. Dinesh, Mr. Ratan Jadhav, Mr. Vipul Gharey, Ms. Luann D'Souza, Ms. Lima Rodrigues, Ms. Amarja Naik, Mr. Akshay Salkar, Ms. Geeta Jalmi, Ms. Mangala Sawal, Ms. Nikita Harmalkar, Mr. Pritesh Khobrekar, Mr. Savio Dias and Ms. Madhuri Gaikwad for making my doctoral journey at the Goa University more lively, scientific and a memorable one.

I am profoundly grateful to Dr. Sagar Patil and Dr. Prajesh Volvoikar for constantly initiating new research ideologies in me and generously resolving my synthetic difficulties during the initial years of doctoral studies. Also, a big thanks to them for providing hands on training in understanding and operating the NMR instrument.

I am obliged to Dr. Diptesh Naik for his constant guidance and motivation throughout my doctoral studies. I am very fortunate to find him as my Ph.D. colleague. I express my special thanks to Dr. Sandesh Bugde for his encouragement, fruitful advices and thoroughly reviewing my research work.

During this delightful journey there were times where I thought of putting my foot down. But there were a group of individuals who made sure I do not lose my balance. These group of individuals are the ones whom I call as my folk of friends namely Mr. Ketan Manderkar, Mr. Vaibhav Satoskar, Mr. Sudesh Morajkar, Ms. Pooja Bhargao, Mr. Shashank Mhaldar, Ms. Neha Parsekar, Mrs. Sinthiya Gawandi, Mrs. Sulaksha Desai, Mrs. Atiba Shaikh. They were the ones who acted as boosters and lit up a spark in me whenever the flame of my confidence flickered.

I am fortunate enough to have a surrounding full of enthusiasm and happiness. Here, I would like to mention that my entire family members stood beside me in good times as well as my bad times. Whichever path I chose, I found them standing beside me patting my back and lending their support. Especially my parents and my younger brother who tried to give me as much as they could and beyond. My brother Ir. Ajay Shetgaonkar, who ignored his pending work and focussed more on my upcoming. My father who pretended to be a tough man so that he teaches how to face difficult hurdles. And my mother, who forgot her sorrows to bring in positiveness around me, the lady who dreamt of seeing me fly very high, the woman who aspired to see the word Doctor to be written in front of my name.

Above all my biggest thank you goes out to the almighty for showering his blessings over me by providing me with a healthy surrounding, fruitful opportunities and all the gem of people who made this journey a great success.

Mr. Abhijit D. Shetgaonkar

*Dedicated to my beloved
family...*

*mum, dad, aju, aai (R.I.P), mama
who always believed in my
inner potential*

TABLE OF CONTENTS

GENERAL REMARKS	i
ABBREVIATIONS	iii
ABSTRACT	vi
Chapter 1 Synthetic studies on polycarbonate and polyurethane dendrimers with functional periphery	
1.1 Introduction	11
1.1.1 Historical overview: Naturally and synthetically evolved dendritic architectures	11
1.1.2 Classification of dendritic polymers	17
1.1.3 Synthetic strategies towards dendrimers/dendrons: from conventional routes to revised and accelerated methodologies	24
1.2 Literature review on polycarbonate and polyurethane dendrimers possessing 1→n (n≥2) branching motif	36
1.3 Experimental	48
1.3.1 Synthetic procedures and characterization of compounds	48
1.4 Results and Discussion	96
1.4.1 General remark on screening and synthesis of integral units of dendrimer	96
1.4.2 Synthesis of 1→2 C branched carbonate linked dendritic motifs using protection-deprotection strategies	96
1.4.3 Synthesis of 1→2/1→4 branched carbonate/urethane dendritic motifs using protection/deprotection free strategies	102
1.5 Conclusions	114
1.6 References	115
Chapter 2 Synthesis, characterization and biodegradation studies on sulphur containing linear and crosslinked polycarbonates	
2.1 Introduction	121
2.1.1 Historical events in research and development of commercial PCs	122
2.1.2 Properties of aliphatic polycarbonate's	125
2.1.3 Methods for synthesis of polycarbonates	126
2.1.4 Applications of linear and crosslinked polycarbonates	134

2.2	Literature review on sulfur containing linear and crosslinked aliphatic polycarbonates	137
2.3	Experimental	146
2.3.1	Methods	146
2.3.2	Synthetic procedures and characterization of compounds	152
2.4	Results and discussion	171
2.4.1	Synthesis and characterization of main chain sulfur functionalized linear APCs.	171
2.4.2	Synthesis and characterization of sulfur containing allylic monomers and development of crosslinked APCs	188
2.4.3	Attempt towards preparation of thermoplastic films of newly developed linear poly (2,2'-sulfonyl diethylene carbonate) (PSOC)	198
2.4.4	Biodegradation studies of sulfur functionalized APCs	205
2.5	Conclusions	225
2.6	References	227
Chapter 3 Application of polymers in Solid State Nuclear Track Detection		
3.1	Introduction	234
3.1.1	Track formation in SSNTDs	235
3.1.2	Highlighting the features of nuclear tracks	237
3.1.3	Theory and mechanisms of latent track formation	237
3.1.4	Track etching geometry and etched-track parameters	240
3.1.5	Determination of bulk etch rate	244
3.1.6	Track revelation and visualization technique	245
3.1.7	Microscopic track counting techniques	248
3.1.8	Merits and demerits of SSNTDs	248
3.1.9	Applications of solid-state nuclear track detection technique	250
3.2	Literature survey	252
3.2.1	Polymeric nuclear track detectors (PNTDs)	252
3.2.2	Criteria for developing polymeric NTDs	257
3.2.3	Sulfur containing allyl monomers and their polymers as highly potential polymeric NTDs	259
3.2.4	General protocol for development of thermoset polymers as NTDs	261
3.2.5	Broad objective	264
3.3	Experimental	265
3.3.1	Instrumental methods	265

3.3.2	Irradiation methods	265
3.3.3	Chemical etching method	267
3.3.4	Etched track counting method	268
3.4	Results and discussion	269
3.4.1	Investigating newly synthesized poly(disulfonyl-carbonate) thermoset polymers for SSNTD applications	269
3.4.2	Investigating newly synthesized poly(urethane-carbonate) highly crosslinked thermoset polymers for SSNTD applications	300
3.5	Conclusions	308
3.6	References	310
	Publications	316

GENERAL REMARKS

- The compound numbers, figure numbers, scheme numbers and reference numbers given in each chapter refer to that particular chapter only.
- All AR grade chemicals were purchased from M/s Spectrochem (India), M/s Sigma–Aldrich (India), M/s Molychem (India), M/s Alfa Aesar (India) and M/s Avra Synthesis (India), M/s Qualigens Fine Chemicals (India), M/s Himedia (India) and used as received.
- Organic solvents were distilled prior to use and stored over specified dehydrated agents whenever necessary.
- Reactions were monitored by thin-layer chromatography (TLC Silica gel 60 F254 purchased from Merck) and visualization of the spots on TLC plates was achieved by I₂ gas, UV chamber and KMnO₄ staining solution.
- Chromatographic purification was conducted by column chromatography using silica gel (60-120 mesh size) or by flash chromatography using silica gel (230-400 mesh size) on Combiflash Companion instrument.
- Preparative size exclusion chromatography was performed over Sephadex[®] G-50, Medium(50-150µm) gel filtration media (Sigma–Aldrich).
- All melting points and boiling points were recorded using Thiele’s tube and are uncorrected.
- Infrared spectroscopy was performed on a Shimadzu Prestige-21 FT-IR spectrometer by KBr sample holder method.
- ¹H NMR and ¹³C NMR experiments were carried out on a Bruker Avance 400 MHz spectrometer at 25°C using deuterated solvent such as CDCl₃, DMSO-*d*₆, D₂O and TMS as an internal standard.
- Electron spray ionization mass spectra (ESI-MS) were obtained using Shimadzu single quadrupole LC-MS-2020 instrument performed in positive ion mode and HRMS were recorded with Micromass Q-ToF ESI instrument.
- Matrix-Assisted Laser Desorption/Ionization Time of Flight Mass Spectrometry (MALDI-ToF-MS) was carried out on Bruker, Autoflex Speed equipped with 355 nm tripled Nd:YAG SmartBeam laser at and 2,5-dihydroxybenzoic acid (DHB) was used as matrices. The spectrum result was recorded in a linear mode.

- Relative number-average molecular weight (M_n) and dispersity index (D_M) of all polymers were measured by Gel Permeation Chromatography (GPC). The GPC measurements were performed on Agilent's infinity 1260 HPLC system equipped with PLgel 5 μ m Mixed-C (300 x 7.5 mm) organic column and refractive index as detector. Tetrahydrofuran (THF) was used as the eluent at a flow rate of 1.0 mL min⁻¹ at 30°C. Polystyrene (PS) with a narrow molecular weight distribution were used as standards for calibration.
- The glass transition temperature (T_g) of polymers were acquired using Netzsch DSC 204 F1 Differential Scanning Calorimeter at a heating and cooling rate of 10 K/ min under nitrogen atmosphere.
- X-ray powder pattern for polymer samples were carried out using a Rigaku Miniflex II powder diffractometer (Ultima IV model) using Cu-K α as target and the sample powders were scanned between 5° and 85° 2 θ .
- Optical glass plates from Schott, Germany and TeflonTM sheets were used for preparation of polymer molds. Polymerization was carried using a polymerization bath controlled using microprocessor-based electronic temperature controller F25 HP from M/s Julabo, Germany.

ABBREVIATIONS

GENERAL ABBREVIATIONS			
anhy.	Anhydrous	L	Litres
aq.	Aqueous	w/w	weight by weight
dil.	Dilute	w/v	weight by volume
conc.	Concentrated	sec.	Seconds
sat.	Saturated	min.	minutes
r.t.	Room temperature	h	Hours
equiv./eq	Equivalent	lit.	Literature
cat.	Catalytic	Calcd	Calculated
%	Percentage	hν	Irradiation
°C	Degree celcius	et al.	Et alia (and others)
m.p.	Melting point	TM	Trade mark
b.p.	Boiling point	®	Registered trade mark
mmol	Millimole	V_T	Track etch rate
g	Grams	V_B	Bulk etch rate
mL	Millilitre	S	Sensitivity
µm	Micrometre	nm	nanometre
sp./spp.	Species	Da	Dalton
OHV	Hydroxyl value	w. r. t.	with respect to
²³⁹Pu	Plutonium	²⁵²Cf	Californium

ANALYTICAL ABBREVIATIONS			
UV	Ultraviolet	s (NMR) s (IR)	Singlet Strong band
NMR	Nuclear Magnetic Resonance	d	Doublet
IR	Infra-red	t	Triplet
FTIR	Fourier Transform Infrared spectroscopy	dd	Doublet of doublet

HPLC	High Performance Liquid Chromatography	dt	Doublet of triplets
TLC	Thin layer chromatography	m (NMR) m (IR)	Multiplet Medium band
GPC	Gel permeation chromatography	w (IR)	Weak band
SEC	Size-exclusion chromatography	brd	Broad signal
HRMS	High resolution mass spectroscopy	stretch	Stretching vibrations
MALDI-TOF	Matrix-assisted laser desorption/ionization time of flight	bend	Bending vibrations
DSC	Differential scanning calorimetry	CDCl₃	Deuterated chloroform
PXRD	Powder X-ray diffraction	DMSO-d₆	Deuterated dimethyl sulfoxide
SEM	Scanning electron microscopy	D₂O	Deuterated water
AFM	Atomic force microscopy	M⁺	Molecular ion
MHz	Megahertz	M_n	Number average molecular weight
$\tilde{\nu}$	wavenumber	M_w	Weight average molecular weight
δ	Delta (Chemical shift in ppm)	DP	Degree of polymerization
ppm	Parts per million	\bar{M}_w/\bar{M}_n	Polydispersity index
m/z	Mass to charge ratio	T_g	Glass transition temperature
J	Coupling constant	T_m	Melting temperature

COMPOUND ABBREVIATIONS			
SSNTDs	Solid state nuclear track detectors	OESDAC	2,2'-(oxybis(ethylenesulfonyl)) diallylcarbonate
PNTDs	Polymeric nuclear track detectors	ETSDAC	2,2'-(ethylenedisulfonyl) diallylcarbonate
PCs	Polycarbonates	APCs	Aliphatic polycarbonates
PUs	Polyurethanes	PEG	Polyethylene glycol

CDI	<i>N,N'</i> -carbonyldiimidazole	ADC	Allyl diglycol carbonate
<i>p</i>-TSA	<i>p</i> -toluenesulfonic acid/ tosylic acid	CR-39	Columbia Resin # 39
DMAP	4-Dimethylaminopyridine	PSDAC	Poly(2,2'-sulfonyldiethanol bis(allyl carbonate))
DCM	Dichloromethane	EGBDC	Ethylene glycol bis (diallyl carbamate)
DMSO	Dimethyl sulfoxide	NADAC	<i>N</i> -allyloxycarbonyl diethanolamine bis (allyl carbonate)
THF	Tetrahydrofuran	PETAC	Pentaerythritol tetrakis(allyl carbonate)
MeOH	Methanol	Pet. Ether	Petroleum ether
<i>t</i>-BuOH	Tertiary butanol	EtOAc	Ethyl acetate
NMO	<i>N</i> -methyl morpholine oxide	DMA	<i>N,N</i> -dimethyl acetamide
Et₃N/TEA	Triethyl amine	CH₃CN	Acetonitrile
BP	benzoyl peroxide	DOP	Diocetyl phthalate
IPP	Isopropylperoxydicarbonate	MSM	Minimal salt medium
DMF	<i>N,N</i> -dimethyl formamide	GS	Ground soil
PSC	Polysulfide carbonate	SS	Sewage soil
PDSC	Polydisulfide carbonate	PSOC	Polysulfonyl carbonate
PDSOC	Polydisulfonyl carbonate	PIDA	Phenyl iodine(III) diacetate
BPA	Bisphenol A		

ABSTRACT

Polycarbonates (PCs) and Polyurethanes (PUs) are one of the significant classes of synthetic polymers and containing repetitive carbonate and urethane (or carbamate) functionalities in its respective polymer network. They find potential applications ranging from high-end engineering plastic to biomaterials. During the course of doctoral research work, our efforts were directed towards synthesis of PC/ PU aliphatic dendritic scaffolds, synthesis of sulfur based aliphatic polycarbonates (APCs) followed by their *in-vitro* biodegradability studies and applicability of selected polymers in area of solid state nuclear track detection (SSNTD).

The thesis entitled “**Synthesis, properties and applications of some polycarbonate and polyurethane polymers**” comprises of three chapters.

The *first chapter* describes our efforts in designing synthetic routes towards some novel dendritic polymers consisting of carbonate and urethane functionalities. This chapter commences with a broad introduction on dendritic polymers, a thorough literature review on dendritic motifs with carbonate/urethane connectivity's, a detailed discussion on synthesis & characterization of newly designed 1→n (n=2,4) branched dendritic motifs using protection-deprotection and accelerated strategies and at the last concluding remarks. For the construction of dendritic motifs, AB₂ type branching monomers were either screened directly from commercial source or synthesized in 1-2 steps. Under protection-deprotection strategies, 1,3-benzylidene acetal and 1,2-acetonide acetal were transformed into reactive AB₂ branching monomers using chloroformylation and CDI coupling methods. Condensation of this reactive acetal with tetra hydroxyl core gave 4-armed [G-1] tetra acetal carbonate in moderate yields (**Figure IA**). However, further acetal deprotection resulted in highly polar, tetra-carbonate polyol, which undergo hydrolytic degradation and intramolecular side reaction to afford starting core back. Hence further iterative process to obtain higher generation PC is restricted. In protection-deprotection free approach, our preliminary attempt to afford AB₂ branching unit from diethanol amine and ethylene glycol bis-chloroformate has been unsuccessful and results in formation of randomly branched oligomer. Finally, an efficient two step method was devised for synthesis of PU/PC dendrimers using *N, N'*-diallyl carbamoyl chloride as AB₂ branching unit. This method is based on iterative steps of per-allylation via carbonate/urethane links followed by

dihydroxylation of the allylic double bonds, generating 1→4 branched polyurethane dendritic motif (**Figure IB**). Both divergent and convergent growth routes were employed to afford urethane/carbonate dendritic motifs in good isolated yields. Thus, incorporation of the current branching motif not only results in dense olefinic periphery at lower generation but also creates a multivalent, multifunctional scaffold to obtain higher generation heterofunctional dendrimers.

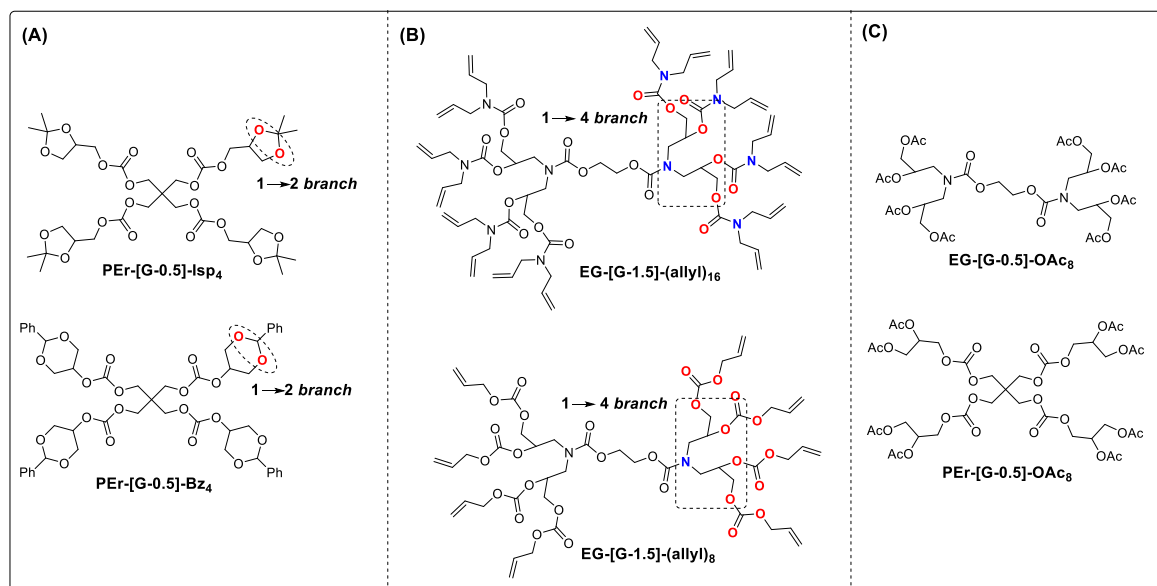


Figure I Carbonate/urethane linked dendritic scaffolds.

Also, some miscellaneous efforts were made to prepare carbonate/urethane linked dendritic motifs (**Figure IC**) using greener diacetoxylating reagent. Although the method was greener, yet it was time consuming.

The *second chapter* deals with design, synthesis and characterization of some sulfur containing linear as well as crosslinked aliphatic polycarbonates (APCs) and evaluation of their *in-vitro* biodegradation properties. Chapter begins with an introductory section on polycarbonates and its applications, a comprehensive literature review on sulfur based linear as well as crosslinked APCs, a detailed discussion on synthetic, polymerization and characterization aspects of sulfur-based APCs, *in-vitro* biodegradation studies and at the end concluding remark. In present study, series of poly(thioether-carbonate) and poly(sulfone-carbonate) linear polymers were synthesized using solution polycondensations followed by sulfide oxidation methods (**Figure IIA**). This Linear APCs were characterized using IR, NMR, MALDI-TOF, GPC, PXRD and DSC techniques. Further, stepwise synthetic and purification approach was adopted to afford sulfone functionalized allyl carbonate

monomers, which were further utilized to fabricate crosslinked thermoset resin using radical polymerization in the presence of peroxide initiator (**Figure IIB**). Additionally, we performed kinetic of polymerization for our new allyl monomer system using Dials kinetic model, in order to generate constant rate polymerization profile. The process of polymerization process was conducted in predesigned mould assembly to furnish hard thermoset films for further applications. Also, attempts were made to cast composite thin film out of linear APC powder sample using spin coating and wet film application techniques.

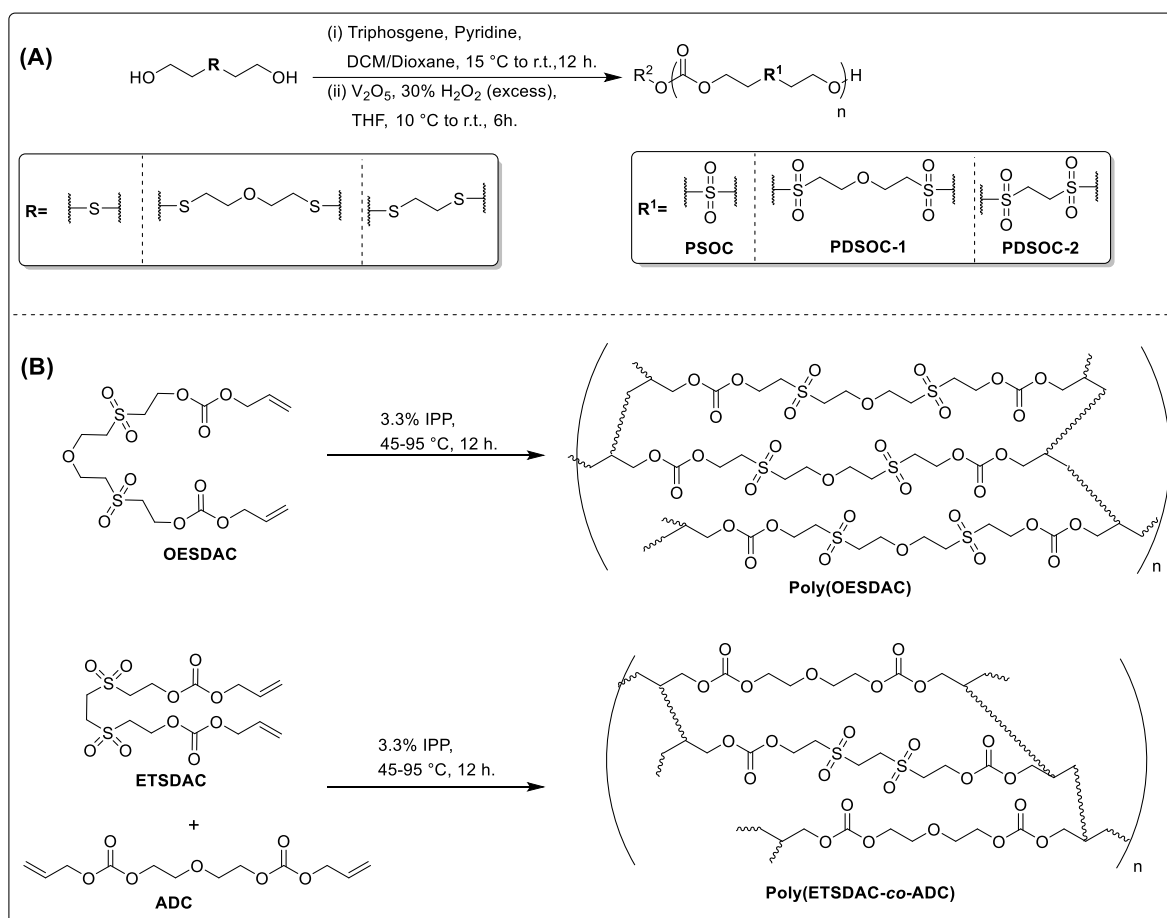


Figure II Synthesis of linear and crosslinked sulfur-based APCs.

Finally, freshly prepared sulfur-based APC polymers were tested for *in-vitro* biodegradation studies using agar plate technique. Here we performed stepwise screening and isolation process, in order to identify the polycarbonate degrading potent microbial strains from garden soil and sewage sludge source collected from two local sites in Goa. In result, most of our APCs showed biodegradability by microorganisms observed with clear zone around the microbial colonies, opacity and surface deterioration of polymer films. Further confirmation of biodeterioration was achieved by scanning electron microscopy. The most

potent microbial colonies showing biodegradation capabilities of polymers were isolated and identified based on molecular identification and phylogenetic analysis. Interestingly the identified stains were not yet reported for biodegradation of APCs.

The *third chapter* describes the development of thermoset polymeric materials for SSNTD application. Also, the effect of increasing radiation sensitive groups and crosslinking on charge particle detection properties of materials has been investigated. This chapter commences with detail introduction on different aspects of SSNTD technique, an in-depth literature survey on polymeric nuclear track detectors (PNTDs), an elaborative discussion on optimization of thermoset polymers for charge particle dosimetry and finally concluding remarks.

In present study, homopolymers of both OESDAC and ETSDAC monomer could not be tested for track detection purpose due difficulties in polymer processing and film defects. While all of their copolymers prepared with ADC were successfully tested for rapid detection of alpha particles and fission fragments. Copolymers were optimized with respect to various track detection parameters such track development time, alpha sensitivity and alpha track efficiency. For OESDAC-ADC copolymers (OESDAC $\geq 40\%$ w/w), track revelation as well as sensitivity studies could be performed under much mild etching condition such as 1 N NaOH at 50°C to 3N NaOH at 60°C. Among all OESDAC-ADC copolymers, 1:1 & 4:6 w/w compositions showed highest sensitivity values, which were higher than previously reported poly(sulfone-carbonate) detector and nearly 3 times greater than commercial CR-39. Furthermore, limited solubility of ETSDAC monomer in ADC restricted us to test only (ETSDAC-ADC, 1:9 w/w) copolymer composition for track detection studies. This copolymer was found to be more sensitive than CR-39 with shorter track development time. In the case of urethane linked thermoset polymer, EGBDC-ADC, 1:9 & 1:8 (w/w) copolymers were successfully tested for alpha and fission track detection and subsequently optimized with respect to track development time and alpha sensitivity. Although copolymers were found more sensitive than CR-39 detector, yet relatively showed lower sensitivity as compared to previously reported poly(urethane-carbonate) detector.

Chapter 1

*Synthetic studies on polycarbonate
and polyurethane dendrimers with
functional periphery*

1.1 Introduction

1.1.1 Historical overview: Naturally and synthetically evolved dendritic architectures

For the past billion years, various architectural complexities have been evolved in the nature. Among this, dendritic structure is one of the most prevalent topologies overserved till today expanding its dimensionality from nano to macro scale. Numerous examples of these patterns may be found in both abiotic systems (e.g., lightning patterns, snow crystals, and erosion fractals) as well as in the biotic world (e.g. tree branching/roots, plant/animal vasculatory systems, and neurons)^[1].

In biological systems^[2], self-explanatory example is the tree which exhibits dual working modes through its dendritic motifs. First, above the ground to enhance the exposure of their leaves to the sunlight for sustaining its growth via photosynthesis. Second, beneath ground in the form of large network of roots serving the purpose to provide strength and collect water and nutrients from the soil. In mammals, tremendous dendritic network of bronchioles and alveoli helps in providing maximum surface for the transfer of oxygen into the bloodstream. On the other hand, transportation of the oxidised blood to the different organs via arterial network progresses into dendritic network. Also, our microscale neural system consists of dendrite structures which play a vital role in receiving and exchange of cellular signals, generating quick stimulus to brain. Although relatively few examples of such architecture are seen at nanoscale level, most notable are amylopectin, glycogen and proteoglycans hyperbranched structures that nature uses for energy storage ^[3]. So, nature has indeed optimized and applied dendritic architectures throughout evolution with great success.

According to historic outlook by Newkome et al.^[4], progressive growth towards the deliberate construction of branched macromolecules have occurred during three general eras. The first period occurred from the late 1860s to the early 1940s, when branched structures were considered responsible for insoluble and stubborn nature of materials formed in polymerization processes. In this era, controlled synthesis, mechanical separation and physical characterization of materials were at primitive stage. Thus, isolation and structural proofing of materials were simply not feasible.

The second period of early 1940s to the late 1970s was an era of hypothetical predictions^[5] of branched macromolecular structures with few initial attempts focusing on their preparation via classical, or single-pot polymerization of functionally differentiated

monomers. This era is marked as conceptual birth phase of present three-dimensional dendritic architecture with the introduction of Molecular Size Distribution and infinite network theory by Flory^[6-9] and Stockmayer^[10,11]. In 1943^[12], Flory proposed the term network cell, which he defined as the most fundamental unit in a molecular network structure. In accordance with original definition- “it is the recurring branch juncture in a network system as well as the excluded volume associated with this branch juncture”. Graessley^[13,14] took the idea one step further by describing assemblies of these network cells as micro-networks. In context to the concept of Flory’s and Graessley’s Gaussian-coil networks, new terms were coined as “branch cells” and “dendritic assemblies” to analogous species that are integral part of branched/dendritic framework^[3]. A comparison of these entities is illustrated in **Figure 1.1**. Successive statistical modelling by Gordon et al., Dušek^[15], Burchard^[16] and others on such branched networks leads to a graph theory designed to mimic the branching morphology in trees. These dendritic models were merged with ‘cascade theory’ in mathematics^[17,18] to provide a reasonable statistic for network-forming events at that time.

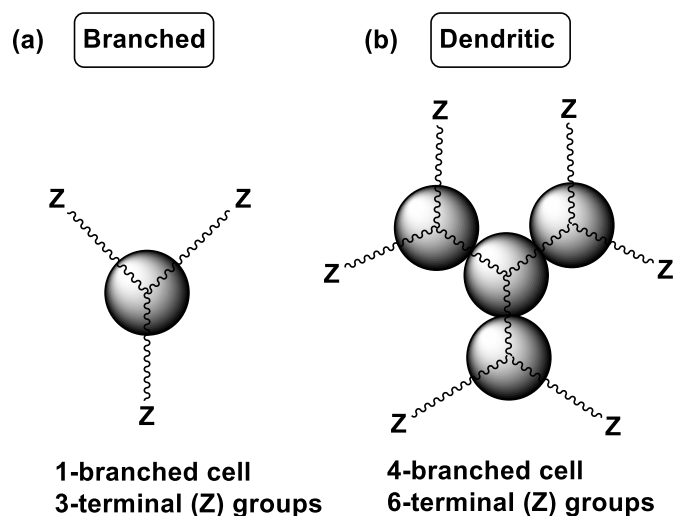


Figure 1.1 Illustrations of (a) branch cell, (b) dendritic assembly of branch cells.

The period from late 1970s and early 1990s, marked as third phase of development in dendritic networks. This stage progresses from preliminary success toward synthesis of low molecular weight dendritic macromolecules to high molecular weight dendritic assemblies with precise control over its size, shape and structure via iterative methodologies. Advancements in physical isolation and purification, as well as the introduction of diverse spectroscopic procedures for structural characterization, played a key role in explaining level of complexities associated with emerging field.

In context to this, following are the crucial milestones recognized in dendritic macromolecular chemistry (**Table 1.1**).

➤ **1978**^[19] - Vögtle “**Cascade**” molecules or **Cascadanes**:

Idea of assembling branches upon branches was first demonstrated by Vögtle et al. in 1978, where they developed repetitive growth protocol for synthesis of well defined, low molecular weight dendritic amines system (<900 Da) at laboratory scale. The scheme was named as “cascade synthesis”, involving sequence of reactions starting with Michael addition of an amine to acrylonitrile, followed by reduction of the nitrile group and amine structures obtained through this process were known as **poly(propyleneimine) (PPI) cascade molecules**. However, strategy suffered through isolation difficulties and poor yield perhaps due to which no subsequent reports on this work could be found until 1980s. Though having a demerit, their work still today is recognized as stepping stone for the research on dendrimeric chemistry.

➤ **1981**^[20,21] - Denkewalter’s **poly(L-lysine)** macromolecules:

In a race to synthesize high molecular weight, branched macromolecules, Denkewalter^[4,22] and co-workers patented a method to synthesize highly branched polypeptide macromolecules. They employed protection/deprotection protocol commonly followed by polypeptide chemists. Synthetic strategy involves stepwise linking of lysine molecules via iterative sequence of deprotection followed by amidation of amino-protected lysine derivative produce asymmetrical **poly(L-lysine)** macromolecule. Therefore, this macromolecular synthesis diverges from a **benzhydrylamine** core and propagates through **N, N'-Bis(tert-butoxycarbonyl)-L-lysine** branching network. Further investigation by Aharoni et al.^[23] confirmed that lysin based dendritic structures are highly monodisperse in nature and possess “**non-draining character**” (i.e., they trapped solvent within the void regions) at higher generations. Authors highly relied on size exclusion chromatography technique and thus failed to provide complete characterization of macromolecules.

➤ **1985**^[24]- Tomalia “**starburst dendrimers**”:

In concurrent investigation on branched structures, the first scientific proof describing broad synthesis and characterization of highly ordered branched macromolecules was published in year 1985 by Tomalia et al at Dow Chemical research laboratories. The authors first time coined a term “**dendrimer**” to describe molecules with tree-like feature originated from Greek terminology “**dendros = tree**” and “**meros = part**”. They were composed of **core**, **repeating units**, and **terminal groups**. Like the divergent cascade synthesis, the synthetic route was initiated by Michael addition of a “core” molecule (ammonia) to three parts of

methyl acrylate, followed by exhaustive amidation of the triester adduct using a large excess of ethylenediamine. Iterative sequence of alternate Michael addition and amidation leads to series of concentric starburst structure known as **poly(amidoamine) (PAMAM)** dendrimers^[3,25]. Level of producing terminal groups were termed as “**Generation**” i.e., every ester stage was denoted as half-generation (0.5, 1.5, 2.5) whereas for amine it's a complete tier (1, 2, 3). High molecular weight, monodisperse macromolecules (i. e., >58 000 Daltons) up to 7th generation (G) were synthesized in excellent yield and purity. However, G>7 resulted in impurities and defects. Structural characterization was established using modern spectroscopy (IR, NMR), mass spectrometry and elemental analysis. Microscopic techniques proved its spheroidal morphology and nanoscale (up to 80 Å) dimensionality. Historically, this divergent methodology established the first commercial route to dendrimers and offers opportunity to observe unique dendrimer properties at higher generations (i.e., G=4 or higher). Their early commercial accessibility has made PAMAM series one of the most widely investigated and has served to promote the field of dendrimer chemistry.

➤ **1985**^[26] – Newkome's “**arborols**”:

Shortly thereafter, in 1985, Newkome et al. an independent synthesis group at Louisiana State University disclosed a new class of cascade molecules with tree like morphology named as “**Arborols**”, derived from the Latin word “**arbor = tree**”. Authors first time utilized ‘**preformed branch cell**’ coupling methodology, where preformed tris-branched reagent was divergently coupled around multifunctional core to afford low molecular weight (i.e., <2000 Daltons) arborol structures. These were **tris-branched polyamide**^[4] monodisperse cascade spheres constituting “unimolecular micelles” with outer surface covered of polar groups and non-polar inner core. Also, water solubility of molecules arises due to multiple hydroxyl groups at periphery. Key synthetic steps involved were nucleophilic substitution followed by amidation of triester. Unfortunately, repetition of this synthetic sequence was precluded by surface steric crowding towards nucleophilic substitution. To date, examples of uni-, di-^[27] and tri-directional^[28] arborols have been registered.

➤ **1988**^[29,30] – Kim & Webster's “**Hyperbranched Polymers**”

After the Flory's classical theory on highly branched polymers by AB_n (n≥2) polymerization^[31] and Kricheldorf's^[32] attempt to synthesis highly branched polyesters by copolymerization of AB and AB₂ type monomers, Kim and Webster first time coined a term “**Hyperbranched Polymers**” in their report on one step homopolymerization of AB_n

monomer to form hyperbranched polyphenylenes. The synthesis utilizes transition metal catalyst to generate the soluble polyphenylene via two complementary aryl–aryl coupling processes^[33]. The hyperbranched polyphenylene produced through Suzuki cross-coupling possessed a high molecular weight (32000 Da) and low polydispersity (1.13) whereas polyphenylene via Kumada type cross-coupling affords relatively low molecular weight (7590 Da) and high polydispersity (1.81-2.3). These hyperbranched polymers exhibited good thermal stabilities and excellent solubility in most of the organic solvents.

- **1990**^[34–36] – Fréchet’s Poly(aryl ether) “**Dendron’s**” and “**Convergent**” methodology:

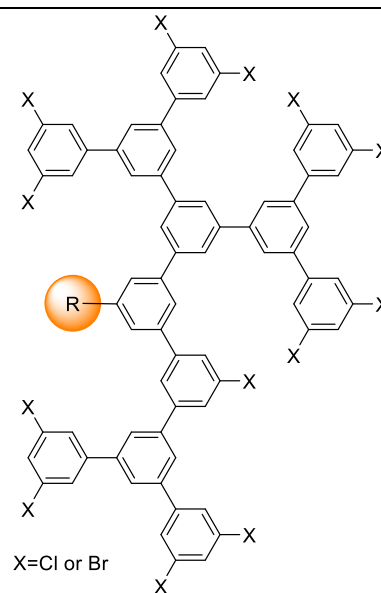
Another breakthrough^[1] on control synthesis of dendritic macromolecules came in 1990, wherein Fréchet and Hawker first time introduced “**convergent**” growth approach to synthesize novel Poly(aryl ether) dendritic macromolecules, which later became complementary method to former divergent strategy. Classical convergent method^[37] primarily focused on construction of perfectly branched “**dendrons**” (dendritic fragments or wedges), which were finally coupled to a core unit after activation of their “**focal point**”. Synthetic steps involved an iterative sequence of phenoxide- based, benzylic bromide Williamson displacement to afford controlled dendritic architecture of benzyl ether network. Dendrimer up to G=6 with M.W. 40,689 Da were synthesized, there by unveiling its unsymmetrical, monodisperse and defect free nature.

These early innovations and discoveries laid a cornerstone of “dendritic polymers” in the world of polymers science and at the same time offered a broad synthetic utility to develop new families of dendritic polymers and to study their properties as well as applications in various areas of science. Thus, the era from 1980s to late 1990s considered as golden revolutionary phase in rapid advancement of highly branched macromolecules. This was evidenced by the remarkably high number of patent applications and original articles published in renowned scientific journals.

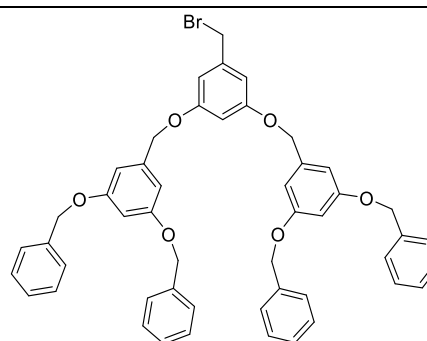
Table 1.1 Crucial milestones in dendritic macromolecular chemistry.

Year	Type	Chemical structure
1978	Vögtle's "Cascadanes"	<p style="text-align: center;">Poly(propyleneimine)</p>
1981	Denkewalter's "Dendritic Polypeptides"	<p style="text-align: center;">Poly(L-lysine)</p>
1985	Tomalia's "Starburst PAMAM Dendrimers"	<p style="text-align: center;">Poly(amidoamine)</p>
1985	Newkome's "Arborols"	<p style="text-align: center;">Polyamide</p>

 1988 Kim & Webster's

“Hyperbranched Polymers”

Polyphenylene

 1990 Fréchet's “Poly(aryl ether)

Dendron's”

Poly(benzyl ethers)
1.1.2 Classification of dendritic polymers

Dendritic polymers^[38,39] are highly branched macromolecules with three-dimensional dendritic network and a large number of end groups. These materials are among the latest additions to the polymer family as consequence of the growing synergy between advanced organic chemistry and polymer synthesis. Dendritic topology is recognized as the fourth major class of polymeric architecture after traditional types i.e., linear, cross-linked and branched architectures. Based on structural growth and variation, they are further divided into four sub-classes: (a) **Dendrons** and **dendrimers**, (b) **hyperbranched polymers** (c) **dendrigrft polymers** and (d) **dendronized polymers**^[40] (**Figure 1.2**). The presence of a highly branched structure gives these polymers unique physical and chemical properties, thereby allowing them to find potential applications in various field such as nanoscience and technology, biomaterials, targeted drug-delivery, polymer electrolytes, coatings, additives, catalysis, sensors, light harvesting and biomimetic applications^[41].

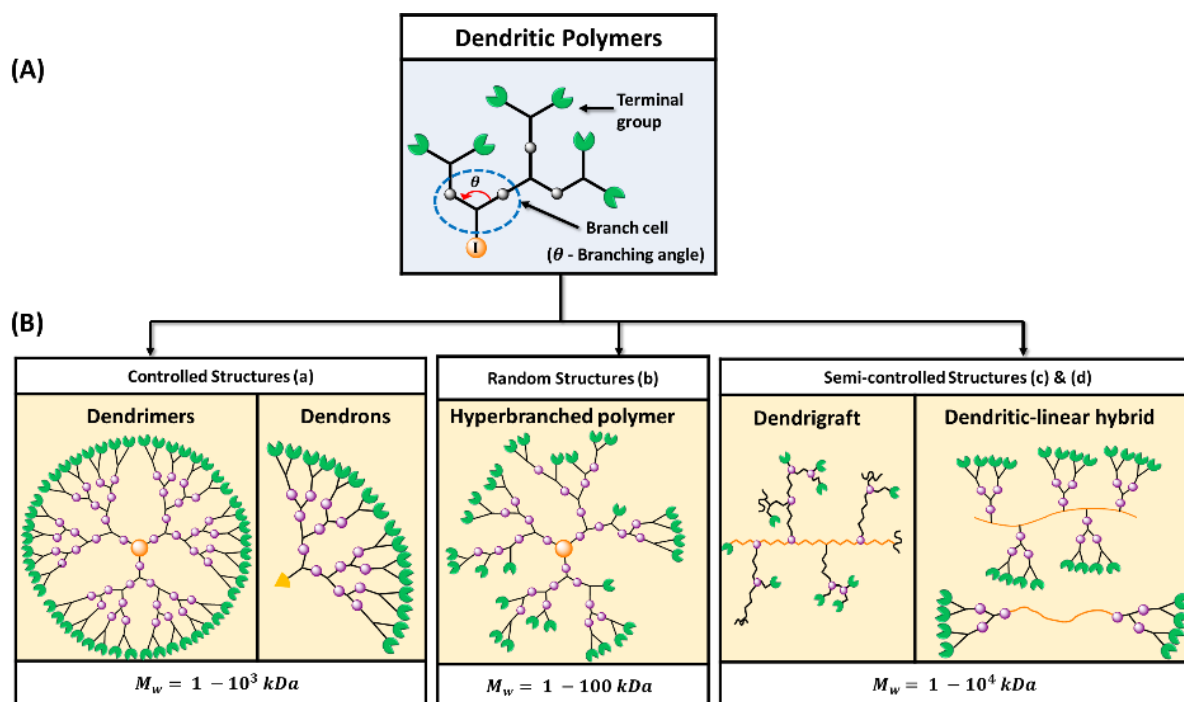


Figure 1.2 Pictorial representation of subclasses of dendritic polymers.

All dendritic systems are open, covalent assemblies of branched cells. The creation of dendritic assemblies and the level of structural control are mainly defined by the propagation strategies as well as by the branch-cell (BC) construction parameters^[42]. This BC parameters are determined by the type of BC monomers and nature of the excluded volume. The BC excluded volume depends on length of the arms, rigidity or flexibility, the symmetry and angle of branching and rotation. The covalent connectivity of dendritic arrays is usually associated to some molecular reference marker or core (I) (**Figure 1.2 A**). In due respect to this, BC arrays are irregular and polydisperse (e.g., $M_w/M_n \cong 2-10$) as in case of hyperbranched polymers and perfectly organized, core-shell type, monodispersed architecture as noted for dendrons /dendrimers ($M_w/M_n \cong 1.0000-1.05$). Dendrigrraft and dendronized polymers reside between these two structural extremes usually manifesting narrow polydispersity's of $M_w/M_n \cong 1.1-1.5$, depending on mode of preparation (**Figure 1.2 B**).

I. Hyperbranched polymers

Hyperbranched polymers (HBP)^[33,40,43] are irregularly or randomly branched macromolecules containing imperfections in the branching points. They have poor control over structure hence we find dendritic as well as linear sites in its macro-structure. Presence of large number of end groups increases the solubility of HBP drastically as compared to its

linear analogues. Traditionally hyperbranched polymers are prepared by polymerization of AB_x type monomers, where $x \geq 2$. Hyperbranched structures are formed as long as A react only with B functionality of another molecule. This methodology is known as “single-monomer methodology (SMM)”. New advancement in SMM strategy was introduced by Fréchet et al., wherein latent AB_2 type monomers were utilized for polymerization. This strategy is known as self-condensing vinyl polymerization (SCVP). Here, monomers possess both initiation and propagation sites, hence can follow two pathways, namely chain growth by vinyl polymerization and step growth by condensation of initiating site. Other SMM methods include self-condensing ring-opening polymerizations (SCROP) and proton-transfer polymerization (PTP).

In another strategy, two types of monomers or monomer pairs are polymerized together below the gel point by controlling monomer stoichiometry or restricting polymer conversion. This is known as double-monomer methodology (DMM) and is further classified based on monomer pairs and reaction pathways: (a) $A_2 + B_3$ methodology, (b) Couple-monomer methodology (CMM). Generally, HBPs are produced by one pot strategy using polycondensations, ring opening polymerizations or addition reaction. Common examples of HBP include poly(phenylenes), polycarbosilanes/siloxanes, Hybrane™ (poly(ester amide)), Boltorns® (bis-MPA polyester), Lupasol™ (poly(ethyleneimine)).

II. Dendrimers and dendrons

Dendrons and dendrimers are the most popular and intensely investigated subsets of dendritic polymers. When dendritic macromolecules are perfectly branched with well-defined size, shape and molecular weight, they are either dendrons or dendrimers. Dendrimers are fractal like macromolecules^[22,44] with regular branching pattern radially symmetric or asymmetric around the center mark. Classical or true dendrimers (PAMAM, PPI type) are core shell type, highly symmetric and attend globular structure at higher level of branching^[3]. Dendrimers are highlighted as well defined, synthetically tailored macromolecules with large number of end groups and a compact molecular structure^[45]. They are constructed in an iterative sequence of reaction steps, in which each iteration step leads to a higher generation material. Much like natural products and proteins, they are nearly monodispersed with predictable molecular weights and nano-scale dimensions. In contrast to linear polymers, these macromolecules do not entangle, showing unusual viscosity and solubility behavior, such as low solution viscosity and high solubility owing to the excessive terminal functional groups^[41].

The framework of a dendrimer consists of regular assembly AB_n monomers where A and B are two different functionalities and $n \geq 2$ ^[46]. Dendrimeric architecture is defined by three distinct structural regions, namely: [1] **Core** [2] **Interior branching or branching cell amplification region** [3] **Periphery or surface**. Each architectural part manifests a specific function, while at the same time defines properties for these nanostructures as they grow to complex level^[38]. A schematic picture of dendrimer structural regions is depicted in **Figure 1.3 b**.

- 1. Core:** central multifunctional structure where dendrimer growth begins by radial emanation of covalent bonds in outward direction. The core expresses size, shape, directionality and multiplicity of the structure, thus affecting the 3D shape of dendrimer (i.e., spherical, ellipsoidal, or cylindrical)^[47].
- 2. Interior or branching cell amplification region:** composed of repetitive AB_n branching units or monomers assembled together to form a covalently branch radial layers or inner shells denoted as **Generations** ($G=1,2, 3...etc.$). Its defined as number of branching points encountered upon moving outward from the core to its periphery^[48]. Plays a key role in propagating the growth of dendrimer, defining amount of interior void space generated and at the same time decides size and molecular mass of branched structure. Also, interior functionality and amount of solvent filled void space highly affect the guest-host properties of dendrimer.
- 3. Periphery or multivalent surface:** is an outer most layer or shell that is decorated with large number of active or passive terminal functional groups which can further undergo step growth polymerization or functionality modification. Depending upon the nature of the end groups, the dendrimers will vary in shape, stability, conformational rigidity/flexibility, solubility, and viscosity. Also, they control entry or departure of guest molecules from the dendrimer interior^[22].

Hence, these three architectural regions essentially govern the physicochemical properties, as well as the overall morphology of dendrimers. It is important to note that as a function of added generation, dendrimer diameters increase linearly whereas the terminal functional groups increase exponentially. As a result of which lower generations dendrimers are generally open, flexible structures, whereas higher generations become dense, less deformable three-dimensional shapes. Polyionic dendrimers do not have a persistent shape and may undergo changes in morphology as a function of increasing generations^[49,50].

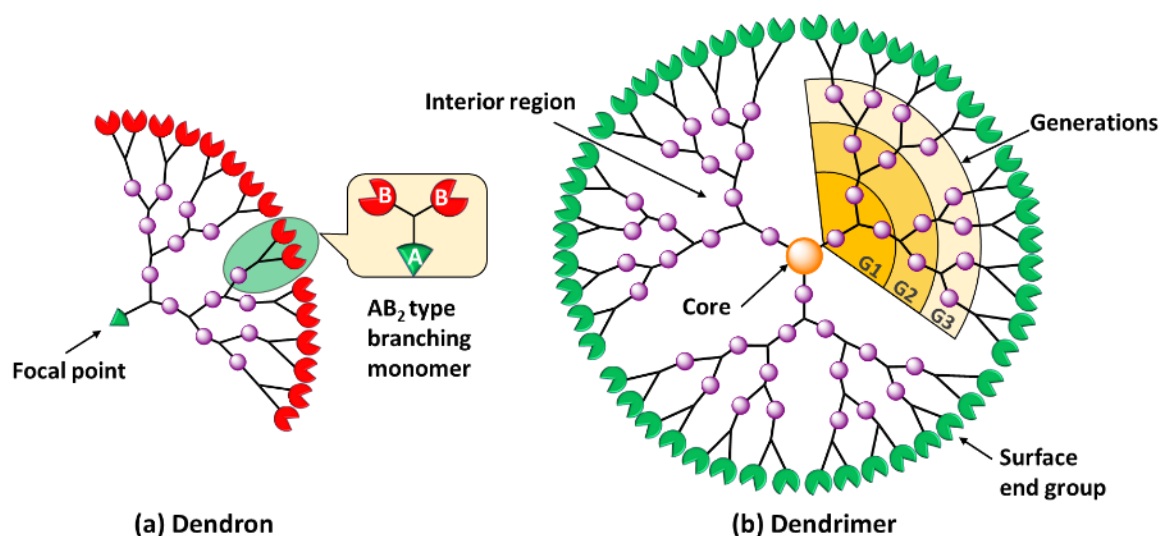


Figure 1.3 Pictorial representation of dendron and dendrimer.

Dendrimer structure can also be divided into its dendritic fragments called as **dendrons**^[2]. These are wedged-shaped sections of a dendrimer going from the core to the periphery. Individually, they do not possess core as such but instead initiates from post-active “focal point” (**Figure 1.3 a**). Hence, a dendrimer can be prepared by assembling two or more dendrons. They are also monodispersed and useful tools in the synthesis of dendrimers by the segment coupling strategy. A type of dendron, which is commercially available and successfully applied in the covalent and non-covalent assembly of dendrimers, are the “Fréchet-type polyether dendrons”^[37].

These structural features make dendrimers distinctly different from their linear and polydisperse analogues and endows with unique functional properties and multivalent cooperativity confined within a small 3-D space. Dendrimers are therefore extremely appealing materials for a wide variety of applications such as sensors, devices, catalysis, diagnostics, drugs and gene delivery systems in areas varying from environmental protection, energy production to human health. Nanomedicine is one of the applications in which dendrimers have been studied and tested, using as a nanocarrier bioactive molecules, imaging agents, or transfection of genes^[51].

Various type of valuable and esthetically pleasing dendritic systems have been developed and thus, a variety of dendritic scaffolds have become accessible with defined nanoscopic dimensions and discrete numbers of functional end groups. Common examples and commercially available dendrimers are as follows: Tomalia-type poly(amidoamine) (PAMAM, Dendritech[®], Sigma-Aldrich[®]), Fréchet-type poly(benzylether), Newkome’s polyamide, Vögtle’s polypropylenimine (PPI) (Astromol, DAB-Sigma-Aldrich[®]),

Denkewalter's poly(L-lysine) (Colcom[®], DGL), Hult's poly(2,2-bis(hydroxymethyl)propionic acid (bis-MPA polyester, Sigma-Aldrich[®]), phosphorous dendrimers (PMMH, Sigma-Aldrich[®]) and Grinstaff's polyester (PGLSA-OH)^[47].

III. Dendrigrraft Polymers

Dendrigrraft polymers^[52,53] are characterized as multi-level branched high molecular weight dendritic polymer, derived from method of successive grafting. This concept of dendrigrraft polymers was introduced independently by two research groups- Tomalia^[54] and Gauthier^[55]. Much like dendrimers, dendrigrraft polymers follows the generation-based growth strategy. However, the distinguishing feature of this polymers is the use of oligomeric or polymeric chains as branching block and their high molecular weight ($M_w \sim 10^4-10^8$) attained in few generations (e.g., G-3). Also, the size of dendrigrraft polymers is typically 10–1000 times larger than dendrimers with nanoscale range of 10 nm to a few hundred nanometres

Another highlighting property of these polymers is their high branching multiplicity, approximately 10-15 as compared to 1-3 in dendrimers or HBPs. Although, they consist of randomly distributed branching points as in HBP, still dendrigrraft polymers show narrow weight distribution (PDI ~ 1.1), but not as controlled as dendrimers. Hence, they are categorized as semi-controlled dendritic architectures, combining the features of dendrimers and HBP.

Dendrigrraft polymers are mainly synthesized using following methodologies based on living cationic or anionic polymerization techniques: (1) divergent 'grafting onto' approach, involves iterative coupling reactions of living polymer chains with a functionalized polymer core to yield comb-branched type polymer (2) divergent 'grafting from' approach, involves introduction of initiating sites on polymer core, followed by activation and growth of polymer side chains from active sites (3) convergent 'grafting through' approach, involves coupling of preformed living polymer chains with difunctional monomer in one-pot step. Common examples of dendrigrraft polymers includes, Comb-burst[®], arborescent polybutadiene, etc.

IV. Linear-dendritic hybrid polymers

This is a class of dendritic polymers^[56]; wherein perfectly branched (dendrons) or imperfectly branched (hyperbranched) dendritic units are coupled with linear polymer chains using either divergent or convergent methodologies. These hybrid polymers combine

the unique properties associated with both dendritic and linear component, thereby advancing the applicability of final material further. Depending on the coupling modes, these polymers are further classified as “linear-dendritic block copolymers” and “dendronized polymers”.

“**Linear-dendritic block polymers (LDBC)**” typically composed of two or more component (linear and dendritic) ^[57,58] in a one-dimensional flexible array. Initial reports on such hybrid materials were published by Newkome^[26,59] and Fréchet^[60] in the late 1980s to early 1990s. The ambivalent character of this architecture leads to distinct properties, which opens a numerous to emerging applications. Such uncertain behaviour could be observed in solutions, where they undergo self-assembly to form spherical micelles or sometime complex supramolecular structures such as cylindrical micelles or vesicles.

Linear–dendritic block copolymers (LDBC) can be synthesized using following methodologies: a) “Coupling strategy”, involve direct coupling dendritic block with mono- or oligo-functional linear polymer chain; b) “Chain-first strategy”, synthesis of terminally functional living polymer chain first, followed by divergent construction of dendritic component and c) “Dendron-first strategy” involves convergent growth synthesis of dendritic component first with chain initiating focal point, for later polymerization of monomer to couple linear polymer chain. Using these strategies diverse linear–dendritic hybrids polymers composed of dendrons or hyperbranched dendritic segments have been reported in the literature.

“**Dendronized polymers**”^[61,62] sometime referred as “rod-shaped polymers”, are macromolecules with multiple dendritic segments attached to a linear backbone and thus differing peculiarly from linear-dendritic block copolymers. They were first introduced in year 1993 by Schlüter et al.^[63] and Percec et al.^[64] They can be considered as special class of comb polymers where “comb-teeth’s” are dendrons assembled covalently on linear polymer chain.

Depending on the size and density of dendrons, the dendronized polymers can orient in either random coil or completely stretched out conformation. Due to the steric hindrance between adjacent dendrons, especially in high generation, these polymers exhibit a wormlike morphology, whose diameter and flexibility are mainly dependent upon the generation of dendrons. Additionally, they possess high aspect ratio as compared to globular dendrimers, forming one-dimensional nanoscopic objects.

Furthermore, they are synthesized using following strategies: (a) “Attached-to-route approach” where dendrons are grown either divergently from polymer chain back bone or

attach convergently grown dendron to polymer chain (b) In “macromonomer route”, dendrons of desired generation having a polymerizable focal point (i.e., the macromonomer) are synthesized first and then set to polymerized to generate polymeric hybrid anchoring side dendrons on each repeating unit. Common examples are Percec-type dendronized polymers, PAMAM, PPI-based linear-dendritic hybrid polymers, bis-MPA polyester based dendronized polymers, Fréchet-type linear-dendritic hybrid polymers, etc.

1.1.3 Synthetic strategies towards dendrimers/dendrons: from conventional routes to revised and accelerated methodologies

Growth process^[46,65,66] of dendrimers is highly influenced by the type of chemistry employed and steric factors especially above G4 or G5 i.e., those related to exponentially growing surface functionalities. One of such factors is the backfolding of the end groups into the interior of the macromolecule. This factor is governed by the dendrimer structure (flexibility and ability of dendrimer structural unit to interact with each other) and reaction conditions such as pH, solvent polarity, pH and ionic strengths^[67]. Another factor that restricts generation growth is the density of surface functionalities. As per dendrimer growth theories by Maciejewski^[68] and later by de Gennes^[69], growth rate of terminal group increases in exponential manner whereas dendrimer radii increases in linear way. Hence, at a certain critical generation, the outer surface of dendrimer becomes densely packed, thereby precluding the ideal branching in dendrimer. This effect is known as “de Gennes dense packing” or “starburst limit effect”. Dendrimer reaching such limit leads to incomplete stoichiometric conversion of end groups to next generation level. This dense packing limit differs with the dendrimer structural features such as valency and size of the core and branching monomers, ability of surface groups to form intramolecular network e.g., hydrogen bonding.

Over past 30 years, synthetic strategies to construct dendrimers and other complex dendritic scaffolds, requiring precise structural control have been well established globally. This could be credited to use of robust and chemo selective organic reactions along with skilful variation of building blocks to generated perfectly branched 3-dimensional macromolecule.

I. Conventional methodologies

Dendrimers and dendrons are typically synthesized using a multiple sequence of iterative “growth or coupling” and “activation” steps. There are two basic synthetic strategies

available to approach dendrimers and dendron, a) Divergent (inside out) b) Convergent (outside in). An overview of these conventional strategies as well as revised approaches will be discussed below.

i. Divergent growth synthesis (inside-out approach)

Dendrimers were first synthesized using divergent strategy^[24,26]. According to this strategy, step wise growth of dendrimers emanates from multivalent core C_n ($n \geq 2$), as starting point and propagates through AB_n type ($n \geq 2$) e.g., AB_2 type branching monomer or building block, where A is an activated group and B is dormant/protected functionalities, which later allows controlled propagation after activation process. In a typical process, excess of active A functionalities of AB_n branching monomer are coupled with reactive sites on core, to generate a first dendritic layer denoted as $[G=1d]$ “dormant” dendrimer. Before going to the next step, this dendrimer is purified using chromatographic techniques. After isolation, dormant/protected B functionalities in dendrimer are activated/deprotected to form $[G=1a]$ “active” dendrimer. In next growth step, newly generated reactive coupling sites were coupled with another new set of AB_n monomers giving rise to second generation dendrimer denoted as $[G=2d]$. Similarly, this dendrimer is purified and activated for next growth step. Thus further, iterative sequence of growth and activation step leads to an increase in generation levels along with exponential increase in end groups. However, the increasing number of end-groups with generation level requires large excesses of monomers, in order to drive the reaction towards completion. Upon reaching desired dendrimer level, peripheral groups are set for further post-modification. For AB_2 type monomer, synthesis proceeds in $1 \rightarrow 2$ branching pattern i.e., every branching site couples two units. Most of the divergent methods are reported on $1 \rightarrow 2$ and $1 \rightarrow 3$ branching monomers^[70,71]. Schematics of divergent growth strategy is shown in **Figure 1.4**.

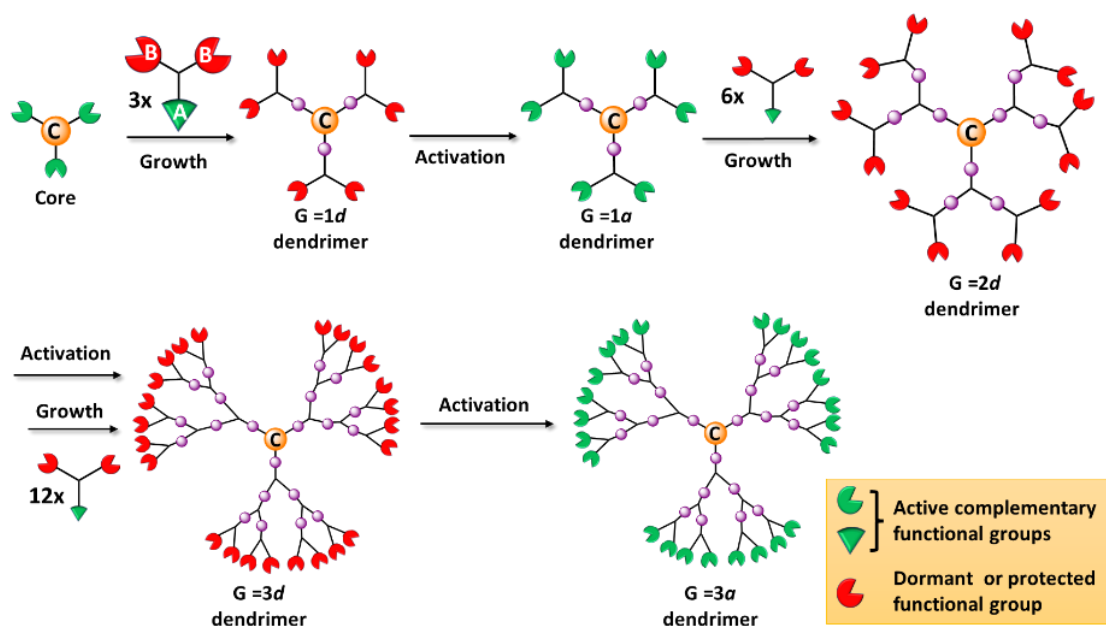


Figure 1.4 Schematics of conventional divergent growth strategy using AB₂ monomer.

A major challenge or difficulty associated with divergent process is to produce the perfectly branched dendrimers at higher generation. Since as a number of generation levels increases the risk of incomplete derivatization during growth or activation step also increases. This mainly arises due to surface crowding or dense packing effect, which give rise to incomplete conversions. As consequence of this, structural defect is observed in dendrimers at higher generations. Additionally, separation of perfectly branched dendrimer from defective dendrimer extremely difficult by standard purification methods because products are identically chemically as well as in size. Nevertheless, defects can be avoided by using robust organic reaction showing high at macromolecular level as well as monitor the progress of the reaction by MS technique.

It should be noted that dendrimer synthesis by divergent process is most practicable approach as it only need an excess of inexpensive reagents. Thus, commercially available dendrimers such as PAMAM^[51], PPI^[72] are still synthesised using this technique. Also, another advantage of divergent process is, it enables full modification of dendrimer surface in a single step, which can afford libraries of surface modified structures with same internal structure for application various field (e.g., drug delivery systems, catalysts, etc.). Such flexibility is less likely to achieve in the below described convergent method.

ii. Convergent growth synthesis (outside-in approach)

Convergent synthesis was first introduced by Hawker and Fréchet^[34,36], as an alternative growth route to construct dendrimers. This a complementary strategy to divergent route, as

it propagates in opposite direction, from periphery towards core i.e., outside-inward path. In this strategy perfectly branched dendritic wedges so called dendrons are synthesized first and finally coupled to multivalent core C_n through activated functionality at convergence point. Dendrons are synthesized based on AB_n type branching monomer, in a similar manner as of divergent approach using growth and activation steps. In a typical synthesis as illustrated in **Figure 1.5**, first generation $[G=1d]$ dendron with dormant functional groups is constructed by coupling A-active site of AB_2 monomer with B-active active site of another AB_2 type. Second generation $[G=2d]$ dendron is obtained by activating A-sites of $[G=1d]$ dendron to form $[G=1a]$ active dendron and subsequent coupling with B-active site of AB_2 monomer. This iterative growth and activation steps are continued until desired sector shaped dendrons is produced. In final step, the dormant group (A-site) at focal point of high generation dendron is activated and coupled with multivalent core to furnish target dendrimer.

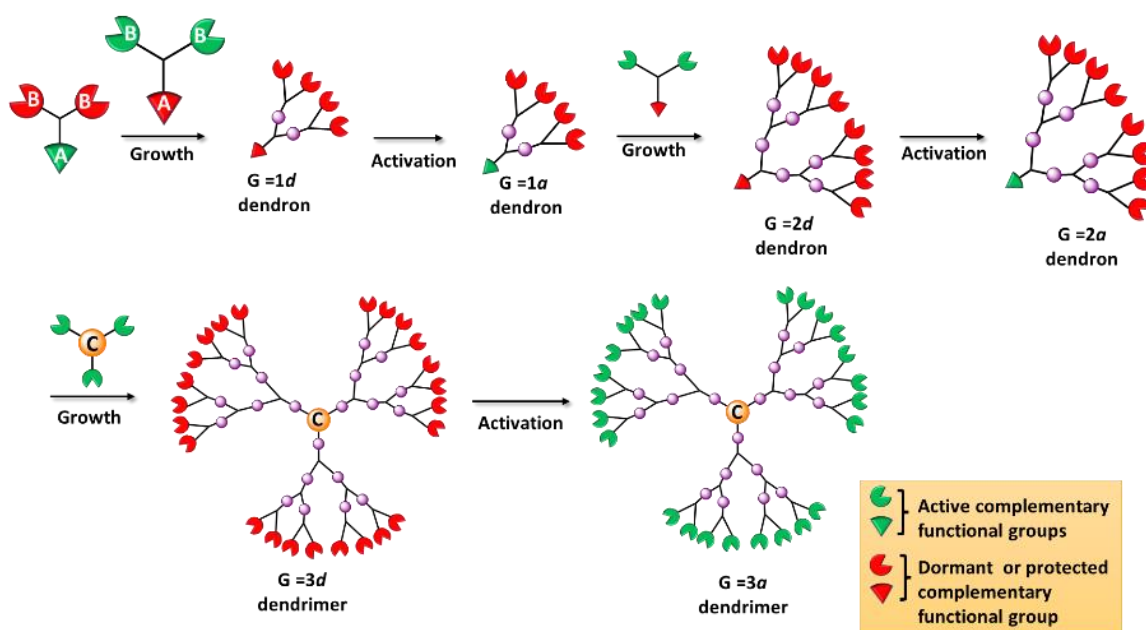


Figure 1.5 Schematics of conventional convergent growth strategy using AB_2 monomer

In comparison with divergent approach, convergent synthesis involves limited number of reactions per generation, thus providing greater control over synthesis, structure, end group functionality and avoid use of large excess of reagent. The use of equimolar or slight excess quantities of reagent is sufficient to drive reaction towards completion. Also, monitoring the growth process in dendron synthesis is much easier because of dendrons having less structural complications compared to dendrimers. Additionally, purification of dendron product is less tedious as compared divergent approach. This because the sizable difference

of molar mass and polarity between the fully derivatized dendron/dendrimer and by-products. As result of all, dendrons and dendrimers with negligible structural defect are produced but up to certain generations.

Highlighting feature of this strategy is ability to assemble different class and size of dendrons onto single core, giving rise to multifunctional dendrimers such as segmented-block dendrimers, surface-block dendrimers, etc^[73]. Additionally, convergent synthesis gives flexibility for changing core unit i.e., same dendron can be assembled to different cores in single step. Hence using this features, library of dendrimers differing in the nature of their core, dendrons, terminal functionalities can be created by convergence approach.

Growing dendron still accompanies with the critical limitations at higher generations. With growing dendron size, reaction efficiency as well as accessibility of convergence point for final coupling step decreases because of the steric hindrance. For this reason, overall yield of dendron decreases and coupling of bulky dendron to core through its activated convergence site leads to incomplete substitution. To overcome these difficulties and drive the final coupling step towards completion, researchers have tried using excess of dendrons and catalyst, harsher reaction conditions and flexible cores to increases its accessibility. However, in a process, loss of high generation dendron during final coupling process leads to low yield of higher generation dendrimers. This restricts the use of convergence synthesis for commercial production of dendrimers. Hence only lower generation dendrimers (<G6) are recommended to construct by convergent method.

II. Accelerated Methodologies

Even though conventional methodologies^[46,56] have successfully produced numerous types of dendrimers, still its iterative sequence of growth and activation makes the dendrimer synthesis tedious, laborious and risk of generating structural defects. Accelerated methodologies mainly focuses on reducing the number of reaction step in dendrimers synthesis to generate perfectly branched structures with sufficient large number of functional groups. This not only lowers the consumption of chemical and starting materials but also makes process more time and cost efficient. As a field of dendrimers is moving towards faster and simpler synthesis, various accelerated approaches are continuously introduced globally to make dendrimer synthesis less laborious and accessible at various scientific levels. Below are important parameters that have been recognized to accelerate the synthesis of dendrimers.

-
- **Choice of building block:** Selection of branching monomer plays a crucial role in deciding the structural composition, multiplicity and functionality of dendrimers. As monomers are used in excess, it is much preferable that these are made commercially available at large scale.
 - **Number of reactions:** Conventional strategies involves two steps, growth and activation, for propagating the growth of a dendrimer. Avoiding the activation steps by using chemoselective reactions would furnish the dendrimer in limited number of steps.
 - **One-pot synthesis:** Coupling monomer with complementary active groups with core in one-pot sequential manner will be always a choice of organic chemist. Hence, progressing in this will not only shortened the synthesis but also overcome the stepwise purifications.

i. Strategies accelerating conventional methods

These strategies are already documented in early 1990s and were devised progressively with an aim to shortened the number of steps and secured the high branching precision in contrast to conventional approaches. Three such approaches were introduced with limited growth and activation steps, namely a) double-stage convergent strategy, b) double-exponential strategy and c) hypermonomer strategy.

a. Double-stage convergent strategy (hypercore approach)

This strategy composed of parallel syntheses of low generation dendrimer and low generation dendrons, which are coupled together in final stage to generated high generation dendrimer. Low generation, activated dendrimer are used as a core, hence it is names as “hypercore” (**Figure 1.6**). In a final step, either a same or different kind of dendron is coupled to the active hyper core to produce homo or hetero-structural dendrimer.

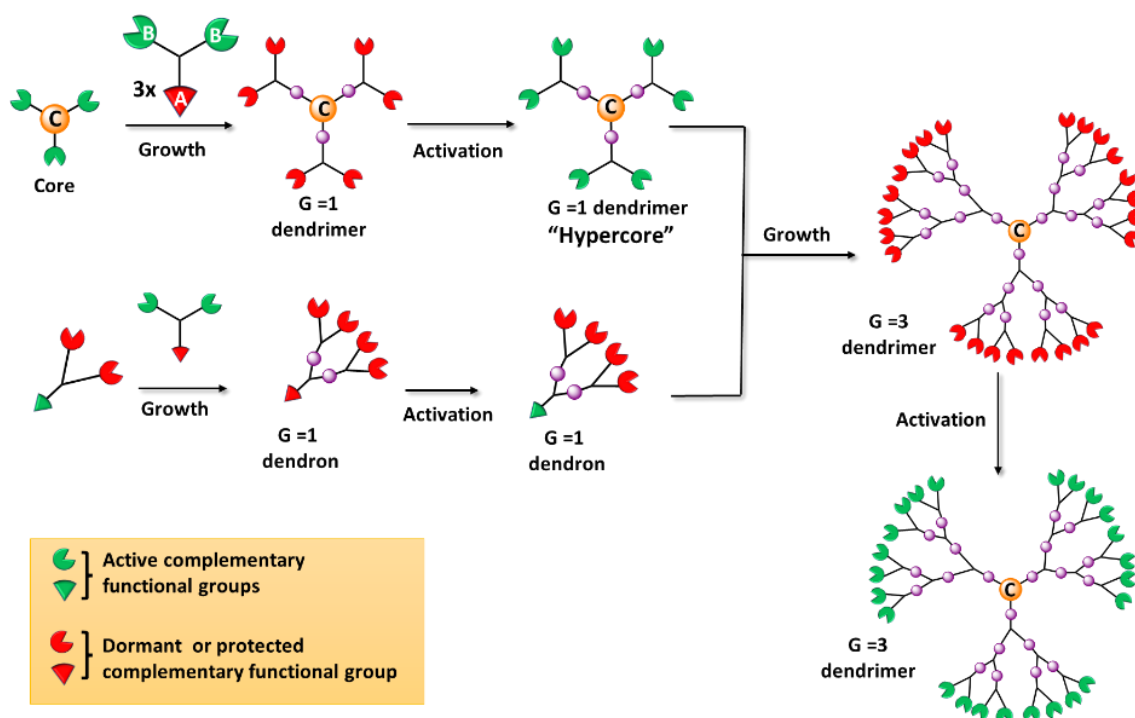


Figure 1.6 Schematics of double stage convergent growth strategy using AB_2 monomer.

This strategy was first introduced by Fréchet group^[74] during the synthesis of G7 double layered poly(benzyl ether) dendrimer. For this purpose, they synthesized G3 hypercore consisting of aliphatic spacers between the benzyl groups. This makes the hypercore flexible and allows efficient coupling with G4 poly (benzyl ether) dendron. Even though synthesis of high molecular weight dendrimer involves limited steps, overall synthesis is time consuming. Since many steps are involved in preparation of dendrons and hypercore. Nevertheless, methodology should be always be considered where the conventional convergent approach is difficult for synthesis of higher generation dendrimers.

b. Double-exponential convergent strategy

This strategy initiates with fully protected AB_n type branching monomer and propagates with two selective activation steps and one coupling step to produce doubly generated dendron ($G1 \rightarrow G3 \rightarrow G7 \dots$). In activation steps, one route targets the selective activation of branching sites i.e., B-sites whereas other activates A-sites at convergence point. In a growth step, branching unit with active A-site is coupled B-sites of another unit, to afford dendron. Iteration of this accelerated activation and growth step leads to highly branched dormant dendron. In order to construct the target dendrimer, A-sites of high generation dendron is activated and coupled with activated multivalent core. Pictorial representation of overall process is shown in **Figure 1.7**.

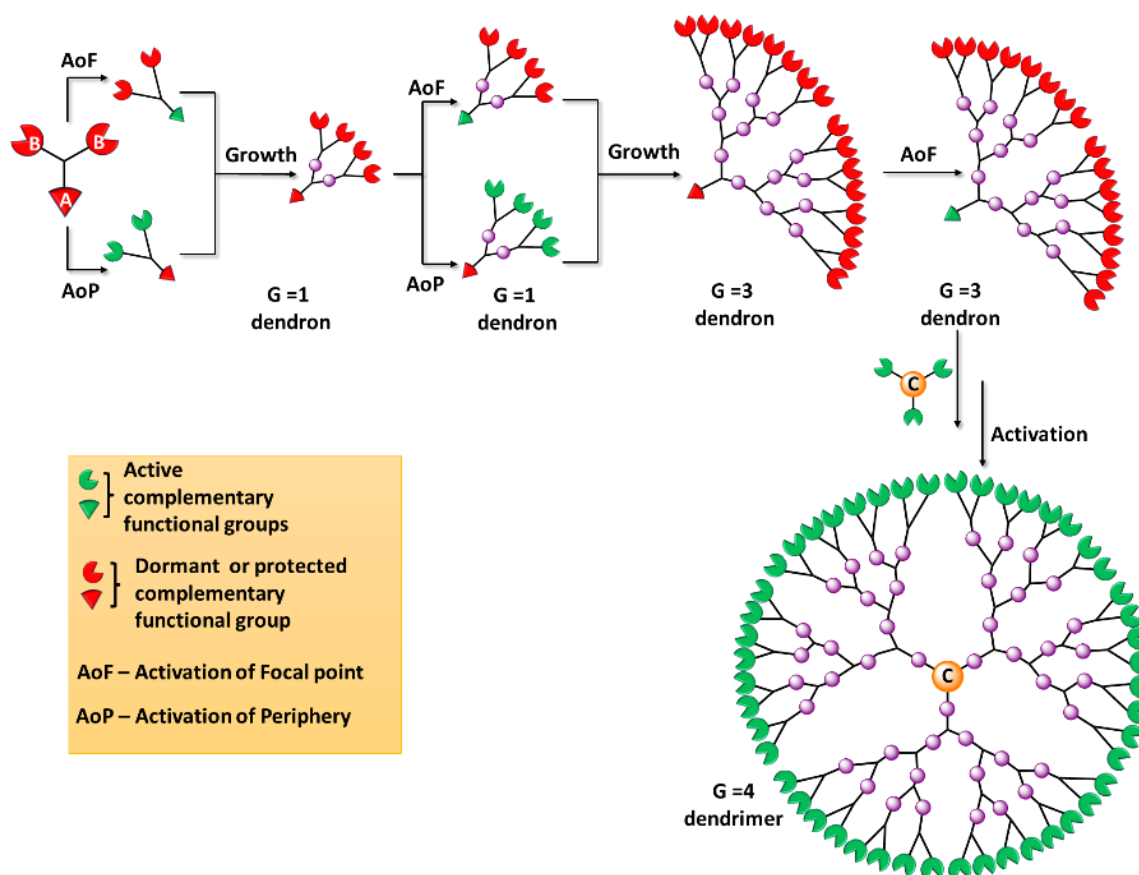


Figure 1.7 Schematics of double exponential convergent strategy using AB_2 monomer.

This concept was first introduced by Moore et al. in 1995, during the synthesis of a G4 poly(phenylacetylene) dendron^[75]. Theoretically, this method could produce G7 dendrimer in 9 steps as compared to conventional convergent synthesis which would require 14 steps. Hence, this method could be considered as one of the rapid approaches to afford high generation dendrons. Using double-exponential method, various class of dendrimers were synthesized, namely poly(ester), poly(amide), poly(ether urethane). Among these G4 aliphatic polyester dendrimers based on bis-MPA branching unit are promising materials and were reported by Hult et al.^[76] However, it was observed that the yield of dendron lowers with increasing dendron size. Commercially, bis-MPA dendrimers are produced using divergent strategy.

c. Hypermonomer strategy

This strategy involves branching monomers with high number of B-functional sites such as AB_4 , AB_8 , etc., in comparison with conventional AB_2 type monomer. Such high functionality monomers were named as “hypermonomers”. Utilizing such hypermonomers,

dendrimers with large number of functional groups are produced in a few synthetic steps. Pictorial representation of hypermonomer strategy is shown in **Figure 1.8**.

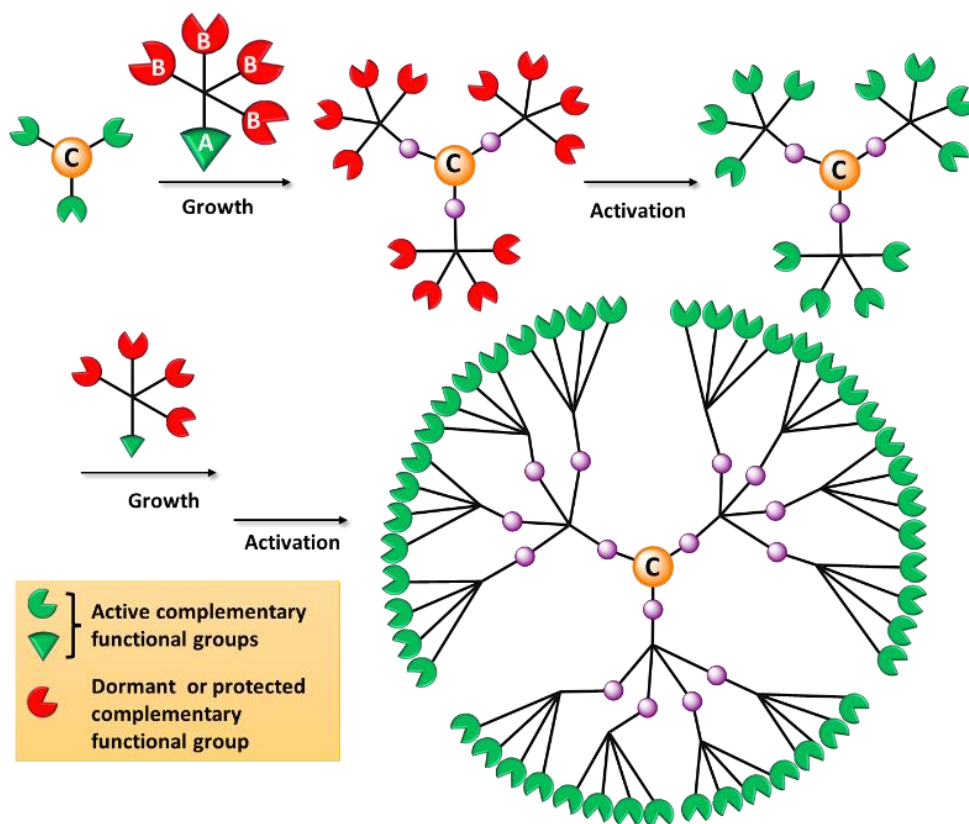


Figure 1.8 Schematics of hypermonomer divergent strategy using AB_4 monomer.

This type of approach was first reported by Fréchet et al.^[77] in 1994. Here, the author utilized AB_4 hypermonomer and coupled with G3 poly (benzyl ether) dendron to afford G5 dendrimers in single coupling step. However, the final dendrimer was obtained in low yield due to steric hindrance and low reaction efficacy. It is also important to note that, hypermonomer used here was nothing but the G2 dendron with carboxylic acid end groups. Other reports include dendrimers-based methyl 3,4,5-trihydroxybenzoate AB_3 monomer^[78] and poly(phenylene) dendrimers based on diene-dienophile type AB_4 monomer^[79]. Generally, the hypermonomer approach is less often used due to time consuming synthesis of dendron as hypermonomer and steric issues.

ii. Chemoselective accelerated growth synthesis towards dendrimers

Although the above revised approaches are seen to accelerate the convention growth process, overall protocol from synthon preparation to final growth steps is time consuming. Thus, in order to have truly accelerated process, one should think of eliminating activation step. This can be achieved by utilizing two or more robust, chemoselective process, which

can work independently in growth of dendrimers. The concept of chemoselectivity is described below for orthogonal and one-pot growth.

a. Orthogonal growth strategy

This strategy employs two different branching monomers i.e., AB_x and CD_x ($x \geq 2$) with complementary coupling sites in divergent or convergent growth synthesis as illustrated in **Figure 1.9**. Combination of this monomer is chosen in such way that, each monomers convergence site selectively couples with peripheral site of other monomer; in other words, A convergence site selectively couples with D peripheral site, similarly C site couples only with D site. Such chemoselective combination and iteration led to layer-block dendrimer/dendron, thereby eliminating the activation steps and overall reduction in number of steps.

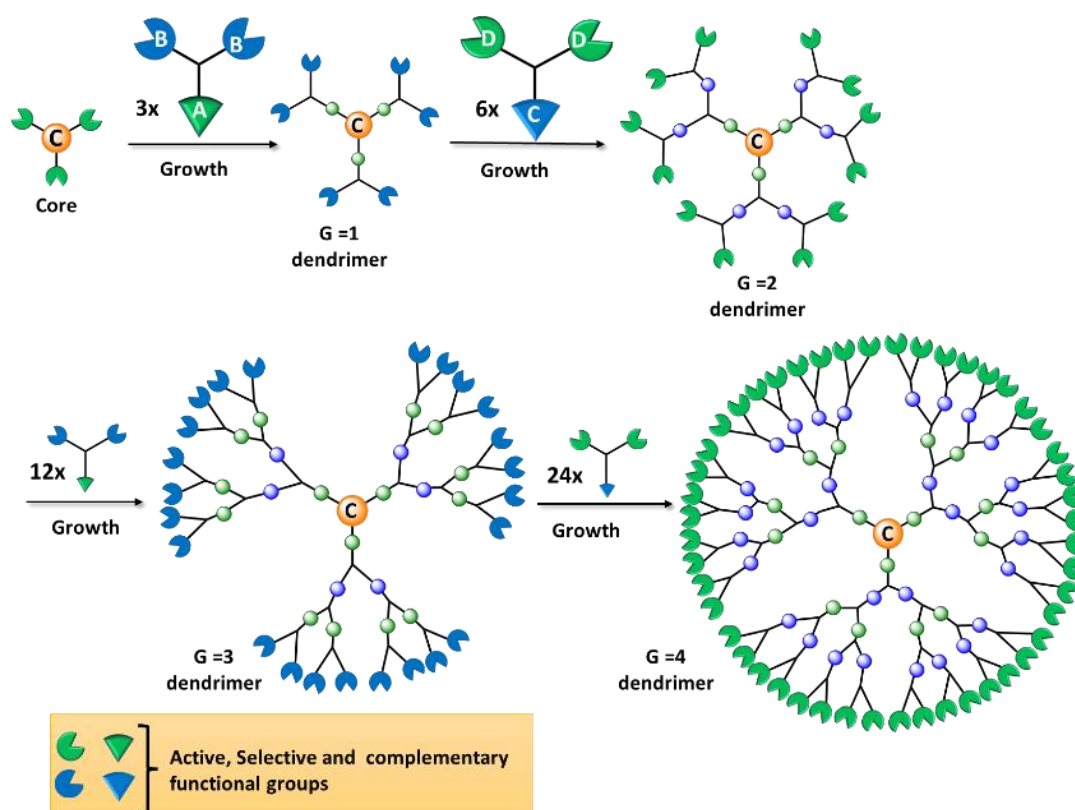


Figure 1.9 Schematics of orthogonal divergent growth strategy using AB_2 - CD_2 monomers

Orthogonal strategy was first attempted by Spindler and Fréchet^[80], while working on synthesis of G3 poly(ether urethane) dendron. They used 3,5-diisocyanatobenzyl chloride and 3,5-dihydroxybenzyl alcohol as AB_2 and CD_2 monomers. However, combine reaction of urethane formation and etherification result in low generation dendrons. The reason being

poor efficacy and chemoselectivity of both reactions. The first effective synthesis of high generation dendrimers via orthogonal strategy was reported by Zimmerman et al.^[81] They employed Mitsunobu esterification and Sonogashira coupling of terminal alkyne with an aryl iodide to afford G4 poly(alkyne ester) dendrons. Additionally, Majoral et al.^[82] reported application of AB₅ and CD₅ hypermonomers in orthogonal strategy, to afford G3 phosphorus-containing dendrimer with 375 end groups just in three steps.

Furthermore, introduction of click chemistry concept in dendrimer synthesis^[83,84], has totally revolutionized synthesis process and made it more attractive. This could be experienced by dramatic increase in the scientific reports dealing with orthogonal and one pot construction of dendrimers using click chemistry. The combine approach of orthogonal and click chemistry was first reported by Malkoch et al.^[85] in 2007, where they synthesis of three different G4 dendrimers consisting of two bis-MPA based and one Fréchet polyaryl type. One of the most promising orthogonal synthesis was reported by Malkoch and Hawker^[86], where they combined thiol-ene and CuAAC click reaction to assemble two AB₂ and CD₂ monomers to generated G6 bis-MPA dendrimer in less than 24 h.

b. One pot growth strategy (NTR and TR methods)

One pot synthesis of dendrimers is considered as ultimate accelerated approach and a primary choice of chemist, which not only reduces laborious steps but prominently confined the purification at final step. This one pot multi-step synthesis is divided into two categories: tandem reactions (TRs) and non-tandem reactions (NTRs). In TR method, chemical reactions take place simultaneously and independent of one another. In NTR method, chemical reactions take place in sequential manner, one after another. Pictorial representation of NT and NTR routes is shown in **Figure 1.10**.

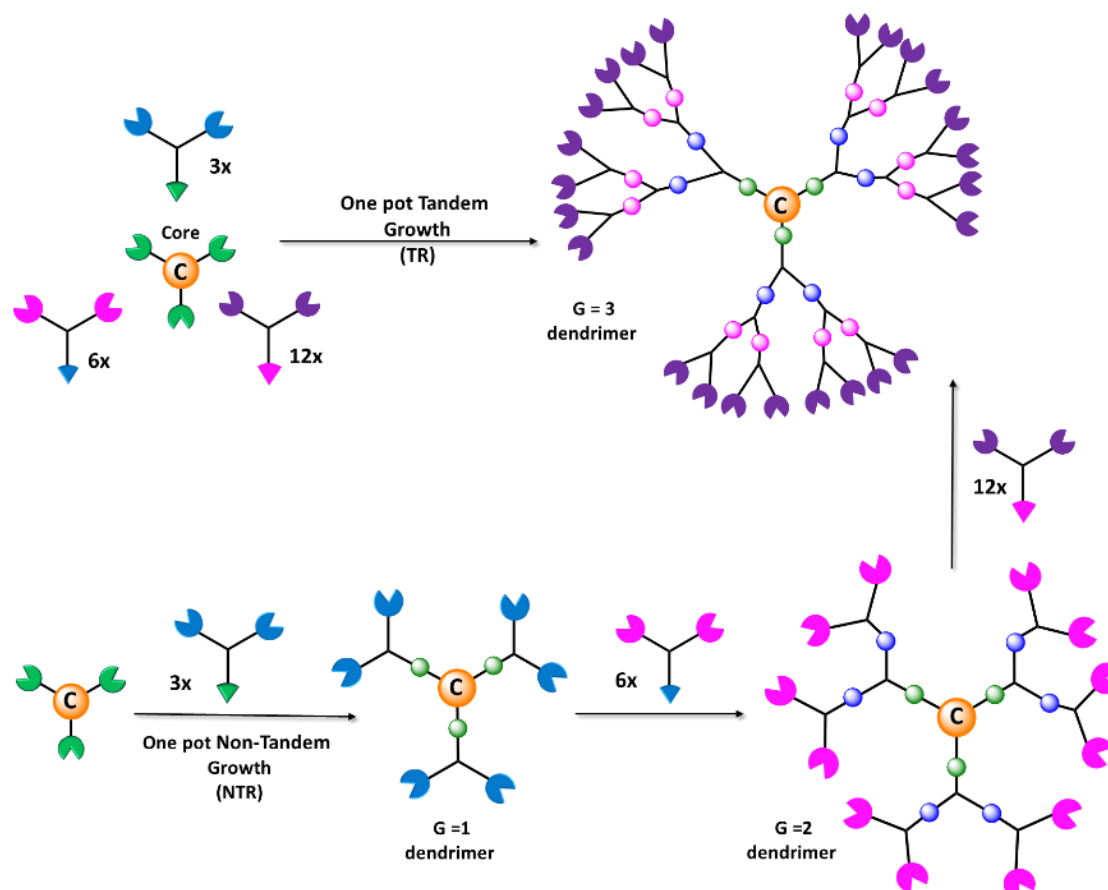


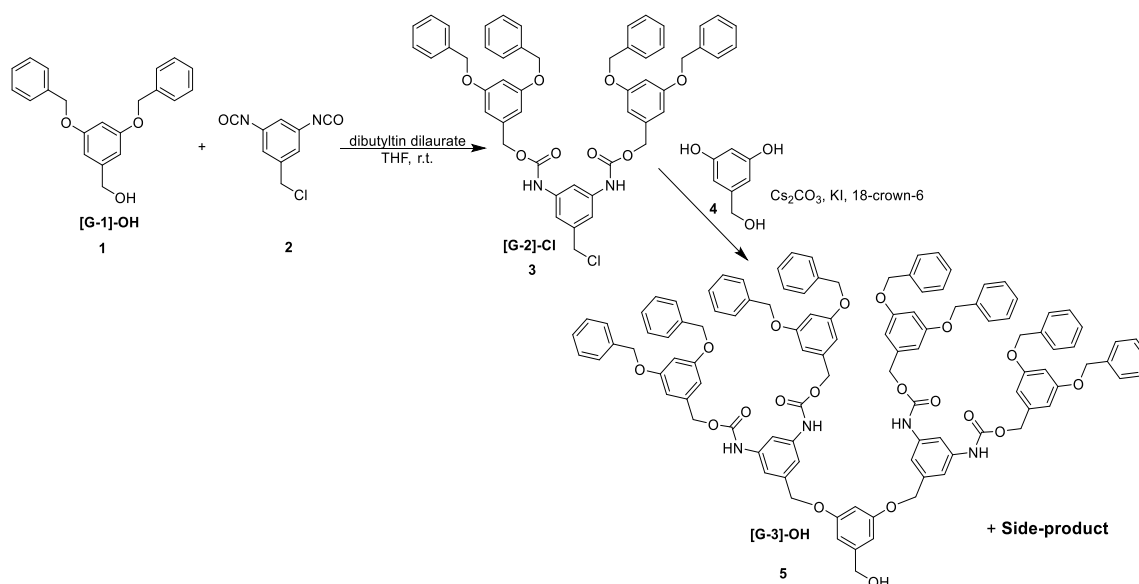
Figure 1.10 Schematics of one pot growth strategy using TR and NTR routes.

The first successful one pot synthesis of dendrimers was reported by Rannard and Davis^[87], who synthesized G3 carbonate dendrimer in four step NTRs convergent growth manner with progressive additions of the reagents. This reaction was performed at 100g scale and obtained dendrimer in 89% yield with final purification step. Moreover, one pot method was also applied for post surface modification of dendrimers as reported by Hawker and co-workers^[88]. Here, authors successfully functionalized terminal amine groups of G4 polypropylenimine dendrimer with PEG groups using amidation and CuAAC click reaction to afford PEG-ylated dendrimer in 78% yield. Despite several advantages in the synthesis of perfectly branched dendrimer via one pot process, it is still challenging. This is due to limitation associated with stoichiometry control over reagent, which produces by-product. A smart choice of chemoselective reactions and purification process can overcome the challenge

1.2 Literature review on polycarbonate and polyurethane dendrimers possessing 1→n (n≥2) branching motif

Extensive research in the field of dendrimer chemistry has generated libraries of dendritic families such as polyesters, polyethers, polyamines, polyamides, polyarylenes, polycarbosilanes, etc. However, the perfectly branched dendritic structure for polycarbonates and polyurethanes have been seldom explored. A literature survey on polyurethane dendrimers notifies, only a few reports dealt with the synthesis of perfect dendrimer structures using conventional isocyanate chemistry. The reason is difficulty in controlling the reactivity between isocyanate and hydroxyl groups in the iterative process thus leading to unwanted side reaction. Also, isocyanates are highly sensitive towards moisture thus handling isocyanate monomers is a tedious task.

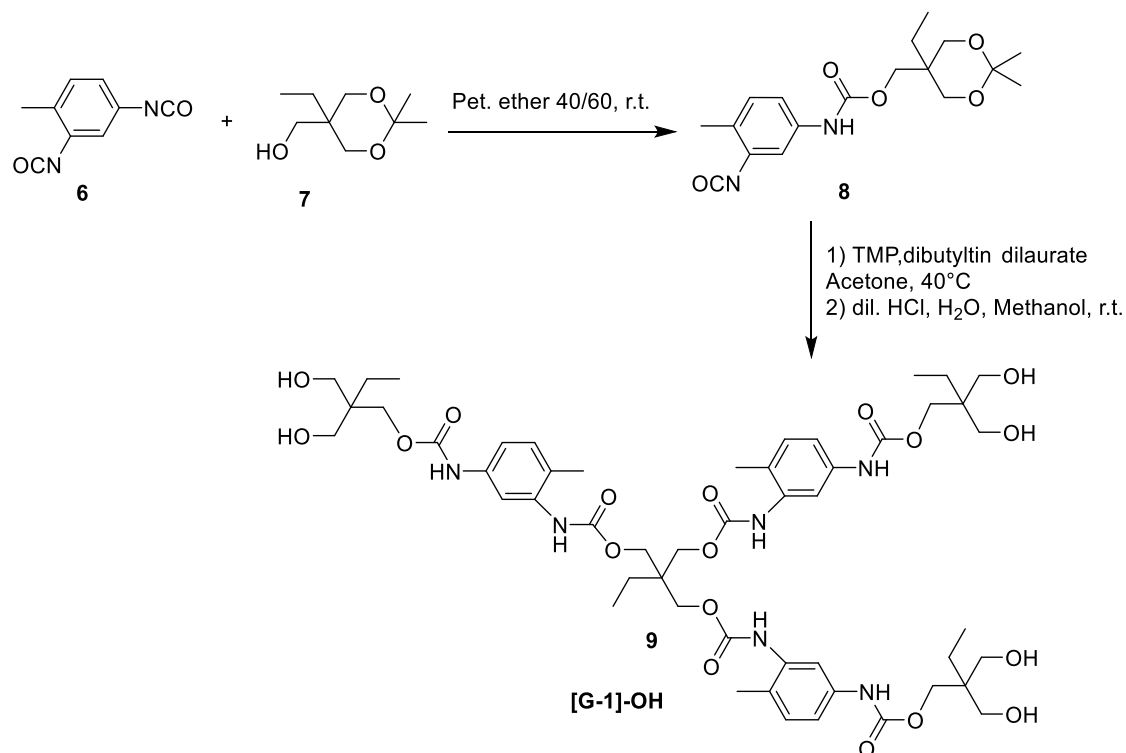
The first report on synthesis of 1→2 *Aryl*-urethane branched poly (aryl ether) was reported by Spindler and Fréchet^[80]. Here, authors utilized two step orthogonal approach to generate G3 urethane branched dendron **5**, by sequential assembling two different monomers i.e., 3,5-diisocyanatobenzyl chloride **2** and 3,5-dihydroxybenzyl alcohol **4** using Isocyanate coupling reaction and Williamson ether synthesis in one pot manner (**Scheme 1.1**). However, in-situ addition of 3,5-dihydroxybenzyl alcohol dendron **3** leads to some irregular growth, due to the side reaction occurring via transesterification of the carbamic ester connectivity.



Scheme 1.1 One pot orthogonal approach towards urethane branched poly(benzyl-ether) dendrimers.

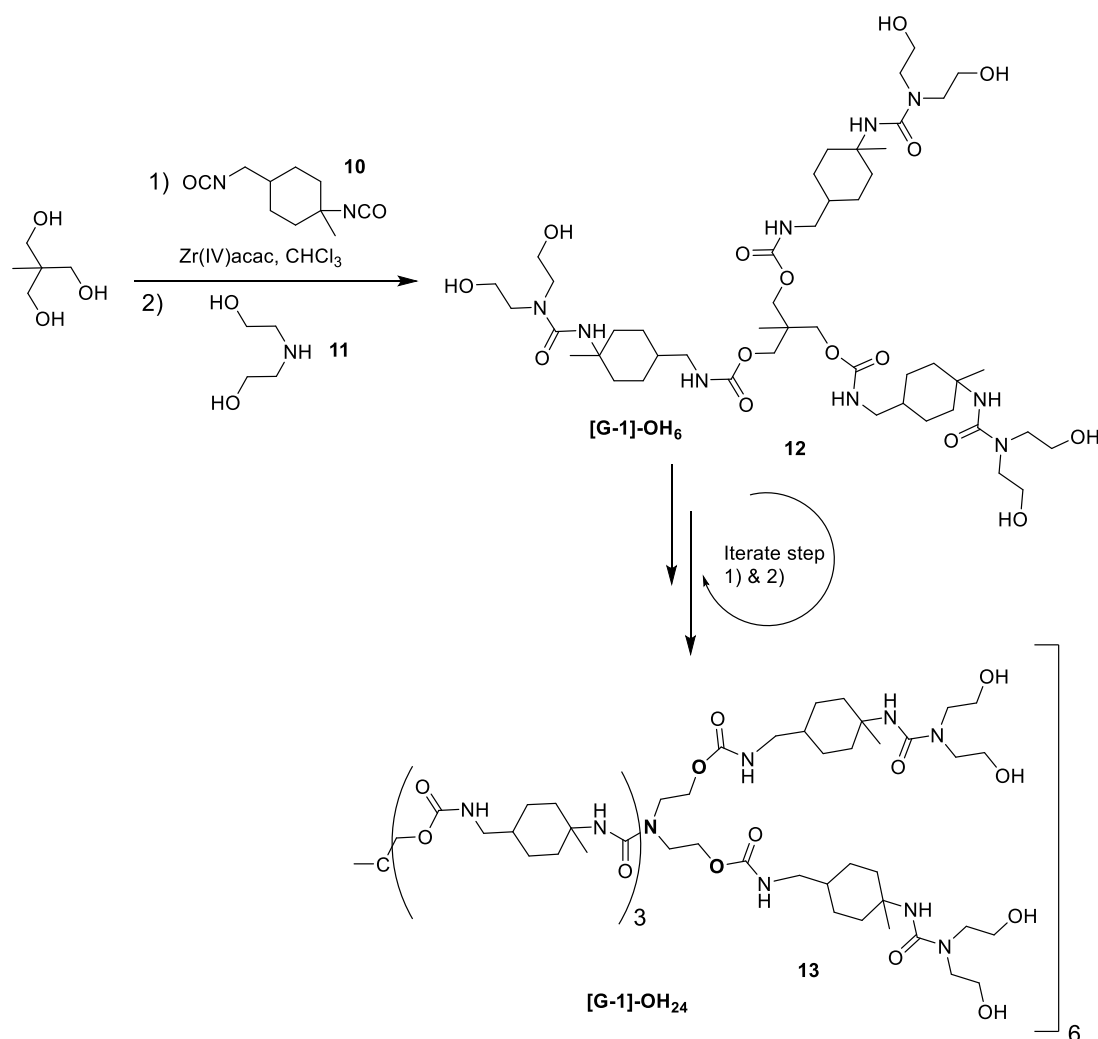
Using similar isocyanate coupling chemistry Bruchmann et al.^[89] reported divergent growth synthesis of G1 polyurethane dendrimer form AB₂ branching monomer **8**. This monomer

was synthesized using readily available raw materials 2,4-toluylene diisocyanate (TDI) **6** and trimethylolpropane (TMP) **7** via isocyanate selectivity and protection group chemistry (**Scheme 1.2**). With this approach hydroxyl group ended dendrimer **9** was obtained in a very effective manner.



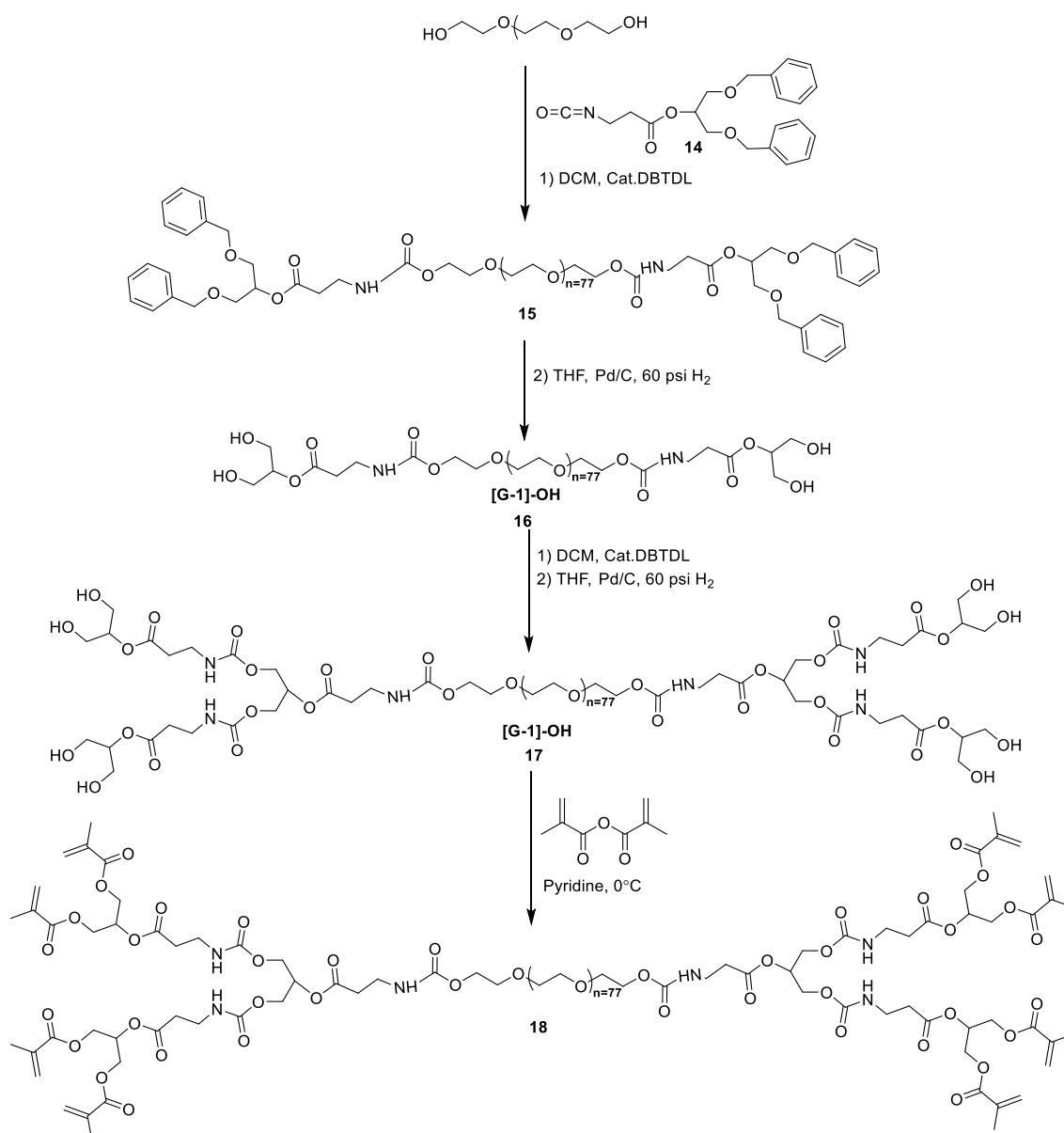
Scheme 1.2 Divergent growth synthesis of G1 polyurethane dendrimer using 2,4-toluylene diisocyanate and trimethylolpropane.

Peerlings et al.^[90] reported 1→2 *N* branched poly(urethane-urea) dendrimers using fast and efficient one pot procedure based on an AB-CD₂ divergent growth coupling strategy. AB are the primary and tertiary isocyanate groups in 4-isocyanatomethyl-1-methylcyclohexylisocyanate (IMCI) monomer **10** and CD₂ is diethanolamine monomer **11** with secondary amine and primary hydroxyl groups. Using the reactivity difference between isocyanate group and sequential coupling reaction with amine and hydroxyls, resulted in third generation dendrimer **13** without any activation or deprotection step (**Scheme 1.3**). Moreover, accurate dosing of monomers allows the construction of dendrimer in 2-3 days with final purification. Besides trimethylol ethane core, 1,10-ferrocene dimethanol was also chosen as a bifunctional core.



Scheme 1.3 Divergent growth synthesis of G3 poly(urethane-urea) dendrimer based on AB+CD₂ selective coupling strategy.

In 2008, Grinstaff group^[91] reported the divergent synthesis of urethane-based dendrimers, utilizing natural metabolites such as glycerol and β -alanine as building units and poly(ethylene glycol) as macro-core. Here, AB₂ monomer **15** was from 1,3-benzyl protected glycerol and succinic anhydride as raw materials and stepwise functionalization to generate isocyanate functionality at focal point. Authors employed two step iterative approach of coupling primary hydroxyl groups with isocyanate followed by deprotection of benzyl groups with catalytic hydrogenation afford urethane branched dendrimers G1 (**16**) and G2 (**17**) (**Scheme 1.4**). Furthermore, these dendrimers were functionalized with acrylic end groups and crosslinked with an eosin-based photo initiator to afford hydrogels. This dendrimer-based hydrogel scaffold showed potential application towards cartilage tissue repair.

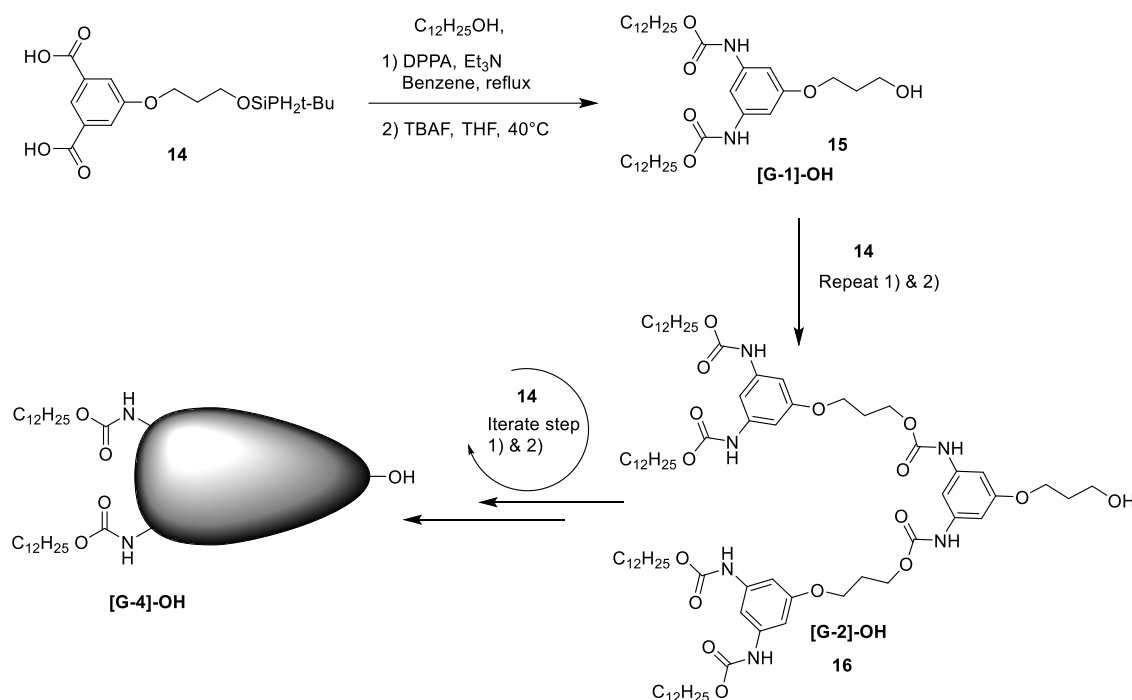


Scheme 1.4 Divergent growth synthesis of G₂ urethane dendrimer based on glycerol and β-alanine.

Furthermore, in order to fix the practical difficulties in handling isocyanate functionality and also as an alternative route to polyurethane dendrimers, several research groups have emerged with isocyanate-free approaches. The Synthetic routes are as follows.

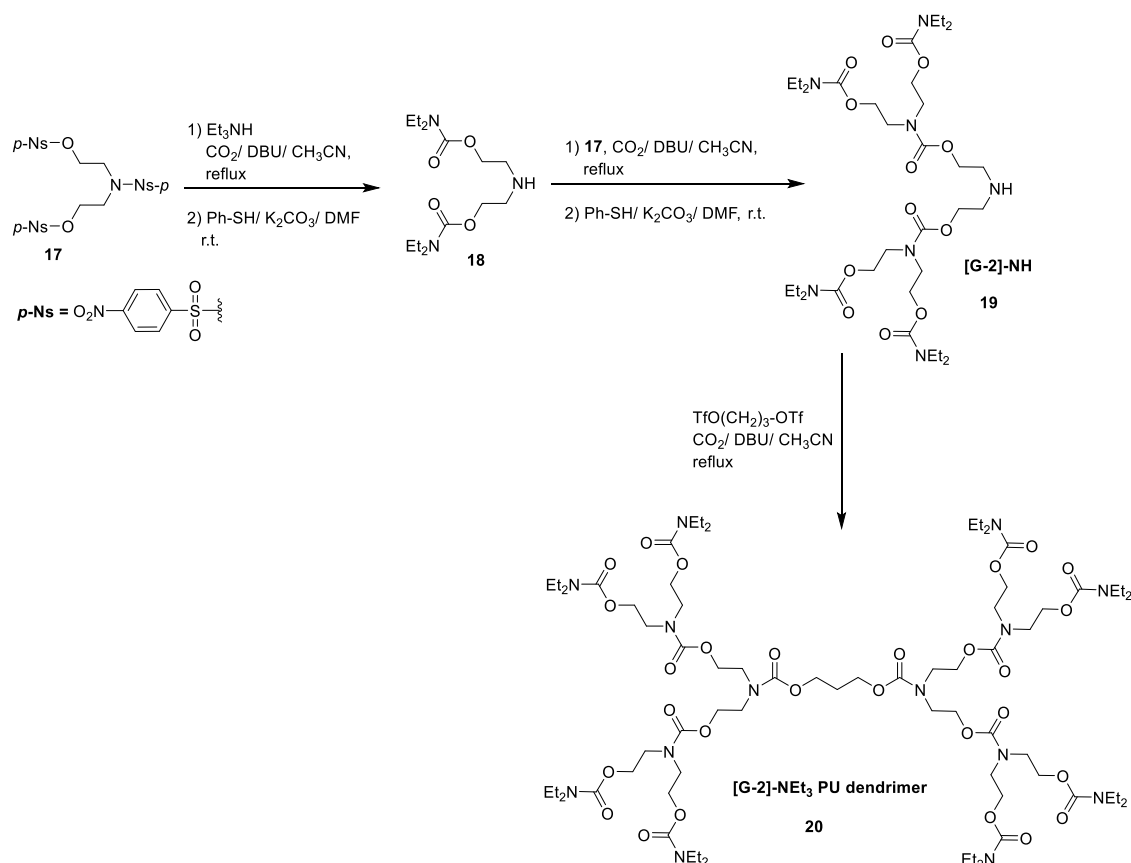
In 1998, R. T. Taylor et al.^[92] reported an isocyanate free route to construct 1→2 *Aryl* branched polyurethane dendrons and dendrimer via Curtius rearrangement. First generation diurethane dendron was synthesized by reacting 5-(*t*-butyldiphenylsiloxy)propyloxy-isophthalic acid AB₂ monomer **14** with diphenylphosphoryl azide (DPPA) and dodecanol through Curtius rearrangement (**Scheme 1.5**). Silyl group deprotection results in activation of group at convergence point i.e., free hydroxyl, which

further undergoes rearrangement with dendron to afford G2 dendron **15**. Using this iterative approach polyurethane dendron up to G4 was synthesized and coupled with 1,3,5-benzenetricarboxylic acid trivalent core to generate G3 polyurethane dendrimer.



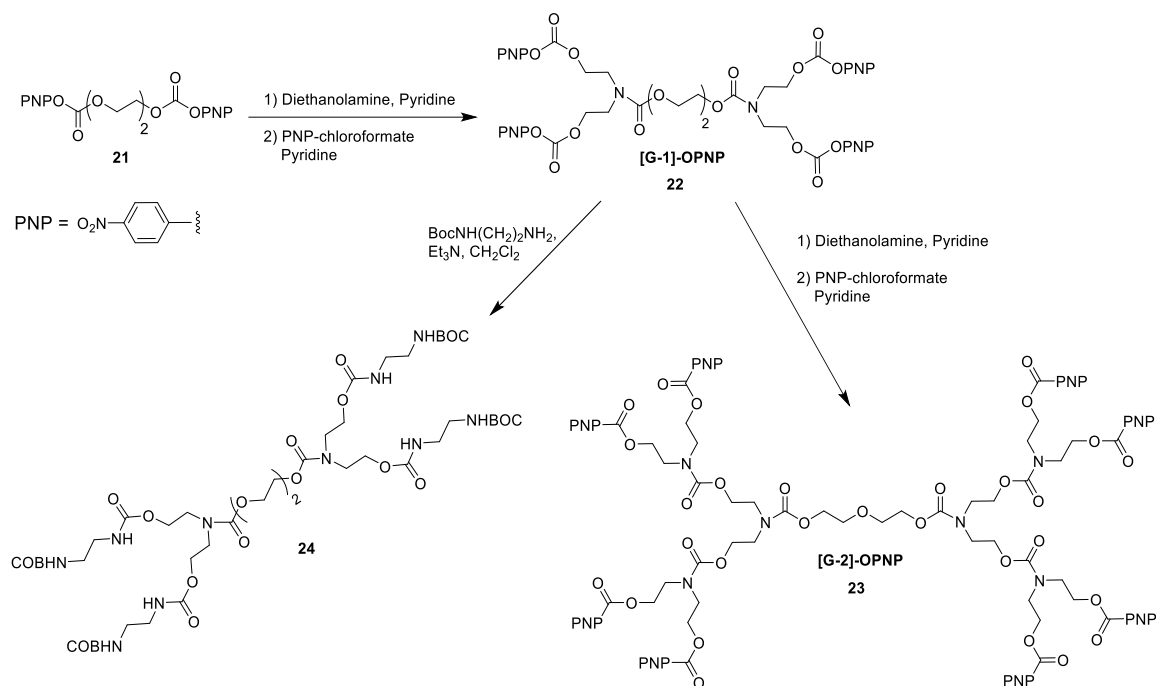
Scheme 1.5 Synthesis of G4 polyurethane dendron using Curtius rearrangement.

P. C. Taylor et al. reported CO_2 insertion method for the synthesis of G2 polyurethane dendron and dendrimer. Author used commercially available diethanolamine as starting material to prepare *O*-activated (B-site) and *N*-protected (A-site) AB_2 monomer **17** by reacting it with *p*-nitrophenylsulfonyl chloride. Activated hydroxyl groups were subjected to nucleophilic attack by in-situ generated carbamate anion formed by reaction of CO_2 with amine. This resulted in formation of *N*-protected secondary diurethane branched product, which upon further *N*-deprotection results in diurethane **18** with activated focal amino group. Under similar CO_2 insertion condition, **18** was reacted with **17** to afford dormant G2 urethane dendron, which upon deprotection produce *N*-activated G2 urethane dendron **19**. Finally, through convergent approach, dendron **19** was coupled with 1,3-propanediol-triflate through CO_2 method to construct G2 polyurethane dendrimer **20** (**Scheme 1.6**).



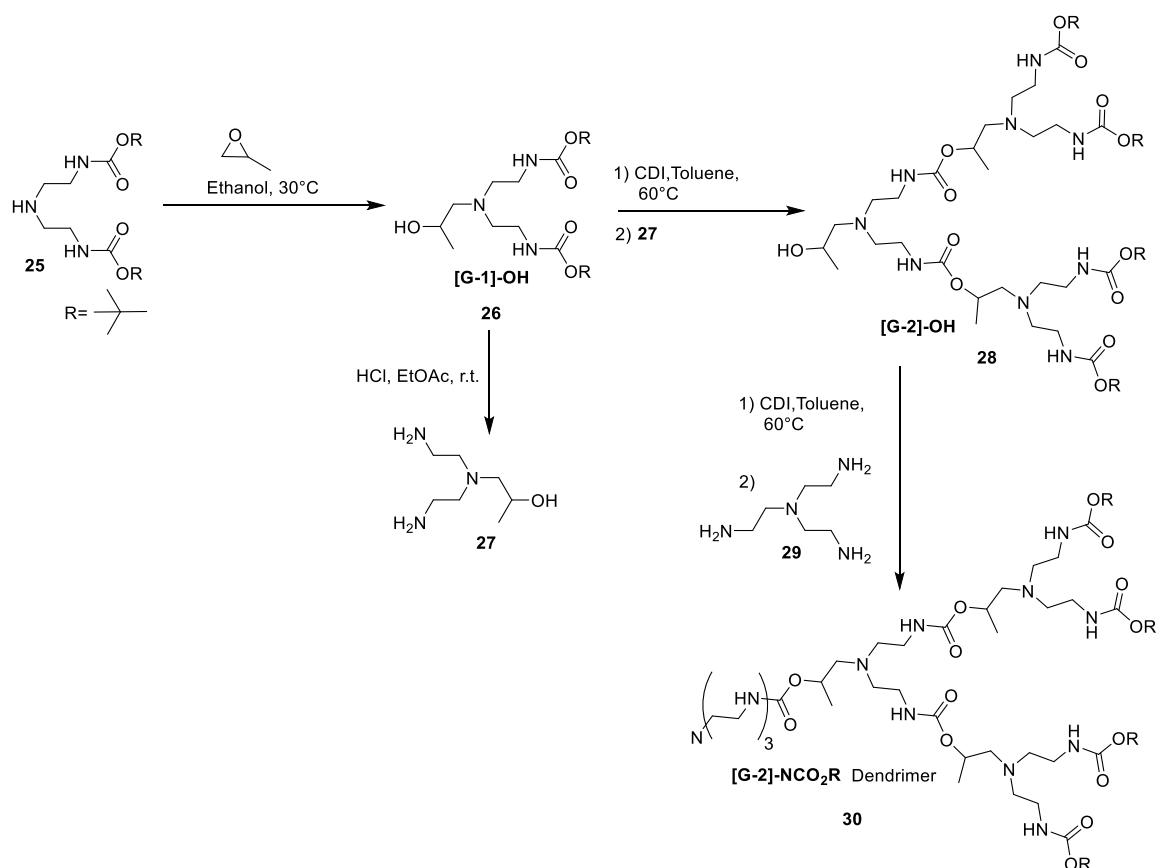
Scheme 1.6 Convergent growth synthesis of G2 secondary polyurethane dendrimer using CO₂ insertion method.

Similar two directional secondary polyurethanes dendrimers were reported by Jones et al.^[93], using diethanol amine as AB₂ monomer and *p*-nitrophenyl (PNP) chloroformate as coupling reagent in a simple divergent growth strategy. Here, author employed two step iterative process of, (i) activation of primary alcohols to PNP carbonate ester, and (ii) selective coupling of secondary amine with PNP ester to produced secondary urethane branched dendrimer. PNP terminated G1 dendrimer **22** was prepared by in-situ reaction of diurethane polyols with *p*-nitrophenyl chloroformate. Similarly, using above iterative protocol, PNP terminated dendrimer up to second generation **23** was synthesized in 68% yield (**Scheme 1.7**). Additionally, reactive PNP-ester also allowed incorporation of other amine bis-nucleophiles such mono-*N*-BOC-ethylenediamine, di[2-(2-hydroxyethoxy)ethyl]amine, to produce functional dendrimer **24**. Hence, showing the potential ability to form multivalent bioconjugates by attaching biologically active molecules.



Scheme 1.7 Divergent growth synthesis of G2 secondary polyurethane dendrimer using amine-PNP-ester coupling.

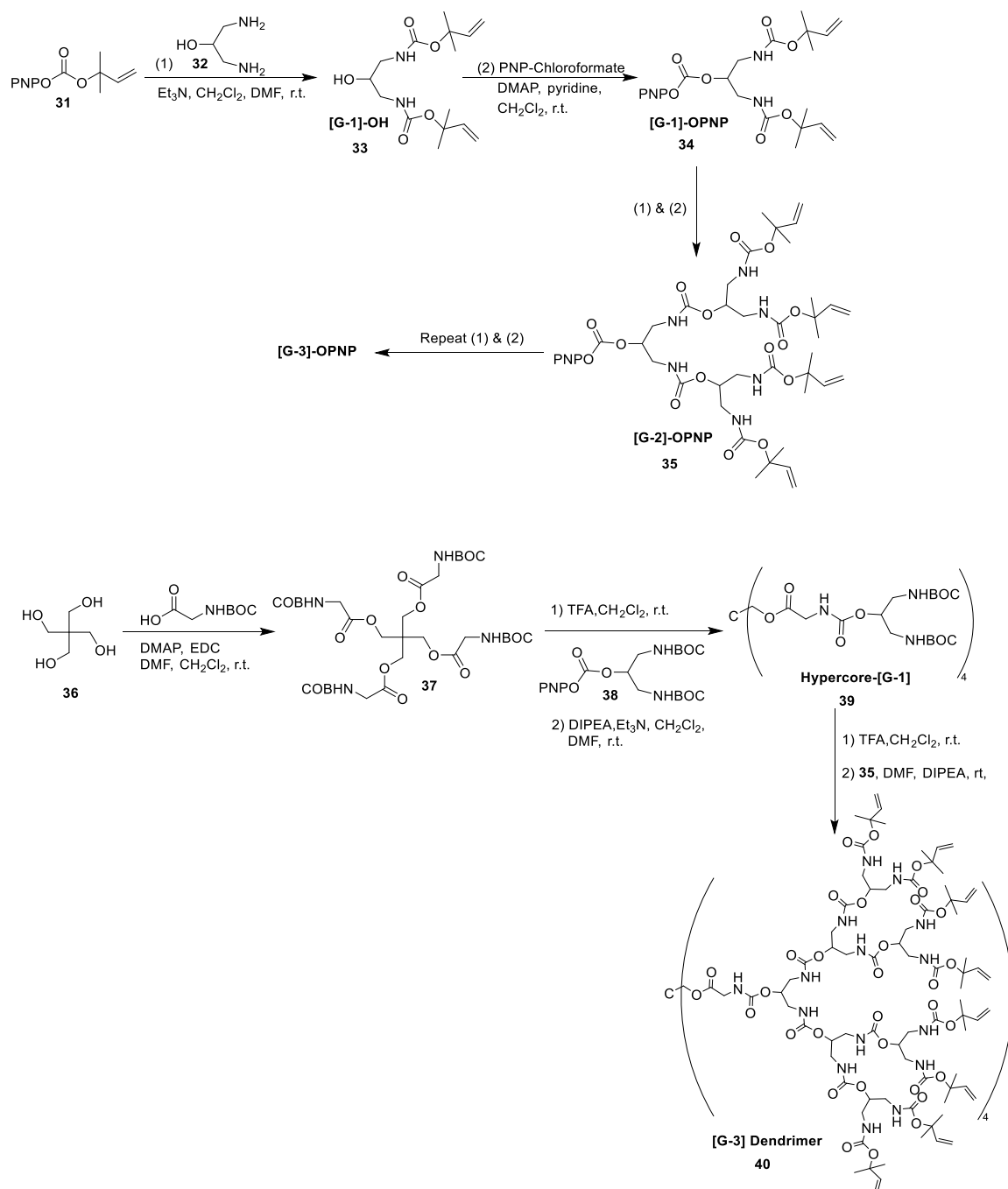
Another ester-amine coupling route towards primary polyurethane dendrons and dendrimers was published by Rannard et al.^[94,95], wherein they utilized 1- [N, N-bis(2-aminoethyl)-amino]-2-propanol (AEAP) as AB₂' branching monomer **27** and carbonyl diimidazole (CDI) as a coupling agent in convergent growth methodology. Here author employed two step iterative process of, (i) activation of primary alcohols (at focal point) to imidazole carboxylic ester, and (ii) selective coupling of primary amines with imidazole carboxylic ester to produced primary urethane branched dendron and dendrimers. Monomer **26** was obtained in 3 synthetic steps, starting with selective *N*- *t*-BOC protection of primary amines in diethylenetriamine with *t*-Butyl imidazole ester, followed by nucleophilic ring opening of 2-methyloxirane forming G1 dendron **26** and finally acid catalysed deprotection of *N*- *t*-BOC group to furnish final monomer **27** (**Scheme 1.8**). Further using the two-step approach (i) & (ii), *t*-BOC protected G2 dendron was prepared in 50% yield and similarly G3 dendron. The focal point activated dendrons were coupled with triamine core i.e., Tris(2-aminoethyl)amine **29** individually to generate G1 to G3 polyurethane dendrimers in low yields.



Scheme 1.8 Convergent growth synthesis of G2 primary polyurethane dendron and dendrimer using amine-imidazole ester coupling.

Lee et al.^[96] reported a combined convergent and divergent growth methods to obtain G4 primary polyurethane dendrimers composed of olefinic periphery. 1,3-Diamino-2-propanol was used as AB₂ branching monomer **32** and PNP-chloroformate as coupling reagent. Authors employed two step activation and growth protocol based on activation of hydroxyl focal group to PNP carbonate ester, followed by amine-ester coupling to afford dendritic structure. In a convergent route, diamine monomer **32** was capped with 2-methyl-3-buten-2-yl functionality via amine-ester coupling to obtain G1 dendron **33**, which upon focal point activation and coupling with diamine monomer produce G2 dendron in 85% yield. Repeating this sequential activation and amine coupling, dendrons up to G3 were synthesized in 75% yield. In a divergent route, G1 *N*-BOC hypercore **39** was prepared by i) esterifying pentaerythritol with *N*-BOC glycine, ii) TFA mediated *N*-BOC deprotection and iii) amine-ester coupling with **38**. Final G3 dendrimer with olefinic periphery **40** was constructed by BOC deprotection and coupling with G2 dendron **35** through activated focal point in moderate yields (**Scheme 1.9**). Additionally, authors proved the immolative nature

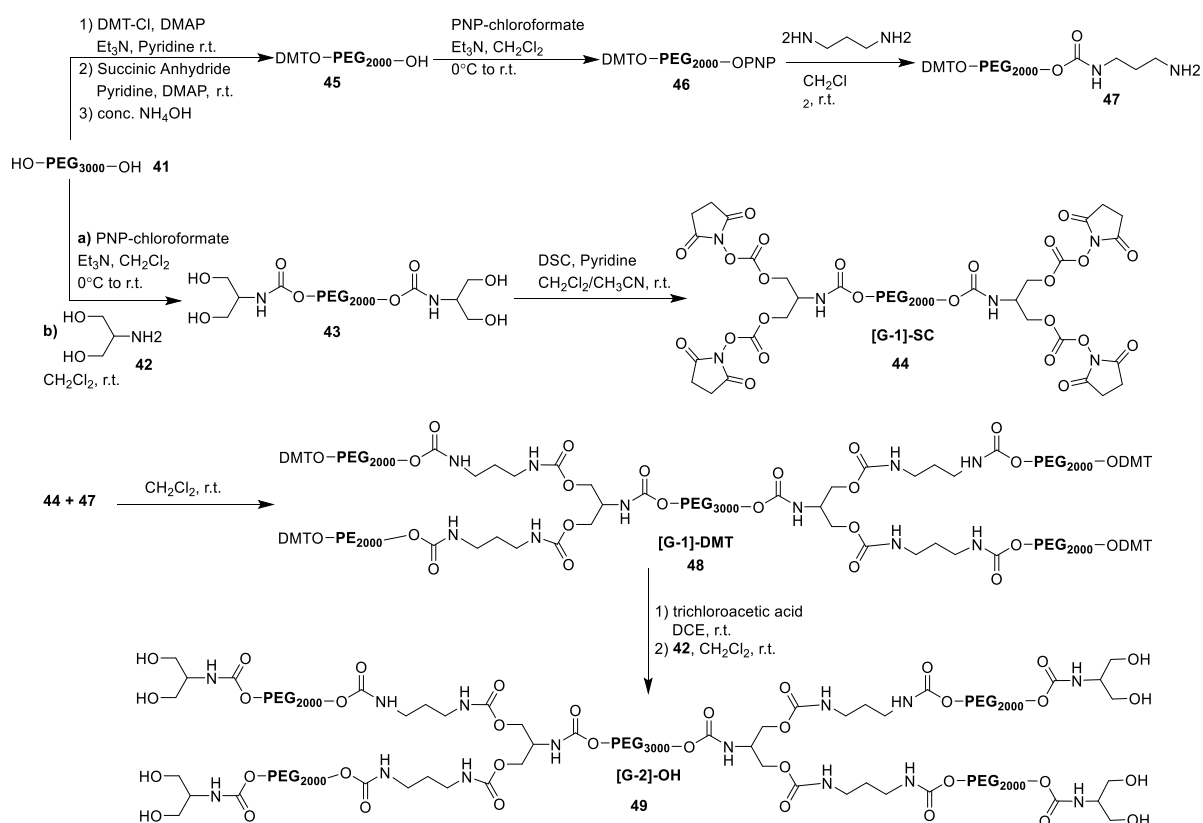
of the urethane groups by performing base hydrolysis and trimethylsilyl iodide/methanol treatment at 40-80°C temperature range.



Scheme 1.9 Convergent growth synthesis of G3 primary polyurethane dendrimer with olefinic periphery.

Ballico et al.^[97] reported a new class of high molecular weight, urethane branched polyethylene glycol (PEG) derivatives by stepwise assembling PEG units in divergent as well as convergent growth process. These are known as Multifunctional polyethylene glycols (Multi-PEGs). Here, 2-aminopropane-1,3-diol **42** was used as branching linker in

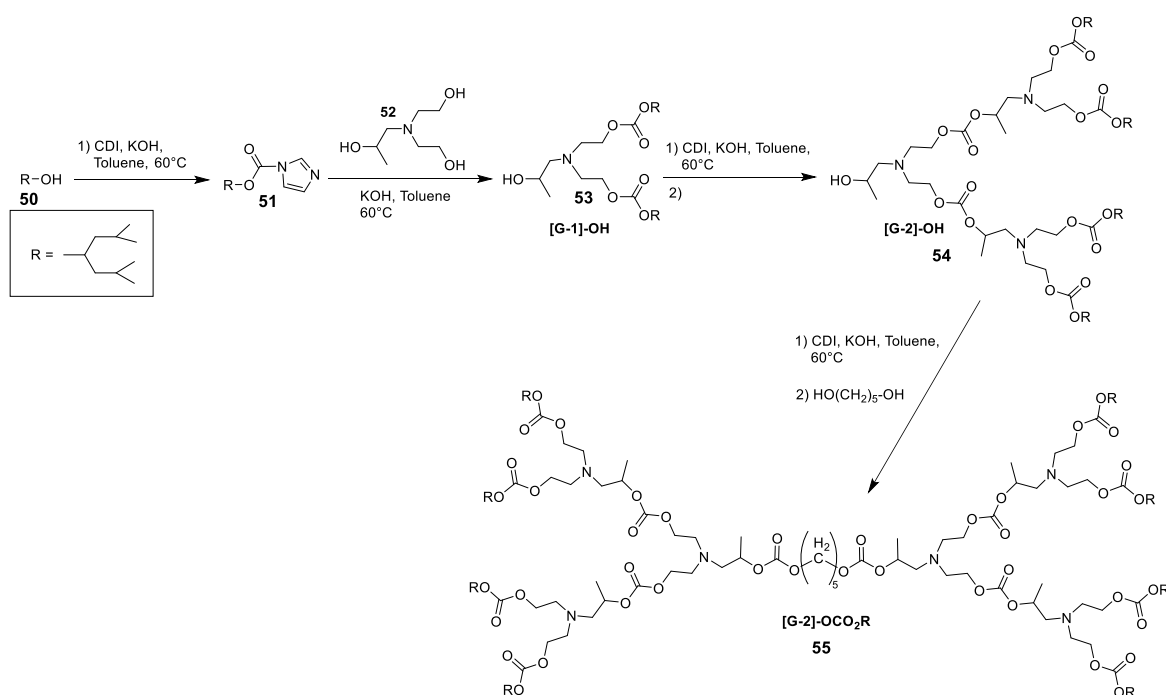
divergent growth whereas 1,3-diamino-2-propanol as branching linker in convergent synthesis. In a typical divergent process (**Scheme 1.10**), tetra hydroxy PEG based core **43** was prepared by first activating the hydroxyl groups of PEG₃₀₀₀ with PNP-carbonate ester followed by selective amine-ester coupling with branching monomer. An amino based PEG fragment **47** was prepared in stepwise manner, starting with selective mono-protection with dimethoxytrityl (DMT) group, followed by isolation steps and activation to PNP-carbonate ester **46**. Finally, this was coupled with 1,3-diamino propane. The tetrahydroxy PEG core was further transformed to tetra-succinimidyl carbonate (SC) ester core **44** and subsequently coupled with PEG based amino fragment **47** to obtain G1 tetra DMT protected penta-PEG derivative **48**. Furthermore, upon acid mediated DMT deprotection, hydroxyl activation by *N,N*-Disuccinimidyl carbonate (DSC) and amine-ester coupling with monomer results in G-2 octa hydroxyl PEG derivative **49**. These new multifunctional, biocompatible and soluble Multi-PEGs were proved to exhibit good physicochemical properties



Scheme 1.10 Divergent synthesis of urethane containing Multi-PEGs.

Dendritic polycarbonates have been known since early work of Bolton and Wooley^[98,99] on 1,1,1-tris(4-hydroxyphenyl) ethane monomer. Since then, very limited reports are found in the literature especially on aliphatic dendritic polycarbonates.

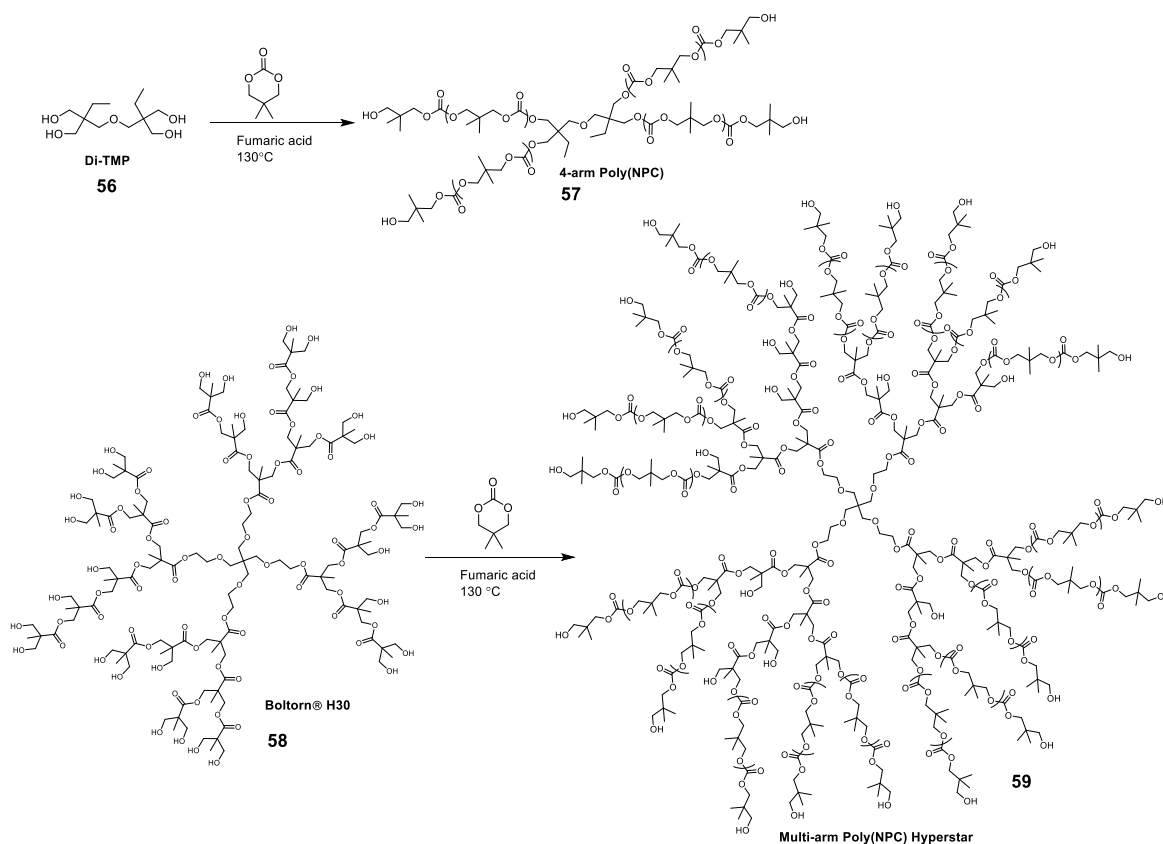
The first ideal aliphatic polycarbonate dendrimer was reported by Rannard and Davis^[87] using efficient one pot process. Authors utilized 1-[*N*, *N*-bis-(2-hydroxyethyl) amino]-2-propanol (HEAP) as AA₂ **52** branching monomer and CDI as coupling reagent in a convergent growth method. One pot synthesis, initiate with preparation of imidazole ester of secondary alcohol and selective reaction with primary hydroxyl of monomer, to obtain G1 dendron **53** with free secondary hydroxyl at focal point. In next course of reaction, secondary hydroxyl was activated to imidazole carbonate ester group and selectively coupled with primary hydroxyls of another mole of monomer, producing G2 dendron **54** with free secondary hydroxyl. Finally, hydroxyl activation in G2 dendron and subsequent in-situ coupling with 1,5-pentane diol, leads to formation of G2 polycarbonate dendrimer **55** 87% yield (**Scheme 1.11**). This method furnished perfectly branched dendrimer with only final step purification. Also, till date this is the only report that deals with synthesis of perfectly branched polycarbonate dendrimer.



Scheme 1.11 Convergent growth synthesis of polycarbonate dendrimer using CDI coupling reaction.

Peter et al.^[100] reported synthesis of star-shaped poly(ester-carbonate) hyperbranched polymer **59** via anionic ring opening polymerization (ROP) of neopentylene carbonate (NPC), initiated by commercially available hydroxy monomers such as hyperbranched polyester (Boltron H₃₀) **58**, Di-trimethylolpropane (di-TMP) **56** and ethoxylated pentaerythritol (PP50). Here ring opening polymerization of cyclic monomer was carried

out in bulk catalyzed by fumaric acid as catalyst at 130 °C (**Scheme 1.12**). Conversion was kept below 90%, in order to avoid cross-linking.



Scheme 1.12 Synthesis of polycarbonate 4-arm and multi-arm hyperstar via ROP.

Above literature review suggested very handful reports on perfectly branched polycarbonates and polyurethanes dendrimers. Additionally, most of the PU and PC dendrimer synthesis involves 1→2 branching sequence and higher branching frameworks are yet to be explored. Hence, in order to understand the synthetic challenges associated with PU/PC dendrimers, at the same time aim to develop new dendritic structures and accompanying methods, we attempted different synthetic strategies to afford 1→2/1→4 branched PU/PC dendritic motifs. The detailed description on their synthesis will be further discussed in **section 1.4** herewith.

1.3 Experimental

1.3.1 Synthetic procedures and characterization of compounds

Caution: All synthetic experiments were strictly performed in fume-hood. Toxic chemicals such as triphosgene, osmium tetroxide, carbamoyl chloride and chloroformates were handled with extreme care.

I. Synthesis of glycerol based AB₂ branching monomers:

i. *cis*-5-hydroxy-2-phenyl-1, 3-dioxane (*cis*-HPD) or *cis*-1,3-*O*-benzylidene glycerol (2)^[101]

In a 2-neck round bottom flask with one neck closed with thermometer socked, was taken glycerol 10 g (0.1086 mol), benzaldehyde 12 g (0.1129 mol) and 10 mL of petroleum ether: benzene mixture. Flask content was refluxed for 5 h at 80°C using Dean-Stark water separator till no more water being formed in the collector. After completion, reaction flask was cooled to room temperature. Mixture was washed with 0.5 M NaOH solution, brine solution and dried over anhy. MgSO₄. Clear mixture was then cooled to -10°C, in order to ppt out white solid. Crude product was filtered off and recrystallized using petroleum ether: toluene (1:1) mixture which gave white shiny silky needles in 21% yield. m.p. =84°C (lit. 82-83°C); ¹H NMR (400 MHz, CDCl₃, 25°C): δ (ppm) = 7.52-7.49 (m, 2H; CH^{Ar}), 7.39-7.37 (m, 3H ; CH^{Ar}), 5.56 (s, 1H; OCHO), 4.21-4.17 (dd, *J*=12Hz and 4Hz, 2H; OCH₂), 4.15-4.12 (dd, *J*=12Hz and 4Hz, 2H; OCH₂), 3.65-3.62(dt, *J*= 8Hz and 4Hz, 1H; CHOH); ¹³C NMR (100 MHz, CDCl₃, 25°C): δ= 137.79(C^{Ar}), 129.12(HC^{Ar}), 128.34(HC^{Ar}), 125.86 (HC^{Ar}), 101.68(OCHO), 72.30(OCH₂), 64.02(CHOH); IR (KBr): ν̃(cm⁻¹)=3284 (m, O-H_{stretch}), 3062 (m, C-H_{stretch}, sp²), 2852 (m, C-H_{stretch}, sp³), 1959-1720(w, overtone, C-H_{bend}, Ar), 1493,1452, 1394(m, C=C_{stretch}, Ar), 1336 (s, O-H_{bend}), 1153, 1085 (s, C-O_{stretch}, ether), 744, 698(s,C-H_{bend}).

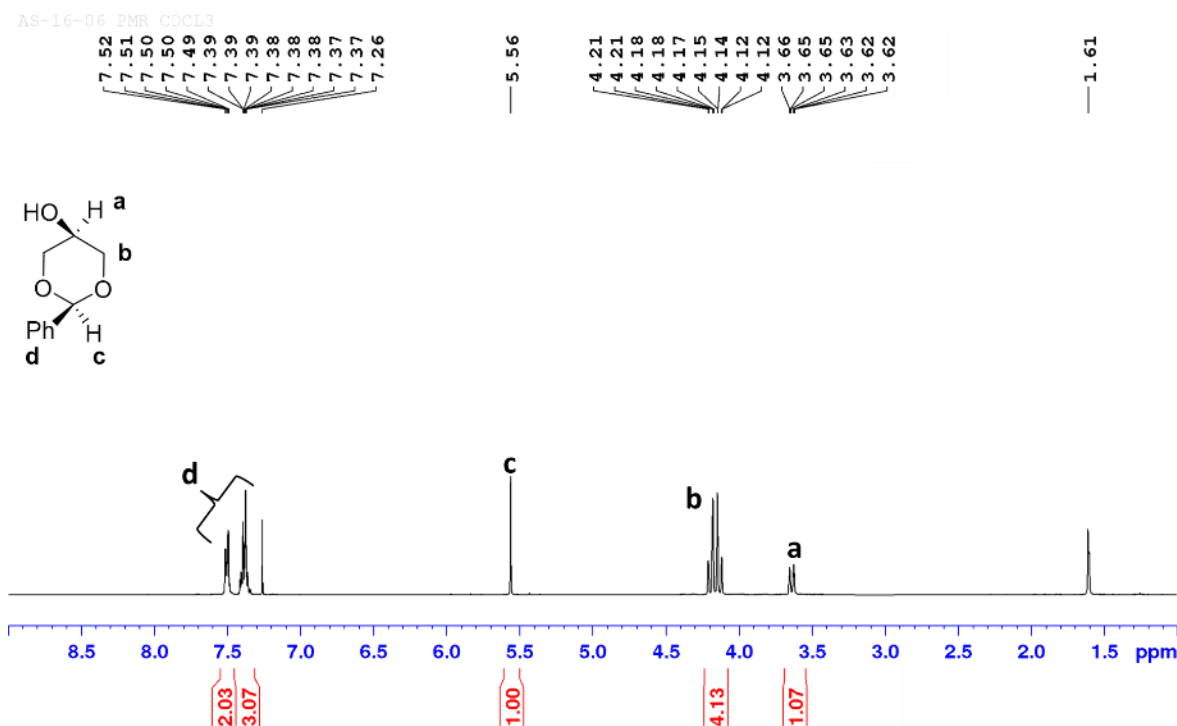


Figure 1.11 ^1H NMR spectrum of *cis*-1,3-*O*-benzylidene glycerol (**2**) in CDCl_3 .

ii. 2,2-dimethyl-1,3-dioxolane-4-methanol or solketal (4**)^[102]**

To a solution of glycerol (10 g, 108.5 mmol), 2,2-dimethoxy propane (13.6 g, 130.3 mmol) in acetone (100 mL), catalytic amount of *p*-TSA (0.22 mmol) was added and stirred at room temperature for 24 h. After the completion of reaction, solvent evaporated to residual oil and extracted with ethyl acetate. Organic layer washed with 10% aq. sodium bicarbonate, water, brine, dried over anhy. sodium sulfate and concentrated under vacuum. Crude oil was purified by distillation at 60-70°C under reduced pressure to afford colourless oil in 88% yield. ^1H NMR (400 MHz, CDCl_3 , 25°C): δ (ppm) = 4.27-4.22(m, 1H; OCH), 4.06-4.03(t, 1H; $J=8\text{Hz}$ OCH₂), 3.81-3.78(t, 1H; $J=8\text{Hz}$ OCH₂), 3.76-3.73(d, 1H ; $J=12\text{Hz}$; CH₂OH), 3.61-3.58(d, 1H ; $J=12\text{Hz}$; CH₂OH), 1.45(s, 3H, CH₃), 1.38(s, 3H, CH₃); IR (KBr): $\tilde{\nu}(\text{cm}^{-1})=3340$ (s, O-H_{stretch}), 2983 (m, C-H_{stretch}, sp^3), 1456(s, C-H_{bend}, *methylene*), 1382(s, C-H_{bend}, *methyl*), 1336 (m, O-H_{bend}), 1183, 1092 (s, C-O_{stretch}, *ether*).

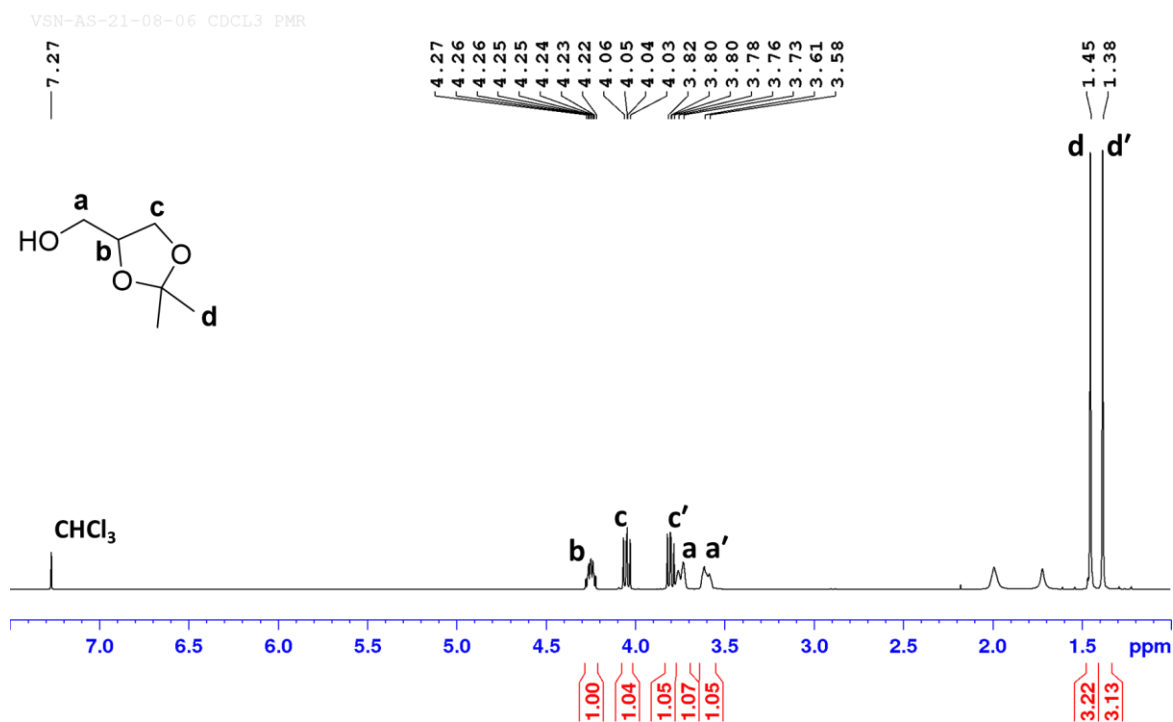


Figure 1.12 ¹H NMR spectrum of 2,2-dimethyl-1,3-dioxolane-4-methanol (**4**) in CDCl₃.

iii. 2,2-Dimethyl-1,3-dioxolan-4-yl)methyl 1*H*-imidazole-1-carboxylate or solketyl imidazole carboxylate (5**)^[103]**

To a solution of solketal (1 g, 7.57 mmol) in 80 mL of dry CH₂Cl₂, *N,N'*-carbonyldiimidazole (1.35 g, 8.32 mmol) was added. The mixture was then stirred for 4 h under an inert atmosphere at room temperature. Solvent layer washed with water, dried over anhy. Na₂SO₄ and evaporated under vacuum to obtain crude viscous yellow oil (98%), which was used in next step without any purification. IR (KBr): $\tilde{\nu}(\text{cm}^{-1}) = 3128(\text{m}, \text{C-H}_{\text{stretch}}, sp^2)$, 2987, 2889(m, C-H_{stretch}, *sp*³), 1768 (vs, C=O_{stretch}), 1525 (w, C=N_{stretch}), 1469 (m, C=C_{stretch}), 1402, 1384(s, C-H_{bend}, *methyl*), 1317, 1284 (s, C-N_{stretch}), 1242 (s, C-O_{stretch}, *ester*), 1178, 1095 (m, C-O_{stretch}, *ether*), 767, 840 (m, C-H_{bend}, *imidazole*).

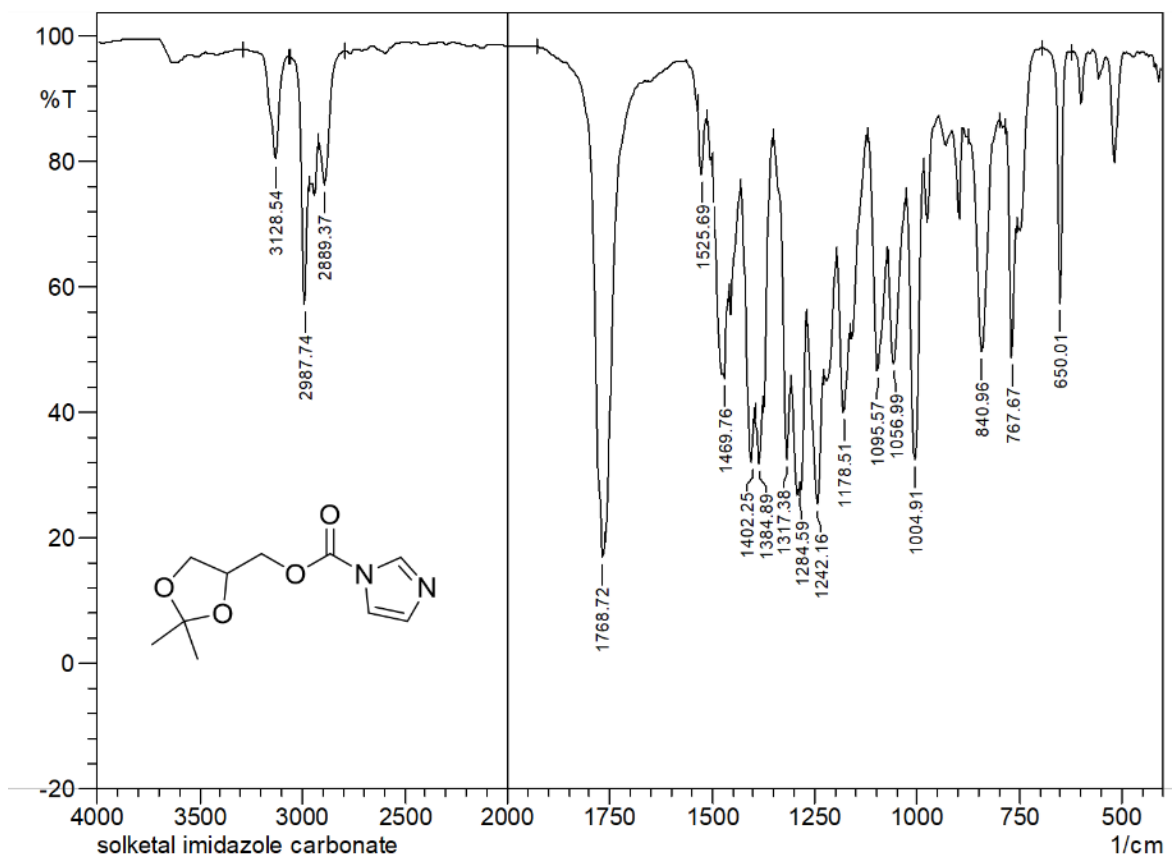


Figure 1.13 IR spectrum of solketyl imidazole carboxylate (**5**) in KBr.

iv. *cis*-2-Phenyl-1,3-dioxan-5-yl chloroformate (**3**)

A solution of triphosgene (0.6 g, 2.2 mmol) in dry dichloromethane (20 mL) was prepared in two neck flask under nitrogen flow. Both the ends of flask were sealed with silicon septum and kept for stirring at -5°C . Upon attaining the desired temperature, pyridine (0.65 g, 8.25 mmol) and *cis*-HPD (1 g, 5.5 mmol) solution in dichloromethane were added dropwise and simultaneously using individual syringes. Addition was performed over a period of 30-40 min, keeping pyridine addition in excess. After complete addition reaction mixture was stirred at same temperature for 45 min. Further mixture was warmed to r.t. and stirred for another 3h. Reaction mixture washed with cold water, brine and dried over anhy. Na_2SO_4 . Solvent evaporated in vacuo to obtain white solid. Crude product was used in next step without any purification. IR (KBr): $\tilde{\nu}(\text{cm}^{-1})=3063, 2991(\text{m}, \text{C-H}_{\text{stretch}}, sp^2), 2862(\text{m}, \text{C-H}_{\text{stretch}}, sp^3), 1948, 1863(\text{w}, \text{overtone}, \text{C-H}_{\text{bend}}, Ar), 1774(\text{vs}, \text{C=O}_{\text{stretch}}), 1496, 1450, 1392(\text{m}, \text{C=C}_{\text{stretch}}, Ar), 1178(\text{s}, \text{C-O}_{\text{stretch}}, ether), 773, 742(\text{m}, \text{C-H}_{\text{bend}}), 690(\text{m}, \text{C-Cl}_{\text{stretch}})$.

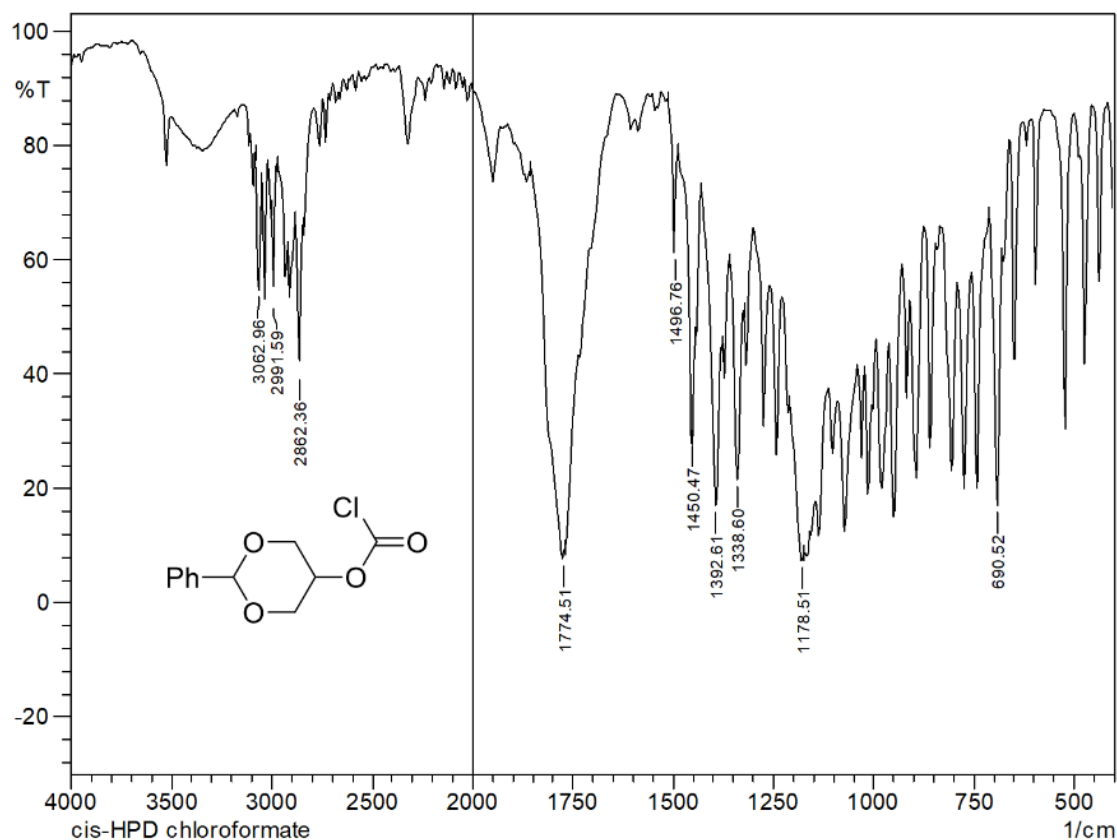


Figure 1.14 IR spectrum of *cis*-2-Phenyl-1,3-dioxan-5-yl chloroformate (**3**) in KBr.

II. Synthesis of dendritic carbonate using protection strategy

i. Synthesis of [G-1] Pentaerythritol tetra acetone carbonate (**7**)

In a two-neck flask, pentaerythritol (0.5 g, 3.67 mmol), triethyl amine (2.22 g, 22.03 mmol), solketyl imidazole carboxylate (4.1 g, 18.36 mmol) was diluted with dry 40 mL DMF and heat at 70°C for 24 h under inert atmosphere. Upon completion, reaction mixture was cooled to r.t, diluted with H₂O/diethyl ether solvent system and organic layer was separated out for further treatment. The aqueous layer was re-extracted with diethyl ether and combined organic layer was washed with aq. LiCl solution and dried over anhy. sodium sulfate. Solvent was evaporated under vacuum and crude product was purified using silica gel chromatography to afford pale yellow thick liquid in 75% yield. $R_f=0.6$ (pet. ether/ethyl acetate 4:6); ¹H NMR (400 MHz, CDCl₃, 25°C): δ (ppm) = 4.31-4.25 (m, 4H; CHO), 4.16 (s, 8H; OCO₂CH₂), 4.11-4.08(d, $J=4$ Hz, 8H; CH₂OCO₂), 4.05-4.01(dd, $J=8$ Hz and 2Hz, 4H; OCH₂), 3.72-43.68(dd, $J=8$ Hz and 2Hz, 4H; OCH₂), 1.37(s, 12H; CH₃), 1.30(s, 12H; CH₃); ¹³C NMR (100 MHz, CDCl₃, 25°C): $\delta=$ 153.41(OCO₂), 137.85(C (CH₃)₂), 72.15(HCO), 67.42(OCO₂CH₂), 65.17(CH₂OCO₂), 64.16(OCH₂), 41.49(C(CH₂)₄), 25.67, 24.28(CH₃); IR (KBr): $\tilde{\nu}$ (cm⁻¹) =2985, 2889(m, C-H_{stretch}, sp^3), 1755 (vs, C=O_{stretch}), 1452(w, C-H_{bend},

methylene), 1371(m, C-H_{bend}, methyl), 1247 (s, C-O_{stretch}, ester), 1159, 1085 (m, C-O_{stretch}, ether); LCMS (ESI) m/z: [M+H]⁺ =769.45.

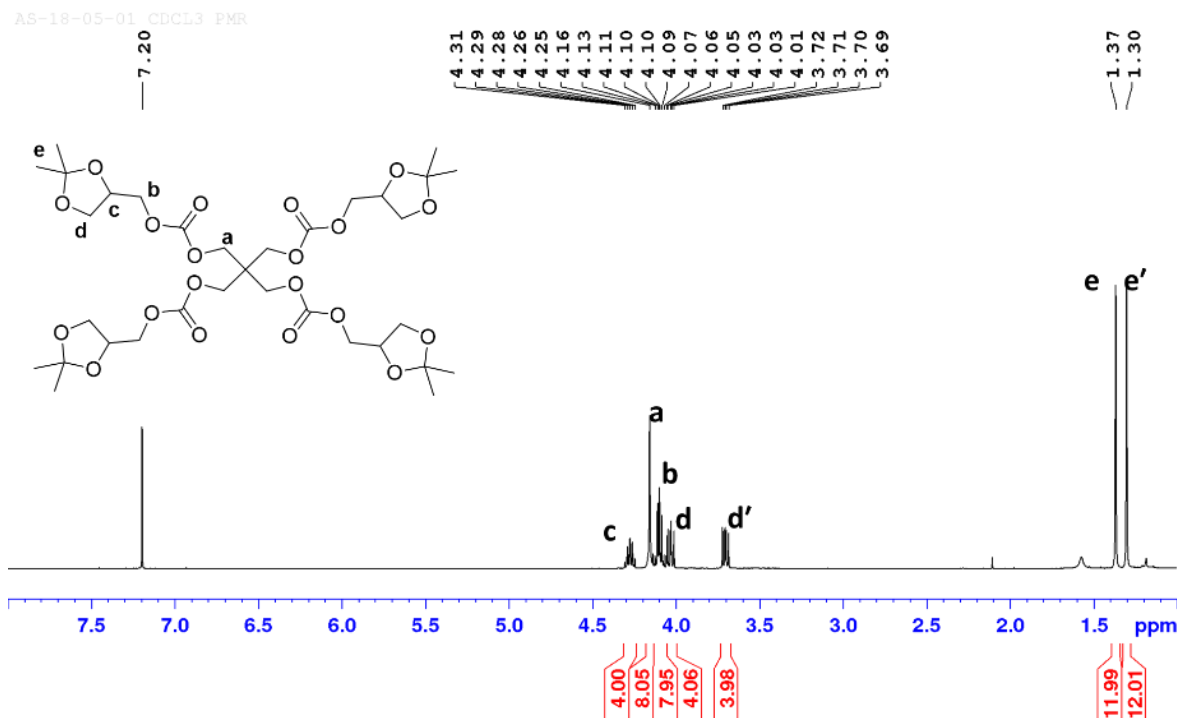


Figure 1.15 ¹H NMR spectrum of [G-1] Pentaerythrityl tetra acetonide carbonate (**7**) in CDCl₃.

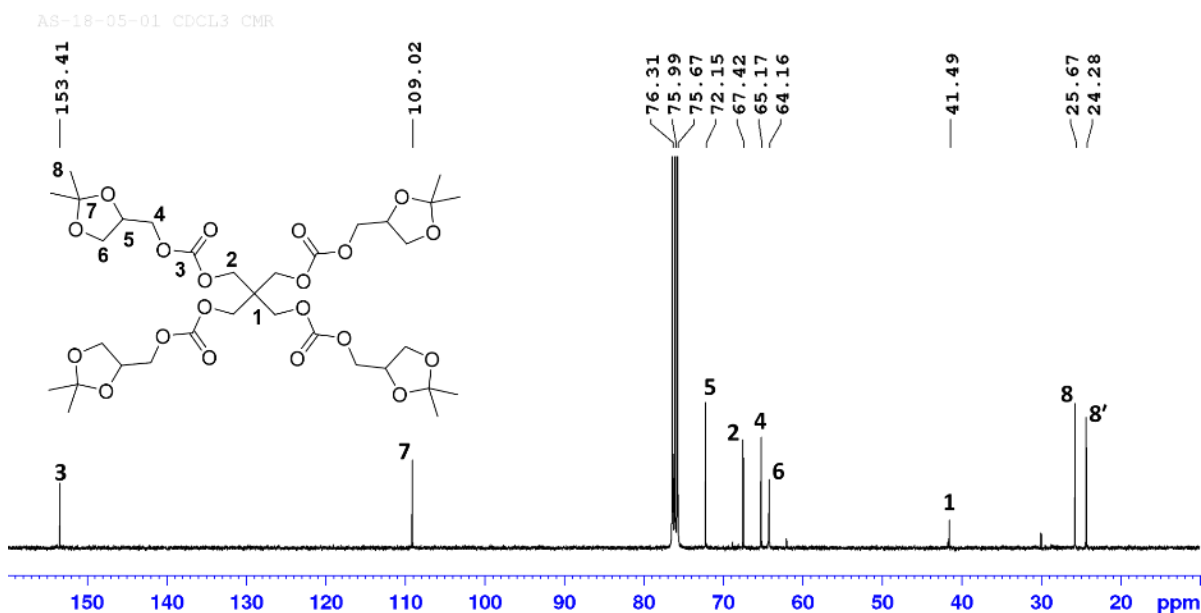


Figure 1.16 ¹³C NMR spectrum of [G-1] Pentaerythrityl tetra acetonide carbonate (**7**) in CDCl₃.

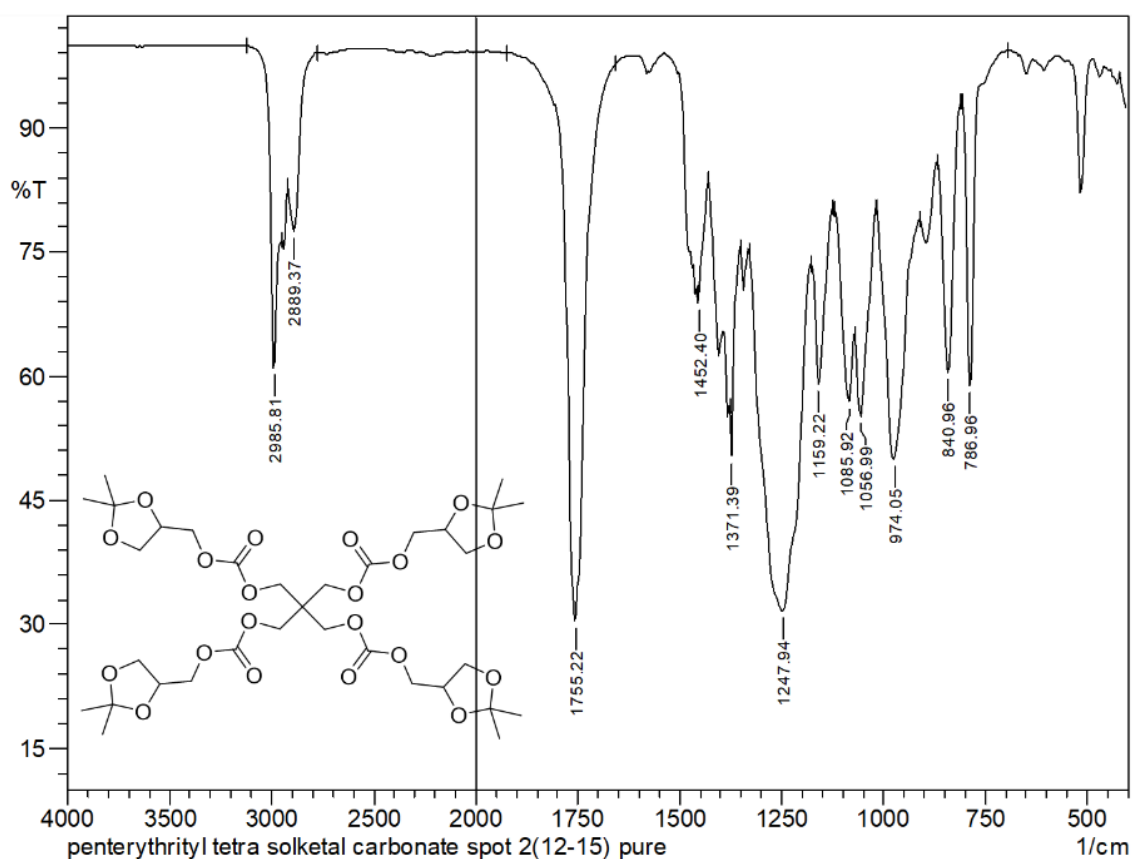


Figure 1.17 IR spectrum of [G-1] Pentaerythrityl tetra acetone carbonate (**7**) in KBr.

ii. Synthesis of [G-1] Pentaerythrityl tetra benzylidene carbonate (**8**)

In a two-neck flask, pentaerythritol (1 g, 7.34 mmol), pyridine (3.48 g, 44.04 mmol), DMAP (0.37 mmol) was placed and diluted with 30 mL dry acetonitrile. The flask mixture was cooled to 0°C and solution of 2-phenyl-1,3-dioxan-5-yl chloroformate (8 g, 33.03 moles) in 30 mL acetonitrile was added drop wise over period of 1 h under inert atmosphere. After complete addition, reaction mixture was warmed to r.t. and stir for another 5 h. Reaction was monitored over TLC. After complete consumption of starting material, solvent was evaporated and extracted with DCM. The resultant organic layer was washed with cold dil. HCl, water, brine and dried over anhy. sodium sulfate. Upon solvent evaporation in vacuo, crude yellow solid obtained was purified using silica gel chromatography to afford white solid in 72% yield. $R_f=0.6$ (pet. ether/ethyl acetate 3:7); $^1\text{H NMR}$ (400 MHz, CDCl_3 , 25°C): δ (ppm) = 7.49 (m, 8H; CH^{Ar}), 7.35-7.33 (m, 12H; CH^{Ar}), 5.48 (s, 4H; OCHO), 4.50 (br, m, 4H; CHOCO_2), 4.32(br, s, 8H; OCO_2CH_2), 4.08(br, dd, $J=12\text{Hz}$, 8H; OCH_2), 4.21, 3.75(br, 8H; OCH_2); $^{13}\text{C NMR}$ (100 MHz, CDCl_3 , 25°C): $\delta=$ 154.77(OCO_2), 137.85(C^{Ar}), 129.13(HC^{Ar}), 128.30(HC^{Ar}), 126.24 (HC^{Ar}), 101.22(OCHO),

69.85(CHCO₂), 68.65(CO₂CH₂), 66.74(CH₂O), 37.49(C(CH₂)₄); IR (KBr): $\tilde{\nu}$ (cm⁻¹)=3062, 2918 (m, C-H_{strech}, *sp*²), 2852(m, C-H_{strech}, *sp*³), 1747 (vs, C=O_{strech}), 1496,1452, 1392(m, C=C_{strech}, *Ar*), 1276, 1238 (s, C-O_{strech}, *ester*), 1153,1083 (s, C-O_{strech}, *ether*), 744, 698 (m,C-H_{bend}); LCMS (ESI) m/z: [M+Na]⁺ =983.10.

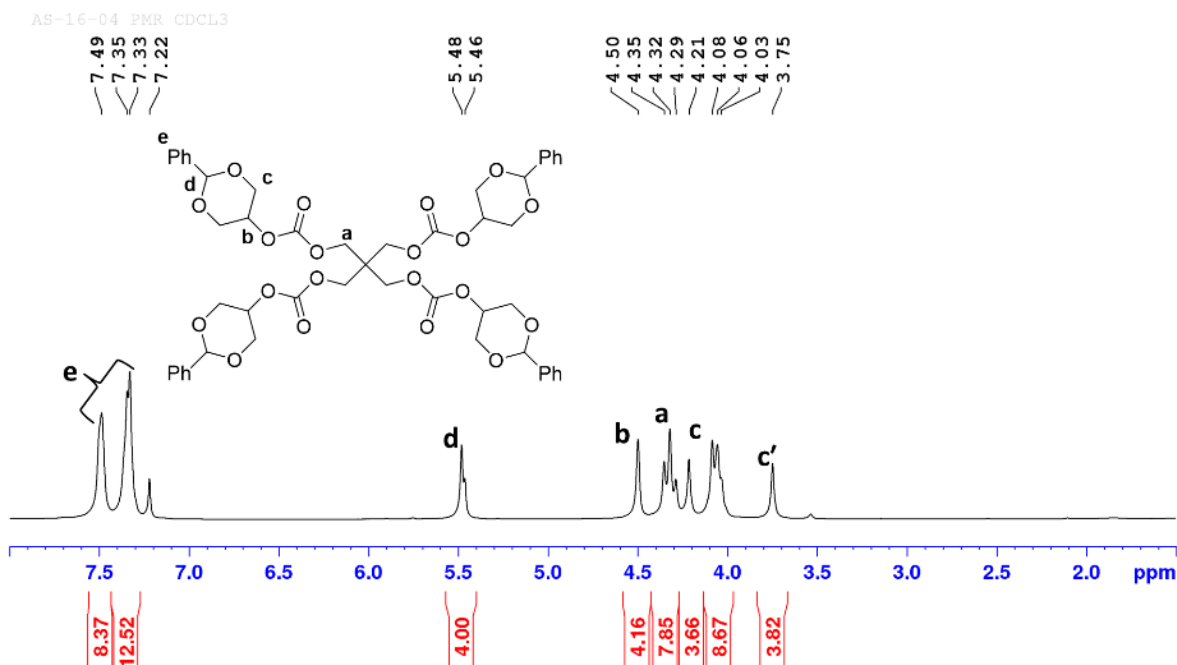


Figure 1.18. ¹H NMR spectrum of [G-1] Pentaerythrityl tetra benzylidene carbonate (8) in CDCl₃

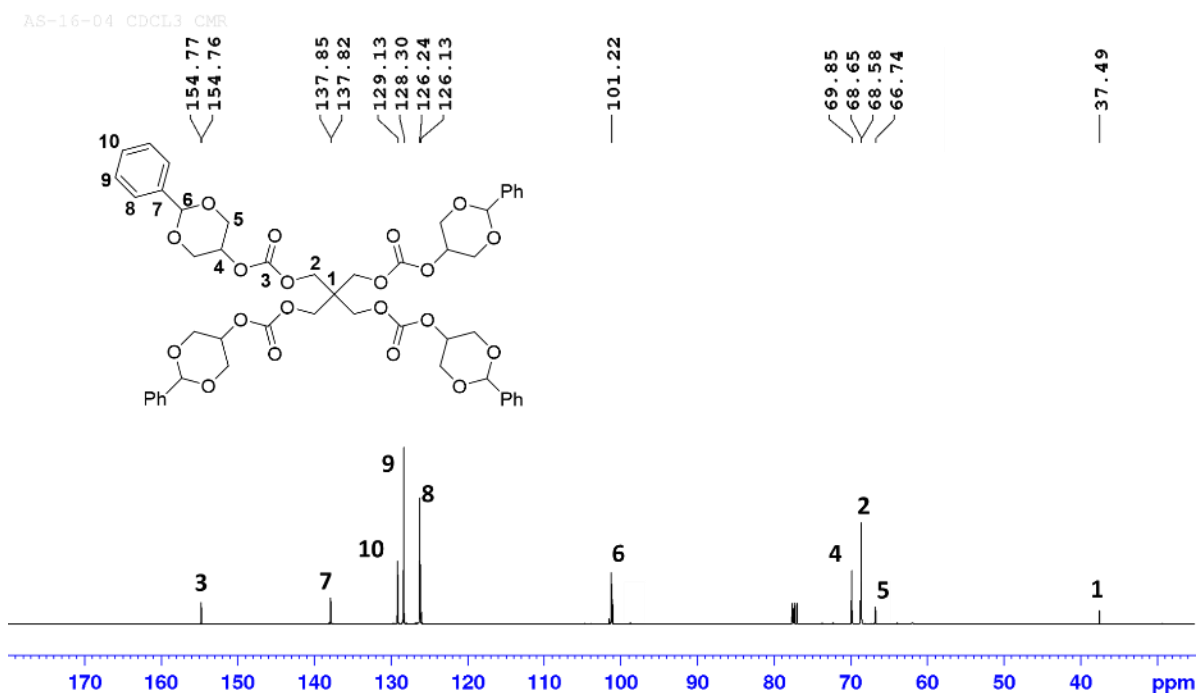


Figure 1.19 ¹³C NMR spectrum of [G-1] Pentaerythrityl tetra benzylidene carbonate (8) in CDCl₃.

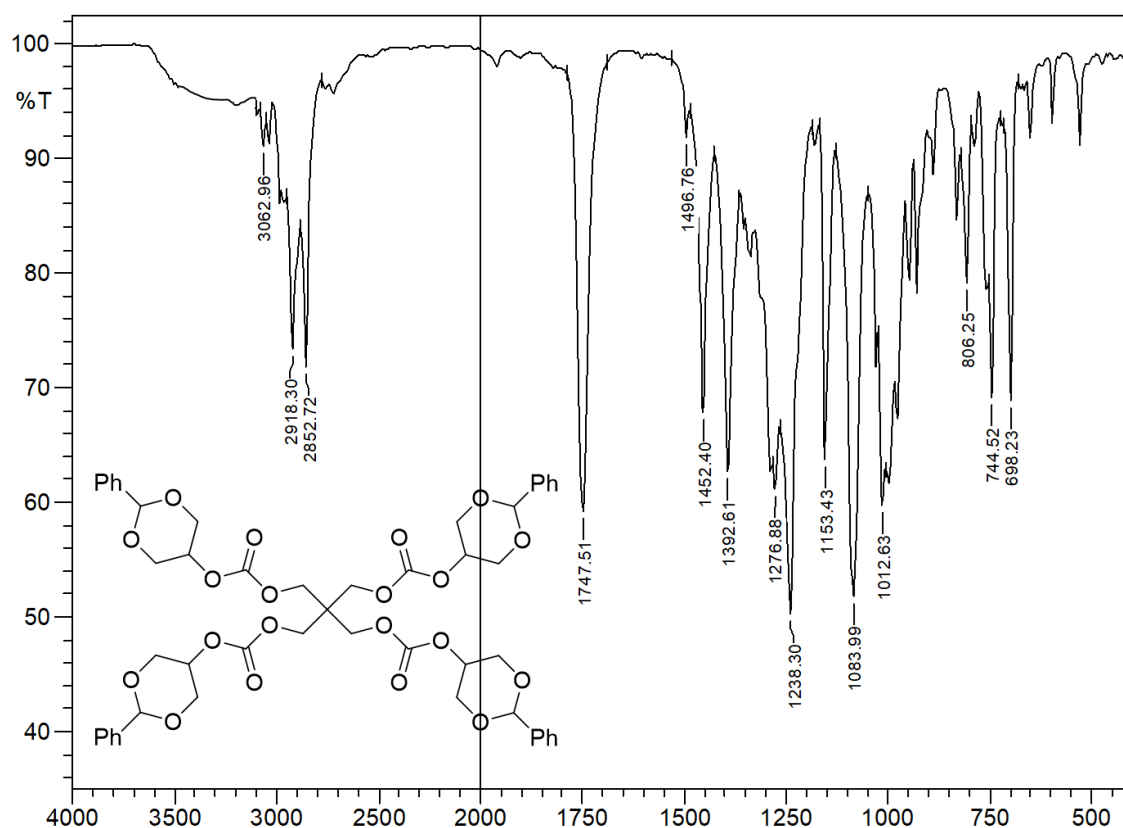


Figure 1.20 IR spectrum of [G-1] Pentaerythrityl tetra benzylidene carbonate (**8**) in KBr.

iii. Synthesis of [G-1] Ethylene glycol bis (benzylidene carbonate) (**15**)

In a two-neck flask, ethylene glycol (0.5 g, 8.05 mmol), pyridine (3.48 g, 24.17 mmol) and DMAP (0.4 mmol) was diluted with 15 mL DCM and kept for stirring at 0°C. To this cold mixture, solution of 2-phenyl-1,3-dioxan-5-yl chloroformate (4.5 g, 18.53 mol) in 15 mL DCM was added drop wise over period of 40 min under inert atmosphere. After complete addition, reaction vessel was warm to r.t. and further stir for 6 h. Upon reaction completion, solvent was evaporated and residue was extraction with DCM. Organic layer was washed with cold dil. HCl, water, brine and dried over sodium sulfate. Solvent evaporated over vacuum and crude yellow solid was purified using silica gel chromatography to afford white solid in 76% yield. $R_f=0.5$ (pet. ether/ethyl acetate 6:4); $^1\text{H NMR}$ (400 MHz, CDCl_3 , 25°C): δ (ppm) = 7.51 (m, 4H; CH^{Ar}), 7.38-7.34 (m, 8H; CH^{Ar}), 5.45 (s, 2H; OCHO), 4.58 (m, 2H; CHOCO_2), 4.42(s, 4H; OCO_2CH_2), 4.40-4.36(dd, $J=12\text{Hz}$ and 1.6Hz, 4H; OCH_2), 4.16-4.12(dd, $J=12\text{Hz}$ and 1.6Hz, 4H; OCH_2); $^{13}\text{C NMR}$ (100 MHz, CDCl_3 , 25°C): $\delta=$ 154.72(OCO_2), 137.70(C^{Ar}), 129.10(HC^{Ar}), 128.25(HC^{Ar}), 126.15 (HC^{Ar}), 101.30(OCHO), 69.77(CHCO_2), 68.63(CO_2CH_2), 65.25(CH_2O); IR (KBr): $\tilde{\nu}(\text{cm}^{-1})=3061$, 2926 (m, C-

H_{stretch} , sp^2), 2852(m, $C-H_{\text{stretch}}$, sp^3), 1751 (vs, $C=O_{\text{stretch}}$), 1452, 1388(m, $C=C_{\text{stretch}}$, *Ar*), 1280, 1265 (vs, $C-O_{\text{stretch}}$, *ester*), 1143, 1080 (m, $C-O_{\text{stretch}}$, *ether*), 744, 696 (m, $C-H_{\text{bend}}$); LCMS (ESI) m/z : $[M+H]^+ = 475.28$.

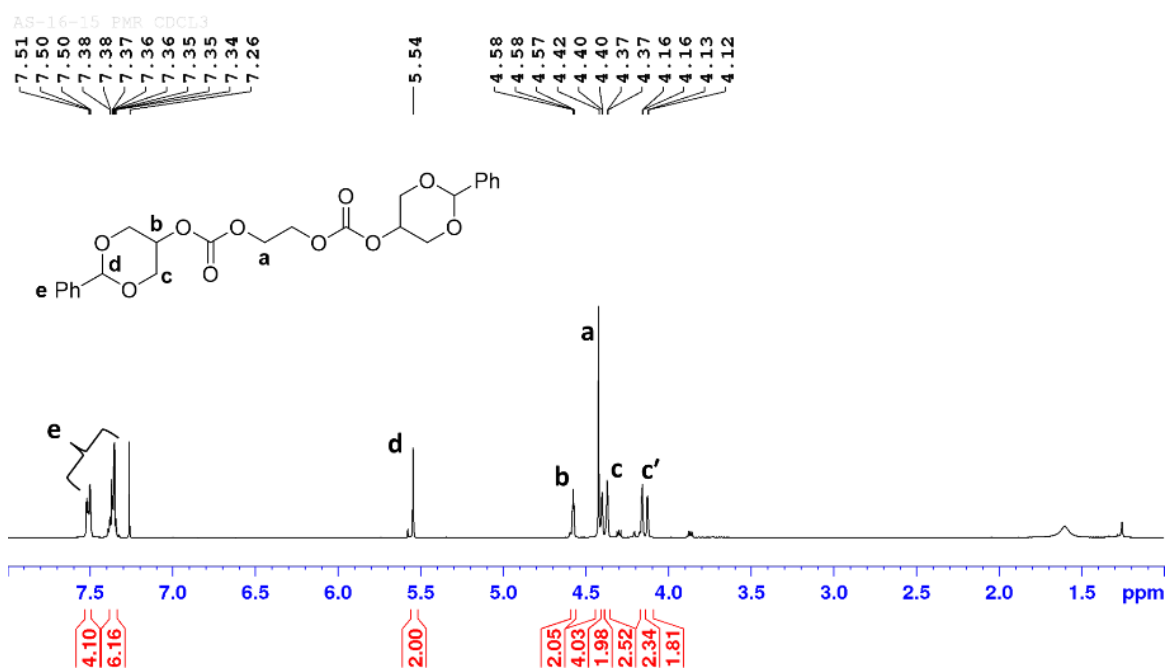


Figure 1.21 ¹H NMR spectrum of [G-1] Ethylene glycol bis (benzylidene carbonate) (15) in CDCl₃.

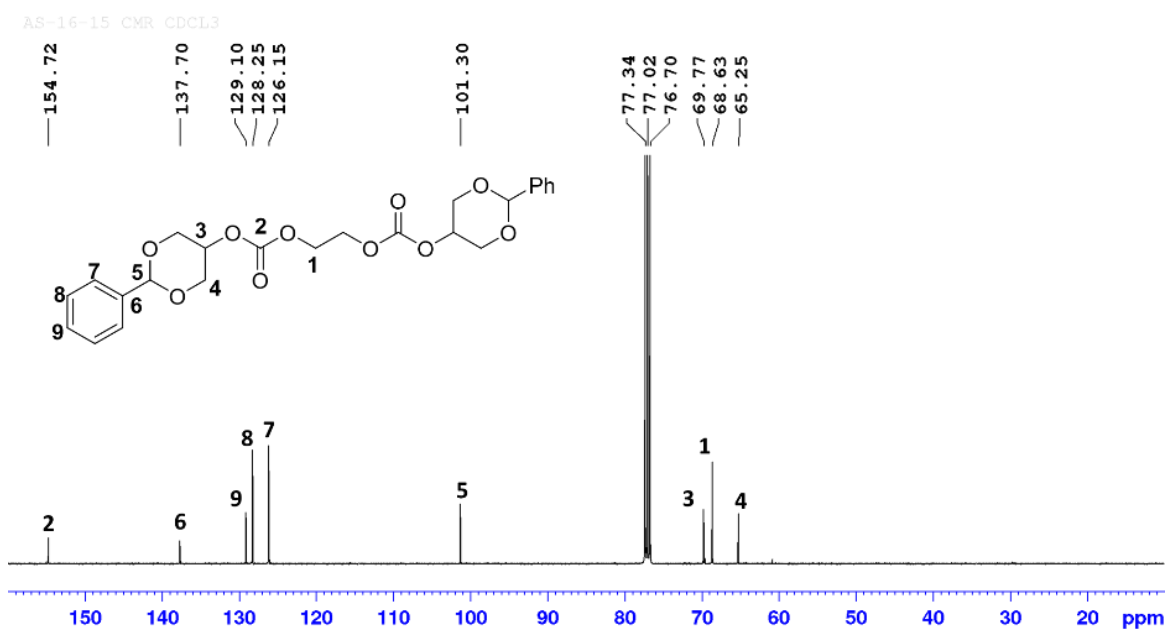


Figure 1.22 ¹³C NMR spectrum of [G-1] Ethylene glycol bis (benzylidene carbonate) (15) in CDCl₃.

III. Procedures for selective deprotection of acetonide and benzylidene groups

i. Methanolysis using solid acid catalyst^[76]

To a solution of acetonide compound (0.2 g, 0.26 mmol) in 5 mL methanol, was added 0.3 g Dowex[®] 50WX2 and the reaction mixture was stirred for 3-4 h at room temperature. After completion, as indicated by TLC, mixture was filtered through glass filter and washed with methanol. Filtrate was evaporated over rotavapor[®] at room temperature. Crude products were subjected to silica gel chromatography in methanol/chloroform eluent system.

ii. Hydrolysis using molecular iodine^[104]

To a solution of acetonide compound (0.2 g, 0.26 mmol) in 5 ml acetonitrile, was added 30 mol% I₂, water (1.56 mmol) and the reaction mixture was stirred for 6-7 h at room temperature. Brown oily layer settled at the bottom of RBF. Solvent layer decanted and washed several times with acetonitrile to fetch yellow oily liquid along with white solid.

iii. Methanolysis using organic acid catalyst

Solution of benzylidene compound (0.2 g, 0.21 mmol) and *p*-toluene sulfonic acid (0.2 mol%) in methanol was stirred for 4 h at 40°C. After completion, mixture was neutralized with Amberlyst A-21, weakly basic resin, filtered and evaporated under reduced pressure.

IV. Synthesis of carbonate and urethane containing dendritic motifs using accelerated strategies

i. Synthesis of dendrimer integral units

a. Synthesis of Ethylene bis(chloroformate) (14)

Two neck round bottom flask was charged with the solution of triphosgene (59.5 g, 200 mmol) in freshly distilled dichloromethane (500 mL). Both the ends of flask were sealed with silicon septum and mixture was kept for stirring at -5 °C. With the help two syringes, pyridine (47.8 g, 604 mmol) and ethylene glycol (15 g, 242 mmol) were added slowly through two necks over a period of 1 h. Care was taken to see that in-situ generated phosgene remains always excess to the alcohol added. After complete addition, mixture was stirred for 0°C for 5 h. Reaction mixture was washed with cold water (2 x 200 mL) and dried over anhy. MgSO₄. Dichloromethane was distilled out and remaining residual liquid was purified under reduced pressure to obtain colourless liquid (80%). b.p. 54°C at 0.3 torr; ¹H NMR (400 MHz, CDCl₃, 25°C): δ=4.5 (s, 4H; CH₂); ¹³C NMR (100 MHz, CDCl₃, 25 °C): δ=150.8 (C=O), 67.7 (CH₂); IR (KBr): $\tilde{\nu}$ (cm⁻¹)=2968 (w, C-H_{stretch}, sp³), 1778 (vs, C=O_{stretch}), 1645 (w, C=C_{stretch}), 1450(m, C-H_{bend}, methylene), 1178, 1145(vs, C-O_{stretch}), 993, 931 (s, C=C_{bend}), 835(s, C-Cl_{stretch}).

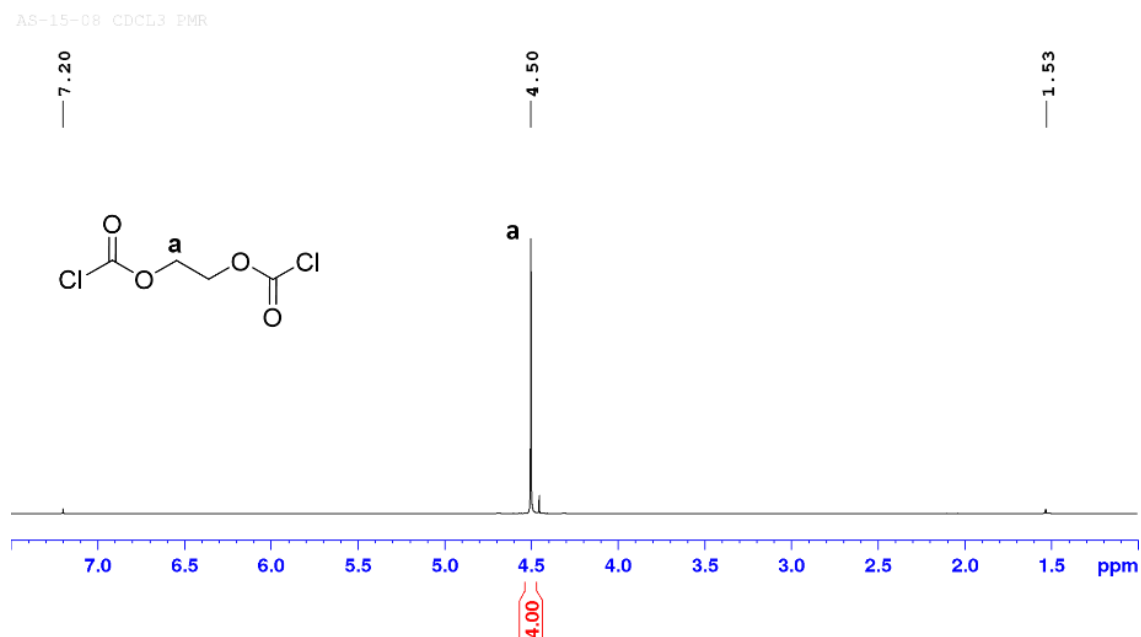


Figure 1.23 ^1H NMR spectrum of Ethylene bis(chloroformate) (**14**) in CDCl_3 .

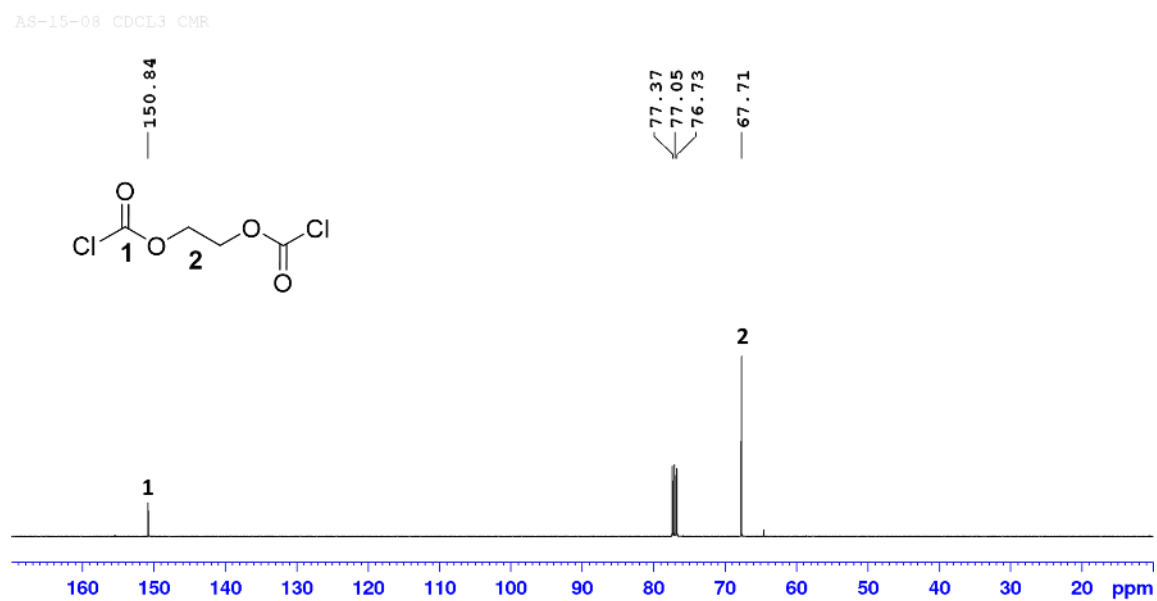


Figure 1.24 ^{13}C NMR spectrum of Ethylene bis(chloroformate) (**14**) in CDCl_3 .

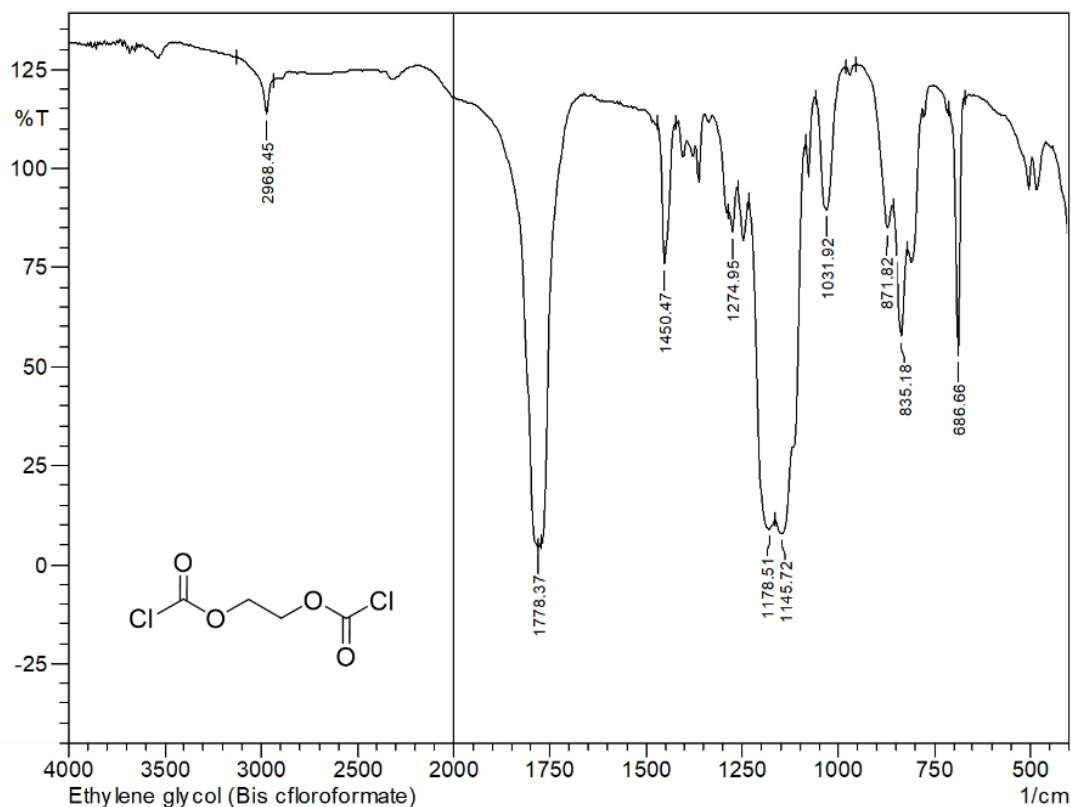


Figure 1.25 IR spectrum of Ethylene bis(chloroformate) (**14**) in KBr.

b. Attempt towards synthesis of urethane linked AB₂ branching unit from diethanol amine and ethylene glycol

In a 2-neck round bottom flask, ethylene bis (chloroformate) (1.94 g, 10.4 mmol) was diluted with 10 mL of dry acetone and cooled to 0°C. To the cold stirring solution, diethanol amine (1 g, 9.5 mmol) in 10 mL acetone was added dropwise over a period of 30 min under inert atmosphere. After complete addition, reaction stirred for more 1.5 h at same temp. Colourless viscous liquid separates out of the solvent system and settles at bottom. Acetone layer was decanted and viscous liquid residue was washed with acetone and dried under vacuum. Combined solvent layer was evaporated to dryness to obtain yellow jelly mass. Both products were analyzed by IR spectroscopy. **Side product 18:** IR (KBr): $\tilde{\nu}(\text{cm}^{-1}) = 3353(\text{vs, brd, O-H}_{\text{stretch}})$, 2963, 2794 (m, C-H_{stretch}, sp^3), 1687 (m, C=O_{stretch}), 1450 (s, C-H_{bend}, *methylene*), 1224 (w, C-O_{stretch}, *urethane*), 1065 (s, C-O_{stretch}, *alcohol*).

Side product 19: IR (KBr): $\tilde{\nu}(\text{cm}^{-1}) = 3371(\text{s, O-H}_{\text{stretch}})$, 2974, 2887(m, C-H_{stretch}, sp^3), 1803 (w, C=O_{stretch}, *chloroformate*), 1753(s, C=O_{stretch}, *ester*), 1691(m, C=O_{stretch}, *urethane*), 1479(m, C-H_{bend}, *methylene*), 1249(s, C-O_{stretch}, *ester*), 1074(m, C-O_{stretch}, *alcohol*).

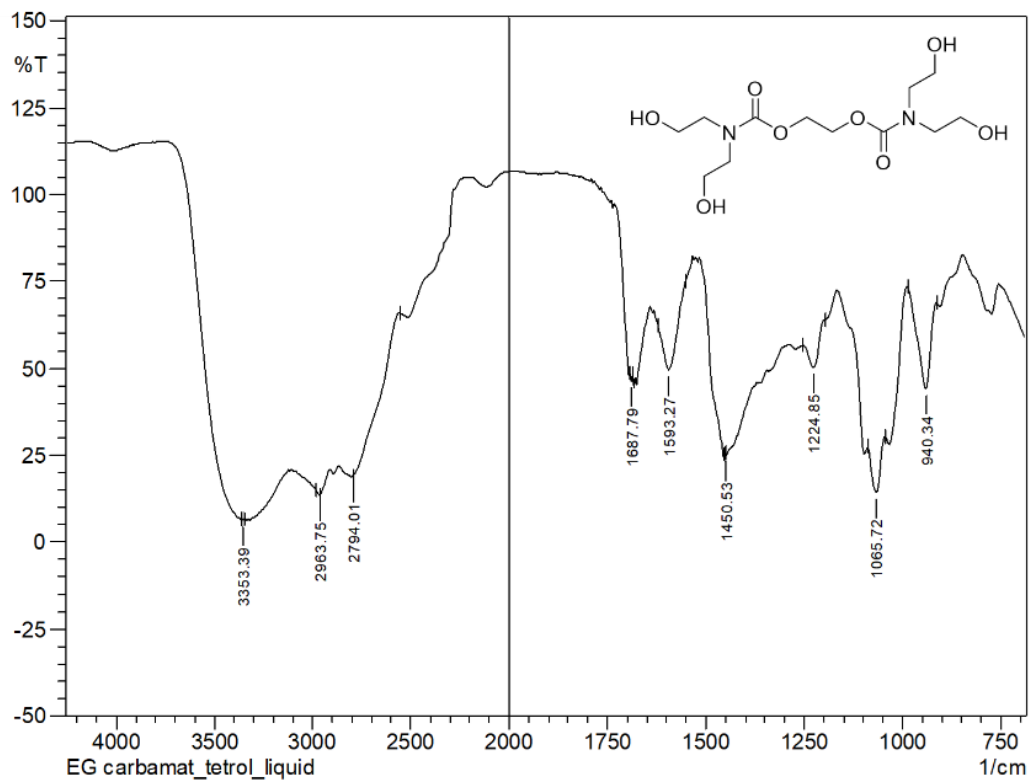


Figure 1.26 IR spectrum of side product (18) in KBr.

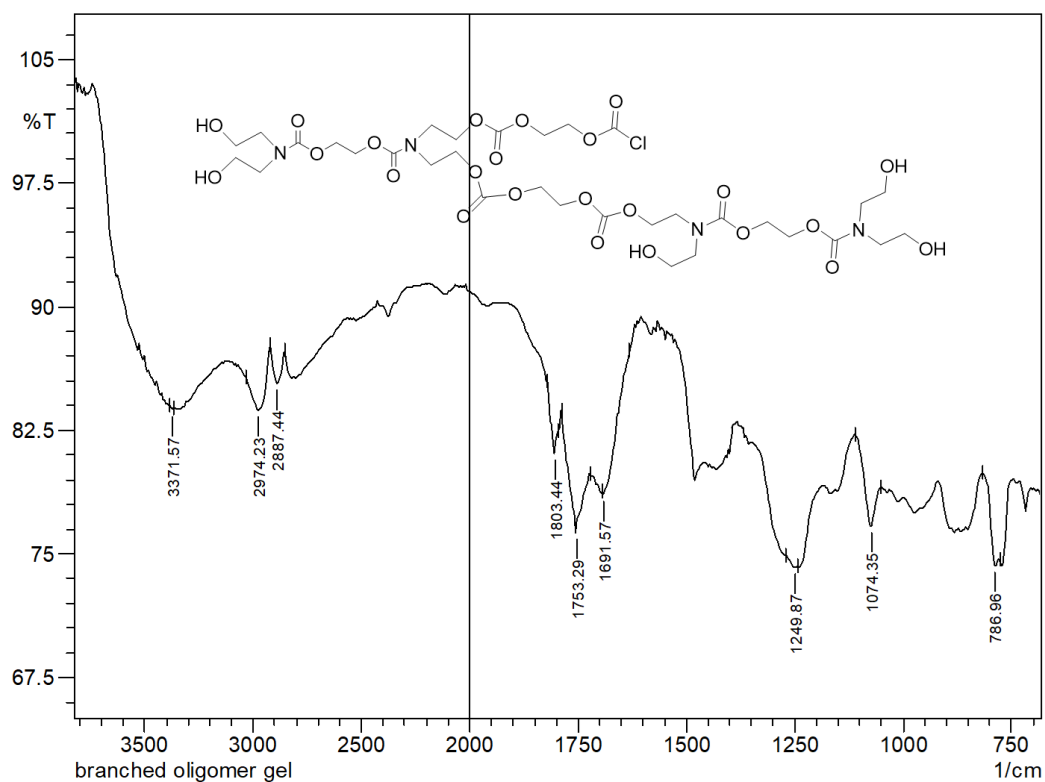


Figure 1.27 IR spectrum of side product (19) in KBr.

c. Synthesis of *N,N*-diallyl carbamoyl chloride (**21**)^[105]

A solution of triphosgene (73.3 g, 247 mmol) in dry dichloromethane (500 mL) was added dropwise to a vigorously stirred solution of *N,N*-diallyl amine (40 g, 412 mmol) in dichloromethane (500 mL) at -15°C in presence of catalytic amount of triethyl amine. After 5 h of complete addition, mixture was slowly warmed to room temperature over a period of 1 h and continued stirring for 12 h at room temperature. Later, nitrogen gas was bubbled through the reaction mixture to scrub excess phosgene into strong alkaline solution. Dichloromethane was distilled out and remaining residual content was purified under reduced pressure to obtain colorless liquid (84%). b.p. 36°C at 0.3 torr; ^1H NMR (400 MHz, CDCl_3 , 25°C): $\delta=5.86\text{-}5.76(\text{m}, 2\text{H}; \text{CH}=\text{CH}_2)$, $5.29\text{-}5.21(\text{m}, 4\text{H}; \text{CH}=\text{CH}_2)$, $4.07\text{-}4.06(\text{d}, J=4\text{ Hz}, 2\text{H}; \text{CH}_2=\text{CHCH}_2)$, $4.0\text{-}3.9(\text{d}, J=4\text{ Hz}, 2\text{H}; \text{CH}_2=\text{CHCH}_2)$; ^{13}C NMR (100 MHz, CDCl_3 , 25°C): $\delta=149.5(\text{C}=\text{O})$, $131.5(\text{CH}=\text{CH}_2)$, $118.8(\text{CH}=\text{CH}_2)$, $52.5(\text{CH}_2=\text{CHCH}_2)$; IR (KBr): $\tilde{\nu}(\text{cm}^{-1})=3086(\text{w}, \text{C-H}_{\text{stretch}}, sp^2)$, $2858(\text{w}, \text{C-H}_{\text{stretch}}, sp^3)$, $1737(\text{vs}, \text{C}=\text{O}_{\text{stretch}})$, $1645(\text{w}, \text{C}=\text{C}_{\text{stretch}})$, $1209, 1176(\text{m}, \text{C-N}_{\text{stretch}})$, $993, 931(\text{s}, \text{C}=\text{C}_{\text{bend}})$, $931(\text{m}, \text{C-H}_{\text{bend}}, \text{alkene})$, $808(\text{w}, \text{C-Cl}_{\text{stretch}})$.

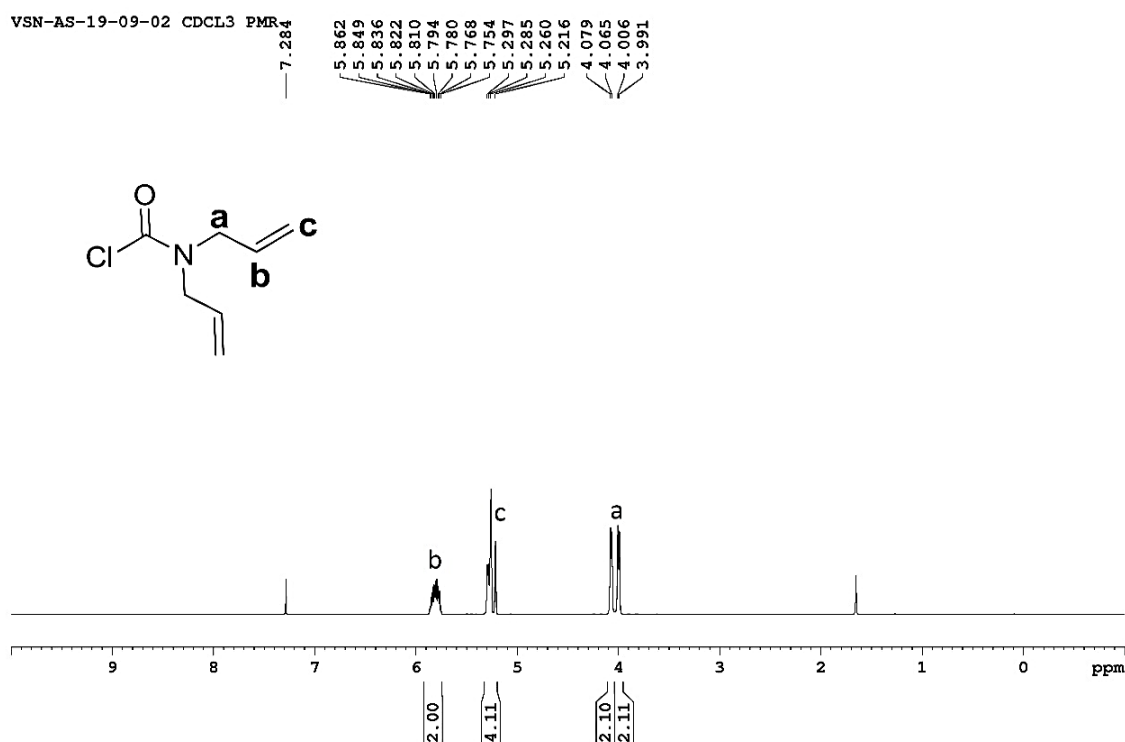


Figure 1.28 ^1H NMR spectrum of *N,N*-diallyl carbamoyl chloride (**21**) in CDCl_3 .

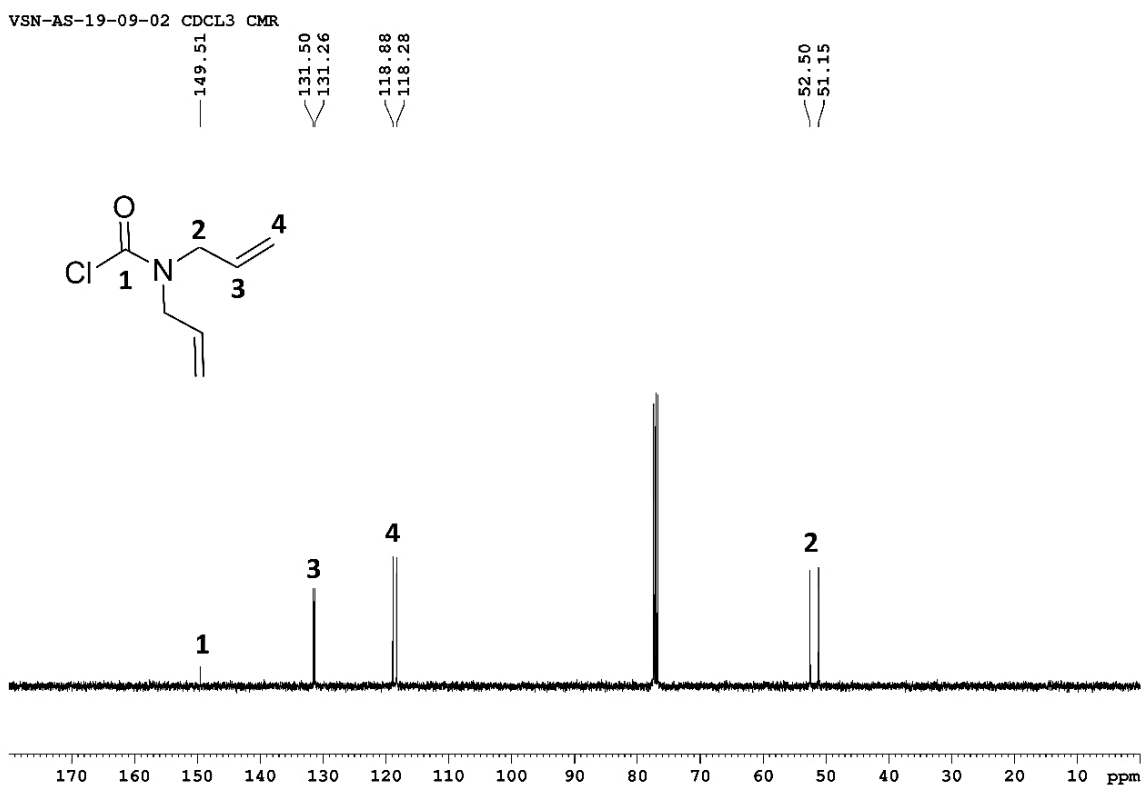


Figure 1.29 ^{13}C NMR spectrum of *N,N*-diallyl carbamoyl chloride (**21**) in CDCl_3 .

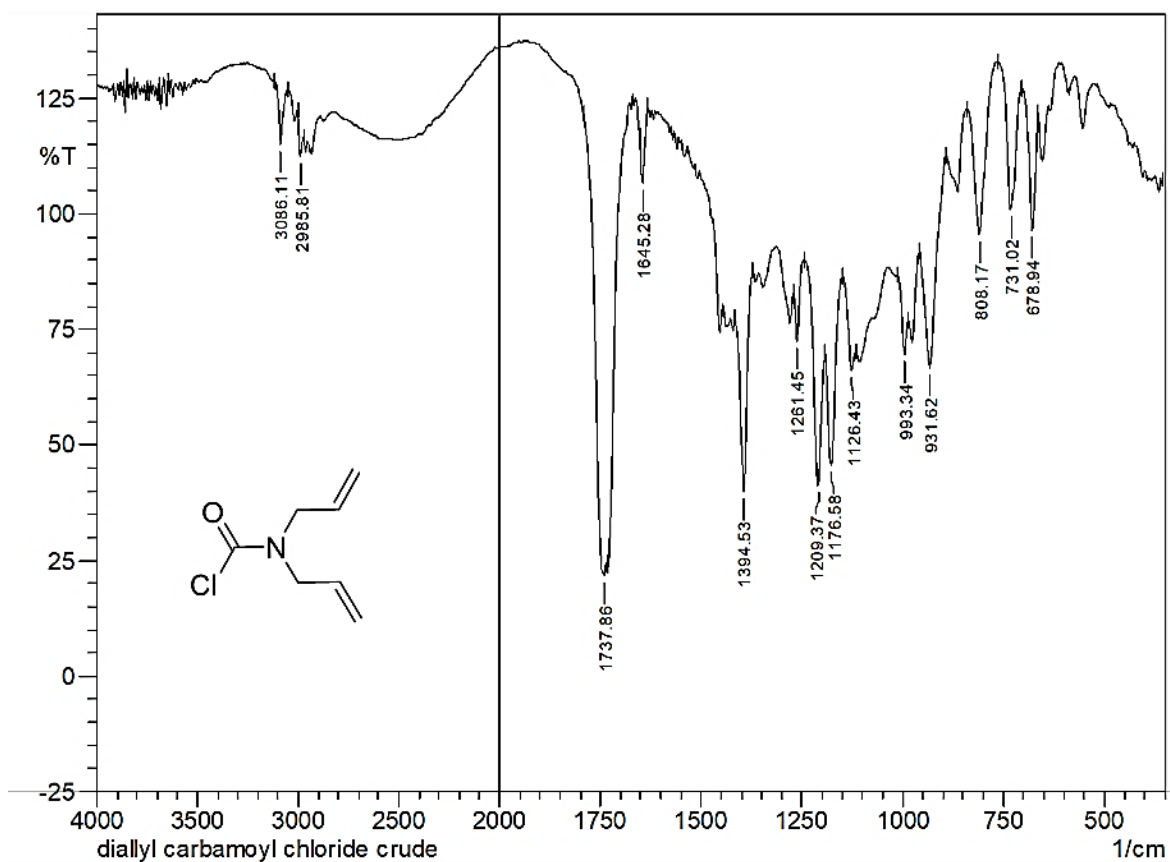


Figure 1.30 IR spectrum of *N,N*-diallyl carbamoyl chloride (**21**) in KBr.

d. Synthesis of Allyl chloroformate chloride (20)

Followed same procedure as mention for ethylene bis(chloroformate) (**14**). Triphosgene (51.2 g, 172 mmol), pyridine (41 g, 516 mmol) and allyl alcohol (20 g, 344 mmol). Azeotropic distillation of dichloromethane was achieved by using Dufton glass fractionating column. Finally crude liquid was purified by distillation under reduced pressure to obtain colorless liquid (37.2 g, 89%). b.p. 34°C at 15 torr; ^1H NMR (400 MHz, CDCl_3 , 25°C): δ = 6.01-5.91 (m, 1H; $\text{CH}=\text{CH}_2$), 5.47-5.39 (dd, $J=16$ and 8 Hz, 1H; $\text{CH}=\text{CH}_2$), 4.08-4.79 (d, $J=4$ Hz, 2H; $\text{CH}_2=\text{CHCH}_2$); ^{13}C NMR (100 MHz, CDCl_3 , 25 °C): δ = 150.5 (C=O), 129.7 ($\text{CH}=\text{CH}_2$), 121.2 ($\text{CH}=\text{CH}_2$), 72.1 ($\text{CH}_2=\text{CHCH}_2$); IR (KBr): $\tilde{\nu}(\text{cm}^{-1})=1775$ (vs, C=O_{stretch}), 1651 (w, C=C_{stretch}), 810(s, C-Cl_{stretch}).

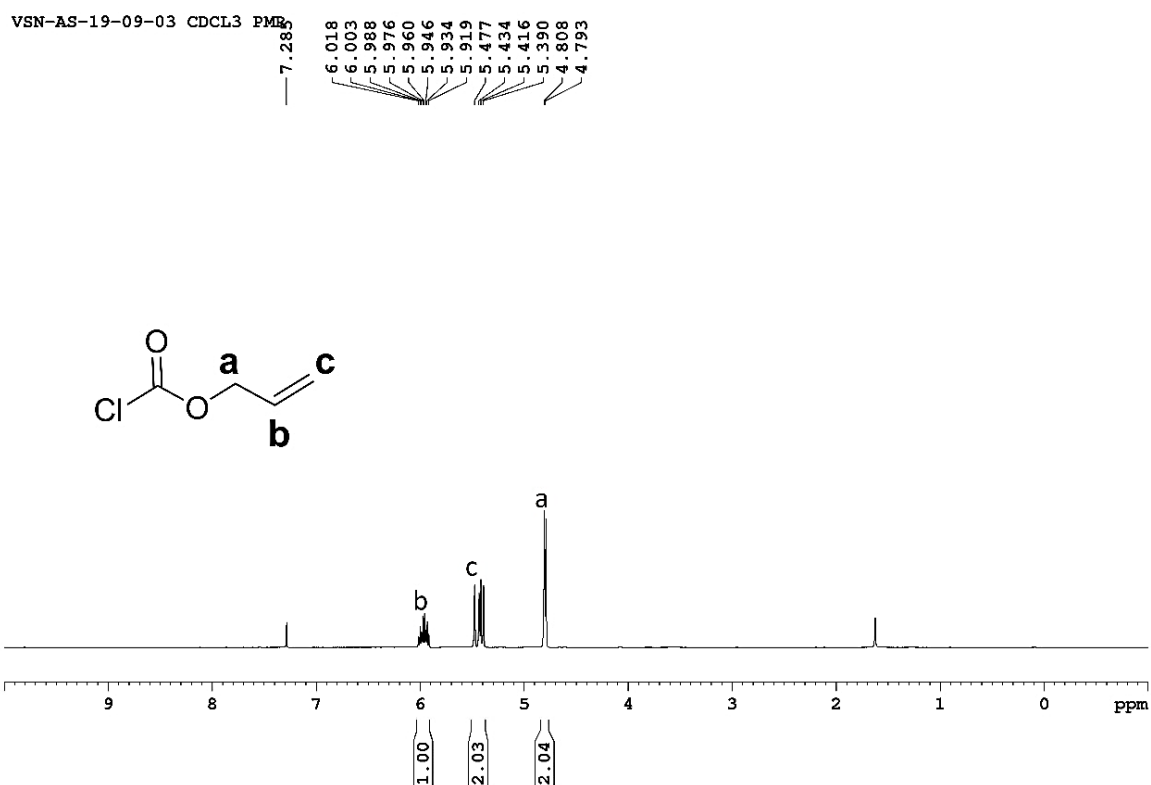


Figure 1.31 ^1H NMR spectrum of Allyl chloroformate (**20**) in CDCl_3 .

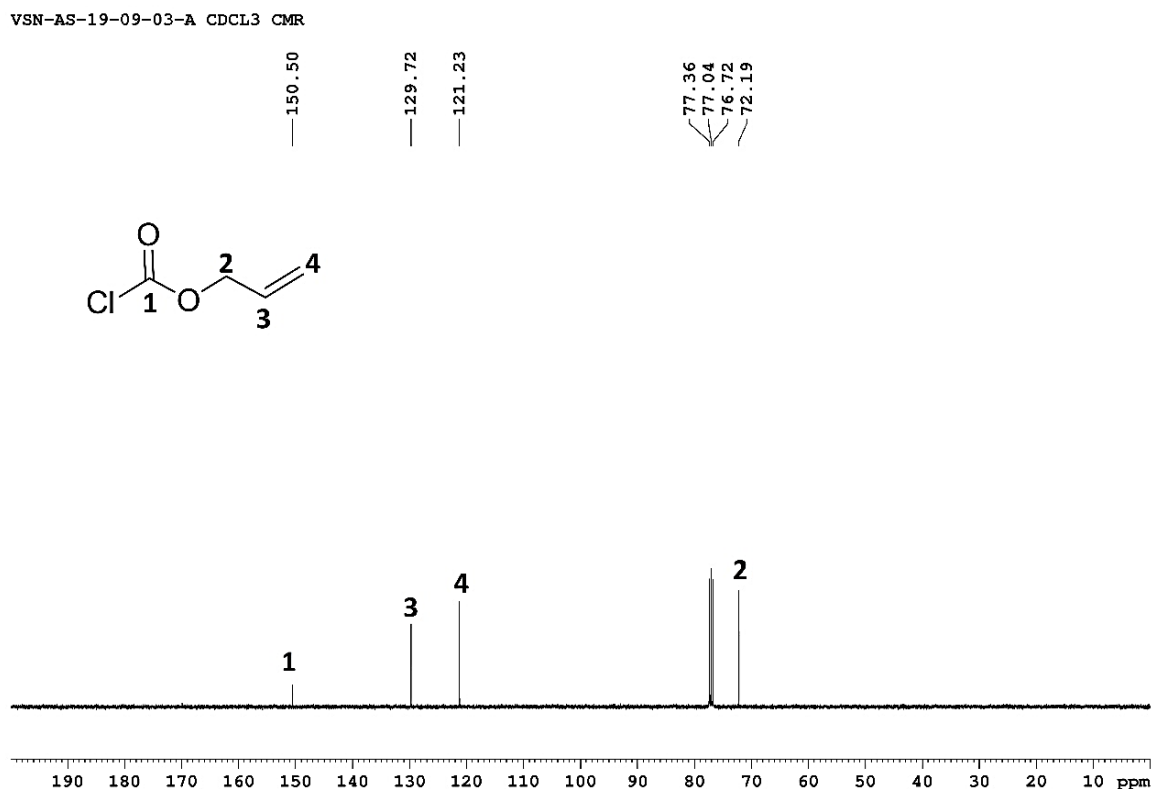


Figure 1.32 ¹³C NMR spectrum of Allyl chloroformate (20) in CDCl₃.

ii. Divergent Growth Synthesis of PU/PC dendrimers using two-step approach.

a. Synthesis of pentaerythritol tetrakis (allyl carbonate) [PETAC] (22)^[106]

In a two-neck flask equipped with pressure equalizer funnel, was placed (5 g, 36.7 mmol) of pentaerythritol, pyridine (14 g, 182.5 mmol) and dry acetonitrile 50 mL. Reacting flask was cooled to 0°C and allyl chloroformate (20 g, 164 mmol) was added dropwise using dropping funnel with drying tube. After addition for 30 min, the mixture was stirred for 1 h at 0°C and then for 4 h at room temperature. The progress of reaction was monitored using thin layer chromatography. After complete conversion, solvent was evaporated and residue was acidified with 1 N HCl. Mixture was extracted twice with diethyl ether and washed with water, brine and dried over anhy. Na₂SO₄. The solvent was removed using rotary evaporator to afford crude yellow product. This product obtained was purified by silica gel chromatography to afford pure colourless viscous oil. *R*_f=0.7 (pet. ether/ethyl acetate 3:7); ¹H NMR (400 MHz, CDCl₃, 25°C): δ (ppm) = 5.98–5.88 (m, 4H; CH=CH₂), 5.39–5.34 (dd, *J*=12Hz and 1.6Hz, 4H; CH=CH₂), 5.30–5.27 (dd, *J*=8Hz and 1.6Hz, 4H; CH=CH₂), 4.63–4.61(dt, *J*=4Hz and 1.6Hz, 8H; CH=CHCH₂); 4.25 (s, 8H; OCH₂); IR (KBr): $\tilde{\nu}$ (cm⁻¹) = 3088(w, C-H_{strech}, *sp*²), 2858(w, C-H_{strech}, *sp*³), 1753 (vs, C=O_{strech}),

1649 (w, C=C_{stretch}), 1454(w,C-H_{bend},*methylene*), 1242 (vs, C-O_{bend}, *ester*), 996 (s, C=C_{bend}), 788 (m,C-H_{bend}, *alkene*).

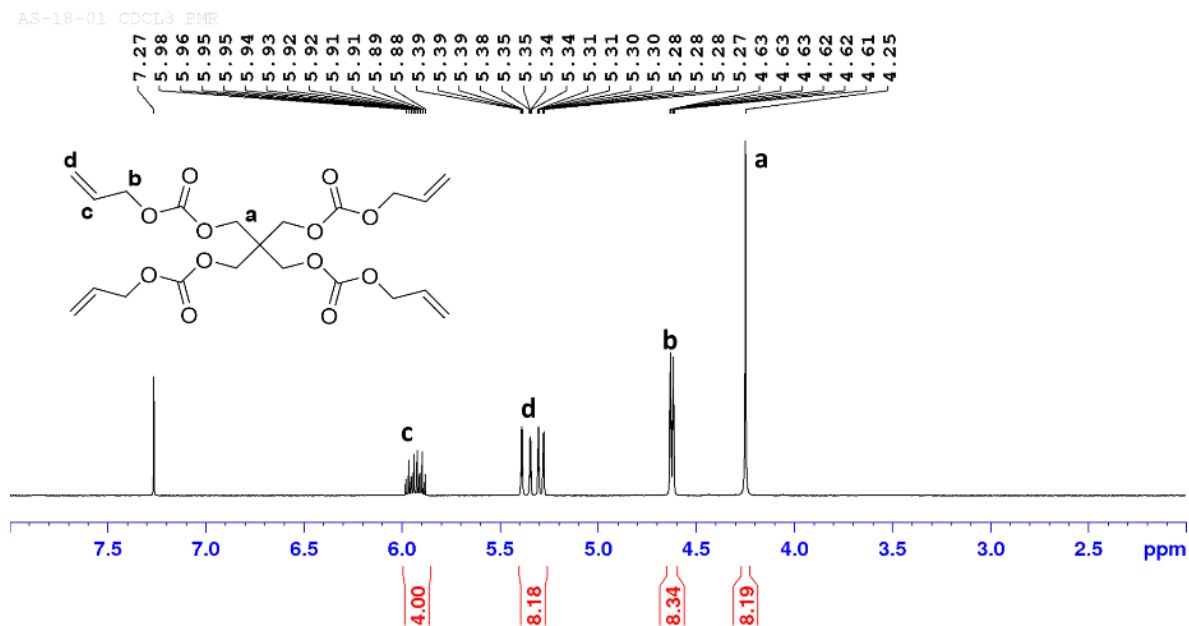


Figure 1.33 ¹H NMR spectrum of pentaerythritol tetra (allyl carbonate) (**22**) in CDCl₃.

b. Synthesis of Ethylene bis (diallyl carbamate) (**24**)

Carbonylation method A: To a homogenous solution of ethylene glycol (5 g, 80.5 mmol) in THF (60 mL) was added NaH (60% in mineral oil, 9.65 g, 240.6 mmol) in portion. The mixture was stirred at 0°C while *N,N*-diallyl carbamoyl chloride (32.1 g, 202 mmol) was added dropwise through addition funnel over a period of 1 h. The reaction mixture was slowly warmed to room temperature and stirred for 3 h. Later, THF was evaporated and mixture extracted with diethyl ether. Organic layer washed with H₂O, brine solution and dried over anhy. MgSO₄.

Carbonylation method B: Reaction flask with drying tube and addition funnel, was charged with dilute solution of *N,N*-diallyl amine (12.5 g, 128 mmol) and triethyl amine (16.2 g, 160 mmol) in dichloromethane (100 mL). To a stirred solution, ethylene bis(chloroformate) (10 g, 53.5 mmol) was added dropwise over a period 30 min 0°C. Mixture was slowly warmed to room temperature and continued stirring for 6 h. After completion of reaction, mixture was neutralized with dil. HCl solution and decanted. Organic layer was washed with water, brine solution and dried over anhy. MgSO₄.

Purification: Crude yellow liquid obtained was purified under reduced pressure of 1 torr at 210°C to yield pure compound as colorless liquid [Method A (94%) and Method B (88%)]. ¹H NMR (400 MHz, CDCl₃, 25°C): δ=5.74 (m, 4H; CH=CH₂), 5.16-5.13 (m, 8H; CH=CH₂), 4.30 (s, 4H; OCO₂CH₂), 3.87-3.81 (d, 8H; CH₂=CHCH₂); ¹³C NMR (100 MHz, CDCl₃,

25°C): $\delta=155.5$ (C=O), 132.3 (CH=CH₂), 117.0 (CH=CH₂), 63.4 (OCH₂), 48.9 (CH₂=CHCH₂); IR (KBr): $\nu(\text{cm}^{-1})=3080$ (m, C-H_{strech}, *sp*²), 2981 (s, C-H_{strech}, *sp*³), 1703 (vs, C=O_{strech}), 1643 (w, C=C_{strech}), 1467(s, C-H_{bend}, *methylene*), 1232 (s, C-N_{strech}), 1153(m, C-O_{strech}), 993(m, C=C_{bend}), 923 (s, C-H_{bend}, *alkene*); HRMS (ESI) *m/z* [M+Na]⁺ calcd for C₁₆H₂₄N₂O₄Na: 331.1634, found: 331.1634.

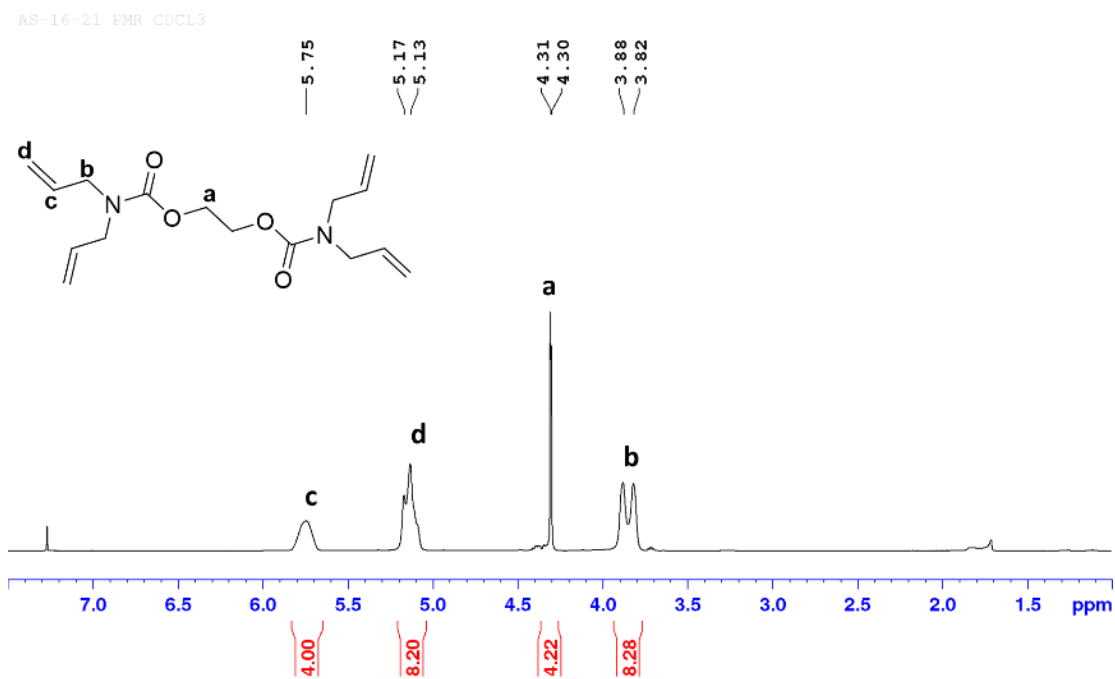


Figure 1.34 ¹H NMR spectrum of Ethylene bis(diallyl carbamate) (**24**) in CDCl₃.

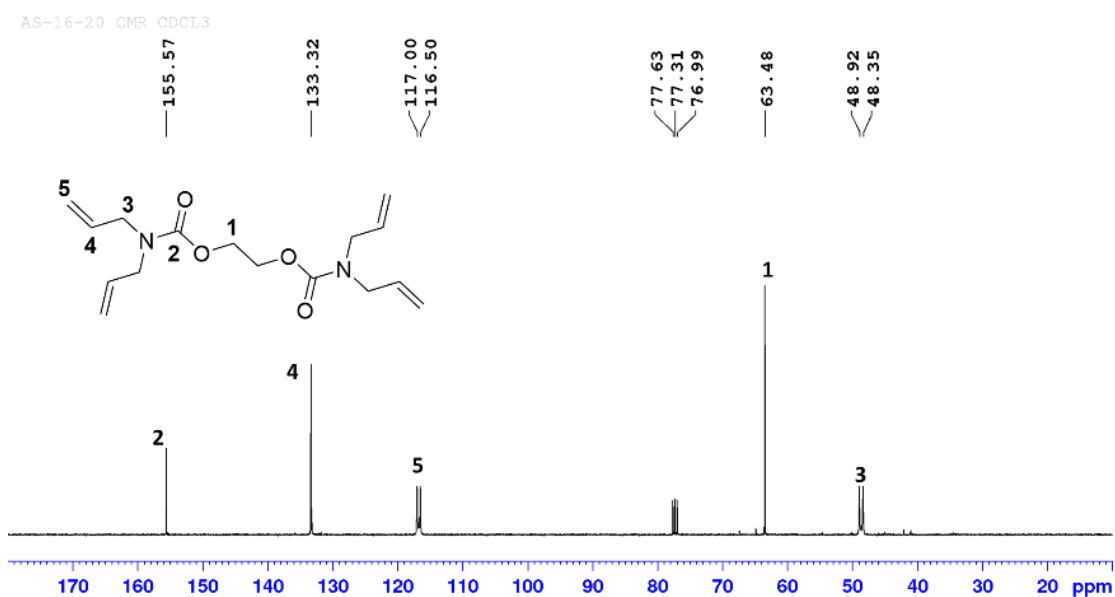


Figure 1.35 ¹³C NMR spectrum of Ethylene bis(diallyl carbamate) (**24**) in CDCl₃.

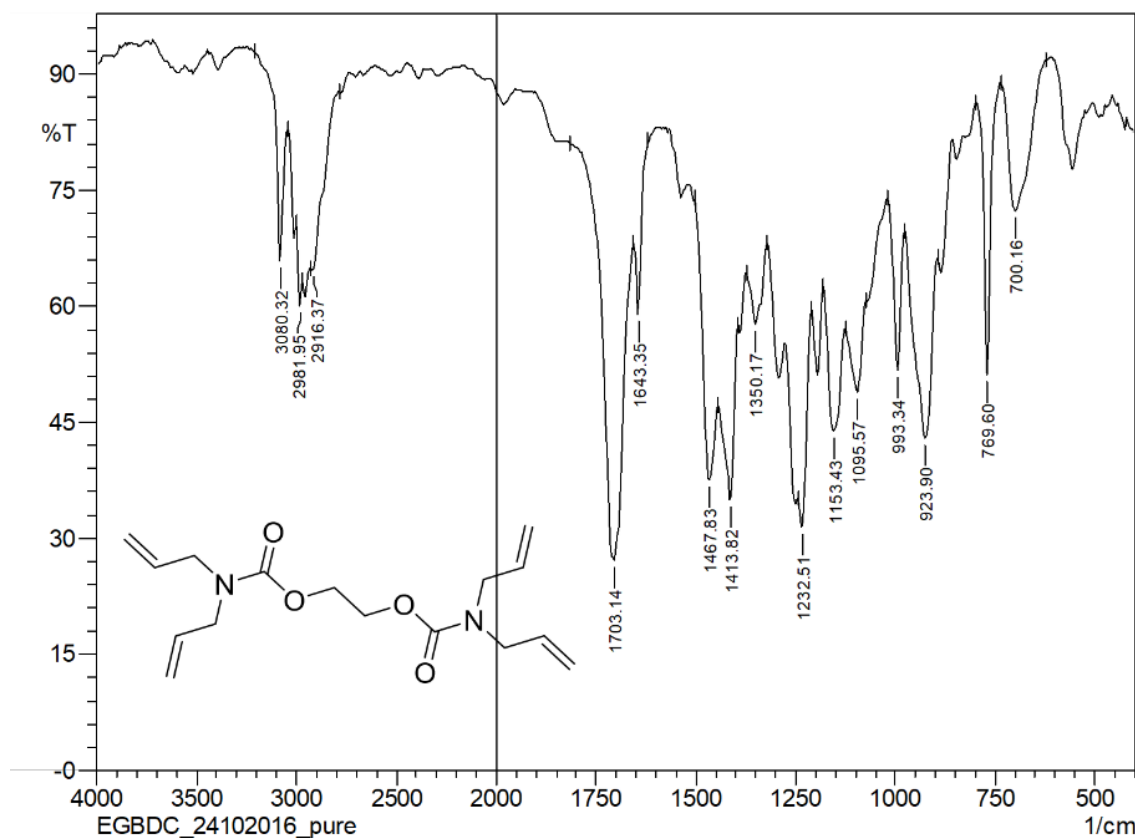


Figure 1.36 IR spectrum of Ethylene bis(diallyl carbamate) (**24**) in KBr.

c. Synthesis of EG-[G-1]-(OH)₈ (**25**)

To a stirred solution of compound **24** (10 g, 32.42 mmol) in a water/acetone/*t*-BuOH mixture (1:1:0.5) was added a solution of *N*-methyl morpholine *N*-oxide (NMO) (50 wt % in water, 33 mL, 143 mmol), followed by solution of osmium tetroxide (4 wt % in water, 2.1 mL, 0.32 mmol). The mixture was stirred at room temperature for 3 h. After completion of reaction, mixture was evaporated with ethanol and toluene to obtain thick brown oil. Crude compound was subjected to silica gel chromatography $R_f=0.6$ ($\text{CHCl}_3/\text{MeOH}$ 1:1) and gel filtration chromatography (Sephadex[®] G-50, water) to afford colorless thick liquid in 90-95% yield. ¹H NMR (400 MHz, D₂O, 25°C): $\delta=4.25\text{--}4.17$ (m, 4H; OHCH), 3.81 (s, 4H; OCH₂), 3.49-3.45 (m, 4H; CH₂OH), 3.39-3.36 (m, 4H; CH₂OH), 3.34-3.31 (m, 4H; CH₂N), 3.22-3.15 (m, 4H; CH₂N); ¹³C NMR (100 MHz, D₂O, 25°C): $\delta=157.7$ (C=O), 70.2, 69.7 (OHCH), 64.13 (OCH₂), 63.2 (CH₂OH), 50.9 (CH₂N); IR (KBr): $\tilde{\nu}(\text{cm}^{-1})=3379$ (vs, O-H_{stretch}), 2943 (m, C-H_{stretch}, *sp*³), 1687 (vs, C=O_{stretch}), 1467 (s, C-H_{bend}, *methylene*), 1234 (s, C-N_{stretch}), 1139 (m, C-O_{stretch}), 1041 (m, C-O_{stretch}, *alcohol*); HRMS (ESI) m/z [$M+\text{Na}$]⁺ calcd for C₁₆H₃₂N₂O₁₂Na: 467.1847, found: 467.1849.

AS-16-22 D2O PMR

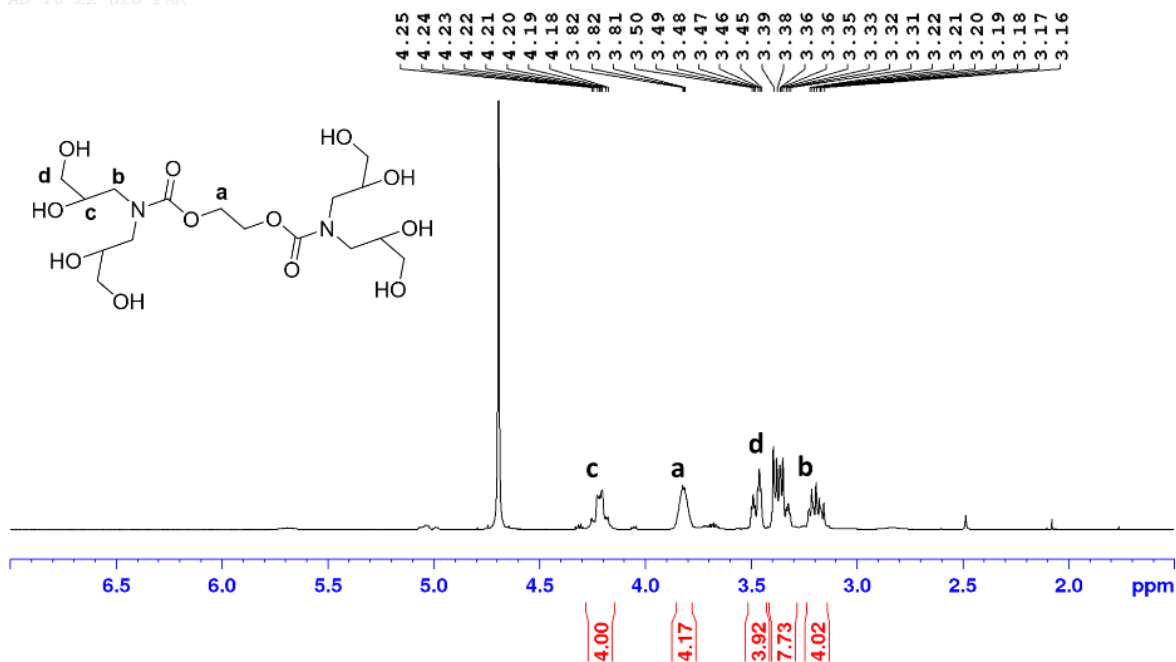


Figure 1.37 ¹H NMR spectrum of EG-[G-1]-(OH)₈ (25) in D₂O.

AS-16-22 D2O CMR

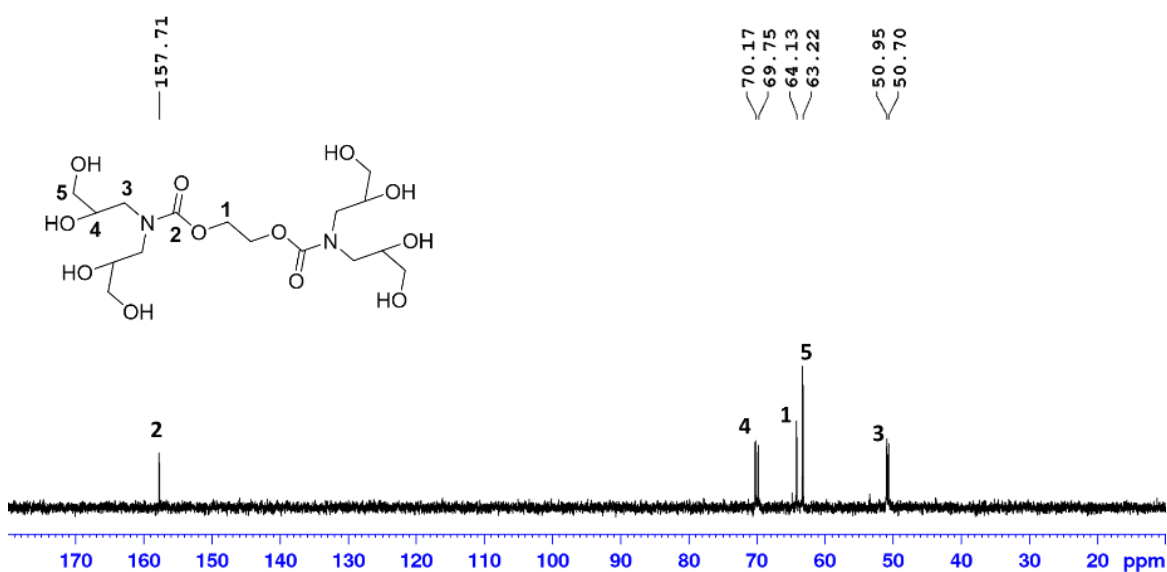


Figure 1.38 ¹³C NMR spectrum of EG-[G-1]-(OH)₈ (25) in D₂O.

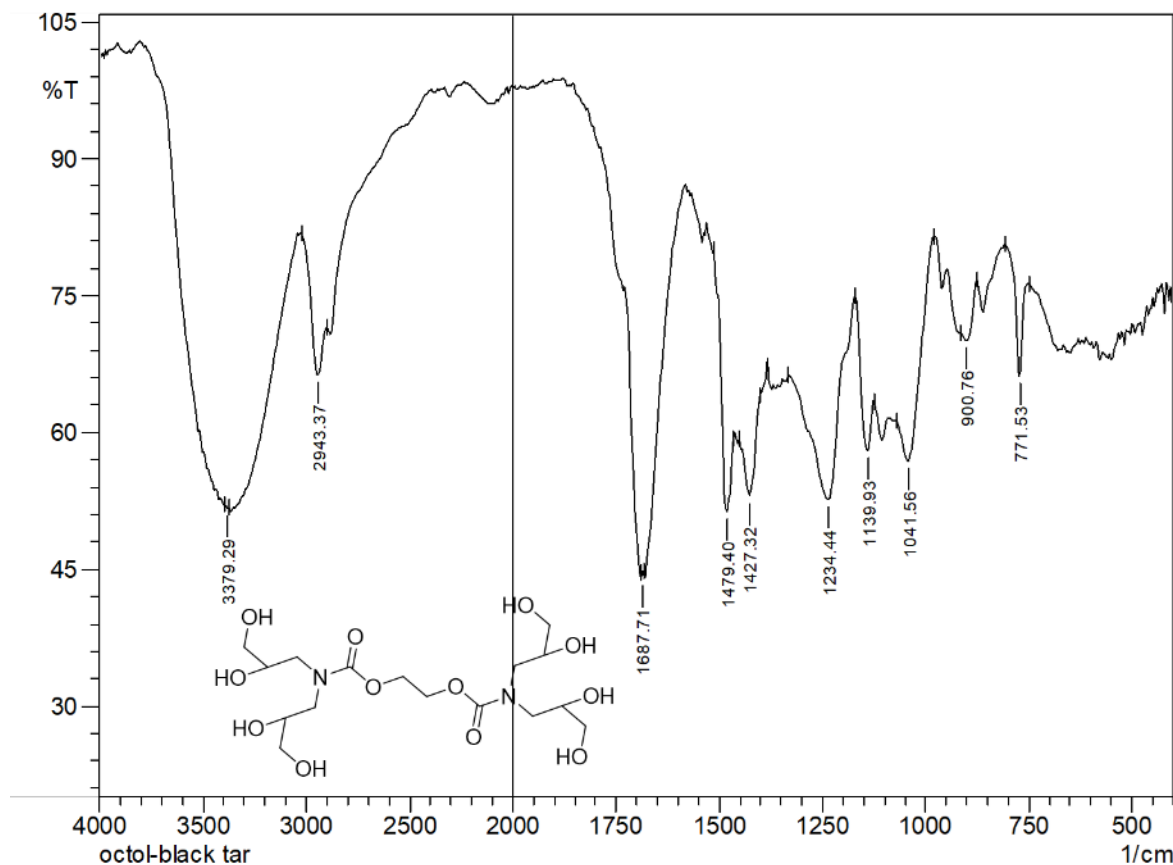


Figure 1.39 IR spectrum of EG-[G-1]-(OH)₈ (**25**) in KBr.

d. Synthesis of EG-[G-1.5]-(allyl)_n dendrimers via per-allylation polyol **25**

EG-[G-1.5]-(allyl)₁₆ (26): To a vigorously stirred homogenous mixture of crude **25** (5 g, 11.2 mmol) and *N,N*-carbonyl chloride **21** (35.91 g, 225 mmol) in dry DMF/THF (1:2, 60 ml) solvent system was added NaH (60% in mineral oil, 4.04 g, 101 mmol) in portions at 0 °C. After stirring for 1 h at same temperature, reaction vessel was gradually warmed to room temperature and continued stirring for 7 h. Later THF was evaporated, residue was dissolved in water/diethyl ether and separated aqueous layer was re-extracted with ether. Combined organic layer was washed with sat. LiCl solution and dried over MgSO₄. The crude brown oil was subjected to silica gel chromatography to provide pale yellow thick liquid in 75% yield. *R_f*=0.6 (hexane/ethyl acetate 4:6); ¹H NMR (400 MHz, CDCl₃, 25 °C): δ=5.80-5.69 (m, 16H; CH=CH₂), 5.16-5.10 (m, 32H, CH=CH₂), 5.06 (m, 4H; OCH), 4.32-4.21 (m, 8H; OCH₂, branch), 4.14-4.07 (m, 4H; OCH₂, core), 3.87-3.78 (m, 32H; NCH₂, terminal), 3.62-3.42 (m, 8H; NCH₂, branch); ¹³C NMR (100 MHz, CDCl₃, 25 °C): δ=155.7 (C=O, terminal), 154.9 (C=O, internal), 133.4 (CH=CH₂), 117.3 (CH=CH₂), 71.2 (OCH), 64.5 (OCH₂, branch), 63.5 (OCH₂, core), 49.1, 48.29 (NCH₂, terminal), 47.8 (NCH₂, branch); IR (KBr): $\tilde{\nu}$ (cm⁻¹)=3080 (m, C-H_{stretch}, sp²), 2981 (s, C-H_{stretch}, sp³), 1712

(vs, C=O_{stretch}, urethane), 1643 (w, C=C_{stretch}), 1462(s, C-H_{bend}, methylene), 1234 (s, C-N_{stretch}), 1153(m, C-O_{stretch}), 993(m, C=C_{bend}), 923 (s, C-H_{bend}, alkene); HRMS (ESI) m/z $[M+Na]^+$ calcd for C₇₂H₁₀₄N₁₀O₂₀: 1451.7321, found: 1451.7336.

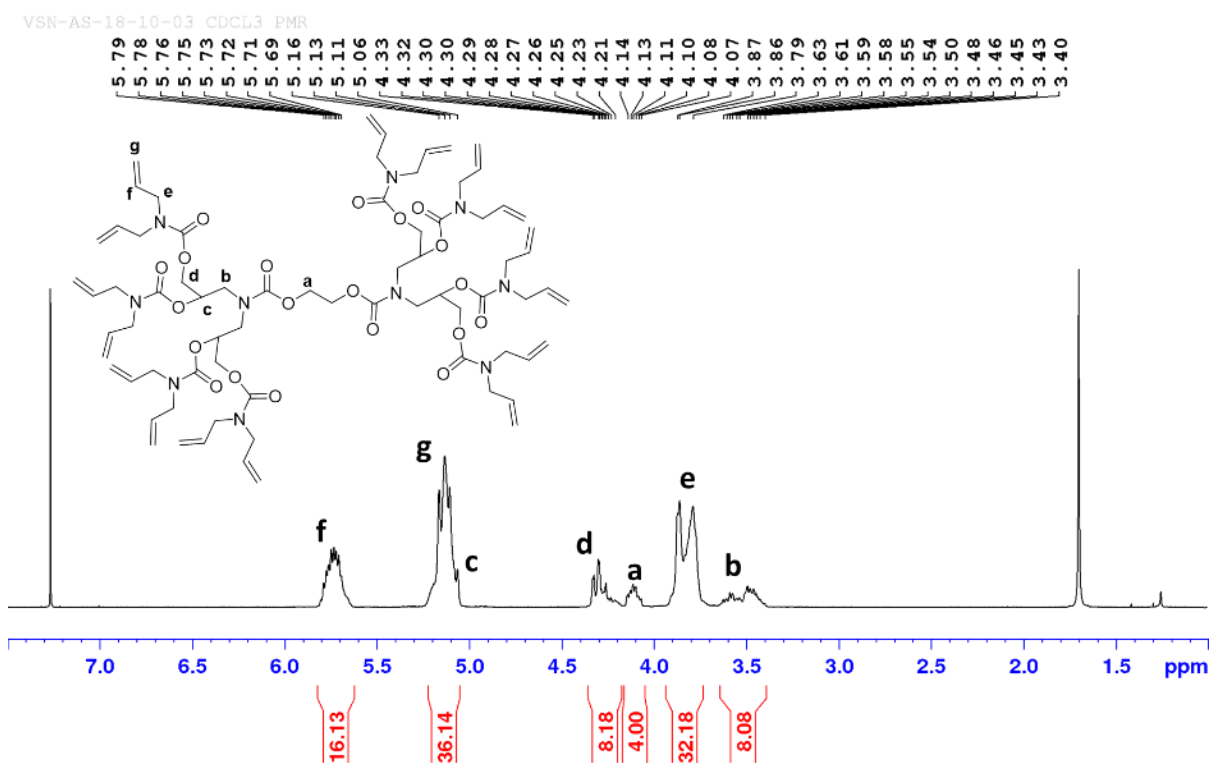


Figure 1.40 ¹H NMR spectrum of dendrimer (26) in CDCl₃.

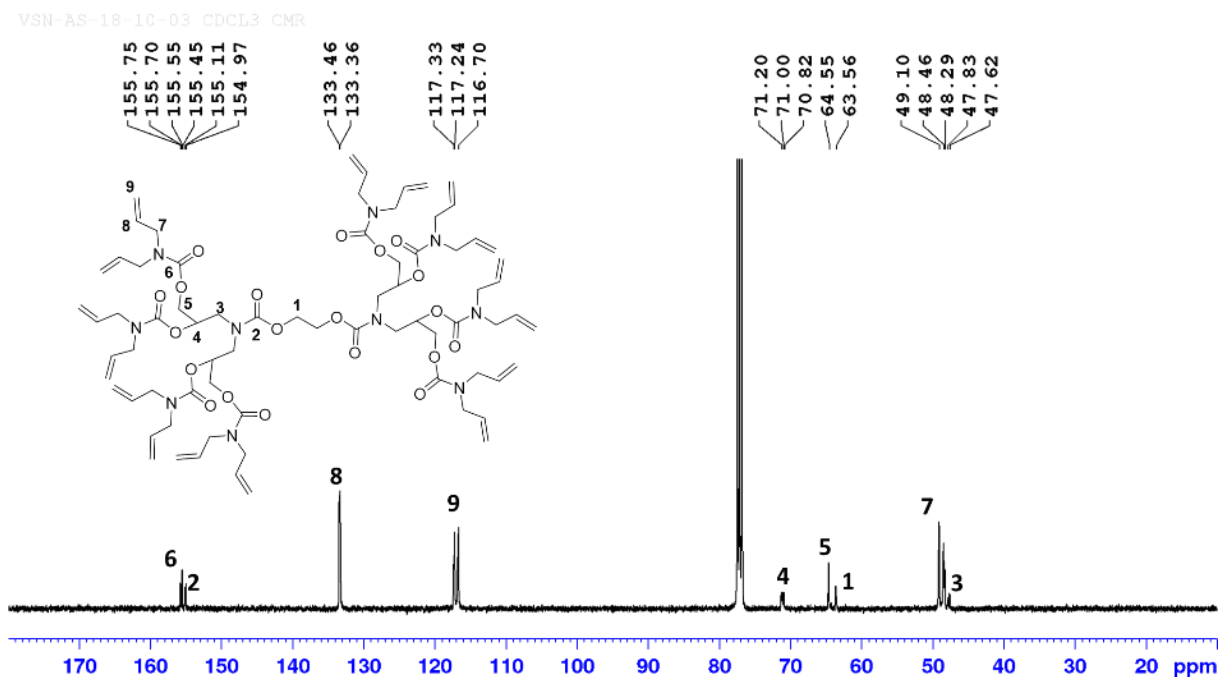


Figure 1.41 ¹³C NMR spectrum of dendrimer (26) in CDCl₃.

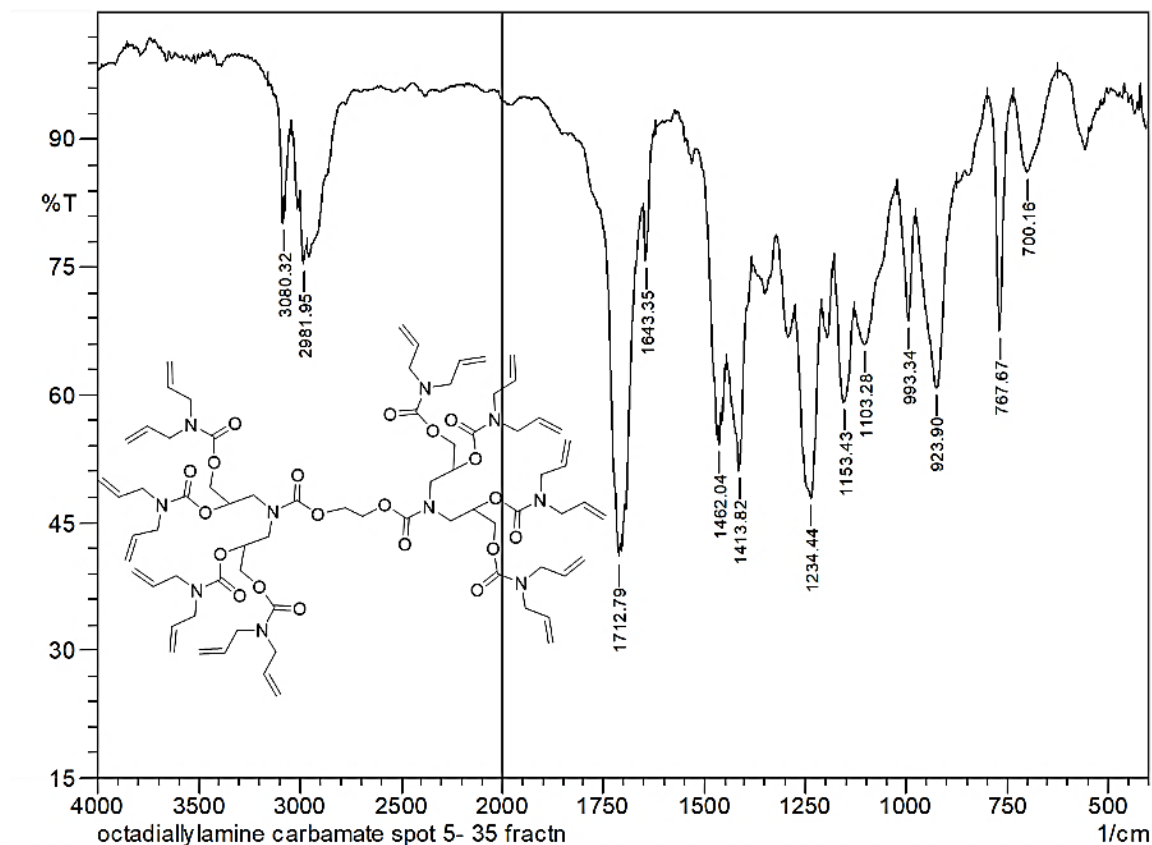


Figure 1.42 IR spectrum of dendrimer (**26**) in KBr.

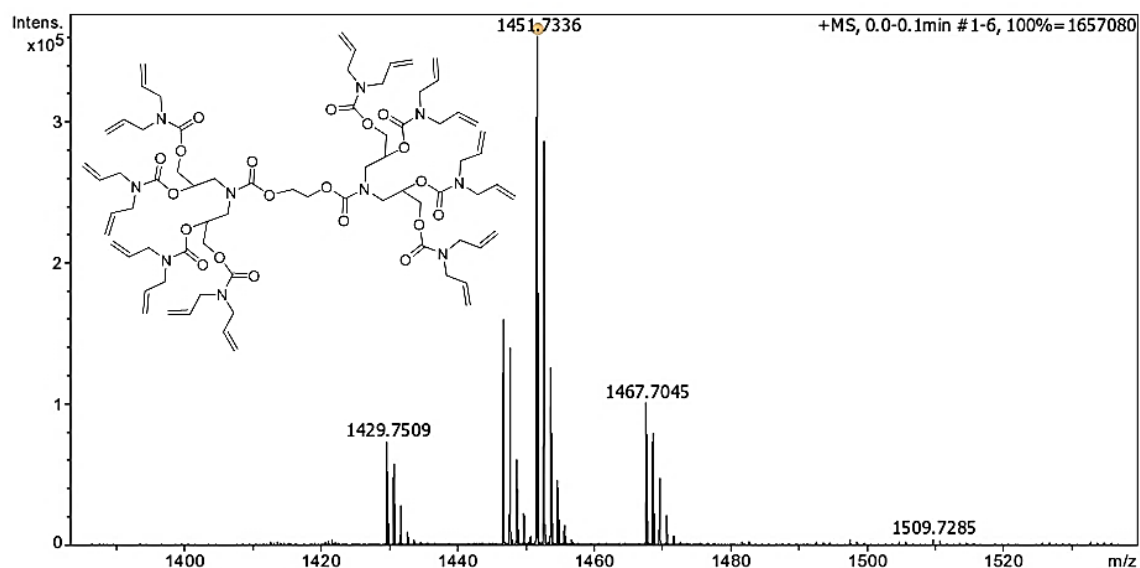


Figure 1.43 HRMS spectrum of dendrimer (**26**).

EG-[G-1.5]-(allyl)₈, (27**):** Reaction flask with drying tube and addition funnel, was charged with crude **25** (5 g, 11.2 mmol) and DMAP (21.9 g, 180 mmol) in dry DMF (60 mL). To a stirred solution was added dropwise allyl chloroformate (21.7 g, 180 mmol) at 0°C over

period of 1 h. After complete addition, mixture was slowly warm to room temperature and continued stirring for 12 h. To stirring mixture, H₂O and diethyl ether were added. Separated aqueous layer was re-extracted with ether. Combined organic layer was washed with H₂O, sat. LiCl solution and dried over MgSO₄. The crude yellow oil was subjected to silica gel chromatography to provide colorless thick liquid in 77% yield. R_f=0.6 (hexane/ethyl acetate 1:1); ¹H NMR (400 MHz, CDCl₃, 25°C): δ=5.97-5.87 (m, 8H; CH=CH₂), 5.39-5.25 (dd, 16Hz and 8Hz, 16H; CH=CH₂), 5.14 (m, 4H, OCH), 4.63-4.61 (d, J=8Hz, 16H; CH₂CH=CH₂), 4.45-4.31 (m, 8H; OCH₂, branch), 3.21-3.16 (m, 4H; OCH₂, core), 3.74-3.37 (m, 8H; NCH₂); ¹³C NMR (100 MHz, CDCl₃, 25°C): δ=155.7 (NCO₂), 154.6 (OCO₂), 131.3(CH=CH₂), 119.1(CH=CH₂), 74.09(OCH), 68.80(CH₂CH=CH₂), 66.35(OCH₂, branch), 64.26(OCH₂, core), 49.31(NCH₂); IR (KBr): ν̄(cm⁻¹)=3086 (w, C-H_{stretch}, sp²), 2956 (m, C-H_{stretch}, sp³), 1753 (vs, C=O_{stretch}, carbonate), 1710 (vs, C=O_{stretch}, urethane), 1649 (w, C=C_{stretch}), 1452(m, C-H_{bend}, methylene), 1276 (vs, C-O_{stretch}, ester), 1157(m, C-O_{stretch}), 954(s, C=C_{bend}), 854 (m, C-H_{bend}, alkene); HRMS (ESI) m/z [M+Na]⁺ calcd for C₄₈H₆₄N₂O₂₈Na: 1139.3538, found: 1139.3543.

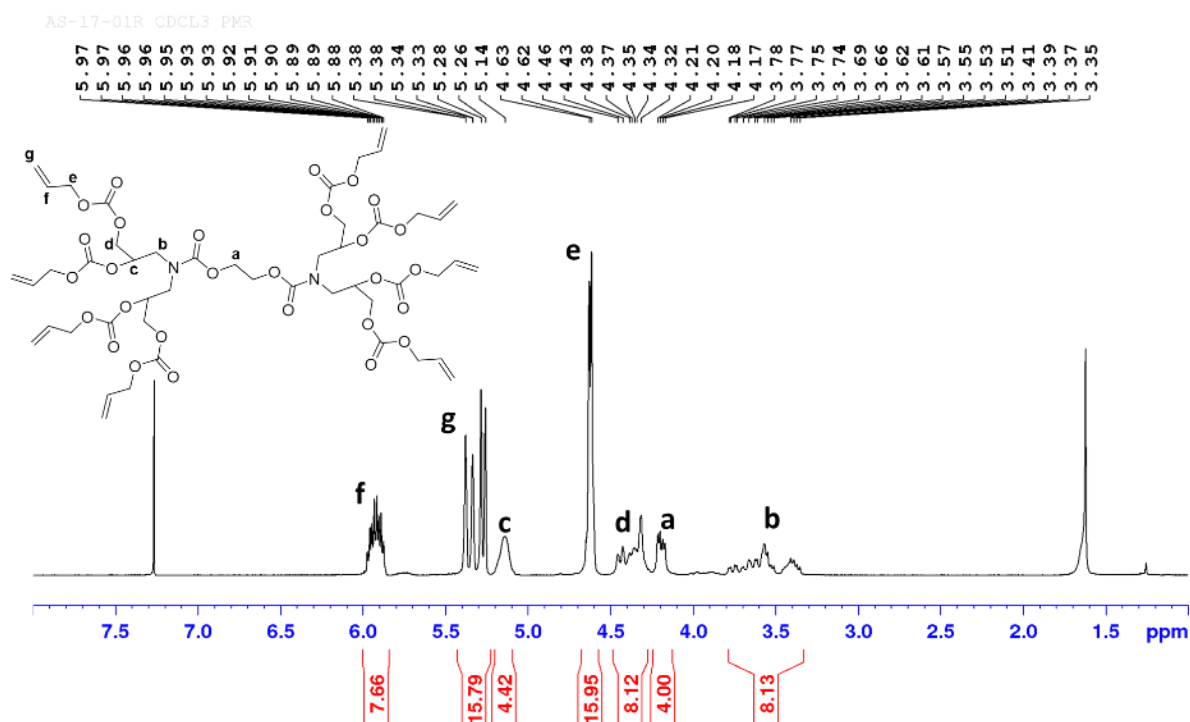


Figure 1.44 ¹H NMR spectrum of dendrimer (27) in CDCl₃.

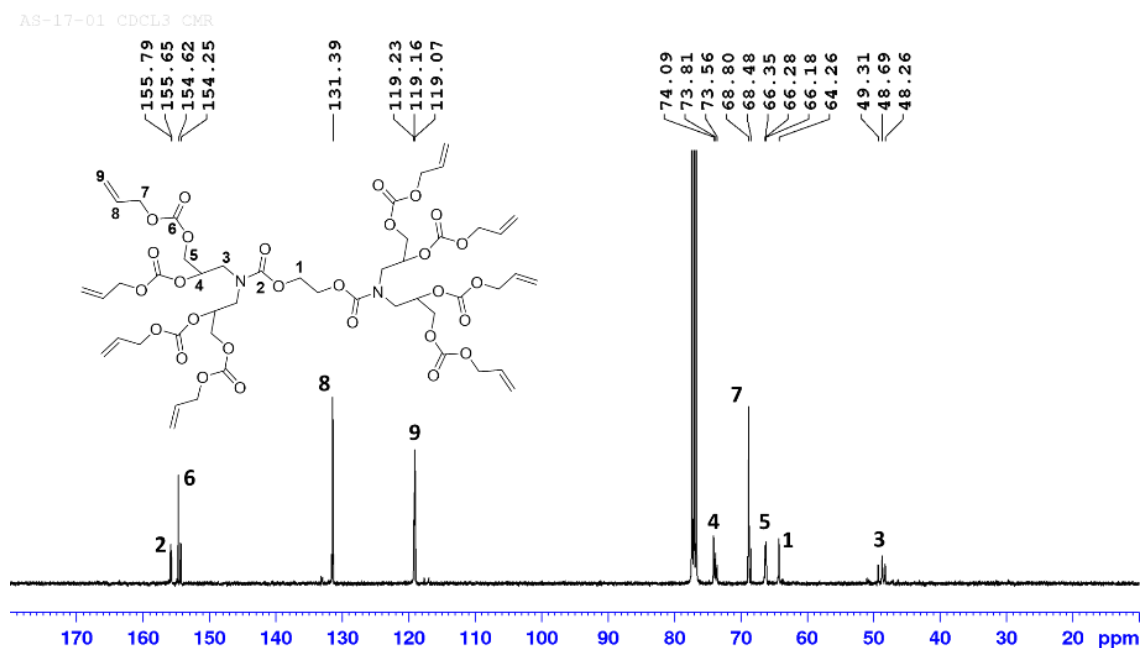


Figure 1.45 ¹³C NMR spectrum of dendrimer (27) in CDCl₃.

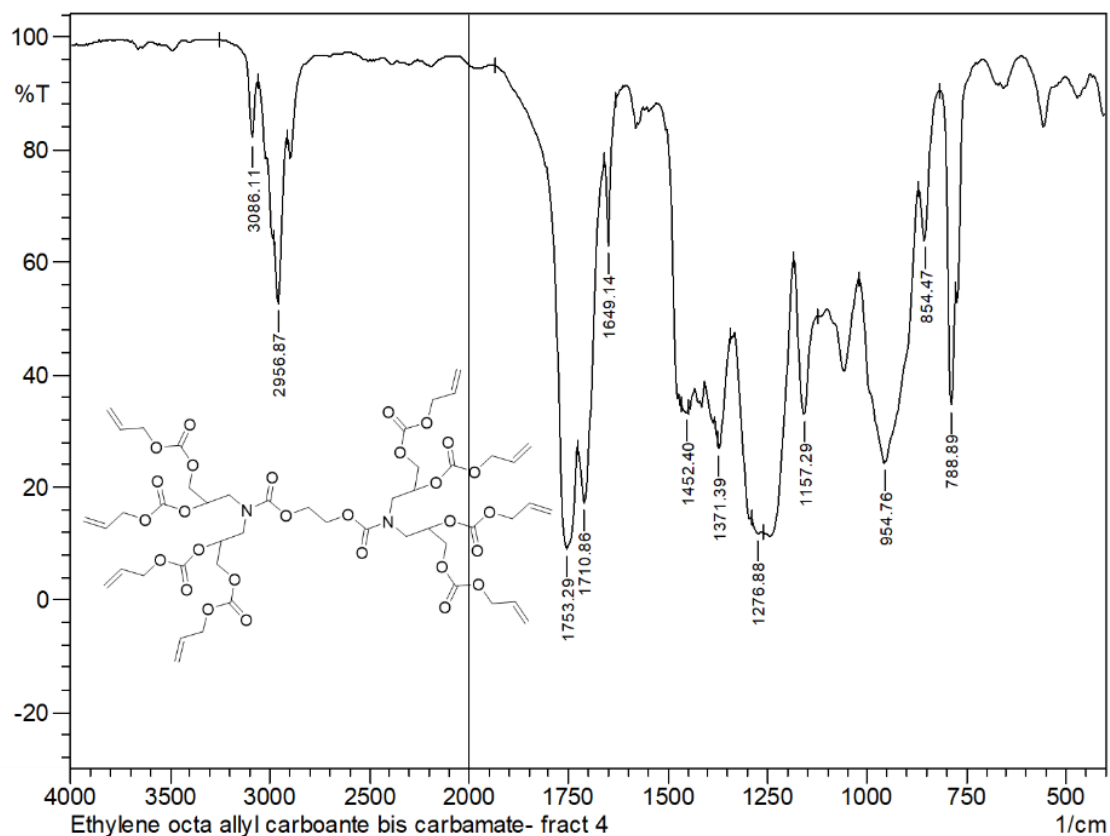


Figure 1.46 IR spectrum of dendrimer (27) in KBr.

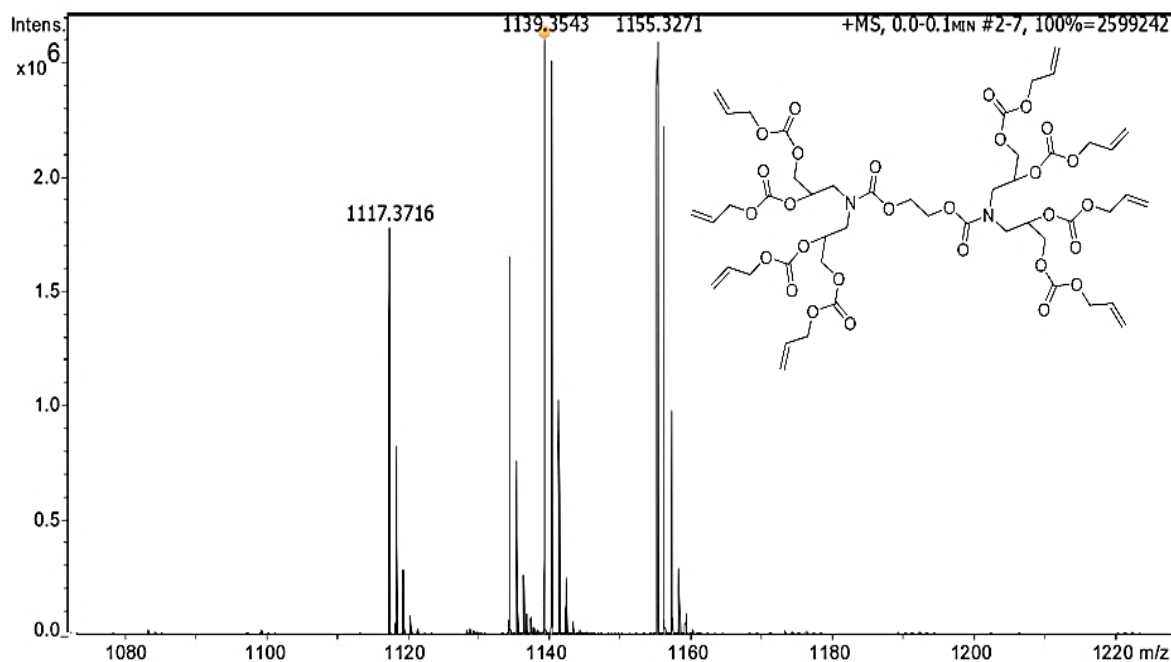


Figure 1.47 HRMS spectrum of dendrimer (27).

iii. Convergent Growth Synthesis of PU/PC dendrimers

a. Synthesis of BOC-*N*-[G-1]-(OH)₄ (29)

To a stirred solution of compound **9** (10 g, 50.7 mmol) in a water/acetone/ *t*-BuOH mixture (1:1) was added a solution of *N*-methyl morpholine *N*-oxide (NMO) (50 wt-% solution in water, 26.1 mL, 111 mmol) followed by a solution of osmium tetroxide (4wt % in water, 1.6 ml, 0.25 mmol). The mixture was stirred at room temperature for 2 h. After completion of reaction, mixture was evaporated with ethanol and toluene to obtain thick brown oil. Crude compound was subjected to silica gel chromatography to afford colorless thick oil in 91% yield. $R_f=0.5$ (CHCl₃/MeOH 9:1); ¹H NMR (400 MHz, CDCl₃, 25°C): δ=3.87 (m, 2H; HOCH), 3.53 (m, 4H; HOCH₂), 3.43-3.40 (m, 2H; CH₂N) 3.10-3.29 (m, 2H; CH₂N), 1.37 (s, 9H; CH₃); ¹³C NMR (100 MHz, CDCl₃, 25°C): δ=156.2 (C=O), 79.7 (C(CH₃)₃), 70.6 (HOCH), 63.2 (HOCH₂), 52.1 (CH₂N), 27.3 (CH₃); IR (KBr): $\tilde{\nu}(\text{cm}^{-1})=3342(\text{vs, O-H}_{\text{stretch}})$, 2974, 2931(m, C-H_{stretch}, *sp*³), 1666 (vs, C=O_{stretch}), 1479(s, C-H_{bend}, *methylene*), 1367(m, O-H_{bend}), 1234 (s, C-N_{stretch}), 1168(m, C-O_{stretch}), 1041(m, C-O_{stretch}, *alcohol*); HRMS (ESI) *m/z* [*M*+Na]⁺ calcd for C₁₁H₂₃NO₆Na: 288.1418, found: 288.1417.

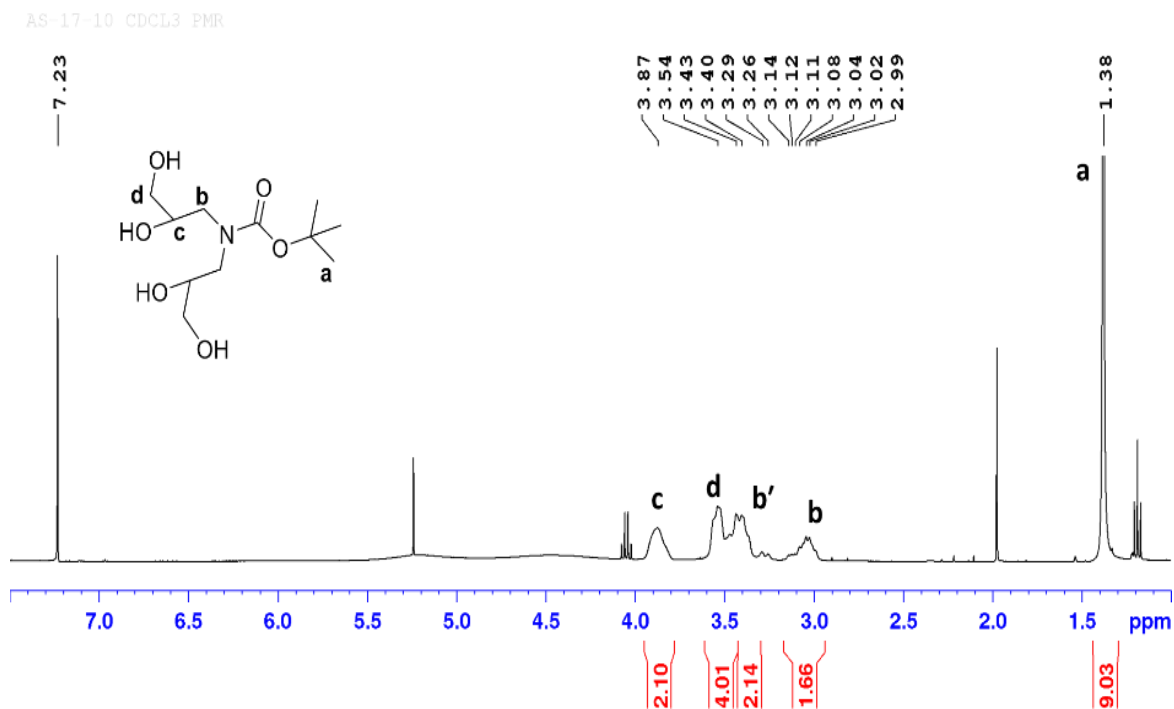


Figure 1.48 ¹H NMR spectrum of BOC-N-[G-1]-(OH)₄ (29) in CDCl₃.

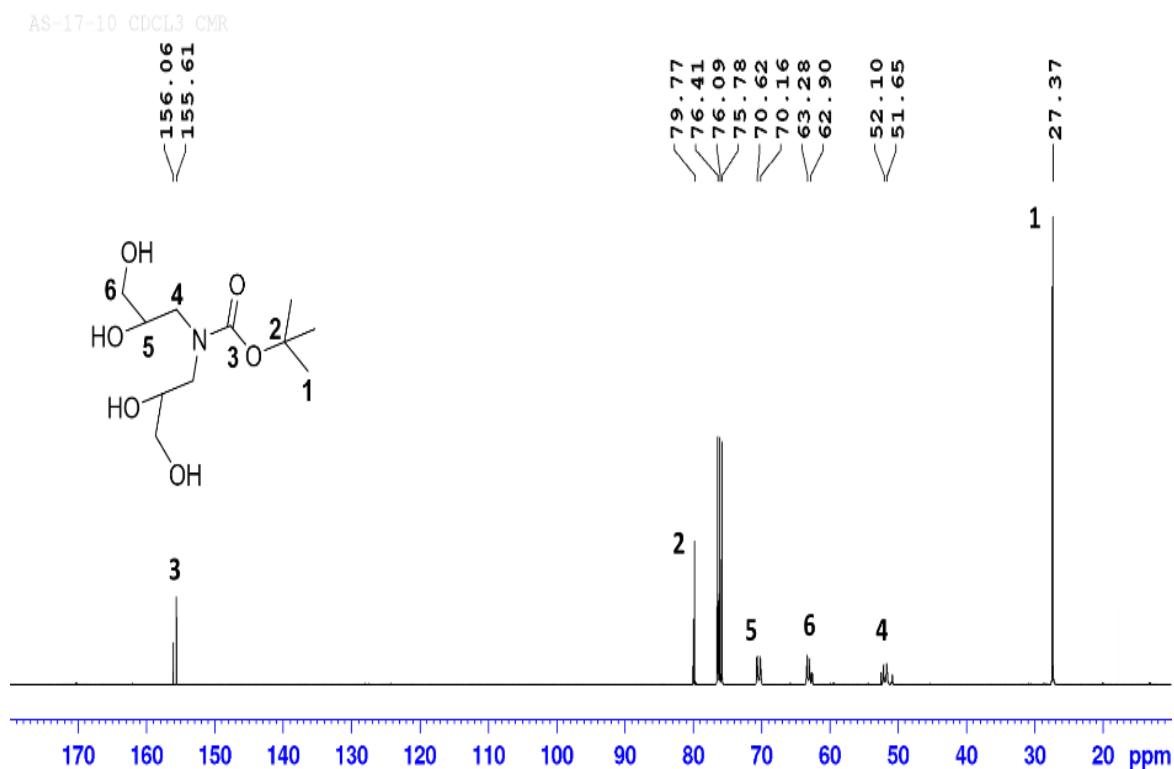


Figure 1.49 ¹³C NMR spectrum of BOC-N-[G-1]-(OH)₄ (29) in CDCl₃.

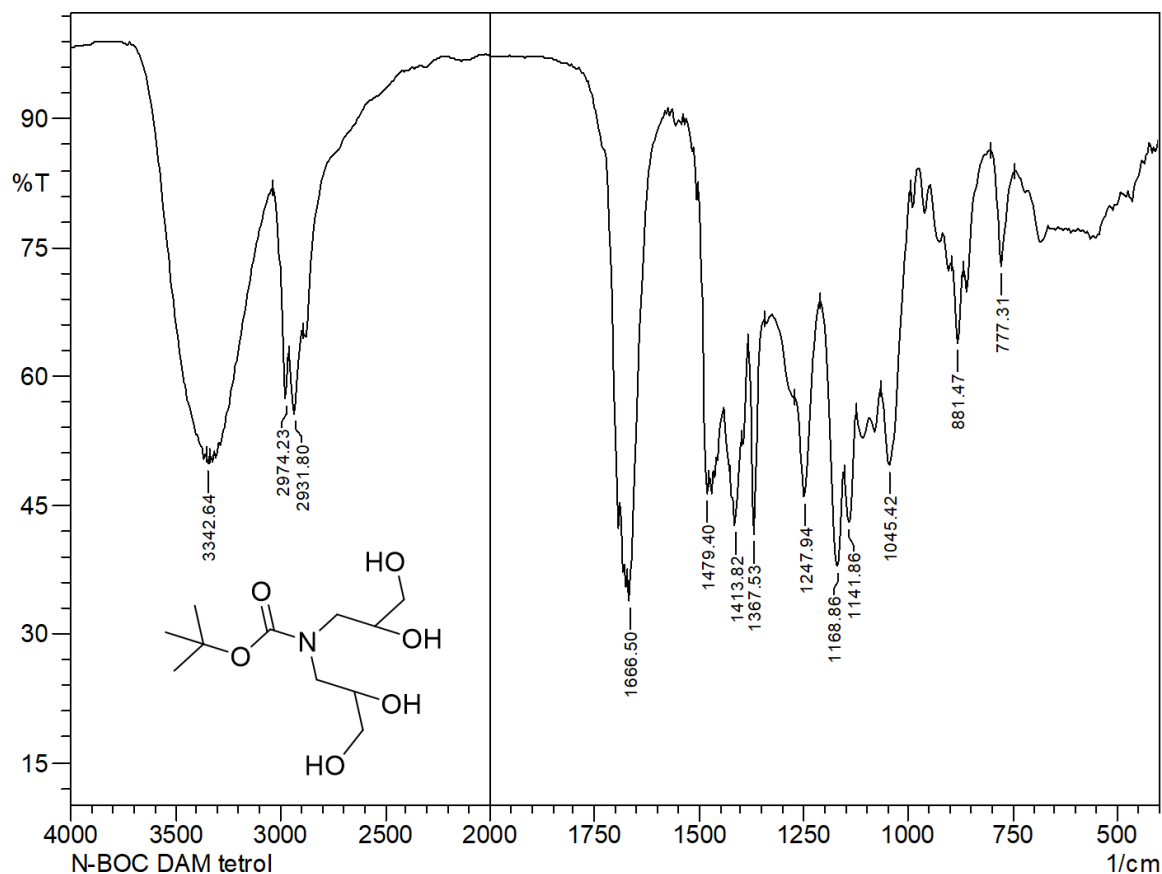


Figure 1.50 IR spectrum of BOC-*N*-[G-1]-(OH)₄ (**29**) in KBr.

b. Synthesis of BOC-*N*-[G-1.5]-(allyl)_n dendrons via perallylation of **29**

BOC-*N*-[G-1.5]-(allyl)₈ (31**):** To a vigorously stirred homogenous mixture of tetrol **29** (5 g, 18.8 mmol) and *N,N*-carbonyl chloride (18 g, 113 mmol) in THF (60 mL) was added NaH (60% in mineral oil, 3.77 g, 94 mmol) in portions at 0°C. After stirring for 1h at same temperature, reaction vessel was gradually warmed to room temperature and continued stirring for 3 h. Later, THF evaporated and mixture extracted with diethyl ether. Organic layer washed with H₂O, brine solution and dried over anhy. MgSO₄. The crude brown oil was subjected to silica gel chromatography to provide pale yellow thick liquid in 92% yield. R_f=0.6 (hexane/ethyl acetate 7:3); ¹H NMR (400 MHz, CDCl₃, 25 °C): δ=5.69-5.64 (m, 8H; CH=CH₂), 5.09-5.04 (m, 16H; CH=CH₂), 5.02 (m, 2H; OCH), 4.24-4.20 (m, 2H; OCH₂), 4.07-3.98 (m, 2H; OCH₂), 3.80-3.6 (m, 16H; NCH₂, terminal), 3.45-3.27 (m, 4H; NCH₂, branch), 1.38 (s, 9H; CH₃); ¹³C NMR (100 MHz, CDCl₃, 25°C): δ=154.5 (C=O, terminal), 153.9(C=O, BOC), 132.3 (CH=CH₂), 116.3 (CH=CH₂), 79.6 (C(CH₃)₃), 70.3 (OCH), 63.9 (OCH₂), 48.04 (NCH₂, terminal), 46.77 (NCH₂, branch), 27.2 (CH₃); IR (KBr): ν̄(cm⁻¹)=3080 (w, C-H_{stretch}, sp²), 2980 (m, C-H_{stretch}, sp³), 1712,1693 (vs, C=O_{stretch}, urethane),

1643 (w, C=C_{stretch}), 1462(s,C-H_{bend}, *methylene*),1234 (s, C-N_{stretch}), 1151(m, C-O_{stretch}),993(m, C=C_{bend}), 925 (m, C-H_{bend}, *alkene*); HRMS (ESI) m/z $[M+Na]^+$ calcd for C₃₉H₅₉N₅O₁₀Na: 780.4154, found: 780.4154.

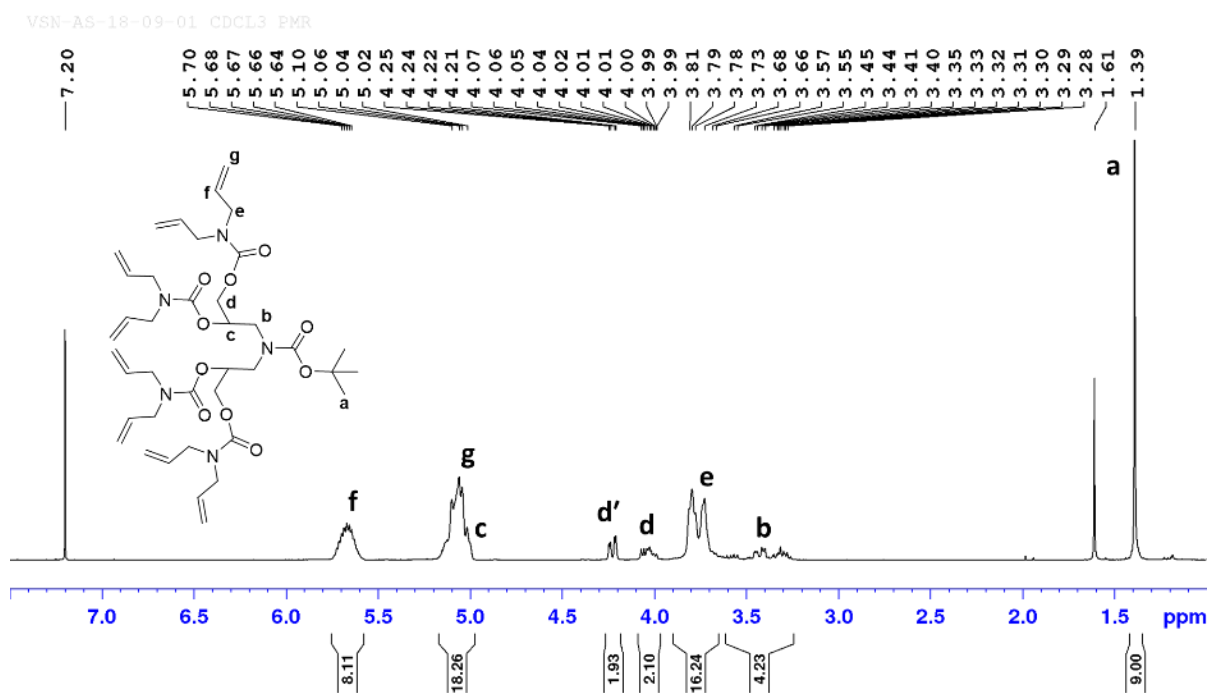


Figure 1.51 ¹H NMR spectrum of dendron (**31**) in CDCl₃.

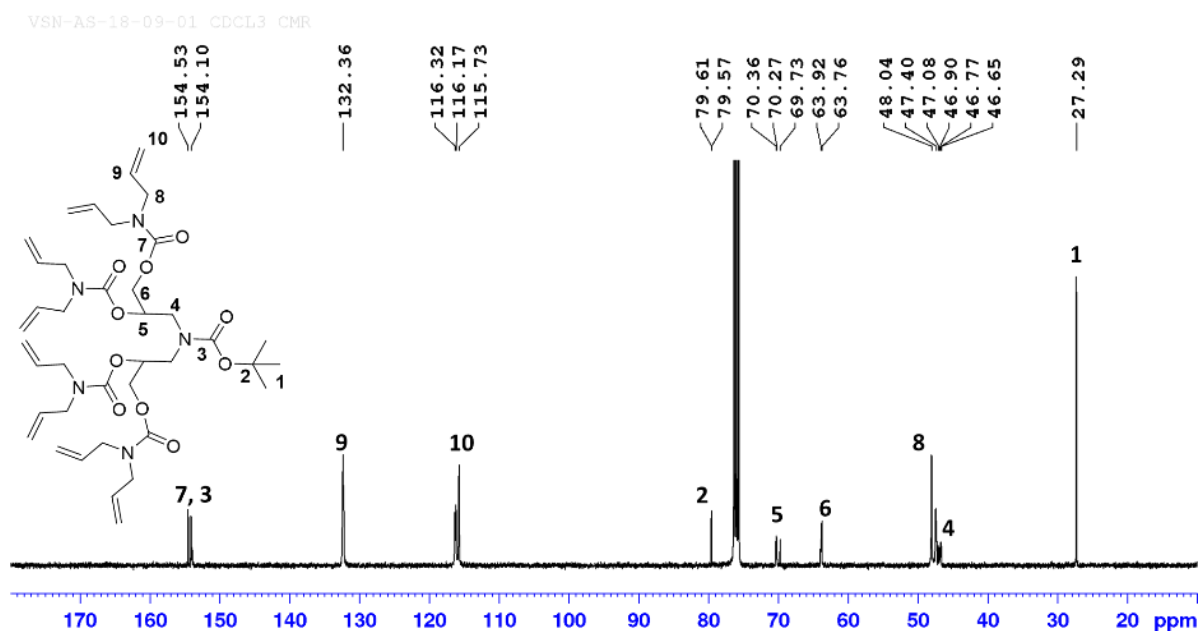


Figure 1.52 ¹³C NMR spectrum of dendron (**31**) in CDCl₃.

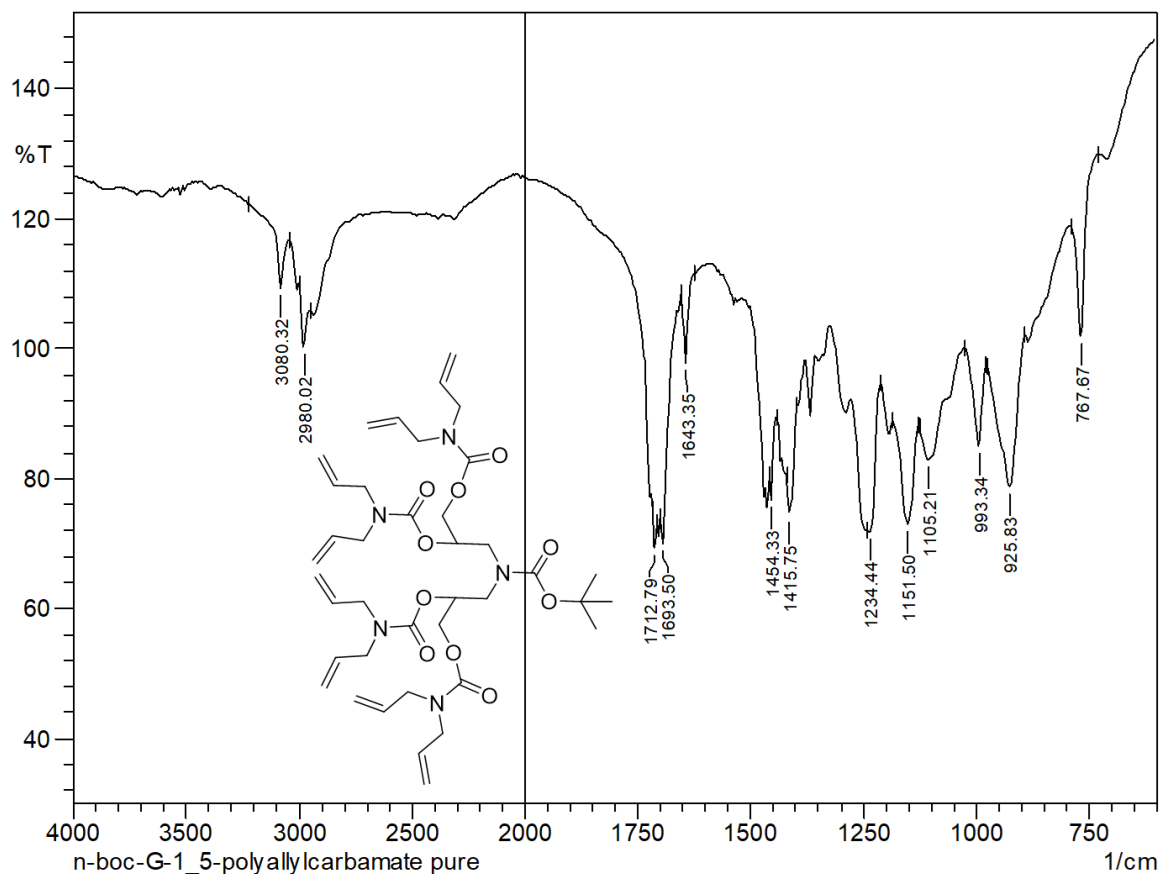


Figure 1.53 IR spectrum of dendron (**31**) in KBr.

BOC-N-[G-1.5]-(allyl)₄ (33**):** Reaction flask with drying tube and addition funnel, was charged with dilute solution of tetrol (5 g, 18.8 mmol) **29** and pyridine (8.92 g, 112 mmol) in THF. To a stirred solution, allyl chloroformate was added dropwise over a period 30 min at 0°C. Mixture was slowly warm to room temperature and continued stirring for 5 h. After completion of reaction, solvent was evaporated and residue was neutralized with dil. HCl solution and extracted with diethyl ether. Organic layer was washed with water, brine solution and dried over anhy. MgSO₄. The crude yellow liquid was purified by silica gel chromatography to provide colourless liquid in 86% yield. R_f = 0.7 (hexane/ethyl acetate 7:3); ¹H NMR (400 MHz, CDCl₃, 25°C): δ = 5.90-5.80 (m, 4H; CH=CH₂), 5.31-5.19 (dd, J = 16 Hz and 8 Hz, 8H; CH=CH₂), 5.06 (m, 2H; OCH), 4.52-4.51 (m, 8H; CH₂CH=CH₂), 4.36-4.29 (m, 2H; OCH₂), 4.1-4.07 (m, 2H; OCH₂), 3.60-3.25 (m, 1H; NCH₂), 1.39 (m, 9H; CH₃); ¹³C NMR (100 MHz, CDCl₃, 25°C): δ = 155.0 (NCO₂), 154.2 (OCO₂), 131.3 (CH=CH₂), 118.9 (CH=CH₂), 81.10 (C(CH₃)₃), 74.13 (OCH), 68.66 (CH₂CH=CH₂), 66.35 (OCH₂), 48.8 (NCH₂), 28.1 (CH₃); IR (KBr): ν̄ (cm⁻¹) = 3088 (w, C-H_{stretch}, sp²), 2978 (m, C-H_{stretch}, sp³), 1753 (vs, C=O_{stretch}, carbonate), 1703 (vs, C=O_{stretch}, urethane), 1649 (w,

C=C_{stretch}), 1454(m, C-H_{bend}, *methylene*), 1240 (vs, C-O_{stretch}, *ester*), 1155(m, C-O_{stretch}), 954(s, C=C_{bend}); HRMS (ESI) m/z $[M+Na]^+$ calcd for C₂₇H₃₉NO₁₄Na: 624.2263; found: 624.2263.

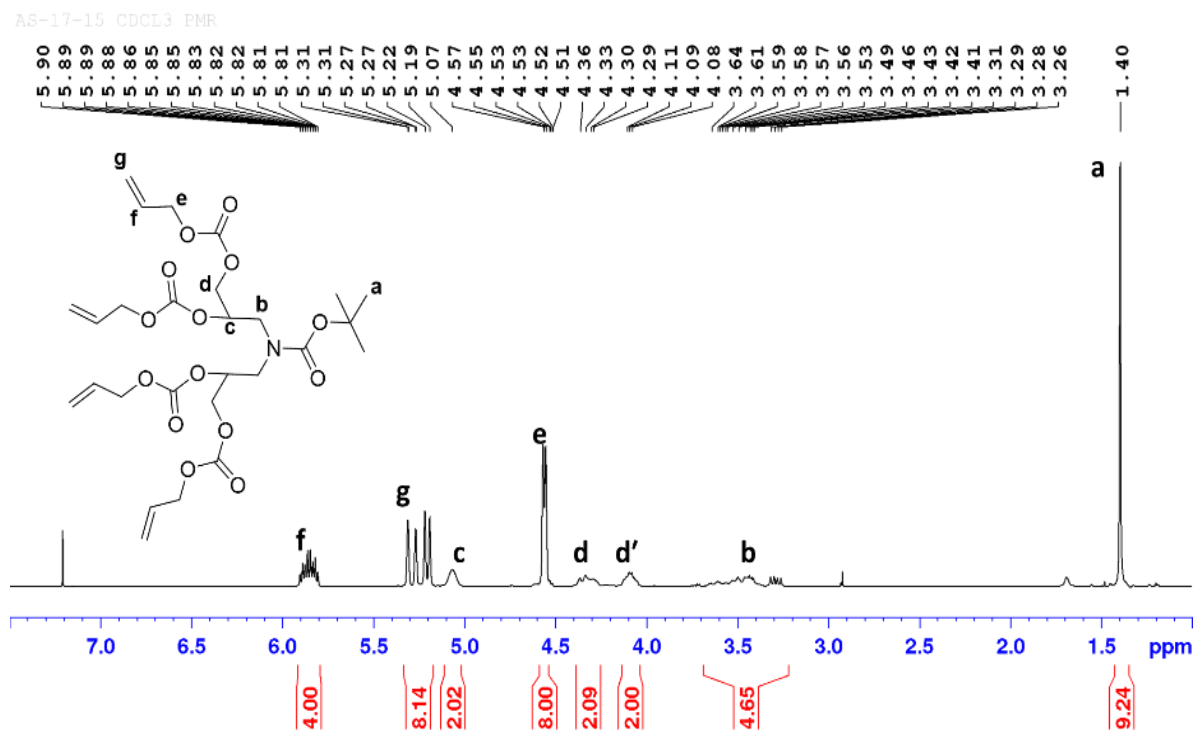


Figure 1.54 ¹H NMR spectrum of dendron (33) in CDCl₃.

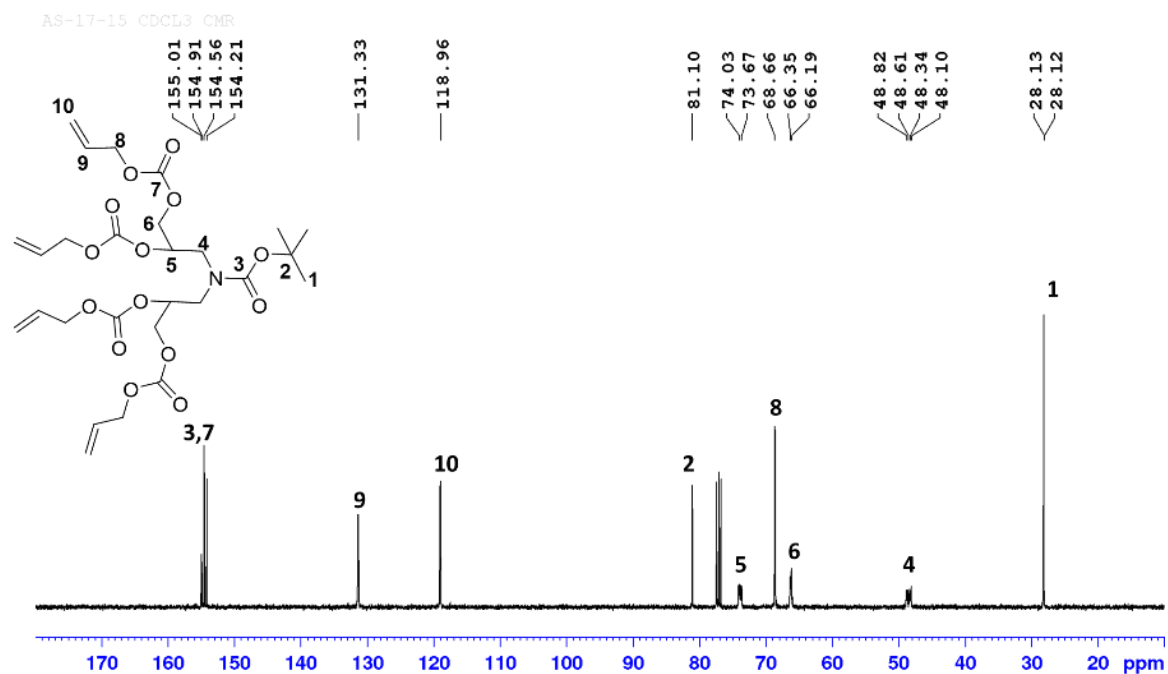


Figure 1.55 ¹³C NMR spectrum of dendron (33) in CDCl₃.

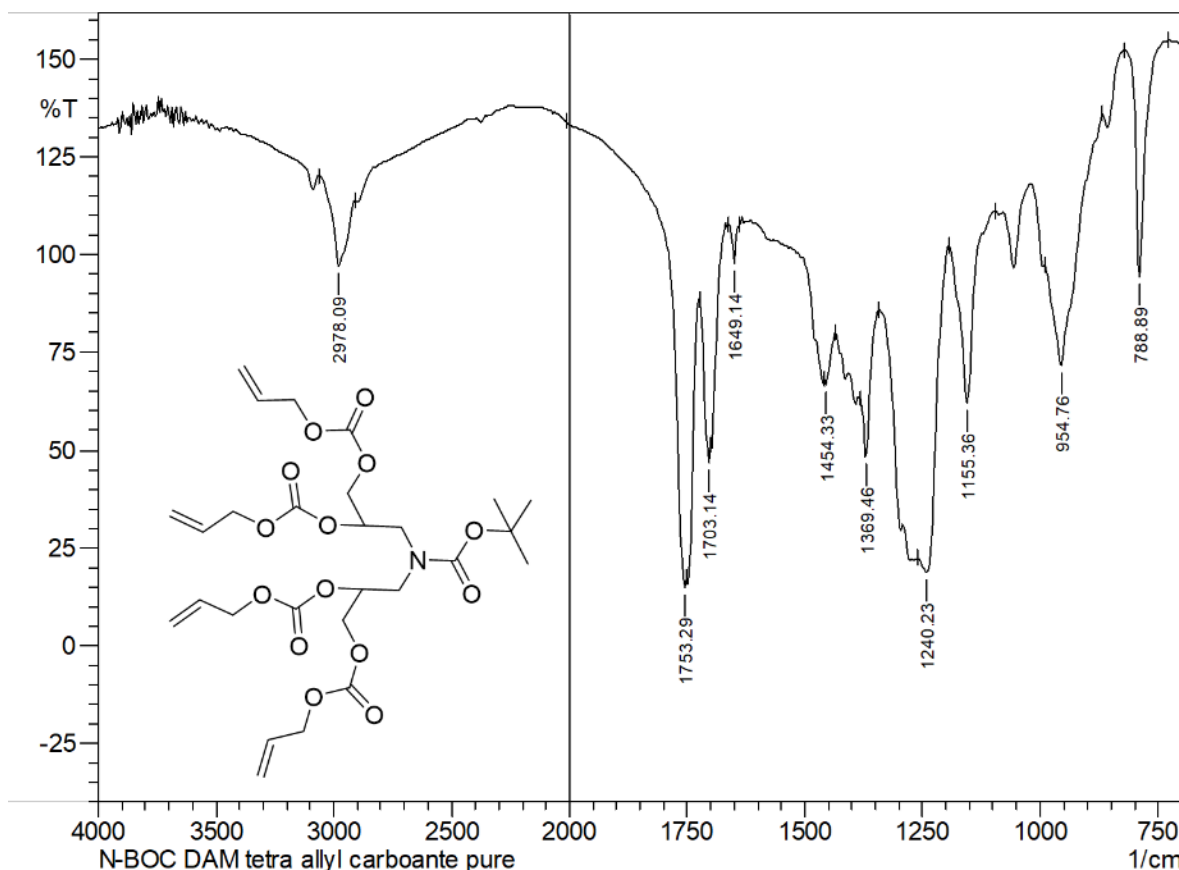


Figure 1.56 IR spectrum of dendron (**33**) in KBr.

c. Synthesis of HN-[G-1.5]-(allyl)_n dendrons via deprotection of *N*-BOC group

To a stirring solution of BOC-*N*-[G-1.5]-(allyl)_n (5 g, 1 equiv.) in dichloromethane (50 mL) was added trifluoroacetic (5 equiv.) acid slowly at room temperature. Mixture was stirred over a period of 3 h. After completion of reaction, solvent was evaporated and crude brown oil was neutralized with sat. NaHCO₃ solution. Resulting mixture was extracted twice with ethyl acetate using phase separator. Combined organic layer was washed with water, brine and dried over anhyd. MgSO₄. Crude brown oil was subjected to silica gel chromatography to yield pure compound as yellow liquid.

Dendron 32: 85%, *R_f*=0.6 (hexane/ethyl acetate 2:8); ¹H NMR (400 MHz, CDCl₃, 25°C): δ= 5.79-5.71 (m, 8H; CH=CH₂), 5.17-5.07 (m, 16H; CH=CH₂), 5.05-5.01 (m, 2H; OCH), 4.32-4.28 (m, 2H; OCH₂), 4.23-4.18 (m, 2H; OCH₂), 3.88-3.78 (m, 16H; NCH₂, terminal), 2.89-2.76 (m, 4H; NCH₂, branch); ¹³C NMR (100 MHz, CDCl₃, 25°C): δ=155.7, 155.4 (C=O), 133.5 (CH=CH₂), 117.3 (CH=CH₂), 72.29 (OCH), 64.98 (OCH₂), 49.5 (NCH₂, terminal), 48.5 (NCH₂, branch); IR (KBr): ν̃(cm⁻¹)=3479 (m, N-H_{stretch}), 3080 (m, C-H_{stretch}, sp²), 2981 (m, C-H_{stretch}, sp³), 1703 (vs, C=O_{stretch}), 1643 (w, C=C_{stretch}), 1462(s, C-

H_{bend} , methylene), 1247 (s, C-N_{stretch}), 1155(m, C-O_{stretch}), 995(m, C=C_{bend}), 925 (m, C-H_{bend}, alkene); HRMS (ESI) m/z $[M+H]^+$ calcd for C₃₄H₅₂N₅O₈: 658.3810; found, $[M+H]^+$ 658.3806.

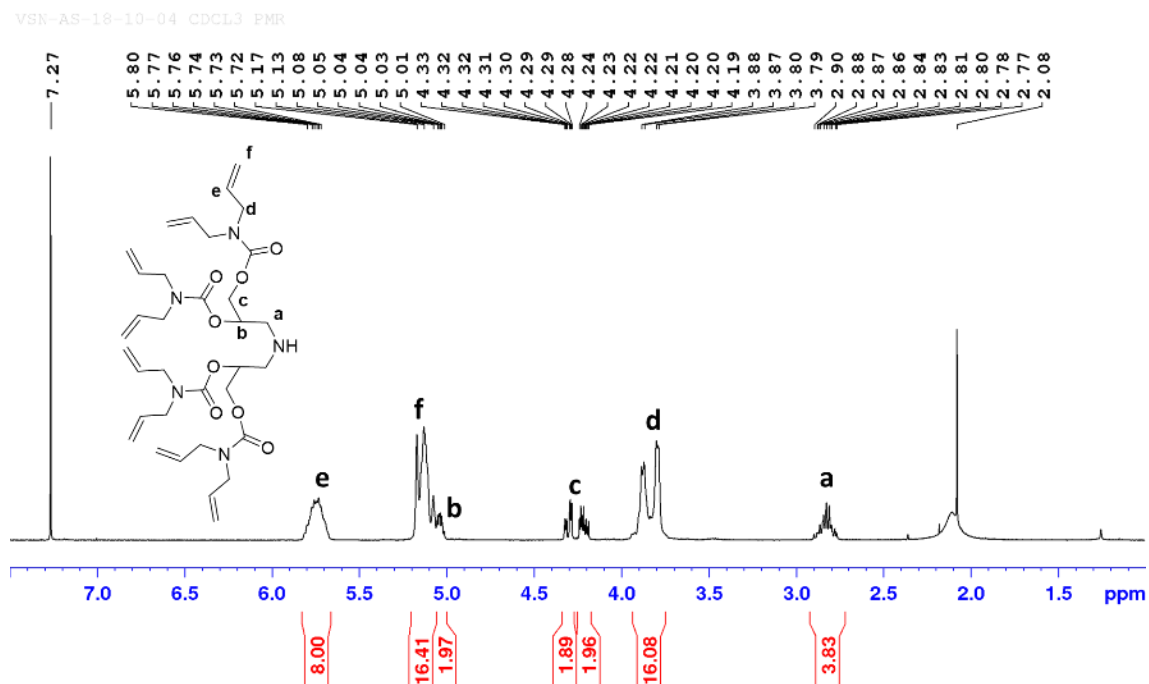


Figure 1.57 ¹H NMR spectrum of dendron (32) in CDCl₃.

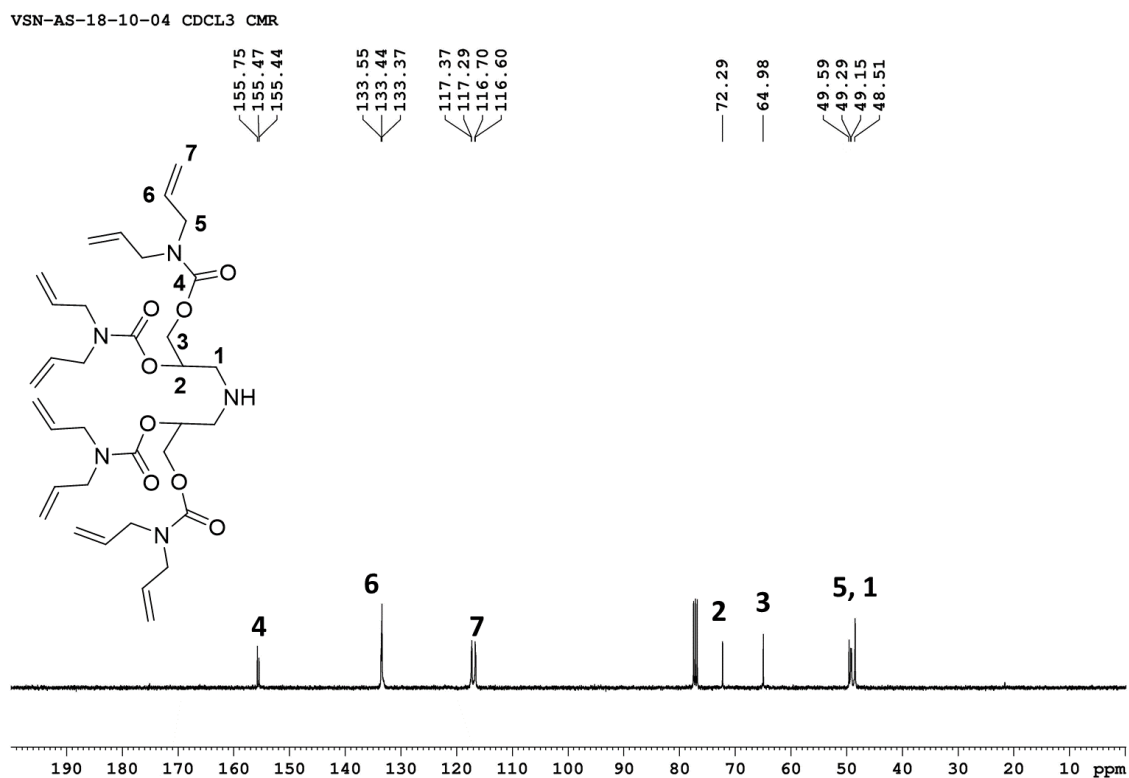


Figure 1.58 ¹³C NMR spectrum of dendron (32) in CDCl₃.

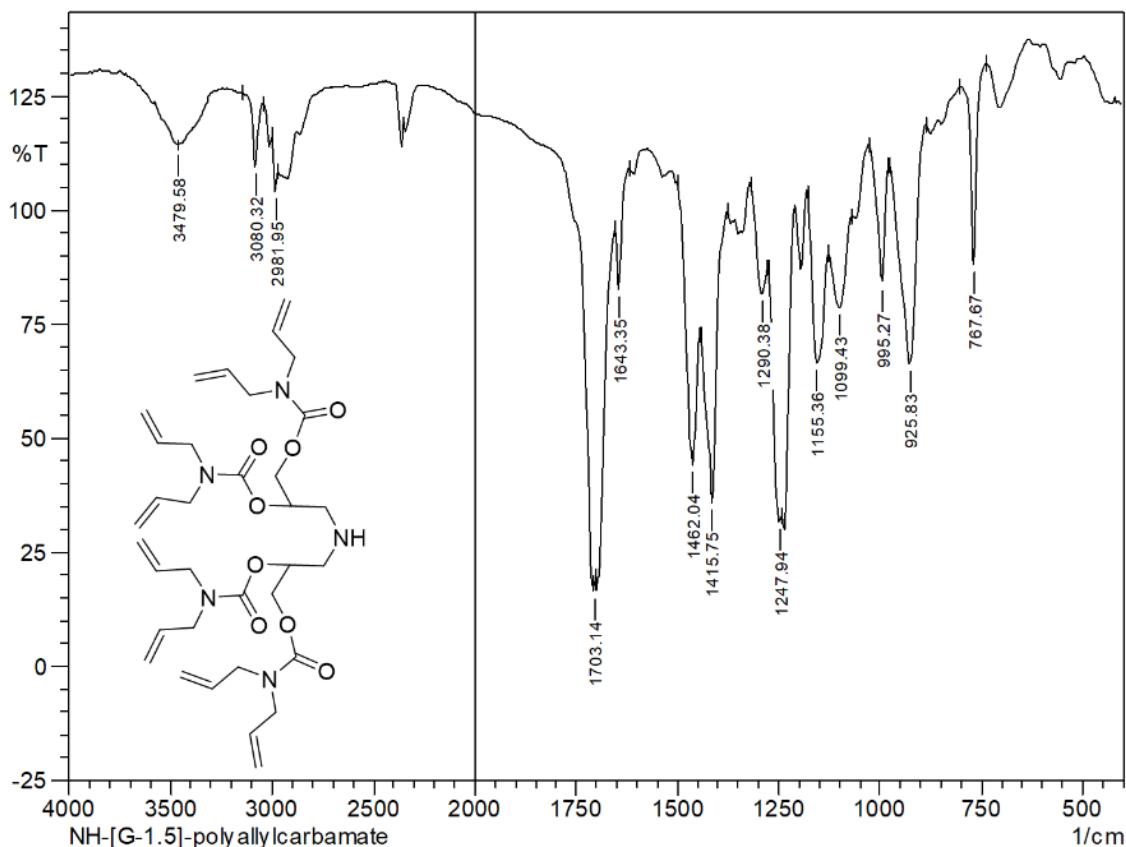


Figure 1.59 IR spectrum of dendron (**32**) in KBr.

Dendron 34: 88%, $R_f=0.7$ (hexane/ethyl acetate 3:7); ^1H NMR (400 MHz, CDCl_3 , 25°C): $\delta=5.97\text{-}5.87$ (m, 4H; $\text{CH}=\text{CH}_2$), $5.39\text{-}5.22$ (dd, $J=16$ Hz and 8Hz, 8H; $\text{CH}=\text{CH}$ dd, $J=16$ Hz and 8Hz, 8H; $\text{CH}=\text{CH}$ dd, $J=16$ Hz and 8Hz, 8H; $\text{CH}=\text{CH}$ dd, $J=16$ Hz and 8Hz, 8H; $\text{CH}=\text{CH}$), 5.15 (m, 2H; OCH), $4.64\text{-}4.6$ (m, 8H; $\text{CH}_2\text{CH}=\text{CH}_2$), $4.19\text{-}4.10$ (m, 4H; OCH_2), $3.55\text{-}3.30$ (m, 4H; NCH_2); ^{13}C NMR (100 MHz, CDCl_3 , 25°C): $\delta=154.9$, 154.6 ($\text{C}=\text{O}$), 131.2 ($\text{CH}=\text{CH}_2$), 119.2 ($\text{CH}=\text{CH}_2$), 73.9 (OCH), 68.8 ($\text{CH}_2\text{CH}=\text{CH}_2$), 66.9 , 66.1 (OCH_2), 52.5 , 48.8 (NCH_2); IR (KBr): $\tilde{\nu}(\text{cm}^{-1})=3477$ (m, $\text{N-H}_{\text{stretch}}$), 3080 (w, $\text{C-H}_{\text{stretch}}$, sp^2), 2954 (m, $\text{C-H}_{\text{stretch}}$, sp^3), 1753 (vs, $\text{C}=\text{O}_{\text{stretch}}$), 1649 (w, $\text{C}=\text{C}_{\text{stretch}}$), 1454 (w, C-H_{bend} , *methylene*), 1242 (vs, $\text{C-O}_{\text{stretch}}$ (*ester*)), 1155 (m, $\text{C-O}_{\text{stretch}}$), 954 (s, C-H_{bend} , *alkene*); HRMS (ESI) m/z $[M+\text{H}]^+$ calcd for $\text{C}_{22}\text{H}_{31}\text{NO}_{12}\text{Na}$: 524.1738 ; found: 524.1737 .

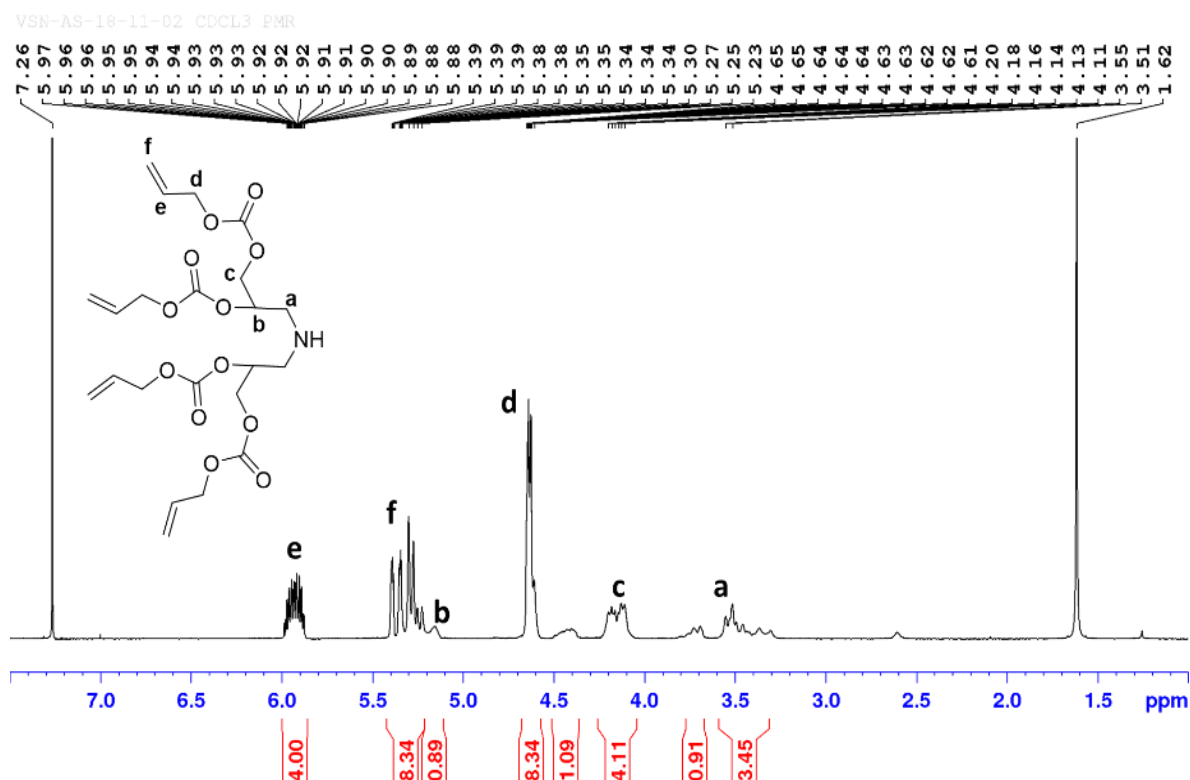


Figure 1.60 ¹H NMR spectrum of dendron (34) in CDCl₃.

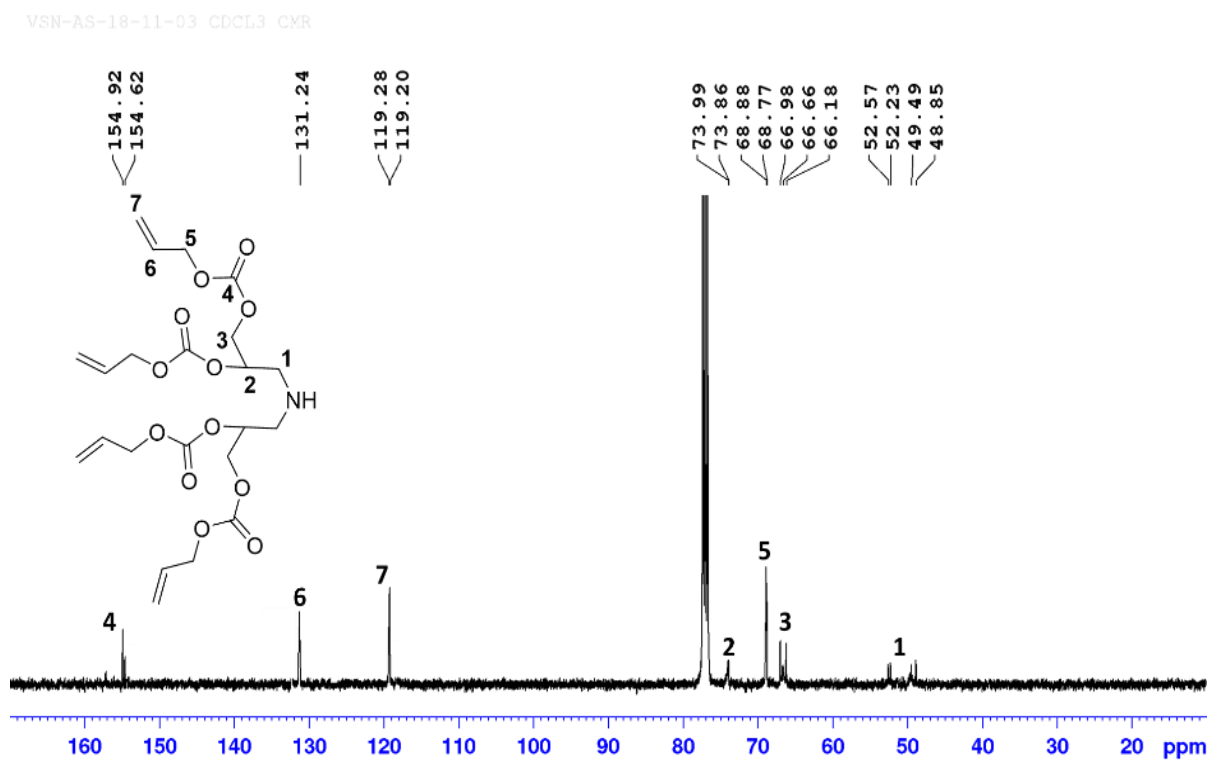


Figure 1.61 ¹³C NMR spectrum of dendron (34) in CDCl₃.

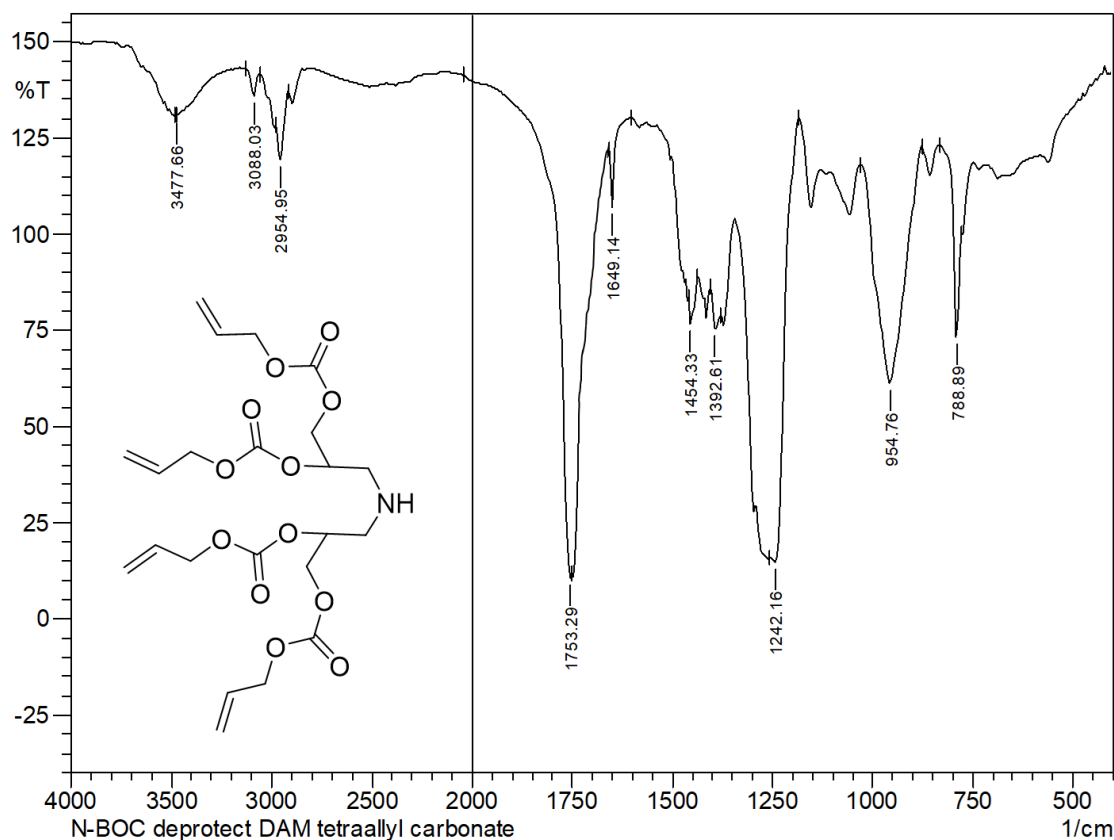


Figure 1.62 IR spectrum of dendron (**34**) in KBr.

d. Synthesis of EG-[G-1.5]-(allyl)_n dendrimers from dendrons (**32**) and (**34**)

Reaction vessel with drying tube and dropping funnel, was charged with solution of dendron HN-[G-1.5]-(allyl)_n (2.2 equiv.), triethyl amine (2.5 equiv.) and cat. DMAP in dichloromethane (30 mL). To a stirring solution, ethylene bis(chloroformate) (2 g, 10.7 mmol, 1 equiv.) in dichloromethane (5 mL) was added dropwise over a period of 10 min at 0°C. After complete addition, mixture was warmed to room temperature and stirring continued for 6-9 h. Later mixture was diluted with dichloromethane and washed twice with H₂O, brine solution and dried over anhy. MgSO₄. After evaporation of solvent, obtained crude was purified over column chromatography to afford pure product in good 80% yield.

V. Synthesis of carbonate and urethane linked polyacetate dendrimers

i. General procedure for diacetoxylation of alkenes^[107]

To a solution of alkene (1 equiv.) and (diacetoxyiodo) benzene (1.2 equiv. per alkene) in acetic acid and acetic anhydride (2 equiv. per alkene) BF₃.OEt₂ was added at room temperature. Reaction mixture was stirred for 16 h and monitored using TLC. After completion, reaction was quenched by adding sodium acetate with stirring for more 15 min.

Reaction mixture concentrated on vacuum to distil out acetic acid. Remaining residue was purified by silica gel chromatography.

ii. [G-0.5] Ethylene tetra (2,3-diacetoxypropyl) bis carbamate (35) or EG-[G-0.5]-OAc

Ethylene bis (diallyl carbamate) (0.5g, 1.6 mmol), (diacetoxyiodo) benzene (2.1 g, 6.5 mmol), acetic anhydride (1.3 g, 12.8 mmol), glacial acetic acid (10 mL), $\text{BF}_3 \cdot \text{OEt}_2$ (1.6 mmol). Isolated as colourless pale yellow viscous liquid in 65% yield. $R_f=0.6$ (pet. ether/ethyl acetate 3:7); $^1\text{H NMR}$ (400 MHz, CDCl_3 , 25°C): δ (ppm) = 5.27–5.21 (m, 4H; AcOCH), 4.32–4.27 (4H; NCO_2CH_2), 4.25–4.09 (m, 8H; CH_2OAc), 3.68–3.48 (m, 8H; NCH_2), 2.11–2.09 (24H; CH_3); $^{13}\text{C NMR}$ (100 MHz, CDCl_3 , 25°C): δ = 170.56(OCO), 157.43(OCO₂), 70.64, 64.05(NCO_2CH_2), 62.87(CH_2OAc), 44.99(NCH_2), 20.94(CH_3); IR (KBr): $\nu(\text{cm}^{-1})$ = 2954(w, C-H_{stretch}, sp^3), 1745 (vs, C=O_{stretch}, acetate), 1732(vs, C=O_{stretch}, urethane), 1444(w, C-H_{bend}, methylene), 1232 (vs, C-O_{stretch}, ester), 1047 (s, C-O_{stretch}); LCMS (ESI) m/z : $[M+\text{Na}]^+ = 803.13$.

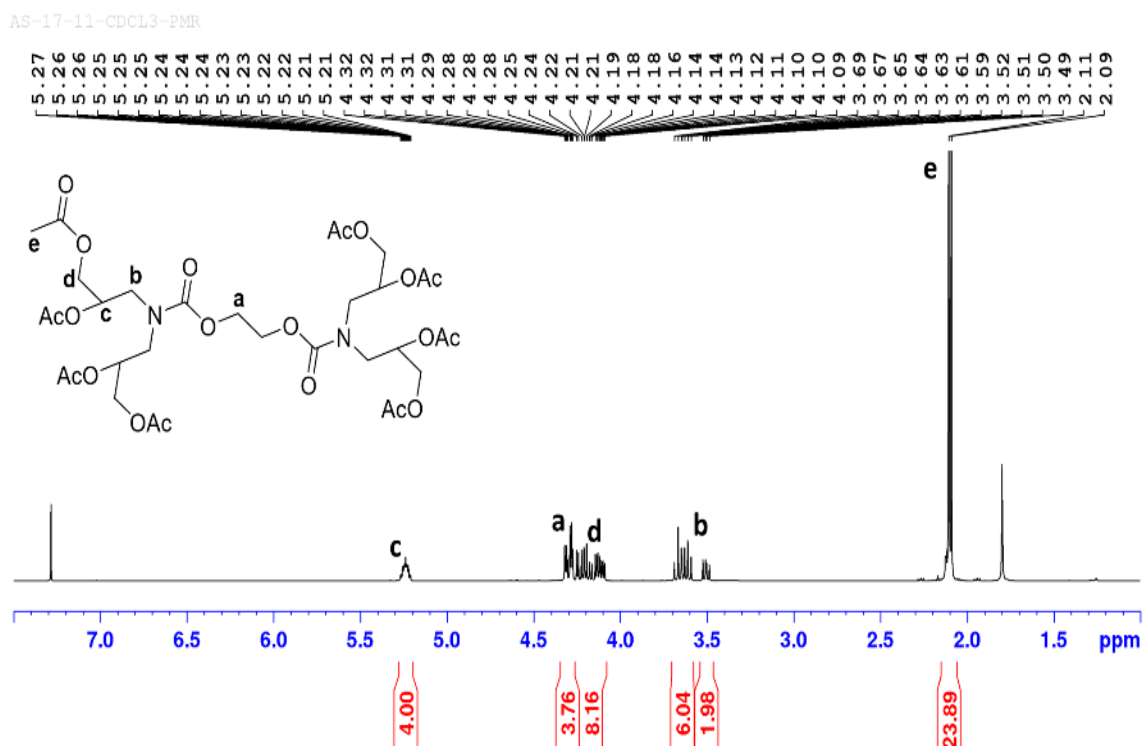


Figure 1.63 $^1\text{H NMR}$ spectrum of dendrimer (35) in CDCl_3 .

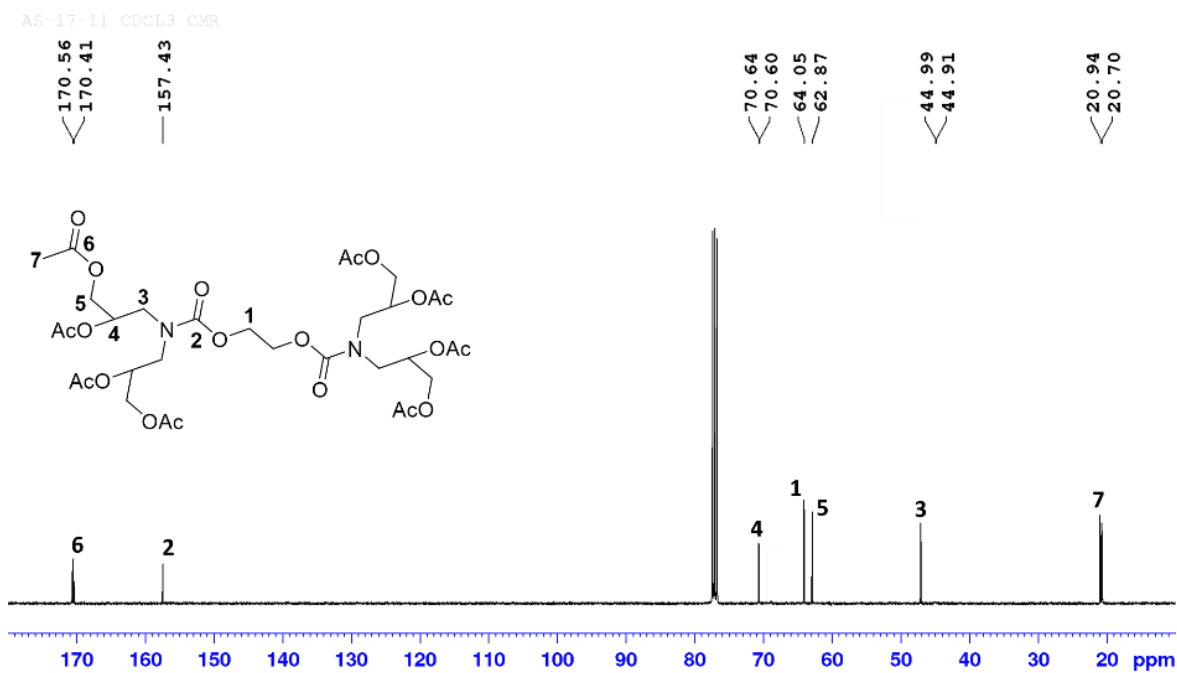


Figure 1.64 ¹³C NMR spectrum of dendrimer (35) in CDCl₃.

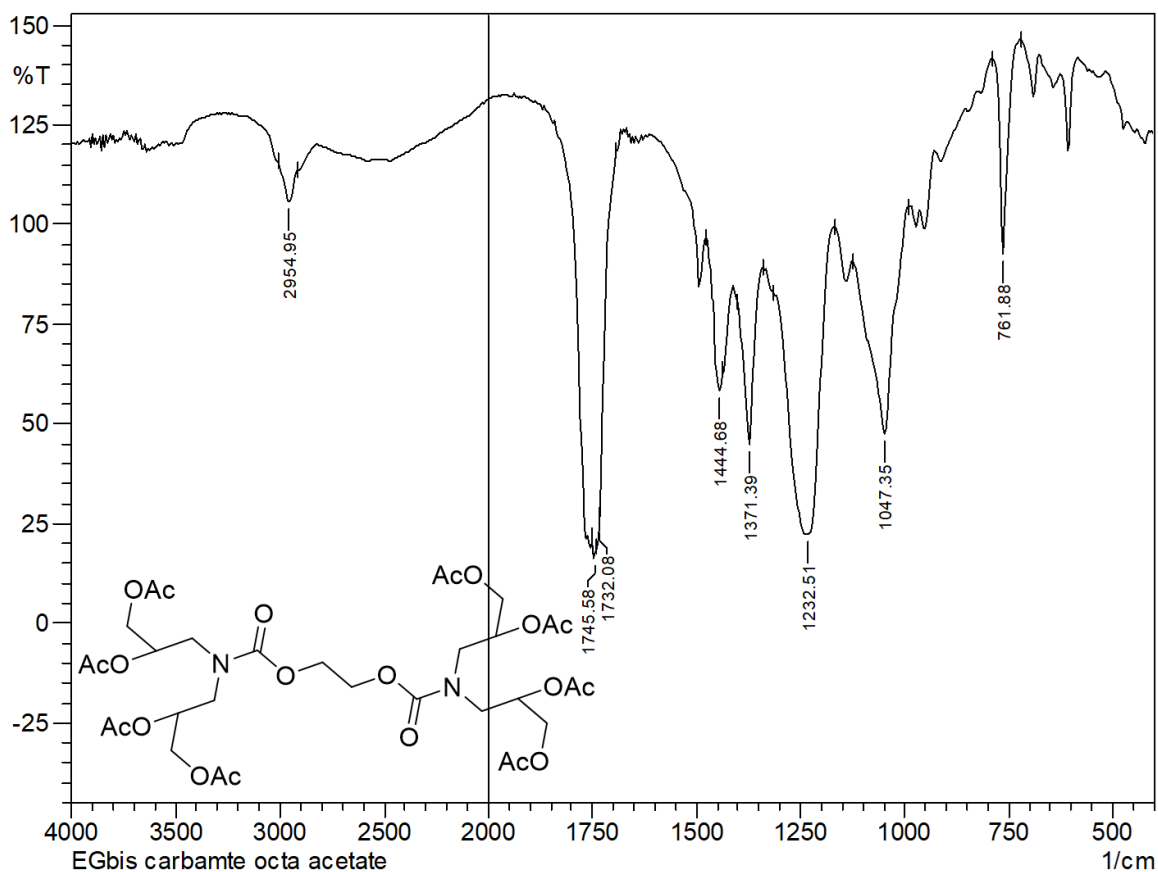


Figure 1.65 IR spectrum of dendrimer (35) in KBr.

iii. [G-0.5] Pentaerythrityl tetra ((2,3-diacetoxypropyl) carbonate) (36) or PEr-[G-0.5]-(1,2)-OAc₈

Pentaerythrityl tetrakis(allyl carbonate) (0.5 g, 1.1 mmol), (diacetoxyiodo) benzene (1.5 g, 4.7 mmol), acetic anhydride (0.86 g, 8.8 mmol), glacial acetic acid (10 mL), BF₃.OEt₂ (1.1 mmol). Isolated as colorless viscous liquid in 51% yield. R_f=0.7 (pet. ether/ethyl acetate 3:7); ¹H NMR (400 MHz, CDCl₃, 25°C): δ (ppm) = 5.28-5.23 (m, 4H; CHOAc), 4.38-4.30 (m, 8H; CH₂OCO₂), 4.25(s, 8H; OCO₂CH₂), 4.22-4.15(m, 8H; AcOCH₂), 2.11(s, 24H; CH₃); ¹³C NMR (100 MHz, CDCl₃, 25°C): δ=170.45(OCO),154.30(OCO₂), 68.75(HCOAc), 66.06(CH₂OCO₂), 65.18(OCO₂CH₂), 61.98(CH₂OAc), 42.77(C(CH₂)₄), 20.86, 20.67(CH₃); IR (KBr): ν̃(cm⁻¹)=2966(w, C-H_{stretch}, sp³), 1768 (vs, C=O_{stretch},carbonate), 1745(vs, C=O_{stretch},acetate), 1444(w,C-H_{bend},methylene), 1249 (vs, C-O_{stretch}, ester), 1097, 1047 (s, C-O_{stretch}); LCMS (ESI) m/z: [M+Na]⁺ = 967.31.

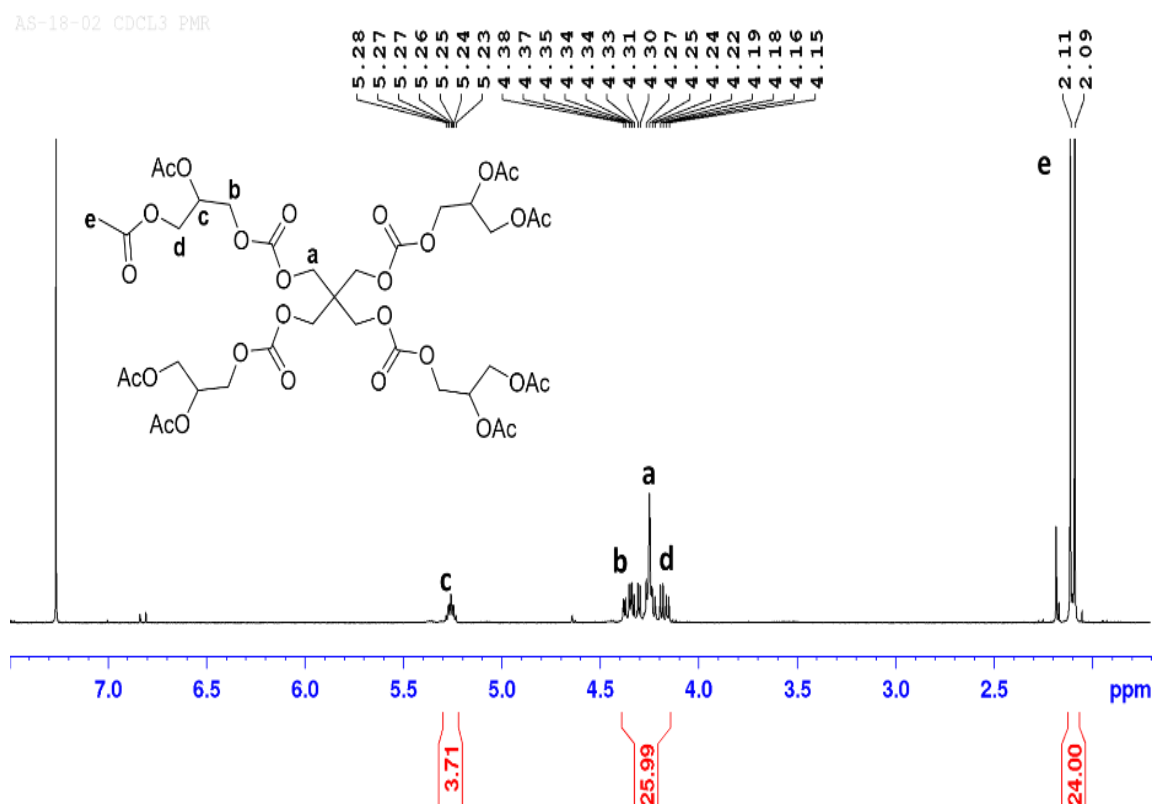


Figure 1.66 ¹H NMR spectrum of dendrimer (36) in CDCl₃.

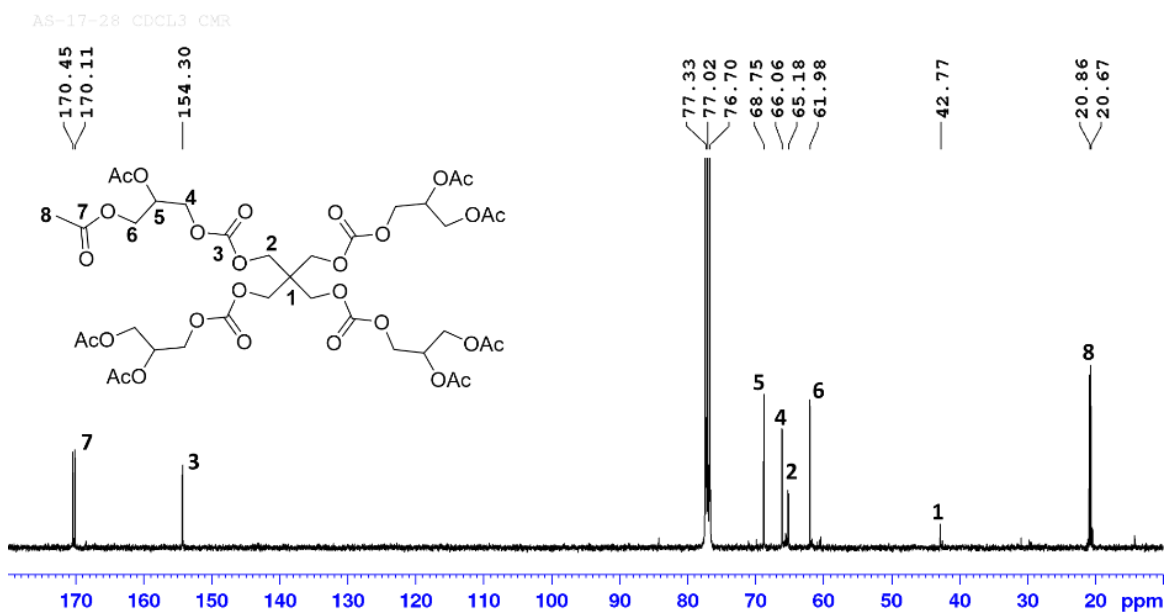


Figure 1.67 ¹³C NMR spectrum of dendrimer (36) in CDCl₃.

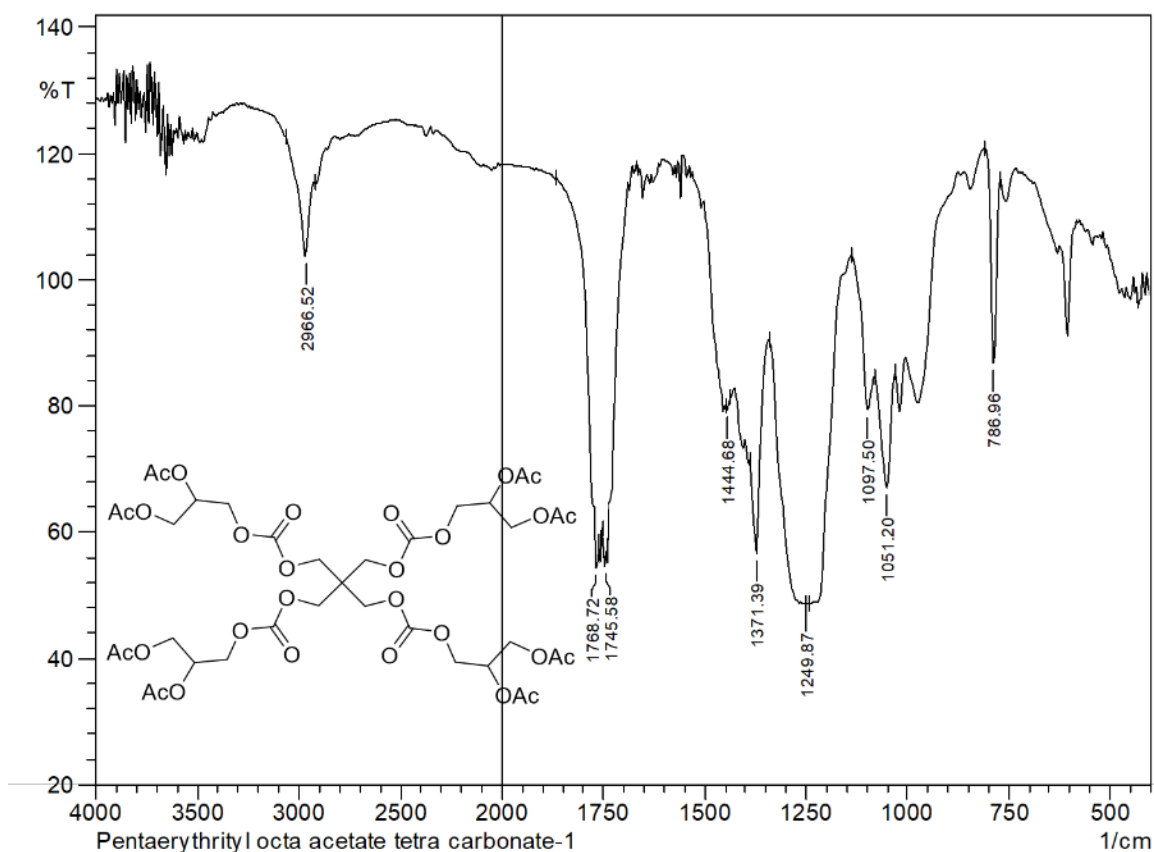


Figure 1.68 IR spectrum of dendrimer (36) in KBr.

Side product (37): ^1H NMR (400 MHz, CDCl_3 , 25°C): δ (ppm) = 5.29-5.24(m, 1H; CHOAc), 4.33-4.29 (dd, $J=8\text{Hz}$ and 4Hz 2H; AcOCH₂), 4.19-4.15 (dd, $J=8\text{Hz}$ and 4Hz 2H; AcOCH₂), 2.11(s, 9H; CH₃); ^{13}C NMR (100 MHz, CDCl_3 , 25°C): $\delta=170.54, 170.14(\text{OCO}), 69.03(\text{HCOAc}), 62.24(\text{CH}_2\text{OAc}), 20.88, 20.69(\text{CH}_3)$; IR (KBr): $\tilde{\nu}(\text{cm}^{-1})=2962(\text{w}, \text{C-H}_{\text{stretch}}, \text{sp}^3), 1745(\text{vs}, \text{C=O}_{\text{stretch}}, \text{acetate}), 1440(\text{w}, \text{C-H}_{\text{bend}}, \text{methylene}), 1226(\text{vs}, \text{C-O}_{\text{stretch}}, \text{ester}), 1051(\text{s}, \text{C-O}_{\text{stretch}})$.

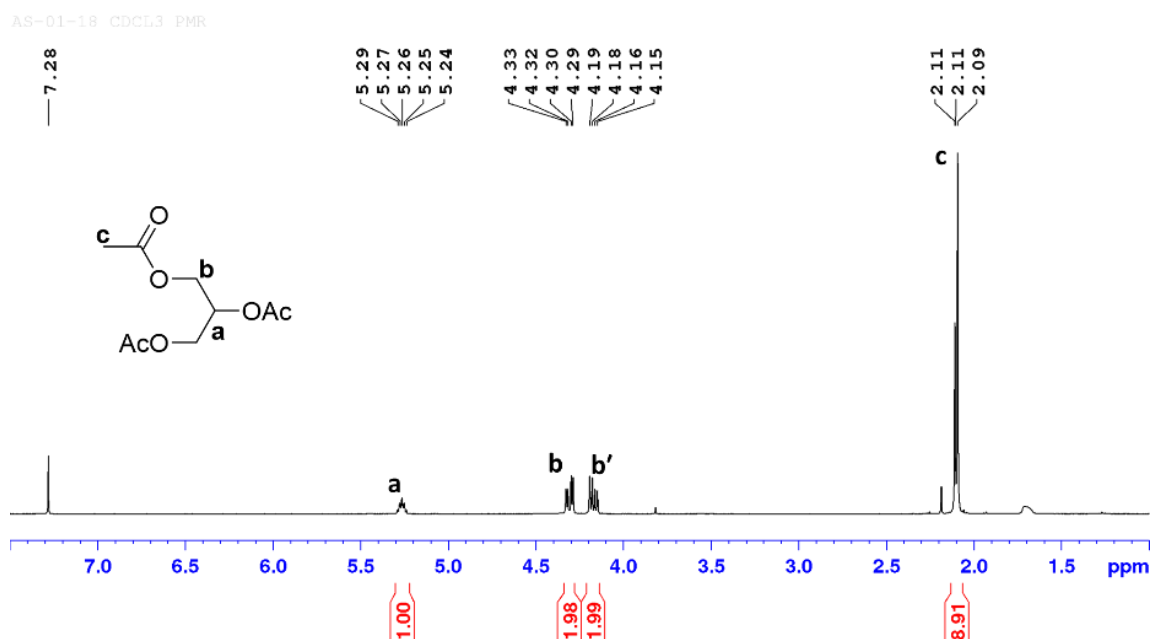


Figure 1.69 ^1H NMR spectrum of compound (37) in CDCl_3 .

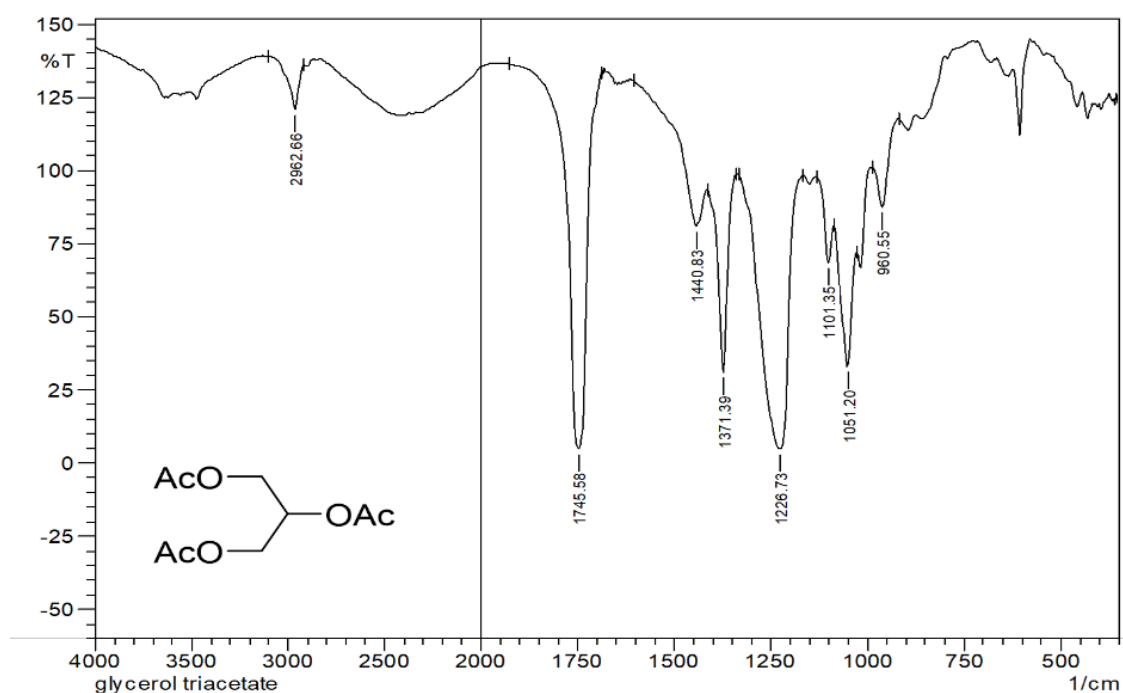


Figure 1.70 IR spectrum of compound (37) in KBr.

iv. Bis(2,3-diacetoxypropyl) carbonate (39)

Diallyl carbonate (0.5 g, 3.5 mmol), (diacetoxyiodo) benzene (2.26 g, 7 mmol), acetic anhydride (1.43 g, 14 mmol), glacial acetic acid (15 mL), $\text{BF}_3 \cdot \text{OEt}_2$ (1.1 mmol). Isolated as pale-yellow viscous liquid in 55% yield. $R_f=0.6$ (pet. ether/ethyl acetate 6:4); ^1H NMR (400 MHz, CDCl_3 , 25°C): δ (ppm) = 4.90-4.85(m, 1H; CHOAc), 4.32-4.28 (dd, $J=8\text{Hz}$ and 4Hz , 2H; CH_2OCO_2), 4.27-4.16(m, 2H; AcOCH_2), 2.07(s, 6H; CH_3); ^{13}C NMR (100 MHz, CDCl_3 , 25°C): $\delta=170.44(\text{OCO})$, $154.37(\text{OCO}_2)$, $73.70(\text{HCOAc})$, $65.97(\text{CH}_2\text{OCO}_2)$, $63.02(\text{CH}_2\text{OAc})$, $20.58(\text{CH}_3)$; IR (KBr): $\tilde{\nu}(\text{cm}^{-1})=2962(\text{w}, \text{C-H}_{\text{stretch}}, \text{sp}^3)$, 1789 (vs, $\text{C}=\text{O}_{\text{stretch, carbonate}}$), 1745 (vs, $\text{C}=\text{O}_{\text{stretch, acetate}}$), 1440 (w, $\text{C-H}_{\text{bend, methylene}}$), $1234, 1172$, (vs, $\text{C-O}_{\text{stretch, ester}}$), $1093, 1055$ (s, $\text{C-O}_{\text{stretch}}$), LCMS (ESI) m/z : $[M+H]^+ = 379.56$.

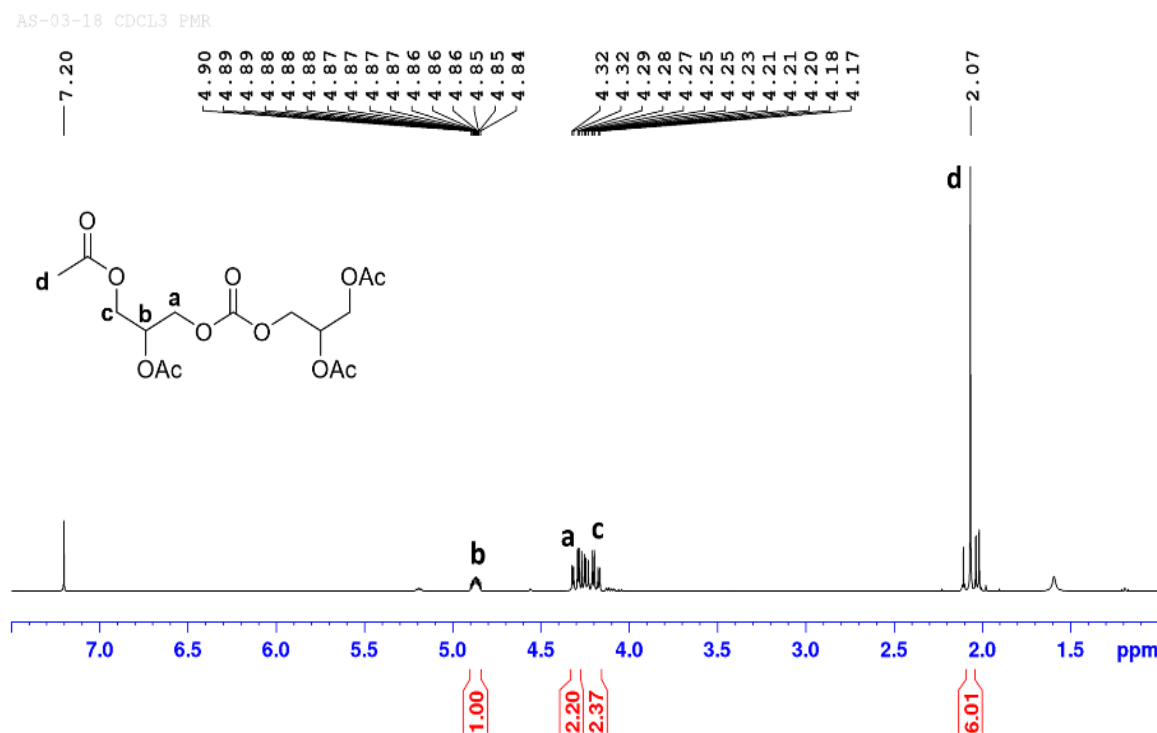


Figure 1.71 ^1H NMR spectrum of compound (39) in CDCl_3 .

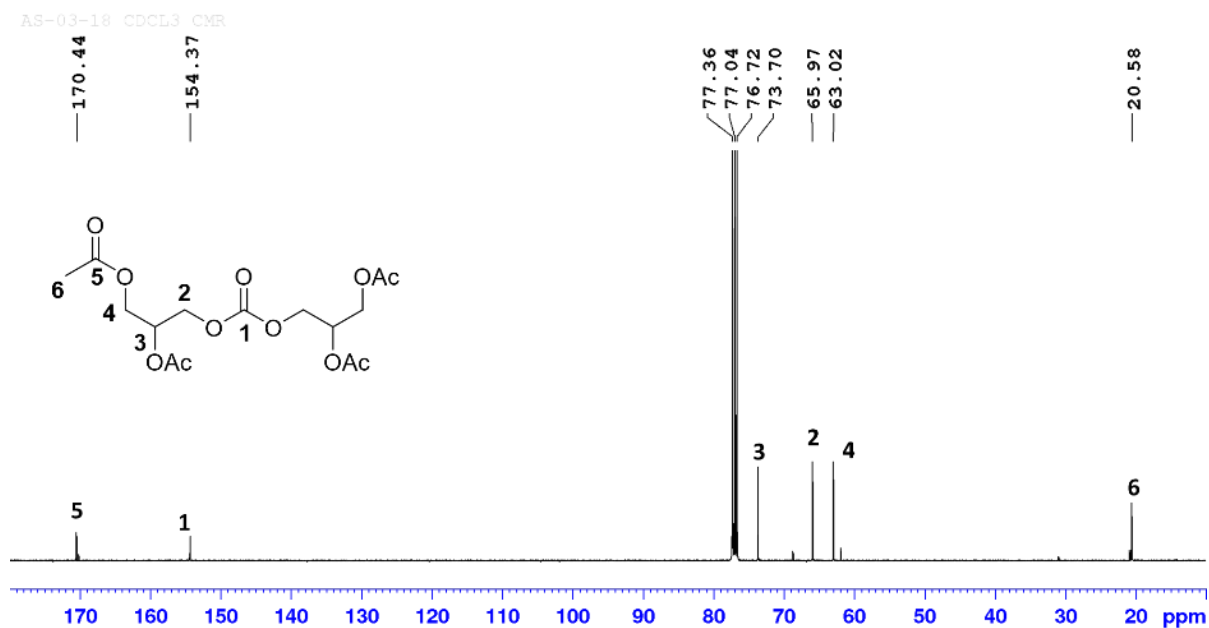


Figure 1.72 ¹³C NMR spectrum of compound (39) in CDCl₃.

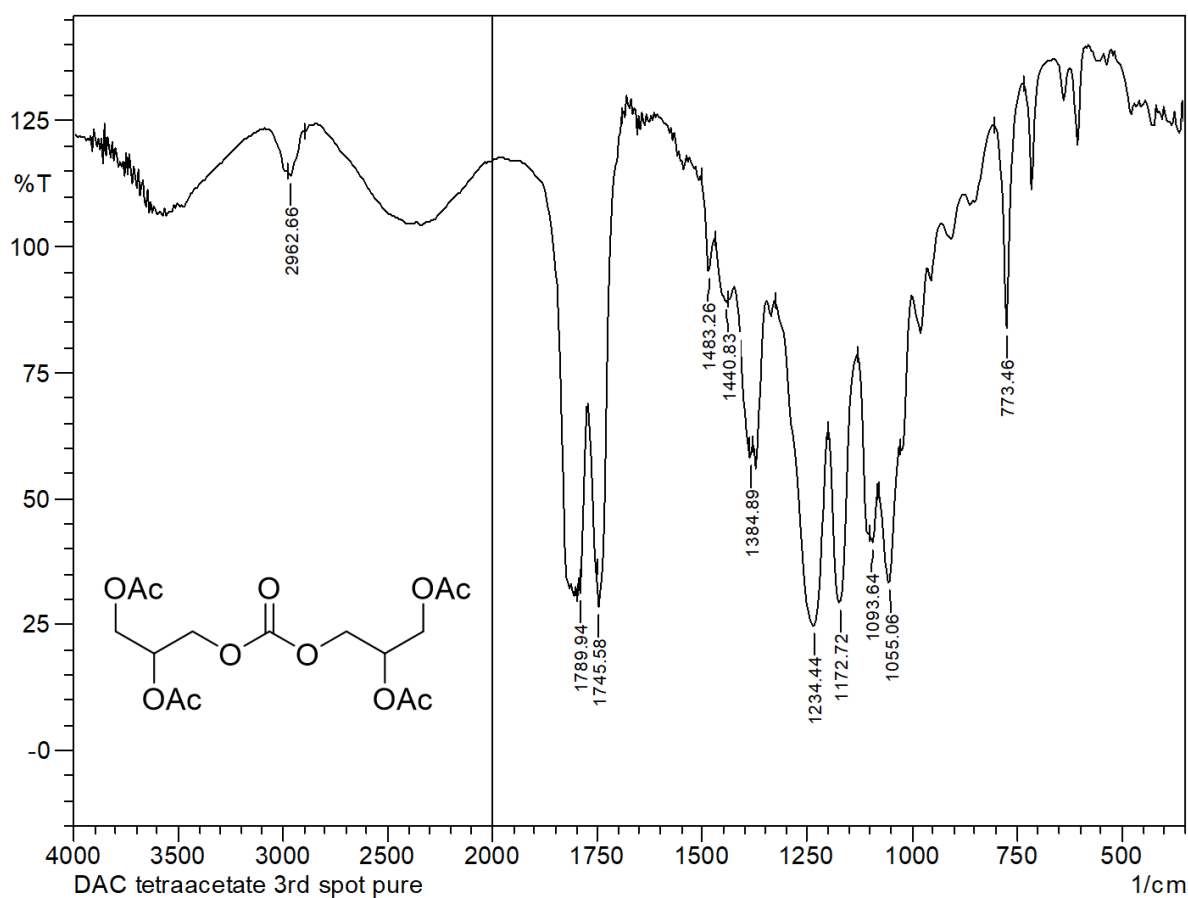


Figure 1.73 IR spectrum of compound (39) in KBr.

VI. Synthesis of bis(2,3-dihydroxypropyl) carbonate (11)**i. Base hydrolysis of Bis(2,3-diacetoxypropyl) carbonate^[108]**

To a stirred solution of tetraacetate (0.1 g, 0.26 mmol) in 20 mL methanol, was added 1 M sodium methoxide methanolic solution dropwise at 0°C over period of 30 min. Stirred at same temp for more 30 min and then stirred for 5 h at 10°C. After completion, reaction mixture was neutralized with Amberlite IR-120 (+H) resin, filtered and concentrated in vacuo. Residue extracted with 2% MeOH/CHCl₃ solution, evaporated to obtain yellow crude oil. Purification by silica gel chromatography to afford colorless oil in 52% yield.

ii. Acid hydrolysis of Bis(2,3-diacetoxypropyl) carbonate

To a stirred solution of tetraacetate (0.1 g, 0.26 mmol) in 10 ml ethanol, was added 5% dil. HCl solution dropwise at 0°C over period of 20 min. Further stirred for 10 h at 10°C. After completion, reaction mixture was neutralized with Amberlyst A-21 weakly basic resin, filtered and concentrated in vacuo. Crude yellow oil subjected to silica gel chromatography to afford target product in 78% yield.

iii. Osmium catalysed dihydroxylation of Diallyl carbonate^[109]

To a mixture of diallyl carbonate (0.5 g, 3.5 mmol), citric acid (1.6 g, 8.5 mmol), NMO (0.9 g, 7.7 mmol) in 10 mL tert-butanol/water (2:1), was added 4% Osmium tetroxide aq. solution (0.018mmol) dropwise at 0°C. Further reaction stirred at 10°C for 3 h. After completion, mixture was treated with Amberlite IRA-400(OH) resin and washed with water. Filtrate was concentrated in vacuo with azeotropic removal of water with ethanol. Resulting crude was purification by silica gel chromatography to afford target product in 76% yield.

Compound 11: R_f=0.7 (Methanol/Chloroform 0.5:9.5). Isolated as colorless pale green oil; ¹H NMR (400 MHz, CDCl₃, 25°C): δ (ppm) = 4.89-4.84(m, 2H; CHOH), 4.56-4.52 (dd, *J*=8Hz, 2H; CH₂OCO₂), 4.32-4.29 (dd, *J*=8Hz and 4Hz, 2H; CH₂OCO₂), 3.82-3.79(dd, *J*=8Hz and 4Hz, 2H; CH₂OH), 3.63-5.59(dd, *J*=8Hz and 4Hz, 2H; CH₂OH); IR (KBr): $\tilde{\nu}$ (cm⁻¹)=3342(vs, O-H_{stretch}), 2931, 2879(m, C-H_{stretch}, sp³), 1481(w, C-H_{bend}, methylene), 1402 (m, O-H_{bend}), 1182(s, C-O_{stretch}, ester), 1085(m, C-O_{stretch}, alcohol).

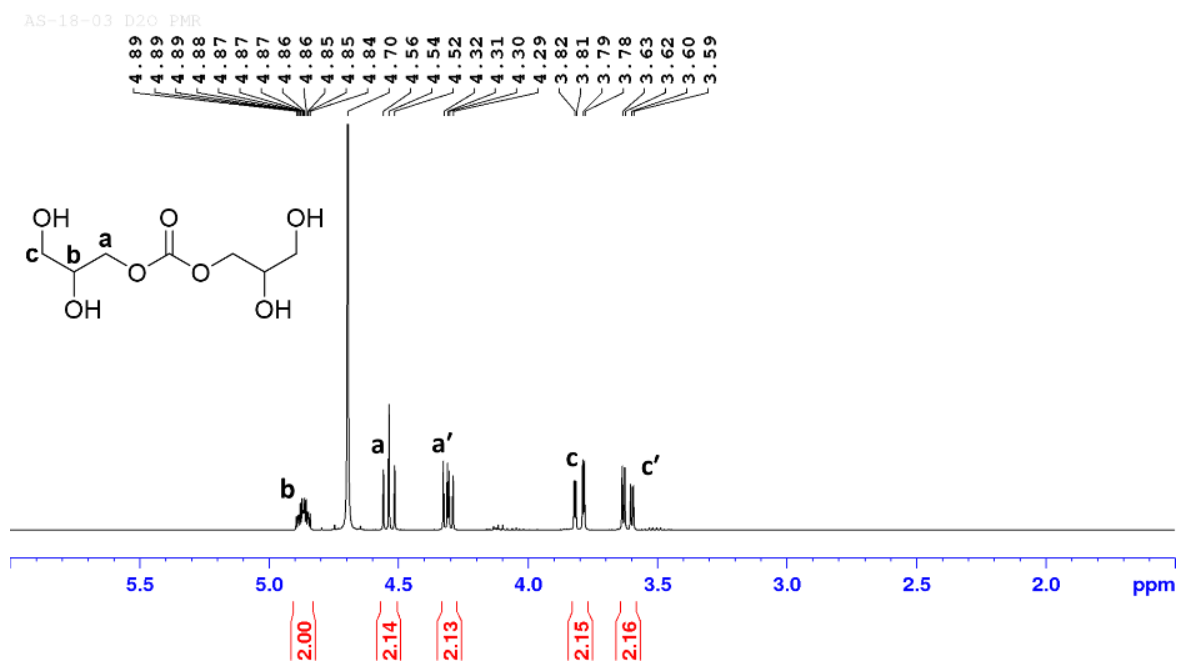


Figure 1.74 ^1H NMR spectrum of compound (11) in CDCl_3 .

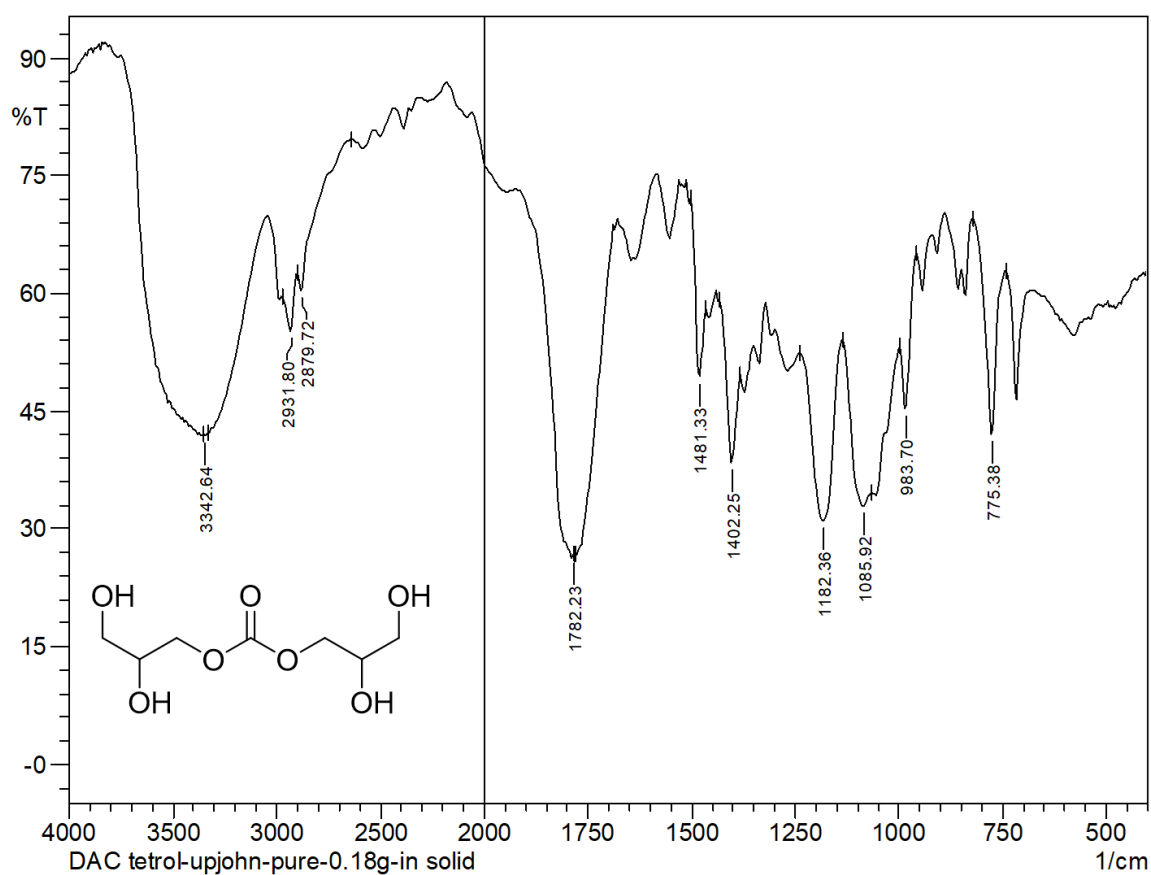


Figure 1.75 IR spectrum of compound (11) in KBr.

VII. Miscellaneous efforts towards synthesis of [G-0.5] Pentaerythrityl tetra ((2,3-dihydroxypropyl) carbonate) or PEr-[G-1] -(1,2)-OH₈ (9).**i. Deacetylation of [G-0.5] Pentaerythrityl tetrakis ((2,3-diacetoxypropyl) carbonate)**

To a stirred solution of polyacetate (0.1 g, 0.1 mmol) in 10 mL ethanol, was added 5% dil. HCl solution dropwise at 0°C over period of 20 min. Progress of reaction was carefully monitored on TLC. Reaction completes after 12 h stirring at 10°C with the formation of new spot along with side products. Further, reaction mixture was neutralized with Amberlyst A-21 weakly basic resin, filtered and concentrated in vacuo. Crude was product analyzed by TLC.

ii. Dihydroxylation of Pentaerythrityl tetrakis (allyl carbonate)^[109]

To a mixture of PETAC (0.5 g, 1.1 mmol), citric acid (0.4 g, 2.2 mmol), NMO (0.57 g, 4.84 mmol) in 8 mL tert-butanol/water (2:1), was added 4% Osmium tetroxide aq. solution (0.011mmol) dropwise at 0°C. Progress of reaction was carefully monitored on TLC. Reaction completes after 6 h stirring at 10°C with the formation of side products only.

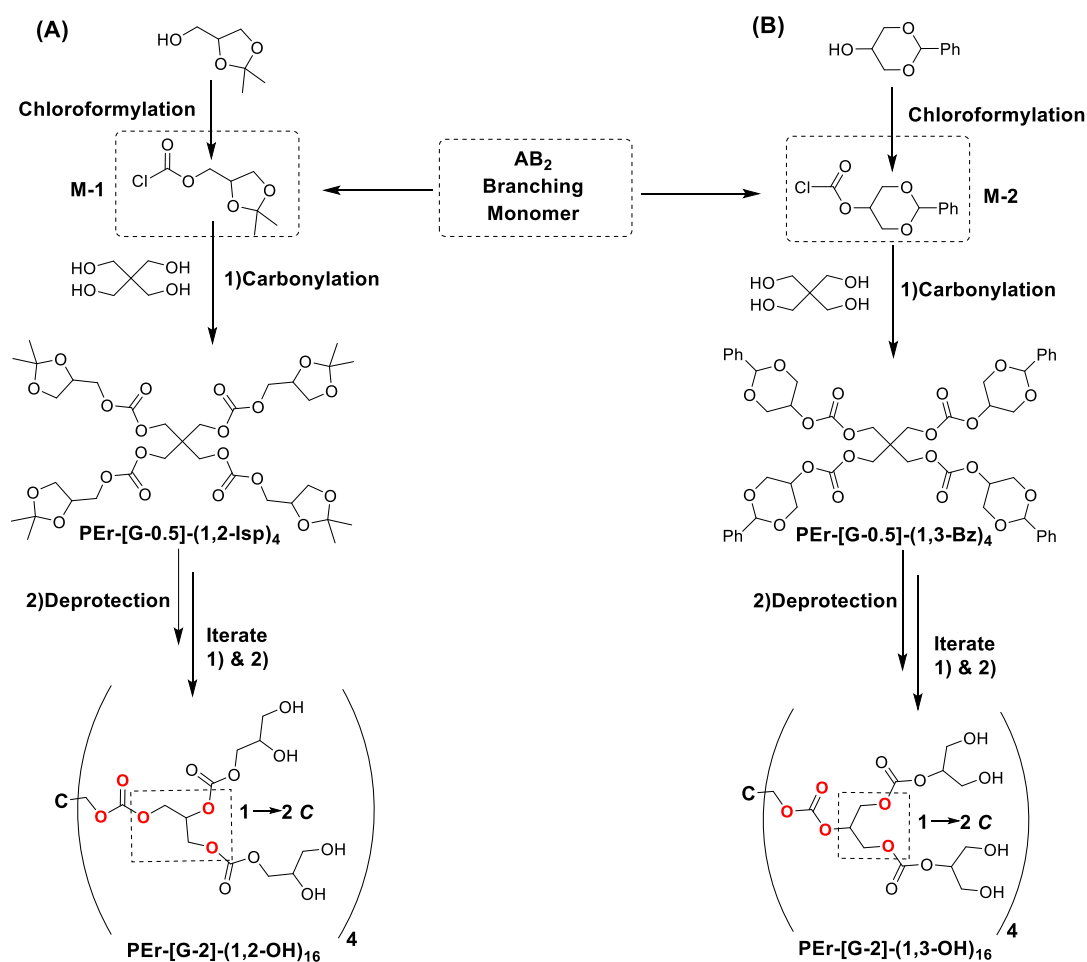
1.4 Results and Discussion

1.4.1 General remark on screening and synthesis of integral units of dendrimer

For the synthesis of polycarbonate and polyurethane dendrimers, choice of the raw material for preparing branching monomers and other building blocks was based on their ease and large-scale commercial availability. We designed these integral units in such a way that, it can follow two or one step sequential iterative protocol required for dendrimer growth and also can be easily obtained in 1-3 step processes. Further, precursor for creating carbonate and urethane linkages was obtained by transforming the branching and other integral units into highly reactive functionalities such chloroformates, carbamoyl chlorides. For this purpose, we employed well known phosgenation protocols, where triphosgene was used as phosgenating agent and a safer alternative to toxic phosgene gas.

1.4.2 Synthesis of 1→2 C branched carbonate linked dendritic motifs using protection-deprotection strategies

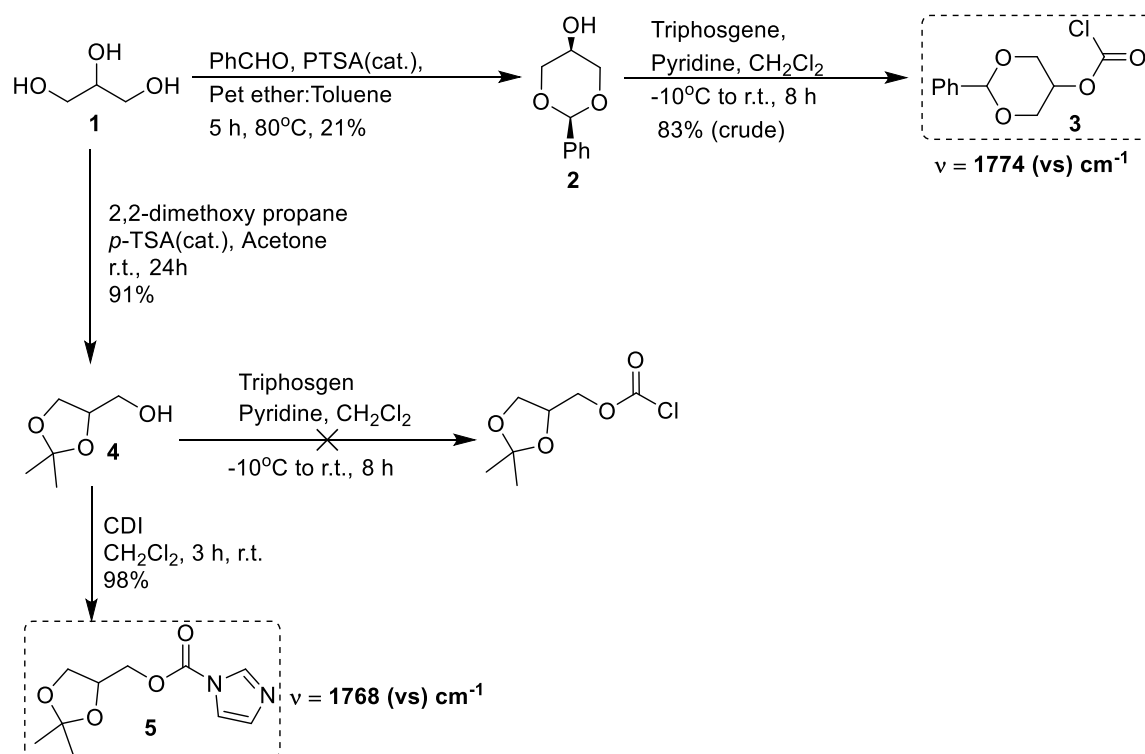
Following divergent growth strategy was designed for synthesis of 4-armed polycarbonate dendritic motifs using glycerol based AB₂ monomers **M-1** and **M-2**.



Scheme 1.13 Divergent growth synthesis of 1→2 C branched Polycarbonates with 1,2- and 1,3-diol end functionalities.

Above divergent growth synthesis involves 2 step iterative process of “growth and activation” i.e.; (i) *O*-carbonylation of hydroxyls and (ii) deprotection of acetal group. Here, glycerol is a key branching unit which facilitates 1→2 glycerol framework through carbonate connectivity’s. Moreover, glycerol is a bioderived, cheap and biocompatible material, which not only easily accessible but more significantly generates the biocompatible dendritic architectures. Most of the glycerol derived dendritic polymers such as polyglycerols, polyester-glycerol’s are excellent biocompatible materials and find potential application in controlled drug delivery and tissue engineering. Our ideology to include carbonate functionality would further enhance its biocompatibility and also provide biodegradable feature to the dendritic system.

I. Synthesis of glycerol based AB₂ branching monomer



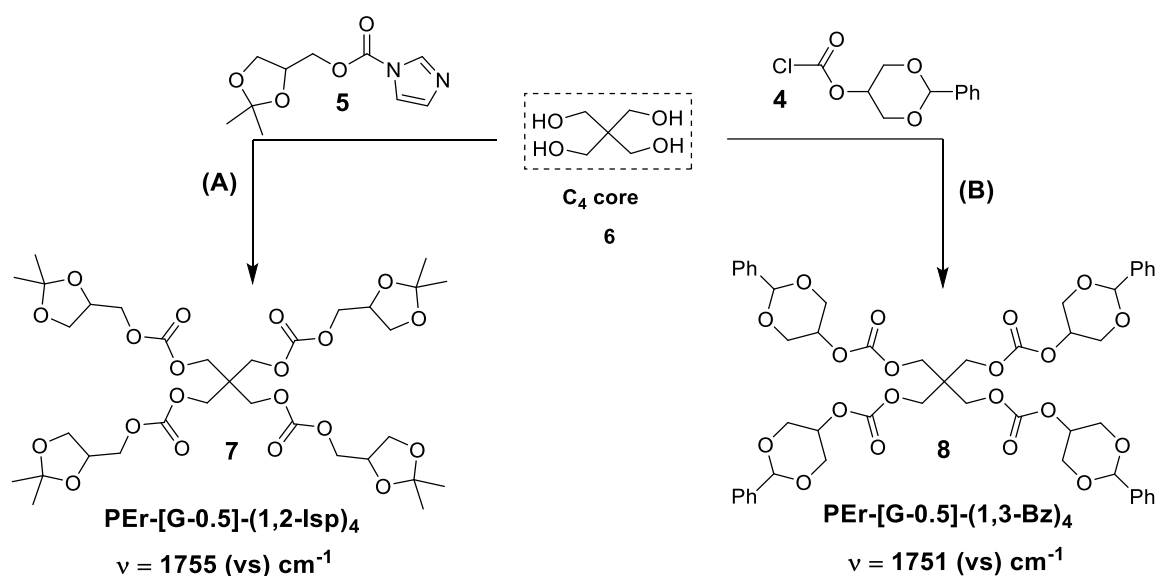
Scheme 1.14 Synthesis of AB₂ type 1,2- and 1,3- branching monomers from glycerol.

Glycerol protected acetals i.e. *cis*-5-hydroxy-2-phenyl-1,3-dioxane (*cis*-HPD), **2** and (2,2-Dimethyl-1,3-dioxolan-4-yl)methanol or solketal, **4** were prepared using known literature procedure^[101,102]. In case of benzylidene acetal reaction, *cis*-1,3 isomer **2** was selectively crystallized from petroleum ether/ toluene mixture as white shiny soft needles, leaving other

isomers into mother liquor. Crude solketal were purified by vacuum distillation at 60-70°C to obtain as colourless liquid. Further, in order to use these hydroxy acetals as AB₂ type branching monomers, they were subjected to chloroformylation reaction, which generates chloroformate groups as reactive A-functionalities. We could successfully afford chloroformate **4** in high yields. However, chloroformylation of solketal **3** resulted in deprotection of acetonide group. Hence, further activation of A-functionality in solketal was performed using esterification reaction with 1,1'-Carbonyldiimidazole (CDI) to form imidazole carbonate ester of solketal **5** in quantitative yields.

I. Synthesis of 4-armed [G-1] tetra acetal carbonate

This is the first growth step towards the 4-direction polycarbonate dendrimer. Step involves, O-carbonylation of tetravalent hydroxy core **C₄** using AB₂ glycerol monomers.



Scheme 1.15 Synthesis of 4-armed tetra acetal carbonate from tetravalent hydroxyl core.

Tetra acetone carbonate **7** was prepared by reacting 4.5 mol equivalent of imidazole carbonate ester of solketal **5** with 1 mol pentaerythritol (PEr) **6** in the presence of either organic or inorganic bases. Using similar mol equivalents, benzylidene chloroformate **4** was reacted with **6** in the presence organic bases to afford tetra benzylidene acetal carbonate **8**. Both the tetra acetal carbonates were obtained in fair to good isolated yields. Furthermore, to improve the reaction time and final yields, we performed optimization study using various reaction conditions and the best optimized entries are highlighted in **Table 1.2** below. It is important to understand here that, reactivity of both carbonate forming functionalities with hydroxyl groups are different. The imidazole esters are comparatively slow reacting electrophile, towards the hydroxyl groups. Hence, we had to provide thermal

energy in the presence of weak organic base such as triethyl amine, in order to drive reaction towards completion. However, insolubility of polar tetrol core **6** in acetonitrile, 1,4-dioxane leads to mixture of product (entry 1A, 3A). Further, using a DMF as polar aprotic solvent, we could achieve complete solubility of **6** along with formation of **7** in good yields (entry 2A). Moreover, using strong base such as NaH and DMF as solvent, we could obtain product **7** at room temperature in relatively less yield but at faster rate (entry 4A).

On the contrary, chloroformates are highly reactive electrophiles, thus carbonylation reaction was smoothly carried out in the presence of organic bases such as pyridine. However, using chlorinated and aromatic solvent, reaction leads to mixture of product due to insolubility of **6** (entry 6B, 7B). Using polar aprotic solvents, we could observe complete formation of final product with a highest yield in acetonitrile (entry 8B). Both **7** and **8**, were purified using silica gel chromatography, eluting in hexane/ethyl acetate solvent system.

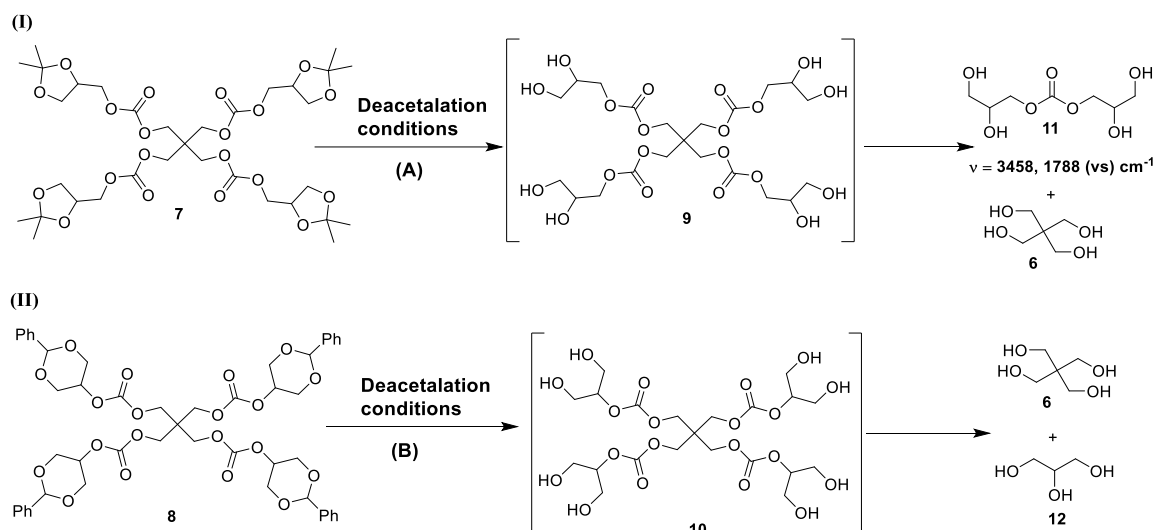
Table 1.2 Reaction conditions employed in *O*-carbonylation of pentaerythritol core.

Entry	Solvent/base/t(h)	Yield ^{ab}
1(A)	CH ₃ CN, Et ₃ N, reflux, 24 h	Mixture
2(A)	DMF, Et₃N, 70°C, 24 h	75%
3(A)	1,4-Dioxane, Et ₃ N, reflux, 24 h	Mixture
4(A)	DMF, NaH, 0°C to r.t. 12 h	65%
5(A)	Dioxane, NaH, 0°C to r.t. 12 h	57%
6(B)	Toluene, Pyridine, DMAP, 0°C to r.t., 12 h	Mixture
7(B)	CHCl ₃ , DMAP, Pyridine, 0°C to r.t. 12 h	Mixture
8(B)	CH₃CN, DMAP, Pyridine, 0°C to r.t., 6 h	72%
9(B)	Acetone, DMAP, Pyridine, 0°C to r.t., 6 h	65%
10(B)	THF, DMAP, Pyridine, 0°C to r.t., 6 h	68%

^aProduct isolated as colourless viscous liquid for conditions (A); ^bProduct isolated as white solid for conditions (B).

II. Attempt towards synthesis of 4-armed [G-1] tetra carbonate polyol

This is the activation step (**Scheme 1.16**) which produce first-generation 1→2 *C* branched carbonate dendrimer with hydroxyl periphery as precursor for next growth or monomer coupling step.



Scheme 1.16 Deprotection of acetal groups to generate [G-1] tetra carbonate dendrimer with (I) 1,2- and (II) 1,3-polyol periphery.

Here, activation step can be performed by deprotection of acetal groups using acid catalysed hydrolysis, methanolysis and transacetalation procedures. Thus, we subjected the G1 tetra acetal carbonates **7** and **8** towards various deacetalation conditions and results were noted table below.

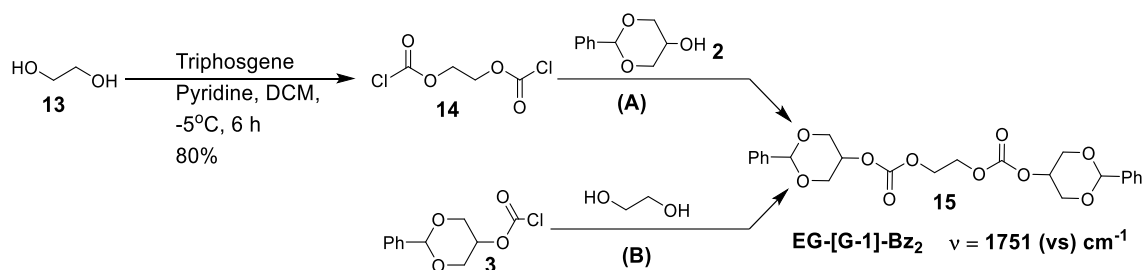
Table 1.3 Reaction conditions for deacetalation of tetra acetal carbonates **7** and **8**.

Entry	Deacetalation conditions	Observation and Results
1(A)	5% aq. HCl/ MeOH, r.t., 8 h	11 (liquid) and 6 (solid)
2(A)	5% aq. HCl/ MeOH, 0°C 15 h	11 (liquid) and 6 (solid)
3(A)	DOWEX [H ⁺], MeOH, r.t., 6 h	New spot (9) along with 11 & 6
4(A)	Amberlite [H ⁺], MeOH, r.t., 3 days.	New spot (9) along with 11 & 6
5(A)	I ₂ (30%), CH ₃ CN, H ₂ O (5 equiv.), r.t., 6 h.	New spot (9) along with 11 & 6
6(A)	Propylene glycol (16 equiv.), <i>p</i> -TSA (10%), CH ₂ Cl ₂ , r.t., 24 h.	Mixture of spots along with 7 on TLC
7(B)	5% aq. HCl/ MeOH, r.t., 20 h	12 and 6
8(B)	DOWEX [H ⁺], MeOH, 50°C, 12 h	New spot (10) along with 12 & 6
9(B)	Propylene glycol (16 equiv.), PTSA (10%), CH ₂ Cl ₂ , r.t., 24 h.	Mixture of spots along with 8 on TLC

Under acid hydrolysis condition (**Table 1.3**, entry 1A, 2A and 7B), we observed hydrolysis of carbonate esters along with acetals groups, which leads to degradation of whole carbonate framework into starting materials **6**, **12** and side product **11**. The formation of this degraded product was revealed by spectroscopic techniques. Side product **11** is the consequence of intramolecular transesterification reaction between two glycerol units, occurring after hydrolytic attack on carbonate linkages. However, under methanolysis conditions (**Table 1.3**, entry 3A, 4A and 8B), we could monitor formation of new identical spot over TLC along with degraded product. This new spot was appeared to be highly polar over TLC analysis. Unfortunately, we were not able to isolate this new product, instead we ended up in obtaining degraded products upon isolation. This shows that degradation mechanism must be going through G1 polyols **9** and **10**. In I_2/CH_3CN reaction (**Table 1.3**, entry 5A), we could locate brown oil separating out of solvent medium. However, further attempt to isolate product through decanting and solvent washing leads to precipitation of white solid which was pentaerythritol **6**. Moreover, intramolecular side product was not observed in deacetylation of **8**. Transacetalation steps (**Table 1.3**, entry 6A and 9B) leads to mixture of products along with starting acetals **7** and **8**. As consequence of above difficulties, we couldn't proceed further with the growth or coupling step.

III. Synthesis of [G-1]-bis benzyldiene carbonate

Two directional, ethylene glycol based G1 carbonate dendrimer **15** was synthesized using two routes as shown in **Scheme 1.17** below.



Scheme 1.17 Synthesis of [G-1]-bis benzyldiene carbonate from divalent core.

First route begins with the synthesis of ethylene glycol bis chloroformate **14** using triphosgene as chloroformylating reagent. The crude product was purified by distillation under reduced pressure to afford colourless liquid **14** in 80% yield. For final coupling step between **14** and *cis*-HPD **2** (2.2 mol equiv.), we screened selected base condition (A), among which best results were obtained for Et₃N/DMAP combination (**Table 1.4**, entry 3A).

Table 1.4 Reaction condition for synthesis of [G-1]-bis benzylidene carbonate, **15**.

Entry	Solvent/base/t(h)	Yield ^a
1(A)	DCM, DMAP, Pyridine, 0°C to r.t., 24 h	No reaction
2(A)	DCM, DMAP, r.t., 24 h	Mixture
3(A)	DCM, Et ₃ N, DMAP, 10°C to r.t., 12 h	64%
4(A)	Acetone, DMAP, Et ₃ N, 10°C to r.t., 12 h	61%
5(B)	DCM, Pyridine, DMAP, 0°C to r.t., 6 h	78%
6(B)	Acetone, Pyridine, DMAP, 0°C to r.t., 6 h	65%

^a Product isolated as white solid.

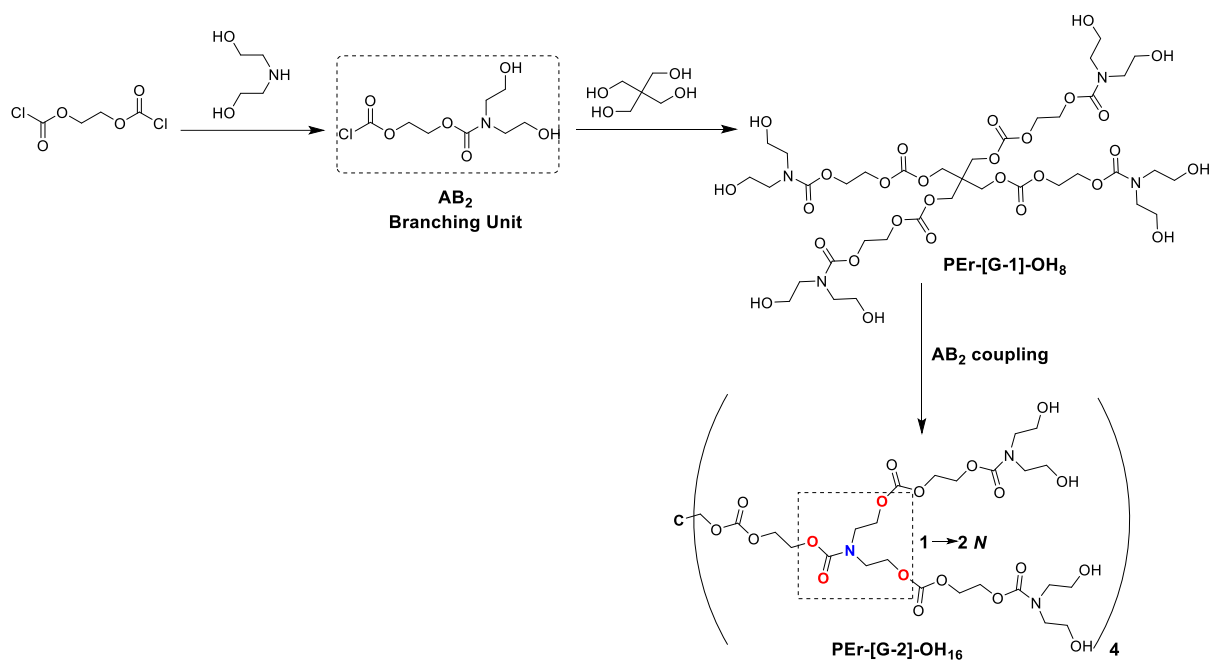
In a second route, benzylidene chloroformate **3** was reacted with ethylene glycol under Pyridine/DMAP base conditions (**Table 1.4**; entry 5-6B), to afford final compound in higher yield as compared to first route. Product **15** was purified by silica gel chromatography eluting in hexane/ethyl acetate solvent system.

Furthermore, we attempted deprotection step on **15** under acid catalysed methanolysis condition, but it suffered similar degradation issue as observed previously for **8**.

1.4.3 Synthesis of 1→2/1→4 branched carbonate/urethane dendritic motifs using protection/deprotection free strategies

I. Strategy towards 1→2 *N* branched poly(carbonate-urethane) dendrimer using one step growth process

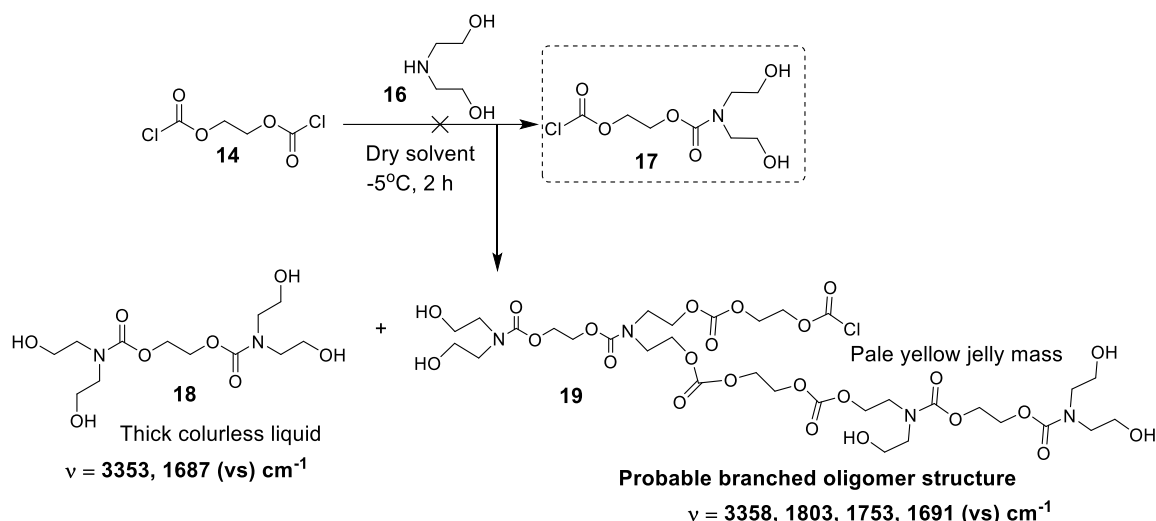
Following divergent strategy (**Scheme 1.18**) was outlined for synthesis of poly(carbonate-urethane) dendritic motifs using AB₂ type branching unit from commercially available diethanol amine (DEA) and ethylene glycol (EG). Methods employs only one growth step of *O*-carbonylation to construct high generation dendrimer.



Scheme 1.18 Proposed synthetic route towards 1→2 branched poly(carbonate-urethane) dendritic motifs.

i. Synthesis of AB₂ branching unit

Synthesis of monomer **17** relied on one step mono-*N*-carbonylation reaction between ethylene glycol bis chloroformate **15** and diethanol amine **16**. However, this planned reaction underwent side reactions such as oligomerization and bis-*N*-carbonylation as shown in **Scheme 1.19**.



Scheme 1.19 Attempted towards synthesis of DEA-EG based AB₂ branching monomer

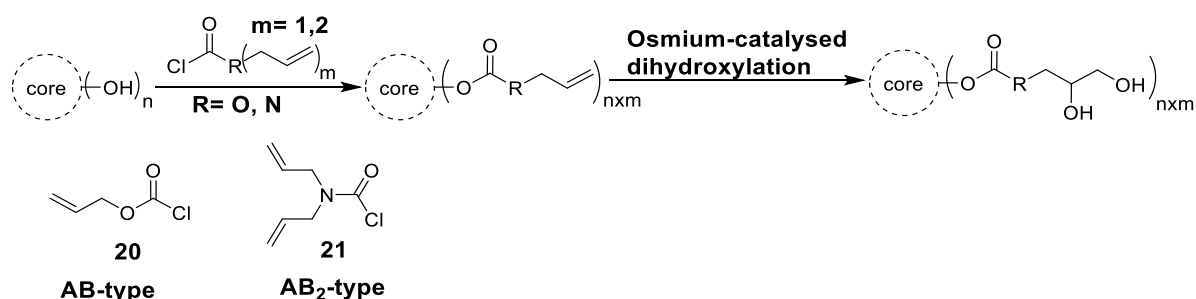
We performed this coupling reaction in two different solvent systems i.e.; acetone and chloroform, which showed similar results. Bis-carbonylated product **18**, precipitated out of

solvent mixture whereas branched oligomer **19** remained soluble in both the solvent system. Product **19** was obtained as yellow jelly mass, upon solvent evaporation and **18** forms highly polar, water-soluble colourless oil. As consequence of above result, we had to discontinue with the scheme further.

II. An efficient protection/deprotection free approach towards 1→n C (n=2, 4) branched PC and PU dendrimers with functional olefinic periphery

A two-step divergent as well as convergent growth approach was devised for synthesis of 1→2 C and 1→4 C branched dendrimers using allylic monomer. Synthetic strategy involves iterative sequence of *O*- carbonyl allylation followed by osmium catalysed dihydroxylation of allylic double bonds to generated target dendrimer.

Similar type of two step approach was employed earlier by Rainer et al. to produce Polyglycerol dendrimer^[110]. Following is our generalized schematics for the two-step process.

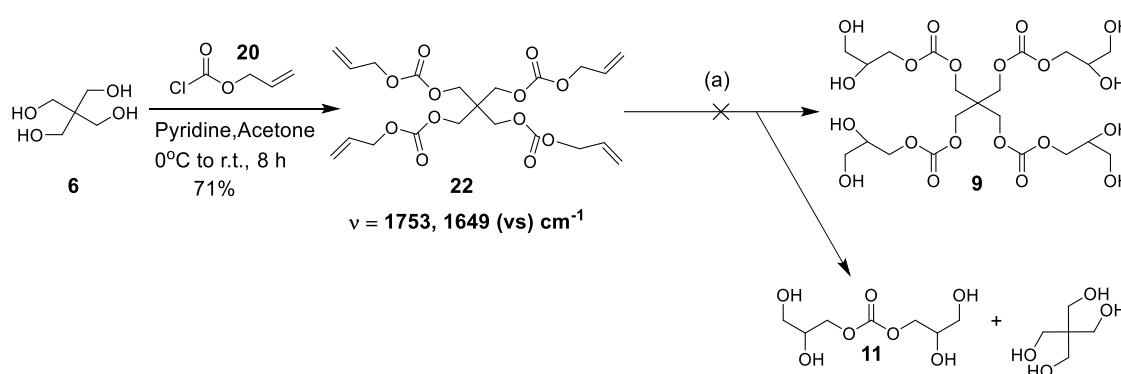


Scheme 1.20 Two-step approach towards 1→2 C and 1→4 C branched PU/PC dendrimer.

This strategy involves use of commercially available AB and AB₂ type allylic monomers either directly or with one step activation of A functionality. Significance of allylic functionality is its ability to induce 1→2 C branching framework in dendrimer synthesis. From the above **Scheme 1.20**, we could generate 1→2 C motifs using mono-allyl monomer and 1→4 C using diallyl monomer. Diallyl monomer is a type hypermonomer which give access to large number of terminal groups at lower generations. Hence, to serve our purpose, we used allyl chloroformate **20** and *N, N'*-diallyl carbamoyl chloride **21** as allylic monomers. Both the monomers **20** and **21** were prepared easily on large scale using chloroformylation method and purification by distillation under reduced pressure.

i. Attempt towards synthesis of 4-armed [G-1] tetra carbonate 1,2-polyol from tetraallyl carbonate

In our first attempt, we tried to employ *O*-carbonyl allylation and dihydroxylation approach to prepare previously proposed 4-armed 1→2 *C* branched polycarbonate dendrimers with hydroxyl periphery. For this purpose, we prepared pentaerythrityl tetra allyl carbonate derivative **22** by reacting 4.5 mol equiv. of allyl chloroformate **20** with 1 mol of pentaerythritol in the presence of pyridine as base. Crude product obtained was purified by silica gel chromatography eluting in pet. ether/ethyl acetate solvent system to fetch final colourless product in 71% yield.



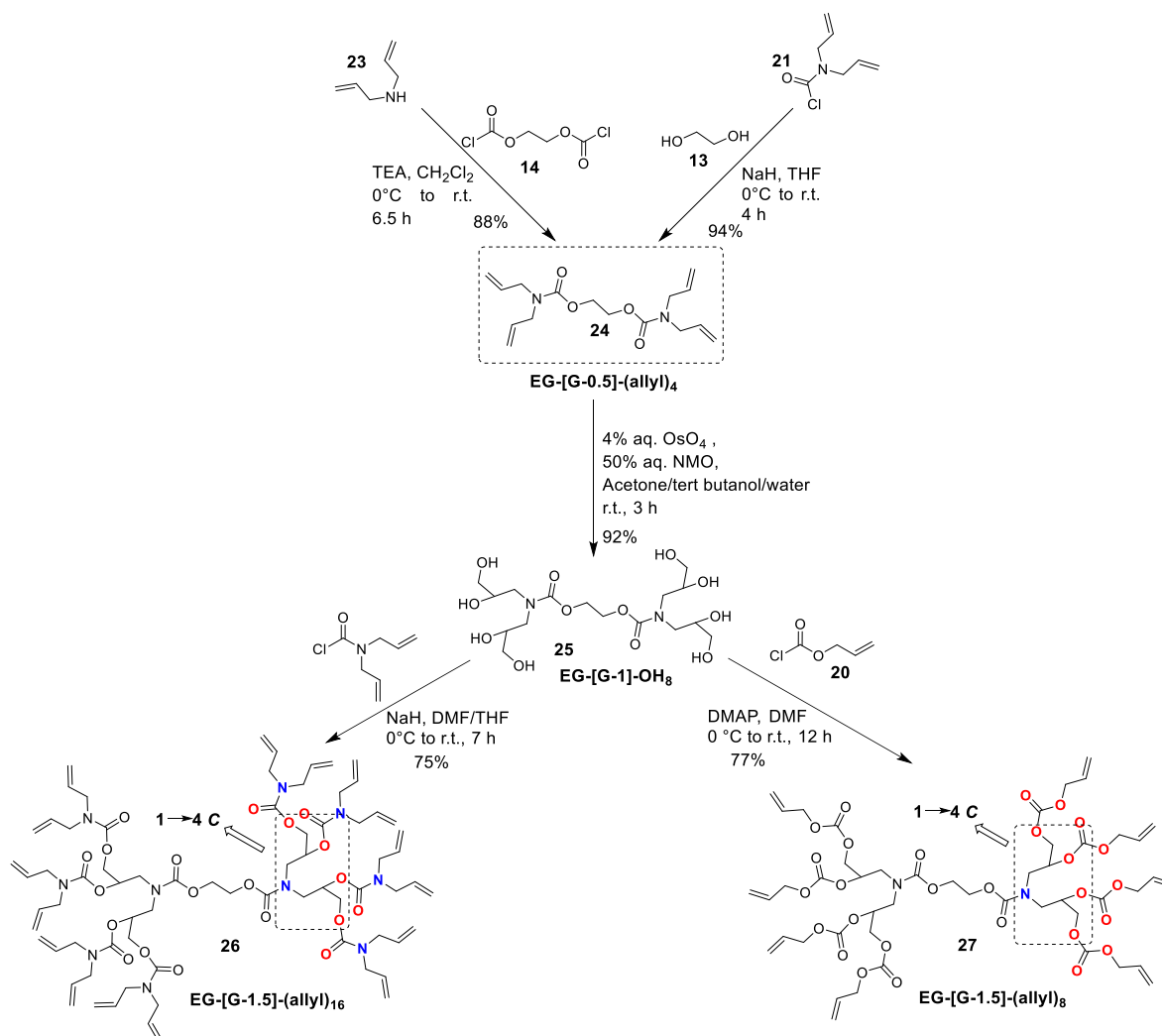
Scheme 1.21 Attempt towards synthesis of [G-1]-1,2-polyol via osmium catalysed dihydroxylation method. (a) 4% aq. OsO₄ (1 mol%), 50% aq. NMO (4.4 equiv.), Acetone/water/tert.butanol, 0°C to r.t., 5h or 4% aq. OsO₄ (1 mol%), 50% aq. NMO (4.4 equiv.), citric acid (4 equiv.), tert.butanol/water, 0°C to r.t., 5 h.

Dihydroxylation of **22** was initially performed using standard Upjohn condition i.e., in the presence of catalytic of osmium tetroxide and stoichiometric amount of *N*-methyl morpholine oxide (NMO) as a co-oxidant. Under given conditions, we couldn't locate formation new spot, instead only degraded products were formed. This is probably due to formation of stoichiometric amount of 4-methylmorpholine, which increases the pH of the system, there by promoting base hydrolysis of carbonate framework. Further, in order to maintain the neutral pH, we performed dihydroxylation reaction in the presence of citric acid as an additive (**Scheme 1.21**). Here, citric acid neutralizes 4-methylmorpholine formed during reaction, thereby maintaining pH at the optimal range. It also acts as a chelating ligand for osmium, keeping the active Os(VI) species in solution and further enhancing product yield^[109].

Using citric acid, although we could locate the formation of new spot but further isolating the same via filtration and evaporation results in degradation of the carbonate framework. This showed that the **9** (Scheme 1.21) is labile and prone towards hydrolytic attack even under neutral pH condition.

ii. Divergent growth synthesis of two directional 1→4 C branched PU/PC dendrimers

Divergent methodology began with two different modes of carbonylation to produce tetrafunctional EG-[G-0.5]-(allyl)₄ dendrimer **24** (Scheme 1.22).



Scheme 1.22 Divergent growth synthesis of 1→4 C branched PU/PC dendritic motifs.

One route shows condensation reaction between *N,N*-diallyl carbamoyl chloride **21** and ethylene glycol in the presence of NaH to afford product **24** in 88% yield. In another route, *N,N*-diallyl amine **23** coupled with ethylene bis(chloroformate) **14** to produce **24** in high yield of 94%. The crude product was purified by distillation under reduced pressure of 1 torr at 210°C. Further, subjecting **24** towards osmium-catalysed dihydroxylation with NMO as

co-oxidant gave a brown tarry crude product, which upon purification with silica gel chromatography afforded EG-[G-1]-(OH)₈, octa functional polyol dendrimer **25** in 92% yield. Also, purification of **25** with Sephadex® gel filtration chromatography fetched the pure compound in 90% yield. Per-allylation of polyol through urethane and carbonate linkages was best effected by using an excess of branching reagents. EG-[G-1.5]-(allyl)₁₆ dendrimer **26** with ideal urethane backbone was synthesized by *O*-carbamoyl-allylation of polyol **25** with carbamylating reagent **21** in the presence of NaH as a base. Similarly, *O*-carbonyloxy-allylation of polyol **25** with an excess of allyl chloroformate **20** and organic base produced EG-[G-1.5]-(allyl)₈ dendrimer **27** with allyl carbonate functionalities. Both dendrimers were subjected to column chromatography to give pure products in good yields.

We observed that per-allylation step operates very effectively with a diol, furnishing target product **24** in high yield (**Scheme 1.22**). Major factors responsible for better reactivity of diols are, their effective solvation in polar aprotic solvents and presence of sterically free hydroxyl groups. On the contrary, polyol **25** is sterically crowded with greater hydroxyl content due to which its solvation strength reduces drastically in oxygen-containing polar aprotic solvents, thereby causing decrease in a reactivity towards electrophiles. Although polyol **25** displays better and complete solubility in solvents such as water and methanol, yet we cannot perform a per-allylation step in such polar protic mediums. Thus, in order to increase the efficacy of per-allylation step, optimization studies were carried out which are summarized in Table below.

Table 1.5 Optimization study on per-allylation of polyol **25** in divergent growth route.

Entry	Electrophile (E=R-Cl) ^[a]	Reaction conditions			PU/PC dendrimer	Results
		Base ^[b] / solvent	T (°C)	t(h)		
1	21, 20 equiv.	NaH, THF	0°C to reflux ^[d]	7	26	Mixture ^[e]
2	21, 20 equiv.	NaH, 1, 4-dioxane	0°C to 100°C ^[d]	7	26	Mixture
3	21, 20 equiv.	NaH, Tetraglyme	0°C to 100°C ^[d]	7	26	Mixture

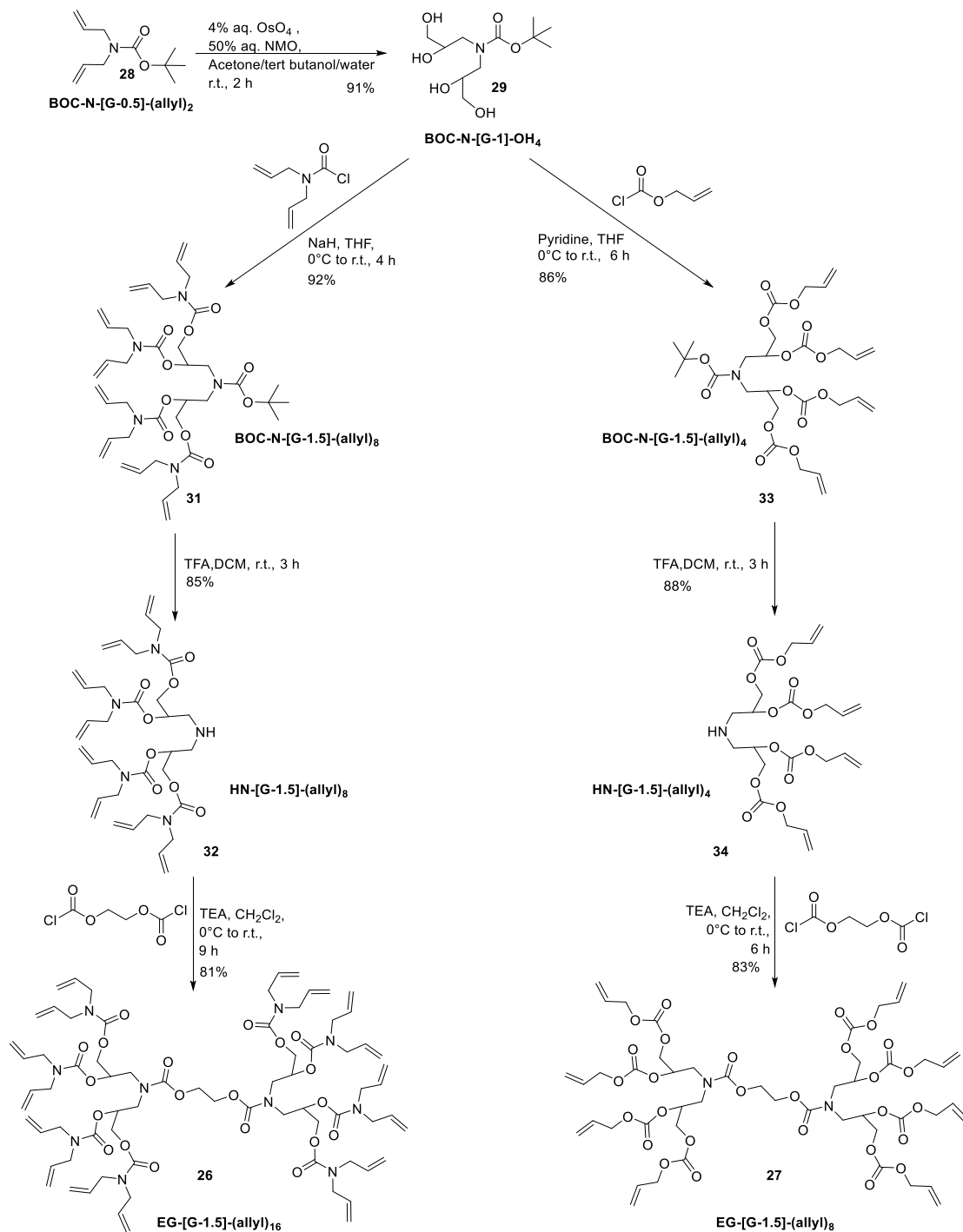
4	21, 20 equiv.	NaH, DMF	0°C to r.t.	7	26	63% T.D. ^[f]
5	21, 20 equiv.	NaH, DMA	0°C to r.t.	7	26	60% T.D.
6	21, 20 equiv.	NaH, DMF/THF (1:2)	0°C to r.t.	7	26	75% T.D.
7	20, 16 equiv.	Pyridine	0°C to r.t.	12	27	66% T.D.
8	20, 16 equiv.	Pyridine/THF (1:1)	0°C to r.t.	12	27	64% T.D.
9	20, 16 equiv.	Pyridine/THF (1:1), cat. DMAP	0°C to r.t.	12	27	73% T.D.
10	20, 16 equiv.	DMAP (16eq.), DMF	0°C to r.t.	12	27	77% T.D.

^[a]Electrophile 21 & 20 were calculated as 2.5 & 2 equiv. per hydroxyl group; ^[b] Condition utilizes: NaH (9 equiv.) and 1:20 ration of polyol to pyridine; ^[d]Reaction mixture stirred for 2 h at r.t.; ^[c]Inseparable mixture of products noted on TLC; ^[f]Isolated yield for target dendrimer (T.D.).

Initially, a combination of THF and NaH with variation in temperature was employed for transformation of polyol **25** to dendrimer **26**. However, reaction ended up in a mixture of spots as monitored by TLC. Also, the use of other oxygen-containing polar aprotic solvents followed the same trend (**Table 1.5**, entry 2 and 3). By changing the solvent to DMF and NaH as a base, we successfully produced dendrimer **26** in 63% yield (**Table 1.5**, entry 4), easily separable on column chromatography. The reaction was best effected by choosing a solvent system as DMF/THF (1:2) and NaH as a base, to fetch target dendrimer in 75% yield (**Table 1.5**, entry 6). In the case of dendrimer **27**, electrophile **20** was more reactive towards polyol **25** than **21** hence per-allylation reaction worked smoothly in the presence of organic bases such as pyridine and 4-Dimethylaminopyridine. Also, pyridine itself was utilized as a solvent due to complete solubility of **25**, affording target dendrimer in 66% yield (**Table 1.5**, entry 7). Notably, the use of the catalytic and stoichiometric amount of DMAP showed further improvement in the yield (**Table 1.5**, entry 9 and 10).

iii. Convergent growth synthesis of two directional 1→4 C branched PU/PC dendrimers

The synthetic route involves simple protection/deprotection step producing target polyenes with improved yields. Synthetic path was initiated by BOC protection of *N,N*-diallyl amine to provide **28** in quantitative yield (Scheme 1.23) as describe by Longshaw et al^[111].



Scheme 1.23 Convergent growth synthesis of 1→4 C branched PU/PC dendritic motifs

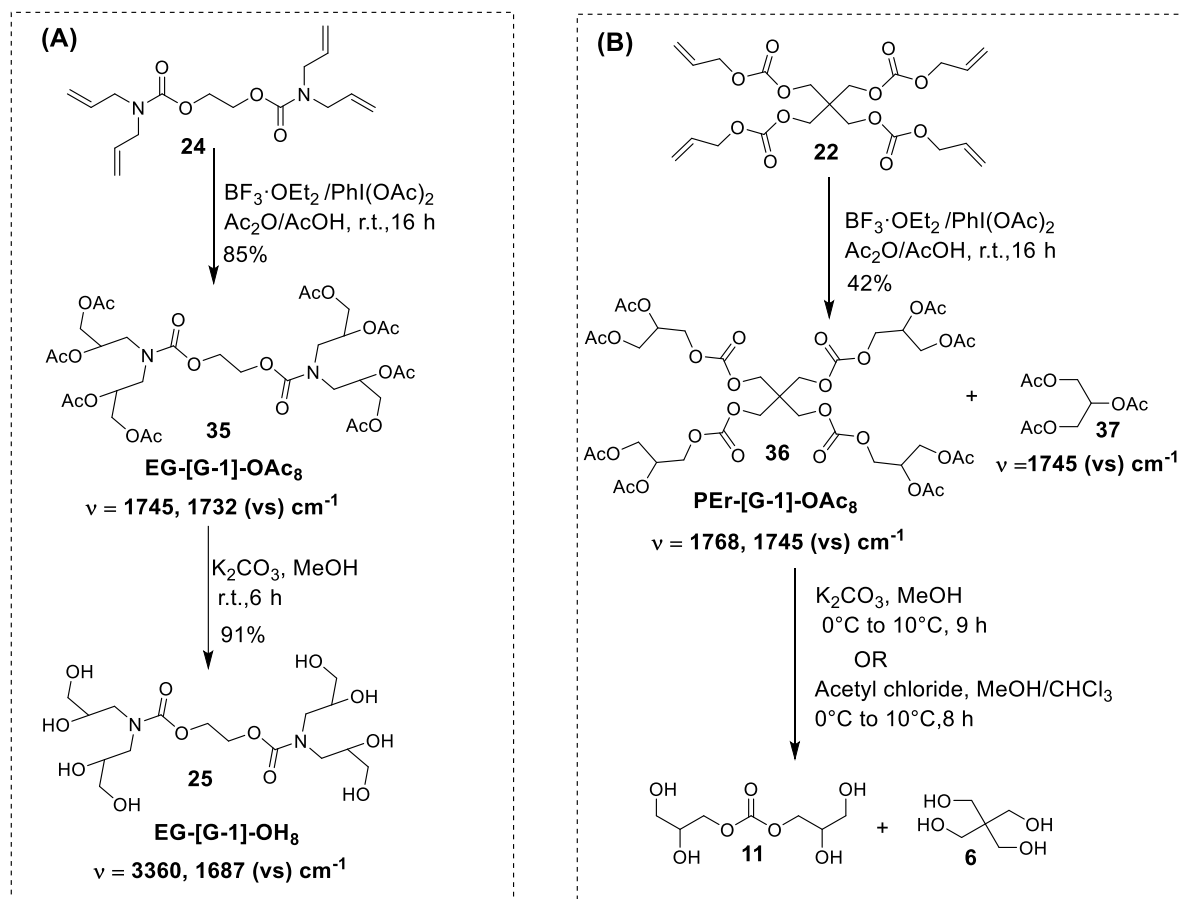
Subjecting **28** towards osmium-catalyzed dihydroxylation with NMO as co-oxidant gave tetrahydroxy dendron **29** in 91% yield (**Scheme 1.23**). Further, *O*-carbamoyl-allylation and *O*-carboxyloxy-allylation steps were performed effectively in a THF solvent system maintaining other reaction parameters same. Resulting crude dendrons **31** and **33** were subjected to column chromatography, to afford the pure product in high yields. Deprotection of step was best achieved in the presence of excess trifluoroacetic acid, producing HN-[G-1.5]-(allyl)_n dendrons **32** and **34** in 85% purified yield. Finally, the process of carbonylation was accomplished by coupling dendrons **32** and **34** with ethylene bis(chloroformate) to generate target EG-[G-1.5]-(allyl)_n dendrimers in relatively good yields.

III. Synthesis of [G-1] urethane/carbonate linked polyacetate dendrimers using achiral hypervalent iodine reagent

Even though the catalytic activity of osmium tetroxide towards the olefinic dihydroxylation is highly efficient and chemo selective, handling this reagent is extremely toxic and fatal in some cases. Hence, considering the fact, we thought of employing lower toxic hypervalent iodine reagent so called (diacetoxyiodo) benzene (**PIDA**) as alkene diacetoxyating agent, which upon deacetylation gives corresponding diol. To serve our purpose, we utilized the method reported by Li and co-workers^[107], for diacetoxylation of terminal and internal alkenes using PIDA in the presence of Lewis acid BF₃·OEt₂. As per report, reaction is selective, scalable and can be performed at room temperature with zero tolerance towards the other functional groups such as ester group.

We applied this reaction condition on two types of tera-allyl branched system i) urethane branched and ii) carbonate branched (**Scheme 1.24**). Typical reaction is carried out under anhydrous condition and at room temperature, utilizing 1 equiv. of PIDA and 0.1 equiv. of BF₃·OEt₂ per alkene. Using these molar calculations, initially we performed reaction with 1 equiv. of allyl compound, 4 equiv. of PIDA and 0.5 equiv. of BF₃·OEt₂. Reaction was monitored over TLC for a period of 12 h. TLC technique indicated consumption of starting material, along with formation of 2 product spot in case of **Scheme 1.24** (a) and 3 spot in case of **Scheme 1.24** (b). Further, assuming the reaction was incomplete, we thought of increasing the catalyst loading to another 0.3 equiv. and again monitored over a TLC. After another 12 h we observed single product spot for urethane-allyl system **24** and 2 spots for carbonate allyl system **22**. Finally, upon workup and purification by silica gel chromatography, **24** gave exclusively polyacetate **35** in 85% yield whereas carbonate allyl system **22** suffered from side reaction, affording target polyacetate **36** in 42% yield and side

triacetate product **37** in 45% yield. Next step was the deprotection of *O*-acetyl groups via acid or base hydrolysis. Hence, we subjected **35** and **36** towards base methanolysis, which resulted in urethane linked [G-1] polyol **25** in nearly quantitative yield. However, carbonate based polyacetates **36** faced degradation issue as seen earlier, exclusively generating degraded products. Similar results were obtained with acid catalysed methanolysis of **36**.

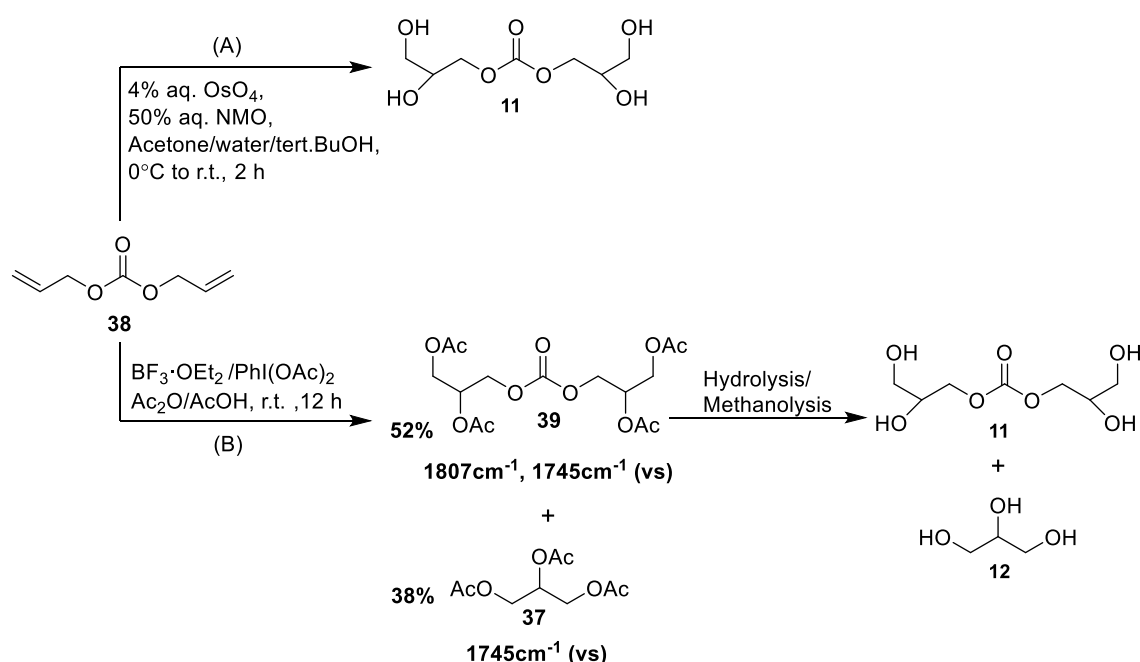


Scheme 1.24 Synthesis of (a) urethane and (b) carbonate based polyacetate dendrimers.

IV. Stability of linear allyl carbonate towards diacetoxylation-deacetylation and dihydroxylation

From the above studies, it is clear that carbonate linkages in polar, hydrophilic, branched polyol network are unstable and vulnerable towards nucleophilic attack, for e.g., by water and methanol. This is mainly due to presence of electrophilic carbonyl centre in carbonate functionalities, which are under the influence of polar glycerol fragment. Thus, beside external nucleophilic attack, carbonates groups also undergo intramolecular nucleophilic attack by primary hydroxyl of glycerol fragment. This intramolecular tetrahydroxy carbonate product **11** formed, is relatively stable under mild base conditions.

In this study, we wanted to prepare tetrahydroxy carbonate **11** from its diallyl carbonate **38** derivative (**Scheme 1.25**) and at the same time, we wish to investigate effect of diacetoxylation-deacetylation and dihydroxylation of alkenes over stability carbonate bond in linear allyl carbonate system. Dihydroxylation of diallyl carbonate **38** was carried out using osmium tetroxide catalyst and NMO as co-oxidant. Under this mild basic condition, we obtained tetrol bis-carbonate **11** in 91% yield, without formation of any degraded product such glycerol. However, for dicetoxylation condition using 2 equiv. of PIDA and 0.4 equiv. of $\text{BF}_3 \cdot \text{OEt}_2$, we observed formation degraded product **37** in nearly 40% yield, thereby reducing the yield of diacetoxylated product **39**.



Scheme 1.25 Synthesis of tetrahydroxy bis-carbonate via (A) dihydroxylation and (B) diacetoxylation-deacetylation route.

Furthermore, we performed deacetylation of **39** under various acid and base conditions and the results are given in table below.

Table 1.6 Deacetylation of tetra acetate bis-carbonate **39**.

Entry	Hydrolysis/Methanolysis conditions	Yield
1	K_2CO_3 , MeOH, 0 °C to 10 °C, 6 h	53% (11) and 40% (12)
2	Acetyl chloride, MeOH/ CHCl_3 (4:1), 0 °C to 10 °C, 8 h	75% (11) and 15% (12)
3	5% dil.HCl, 0°C to 10°C, 9 h	78% (11) and 10% (12)

Acid catalysed methanolysis of **39** afford target tetrahydroxy carbonate in 75% yield along with the formation degraded product **12** in low yield (**Table 1.6**, entry 2-3). Also, acid catalysed hydrolysis of **39** showed similar results, forming target tetrahydroxy compound in 78% yield and side product in 10% yield. On the contrary, methanolysis in the presence of K_2CO_3 as base leads to increase in the formation of degraded product, thereby reducing the yield of final tetrahydroxyl compound. Thus, overall study indicates that, carbonate bond in a rigid linear allyl system is tolerant towards nucleophilic attack under mild basic and acidic conditions as compared to branched system.

1.5 Conclusions

1. We have successfully transformed commercially available triols, amino diols, allyl alcohols/amines into branching AB /AB₂ monomers using 1-2 step functional group transformation protocols.
2. We have successfully synthesized first generation tetra acetal carbonate dendrimers by coupling 1,2-and 1,3-glycerol protected AB₂ monomers to 4-armed tetrahydroxyl core using *O*-carbonylation method. However, further attempt to prepare higher generation hydroxy terminated polycarbonate dendrimers is unsuccessful due to degradation of carbonate framework under acid and base catalysed activation step. Thus, we could not proceed with the divergent growth strategy outlined for synthesis of 1→2 *C* branched polycarbonate dendrimers.
3. Attempt towards the preparation of diethanol amine-ethylene glycol based AB₂ is unsuccessful, due to formation unwanted branched products. Hence, we could not proceed with our outlined accelerated divergent growth strategy for synthesis of carbonate-urethane dendrimers.
4. Finally, we have successfully implemented a protection-deprotection free strategy based on simple two step iterative process of carbonyl-allylation followed by dihydroxylation of allyl bonds, for the synthesis of PU/PC dendrimers. This strategy is the first of its kind to construct such aliphatic dendrimers with urethane backbone and dense olefinic periphery at lower generations.
5. Using this two-step approach, we have successfully demonstrated post generative synthetic induction 1→4 *C* branching motif in divergent as well as convergent growth routes. Functionalisation with allyl carbonates periphery results in urethane-carbonate framework providing further access to 1→2 *C* branching.
6. Remarkably, this allylated PC/PU dendrimers would serve as a useful multivalent scaffold platform for synthesis of higher generation hetero-functional dendrimers using classical as well as click-chemistry methods.
7. We have also successfully synthesized carbonate/urethane linked [G-1] polyacetate dendrimers using hypervalent Iodine reagent, which would be an alternative method to osmium catalysed dihydroxylation in activation step.
8. We have successfully characterised all intermediates and dendritic scaffolds using spectroscopic and mass spectrometry methods.

1.6 References

- [1] D. A. Tomalia, J. M. J. Fréchet, *J. Polym. Sci. Part A Polym. Chem.* **2002**, *40*, 2719–2728.
- [2] U. Boas, J. B. Christensen, P. M. H. Heegaard, *Dendrimers in Medicine and Biotechnology*, Royal Society Of Chemistry, Cambridge, **2007**.
- [3] D. A. Tomalia, A. M. Naylor, W. A. Goddard, *Angew. Chemie Int. Ed. English* **1990**, *29*, 138–175.
- [4] G. R. Newkome, C. N. Moorefield, F. Vögtle, *Dendrimers and Dendrons*, Wiley, **2001**.
- [5] G. R. Newkome, C. N. Moorefield, F. Vögtle, in *Dendrimers and Dendrons*, John Wiley & Sons, Ltd, **2001**, pp. 23–37.
- [6] P. J. Flory, *J. Am. Chem. Soc.* **1941**, *63*, 3083–3090.
- [7] P. J. Flory, *J. Am. Chem. Soc.* **1941**, *63*, 3091–3096.
- [8] P. J. Flory, *J. Am. Chem. Soc.* **1941**, *63*, 3096–3100.
- [9] P. J. Flory, *J. Am. Chem. Soc.* **1942**, *64*, 2205–2212.
- [10] W. H. Stockmayer, *J. Chem. Phys.* **1943**, *11*, 45–55.
- [11] W. H. Stockmayer, *J. Chem. Phys.* **1944**, *12*, 125–131.
- [12] P. J. Flory, J. Rehner, *J. Chem. Phys.* **1943**, *11*, 521–526.
- [13] W. W. Graessley, *Macromolecules* **1975**, *8*, 186–190.
- [14] W. W. Graessley, *Macromolecules* **1975**, *8*, 865–868.
- [15] K. Dušek, *Die Makromol. Chemie* **1979**, *2*, 35–49.
- [16] W. Burchard, *Macromolecules* **1972**, *5*, 604–610.
- [17] I. J. Good, *Math. Proc. Cambridge Philos. Soc.* **1949**, *45*, 360–363.
- [18] I. J. Good, *Proc. R. Soc. London. Ser. A. Math. Phys. Sci.* **1963**, *272*, 54–59.
- [19] E. Buhleier, W. Wehner, F. Vögtle, *Synth.* **1978**, *1978*, 155–158.
- [20] R. G. Denkewalter, J. Kolc, W. J. Lukasavage, *Macromolecular Highly Branched Homogeneous Compound Based on Lysine Units*, **1981**.
- [21] R. G. Denkewalter, J. Kolc, W. J. Lukasavage, *Preparation of Lysine Based Macromolecular Highly Branched Homogeneous Compound*, **1982**.
- [22] F. Vögtle, G. Richardt, N. Werner, *Dendrimer Chemistry*, Wiley-VCH Verlag GmbH & Co. KGaA, Weinheim, **2009**.
- [23] S. M. Aharoni, C. R. Crosby, E. K. Walsh, *Macromolecules* **1982**, *15*, 1093–1098.

- [24] D. A. Tomalia, H. Baker, J. Dewald, M. Hall, G. Kallos, S. Martin, J. Roeck, J. Ryder, P. Smith, *Polym. J.* **1985**, *17*, 117–132.
- [25] D. A. Tomalia, H. Baker, M. Hall, G. Kallos, S. Martin, J. Ryder, P. Smith, *Macromolecules* **1986**, *19*, 2466–2468.
- [26] G. R. Newkome, Z. Yao, G. R. Baker, V. K. Gupta, *J. Org. Chem.* **1985**, *50*, 2003–2004.
- [27] G. R. Newkome, G. R. Baker, S. Arai, M. J. Saunders, P. S. Russo, K. J. Theriot, C. N. Moorefield, L. E. Rogers, J. E. Miller, *J. Am. Chem. Soc.* **1990**, *112*, 8458–8465.
- [28] G. R. Newkome, Z. Yao, G. R. Baker, V. K. Gupta, P. S. Russo, M. J. Saunders, *J. Am. Chem. Soc.* **1986**, *108*, 849–850.
- [29] Y. H. Kim, O. W. Webster, *Polym Prepr* **1988**, *29*, 310–311.
- [30] Y. H. Kim, O. W. Webster, *J. Am. Chem. Soc.* **1990**, *112*, 4592–4593.
- [31] P. J. Flory, *J. Am. Chem. Soc.* **1952**, *74*, 2718–2723.
- [32] H. R. Kricheldorf, Q.-Z. Zang, G. Schwarz, *Polymer (Guildf)*. **1982**, *23*, 1821–1829.
- [33] C. R. Yates, W. Hayes, *Eur. Polym. J.* **2004**, *40*, 1257–1281.
- [34] C. Hawker, J. M. J. Fréchet, *J. Chem. Soc. Chem. Commun.* **1990**, 1010–1013.
- [35] C. J. Hawker, J. M. J. Fréchet, *Macromolecules* **1990**, *23*, 4726–4729.
- [36] C. J. Hawker, J. M. J. Fréchet, *J. Am. Chem. Soc.* **1990**, *112*, 7638–7647.
- [37] S. M. Grayson, J. M. J. Fréchet, *Chem. Rev.* **2001**, *101*, 3819–3868.
- [38] D. A. Tomalia, J. M. J. Fréchet, *Dendrimers and Other Dendritic Polymers*, John Wiley & Sons, Ltd, Chichester, UK, **2001**.
- [39] D. A. Tomalia, *Mater. Today* **2005**, *8*, 34–46.
- [40] C. Gao, D. Yan, *Prog. Polym. Sci.* **2004**, *29*, 183–275.
- [41] A. Carlmark, C. Hawker, A. Hult, M. Malkoch, *Chem. Soc. Rev.* **2009**, *38*, 352–362.
- [42] D. A. Tomalia, *Prog. Polym. Sci.* **2005**, *30*, 294–324.
- [43] M. Jikei, M. Kakimoto, *Prog. Polym. Sci.* **2001**, *26*, 1233–1285.
- [44] G. R. Newkome, E. He, C. N. Moorefield, *Chem. Rev.* **1999**, *99*, 1689–1746.
- [45] E. Abbasi, S. Aval, A. Akbarzadeh, M. Milani, H. Nasrabadi, S. Joo, Y. Hanifehpour, K. Nejati-Koshki, R. Pashaei-Asl, *Nanoscale Res. Lett.* **2014**, *9*, 247.
- [46] M. V. Walter, M. Malkoch, *Chem. Soc. Rev.* **2012**, *41*, 4593–4609.
- [47] M. A. Mintzer, M. W. Grinstaff, *Chem. Soc. Rev.* **2011**, *40*, 173–190.
- [48] J. D. amou. K. Twibanire, T. B. Grindley, *Polymers (Basel)*. **2012**, *4*, 794–879.

- [49] M. L. Mansfield, L. I. Klushin, *Macromolecules* **1993**, *26*, 4262–4268.
- [50] M. K. Bhalgat, J. C. Roberts, *Eur. Polym. J.* **2000**, *36*, 647–651.
- [51] Z. Lyu, L. Ding, A. Y.-T. Huang, C.-L. Kao, L. Peng, *Mater. Today Chem.* **2019**, *13*, 34–48.
- [52] S. J. Teertstra, M. Gauthier, *Prog. Polym. Sci.* **2004**, *29*, 277–327.
- [53] M. Gauthier, *J. Polym. Sci. Part A Polym. Chem.* **2007**, *45*, 3803–3810.
- [54] D. A. Tomalia, D. M. Hedstrand, M. S. Ferritto, *Macromolecules* **1991**, *24*, 1435–1438.
- [55] M. Gauthier, M. Moeller, *Macromolecules* **1991**, *24*, 4548–4553.
- [56] M. Malkoch, S. García-Gallego, in *Dendrimer Chem. Synth. Approaches Toward Complex Archit.*, Royal Society Of Chemistry, **2020**, pp. 1–20.
- [57] F. Wurm, H. Frey, *Prog. Polym. Sci.* **2011**, *36*, 1–52.
- [58] I. Gitsov, *J. Polym. Sci. Part A Polym. Chem.* **2008**, *46*, 5295–5314.
- [59] G. R. Newkome, G. R. Baker, M. J. Saunders, P. S. Russo, V. K. Gupta, Z. Yao, J. E. Miller, K. Bouillion, *J. Chem. Soc. Chem. Commun.* **1986**, 752.
- [60] I. Gitsov, K. L. Wooley, J. M. J. Fréchet, *Angew. Chemie Int. Ed. English* **1992**, *31*, 1200–1202.
- [61] A. D. Schlüter, J. P. Rabe, *Angew. Chemie Int. Ed.* **2000**, *39*, 864–883.
- [62] Y. Chen, X. Xiong, *Chem. Commun.* **2010**, *46*, 5049.
- [63] R. Freudenberger, W. Claussen, A.-D. Schlüter, H. Wallmeier, *Polymer (Guildf)*. **1994**, *35*, 4496–4501.
- [64] V. Percec, J. Heck, D. Tomazos, F. Falkenberg, H. Blackwell, G. Ungar, *J. Chem. Soc. Perkin Trans. 1* **1993**, 2799.
- [65] F. Vögtle, G. Richardt, N. Werner, in *Dendrimer Chem.*, John Wiley & Sons, Ltd, **2009**, pp. 25–48.
- [66] M. Sowinska, Z. Urbanczyk-Lipkowska, *New J. Chem.* **2014**, *38*, 2168.
- [67] U. Boas, J. B. Christensen, P. M. H. Heegaard, *J. Mater. Chem.* **2006**, *16*, 3785.
- [68] M. Maciejewski, *J. Macromol. Sci. Part A - Chem.* **1982**, *17*, 689–703.
- [69] P. G. de Gennes, H. Hervet, *J. Phys. Lettres* **1983**, *44*, 351–360.
- [70] G. R. Newkome, C. D. Shreiner, *Polymer (Guildf)*. **2008**, *49*, 1–173.
- [71] G. R. Newkome, C. Shreiner, *Chem. Rev.* **2010**, *110*, 6338–6442.
- [72] E. M. M. de Brabander-van den Berg, E. W. Meijer, *Angew. Chemie Int. Ed. English*

- 1993**, 32, 1308–1311.
- [73] C. J. Hawker, J. M. J. Fréchet, *J. Am. Chem. Soc.* **1992**, 114, 8405–8413.
- [74] K. L. Wooley, C. J. Hawker, J. M. J. Fréchet, *J. Am. Chem. Soc.* **1991**, 113, 4252–4261.
- [75] T. Kawaguchi, K. L. Walker, C. L. Wilkins, J. S. Moore, *J. Am. Chem. Soc.* **1995**, 117, 2159–2165.
- [76] H. Ihre, A. Hult, J. M. J. Fréchet, I. Gitsov, *Macromolecules* **1998**, 31, 4061–4068.
- [77] K. L. Wooley, C. J. Hawker, J. M. J. Fréchet, *Angew. Chemie Int. Ed. English* **1994**, 33, 82–85.
- [78] V. S. K. Balagurusamy, G. Ungar, V. Percec, G. Johansson, *J. Am. Chem. Soc.* **1997**, 119, 1539–1555.
- [79] F. Morgenroth, *Chem. Commun.* **1998**, 1139–1140.
- [80] R. Spindler, J. M. J. Fréchet, *J. Chem. Soc., Perkin Trans. 1* **1993**, 913–918.
- [81] F. Zeng, S. C. Zimmerman, *J. Am. Chem. Soc.* **1996**, 118, 5326–5327.
- [82] V. Maraval, R. Laurent, P. Marchand, A.-M. Caminade, J.-P. Majoral, *J. Organomet. Chem.* **2005**, 690, 2458–2471.
- [83] M. Arseneault, C. Wafer, J.-F. Morin, *Molecules* **2015**, 20, 9263–9294.
- [84] G. Franc, A. K. Kakkar, *Chem. Soc. Rev.* **2010**, 39, 1536.
- [85] P. Antoni, D. Nyström, C. J. Hawker, A. Hult, M. Malkoch, *Chem. Commun.* **2007**, 2249–2251.
- [86] P. Antoni, M. J. Robb, L. Campos, M. Montanez, A. Hult, E. Malmström, M. Malkoch, C. J. Hawker, *Macromolecules* **2010**, 43, 6625–6631.
- [87] S. P. Rannard, N. J. Davis, *J. Am. Chem. Soc.* **2000**, 122, 11729–11730.
- [88] M. Malkoch, K. Schleicher, E. Drockenmuller, C. J. Hawker, T. P. Russell, P. Wu, V. V. Fokin, *Macromolecules* **2005**, 38, 3663–3678.
- [89] B. Bruchmann, F. Wingerter, H. Graf, S. Wolff, *Highly Functionalized Polyurethanes*, **1995**, US5981684A.
- [90] H. W. I. Peerlings, R. A. T. M. Van Benthem, E. W. Meijer, *J. Polym. Sci. Part A Polym. Chem.* **2001**, 39, 3112–3120.
- [91] L. Degoricija, P. N. Bansal, S. H. M. Söntjens, N. S. Joshi, M. Takahashi, B. Snyder, M. W. Grinstaff, *Biomacromolecules* **2008**, 9, 2863–2872.
- [92] R. T. Taylor, U. Puapaiboon, *Tetrahedron Lett.* **1998**, 39, 8005–8008.
- [93] D. S. Jones, M. E. Tedder, C. A. Gamino, J. R. Hammaker, H.-T. Ton-Nu,

- Tetrahedron Lett.* **2001**, *42*, 2069–2072.
- [94] W. J. Feast, S. P. Rannard, A. Stoddart, *Macromolecules* **2003**, *36*, 9704–9706.
- [95] A. Stoddart, W. J. Feast, S. P. Rannard, *Soft Matter* **2012**, *8*, 1096–1108.
- [96] J.-K. Lee, Y.-W. Suh, M. C. Kung, C. M. Downing, H. H. Kung, *Tetrahedron Lett.* **2007**, *48*, 4919–4923.
- [97] M. Ballico, S. Drioli, G. M. Bonora, *European J. Org. Chem.* **2005**, *2005*, 2064–2073.
- [98] D. H. Bolton, K. L. Wooley, *Macromolecules* **1997**, *30*, 1890–1896.
- [99] D. H. Bolton, K. L. Wooley, *J. Polym. Sci. Part A Polym. Chem.* **2002**, *40*, 823–835.
- [100] P. Löwenhielm, H. Claesson, A. Hult, *Macromol. Chem. Phys.* **2004**, *205*, 1489–1496.
- [101] Z. Zheng, M. Luo, J. Yu, J. Wang, J. Ji, *Ind. Eng. Chem. Res.* **2012**, *51*, 3715–3721.
- [102] S. K. Karmee, *Synth. Commun.* **2013**, *43*, 450–455.
- [103] Y. Suzuki, K. Kowata, Y. Komatsu, *Bioorg. Med. Chem. Lett.* **2013**, *23*, 6123–6126.
- [104] J. S. Yadav, M. Satyanarayana, S. Raghavendra, E. Balanarsaiah, *Tetrahedron Lett.* **2005**, *46*, 8745–8748.
- [105] M.-Y. Huang, J. Lin, Z.-J. Huang, H.-G. Xu, J. Hong, P.-H. Sun, J.-L. Guo, W.-M. Chen, *Medchemcomm* **2016**, *7*, 658–666.
- [106] V. K. Mandrekar, G. Chourasiya, P. C. Kalsi, S. G. Tilve, V. S. Nadkarni, *Nucl. Instruments Methods Phys. Res. Sect. B Beam Interact. with Mater. Atoms* **2010**, *268*, 537–542.
- [107] W. Zhong, J. Yang, X. Meng, Z. Li, *J. Org. Chem.* **2011**, *76*, 9997–10004.
- [108] S. J. Meunier, Q. Wu, S.-N. Wang, R. Roy, *Can. J. Chem.* **1997**, *75*, 1472–1482.
- [109] P. Dupau, R. Epple, A. A. Thomas, V. V. Fokin, K. B. Sharpless, *Adv. Synth. Catal.* **2002**, *344*, 421–433.
- [110] A. D. Shetgaonkar, V. S. Nadkarni, *ChemistrySelect* **2019**, *4*, 12210.
- [111] A. I. Longshaw, F. Adanitsch, J. A. Gutierrez, G. B. Evans, P. C. Tyler, V. L. Schramm, *J. Med. Chem.* **2010**, *53*, 6730–6746.

Chapter 2

Synthesis, characterization and biodegradation studies on sulfur containing linear and crosslinked aliphatic polycarbonates

2.1 Introduction

Polycarbonates (PCs) are important class of synthetic organic polymers containing repeated carbonate [-O-(C=O)-O-] linkages (**Figure 2.1**) in its main chain backbone. PCs are broadly classified into two types i.e., Aliphatic polycarbonates (APCs) and Aromatic polycarbonates. Currently, they are one of the most versatile and commonly available thermoplastic polymers with applications ranging from high-end engineering materials to biomaterials^[1].

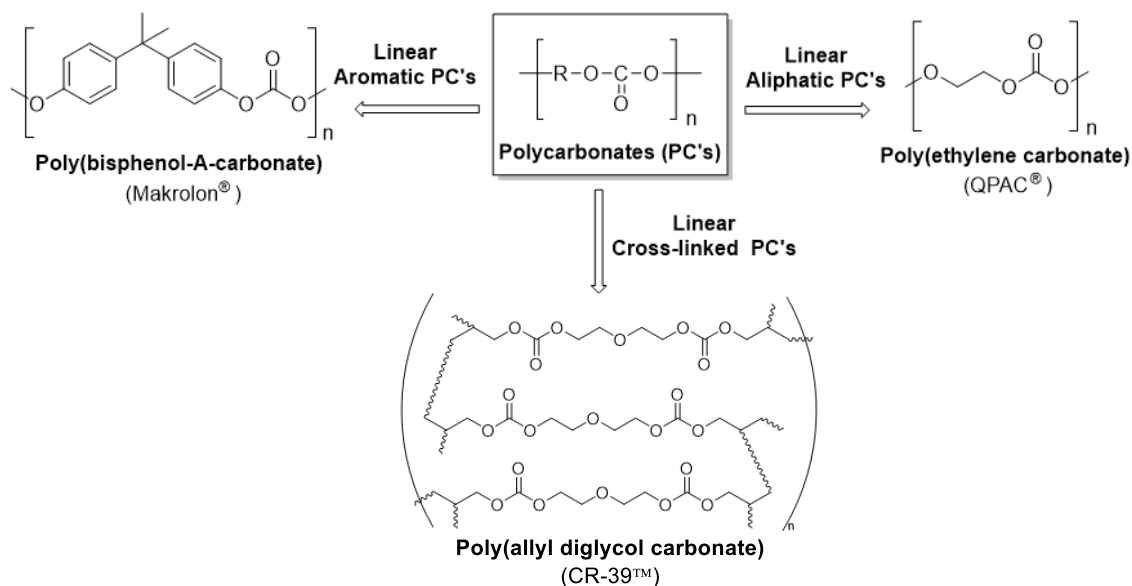


Figure 2.1 Classification of polycarbonates.

Commonly employed synthetic routes for preparation of polycarbonates include phosgene condensation, transesterification, ring-opening polymerization (ROP) and CO₂/epoxides polymerization^[2]. Most of the Bisphenol A (BPA) based PCs have been currently manufactured in the Interfacial phosgene process^[3]. This process has some advantages including easy synthesis, modest reaction conditions, and excellent properties of products. However, it suffers from drawbacks such as the usage of highly toxic phosgene and chlorinated solvents. In recent years, industries are focussing on developing environmentally benign synthetic processes for BPA based PCs including use of carbon dioxide as a phosgene alternative from viewpoint of green chemistry and reduction of greenhouse gases^[4]. Aliphatic polycarbonates are commonly prepared using ring opening polymerization (ROP) of cyclic carbonates. For this purpose, various sized functional cyclic carbonates have been synthesised based on corresponding diols and catalyst/initiators for ROP mechanisms^[5]. Advantage being control on polymerization, high polymerization rates and most highlighting is the formation of functionalised aliphatic polycarbonate backbone for

polymer modification. The polycarbonate chemistry has been extensively developed globally as indicated by comprehensive study of PCs by Brunelle^[6,7] and review articles by others^[8,9].

Among all PCs, linear aromatic polycarbonates especially BPA based, have garnered special attention in terms of large-scale commercial production and utilization. This due to its high performing characteristics such high thermal capabilities, extreme toughness and enhanced optical clarity. Hence, BPA based PCs are successful engineering plastics ranging its utility from small consumer products to automotive and construction businesses^[10]. In contrast to aromatic PCs, linear aliphatic PCs have received limited attention from industries due to its low thermal capacities and hydrolytic stability.

For past few decades, aliphatic polycarbonates have gained increasing interest in biomedical applications due to their biodegradability, low toxicity and biocompatibilities. Hence, then seen draw backs such as low glass-transition temperatures, degradability and elasticity, have turned into competitive advantages over other commercial polymers^[11]. Also, aliphatic PCs derived from CO₂^[9] and biomass-based^[12] materials are under limelight, looking at as promising substitute for the present-day non-renewable source derived plastics. Its current industrial applications are limited to low molecular weight PC polyols, macromonomers for polyurethanes and other copolymers production.

2.1.1 Historical events in research and development of commercial PC's

Birnbaum and Lurie^[13] first reported the synthesis of Polycarbonate by polycondensation of resorcinol with phosgene in the presence of pyridine as solvent. Further, this phosgene method was extended to hydroquinone by Einhorn^[14]. Attempts were also made to prepare PCs from catechol which led to five membered cyclic carbonates only. A few years later, Bischoff and Hendenström^[15] synthesized similar aromatic PCs using method of solventless transesterification between bisphenols and diphenyl carbonate (DPC). The hydroquinone polymer was brittle, crystalline, insoluble in most solvents, and with melting range >280°C. The PCs from resorcinol were glassy and brittle, also it crystallizes from solution and melts in range of 190–200°C. However, both these PCs were apparently of low molecular weight, proving difficulties in further processing and development on commercial scale. In fact, research on polycarbonates^[2,6] was lacking in the literature for nearly about 30 years after this initial discovery of aromatic PCs.

Later in early 1930s, Wallace Carothers laboratory^[16,17] at DuPont initiated the preparation of aliphatic polycarbonates. They employed two methods for preparation: direct

transesterification of alkyl diols with diethyl carbonate and ring opening polymerization of low molecular weight cyclic PCs with approach of distillative transesterification-depolymerization. Work was further extended to 1940s, where 1,6-hexanediol based polycarbonates were synthesized via transesterification method with dibutyl carbonate^[18]. This aliphatic PCs were waxy solids, low melting, low molecular weight and prone to hydrolysis, which were considered inferior to the properties exhibited by many other polymers such as polyamide, polyesters, poly (methyl methacrylate) mainly developed for fibre application in that era. Hence, APCs were not only remained unexplored commercially but at the same lack attention from research field as well until 1990s.

In 1941, the Pittsburgh Plate Glass Co. (PPG)^[19] commercially introduced a first crosslinked polycarbonate thermoset resin known as poly (allyl diglycol carbonate) (PADC) or CR-39, for eye glass lenses. This was developed by its subsidiary, Columbia-Southern Chemical Corporation as 39th formulation of thermosetting plastic. Thus, it was designated and commercially made available as Columbia Resin # 39 (CR-39). Homopolymer was prepared by peroxide-initiated free radical polymerization of allyl diglycol carbonate (ADC) tetrafunctional monomer. CR-39 resin showed enhanced scratch resistance and optical properties^[20]. PADC was the first polycarbonate plastic which was made commercially available. Currently it is also sold under a various trade- names such as PM-500TM, LanTrak[®], Homalite H-911, etc.

Later in 1950s, with the increasing commercial demands for new polymeric materials, the chemistry of aromatic polycarbonates was revisited, wherein two corporate groups H. Schnell^[21,22] of Bayer AG (Germany) and D. W. Fox at General Electric Company (USA) independently discovered a bisphenol A (BPA) polycarbonate and its derivatives from 4,4'-dihydroxydiaryllkanes. For preparation, both transesterification using DPC and interfacial phosgene polycondensation methods were examined. However, PCs produced using transesterification method suffers from various drawbacks such as poor resin colour, low thermal stability, low hydrolytic resistance and lower molecular weight.

BPA based aromatic PCs exhibited excellent properties such as extreme toughness, elevated glass transition temperature, solvent resistance and optical transparency. Among all derivatives Bisphenol A polycarbonate proved superior and cost effective. Bayer AG, was the first to report the properties of polycarbonates series with patents issuing as early as 1954. After a period of litigation process, U.S. patents were issued to Bayer AG for an interfacial process for polycarbonates preparation along with multiple claims to various polycarbonates^[23]. GE was issued patent for transesterification process and resulting

polycarbonate product^[24]. Bayer AG started commercial production of BPA based PCs under trade name Makrolon[®] in Germany, 1958 and United states in 1960. At the same time, General Electric begun its U.S. commercial production under trade name Lexan[®] in 1960. Since then, extensive research was carried out on process development of polycarbonates.

In 1993, GE Plastic Japan^[25,26] developed a new transesterification process for polycarbonates called as melt process. Here, condensation process between BPA and DPC was performed under a melt state without any solvents. This process resulted in colourless and high molecular-weight polycarbonates. Since this initial process, the various new developments were made in the melt process and till date have been successfully used as alternatives for the interfacial processes. Although Bayer AG and GE remains the principal producers, at least 50 new PCs producing companies have patented some aspect of polycarbonate chemistry. Currently, BPA polycarbonates are commercially available under various trade names such as Lexan[™], Makrolon[®], Calibre[®], Panlite[®], Novarex[®], etc. Millions of tons of BPA-based PCs are currently manufactured and utilized globally every year.

As mentioned above, aliphatic PCs had less commercial interest because of their modest properties. In 1968, Inoue et al.^[27,28] introduced a direct synthesis method for aliphatic PCs by one-step copolymerization of carbon dioxide and oxirane such as propylene oxide. Recently, this process has garnered special attention from industries for commercial production of poly (ethylene carbonate) and poly (propylene carbonate). These aliphatic PCs are sold under trade name of QPAC[®]25 and QPAC[®]40 by Empower Materials Inc. as world cleanest thermal decomposable binder. Here, manufacturers are working on green chemistry concept of direct fixation of carbon dioxide into polymeric system thereby reduction of greenhouse gas effects.

In recent years, some engineering thermoplastic PCs have been developed based on alicyclic rigid diols^[10]. Among this aliphatic PCs prepared from biomass derived diols such as Isosorbide (a sugar derivative) have been successful produced on commercial scale. In 2012 Mitsubishi Chemical Co.^[29] became the first one to commercialized bio-based PC under trade name DURABIO[™] and later by Teijin Ltd. under the trade name PLANEXT[®], mainly derived from Isosorbide (ISB) monomer. This ISB based PCs^[30] are high engineering thermoplastics which currently serve as commercial replacement for non-renewable plastic such as BPA-PCs. At present, industries are working on developing such bio-engineering thermoplastic PCs based on bioderived rigid monomer as an alternative to fossil fuel source.

2.1.2 Properties of aliphatic polycarbonate's

A) Linear aliphatic PC's (APC's)^[2]

PCs derived from acyclic diols are generally semicrystalline and elastic structure with oily or crystalline appearance. They are low melting (<120°C), low heat resistances and low tensile strengths. APCs are easily soluble in common organic solvents such as chloroform, methylene chloride, benzene, acetone, and acetic acid. On the other hand, these polymers are insoluble in alcohols, ethers, or aliphatic hydrocarbons. Many of these polymers are prone to biodegradation due to flexible aliphatic backbone. APCs derived from rigid, bulky cyclic aliphatic diols are amorphous and high melting. They exhibit useful properties such as high glass transition temperature (120-150°C)^[10], high scratch resistance and are stable under weathering conditions. Also, these APCs are relatively resistance to hydrolytic degradation as compared to the acyclic derivatives. However, these rigid based APCs show poor performance towards chemical, impact resistance and also difficulties in biodegradation^[31]. They have high solubility towards organic solvents. In recent years, researchers have developed a stereoregular polymerization for APCs derived from carbon dioxide and epoxides that have enhanced the melting points and mechanical strength of polymers. They also generally possess low gas permeabilities.

B) Cross-linked aliphatic PCs^[32]

PCs derived from diallyl carbonate monomers are densely crosslinked, thermosetting and amorphous in nature. They exhibit high mechanical, scratch resistance and excellent optical properties. Among this, CR-39 or PADC polymer is most commercially explored and popular thermosetting PC material. It is known for its superior optical properties compare to all other plastic materials and has refractive index of 1.501. Polymer material is transparent to visible light and absorbs several wavelengths in the UV and IR spectral ranges. Combining optical properties (similar to glasses) with high abrasion resistance and light weight ($d = 1.32 \text{ g/cm}^3$) makes polymer highly suitable to utilize as durable lens material. CR-39 lenses are resistant to heat distortion up to 130°C and thus can be used continuously at such elevated temperatures. Also, this polymer is highly resistant to welding sparks, where glasses fail to tolerate such heat sparks. CR-39 polymer has a high resistance against acids (except oxidizing acids) and alkali and insoluble in the most the common organic solvents. Also, it is resistant to other chemicals, aging, and material fatigue.

2.1.3 Methods for synthesis of polycarbonates

I. Linear polycarbonates

Synthesis of linear PCs are primarily carried out using following well established methods^[2]:

1. Phosgene condensation process (interfacial and solution phase synthesis)
2. Bulk transesterification process (melt phase synthesis)
3. Oxidative carbonylation process
4. Ring opening polymerization (ROP) of cyclic carbonate monomers
5. CO₂ insertion process

The processes (1), (2), (3) and (4) can be utilized to produce both aromatic and aliphatic PCs whereas method (5) has been exclusively applied for APCs synthesis in current scenario.

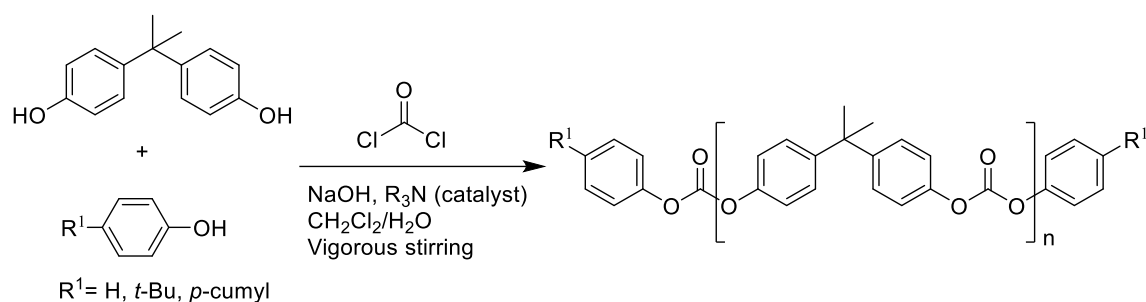
1. Phosgene condensation process (Interfacial and Solution phase polymerisation)

This polymerization process utilizes carbonyl halides and diols as monomeric materials. The interfacial synthesis is conducted in a two-phase, separated liquid systems i.e., organic solvent and water, with the reaction occurring at the interface of two phases. Among the various carbonyl halides, phosgene is the most reactive, and the reaction between phosgene and aromatic diols proceeds efficiently even at room temperature and yielding high-molecular-weight polymer. This is the most widely practiced method for commercial production of BPA polycarbonates.

Interfacial process^[3,6] is performed by reacting phosgene³ gas with slurry of aq. NaOH, bis-phenols and dichloromethane, in the presence of catalytic amount of organic base such as trialkylamine or pyridine. In a typical process, ionic species formed reside in the aqueous phase, while oligomeric product are transferred to the organic phase. As reaction proceeds at aqueous-organic interface, molecular weight of the oligomers continues to grow in the organic phase. Mechanistically, the reaction proceeds through acylammonium salt, which enhances the reaction rates, resulting in high molecular weight polymers. The reaction is usually over-phosgenated in order to ensure complete consumption free phenolic groups and excess phosgene is hydrolysed forming sodium carbonate. If a reaction is performed in the presence of phase transfer catalyst instead of amine bases, reaction utilizes 1-2% of excess phosgene. To control molecular weight of growing polymer, monophenolic chain terminators such phenol, *p-t*-butylphenol, or *p-cumyl*phenol, are often added to a reaction mixture to end the chain extension. The pH of the reaction must be carefully controlled throughout the process, because high pH can lead to hydrolysis of phosgene, intermediate

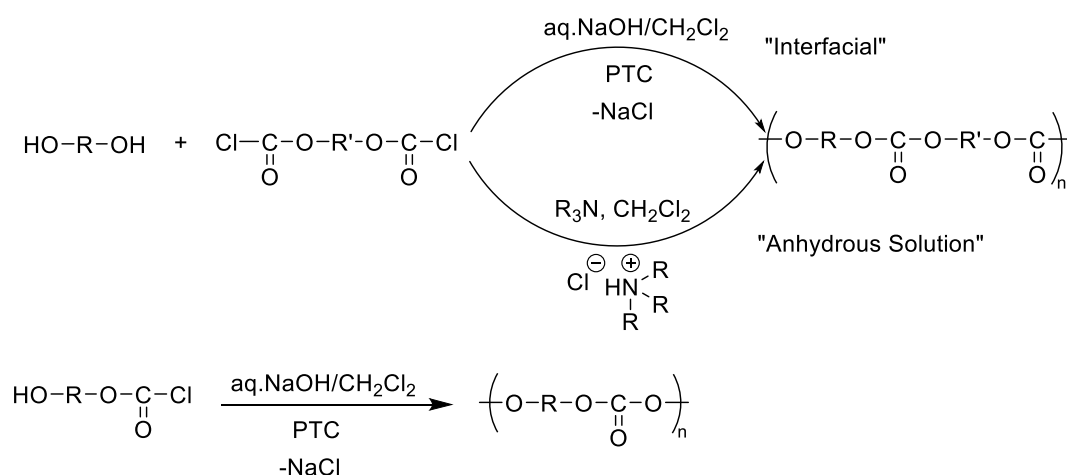
chloroformates, or PC itself, whereas low pH results in very slow reaction rates and residual amount of chloroformates.

Reaction is stopped by separating the aqueous brine layer, washing organic layer with aq. acid and water. The polycarbonate product in dichloromethane is purified by various techniques such as steam crumbing, anti-solvent precipitation, devolatilization, etc.^[33]. This interfacial process, readily produces a transparent PC with molecular weights of 20,000-1,50,000 Da and polydispersities typically range from 2.2 to 2.8. The typical process is shown in **Scheme 2.1**.



Scheme 2.1 Interfacial synthesis of BPA Polycarbonates.

Bischloroformates^[3] and monochloroformates of diols are also applicable as carbonyl halides in the polymerization (**Scheme 2.2**). When interfacial synthesis is performed with equimolar quantities of bischloroformate and bisphenol in the presence of PTC, an alternating polymer are achieved. On the contrary, in the presence of amine catalyst's reaction generates more of random polymers, due to hydrolysis reactions, thereby forming free phenols.



Scheme 2.2 Interfacial Solution phase synthesis of Co-polycarbonates.

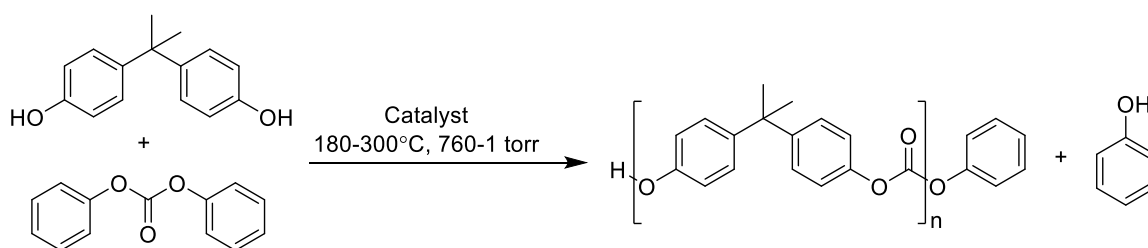
Under anhydrous solution phase process^[3], polymerization is conducted with equimolar amounts of carbonyl halides (bischloroformate or phosgene) and bisphenols in

the presence of two or more equivalents of tertiary amine to absorb generated HCl. Care must be taken to control the temperature, since the acylammonium salts formed in the reaction are susceptible to side reaction, leading to a urethane and alkyl chloride. At laboratory scale it is convenient to use phosgene alternatives such as diphosgene, triphosgene, and resulting bischloroformates.

2. Bulk transesterification process (melt and liquid phase polymerization)

Transesterification synthesis^[2] uses organic carbonate and diols as starting materials and polycondensation is performed at elevated temperatures with elimination alcohols. The melt process involves base-catalysed transesterification reaction between diols and organic carbonates such as dialkyl/diaryl carbonates in a molten state. In a typical BPA-based PC synthesis, diphenyl carbonate (DPC) is used as organic carbonate (**Scheme 2.3**). Other carbonate source, such as dimethyl carbonates, cannot be used due to high reaction temperature and reduced pressure.

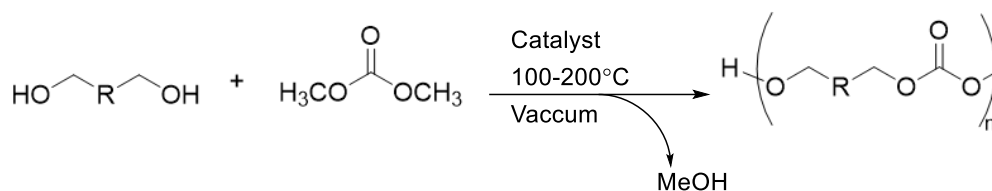
In the initial stage of the reaction, diphenyl carbonate and BPA are reacted with small amounts (<0.01%) of basic catalyst such as Na, K, Li, tetraalkylammonium, or tetraalkylphosphonium hydroxides or carbonates in a melt reactor^[6]. A slight stoichiometric excess of DPC is employed to achieve high molecular weight and also to compensate for any minor loss caused due to devolatilization from the reactor. As the starting materials pass through the stages of reaction, the temperature of reaction is increased and higher vacuum is employed in order to facilitate removal of the phenol by-product, driving the equilibrium toward polycarbonates. In final stages, the polymer melt becomes highly viscous, thus specialized equipment's such as wiped film evaporators, helicone reactors, multiple vacuum-vent extruders are used to facilitate mass transfer of phenol by-product through surface renewal of the melt. When a desired melt viscosity is achieved, the polymerization is terminated by cooling the reactor to ambient pressure or end capping the polymer chain by the addition of phenyl moieties, which can be achieved up to 60-90%^[3].



Scheme 2.3 Synthesis of BPA-PC by Melt phase polycondensation.

The melt process is employed to manufacture high quality, low to medium molecular weight PCs, especially optical grade. Further high molecular weight PCs can be achieved from prepolymer using solid state polymerization (SSP)^[1,3]. In this method, PC prepolymer ($M_w = 2000\text{--}20\,000$ Da) are heated above their glass transition temperature but below its melting temperature under reduced pressure or in a stream of an inert gas. This process facilitates high chain mobility, preventing PC to melt and merge, affording excellent quality polymers.

Transesterification process is an alternative industrial method to interfacial synthesis and offers several advantages beside elimination of solvents and toxic phosgene^[6]. PCs of narrow polydispersity are produced due to lower equilibrium levels of low molecular weight species. Least involvement of impurities such as salts, amines, solvents etc. In melt synthesis, PCs can also be pelletized directly without any prior washing.



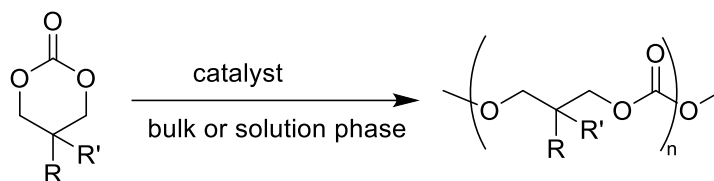
Scheme 2.4 Synthesis of aliphatic PCs by transesterification.

Bulk transesterification method^[34–36] is also employed to prepare high molecular weight APCs, from dialkyl carbonates and aliphatic diols in two-step process. With a development of novel $\text{TiO}_2/\text{SiO}_2$ -poly (vinyl pyrrolidone)-based catalyst (TSP-44), high weight-average molecular weight ($M_w = 166,000$ Da) and narrow polydispersity (≤ 1.86) APCs were achieved namely, poly (butylene carbonate), poly (pentamethylene carbonate), and poly (hexamethylene carbonate)^[11]. Hence, transesterification process is preferred method to produce high molecular weight aliphatic homo and copolymers.

3. ROP of cyclic carbonate monomers

ROP^[11] of cyclic carbonates is the most effective and practiced method for the synthesis of aliphatic polycarbonates with good reproducibility, control molecular weights with narrow PDI and improved mechanical properties. The polymerization is living type, with typical initiation and propagate steps and forms medium to high molecular weight polymer with active chain ends without formation of any by-product. The most commonly used cyclic carbonates for ROPs are the 5 and 6-membered ring monomers^[5] (**Scheme 2.5**), which undergo enthalpy driven ring opening polymerization due to ring strain. Contrary strain-

less macrocyclic carbonates such cyclic dimer, trimer, etc follows entropy driven ROP to produce high molecular weight PCs^[37,38].



Scheme 2.5 Synthesis of APC using Ring opening polymerization.

ROP can be performed in the melt or in solution phase following various mechanisms namely, cationic, anionic, coordination–insertion, enzymatic, monomer and initiator dual activation. Several catalysts are available for the ROP of cyclic carbonates such as transition-metals, alkyl halides, basic/acidic organocatalysts and enzyme catalysts. Organic base catalysts, tertiary amines, amidines, guanidines, phosphazenes, *N*-heterocyclic carbene, thiourea (TU)/ amines, and the organic acid catalysts diphenyl phosphate, sulfonic acid, and triflic acid (TFA) are found to be very effective catalysing ROP^[11].

Melt polymerization of the BPA cyclic macrocycles^[39,40] can be achieved at 200–300°C and solution polymerization at ambient temperature. Here, ROP is entropy driven, leading to high molecular weight polymer ^[2] ($M_w \geq 700000$ Da) and PDI reaches to 2.0. especially in melt phase synthesis. Since the melt viscosity of PC is very high, techniques such as pultrusion, resin-transfer molding has been employed to produce reinforced polymers. Bulk ROP of aliphatic cyclic carbonates under different ring opening pathways resulted in high molecular weight polymers ($M_w \geq 150000$ Da) with PDI less than 2 at temperature 100-130°C^[8].

APCs are of special interest in biomedical applications due to their controlled polymer structure and slow hydrolytic degradation. Diverse availability functional 6-8 membered cyclic carbonates^[41] allow an effective way to incorporate various functionalities in polycarbonate backbone controlling the molar mass and PDIs by changing the monomer/initiator ratio. Additionally, ROP is one of the best routes to produce copolymers with a tunable property depending on application.

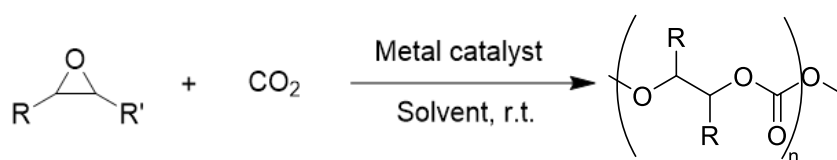
4. CO₂ insertion process (copolymerization process)

Carbon dioxide is the most abundant, cheap and renewable carbon resources on planet earth and also vast quantities of CO₂ are generated every day worldwide. Technologies for the chemical utilization of CO₂ have been widely developed, not only from the point of innovative materials but also for fixing environmental issues. In PC synthesis ^[2], carbon

dioxide has potentially used as carbonyl source for generation of carbonate functionalities. So far, researchers have proposed the following CO₂ based methods for direct PC synthesis: (1) Copolymerization of CO₂ with cyclic ethers, and (2) Polycondensation of CO₂ with aliphatic dihalides.

i) Copolymerization of CO₂ with cyclic ethers

Till date, the selective conversion of CO₂ and epoxides into degradable PCs has been regarded as a promising greener and sustainable route to polycarbonates production. This copolymerization technique ^[11] was first introduced by Inoue et al. in 1969, using zinc compound as catalyst. Since its discovery, this method has become one of the most well-studied and pioneering technologies for the large-scale utilization of CO₂ in any chemical synthesis.



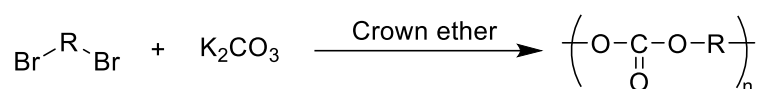
Scheme 2.6 Synthesis of APC using copolymerization of carbon dioxide with epoxides.

In a typical synthetic route, zinc catalyst was prepared by the equimolar reaction between diethylzinc and water and subsequent polymerization was performed in an autoclave using pressurized CO₂ (5.0 MPa), epoxide, dioxane as a solvent and catalyst at room temperature. The resulting PC has a sufficiently high molecular weight ($M_w = 50$ -150KDa) and composed of an alternating copolymer structure. Mechanistically, copolymerization was triggered by epoxide ring opening with metal catalyst, followed by CO₂ insertion into newly generated metal-oxygen bond. Process is repeated in alternating fashion to the active terminal of the growing polymer chain. Other than ZnEt₂-H₂O catalyst, number of active homogeneous metal catalysts have been reported, including zinc-phenoxide derivatives, aluminium-porphyrin complex, β -diiminate-zinc catalysts, chromium and cobalt salen catalysts. Among this, cobalt salen catalytic system were found most efficient and reactive under mild conditions (e.g., 0.1 MPa CO₂ pressure) and generating copolymers with more than 99% carbonate linkages with excellent regiochemical control. Unlike catalyst various epoxide were examined for copolymerization including propylene oxide, epichlorohydrin's, cyclohexene oxide, styrene oxide, indene oxide, limonene oxide and oxetane. Five-membered cyclic ethers do not show copolymerization reactivity with CO₂.

Glass transition temperatures of poly (propylene carbonate) (PPC) and poly (cyclohexene carbonate) are 30–40°C and 110–120°C, respectively. Poly (ethylene carbonate) and PPC display biodegradability. Most of these APCs are amorphous, and have low tensile strengths and heat resistances, thus they lack in practical applicability.

ii) Polycondensation of CO₂ with aliphatic dihalides

In this method^[2], organic dihalides, such as aliphatic dibromides condense with potassium carbonate in the presence of phase-transfer catalysts, such as crown ether, to produce PCs as shown **Scheme 2.7**.



Scheme 2.7 Synthesis of APC using polycondensation of CO₂ with aliphatic halide.

This polycondensation occurs in a solid-liquid binary phase. Crown ethers namely 18 crown-6 are commonly used as phase-transfer catalysts, yielding low molecular weight PCs.

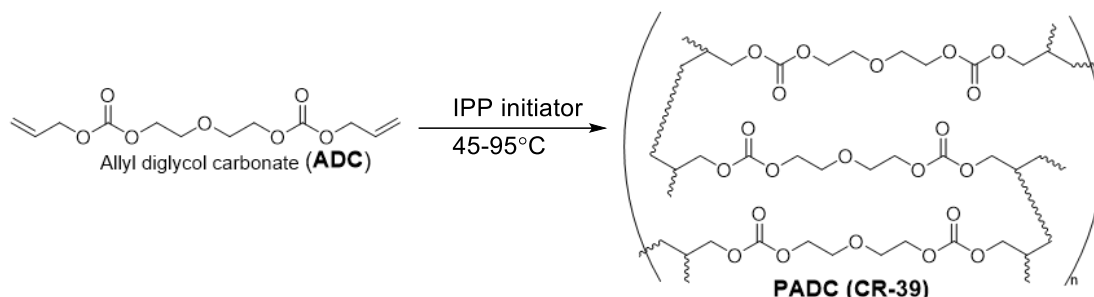
II. Cross-linked aliphatic polycarbonates

Cross-linked PCs are synthesized using following methods:

i. Radical addition polymerization of allylic carbonate monomers

Compared to vinylic counterparts, allyl monomers show slower reactivity towards radical polymerization^[42,43]. This is mainly due to the presence of active allylic hydrogen next to ethylic group, which under degradative chain transfer reaction which terminates the growing polymer chain, producing resonance stabilized allyl radical inefficient in propagating polymer chain. This is called as auto inhibition process, which influence the molecular weight of the polymer and lowers the number of crosslinks. Hence, the mono-allyl monomers result in viscous liquids having low degree of polymerization. However, allylic monomers having two or more allylic groups could efficiently produce hard crosslinked solid resin, inspite of degradative chain transfer. Like other allylic monomers, allylic carbonates too undergo radical induced addition polymerization. Using a suitable radical initiator, and curing condition, polyfunctional allyl monomer is successfully transformed to thermoset homopolymer. CR-39 is the product of the radical initiated homo-polymerization of the polyfunctional monomer i.e., allyl diglycol carbonate (ADC) monomer. The two most widely used radical initiators are benzoyl peroxide (BP) and IPP (diisopropyl peroxydicarbonate). BP is less volatile with higher decomposition temperature as compared to IPP. Also, CR-39 prepared from BP has a higher yellowness index^[32].

In typical polymerization process, generated radicals initiate the polymerization process by reacting with olefinic bonds. Resulting chain radicals propagates the process to produce a three-dimensional cross-linked network consisting of polyallyl chains interconnected by alkene ether carbonate links (**Scheme 2.8**).



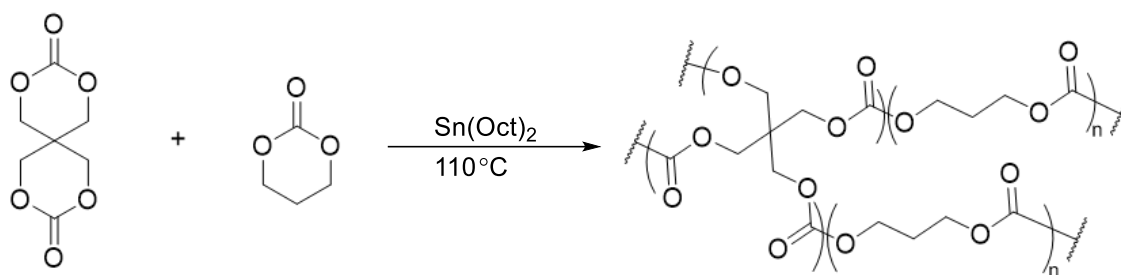
Scheme 2.8 Synthesis of cross-linked ADC polycarbonate using radical polymerization.

The average length of polyallyl chains is relatively short (DP~ 80) due to degradative chain transfer and polymerization does not reaches 100% conversion because the polymer system enters the glassy state first, leaving unreacted allyl functions in a viscous cluster^[32]. Resins are cured maximum at 95°C using IPP initiator for 12 and 24h using control heating program and polymerization is usually conducted using casting technique in a rectangular or square shaped mold.

ii. Ring opening polymerization using multifunctional crosslinkers

Here, degradable cross-linked polycarbonates^[44] are synthesized using two approaches: 1) one-pot reaction, via the copolymerisation of monomers with cross-linkers and 2) multi-step methods by crosslinking PC prepolymers with cross-linkers. One-step methods eliminates the processing steps and allow direct conversion of monomers to cross-linked PCs.

In a one-step methodology, cross-linked aliphatic polycarbonates were obtained via ROP of bifunctional cyclic carbonate in the presence of tetrafunctional cross-linking agents (ether linked bis(cyclic carbonates)^[45,46], spiro-bis (cyclic carbonate)^[47] and Sn(Oct)₂ (**Scheme 2.9**). Co-polymerisations were carried out in bulk at 110-130°C, to afford crosslinked PC network ranging from elastomeric amorphous to strong low crystalline.



Scheme 2.9 Synthesis of cross-linked aliphatic polycarbonate using one pot ROP of trimethylene carbonate in the presence of crosslinker.

Multistep approach^[44] is an alternative to above method and allows fine tuning of prepolymer in order to impart specific properties to target cross-linked polycarbonate. In a typical method, linear or branched polycarbonate prepolymer is synthesized first using ROP of cyclic carbonates with diol or triols in the presence of metal catalyst. The obtained prepolymer is further reacted with multifunctional crosslinker such as bis(cyclic carbonates), acrylates to either obtain cross-linked network via ROP or photo induce radical polymerization^[48]. The resultant PC materials exhibits excellent elastomeric properties such as low moduli and high strength.

2.1.4 Applications of linear and crosslinked polycarbonates

➤ Aromatic PCs based on BPA^[2,33]

BPA-based PCs are high engineering thermoplastic materials having broad range of application, such as:

- **Optical applications**

PC are used as support material in optical information media such CDs, DVDs. Application demands for PC with light scattering $<0.3 \text{ cd/m}^2$, transparency $>87\%$ spectral light transmission and yellow index <4.5 . In the CDs, data is stored in the form of microscopic pits, which as are transcribed on the PC substrate using a compression-assisted injection moulding technique. Other application includes lens material and automobile light cover.

- **Construction and housing:**

Commercial grade PCs such as CALIBRE 600 and 302 are specially formulated for fabrication of sheets, which are used in construction applications such as laminated walls, windows, IR-reflective insulation and skylight roofing. Other uses of PC sheet include household applications such as table and desk cover.

- **Electrical and electronic applications**

PC is used extensively in electrical and telecommunication devices where heat resistance and toughness are needed. Furthermore, special grades of PC for e.g., CALIBRE 800 having an ignition-resistant additive package and impact modifiers are specifically formulated for these applications.

- **Automotive applications**

BPA based PC finds demanding application in automotive sector due to their combine properties of transparency, high toughness and heat resistance. Examples of such applications includes, instrument panels, windscreens, head lamp covers and housings, windscreens, etc. Furthermore, in order to enhance the properties additives such as UV, ignition resistance components are added, considering sunlight exposure and fire hazards.

- **Aliphatic polycarbonates**

Although, most of APCs could not match the high performing properties of aromatic PCs, they still find potential applications in biomedical sector, due to their controlled biodegradability, biocompatibility and tunable mechanical and chemical properties. Biomedical application includes tissue engineering scaffolds, biodegradable elastomers, hydrogels, drug-delivery carriers in the form of micelles and biomedical devices.

- **Drug delivery nanocarriers**^[8,50]

Among several biodegradable polymeric drug delivery systems, APCs attains special interest, due to their excellent biocompatibility, non-toxic degradation products, and ease of functionalization. Like other amphiphilic drug delivery, APC amphiphiles are composed short block hydrophobic (polycarbonate) and long block hydrophilic (PEG) component, which can be further self-assembled into two nanocarrier systems: 1) Micelles and 2) Polymersomes. Micelles allow loading of only hydrophobic drug to hydrophobic polycarbonate through physical encapsulation whereas polymersomes can encapsulate both hydrophilic as well as hydrophobic drugs. Various block or grafted copolymer APCs are reported to enhance drug-loading capacity and selective drug release to targeted tissues appearing in several reviews.

- **Hydrogels**^[11]

Hydrogels are cross-linked 3D polymeric networks with the intrinsic ability to absorb/hold water up to 99% of their weight. This unique feature and the capability to readily tune their mechanical properties make the materials applicable in the area of personal care products, cell encapsulation, ophthalmic prostheses, and tissue regeneration. APCs themselves are typically hydrophobic; thus, copolymerization with hydrophilic component result in APC-

based hydrogels. Various physically and chemically crosslinked APC-based hydrogels are reported with altering mechanical properties, hydrophobicities, and degradation profiles. In early reports, APC based hydrogels were prepared using ROP of cyclic carbonates using bis- (cyclic carbonate)-PEG macromonomer. Non-covalently crosslinked APC based hydrogels were achieved using non-covalent interaction such as ionic and hydrogen bonding between chemical functionalities in amphiphilic network. Photopolymerization has evolved as an alternative strategy for in situ hydrogel preparation generating a strong network,

- **Medical devices and cell culture scaffolds**^[8]

Tough tissue engineering scaffolds based on cross-linked APCs were prepared using solvent casting, electrospinning, sintering, and 3D printing techniques. Among them, Stereolithography (SLA) a 3D printing technique has been widely used for preparation of a well-defined porous matrix and biomimetic scaffold based on APC. In this method, photo-cross linkable APC macromonomer is subjected to solidification upon irradiation with laser beam. Upon computer-controlled program, sequential photo-crosslinking of the layers through the masks was performed to generate a 3D structure. This scaffold system has been employed for cartilage regeneration, microvascular grafts, orbital floor implants, and bone regeneration.

- **Optical and nuclear track etching application**^[32]

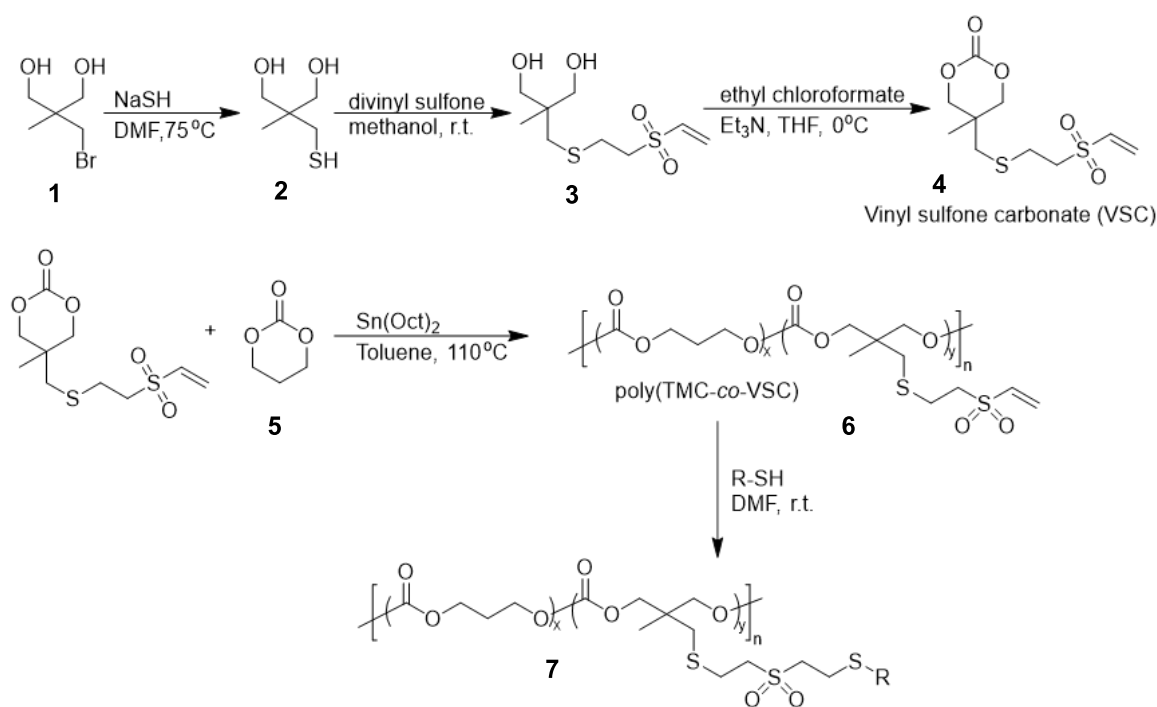
Highly crosslinked APC such as CR-39 polymer are widely used for casting transparent sheets and optical lenses due to their excellent scratch resistance, impact strength, and superior optical properties. Due to their high durability these materials are used for manufacturing of sport-action lenses. Other applications of this materials are Cokin filter systems, molding materials, electric devices of high resistance, and flame-retardant materials. Also, an alternate use of such polymers is widely recognized in nuclear track etching technology, such as porous membrane manufacturing and dosimetry of protons, neutrons and heavy ions.

In track etching method, thermoset APC material is irradiated with energetic charge particles, resulting in formation of linear damaged tracks across the irradiated area of polymer film. Further, these tracks are transformed into pores using a selected wet chemical etchant.

2.2 Literature review on sulfur containing linear and crosslinked aliphatic polycarbonates

Among various functional APCs, sulfur functionalized polycarbonates have emerged as an important class of biomaterials with targeted applications in controlled drug delivery, inflammation targeting and biomedical devices. Such sulfur based linear APCs are mainly synthesised using ring opening polymerization of cyclic carbonate^[50], post-polymerization modification^[51], CO₂/epoxide copolymerization^[52] and step growth polymerization via thio-ene chemistry, which will be discussed herewith.

Wang et al.^[53] reported a versatile and robust synthesis of vinyl sulfone functionalized biodegradable APC copolymer using Sn(Oct)₂ catalysed ring opening polymerization of newly designed vinyl sulfone carbonate (VSC) cyclic monomer **4** with trimethylene carbonate **5**. VSC monomer was prepared using series of synthetic steps as shown in **Scheme 2.10**.

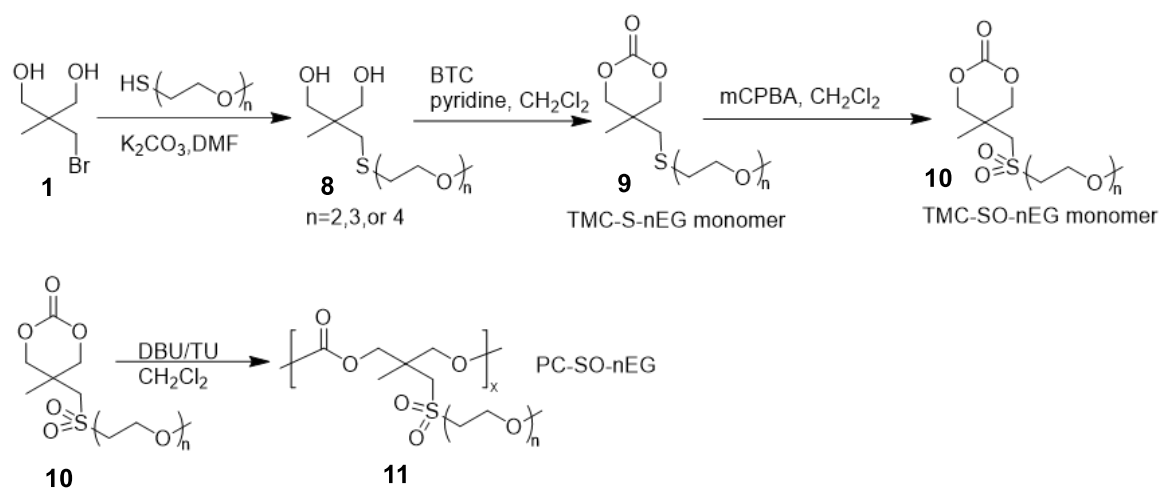


Scheme 2.10 Synthesis of vinyl sulfone carbonate monomers and its PC copolymer.

VSC monomer **4** was also copolymerized with ϵ -caprolactone and L-lactide to afford copolymers with controlled molecular weight and functionalities. Additionally, post polymer functionalization was carried out using Michael type addition of thiol-containing molecules (e.g., 2-mercaptoethanol, cysteine, cystamine, GRGDC, PEG-SH, etc.) to vinylic sulfone functionality without any catalyst under mild condition, thereby providing access to

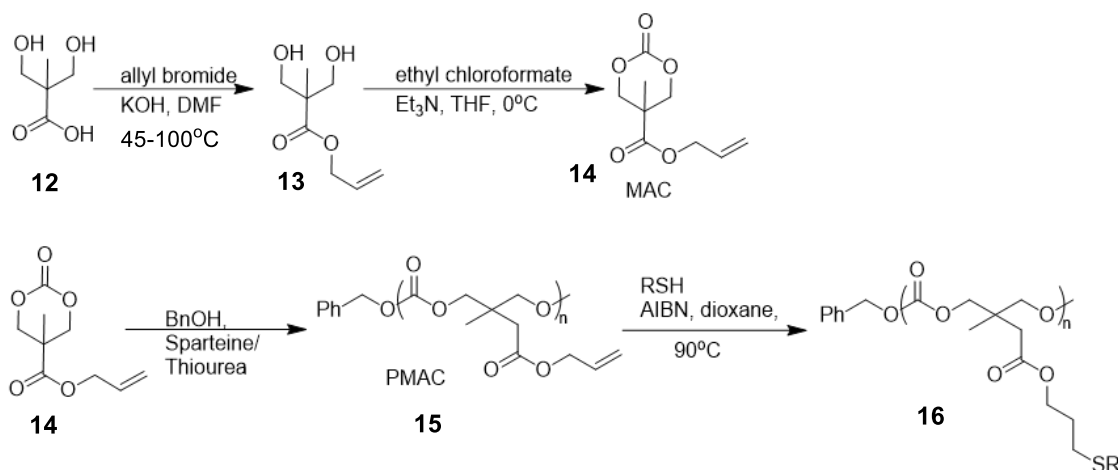
advanced functional biopolymers **7**. Coatings of VS based PCs allows efficient, and clean surface functionalization in aqueous conditions, and thus opens new path way towards functionalized medical implants and tissue scaffolds. The preliminary cell culture studies showed that VS-functionalized poly(VSC-*co*-CL) film is non-toxic and biocompatible.

Yu et al.^[55] reported series of thermoresponsive copolycarbonates using organo-catalytic ring opening of cyclic trimethylene carbonate (TMC) monomers bearing oligo ethylene glycol (OEG), connected through thioether or/and sulphone functionalities **9** and **10**. Synthetic steps involve in monomer synthesis is shown in **Scheme 2.11**. Author utilized 1,8-diazabicyclo[5.4.0]undec-7-ene(DBU)/*N*-(3,5-trifluoromethyl)phenyl-*N*-cyclohexylthiourea (TU) as the organic catalyst with 1,4-benzenedimethanol as initiator. This PC-OEGs with varying OEG chain lengths, thioether and sulfone **11** linkages were studied for lower critical solution temperature (LCST) properties over a temperature range of 0 °C to 46 °C (3 g L⁻¹ in aqueous solution). Also, Polycarbonates were subjected to cytotoxicity assay, indicating low little toxicity. PC-OEGs with hydrophobic thioether linkages showed LCST at low temperature whereas hydrophobic sulfone polymers showed relatively high temperatures. With unique properties, this APC were directed as promising candidates for biomedical applications.



Scheme 2.11 Synthesis of TMC-SO-nEG monomer and its PC polymer.

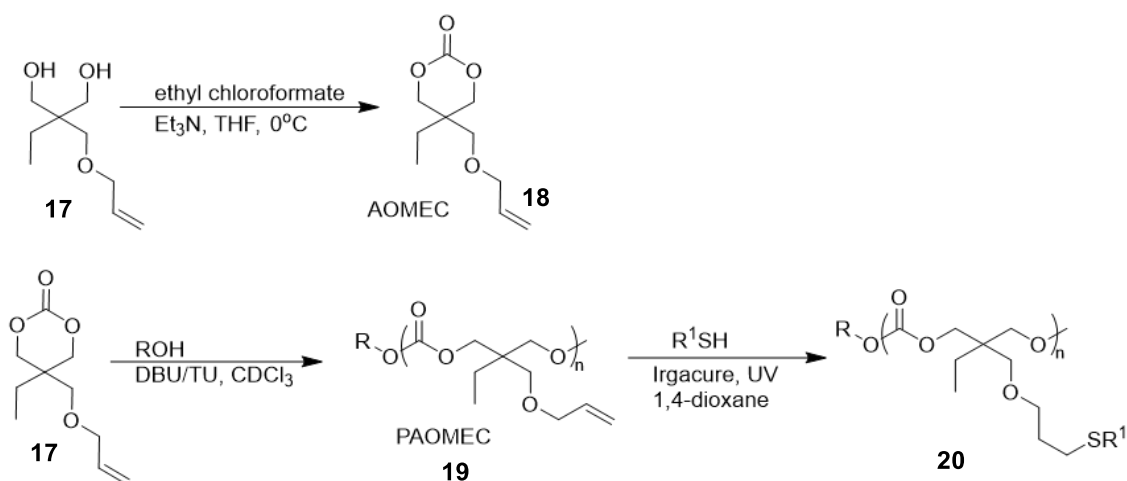
Tempelaar et al.^[55] reported synthesis of allyl-functionalized PC homopolymer **15** using ring opening polymerization of 5-methyl-5-allyloxycarbonyl-1,3-dioxan-2-one (MAC) **14** cyclic carbonate in the presence of bifunctional organo-catalytic system 1-(3,5-bis(trifluoromethyl)phenyl)-3-cyclohexylthiourea/(-)-sparteine. Telechelic and Block copolymer were prepared using 1,3-propanediol, 2-hydroxyethyl disulfide and poly(ethylene oxide) initiators.



Scheme 2.12 Synthesis of MAC monomer and PC polymer.

The resultant allyl ester-functional polymers showed low polydispersities and high end-group fidelity. Post polymer functionalization was performed via radical initiated addition of thiols to pendant allyl groups to afford range of functional PCs **16** through mild and selective routes.

Thomas et al.^[56] reported series of APCs homopolymer bearing pendent allyl ether groups **19**, using dual organocatalytic ROP methodology of 2-allyloxymethyl-2-ethyltrimethylene carbonate (AOMECE) **18** cyclic carbonate monomer. 1,8-diazabicyclo [5.4.0] undec-7-ene (DBU) and 1-(3,5-bis(trifluoromethyl)-phenyl)-3-cyclohexylthiourea (TU) were used as organocatalytic system with alcohol as initiator (**Scheme 2.13**).

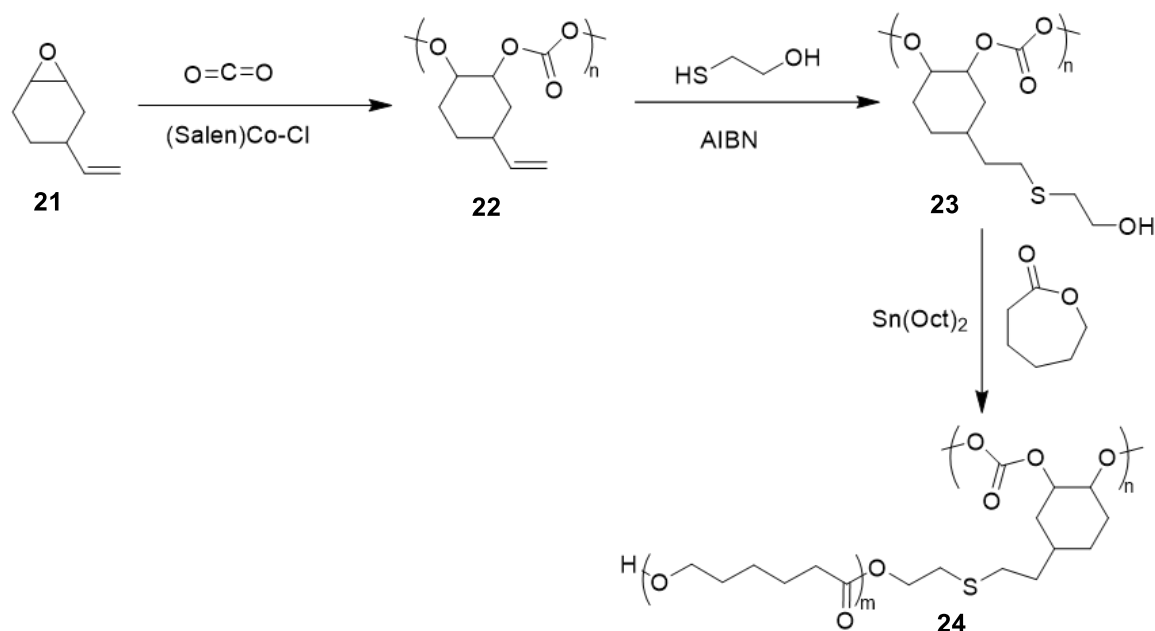


Scheme 2.13 Synthesis of AOMECE monomer and PC polymers.

Post-polymer functionalisation of PAOMECE **19** with thiol substrates were conducted using photo-initiated radical thiol-ene coupling reactions, to afford thermoresponsive APC graft

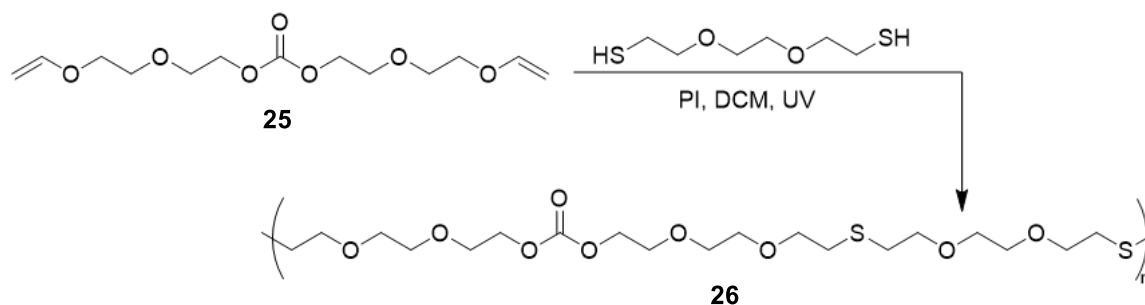
polymer **20**. Functionalization with thiol-terminated PEG substrate results in PCs exhibiting lower critical solution temperature (LCST).

Zhang et al.^[57] reported synthesis of aliphatic polycarbonate with hydroxyl side groups (**23** and **24**), which was used as precursor for preparation brush copolymers with well define structure and almost 100% grafting density. This approach involved three steps: 1) living alternating copolymerization of carbon dioxide/4-vinyl-cyclohexene-1,2-epoxide catalysed by (salen)Co(III)Cl complex without using any cocatalysts, 2) thiol-ene click functionalization of side vinyl group to hydroxyl group and 3) ring opening polymerization of ϵ -Caprolactone (ϵ -CL) initiated by side hydroxyl groups to afford a PCL side chain (**Scheme 2.14**). Both the backbone and side chain of this brush copolymers are degradable and biocompatible.



Scheme 2.14 Synthetic route towards brush copolymers with polycarbonate as backbone and polycaprolactone as side chains.

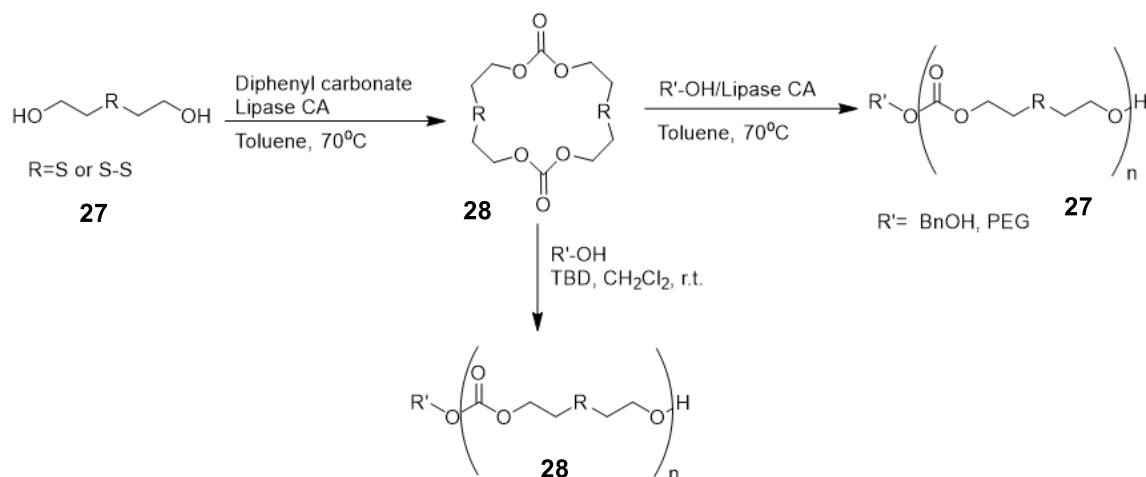
Sarapas and Tew^[58], reported a novel approach to afford main chain carbonate and thioether functionalized polymers using a step growth thio-ene polymerization at ambient temperature. In this method, carbonate functionalized divinyl ether and triethylene glycol dithiol monomers are polymerized using photoinitiated thio-ene click chemistry (**Scheme 2.15**). Also, this approach is an efficient way to incorporate thioether and carbonate linkages into polymer main chain, differing from conventional methods, which mainly involves side chain functionalization either through monomer design or post polymer modification.



Scheme 2.15 Photo initiated step growth thio-ene polymerization.

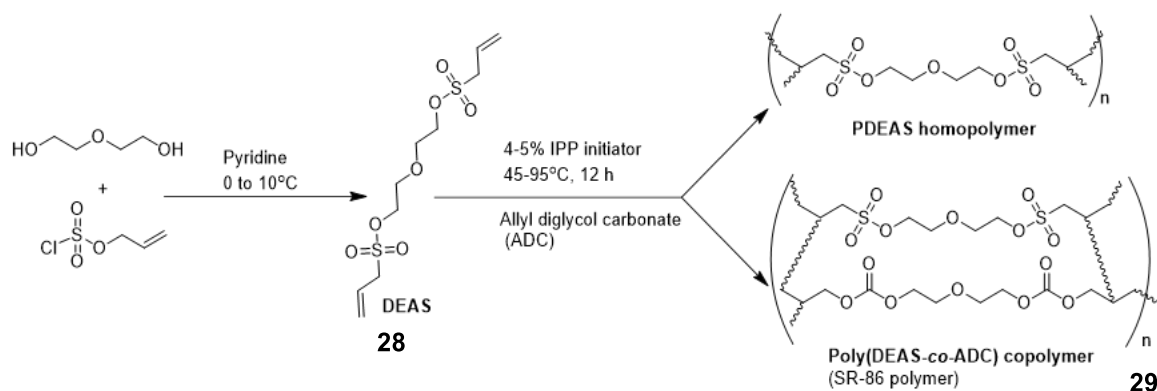
Additionally, the redox properties of thioethers makes resulting polymer redox active, at the same time varies the polymer polarity and solubility with controllable oxidation of thioethers to either sulfoxide or sulfone.

Recently, Lang and Zhang research group reported series of main chain sulfur functionalized homo and copolycarbonates using enzyme and organocatalysed ROP of sulfur based macrocyclic carbonate, for target application as ROS-responsive nanocarriers in cancer treatment. Thioether and disulfide macrocyclic carbonate monomers **28** were synthesized using enzyme (lipase CA) catalyze intermolecular cyclization of 2,2'-thiodiethanol and 2-hydroxyethyl disulfide **27** with diphenyl carbonate^[59] (**Scheme 2.16**). Using the same enzyme, ROP of macrocycles was performed using alcohol as initiator in toluene. PEG monomethyl ether macro-initiator results in amphiphilic thioether block copolymer **27**, which self-assembles into well define nanostructure displaying excellent reactive oxygen species (ROS) responsiveness^[60]. Also, this diblock copolymers showed negligible cell toxicity, proving its biocompatibility. ROP of thioether^[61] and disulfide^[62] macrocycles were performed in more effective and controlled manner using 1,5,7-triazabicyclo[4.4.0] dec-5-en (TBD) as organic catalyst and alcohol as initiator in dichloromethane solvent. Further, they were also copolymerized with various cyclic esters and carbonate to afford polymers with tunable properties. Above ROP methods fetched sulfur-based APC homopolymer **28** and copolymers, with predictable molecular weight, narrow polydispersivities and control copolymer compositions.



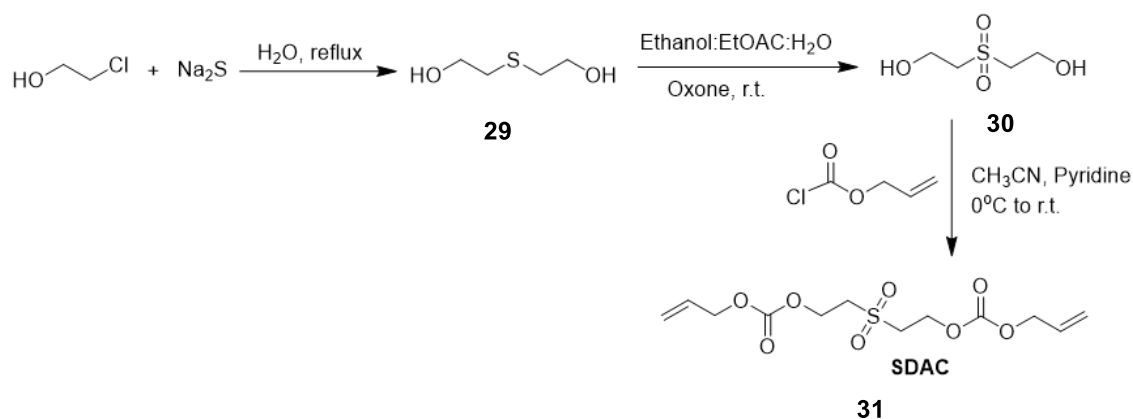
Scheme 2.16 synthesis and ROP of sulfur functionalized macrocyclic carbonate.

Most of the sulfur containing cross-linked APCs are synthesized either in one step or multi-step approach using radical polymerization^[44,63]. Highly cross-linked hard thermoset APCs containing sulfonate, sulfone functionalities have been reported for application in charge particle detection. These hard resins are mainly obtained using one step radical polymerization of sulfonate/sulfone functionalized allyl monomers in the presence of peroxide initiators and under control heating^[64]. Till date, this are the most radiation sensitive materials available as polymeric nuclear track detectors (PNTDs). Fuji et al.^[65] reported sulfonate functionalized allylic monomer, namely diethylene glycol bis (allyl sulfonate) (DEAS) **28** and was copolymerized with allyl diglycol carbonate (ADC) in a ratio of 10:90 [SR-86 (10)] and 20:80 wt% [SR-86 (20)] using 5% IPP initiator (**Scheme 2.17**). These copolymers were used as PNTDs. Mandrekar et al.^[66] extended Fuji's work and synthesized homopolymer of DEAS and also several copolymers with ADC **29** in the higher concentration of DEAS. Two sets of copolymers were prepared using 4% IPP and 5% BP initiator using 12 h constant rate heating profile. This DEAS-ADC copolymer were highly sensitive towards charge particle detection but short shelf life.

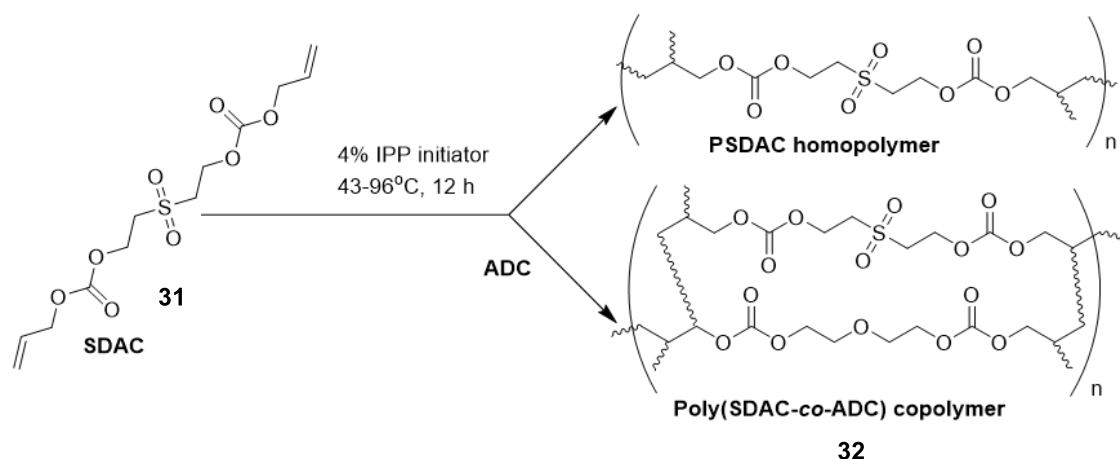


Scheme 2.17 Radical homo and copolymerization of DEAS.

Recently, Naik and Nadkarni^[67] reported main chain sulfone containing APCs using one step radical induced bulk polymerization of newly designed monomer 2,2'-sulfonyldiethanol bis (allyl carbonate) (SDAC). SDAC monomer **31** was prepared using three synthetic steps (**Scheme 2.18**) and subsequently homo and copolymerised **32** with ADC using 4% IPP initiator under 12 h constant heating rate (**Scheme 2.19**). Acquire polymer films were tested for track detection application. All polymers were highly sensitive, stable, optically clear and had a longer shelf life.

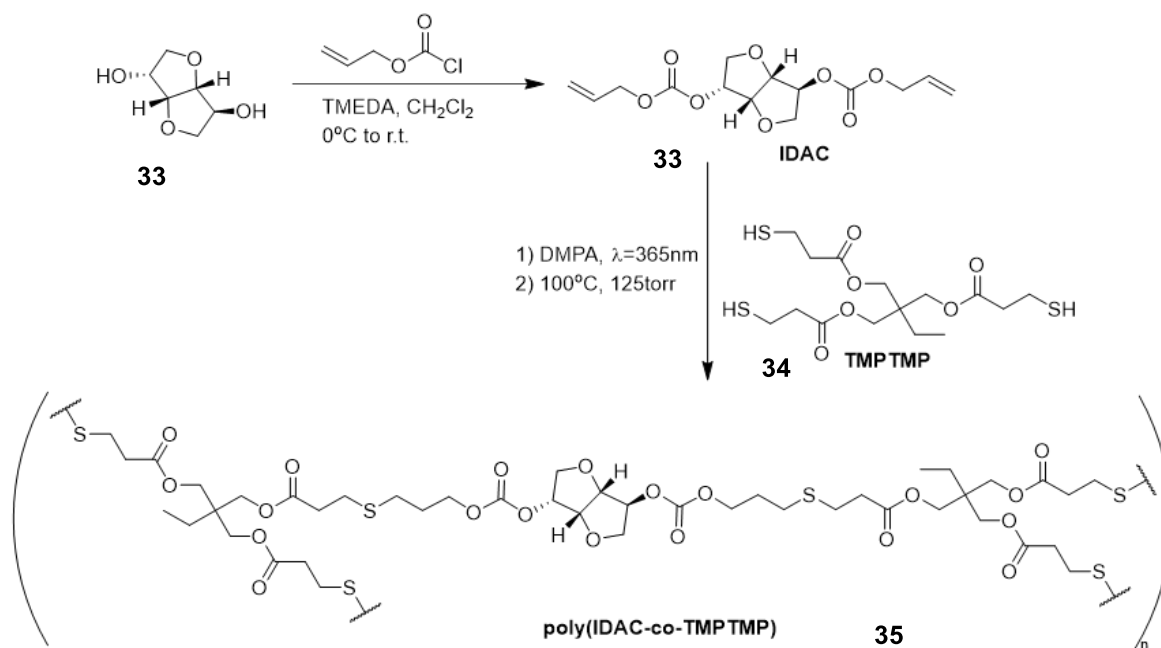


Scheme 2.18 Synthesis of SDAC monomer.



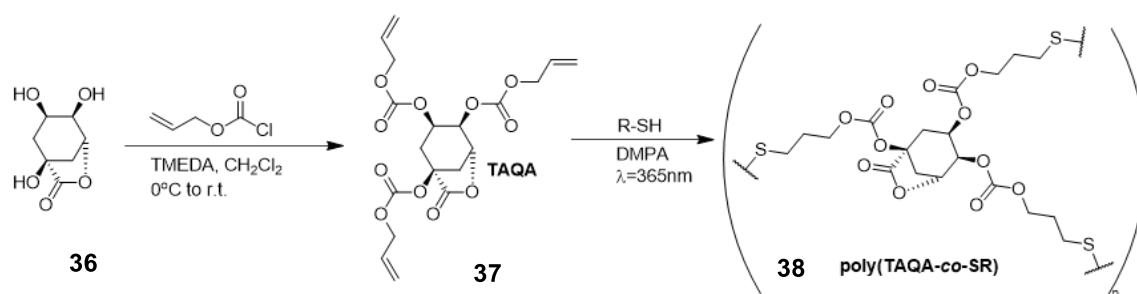
Scheme 2.19 Synthesis of crosslinked SDAC homo and copolymer.

We see very limited and recent literature report on sulfur containing crosslinked flexible APCs prepared using one step methodology. Wooley and co-workers reported series of cross-linked poly(thioether-*co*-carbonate) networks by photocatalyzed thio-ene radical copolymerization of di/tri-allyl carbonates with multifunctional thiols in the presence of photoinitiator and UV source. Allyl carbonate monomers were synthesized from aliphatic diols/triols derived from natural sources. Cross-linked copolymer network prepared from isosorbide diallyl carbonate **33** (IDAC) ^[68] monomer and trimethylolpropane tris(3-mercaptopropionate) (TMPTMP) **34** crosslinker (**Scheme 2.20**), resulted in optically-transparent elastomer **35** with rubbery modulus varying from 6.5 to 7.1MPa and T_g below room temperature.



Scheme 2.20 Synthesis of the IDAC monomer and the cross-linked poly(thioether-co-carbonate) network.

Similarly, crosslinked copolymeric networks synthesized from triallyl carbonate quinic acid (TAQA) monomer^[69] and various thiol crosslinkers (**Scheme 2.21**), resulted in wide range of thermomechanical properties such as rubbery modulus values from 3.8 to 20 MPa and T_g from -18 to 65°C.



Scheme 2.21 Synthesis of the TAQA monomer and the cross-linked poly(thioether-co-carbonate) network.

These poly(thioether-co-carbonate) cross-linked systems are hydrolytically degradable to environmentally friendly products and exhibits properties essentially required for utility in biomedical and renewable plastic applications.

Literature survey suggested, most of reports are focused on synthesis of side chain thioether functionalized linear APC while main chain thioether-APCs are seldomly explored. Further, none of these have been tested as PNTDs. Thus, with an envision and our interest to develop new sulfone based thermoplastic and thermoset material as an efficient PNTDs, which would be replacement for commercial plastic detectors such as cellulose nitrate (CN), CR-39, we planned for synthesis of new poly(sulfone-carbonate) linear and cross-linked copolymers using known polymerization methods.

Additionally, with a keen interest to understand biodegradation feature of our newly synthesized aliphatic polycarbonates, we performed preliminary biodegradation studies on these polymers, which will be discussed in this chapter.

2.3 Experimental

Synthesized monomers were purified using various techniques such as treatment with activated charcoal followed by vacuum distillation, silica-gel chromatography and recrystallization for solids. Benzoyl peroxide (BP) and isopropylperoxydicarbonate (IPP) were used as initiator for radical polymerization. Benzoyl peroxide was recrystallized chloroform and methanol mixture (3:1 v/v) at room temperature. IPP being highly unstable at room temperature, was used without further purification. AR grade dioctyl phthalate (DOP) was used as plasticizer after desiccating over 3A molecular sieves.

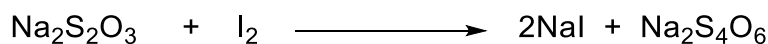
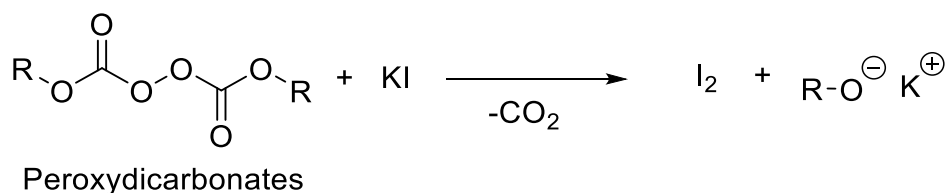
Glass plates (Schott, Germany), thin Teflon sheets 500 μm thickness and Wacker® Metroark silicone sealant were used in the preparation of glass mold for polymerization. For casting the thermoplastic polymer films, Polyester 100-micron transparent sheets of 15 cm x 15 cm size (M/s Oddy®, India) were used as solid support.

2.3.1 Methods

I. Titrimetric estimation

i. Determination of percent purity/concentration of peroxide initiator^[64,70]

Method involves treatment of known amount of initiator (30-50 mg) dissolved in acetic anhydride with solid KI. The mixture was swirled for 30 seconds and kept in dark for 30 minutes. Later, the mixture was diluted with glacial acetic acid and water. In this process, the liberated iodine was titrated against standard 0.01 N $\text{Na}_2\text{S}_2\text{O}_3$ solution using 1% starch indicator. Following are the chemical reactions are involved in the reaction:



From above relation, 2000 mL of 1 N $\text{Na}_2\text{S}_2\text{O}_3$ equals to molecular weight of the peroxydicarbonate initiator. Thus, the above relation can be conveniently used to estimate the percent purity of peroxide initiator. Additionally, this method can be used to determine the residual amount of peroxide left in the polymerization mixture. Hence helps in studying the kinetic of radical polymerization. Under kinetic studies known weight of polymerizing mixture was dissolved in acetic anhydride and treated with solid KI. Further testing protocol

remains same as mentioned above. End point blue to colourless. The percent concentration/purity of peroxide initiator can be determined using following equation:

$$\text{Percent initiator} = \frac{B.R. \times N \times M.W.}{Wt. \times 2000} \times 100 \quad (2.1)$$

where, B.R. is the volume of burette reading in mL.

N is the Normality of Na₂S₂O₃ solution.

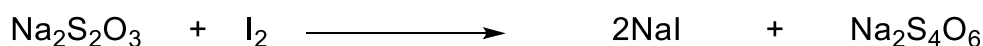
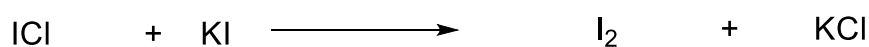
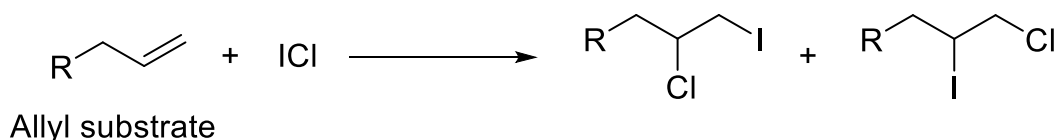
M.W. is the molecular weight of the initiator

Wt. is the sample weight in grams.

ii. Determination of unsaturation^[64,71]

The amount of unsaturation in a given sample or the amount of monomer converted to the polymer can be estimated by Wij's iodometric estimations. This method is also useful in determining the purity of olefinic monomers.

Wij's method involves a back titration of liberated iodine with standardized 0.1 N Na₂S₂O₃ solution. A known weight of sample (30-50 mg) was dissolved in chloroform and a known amount of Wij's reagent i.e., ICl in acetic acid was added. The resulting mixture was kept in the dark for 1 h and later 5 mL of 20% KI solution was added to the mixture. The liberated iodine from unreacted ICl was then titrated against standard 0.1 N Na₂S₂O₃ solution using starch indicator. End point was noted based on colour change from blue to colourless. Following are the chemical reactions involved in the process:



From the above relations, 2000 mL of 1N Na₂S₂O₃ = 1I₂ = n X C =C, i.e., molecular weight of the allyl monomer, *n* stands for number of double bonds. This method is used for the estimation of residual unsaturation present in a polymerizing mixture. Thus, it helps in studying the kinetic of radical polymerization in terms of percent monomer conversion to polymer. Under kinetic study, 30 - 50 mg of polymerizing mixture was dissolved in chloroform and further analyzed as per above mentioned procedure. Reading corresponding to blank was subtracted from the main reading.

$$\text{Unsaturation value} = \frac{(\text{Blank} - \text{Main reading}) \times N \times M.W.}{\text{Wt.} \times 2000} \quad (2.2)$$

where, N is the Normality of Na₂S₂O₃ solution.

M.W. is the molecular weight of the initiator

Wt. is the sample weight in grams.

iii. Determination of hydroxyl value (OHV) and number average molecular weight of polymer^[72]

The hydroxyl values for macrodiols (polymer with hydroxyl end group) were determined using titrimetric methods as per the ASTM method E 222. KOH (28.05 g, 0.500 mol) was dissolved in distilled water (100 mL) and then diluted with ethanol to prepare a 0.5 N KOH solution. A corrected concentration of KOH solution was obtained by standardization with potassium hydrogen phthalate as primary standard. An acylating mixture i.e., pyridine-acetic anhydride (500 mL) was prepared freshly by mixing three parts pyridine and one part of acetic anhydride.

For the sample titration, dried polymer sample was (20-30mg) treated with acylating mixture (5.0 mL) and then heated to reflux for 1 h. Later distilled water (1 mL) was added and heated again to reflux for 20-30min. Finally, the sample mixture was cooled to room temperature and was titrated against 0.5 N KOH solution till end point using phenolphthalein as indicator. For the blank titration, acylating mixture (5.0 mL) was mixed with distilled water (1 mL) and later titrated with 0.5 N KOH solution.

Hydroxyl value (OHV) for a given polymer sample is calculated using following equation:

$$\text{OHV} \left(\text{mg} \frac{\text{KOH}}{\text{g}} \right) = \frac{(\text{Blank} - \text{Main reading}) \times C \times 56.11}{D} \quad (2.3)$$

where, C is the corrected Normality of KOH solution.

D is the sample weight in grams.

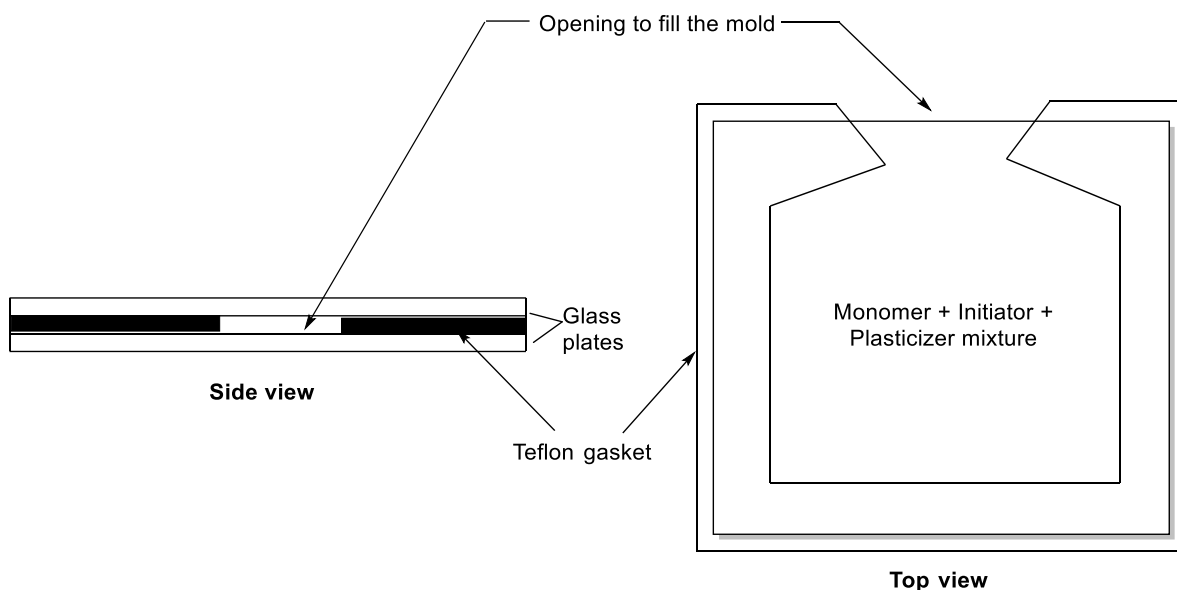
Number average molecular weight (M_n) of the polymer sample is determined using following equation:

$$M_n \left(\frac{\text{g}}{\text{mol}} \right) = \frac{56.11 \times 1000 \times 2(\text{no. of OH groups per polymer chain})}{\text{OHV}} \quad (2.4)$$

II. Polymerization and casting techniques

i. Polymerization mold assembly^[64]

A typical glass mold was prepared by sandwiching rectangular shaped Teflon gasket between the two optical glass plates previously greased along its sides as shown in figure below. Teflon used here was 500 μm thickness and width of 1.5-2.0 cm. A small opening to the Teflon gasket was made, in order to inject monomer mixture into the mold. The mold was kept under polymer press overnight to ensure uniform greasing and leak-proof during the filling of monomer and polymerization.



ii. Preparation of crosslinked thermoset film by radical cast polymerization technique^[73]

A homogenous mixture of pre-filtered (using 0.45 μm nylon filter), degassed monomer, IPP initiator and 0.5% DOP plasticizer was injected slowly into a glass mold with the help of plastic syringe. Glass mold was sealed leakproof using a binder. Radical polymerization was initiated by placing mold into a programmable heating bath and subjecting it to pre-calculated 12 h constant rate heating profile. After completion of heating, the mold was cooled to room temperature over period of 5 h. The glass plates were carefully detached to afford clear polymer film.

iii. Techniques employed in casting thermoplastic thin film on solid support

a) Spin coater

Thin polymer film was prepared using Spin Coater manufactured by M/s Indo-German Industries, Mumbai having a following specifications:

- 0.5 HP three phase, 2880 RPM, flame proof motor
- Chuck of Casting with Magnets
- Electronic timer to set the time of rotation
- A variable frequency drive (VFB) to regulate the RPM of the motor from 0-2880 RPM. VFB has fans for cooling along with MCB, contactor
- Size of machine 3 ft x 3 ft x 3 ft (L x W x H) with trolley wheels
- Tin plate (6'x 6' approx) for fixing a polyester support.

b) Motorized wet film applicator

Polymer thin films were also cast using Elcometer 3525 - adjustable baker film applicator (0-100 μm), attached to motorized assembly i.e., Elcometer 4340 Automatic wet film applicator machine (Made in GB). These are widely used for testing paint, varnish, cosmetics, glue etc. This machine provides great consistency and reproducibility to cast film on various supports such as contrast charts, steel sheet, plastic foils and glass.

c) Polymer press assembly

Several attempts were made during our study to cast a thick polymer film by technique of compression molding. To produce polymer film out of powder or granules, sample was heated and simultaneously pressurized in steel die having a gasket of suitable thickness. This process was performed in Polymer press assembly (manual)-15 Ton (Model: PF M 15) manufactured by Techno Search Instruments, Mumbai equipped with PID temperature controller (ambient to 350°C), 15 Ton max. pressure and water circulation for cooling.

III. *In-vitro* biodegradation methods

i. Sample collection

The soil samples used in this study were collected from two different locations in Goa, India, *viz.* drainage system in the backyard of Science Block-E building, Goa University, Panaji, Goa, India and sludge soil from sewage treatment plant, Tonca, Panaji, Goa, India. Each soil samples were collected in sterile container and to sustain the biological activity of soil they were kept at 4°C in the refrigerator.

ii. Primary screening and isolation

We used enrichment culture technique^[74-76] in order to isolate the polycarbonate degrading microorganism. For this purpose, MSM (Mineral salt medium) enrichment broth was prepared containing APC as sole carbon source and energy source. The MSM contains (per 1000 mL distilled water, pH 7.0): KH_2PO_4 , 3.0 g; Na_2HPO_4 , 6.0 g; NaCl, 5.0 g; NH_4Cl , 2.0

g; MgSO₄, 0.1 g. APC samples were used in the powdered form. Enrichment media is prepared in 100 mL Erlenmeyer flasks, consisting of 50 mL of MSM supplemented with 1% of APC polymer and 1% soil sample was prepared. MSM broth with 1% polymer without inoculum source was used as control. All the flasks were mixed thoroughly and incubated at 30°C for 21 days on rotary shaker at 100 rpm. Broth media is used as inoculum source for screening and isolation of microbial strains using agar plate test.

Sterile MSM agar plate supplemented with 1% powdered polymer sample was prepared on petridish (8 cm × 1.5 cm), consisting of KH₂PO₄, 3.0 g; Na₂HPO₄, 6.0 g; NaCl, 5.0 g; NH₄Cl, 2.0 g; MgSO₄, 0.1 g; Agar 15.0 g in 1000 mL distilled water maintaining the pH=7.0. A 100 µL sample from respective MSM broth culture media was dispensed and spread plated over a APC-agar plate using a bended glass rod. This inoculated agar plates were incubated at 30°C in aerobic incubator until colonies were observed. Microbial growth specifically colonies showing clear zones of inhibition was located.

iii. Secondary screening of isolates using modified cross-streak technique^[77,78]

Sterile MSM agar plates with no carbon supplement were prepared using a standard protocol. The polymer sample in the form of film or powder were placed at the centre of agar plate. The selected microbial isolates from primary screening method, were streaked perpendicular to the polymer sample and the inoculated agar plates were incubated at 30°C for a period of 2 weeks with constant periodic monitoring. (Note: the giant colony of microorganism that is streaked at the centre of the plate in the standard Cross-streak plate technique procedure, was substituted by the polymer sample). Microbial growth was observed for further qualitative analysis.

iv. Biodegradability test for APC films by potent isolates^[79]

To examine the biodegradability of APC films by the isolated strains, MSM agar plates with polymer film (1 cm x 1 cm) at the centre of the agar plate were prepared. This APC agar plates were inoculated with the respective isolate by spread plating technique and incubated at 30°C for period of 3 weeks under constant periodic check for microbial growth. Further, the APC films were observed by scanning electron microscopy (SEM) to monitor the extent of APC degradation and also to identify the degradation patterns, morphology of the isolated strains. Under SEM analysis polymer samples were fixed on aluminium stubs, and sputtered with gold. The gold coated samples were further analysed for SEM imaging

v. Characterization of potent bacterial isolates by 16S rRNA Gene sequencing and analysis

Molecular identification of the most potent isolated bacterial strains was carried out using bacterial 16s rRNA gene sequencing. 27F and 1492R primers were used for amplification of the 16s rDNA gene and BLAST analysis was carried out for the nucleotide sequencing results. The phylogenetic tree was constructed using the neighbour-joining method using MEGA version 7.0.

2.3.2 Synthetic procedures and characterization of compounds

I. Synthesis of sulfur containing monomers

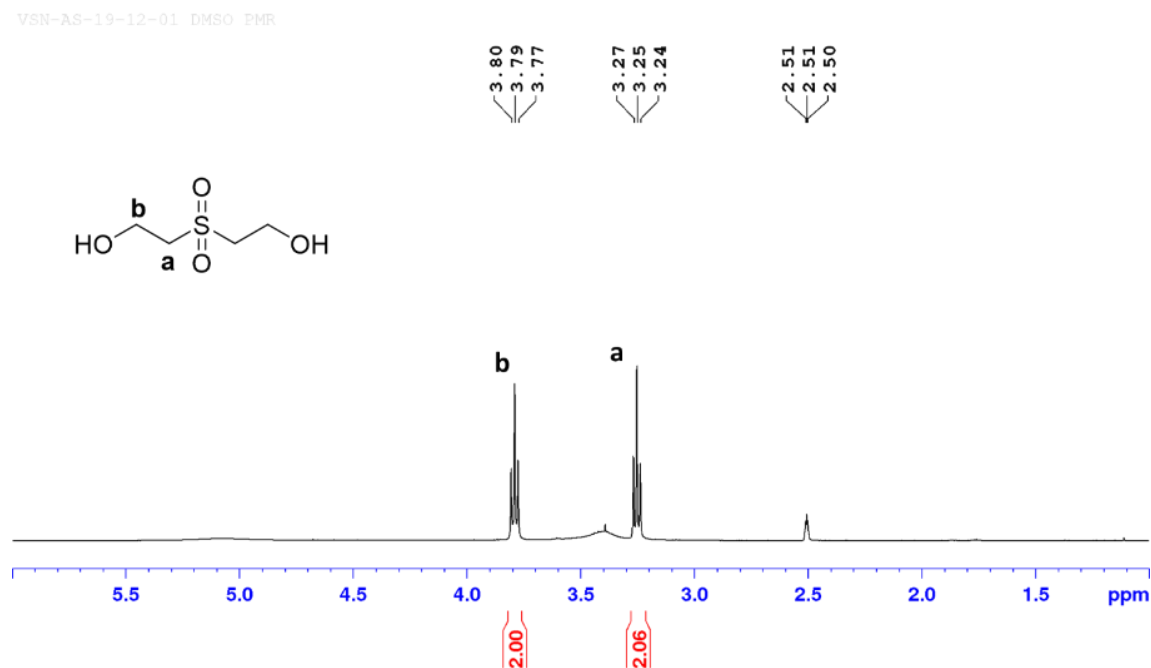
i. Synthesis of 2,2'-thiobis(ethan-1-ol) or β -thiodiglycol (2)^[80]:

Three neck RBF fitted with overhead stirrer and thermometer, charge with 300 mL of 20% (60 g, 0.745 mol) 2-chloroethanol solution and 200 mL of water. The reaction flask was placed in a cooling bath to maintain the temperature below 20°C. To stirring solution, 32.1 g (0.411 mol) sodium sulfide was added in portions over period of 2 h, maintaining the temperature between 30-35°C. After complete addition, mixture was stirred for another 1h. Later mixture was heated to 90-95°C for 45 min using a reflux condenser and the solution was set for reflux. The flask was then cooled to room temperature and neutralized by adding conc. HCl dropwise. Mixture was filtered and concentrated over rotary evaporator under reduced pressure. Residual liquid was further concentrated with ethanol and toluene to remove maximum amount of water. Finally, crude liquid product was distilled under reduced pressure of 0.2 torr at 80°C, to afford colourless liquid in 61% yield. ¹H NMR (400 MHz, CDCl₃, 25°C): δ (ppm) = 3.8-3.76(t, 2H; OCH₂), 2.78-2.75 (t, 2H; SCH₂); ¹³C NMR (100 MHz, CDCl₃, 25 °C): δ = 61.28(OCH₂), 35.01(SCH₂); IR (KBr): $\tilde{\nu}$ (cm⁻¹) = 3346(vs, O-H_{stretch}), 2922,2877(m, C-H_{stretch}, sp³), 1062(s, C-O_{stretch}).

ii. Synthesis of 2,2'-sulfonylbis(ethan-1-ol) (3)

To a cold stirred solution of thiodiglycol (10 g, 81.8 mmol) and V₂O₅ (5 mol%) in methanol 200 mL, was added 30 mL of 28% hydrogen peroxide (245.5 mmol) dropwise over a period of 1 h. Mixture further stirred at room temperature for 5 h and filtered through celite. Filtrate was concentrated in vacuo to obtain brown residue, which was purified using silica gel chromatography. R_f=0.7 (Methanol/Chloroform 25:75). Isolated as colourless pale-yellow oil in 78% yield. ¹H NMR (400 MHz, CDCl₃, 25°C): δ (ppm) = 3.8-3.77(t, 2H; CH₂OH), 3.26-3.23(t, 2H; SO₂CH₂); ¹³C NMR (100 MHz, CDCl₃, 25°C): δ = 55.31(CH₂OH),

50.73(SO₂CH₂); IR (KBr): $\tilde{\nu}$ (cm⁻¹) = 3456(vs, O-H_{strech}), 2929(m, C-H_{strech}, *sp*³), 1313, 1278 (vs, S=O_{strech}), 1118(s, C-O_{strech}).



iii. Synthesis of 2,2'-sulfonylbis (ethyl chloroformate) (**4**)

In 2 neck RBF, was placed solution of triphosgene (6.7 g, 22.7 mmol) in THF/CH₃Cl (1:1) 80 ml Both the ends of the flask were sealed with silicon septum and mixture was cooled to -5°C. To a stirring solution, 2,2'-sulfonylbis(ethanol) (5 g, 32.4 mmol) in THF and pyridine (5.6 g, 71.3 mmol) in CH₃Cl was added dropwise over a period of 90 min. During addition pyridine should be kept in excess as compared to alcohol. Reaction further stirred at same temperature for 1 h, later slowly warmed to r.t. and stirred for another 4 h. Mixture was diluted with chloroform, washed with ice cold water, dried over Na₂SO₄ and solvent was distilled under reduced pressure. Crude light brown liquid obtained was used in next step without any purification. IR (KBr): $\tilde{\nu}$ (cm⁻¹)= 2989, 2937(m, C-H_{strech}, *sp*³), 1782(vs, C=O_{strech}), 1323,1292(vs, S=O_{strech}), 1157,1124(s, C-O_{strech}), 854(m, C-Cl_{strech}).

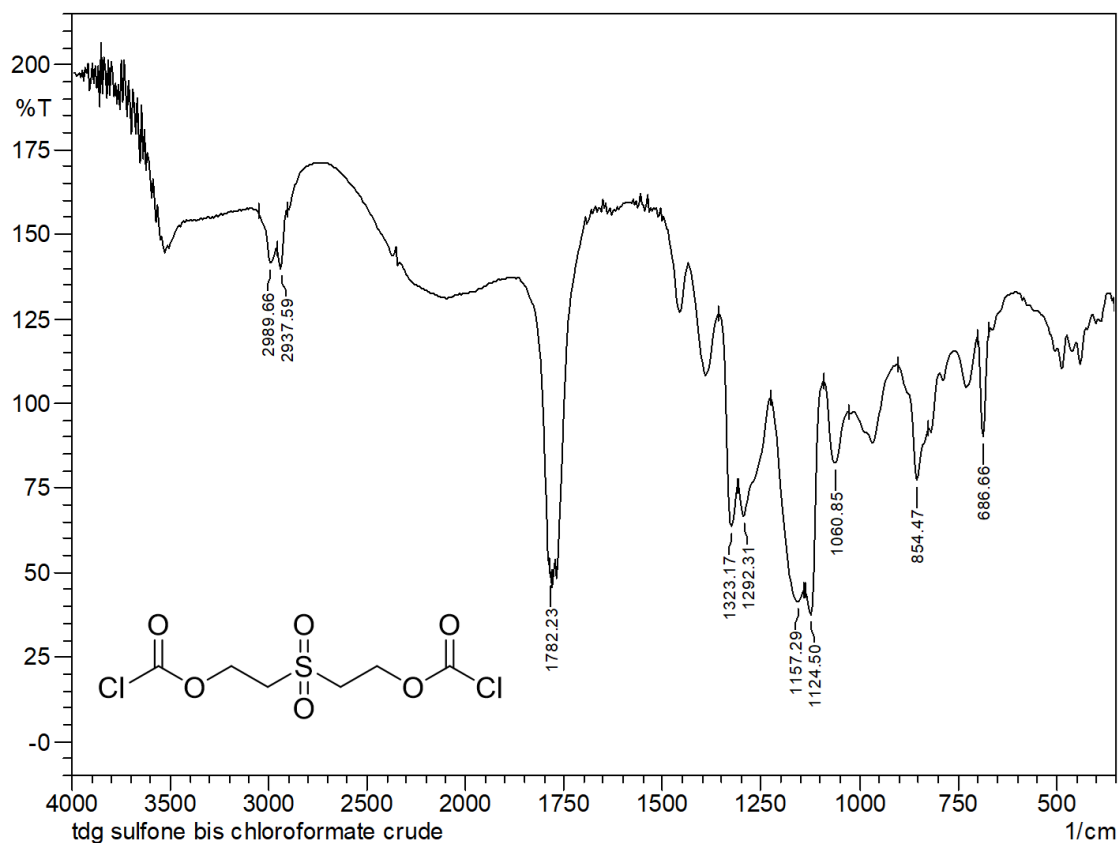


Figure 2.3 IR spectrum of 2,2'-sulfonylbis(ethyl chloroformate) (**4**) in KBr.

iv. Synthesis of 2,2'-(ethylenedithio)diethanol(**13**)^[81]

To a 3 neck RBF equipped with double surface walled reflux condenser, pressure equalizing funnel and thermometer was added 400 mL of absolute ethanol and reaction vessel assembly was placed in cooling bath. To the stirred ethanol solution, was added small pieces of sodium metal (18.4 g, 0.8 mol) in portions, till it completely dissolved to obtain fresh sodium ethoxide solution. 2-mercaptoethanol (62.4 g, 0.8 mol) was added quickly and the reaction mixture was heated to 50°C. To this 1, 2-dibromoethane (75.2 g, 0.4 mol) was added dropwise using addition funnel over a period of 1 hour. After complete addition, mixture was refluxed for 90 min. Upon completion, reaction mixture was cooled to room temperature and was filtered through celite. The filtrate was concentrated to obtain crude white solid. Crude product was recrystallized using toluene/acetonitrile to obtain white shiny solid in 75% yield. ¹H NMR (400 MHz, CDCl₃, 25°C): δ (ppm) = 3.78-3.74(t, 2H; CH₂OH), 2.78-2.76 (m, 4H; SCH₂); ¹³C NMR (100 MHz, CDCl₃, 25 °C): δ= 60.82(CH₂OH), 32.07(SCH₂); IR (KBr): $\tilde{\nu}$ (cm⁻¹) = 3279(vs, O-H_{stretch}), 2957(m, C-H_{stretch}, sp³), 1051(s, C-O_{stretch}).

v. Synthesis of 2, 2'-(oxybis(ethylenethio))diethanol (10)^[81]

Two neck RBF equipped with dropping funnel and reflux condenser, was charged with solution of sodium hydroxide (40 g, 1 mol) in 40 mL water and 330mL absolute ethanol. To stirring mixture, 2-mercaptoethanol (78 g, 1 mol) was added quickly and heated to 50°C. Using dropping funnel, 2-chloroethyl ether (71.5 g, 0.5mol) was added over a period of 1 h. Further, the reaction mixture was refluxed for 1h and allowed to cool at room temperature. Mixture filtered through celite and filtrate was concentrated in vacuo to obtain crude product. This was purified by distillation under reduced pressure of 0.5 tor at 160°C to obtain pale yellow liquid in 85% yield. ¹H NMR (400 MHz, CDCl₃, 25°C): δ (ppm) = 3.78-3.75(t, 2H; CH₂OH), 3.68-65(t, 2H; OCH₂), 2.79-2.77(m, 4H; SCH₂); ¹³C NMR (100 MHz, CDCl₃, 25 °C): δ= 70.75(OCH₂), 61.06(CH₂OH), 35.66(CH₂S), 31.58(SCH₂); IR (KBr): $\tilde{\nu}$ (cm⁻¹) = 3368(vs, O-H_{stretch}), 2920, 2867(vs, C-H_{stretch}, sp³), 1103, 1043(vs, C-O_{stretch}).

vi. Synthesis of 2,2'-(ethylenedithio) diallylcarbonate (19)

Round bottom flask, charged with solution of 2,2'-(ethylenedithio)diethanol (10 g, 55 mmol) and pyridine (13 g, 165 mmol) in 150 mL of acetone. The reaction mixture was cooled to 0 °C with and allyl chloroformate (16.6 g, 137.5 mmol) was added dropwise using pressure equalizing funnel over a period of 45 min. After complete addition, stirring was continued to 0°C for 1 h and then at room temperature for another 4 h. Progress of reaction was monitored by TLC. After complete conversion, solvent was evaporated in vacuo and residue was acidified with 2 N HCl solution. The mixture was extracted twice in diethyl ether, washed with brine and dried over sodium sulphate. The solvent was evaporated in vacuo to obtain crude yellow liquid product. Crude was purified using silica gel chromatography to afford pale yellow oil in 81% yield. R_f=0.7 (Pet. Ether/ EtOAc, 70:30); ¹H NMR (400 MHz, CDCl₃, 25°C): δ (ppm) = 5.97–5.88 (m, 2H; CH=CH₂), 5.39-5.23 (m, 4H; CH=CH₂), 4.64-4.59(m, 4H; CH₂-CH=CH₂), 4.31-4.23(m, 4H; OCH₂), 2.84-2.76(m, 8H; SCH₂); IR (KBr): $\tilde{\nu}$ (cm⁻¹) = 3084(w, C-H_{stretch}, sp²), 2953(m, C-H_{stretch}, sp³), 1747(vs, C=O_{stretch}), 1649(w, C=O_{stretch}), 1257(vs, C-O_{stretch}, ester).

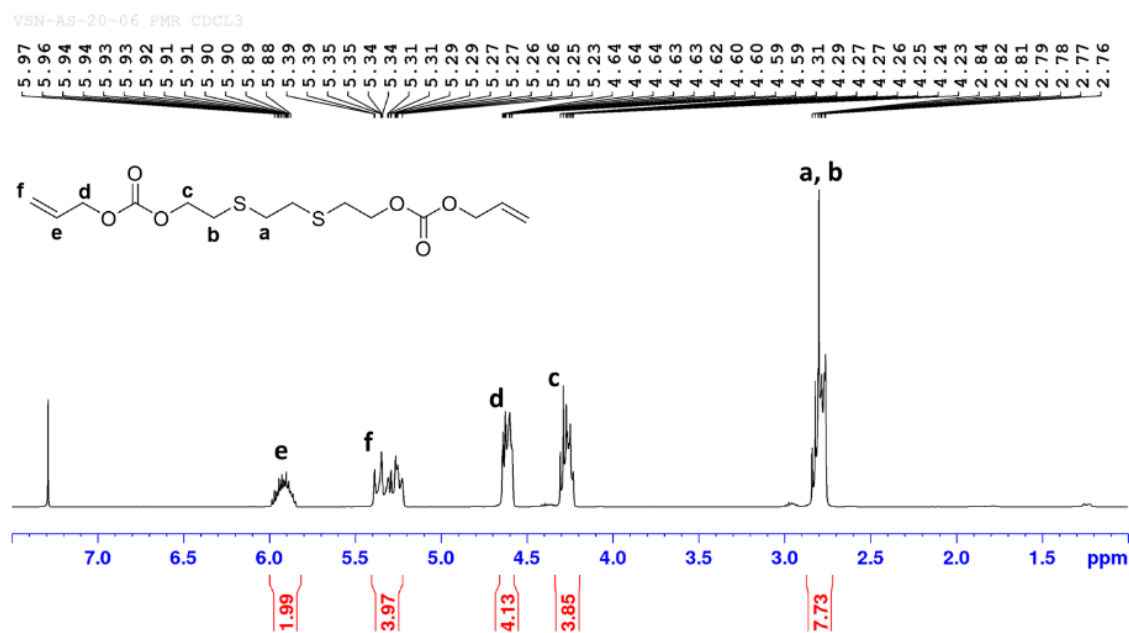


Figure 2.4 ^1H NMR spectrum of 2,2'-(ethylenedithio) diallylcarbonate (**19**) in CDCl_3 .

vii. Synthesis of 2, 2'-(oxybis(ethylenethio)) diallylcarbonate (**17**)

In a 2 neck RBF fitted with overhead stirrer and pressure equalizing funnel, was added 2, 2'-(oxybis(ethylenethio))diethanol (41 g, 181 mmol), pyridine (43 g, 543 mmol) and 200 mL of acetone. Resulting homogenous mixture was cooled to 0 °C and allyl chloroformate was added dropwise over a period of 2 h with vigorous stirring. Further stirring was continued for more 90 min at 0°C and then to room temperature for 6 h. After completion of reaction as indicated by TLC, solvent was evaporated in vacuo and residue was acidified with 2 N HCl. Mixture was extracted twice with diethyl ether, washed with brine and dried over sodium sulphate. Crude product was purified by silica gel chromatography to afford colorless oil in 88% yield. $R_f=0.6$ (Pet. Ether/ EtOAc, 70:30); ^1H NMR (400 MHz, CDCl_3 , 25°C): δ (ppm) = 5.95–5.90 (m, 2H; $\text{CH}=\text{CH}_2$), 5.39-5.26 (dd, $J=16\text{Hz}$ and 8Hz, 4H; $\text{CH}=\text{CH}_2$), 4.64-4.62(m, 4H; $\text{CH}_2-\text{CH}=\text{CH}_2$), 4.31-4.27(t, 4H; OCO_2CH_2), 3.67-3.63(t, 4H; OCH_2), 2.86-2.82(t, 4H; CH_2S), 2.78-2.74(t, 4H; SCH_2); IR (KBr): $\tilde{\nu}(\text{cm}^{-1})= 3084(\text{w}, \text{C}-\text{H}_{\text{stretch}}, sp^2)$, 2953(m, $\text{C}-\text{H}_{\text{stretch}}, sp^3$), 1747(vs, $\text{C}=\text{O}_{\text{stretch}}$), 1649(vs, $\text{C}=\text{O}_{\text{stretch}}$), 1257(vs, $\text{C}-\text{O}_{\text{stretch}}, \text{ester}$), 1109(s, $\text{C}-\text{O}_{\text{stretch}}, \text{ether}$).

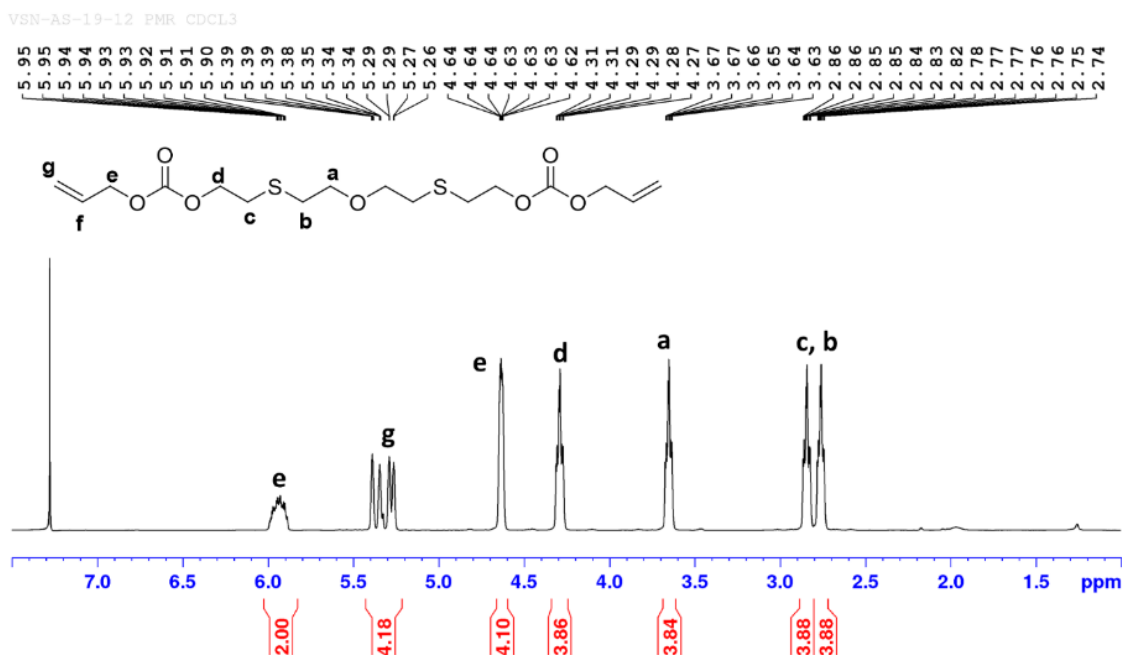


Figure 2.5 ¹H NMR spectrum of 2, 2'-(oxybis(ethylenedioxy)) diallylcarbonate (17) in CDCl₃.

viii. Oxidation of dithio diallylcarbonate (18) & (20)

To a cold stirred solution of dithio diallylcarbonate (1 equiv.) and V₂O₅ (5 mol%) in methanol, was added 28% hydrogen peroxide (6 equiv.) dropwise over period of 1-2 h. Mixture further stirred at room temperature 4-5 h and after complete conversion filtered through celite. Filtrate was concentrated in vacuo.

2,2'-(ethylenedisulfonyl) diallylcarbonate (20): 2,2'-(ethylenedioxy) diallylcarbonate (10 g, 28.5 mmol) in 120 mL methanol, 28% hydrogen peroxide (21 mL, 171.2 mmol). R_f=0.6 (Pet. Ether/ EtOAc, 30:70), Isolated as white shiny solid in 78%; m.pt. 91°C; ¹H NMR (400 MHz, CDCl₃, 25°C): δ (ppm) = 5.98–5.88 (m, 2H; CH=CH₂), 5.41-5.30 (dd, *J*=16Hz and 8Hz, 4H; CH=CH₂), 4.67(d, 4H; CH₂-CH=CH₂), 4.65-4.59(t, 4H; OCO₂CH₂), 3.60(s, 4H; SO₂CH₂), 3.46-3.44(t, 4H; CH₂SO₂), ¹³C NMR (100 MHz, CDCl₃, 25°C): δ (ppm) = 153.97 (C=O), 130.91(CH=CH₂), 119.81 (CH=CH₂), 69.27(CH₂-CH=CH₂), 60.88(OCO₂CH₂), 52.95(SO₂CH₂), 47.24(CH₂SO₂); IR (KBr): ν̃(cm⁻¹)= 3086(w, C-H_{strech}, *sp*²), 2992, 2947(m, C-H_{strech}, *sp*³), 1747(vs, C=O_{strech}), 1649(w, C=C_{strech}), 1315, 1287(s, S=O_{strech}), 1234,1140,1107(s, C-O_{strech}).

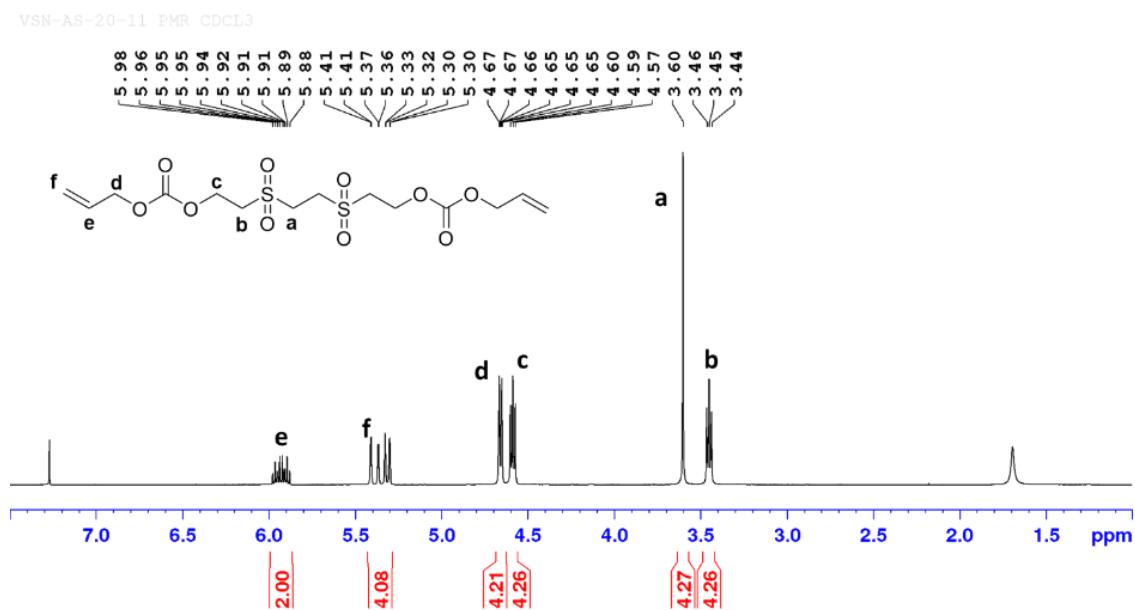


Figure 2.6 ¹H NMR spectrum of 2,2'-(ethylenedisulfonyl) diallylcarbonate (**20**) in CDCl₃.

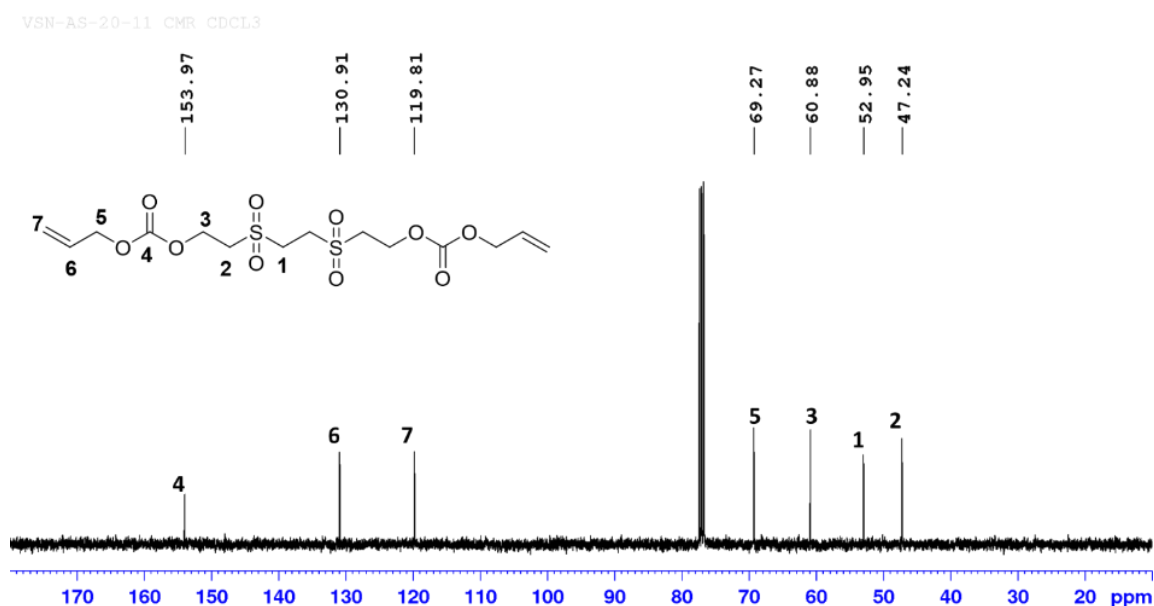


Figure 2.7 ¹³C NMR spectrum of 2,2'-(ethylenedisulfonyl) diallylcarbonate (**20**) in CDCl₃

2, 2'-(oxybis(ethylenesulfonyl)) diallylcarbonate (18): 2, 2'-(oxybis(ethylenethio)) diallylcarbonate (21 g, 53.2 mmol) in 250 mL methanol, 28% hydrogen peroxide (39 mL, 319.2 mmol). *R_f*=0.5 (Pet. Ether/ EtOAc, 30:70); Isolated as colorless viscous liquid in 81%; ¹H NMR (400 MHz, CDCl₃, 25°C): δ (ppm) = 5.99–5.89 (m, 2H; CH=CH₂), 5.41–5.31 (dd, 4H, *J*=16Hz and 8Hz; CH=CH₂), 4.67–4.65(d, 4H; CH₂-CH=CH₂), 4.59–4.56(t, 4H; OCO₂CH₂), 4.0–3.97(t, 4H; OCH₂), 3.50–3.47(t, 4H; CH₂SO₂), 3.36–3.34(t, 4H; SO₂CH₂);

^{13}C NMR (100 MHz, CDCl_3 , 25°C): δ (ppm) = 154.12(C=O), 131.10(CH=CH₂), 119.68(CH=CH₂), 69.09(CH₂-CH=CH₂), 64.75(OCO₂CH₂), 61.26(OCH₂), 54.36(CH₂SO₂), 53.72(SO₂CH₂); IR (KBr): $\tilde{\nu}$ (cm⁻¹)= 3086(w, C-H_{strech}, *sp*²), 2988, 2882(m, C-H_{strech}, *sp*³), 1750(vs, C=O_{strech}), 1649(w, C=C_{strech}), 1322 (s, S=O_{strech}), 1266(s, C-O_{strech}, *ester*), 1130(s, C-O_{strech}, *ether*).

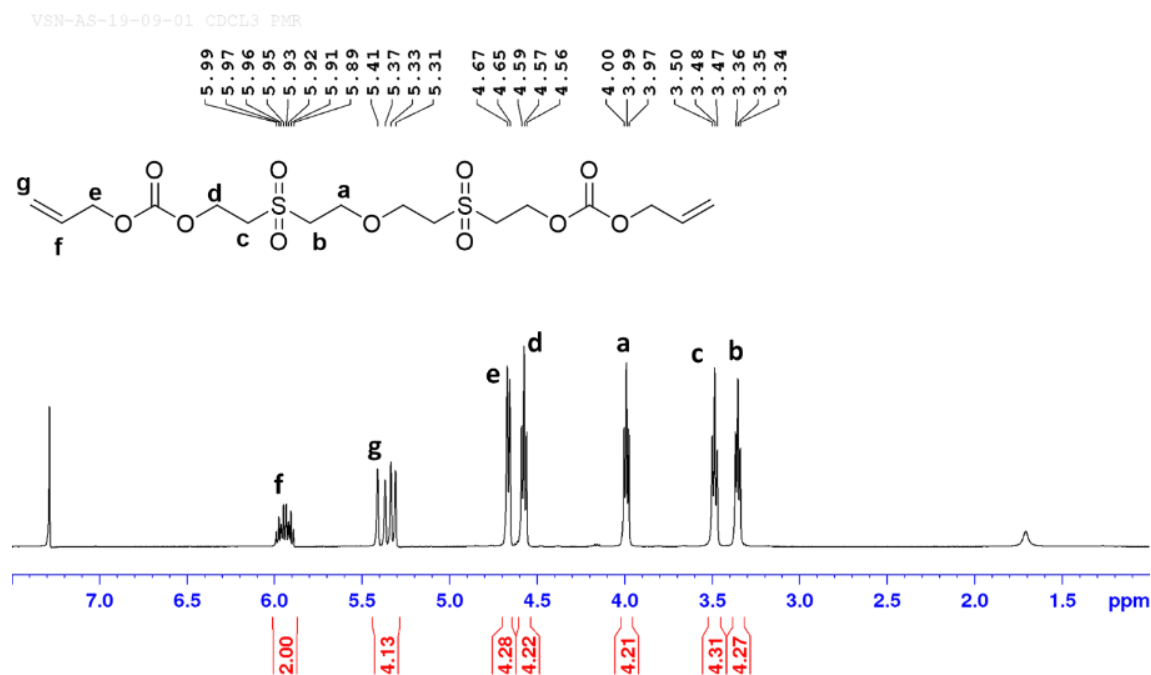


Figure 2.8 ^1H NMR spectrum of 2, 2'-(oxybis(ethylenesulfonyl)) diallylcarbonate (**18**) in CDCl_3 .

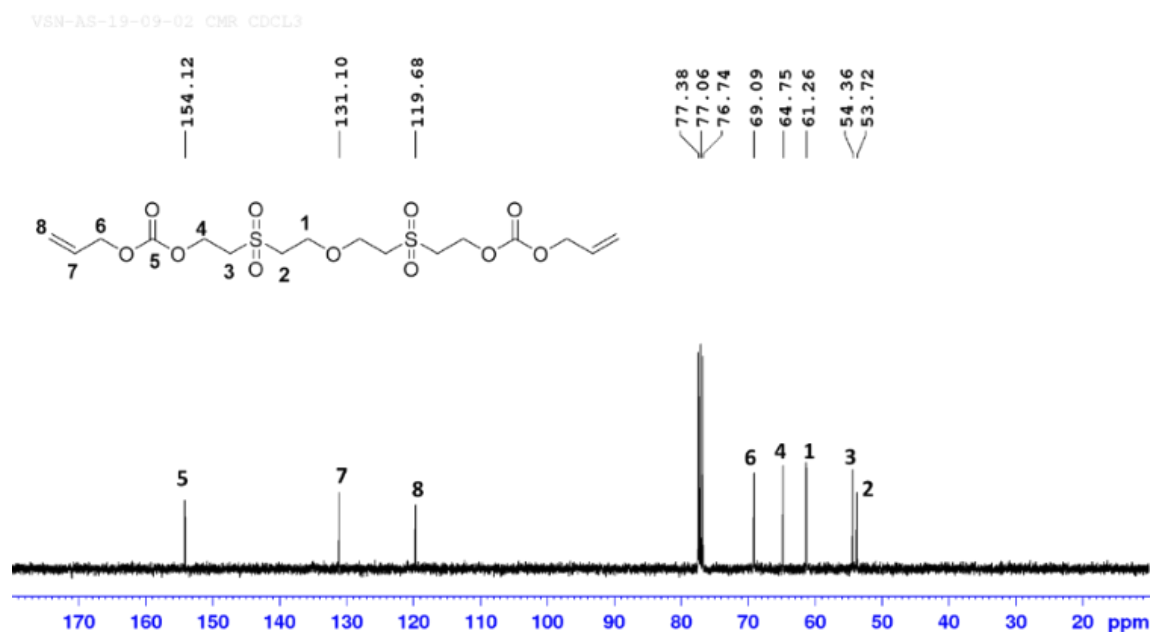


Figure 2.9 ^{13}C NMR spectrum of 2, 2'-(oxybis(ethylenesulfonyl)) diallylcarbonate (**18**) in CDCl_3 .

II. Synthesis of allyl diglycol carbonate (ADC)^[42,64]

Synthesized using the known literature report. A typical procedure consists of two-neck flask equipped with pressure equalizing funnel, was placed solution of diethylene glycol (10.0 g, 94.2 mmol), pyridine (22 mL, 283.7 mmol) in dichloromethane 80 mL. Reaction flask was cooled to 0°C . To a stirring solution, allyl chloroformate (28.4 g, 235.6 mmol) was added drop wise using dropping funnel connected with drying tube. After addition for 40 min, stirring was continued for another 1 h at 0°C and then 3 h at room temperature. Salt formed was filtered and washed with dichloromethane. Filtrate was stirred with 1:1 dil. HCl for 30 min and transferred to separating funnel. Organic layer was washed with water, brine water and dried over anhy. Na_2SO_4 . Solvent was removed using rotary evaporator. Crude yellow product was purified using distillation under reduced pressure of 0.5 torr at $140\text{--}145^\circ\text{C}$ to afford colourless liquid in 85% yield. ^1H NMR (400 MHz, CDCl_3 , 25°C): δ (ppm) = 5.98–5.88(m, 2H; $\text{CH}=\text{CH}_2$), 5.39–5.25 (dd, 4H, $J=16\text{Hz}$ and 8Hz ; $\text{CH}=\text{CH}_2$), 4.62–4.64(d, 4H; $\text{CH}_2\text{-CH}=\text{CH}_2$), 4.31–4.29(t, 4H; OCO_2CH_2), 3.75–3.72(t, 4H; OCH_2); IR (KBr): $\tilde{\nu}$ (cm^{-1}) = 3086(w, $\text{C-H}_{\text{stretch}}$, sp^2), 2956(m, $\text{C-H}_{\text{stretch}}$, sp^3), 1747(vs, $\text{C=O}_{\text{stretch}}$), 1649(w, $\text{C=C}_{\text{stretch}}$), 1257(s, $\text{C-O}_{\text{stretch}}$, *ester*), 1141(s, $\text{C-O}_{\text{stretch}}$, *ether*).

III. Synthesis of sulfur containing linear aliphatic polycarbonates.

i. Attempt towards synthesis of poly (sulfonyl diethylene carbonate).

a. Solution polycondensation of 2,2'-sulfonylbis(ethan-1-ol) and triphosgene,

In RBF, 2,2'-sulfonylbis(ethanol) (1 g, 6.4 mmol) and pyridine (1.01 g, 12.8 mmol) dissolved in 6 mL THF, flask sealed with silicon septum and cooled to 0°C . Dropwise addition of triphosgene (0.7 g, 2.3 mmol) solution in 3 mL THF through septum using syringe over a period of 1 h. Precipitation of white sticky solid from solvent medium settling at bottom. Reaction mix. Warm to room temperature and stirred for 3 h. After completion solvent decanted and sticky solid washed with THF. Sticky residue was precipitated in acetonitrile/water to afford white powder (41% yield). m.p. $100\text{--}110^\circ\text{C}$.

b. Solution polycondensation of 2,2'-sulfonylbis(ethanol) and 2,2' sulfonylbis (ethyl chloroformate),

To a 3 neck RBF equipped with overhead stirrer and pressure equalizer addition funnel, was added 2,2'-sulfonylbis(ethanol) (0.5 g, 3.2 mmol), pyridine (1.26 g, 16 mmol), DMAP (78

mg, 0.64 mmol) and 10 mL of THF under a continuous nitrogen flow. The resulting homogenous mixture was cooled to 15°C. To this cooled mixture solution of 2,2' sulfonylbis (ethyl chloroformate) (1 g, 3.52 mmol) in 5 mL THF was added dropwise over a period of 40 min under nitrogen flow. After 15 min of addition, white sticky solid precipitates from solvent medium. After complete addition, reaction vessel was warmed to room temperature and stirred for another 2 h. Finally, solvent was decanted and sticky solid was washed with THF. Sticky residue was precipitated in acetonitrile/water to afford white powder (45% yield). m.p. 105-110°C.

c. Interfacial polycondensation of 2,2'-sulfonylbis(ethanol) and 2,2' sulfonylbis (ethyl chloroformate).

In two neck RBF equipped with overhead stirrer, was added 2,2'-sulfonylbis(ethanol) (1 g, 6.5 mmol), DMAP (20 mol%) and NaOH (0.78 g, 19.5 mmol) dissolved in 8 mL water. To rapidly stirred flask solution, was added 2,2' sulfonylbis (ethyl chloroformate) (2.17 g, 7.8 mmol) in 4 mL of chloroform at room temperature. Mixture stirred for 1 h. and poured in excess water. White solid was filtered, dried in vacuo at 50°C (61% yield). m.p. 110-115°C.

Oligo-SOC (5): ^1H NMR (400 MHz, CDCl_3 , 25°C): δ (ppm) = 4.49-4.46(t, 14H; $\text{OCH}_2\text{CH}_2\text{SO}_2$), 3.81-3.77(t, 2H; OHCH_2), 3.61-3.58(t, 14H; $\text{OCH}_2\text{CH}_2\text{SO}_2$), 3.38-3.25(t, 2H; $\text{HOCH}_2\text{CH}_2\text{SO}_2$); M_n (NMR) = (DP=7); IR (KBr): $\tilde{\nu}(\text{cm}^{-1})$ = 3518(w, $\text{O-H}_{\text{stretch}}$), 2995, 2945(m, $\text{C-H}_{\text{stretch}}$, sp^3), 1755(vs, $\text{C=O}_{\text{stretch}}$), 1321(s, $\text{S=O}_{\text{stretch}}$), 1236(s, $\text{C-O}_{\text{stretch}}$, ester), 1126, 1064(s, $\text{C-O}_{\text{stretch}}$, ether).

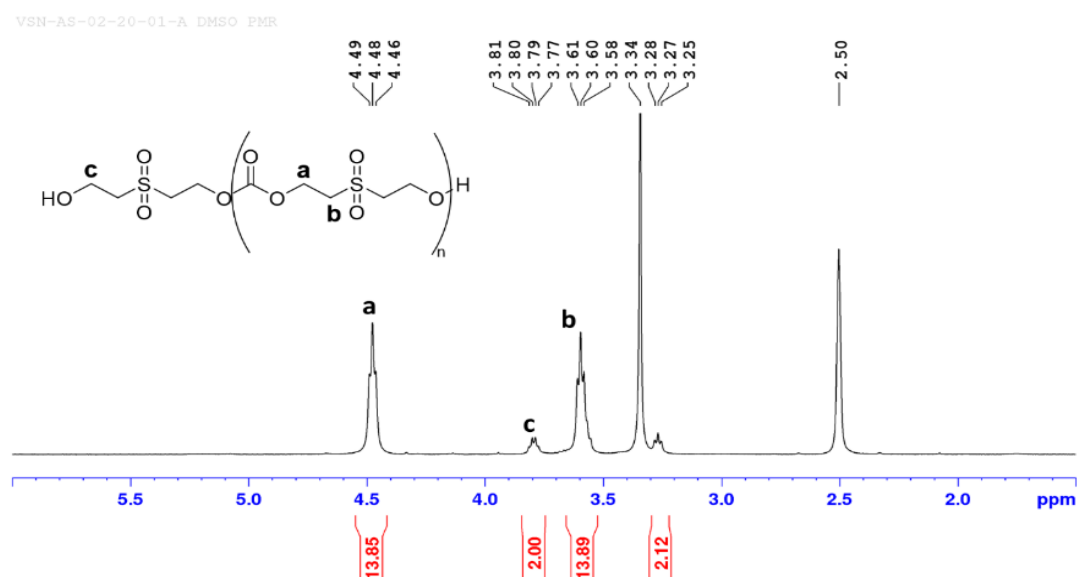


Figure 2.10 ^1H NMR spectrum of Oligo-SOC (5) in DMSO-d_6 .

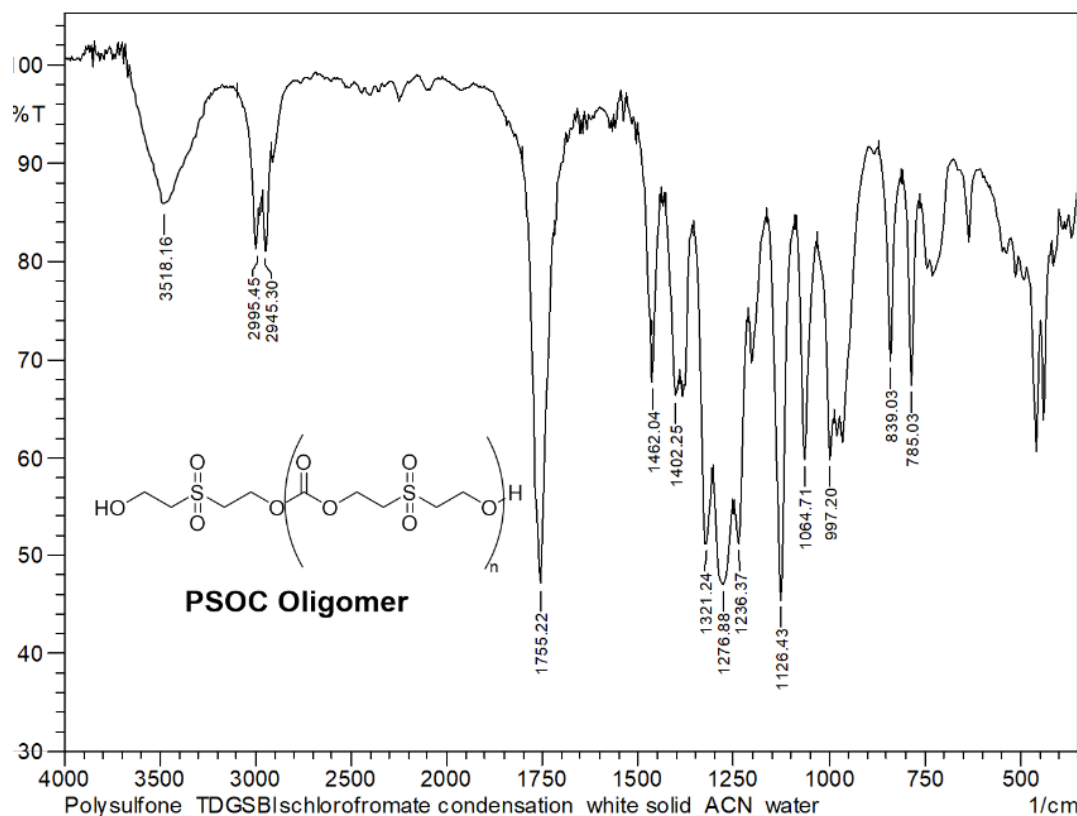


Figure 2.11 ^1H NMR spectrum of Oligo-SOC (**5**) in KBr.

ii. General procedure for synthesis of poly (thioether carbonate) linear polymers using solution polycondensation.

In two neck RBF fitted with pressure equalizer funnel was placed thioether diol (1equiv.), pyridine (4 equiv.) and dichloromethane solvent (50 mL). Mixture was cooled to 15 °C and triphosgene (0.45 equiv.) solution in 30 ml dichloromethane solvent was added dropwise over a period of 8 h. After complete addition mixture warmed to room temperature and continued stirring for another 4-5 h. Reaction was treated with 10% dil. HCl solution and extracted twice with excess of dichloromethane. Organic layer was washed with water, brine and dried over sodium sulphate. Maximum solvent removed under normal distillation at 1 atmosphere pressure. Residual solvent was removed under vacuo to afford crude product.

Poly (2,2'-thio diethylene carbonate), PSC (6**):** 2,2'-thiobis(ethanol) (10 g, 82 mmol), pyridine (26 g, 328 mmol), triphosgene (11 g, 37 mmol). Crude product reprecipitated in DCM/hexane to afford densely viscous brown liquid in 97% yield. IR (KBr): $\tilde{\nu}(\text{cm}^{-1})=2960(\text{m}, \text{C-H}_{\text{stretch}}, \text{sp}^3)$, 1745(vs, $\text{C}=\text{O}_{\text{stretch}}$), 1267(s, $\text{C-O}_{\text{stretch}}$, ester), 1062(s, $\text{C-O}_{\text{stretch}}$, ether).

Poly (2, 2'-(oxybis(ethylenethio)) diethylene carbonate), PDSC-1 (11): 2, 2'-(oxybis(ethylenethio)) diethanol (10.23 g, 45.2 mmol), pyridine (14.3 g, 181 mmol), triphosgene (6 g, 20.3 mmol). Crude product reprecipitated in DCM/hexane to afford viscous liquid in 93% yield. IR (KBr): $\tilde{\nu}(\text{cm}^{-1}) = 2920(\text{m}, \text{C-H}_{\text{stretch}}, sp^3)$, 1745(vs, C=O_{stretch}), 1263(s, C-O_{stretch}, ester), 1107(w, C-O_{stretch}, ether).

Poly (2,2'-(ethylenedithio) diethylene carbonate), PDSC-2 (14): 2,2'-(ethylenedithio)diethanol (10 g, 54.8 mmol), pyridine (17.34 g, 219 mmol) dissolved in 1,4-dioxane/dichloromethane (2:1) and triphosgene (7.33 g, 24.7 mmol) solution in dichloromethane was added. Crude white sticky solid reprecipitated in methanol/chloroform/ethyl acetate solvent system to afford free flowing white solid in 81% yield. IR (KBr): $\tilde{\nu}(\text{cm}^{-1}) = 2958(\text{m}, \text{C-H}_{\text{stretch}}, sp^3)$, 1745(vs, C=O_{stretch}), 1267(s, C-O_{stretch}, ester), 1072(w, C-O_{stretch}, ether).

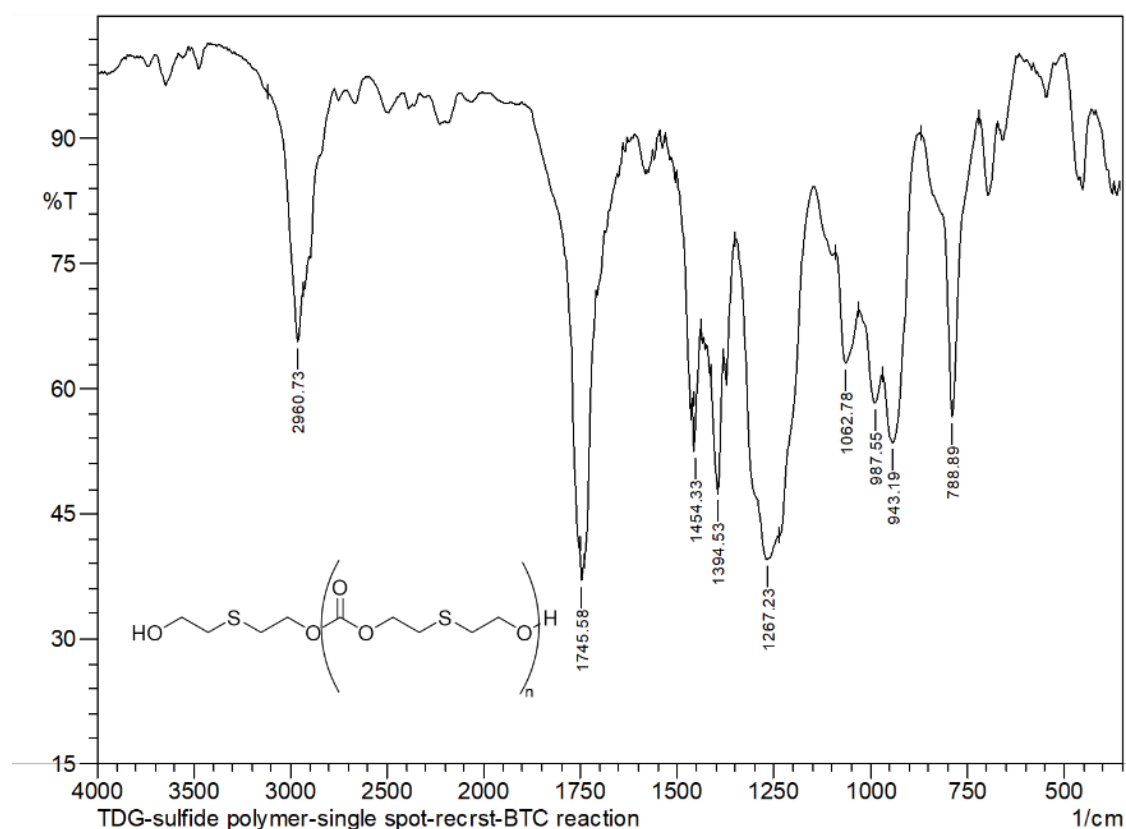


Figure 2.12 IR spectrum of Poly (2,2'-thio diethylene carbonate), PSC (6) in KBr.

Acquired Software :EZChrom Elite Build 3.3.2.1037

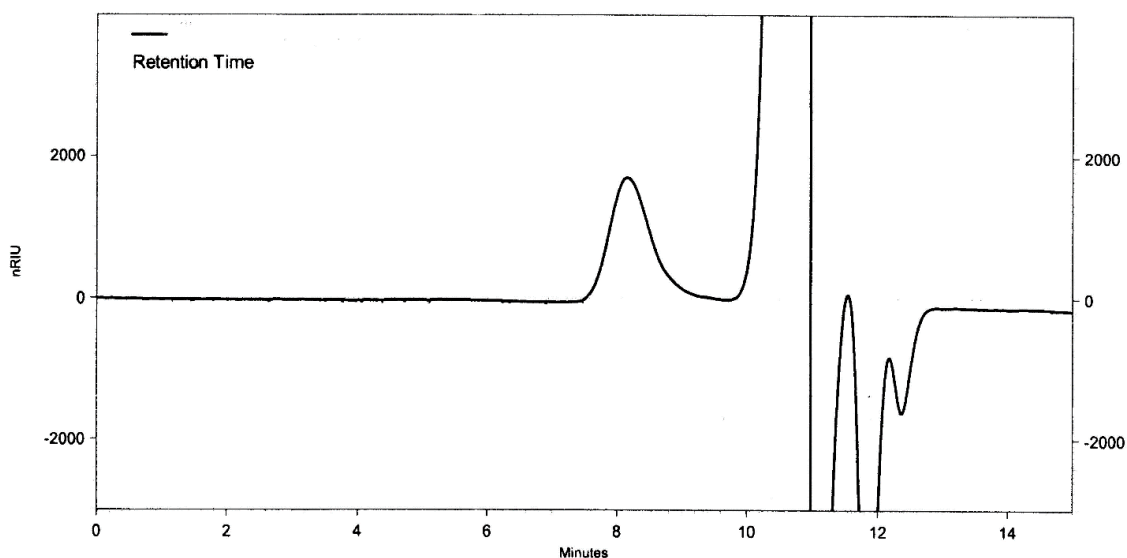


Figure 2.13 GPC chromatogram of Poly (2,2'-thio diethylene carbonate), PSC (6) eluted with THF

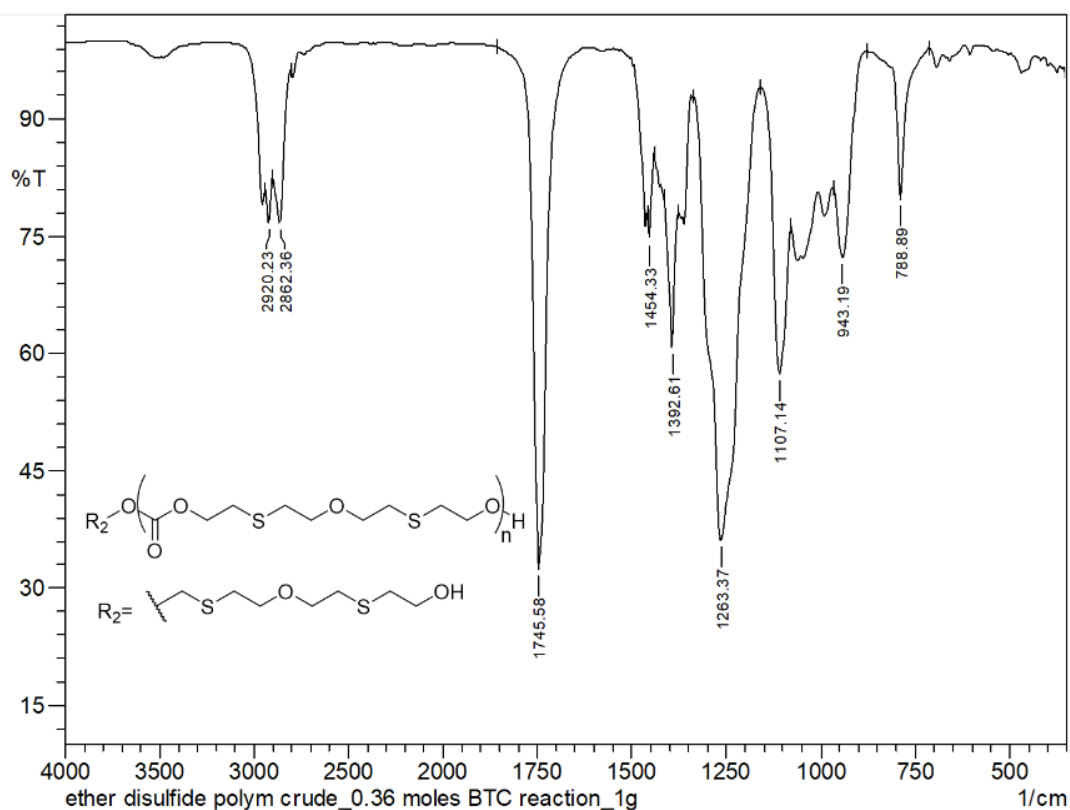


Figure 2.14 IR spectrum of poly (2, 2'-(oxybis(ethylenethio)) diethylene carbonate), PDSC-1 (11) in KBr.

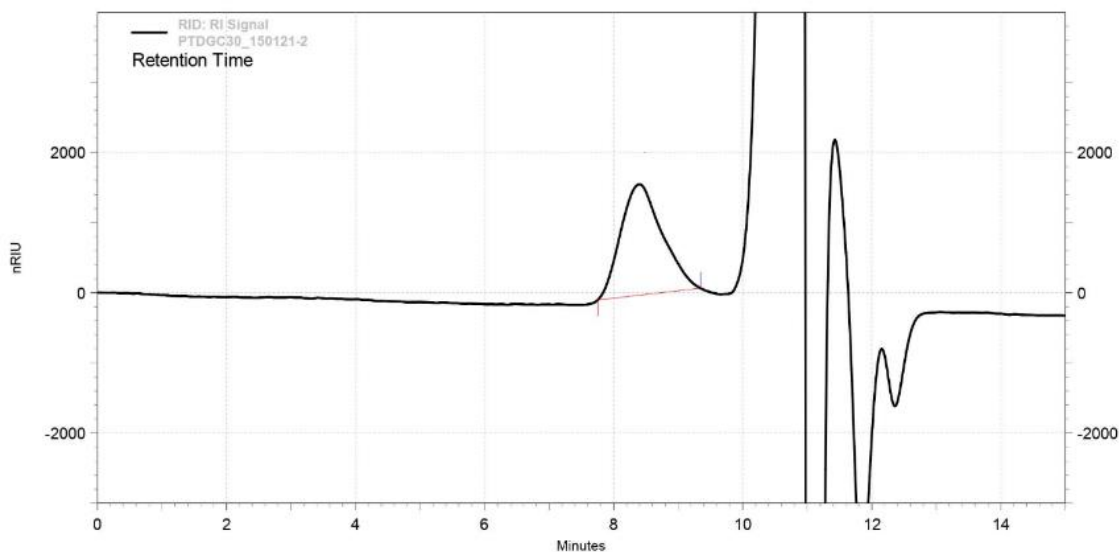


Figure 2.15 GPC chromatogram of poly (2, 2'-(oxybis(ethylenedioxy)) diethylene carbonate), PDSC-1 (**11**) eluted with THF.

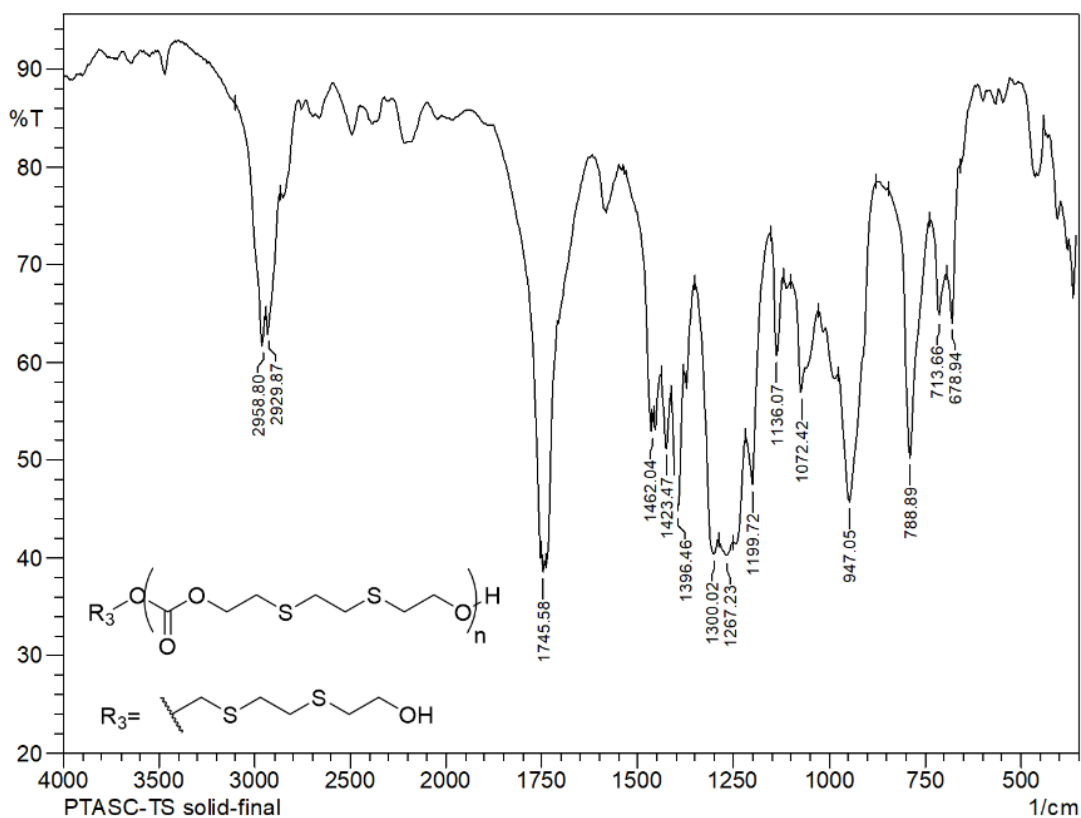


Figure 2.16 IR spectrum of Poly (2,2'-(ethylenedioxy) diethylene carbonate), PDSC-2 (**14**) in KBr.

iii. General procedure for synthesis of poly (sulfonyl carbonate) linear polymers

To a cold stirred solution of poly(thioether-carbonate) and V_2O_5 (5 mol%) in 200 mL THF, was added 28% hydrogen peroxide (20-30-fold excess) in portion over a period of 2h. Mixture further stirred at room temperature 7 h.

Poly (2,2'-sulfonyl diethylene carbonate), PSOC (7): Poly (2,2'-thio diethylene carbonate) (11 g, 74 mmol). White solid product precipitates in reaction medium, filtered through Buckner funnel and solid was washed with hot water, THF and dried in vacuo to obtain white solid in 88% yield. ^{13}C NMR (100 MHz, $CDCl_3$, $25^\circ C$): δ (ppm) = 153.80(C=O), 61.49($O_2COCH_2CH_2SO_2$), 52.75($O_2COCH_2CH_2SO_2$); IR (KBr): $\tilde{\nu}(cm^{-1})$ = 2995, 2943(m, C-H_{stretch}, sp^3), 1753(vs, C=O_{stretch}), 1321 (s, S=O_{stretch}), 1276(s, C-O_{stretch}, *ester*), 1064,997(s, C-O_{stretch}, *ether*).

Poly (2, 2'-(oxybis(ethylenesulfonyl)) diethylene carbonate), PDSOC-1 (15): Poly (2, 2'-(oxybis(ethylenethio)) diethylene carbonate) (10 g, 39.5 mmol). Sticky solid precipitates in reaction mixture and settles at the bottom. Solvent medium decanted, residue washed with hot THF/ H_2O (1:1) to obtain colourless sticky solid in 78% yield. ^{13}C NMR (100 MHz, $CDCl_3$, $25^\circ C$): δ (ppm) = 153.80(C=O), 64.39 ppm (-OCOCH₂CH₂SO₂CH₂CH₂O-), 61.51 ppm (-OCOCH₂CH₂SO₂CH₂CH₂O-), 53.73(-OCOCH₂CH₂SO₂CH₂CH₂O-) and 52.97 ppm (-OCOCH₂CH₂SO₂CH₂CH₂O-); IR (KBr): $\tilde{\nu}(cm^{-1})$ = 2987, 2933(m, C-H_{stretch}, sp^3), 1755(vs, C=O_{stretch}), 1319(s, S=O_{stretch}), 1271(s, C-O_{stretch}, *ester*), 1126(s, C-O_{stretch}, *ether*).

Poly (2,2'-(ethylenedisulfonyl) diethylene carbonate), PDSOC-2 (16): Poly (2,2'-(ethylenedithio) diethylene carbonate) (10 g, 48 mmol). White solid product precipitates in reaction medium, filtered through Buckner funnel and solid was washed with hot water, THF and dried in vacuo to obtain white solid in 82% yield. ^{13}C NMR (100 MHz, $CDCl_3$, $25^\circ C$): δ (ppm) = 153.80(C=O), 61.34 ppm (-OCOCH₂CH₂SO₂CH₂CH₂SO₂-), 51.82 ppm (-OCOCH₂CH₂SO₂CH₂CH₂SO₂-), 46.3 ppm (-OCOCH₂CH₂SO₂CH₂CH₂SO₂-); IR (KBr): $\tilde{\nu}(cm^{-1})$ = 2993, 2943(m, C-H_{stretch}, sp^3), 1753(vs, C=O_{stretch}), 1284(s, S=O_{stretch}), 1114(s, C-O_{stretch}, *ether*).

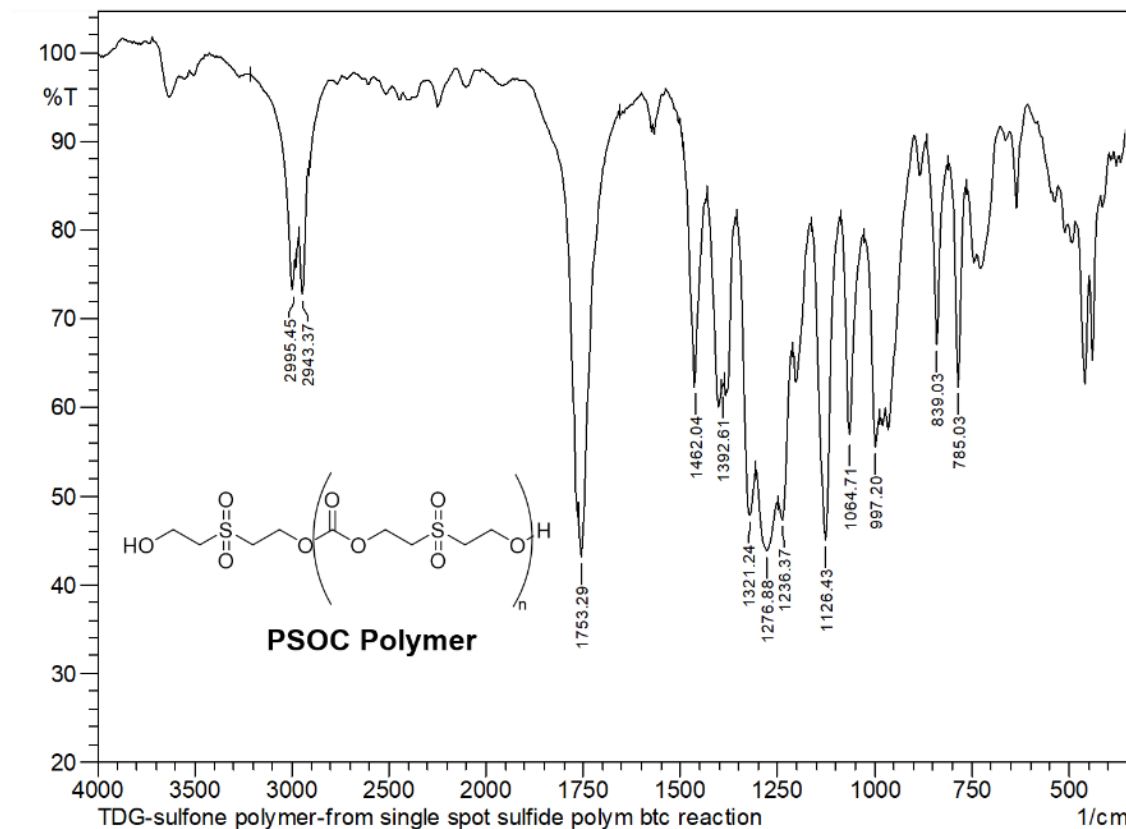


Figure 2.17 IR spectrum of poly (2,2'-sulfonyl diethylene carbonate), PSOC (7) in KBr.

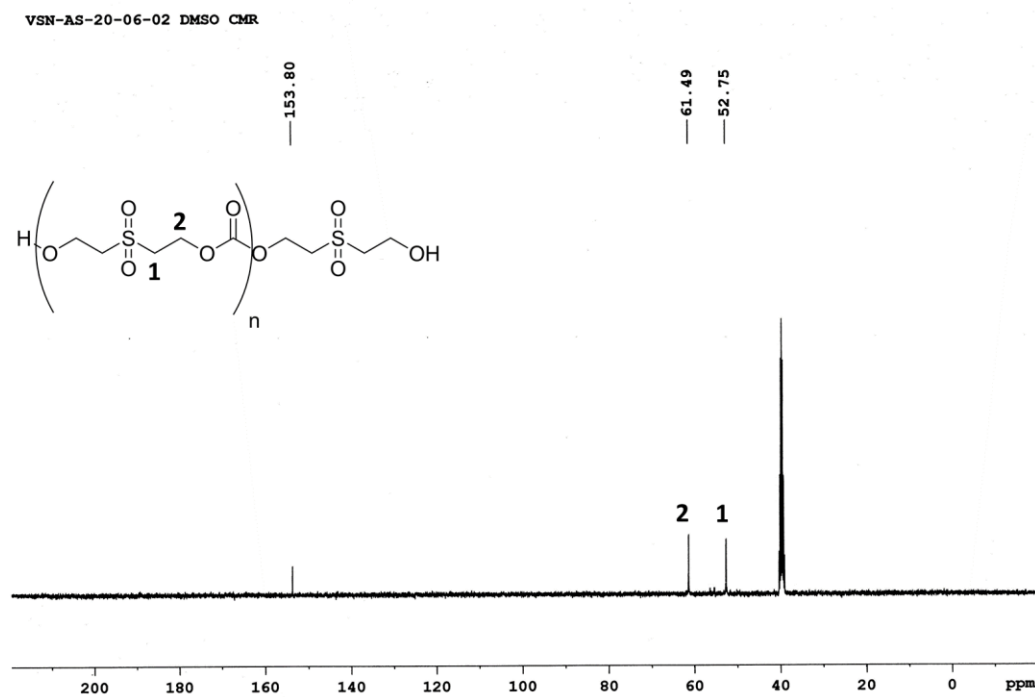


Figure 2.18 ¹³C NMR spectrum of poly (2,2'-sulfonyl diethylene carbonate), PSOC (7) in DMSO-d₆.

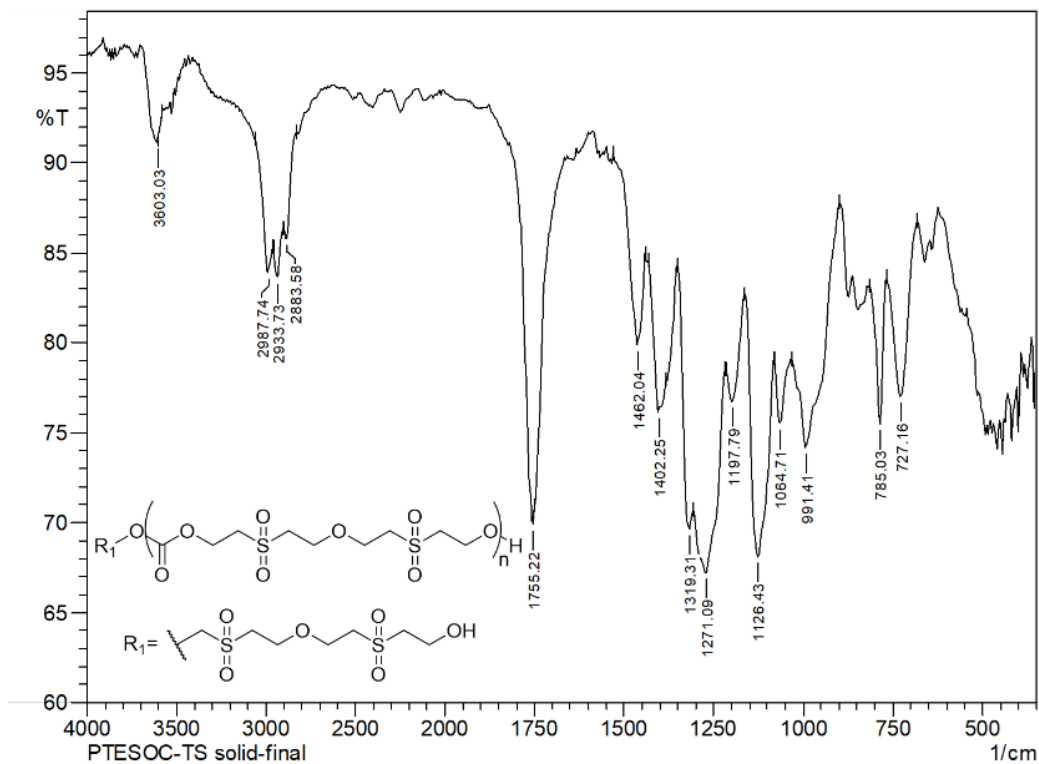


Figure 2.19 IR spectrum of poly(2, 2'-(oxybis(ethylenesulfonyl)) diethylene carbonate), PDSOC-1 (15) in KBr.

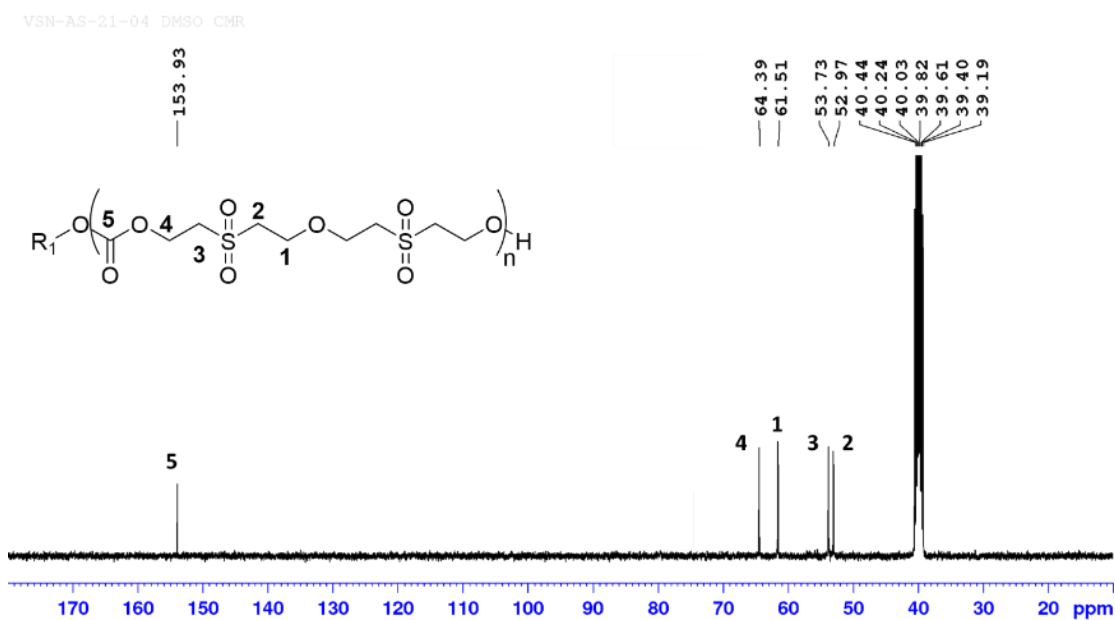


Figure 2.20 ^{13}C NMR spectrum of poly(2, 2'-(oxybis(ethylenesulfonyl)) diethylene carbonate), PDSOC-1 (15) in DMSO-d_6 .

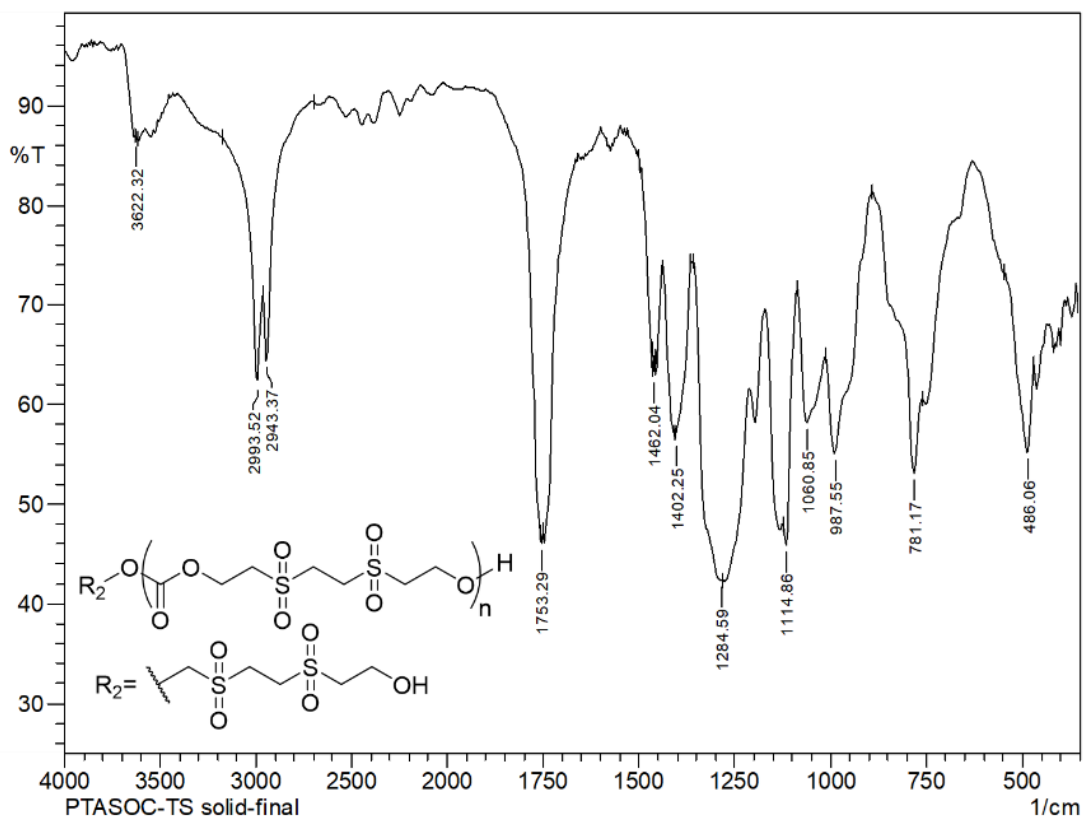


Figure 2.21 IR spectrum of poly (2,2'-(ethylenedisulfonyl) diethylene carbonate), PDSOC-2 (**16**) in KBr.

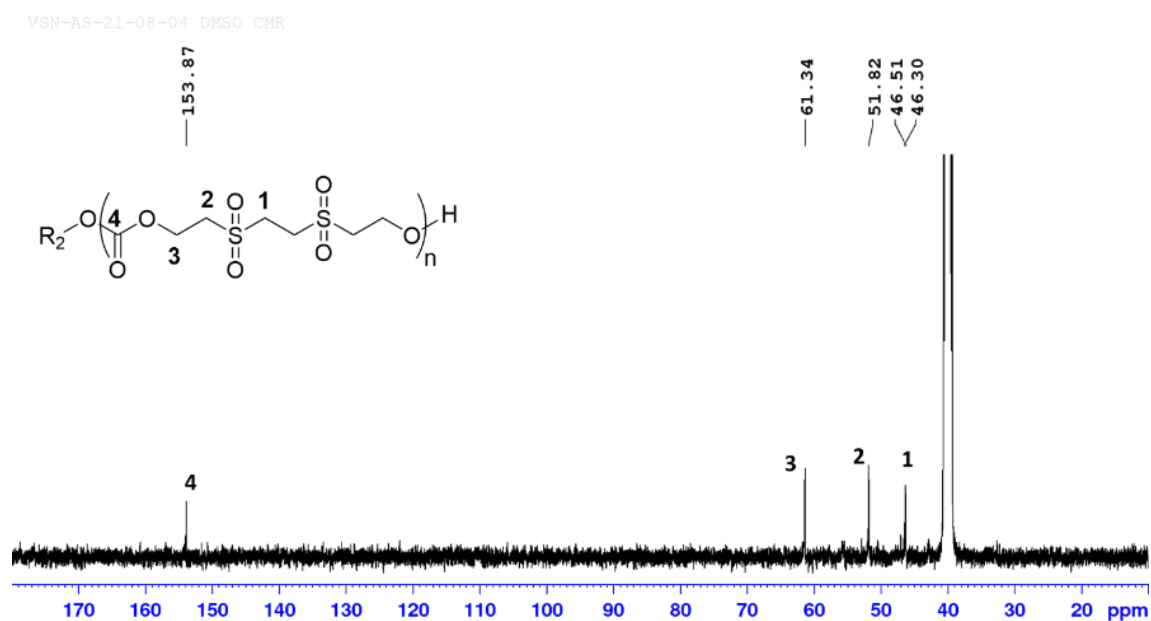


Figure 2.22 ^{13}C NMR spectrum of poly (2,2'-(ethylenedisulfonyl) diethylene carbonate), PDSOC-2 (**16**) in DMSO-d_6 .

IV. Synthesis of isopropylperoxydicarbonate (IPP) initiator for radical polymerization

IPP was prepared using reported method using two synthetic steps.

Step 1: Synthesis of isopropyl chloroformate (IPCL)⁴²

Two neck flask was charged with solution of triphosgene (19 g, 632 mmol) in 150 mL of dichloromethane and flask necks were sealed with silicon septum. The mixture was cooled to -5°C. With the help of two individual syringes isopropyl alcohol (10 g, 172 mmol) and pyridine (15 mL, 189.2 mmol) were added dropwise through the silicon septum, keeping pyridine addition in excess. After complete addition, reaction mixture was stirred for 4 h at 0°C. Reaction was stopped by pouring mixture into ice cold water and transferred to separatory funnel. Organic layer was washed twice with ice cold water, brine and dried over anhy. Na₂SO₄. Dichloromethane was removed by normal distillation using fractionating column to afford crude brown product. Crude product was purified by distillation under reduced pressure at 45°C to afford colourless liquid.

Step 2: Synthesis of isopropyl peroxydicarbonate (IPP) using IPCL⁸³

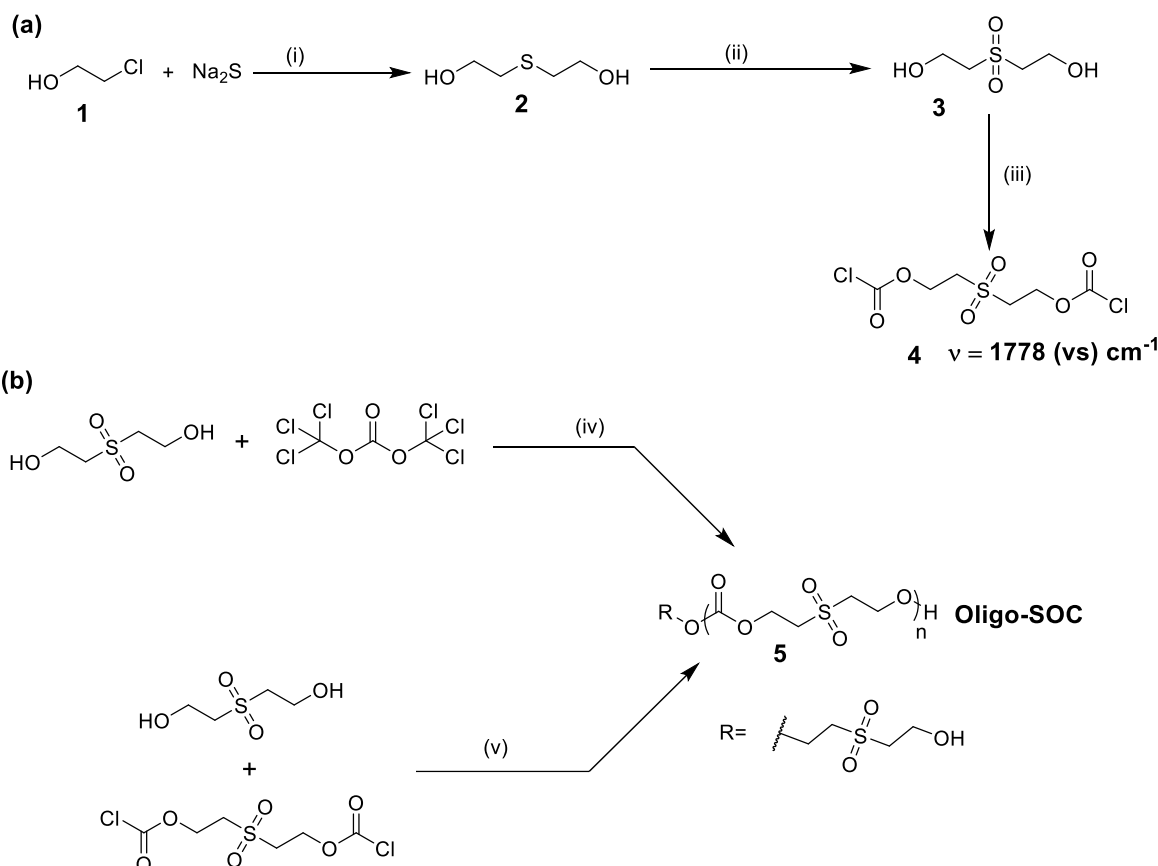
In a conical flask, was placed solution of NaOH (1.5 g, 37.5 mmol) in 2 mL of water and cooled to 0°C. To a stirred solution, 28% aq. H₂O₂ solution was added dropwise, maintaining the temperature below 10°C. Addition of aq. H₂O₂ results in formation of Na₂O₂ as a white paste, which was used in next step without any purification. In another flask, IPCL (5 g, 40.8 mmol) was placed and cooled to 0°C. To the stirred solution of IPCL was added Na₂O₂ drop wise, maintaining temperature between below 10°C. After complete addition, mixture was stirred vigorously for 1 h at 0°C. Later mixture was extracted with cold dichloromethane and transferred to separatory funnel. Organic layer was washed with water, brine and dried over anhydrous Na₂SO₄. Maximum amount of dichloromethane removed under low vacuum at 20°C to afford colourless liquid. Percent purity of IPP was determined using iodometric titration and purity above 75% was used further for cast polymerization. IPP being unstable at room temperature, it was stored below 10°C.

2.4 Results and discussion

2.4.1 Synthesis and characterization of main chain sulfur functionalized linear APCs.

I. An attempt toward synthesis of poly (2,2'-sulfonyl diethylene carbonate) by condensation polymerization

Our primary interest was to synthesize main chain sulfone functionalized APC, thus we outlined following scheme for the synthesis of sulfonyl monomers and poly(sulfone-carbonate) polymers.

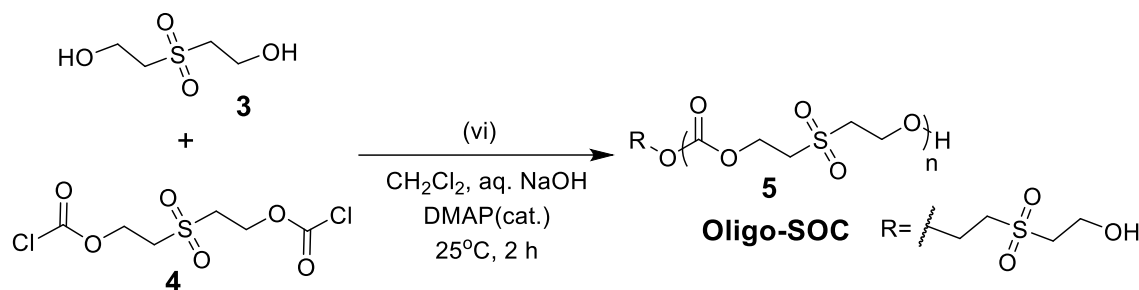


Scheme 2.22 Synthesis of (a) 2,2'-sulfonylbis(ethanol) and 2,2' sulfonylbis (ethylene chloroformate) monomers, (b) poly (2,2'-sulfonyl diethylene carbonate) polymer using solution polycondensation. (i) H_2O , reflux, 1 h; (ii) Oxone, diethyl amine (cat.), CH_3CN/H_2O (1:2), 30 min or V_2O_5 , MeOH, aq. H_2O_2 , 4 h; (iii) Triphosgene (1 equiv.), THF/ CH_2Cl_2 , $0^\circ C$ to r.t., 5 h; (iv) Pyridine (2 equiv.), THF, $0^\circ C$ to r.t., 2 h; (v) Pyridine (5equiv.)/DMAP (cat.), THF, $0^\circ C$ to r.t., 2 h.

Synthetic strategy towards sulfonyl monomers began with the preparation of thiodiglycol **2** intermediate, by reacting ethylene chlorohydrin with sodium sulfide in aqueous medium (**Scheme 2.22a**). The crude yellow product was purified by distillation under reduced

pressure of 0.2 torr at 80°C, to receive colorless liquid in 60-65% yield. Thiodiglycol sulfone monomer **3** was prepared by simple one step sulfide oxidation step. Method reported for synthesis of **3** utilizes oxone as oxidant, yielding product in 65% yield. This method involves excess of oxone reagent and some sulfoxide product remained unoxidized. Hence, we employed a modified strategy reported by Kupwade et al.^[83], where they used 1.5equiv. of oxone reagent per sulfide group in the presence of catalytic amount of diethyl amine. Using the same method, we were able to obtain purified sulfone product in 87% yield as pale-yellow product. Also, we tried an alternative method for sulfide oxidation reported by Choi et al.^[84], where H₂O₂ as oxidant in the presence of solid metal oxide catalyst such as V₂O₅. This reaction affords final purified product in 81% yield. For both method purification was carried out by silica gel chromatography. Thiodiglycol monomer **3** was further subjected to chloroformylation using phosgenation method to give sulfonylbis (ethylene chloroformate) monomer **4** in 78% crude yield. This was used in polymerization step without any purification.

In polymerization step, we attempted two step-growth polycondensation methods i.e., solution and interfacial (**Scheme 2.22b**). In solution polycondensation, thiodiglycol monomer **3** was polymerized with carbonylating reagent such as phosgene and bischloroformate monomer **4** in the presence of stoichiometric amount of pyridine as base and HCl scavenger and catalytic amount of DMAP. However, due to limited solubility of oligomeric chains forming in the reaction, results in precipitation of sticky white solid out of the solvent medium, making reaction medium difficult to stir. This sticky solid was reprecipitated in acetonitrile/water medium to afford white solid, which was further analyses for molecular weight using end group analysis, thereby confirming low molecular weight (DP=7) oligomeric product **5** (section 2.3.2III.i **Figure 2.10**).



Scheme 2.23 Synthesis of poly (2,2'-sulfonyl diethylene carbonate) polymer using interfacial polycondensation. (vi) CH₂Cl₂, aq. NaOH, DMAP (cat.), 25 °C, 2 h.

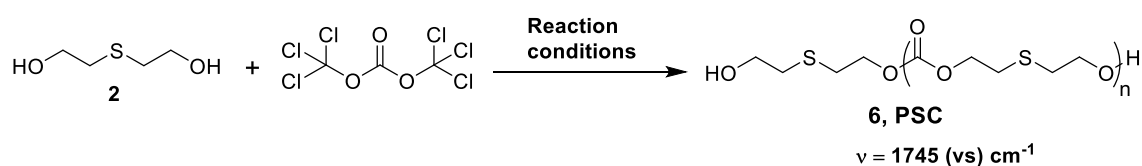
Interfacial polycondensation was performed using overhead mechanical stirrer. In this biphasic process, aqueous solution of thiodiglycol monomer **3**, sodium hydroxide and DMAP was rapidly stirred with sulfonyl bis (ethylene chloroformate) monomer **4** dissolved in organic medium such as chloroform (**Scheme 2.23**)

Similar observation was noted as seen in case of solution polymerization method. Sticky white solid was seen adhering to the glass walls of reaction vessel. Reprecipitation of this sticky material resulted in powder solid, which was also analysed for end group analysis.

II. Synthesis and characterization of Poly (2,2'-thio diethylene carbonate) using solution polycondensation methodology

Looking at difficulties encountered in our initial attempt towards synthesis of poly(sulfone-carboante) polymer, we thought of changing our strategy to two-step approaches. In our new approach, we planned to synthesize poly(thioether-carbonate) polymer first and then subjecting this to sulfide oxidation in second step to fetch desire sulfone-based polycarbonate polymer.

In a solution polycondensation, thiodiglycol **2** was polymerized with phosgene in the presence of excess of pyridine under anhydrous conditions (**Scheme 2.24**). In order to curtail the potential health hazards and safety issues associated with direct handling phosgene gas, we utilized methods of in-situ generation of phosgene in reaction medium through its solid analogue i.e., triphosgene. Reaction was terminated by aqueous workup and precipitated in dichloromethane/hexane solvent system to afford highly viscous liquid. It was essential here to maintain slow rate of addition of triphosgene at ambient temperature, because at quicker addition rate and lowering of temperature leads to decrease in average molecular weight of and yield of resultant polymer.



Scheme 2.24 Synthesis of Poly (2,2'-thio diethylene carbonate) (**PSC**)

Further, to understand the effect of varying stoichiometric ratio of carbonylating reagent i.e., triphosgene, we performed an optimization study at several stoichiometric ratios of triphosgene as depicted in **Table 2.1**.

Table 2.1 Optimization of carbonylation condition in polycondensation of thiodiglycol **2**.

Entry	Reaction conditions with pyridine (4eq) ^a	% Conversion ^b & Yield	M_n (Da) (NMR) ^b	M_n (Da) (OHV) ^c	M_n (Da) & \overline{M}_w (GPC) ^d
1	2 (0.3equiv.), 15°C to r.t., DCM, 12 h	94.9% (DP=19.5) & 81%	2909	2801	-
2	2 (0.36equiv.), 15°C to r.t., DCM, 12 h	98.3% (DP=58.5) & 96%	8727	8836	11261 & 1.46
3	2 (0.4equiv.), 15°C to r.t., DCM, 12 h	98.4% (DP=64) & 97%	9547	9502	12088 & 1.43
4	2 (0.4equiv.) 15°C to r.t., THF, 12 h	98.1% (DP=52) & 87%	7757	7501	9960 & 1.58

^a Initial triphosgene addition was carried out at 15°C for 1h, to control exothermic evolution of phosgene gas at preliminary stage; ^bDetermined by ¹H NMR spectroscopy; ^c calculated from hydroxyl value; ^d determined in THF by PS calibrated GPC.

Low molecular weights and percent monomer conversion rates were obtained at equimolar ratio carbonylating reagent with respect to thioether monomer, whereas highest molecular weight and percent conversion rate of 98% was observed at 10 mol% excess of triphosgene (**Table 2.1**). Variation in triphosgene ratio also affected the final yield of the polymeric product. Hence, our result complies with literature facts that, polycondensation reaction are necessary to be conducted at excess feed ratio of carbonylating reagent.

NMR technique proved to be a crucial technique in determining chemical structure, degree of polymerization and molecular weight of polymer. For chemical structural analysis of polymer, we employed ¹H NMR, ¹³C NMR and IR spectroscopy techniques. As seen in **Figure 2.23** ¹H NMR spectra of thiodiglycol and poly (2,2'-thio diethylene carbonate) in CDCl₃, characteristic triplet peaks appearing at 4.28-4.31ppm and 2.82-2.86 ppm were assigned to methylene protons of (OCH₂CH₂S) and (OCH₂CH₂S) in structural repeating unit, showcasing an evident chemical shift as compared to the peaks of thiodiglycol monomer. Peak appearing at 3.68 ppm was assigned to methylene peak attached to end hydroxyl group, confirming the linear polymer growth.

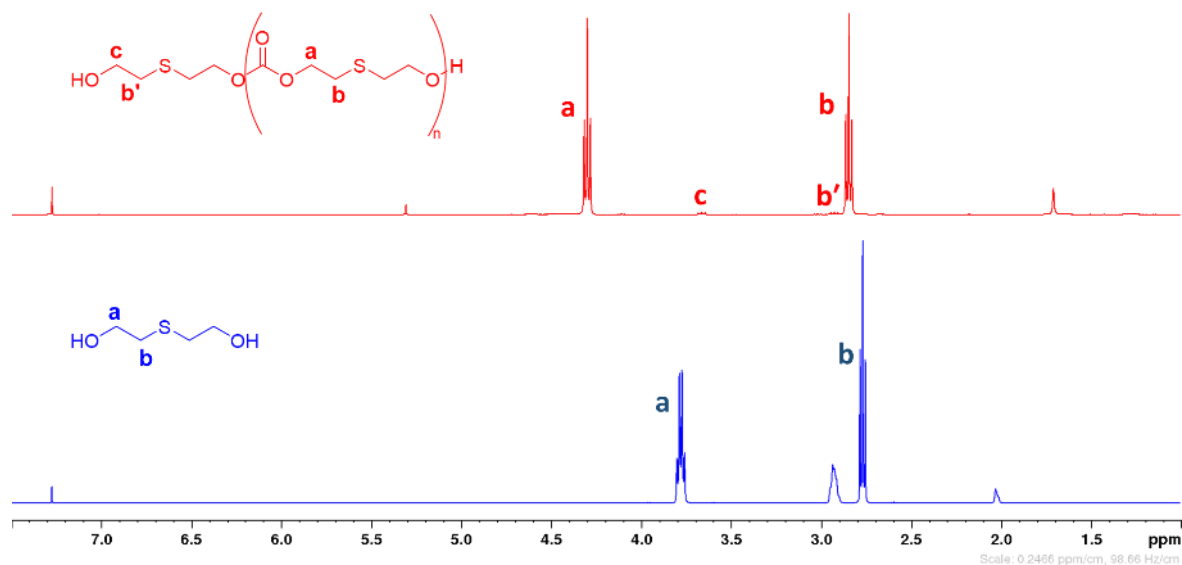


Figure 2.23 ^1H NMR spectra of thiodiglycol and poly (2,2'-thio diethylene carbonate) in CDCl_3 .

Similarly, distinctive three carbon signals were observed for PSC polymer at 154.72 ppm ($-\text{O}\underline{\text{C}}\text{OO}-$), 66.92 ppm ($\text{O}\underline{\text{C}}\text{H}_2\text{CH}_2\text{S}$) and 30.7 ppm ($\text{OCH}_2\underline{\text{C}}\text{H}_2\text{S}$) (**Figure 2.24**). IR spectroscopy confirms the formation of carbonate bonds appearing at carbonyl stretching frequency of 1745 cm^{-1} (section 2.3.2III.ii; **Figure 2.12**).

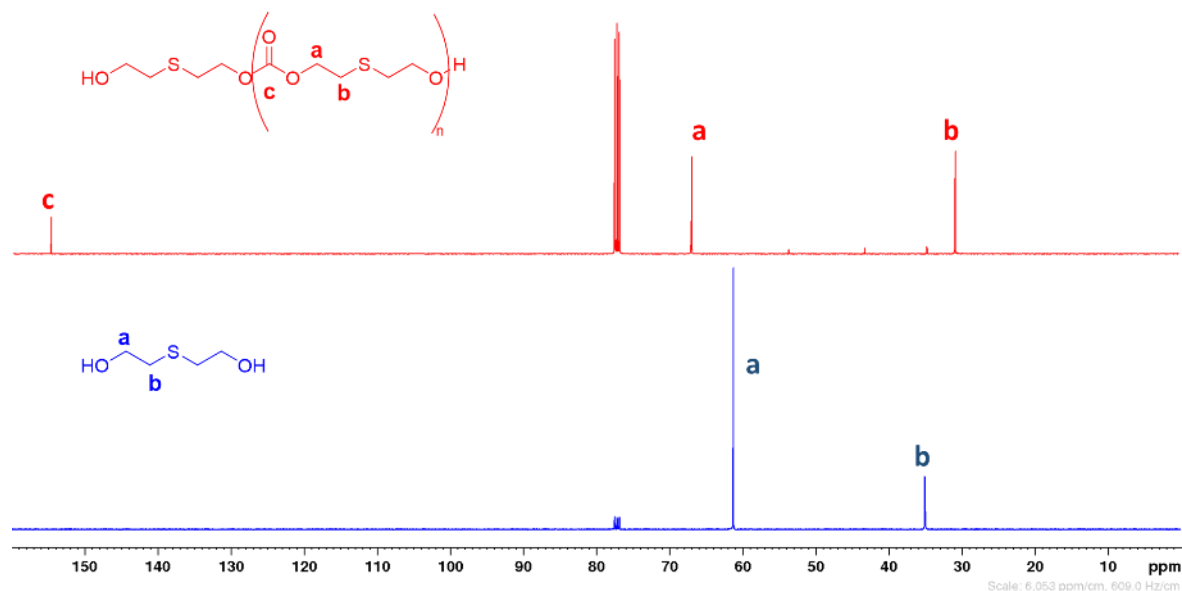


Figure 2.24 ^{13}C NMR spectra of thiodiglycol and poly (2,2'-thio diethylene carbonate) in CDCl_3

Average molecular weight determined by NMR and hydroxyl value (OHV) estimation technique is based on the end group analysis. Hydroxyl value was determined by iodometric

titration and this value was utilized to calculate number average molecular weight (M_n), which are closely related M_n (NMR) values (section 2.3.11.iii). Titrimetric analysis was performed in triplicates in order to minimize manual errors. Alternatively, molecular weights were also determined using GPC technique (Table 2.1).

It was important to note here that M_n values determined by NMR and GPC are inconsistent with each other, which can be attributed to the different hydrodynamic volumes of synthesized aliphatic polycarbonates relative to the polystyrene polymer standards. Moreover, polymers showed monomodal and narrow weight distribution curves.

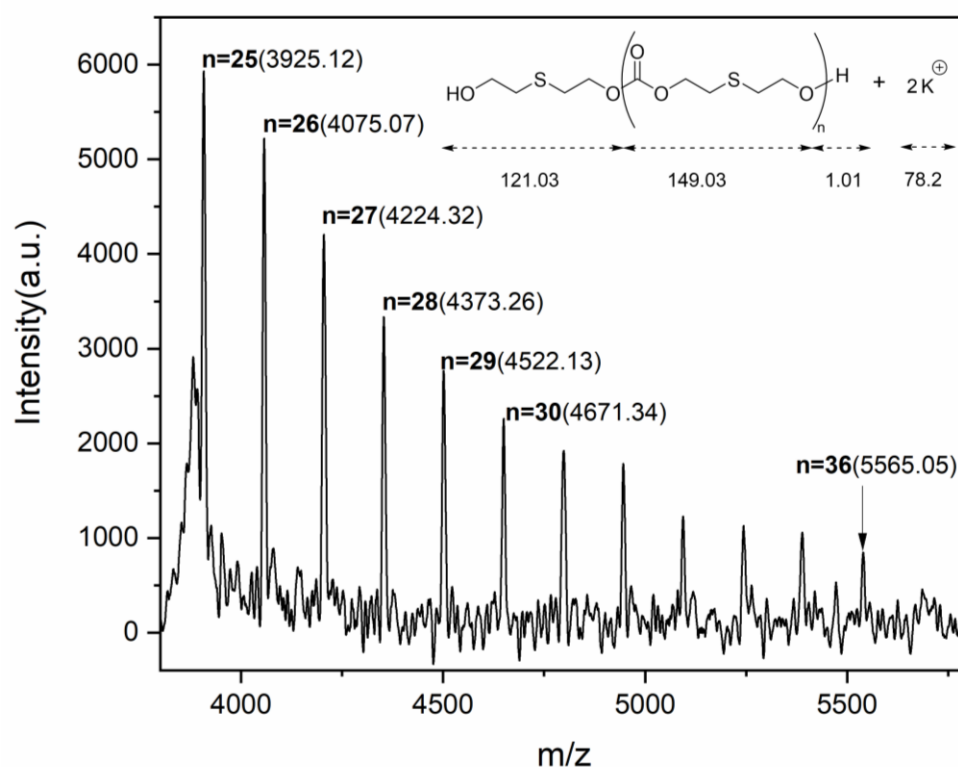


Figure 2.25 MALDI-TOF Mass spectrum of Poly (2,2'-thio diethylene carbonate).

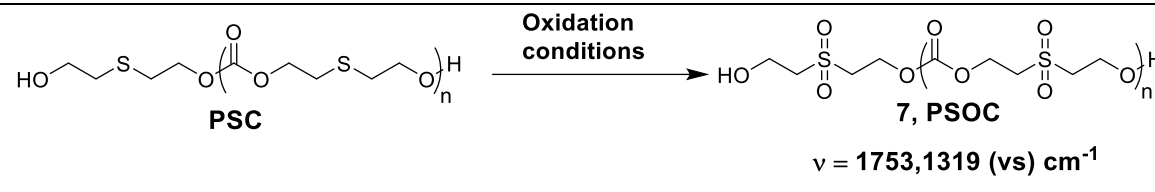
Furthermore, polymer composition was determined using MALDI-TOF mass spectrometry, which could provide clear evidence on the end groups and repeating units. From the mass spectrum as shown in **Figure 2.25**, each peak signifies the growing polymer chains with the mass difference between peaks are consistent with molar mass of the repeating unit i.e., $m/z = 149$. It was worth noting that, each molecular ion peaks appearing in the MS were in a good agreement with expected mass of the linear chain having two hydroxyl ends, calculated as $M_n = 122.04 + 149.03 \cdot n + 78.2$ ($2K^+$). Therefore, these above results prove that step

growth polycondensation reaction proceeded in highly controlled manner with formation of linear chain polymer under slow addition process.

III. Synthesis of poly (2,2'-sulfonyl diethylene carbonate) via sulfide oxidation of PSC polymer

Target poly (sulfone-carbonate) polymer was obtained by simple oxidation step. This sulfide oxidation step was performed using 20 to 30-fold excess of aqueous hydrogen peroxide as oxidant and V_2O_5 as catalyst (**Table 2.2**). Oxidant was calculated as per the obtained degree of polymerization of polycarbonate. In reaction medium polymer precipitates out as white solid, which was purified by reprecipitation in DMF/ H_2O solvent system. Solid was dried under high vacuum and characterized by IR, NMR and OHV analysis. Also, solid had a solubility limited to polar aprotic solvents such as DMF and DMSO.

Table 2.2 Synthesis and molecular weight analysis of poly (2,2'-sulfonyl diethylene carbonate) (PSOC).

					
Entry	Oxidation condition	% Monomer conversion^a	Yield^b	M_n (Da) (NMR)^a	M_n (Da) (OHV)^c
1	V_2O_5 (5 mol%), 30% H_2O_2 (30-fold excess), THF, 1 °C to r.t., 6 h.	98.3% (DP=60)	88%	10,871	10,252
^a Determined by 1H NMR spectroscopy; ^b isolated yield; ^c calculated from hydroxyl value.					

Chemical structure of the sulfone-carbonate polymer **7**, was determined by NMR and IR spectroscopy. As depicted in **Figure 2.26**, oxidation of sulfur resulted in shift of triplets corresponding to methylene protons, towards downfield region. Thus, peaks appearing at 4.46-4.49 ppm and 3.58-3.60 ppm were assigned to methylene protons of ($O\text{CH}_2\text{CH}_2\text{SO}_2$) and ($O\text{CH}_2\text{CH}_2\text{SO}_2$) in repeating units and 3.92 ppm to methylene next to hydroxyl end group. In IR spectrum, the SO_2 stretching band appeared at 1319cm^{-1} and carbonyl of carbonate linkages at 1753cm^{-1} (section 2.3.2III.iii; **Figure 2.17**). Average mass for the polymer **7** was calculated using end group analysis from NMR and hydroxyl value estimations.

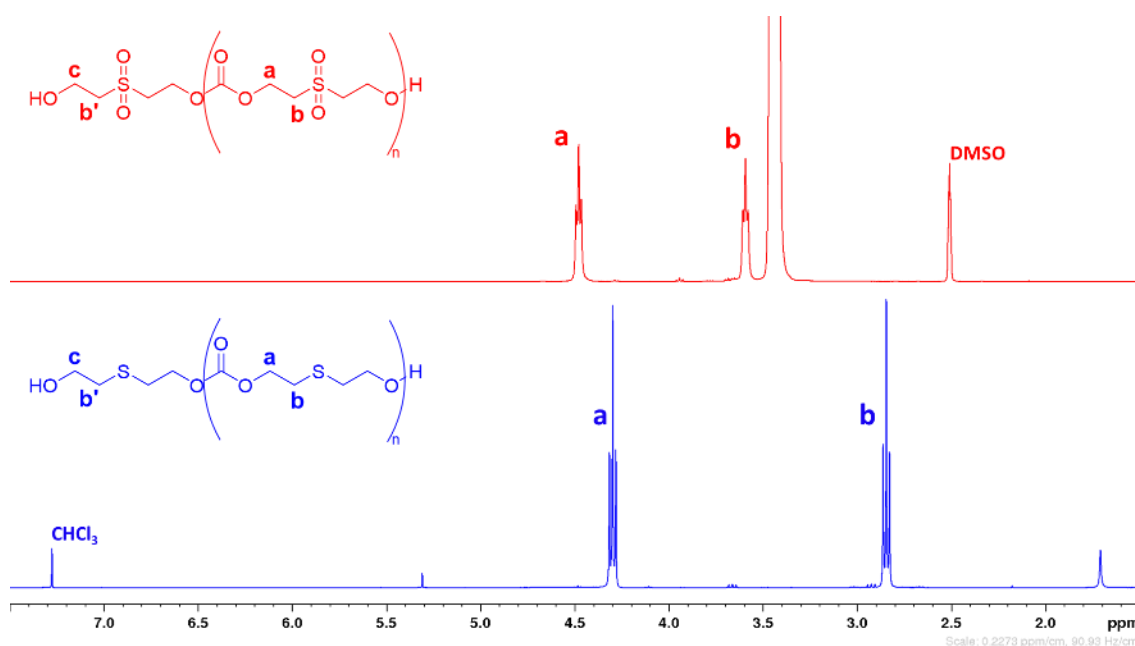
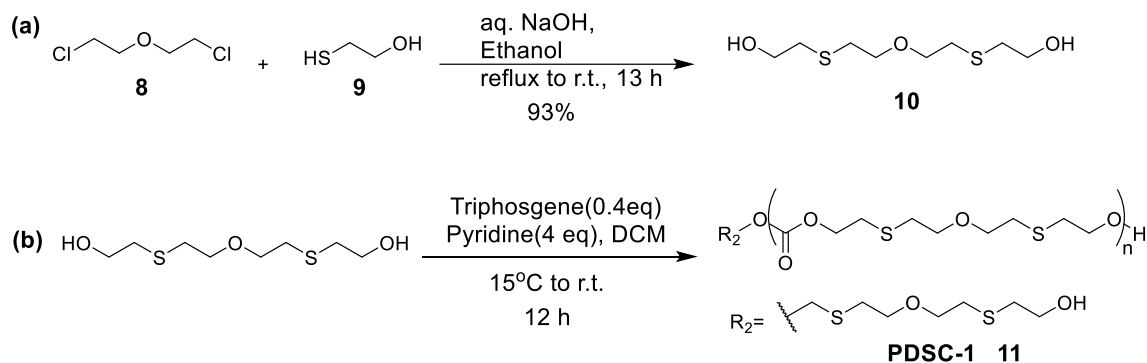


Figure 2.26 ^1H NMR spectra of poly (2,2'-sulfonyl diethylene carbonate) in DMSO-d_6 vs poly (2,2'-thio diethylene carbonate) in CDCl_3 .

IV. Synthesis and characterization of bis (thioether-carbonate) polymers using solution polycondensation method

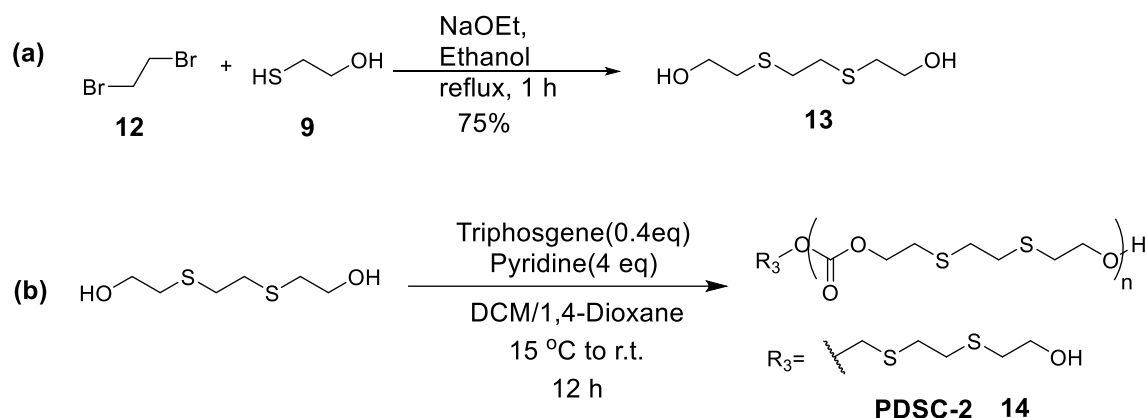
Looking at the success in obtaining the above mono (thioether-carbonate) polymers using solution polycondensation method, here we synthesized new types of thioether-carbonate polymers possessing two thioether moieties linked by ether or ethylene linkage in its structurally repeating units.



Scheme 2.25 . Synthesis of (a) 2, 2'-(oxybis(ethylenethio)) diethanol monomer; (b) Poly (2, 2'-(oxybis(ethylenethio)) diethylene carbonate) polymer.

Ether bridged polymer was synthesized from 2,2'-(oxybis(ethylenethio)) diethanol monomer **10** whereas ethylene bridged polymer was obtained from 2,2'-(ethylenedithio)diethanol **13** as shown in **Scheme 2.25** and **Scheme 2.26**.

Dithiadiol monomers **10** and **13** were prepared by classical nucleophilic displacement reaction between dialkyl halides (**8** and **12**) and 2-mercaptoethanol **9** in the presence of strong bases such as NaOH, NaOEt. Formation of dithiadiols proceed through the thiolate salt⁸². Also, reactions were smoothly carried out above 50 g scale. Monomer **10** was purified by distillation under reduced pressure to afford 93% yield, whereas crude solid monomer **13** was purified recrystallization in acetonitrile/toluene mixture to fetch white product in 75% yield.



Scheme 2.26 Synthesis of (a) 2,2'-(ethylenedithio)diethanol monomer; (b) Poly (2,2'-(ethylenedithio) diethylene carbonate) polymer

Polycondensation reaction were performed under similar condition as discussed previously using triphosgene as carbonylation agent in the presence of base. Only in case of ethylene bridged dithioether-carbonate polymer **14**, 1,4-dioxane was used as a solvent in combination with dichloromethane, due to low solubility of dithiaalkanediol monomer **13**. Polymer **11** was obtained as crude brown liquid, which was purified by silica gel filtration using ethyl acetate/hexane eluent system, whereas crude solid polymer **14** was purified precipitation in ethyl acetate/chloroform solvent system to afford white solid in 91% yield. Both monomers and polymers were analysed for their chemical structure using IR and NMR spectroscopy. For polymer **11** (**Figure 2.27**), characteristic, intense triplet's peaks were assigned to methylene protons of structural repeating unit (CRU) appearing at 4.28-31 ppm (-OCOCH₂CH₂SCH₂CH₂O-), 3.65-68 ppm (-OCOCH₂CH₂SCH₂CH₂O-), 2.84-87 ppm (-OCOCH₂CH₂SCH₂CH₂O-) and 2.75-78 ppm (-OCOCH₂CH₂SCH₂CH₂O-). Peak observed at 3.72-75 ppm was assigned to methylene peak attached to end hydroxyl group, thus confirming linear polymer chain formation in comparison with peaks observed for 2, 2'-(oxybis(ethylenethio)) diethanol monomer **10**.

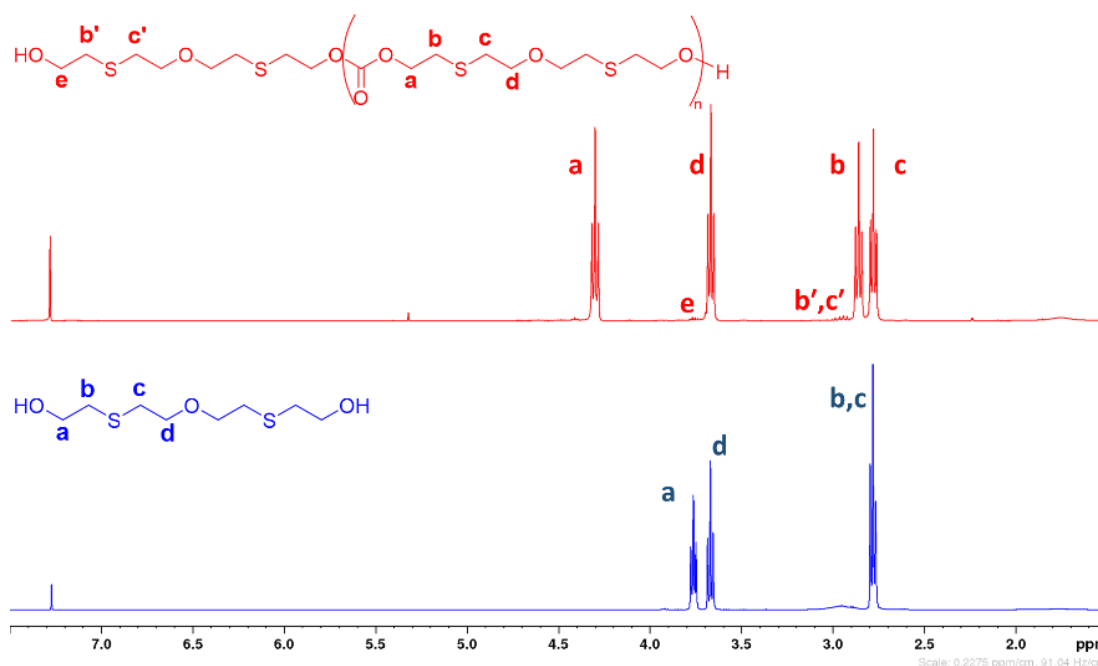


Figure 2.27 ¹H NMR spectra of 2, 2'-(oxybis(ethylenethio)) diethanol monomer and poly(2, 2'-(oxybis(ethylenethio)) diethylene carbonate) polymer in CDCl₃.

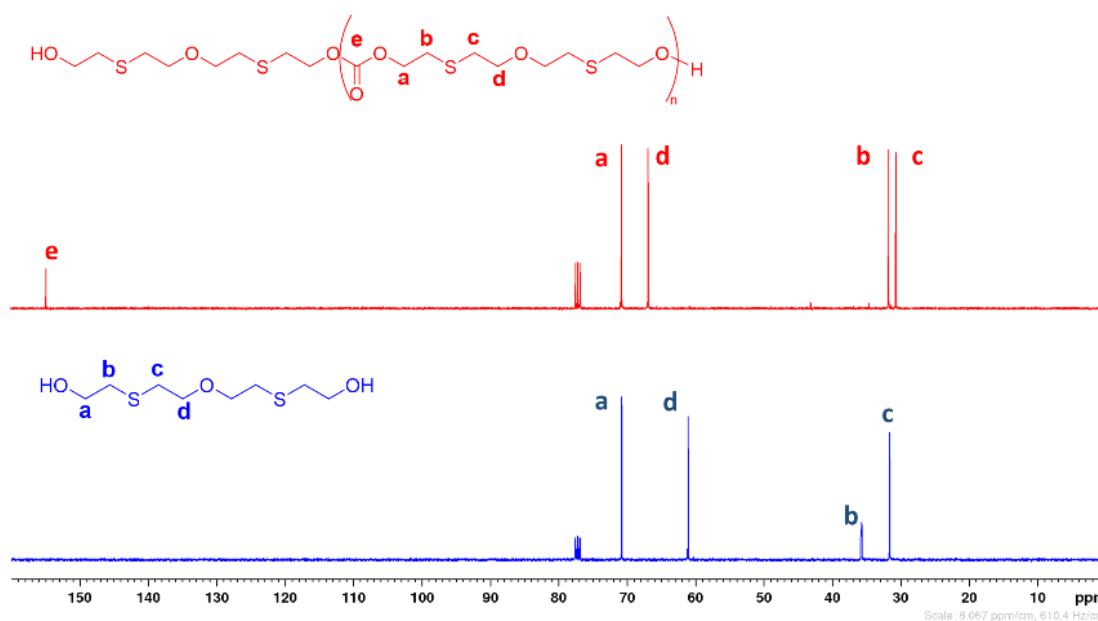


Figure 2.28 ¹³C NMR spectra of 2, 2'-(oxybis(ethylenethio)) diethanol monomer and poly(2, 2'-(oxybis(ethylenethio)) diethylene carbonate) polymer in CDCl₃.

In ¹³C NMR spectrum (**Figure 2.28**) peaks observed for each distinctive methylene carbon of CRU with chemical shift values 154.74 ppm (-OCCOO-), 77.16 ppm (-OCCOCH₂CH₂SCH₂CH₂O-), 70.77 ppm (-OCCOCH₂CH₂SCH₂CH₂O-), 31.82 (-OCCOCH₂CH₂SCH₂CH₂O-) and 30.77 ppm (-OCCOCH₂CH₂SCH₂CH₂O-). Additionally,

formation of carbonyl linkages in polymer structure is supported by carbonyl stretching band appearing in IR spectrum at 1745 cm^{-1} (section 2.3.2III.ii; **Figure 2.14**).

Similarly, for ethane bridged dithioether carbonate polymer **14**, a distinct, intense triplet peak appearing at 4.39-4.42 ppm corresponds methylene protons attached to carbonate bond ($-\text{OCO}\underline{\text{CH}_2}\text{CH}_2\text{SCH}_2\text{CH}_2\text{S}-$) in CRU (**Figure 2.29**). Methylene protons attached to thioether appeared at 3.73-3.78 ppm ($-\text{OCOCH}_2\underline{\text{CH}_2}\text{SCH}_2\text{CH}_2\text{S}-$).

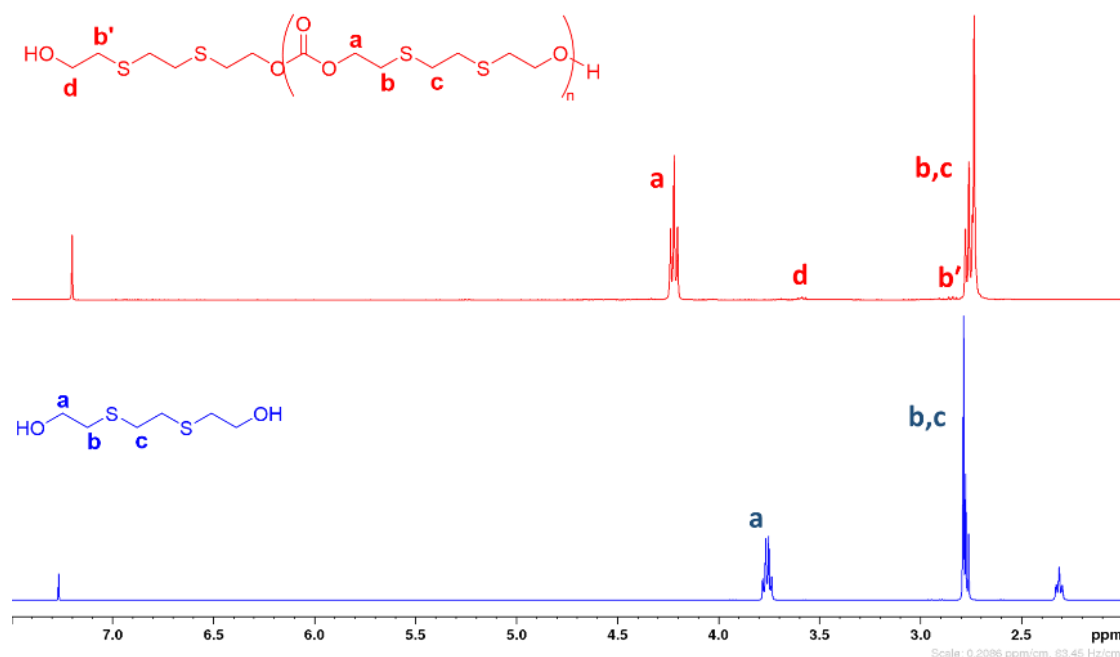


Figure 2.29 ^1H NMR spectra of 2,2'-(ethylenedithio)diethanol monomer and Poly (2,2'-(ethylenedithio) diethylene carbonate) polymer in CDCl_3

In ^{13}C NMR spectrum (**Figure 2.30**), we found 4 intense peaks appearing at 154.73 ppm ($-\text{OCO}\underline{\text{O}}-$), 66.92 ppm ($-\text{OCO}\underline{\text{C}}\text{H}_2\text{CH}_2\text{SCH}_2\text{CH}_2\text{S}-$), 32.45 ppm ($-\text{OCOCH}_2\underline{\text{C}}\text{H}_2\text{SCH}_2\text{CH}_2\text{S}-$) and 30.4 ppm ($-\text{OCOCH}_2\text{CH}_2\underline{\text{S}}\text{CH}_2\text{CH}_2\text{S}-$). In IR spectrum, band at 1745 cm^{-1} assigned to carbonyl stretching frequency of carbonate (section 2.3.2III.ii; **Figure 2.16**).

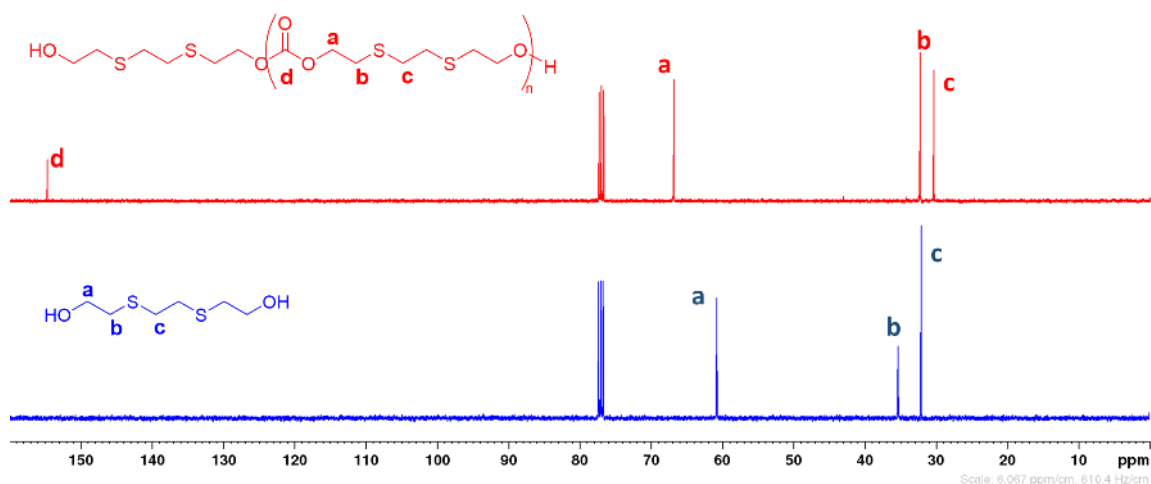


Figure 2.30 ^{13}C NMR spectra of 2,2'-(ethylenedithio)diethanol monomer and poly (2,2'-(ethylenedithio) diethylene carbonate) polymer in CDCl_3 .

Furthermore, using end group analysis by ^1H NMR and OHV estimations, number average molecular weight was calculated, which were closely correlated with each other as noted in **Table 2.3**. Also, GPC technique was employed to determine average molecular weights and polydispersity index (\mathcal{D}_M). Narrow distributions curves were obtained for both polymers and alike PSC polymer, notable difference between M_n values by NMR and GPC were observed, due to difference in hydrodynamic values of PSDC polymer and PS calibrant.

Table 2.3 Average molecular weight analysis for polymer **11** and **14**.

PDSC	%Monomer conversion ^a	Yield ^b	M_n (Da) (NMR) ^a	M_n (Da) (OHV) ^c	M_n (Da) & \mathcal{D}_M (GPC) ^d
PDSC-1	96.9% (DP=32.6)	93%	8259	8501	10,259 & 1.67
PDSC-2	96.8% (DP=31)	91%	6488	6628	8138 & 1.49

^a Determined by ^1H NMR spectroscopy; ^b isolated yields; ^c calculated from hydroxyl value;

^d determined in THF by PS calibrated GPC.

MALDI-TOF-MS analysis of PDSC polymers confirms its linear chain structure and showed controlled progression of step growth polycondensation. For e.g., polymer **11**, the mass differences between two adjacent peaks were well accord with the expected molecular weight of the CRU i.e., $m/z = 253$ and each molecular ion peaks appearing in the MS were agreed well with expected mass of the linear chain having two hydroxyl ends (**Figure 2.31**).

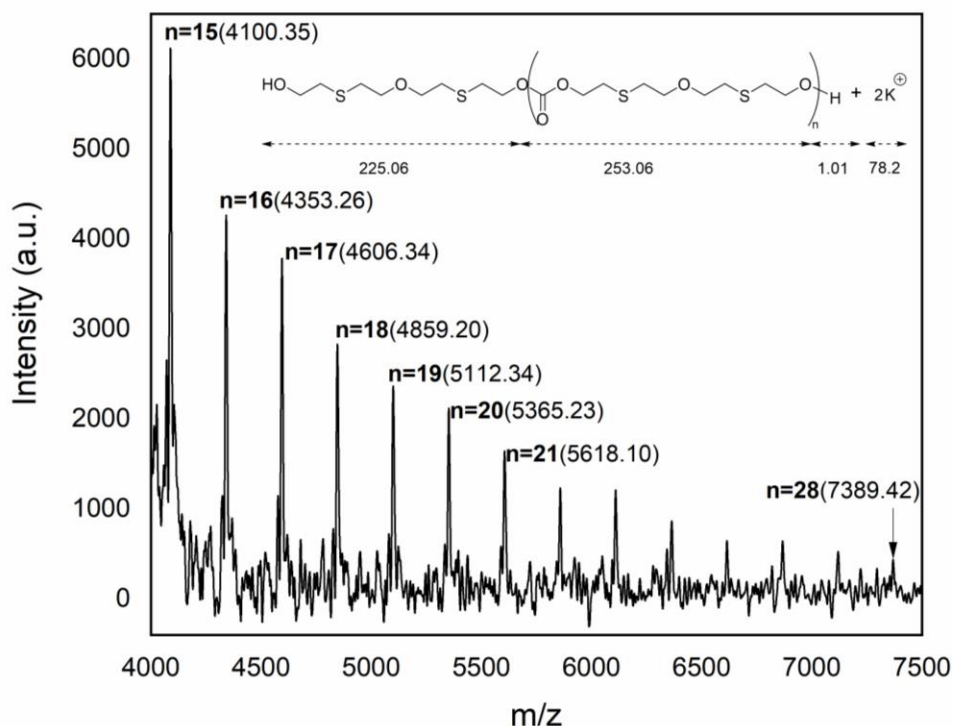
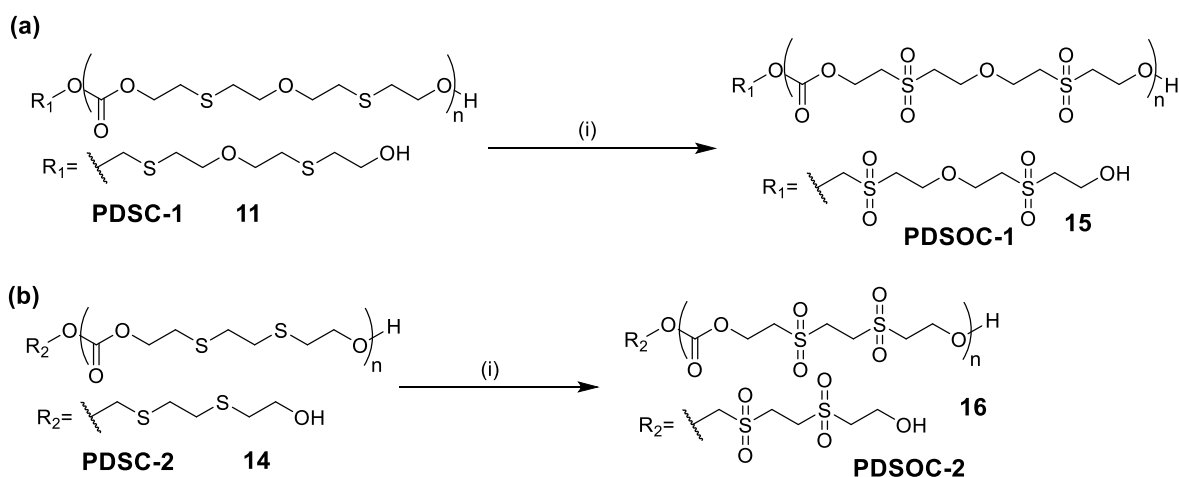


Figure 2.31 MALDI-TOF Mass spectrum of Poly (2,2'-thio diethylene carbonate).

V. Synthesis and characterization of bis-sulfonyl-carbonate polymers via oxidation of sulfide functionality

Oxidation PDSC polymers were performed using 20-fold excess of hydrogen peroxide as oxidant and vanadium pentoxide as catalyst (**Scheme 2.27**).



Scheme 2.27 Synthesis of disulfonyl-carbonate polymers (PDSOC) (a) Poly (2, 2'-(oxybis(ethylenesulfonyl)) diethylene carbonate); (b) Poly (2,2'-(ethylenedisulfonyl) diethylene carbonate). (i) V_2O_5 (5 mol%), 30% H_2O_2 (20-fold excess), THF, 10 °C to r.t., 6 h.

Polymer **15** was precipitated out of reaction mixture as thick colourless liquid, which was purified by reprecipitating in DMF/EtOAc mixture to afford hard sticky transparent solid upon drying high vacuum. On the other hand, polymer **16** was precipitated as white solid from reaction mixture and later purification by reprecipitation in DMSO/Methanol mixture. Unlike PSOC polymer, PDSOC had a solubility confined to polar aprotic solvents like DMF, DMSO.

Chemical structure of PDSOC polymers and complete oxidation was determined using IR and NMR spectroscopy. Oxidation of sulfide to sulfonyl functionalities resulted in increase of chemical shift values for methylene protons in CRU. For polymer **15**, characteristic triplet peaks in ^1H NMR spectrum (Figure 2.32) were positioned at 4.45-48 ppm (-OCO $\underline{\text{CH}_2}$ CH $_2$ SO $_2$ CH $_2$ CH $_2$ O-), 3.80-83 ppm (-OCOCH $_2$ CH $_2$ SO $_2$ CH $_2$ $\underline{\text{CH}_2}$ O-), 3.56-59 ppm (-OCOCH $_2$ $\underline{\text{CH}_2}$ SO $_2$ CH $_2$ CH $_2$ O-) and 3.43-45 ppm (-OCOCH $_2$ CH $_2$ SO $_2$ $\underline{\text{CH}_2}$ CH $_2$ O-). In ^{13}C NMR spectrum (section 2.3.3-III-C; Figure 2.20), peaks at 153.94 ppm (-OCO-) corresponds to carbonyl carbon, whereas rest methylene protons appeared at 64.39 ppm (-OCO $\underline{\text{CH}_2}$ CH $_2$ SO $_2$ CH $_2$ CH $_2$ O-), 61.51 ppm (-OCOCH $_2$ CH $_2$ SO $_2$ CH $_2$ $\underline{\text{CH}_2}$ O-), 53.73 ppm (-OCOCH $_2$ $\underline{\text{CH}_2}$ SO $_2$ CH $_2$ CH $_2$ O-) and 52.97 ppm (-OCOCH $_2$ CH $_2$ SO $_2$ $\underline{\text{CH}_2}$ CH $_2$ O-).

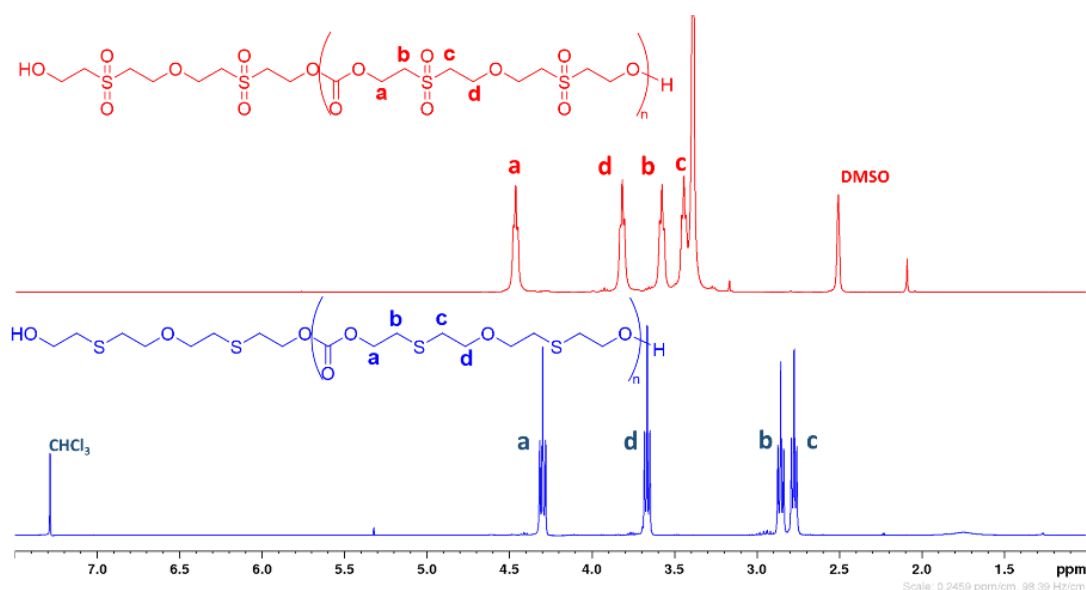


Figure 2.32 ^1H NMR spectra of Poly (2, 2'-(oxybis(ethylenesulfonyl)) diethylene carbonate) in $\text{DMSO-}d_6$ vs Poly (2, 2'-(oxybis(ethylenethio)) diethylene carbonate) in CDCl_3 .

For polymer **16**, two distinct triplets appeared at 4.5 ppm (-OCO $\underline{\text{CH}_2}$ CH $_2$ SO $_2$ CH $_2$ CH $_2$ SO $_2$ -) and 3.72-74 ppm (-OCOCH $_2$ $\underline{\text{CH}_2}$ SO $_2$ CH $_2$ CH $_2$ SO $_2$ -). Also, a characteristic singlet peaks

was seen to appear at 3.63 ppm ($-\text{OCOCH}_2\text{CH}_2\text{SO}_2\text{CH}_2\text{CH}_2\text{SO}_2-$) corresponding to ethylene protons (

Figure 2.33).

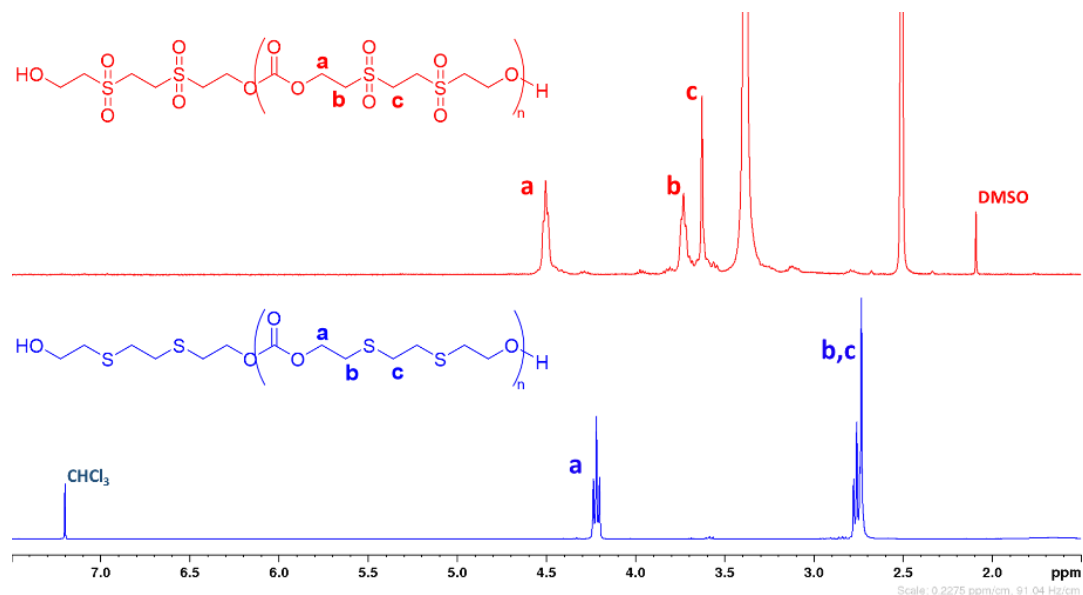


Figure 2.33 ^1H NMR spectra of Poly (2,2'-(ethylenedisulfonyl) diethylene carbonate) in $\text{DMSO-}d_6$ vs poly (2,2'-(ethylenedithio) diethylene carbonate) in CDCl_3

Accordingly, four peaks were located in ^{13}C NMR spectrum (section 2.3.3-III-C; **Figure 2.22**), which corresponds to one carbonyl and three methylene carbon with chemical shift values 153.87 ppm ($-\text{O}\underline{\text{C}}\text{OO}-$), 61.34 ppm ($-\text{OCO}\underline{\text{C}}\text{H}_2\text{CH}_2\text{SO}_2\text{CH}_2\text{CH}_2\text{SO}_2-$), 51.82 ppm ($-\text{OCOCH}_2\text{CH}_2\text{SO}_2\text{CH}_2\text{CH}_2\text{SO}_2-$) and 46.3 ppm ($-\text{OCOCH}_2\text{CH}_2\text{SO}_2\text{CH}_2\text{CH}_2\text{SO}_2-$). For both polymers, carbonyl stretching frequency appeared at $1753\text{--}1755\text{ cm}^{-1}$ whereas sulfonyl group appeared at 1319 cm^{-1} (section 2.3.2III.iii; **Figure 2.19** and **Figure 2.21**).

Table 2.4 Average molecular weight analysis for polymer **15** and **16**.

PDSOC	% Monomer conversion ^a	Yield ^b	M_n (Da) (NMR) ^a	M_n (Da) (OHV) ^c
PDSOC-1 (15)	96.4% (DP=27.9)	78%	8848	8191
PDSOC-2 (16)	96% (DP=24.8)	85%	6787	6125

^a Determined by ^1H NMR spectroscopy; ^b isolated yields; ^c calculated from hydroxyl value.

Number average molecular weight (M_n) for polycarbonate **15** and **16** were calculated by end group analysis using ^1H NMR and hydroxyl value estimations. M_n by both methods were closely related to each other as noted in **Table 2.4**.

Newly synthesized sulfur containing linear APCs were thermally characterized for its glasstransition (T_g) temperature using Differential Scanning Calorimetry. Poly(thioether carbonate) polymers, showed T_g at low temperature scale. PDSC-1 polymer showed a lowest value of -51.6°C (**Figure 2.34**), indicating influence of diethylene ether chain in main chain backbone, which increases the flexibility of chain and lowers the T_g .

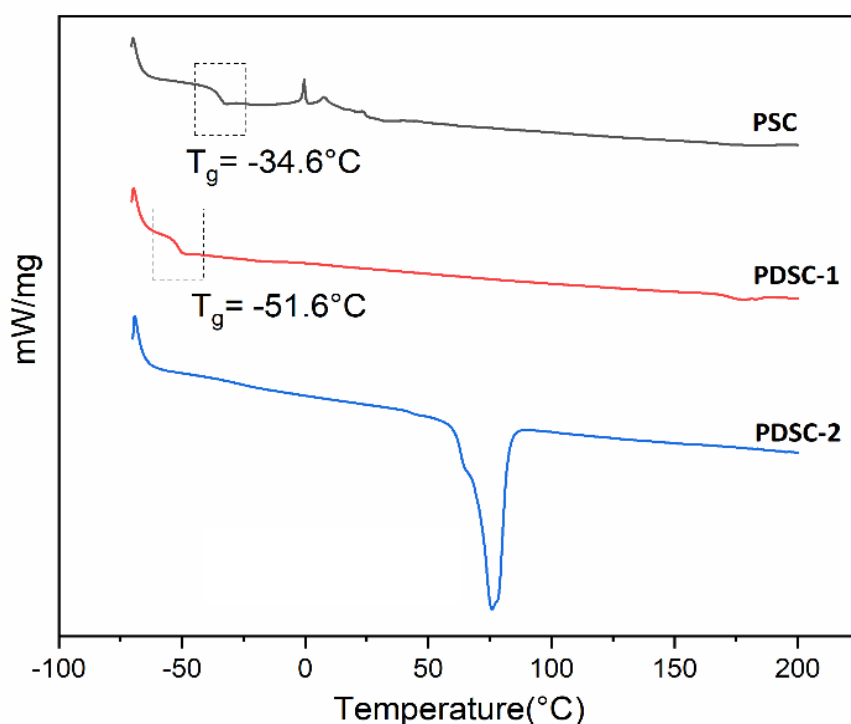


Figure 2.34 DSC thermogram of main chain thioether based APCs.

On the contrary, sulfone functionalized APCs showed high values of T_g compared to their sulfide analogue's (**Figure 2.35**). This could be attributed to the decrease in chain flexibility, caused by sulfone moieties. Additionally, solid polymers such as PDSC-2 and PSOC polymers showed a narrow melting peak (T_m) at 75.8°C and 127°C , indicating high crystalline nature of polymers. However, PDSOC-1 polymer showed broad and diminishing melting curve at 55°C , this could be due to high amorphous character of polymer.

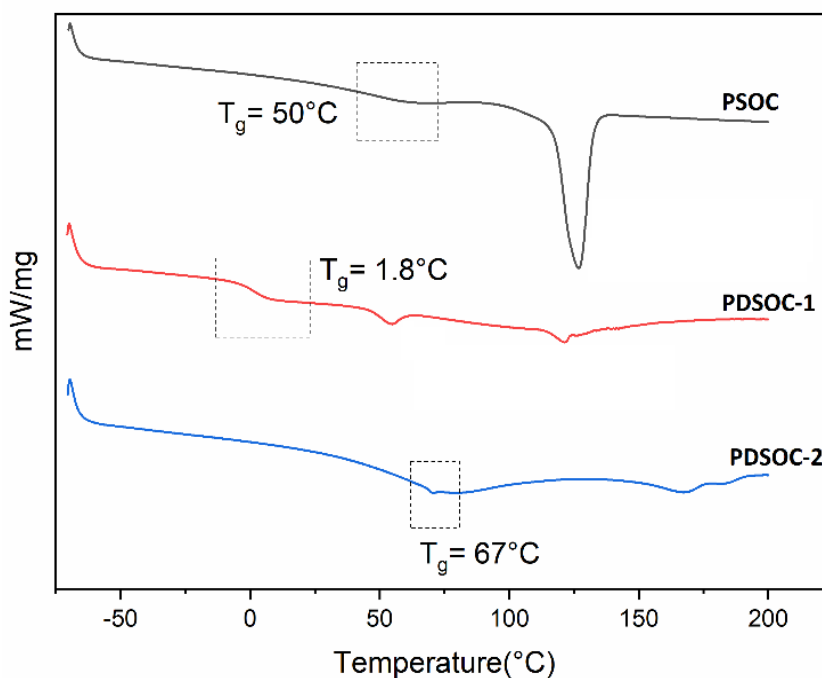


Figure 2.35 DSC thermogram of main chain sulfone-based APCs.

Supporting study to the morphology of polymers was provided by recording its powder XRD pattern as shown in **Figure 2.36**. XRD analysis revealed that, PSOC and PDSOC-2 polymers possess more crystalline nature as compared to PDSOC-1 polymer. Due to waxy sticky form of the PDSOC-1 polymer we were unable to record its PXRD pattern.

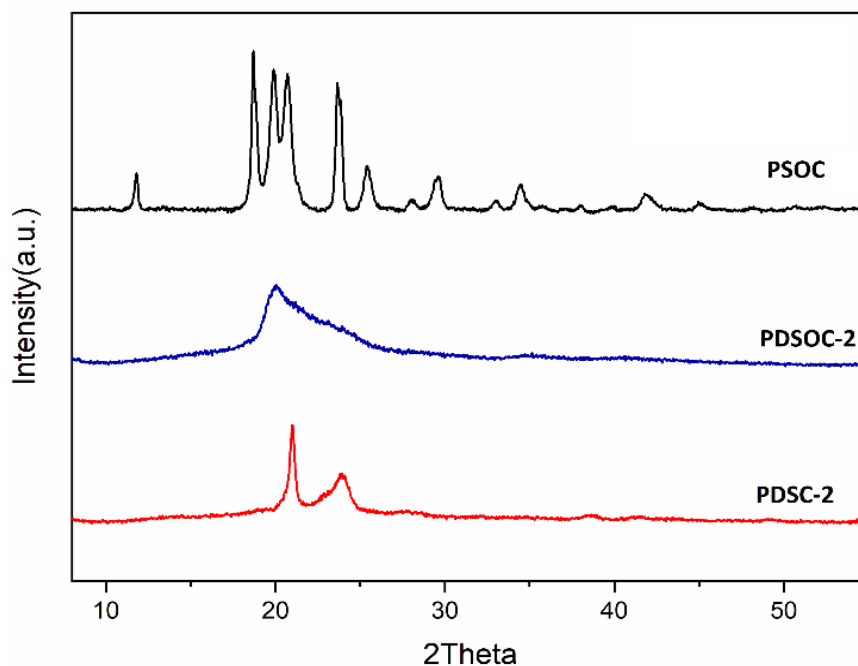
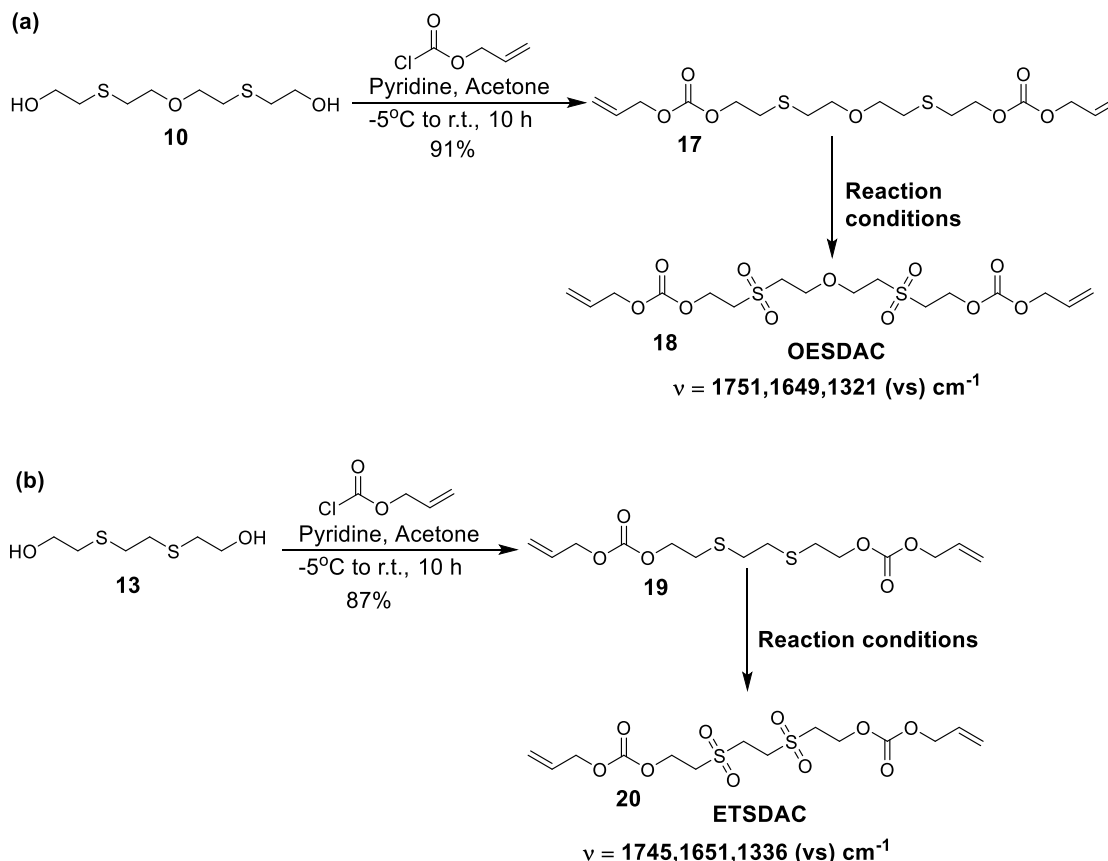


Figure 2.36 PXRD pattern for main chain sulfur functionalized APCs.

2.4.2 Synthesis and characterization of sulfur containing allylic monomers and development of crosslinked APCs

I. Synthesis of sulfone functionalized allyl carbonate monomers (SOAC).

Tetrafunctional (-C=C-) sulfone functionalized monomers were synthesized from dithiadiol **10** and **13** as starting substrates, using two step approach as depicted in **Scheme 2.28**.



Scheme 2.28 Synthesis of sulfone functionalized allyl carbonate monomers (SOAC), (a) 2,2'-(oxybis(ethylenesulfonyl)) diallylcarbonate (OESDAC); (b) 2,2'-(ethylenedisulfonyl) diallylcarbonate (ETSDAC).

Synthesis began with *O*-carbonylation of dithiadiol monomers **10** and **13** using allyl chloroformate as carbonylating reagent and pyridine as base as well as acid scavenger to afford dithiadiallyl carbonate intermediates **17** and **20**. These crude products were subjected to silica gel chromatography to afford pure liquid product. Purification of **17** was achieved by eluting pure colourless liquid in Pet. Ether/ EtOAc, 70:30 solvent system in 90% yield. Similarly, crude **20** was eluted as pale-yellow liquid in 87% yield using Pet. Ether/ EtOAc, 70:30) solvent system.

Further, in order to prepare SOAC monomers **18** & **20**, we employed two oxidant conditions as noted in **Table 2.5**. Both methods could furnish selectively sulfone product in

high yield. Crude sulfone product of **18** was purified by silica gel chromatography, eluting in Pet. Ether/ EtOAc, 80:20, solvent system to fetch colorless viscous liquid in 81-87% yield. On the other hand, crude sulfone product of **20** was recrystallized in toluene/acetonitrile mixture to afford pure white shiny product in 82% yield.

Table 2.5 Oxidation conditions for conversion of sulfide to sulfone.

Entry	Reaction conditions	% Isolated yields	
		OESDAC (18)	ETSDAC (20)
1	Oxone (4 equiv.), DEA (cat.), CH ₃ CN/ H ₂ O, r.t., 30min.	87%	82%
2	V ₂ O ₅ (cat.), 30% H ₂ O ₂ , MeOH, 4 h.	81%	78%

II. Synthesis of sulfone functionalized cross-linked aliphatic polycarbonates

The radical polymerization of allyl monomers is usually carried out using organic peroxide initiators such as benzoyl peroxide (BP) or isopropyl peroxydicarbonate (IPP). The polymerization using BP initiator results in high cross-linking in polymer because of an access to higher curing temperatures. However, for thermosetting aliphatic polymers with an application as plastic nuclear track detector, use of BP initiator is known to result in decrease in radiation sensitivity of plastic material^[66]. On the other hand, IPP has low decomposition temperature (35-40°C), which allows the polymerization at lower temperature and produce thermoset resin sensitive to charge particle detection. Therefore, for such application thermoset polymers are usually prepared using IPP initiator. Moreover, the polymers cured with IPP initiator do not lead to maximum crosslinks as the polymerization slowly diminishes with the vitrification of the polymer network^[42].

Before proceeding with polymer preparation using casting technique, it is essential to check the stability of monomer in initiator. Usually, allyl carbonate monomers are most stable and can be polymerized smoothly in the presence of BP and IPP. Also, in recent studies sulfone-carbonate monomer were proved to be stable and could furnish hard crosslinked resin in the presence of IPP.^[67] Hence, in our study we utilized IPP for radical polymerization sulfone-carbonate monomers. Initially, we conducted radical polymerization in test tubes, in order to confirm the hardness of the gel. We performed this test in the presence of 4% IPP concentration with slow heating from 50-70°C and result were noted in table below.

Table 2.6 Test tube radical homo- and co-polymerization of SOAC monomers with ADC.

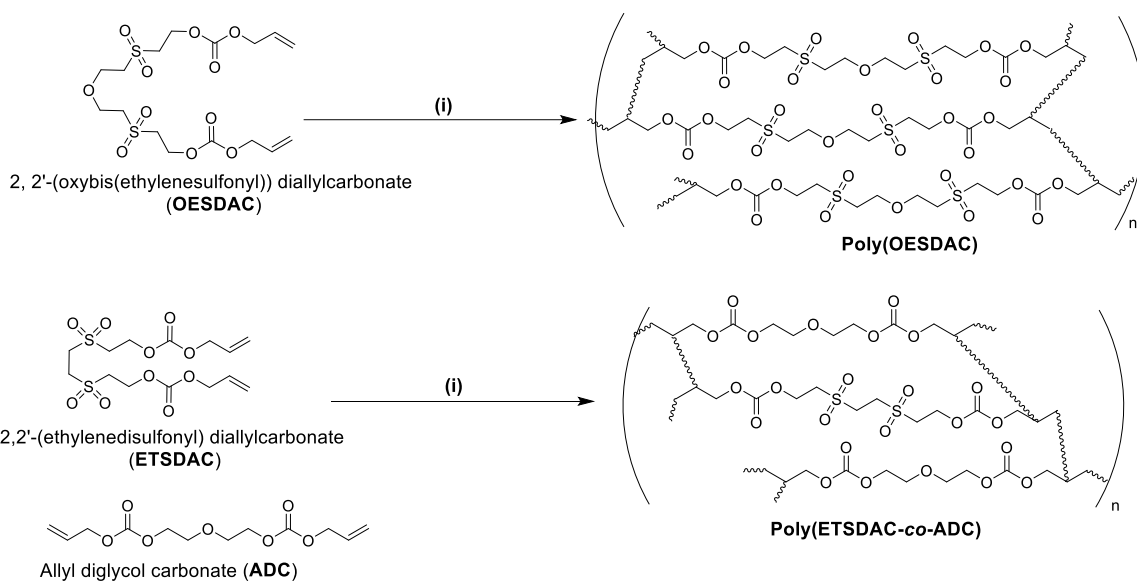
Sr. No.	Monomer composition (w/w%)	Initiator conc. (w/w%)	Temperature (°C)	Observation and results
1	OESDAC	4	50-80	Gelation after 30 min at 50°C and soft resin after 4h at 70-80°C
2	OESDAC: ADC (1:1)	4	50-80	Gelation after 30min at 50°C and hard resin after 4 h at 70-80°C
3	ETSDAC: ADC (1:9)	4	50-80	Gelation after 3 h at 50 °C and hard resin after 4 h at 70-80°C

^aMonomers were purged with N₂ gas; ^btemperature of oil bath.

Since ETSDAC monomer is solid and had melting point 90-92°C, we couldn't polymerise the monomer using IPP initiator. However, one could try polymerizing at melting temperature using BP initiator. Also, we could prepare only one monomer composition of ETSDAC with ADC. This is because the solid ETSDAC was soluble up to 10% w/w into ADC monomer, even after sonication, heating with N₂ purging, etc. Thus, above test confirmed polymerizing capabilities of SOAC monomers.

i. Preparation of test PC thermoset polymer films using cast polymerization

SOAC monomer compositions were cast homo- and co-polymerized with ADC using 12-hour constant rate polymerization profile previously developed for ADC, PSDAC and poly (SDAC-co-ADC) polymers^[42,64] in the presence of 4% IPP initiator and 1% dioctyl phthalate (DOP) as plasticizer (**Scheme 2.29**).



(Note: above structure representation of polymer is merely indicative)

Scheme 2.29 Radical polymerization of SOAC monomers in the presence of peroxide initiator. (i) 4 % isopropyl peroxydicarbonate (IPP) initiator, 1% DOP, 45-95 °C, 12 h.

Although POESDAC homopolymer was relatively soft in nature (**Table 2.7**), rest all the copolymeric films were optically clear and hard enough to be used as plastic nuclear track detector.

Table 2.7 Curing conditions used for polymerization and physical properties of different test polymers.

Sr. No.	Polymer composition (w /w)	Heating profile (Temperature range)	Avg. thickness (μm) ^a	Colour and hardness
1	POESDAC	PSDAC polymerization profile (40-95°C)	653±10	Light brown and soft film
2	3:7 OESDAC: ADC	PSDAC-ADC polymerization profile (45-95°C)	663±10	Colourless and hard film
3	4:6 OESDAC: ADC	PSDAC-ADC polymerization profile (45-95°C)	547±10	Pale yellow and hard film
4	1:1 OESDAC: ADC	PSDAC-ADC polymerization profile (45-95°C)	601±10	Pale yellow and hard film

5	6:4 OESDAC: ADC	PSDAC-ADC polymerization profile (45-95°C)	526±10	Pale yellow and hard film
6	1:9 ETSDAC: ADC	ADC polymerization profile (40-95°C)	529±10	Colourless and hard film

^afilm thickness were calculated using ELCOMETER thickness gauge.

III. Kinetics of allyl polymerization and development of a constant rate polymerization profiles

Like any other radical induced olefinic addition polymerization, allylic polymerization involves several processes such as initiation, propagation, etc, occurring at rapid rates during initial stages. This process is exothermic in nature and favours increase in the rate further.

Thus, uncontrolled and rapid curing temperature leads to elevation in exothermic heat evaluation, thereby causing defects in polymer matrix such as cracking of film. Also, excessive temperature declines the activity of polymerization catalyst. It is well known that allylic polymerization causes reduction in bulk volume, hence in PADC polymerization shrinkage up to 14% is observed^[43].

Constant rate polymerization, controls the heat evaluation and considerably reduces such defects. However, the time required for polymerizations extends to longer durations. In order to address such issue, Dial et al.^[85] examined the kinetics of allylic polymerization in ADC system using IPP as initiator. They found that rate of monomer conversion to that of initiator decomposition is of first order. Dial et al. heated polymerizing mixture in series of test tubes at constant temperature and determined monomer consumption and initiator decomposition using titrimetric analysis. From the data obtained, authors derived first order kinetic equations and based on this special heating profiles were constructed. Using this heating profiles, constant rate of polymerization and heat evolution was achieved, preventing sudden rise in temperature.

Constant rate a polymerization profiles were based on following set of Dials kinetic equations:

$$K_4 = Z_3 e^{-E_3/RT} (M_0 - K_4 t) \sqrt{C_0 - \frac{K_4 t}{Z_1 e^{-E_3/RT}}} \quad (2.5)$$

$$E_1 = \frac{T_1 T_2}{T_1 - T_2} \text{Log}_e \frac{K_1}{K'_1} \quad (2.6)$$

$$K_1 = Z_1 e^{-E_1/RT} \quad (2.7)$$

$$K_3 = -\frac{1}{t} \left[\frac{1}{\sqrt{C_0 - \frac{M_0}{K_1}}} \text{log}_e \frac{\sqrt{C_0 - \frac{M_0}{K_1} + \frac{M}{K_1}} - \sqrt{C_0 - \frac{M_0}{K_1}}}{\sqrt{C_0 - \frac{M_0}{K_1} + \frac{M}{K_1}} + \sqrt{C_0 - \frac{M_0}{K_1}}} - \frac{1}{\sqrt{C_0 - \frac{M_0}{K_1}}} \text{log}_e \frac{\sqrt{C_0} - \sqrt{C_0 - \frac{M_0}{K_1}}}{\sqrt{C_0} + \sqrt{C_0 - \frac{M_0}{K_1}}} \right] \quad (2.8)$$

$$E_3 = \frac{T_1 T_2}{T_1 - T_2} \text{Log}_e \frac{K_3}{K'_3} \quad (2.9)$$

$$K_3 = Z_3 e^{-E_3/RT} \quad (2.10)$$

Where, K_1 is the slope, K_3 is the rate of reaction and K_4 is rate of polymerization. Z_1 and Z_3 are Arrhenius constants; E_1 and E_3 are corresponding activation energies; M_0 and C_0 are initial concentrations of monomer and initiator and R is gas constant. Temperature (T) at a given time t is calculated using above equations. Dial et. al. calculated this kinetic parameter for ADC monomer using 3.3 % IPP at three different set of temperature i.e., 40, 50 and 60°C. Our research group at Goa University have successfully, employed this kinetic model to generate constant heating and polymerization profile for various tetra-, hexa-, octa-functional monomers^[86]. Recently, Naik and Nadkarni^[67] have successfully utilized this kinetic model for generating constant rate heating profiles for SDAC and SDAC-ADC (4:6w/w), sulfone-carbonate allylic system.

Kinetic study mainly involves examining concentration of monomer and initiator at different temperature and time intervals. Residual initiator and monomer concentration was determined by iodometric titrations.

IV. Polymerization kinetics of OESDAC-ADC allylic system using IPP initiator

With the help of polymerisation protocols developed by in our laboratory, we decided to study rate of polymerization of newly prepared sulfone-carbonate allylic system by extending the Dial's kinetic model. For this purpose, we chose (OESDAC-ADC, 1:1w/w) as monomer composition. Before actually beginning with kinetic study, the gelation time of monomer composition was determined at fixed initiator composition and different temperature conditions as a function of time. Typically, monomer with known IPP

concentration was placed in three different test tubes and purged with dry nitrogen. Test tubes were tightly stoppered and immersed in temperature-controlled water bath at three different temperatures. Time required for gel formation was observed as listed in **Table 2.8**.

Table 2.8 Time to observe immobile gel for OEDSAC: ADC (1:1) monomer composition at different temperature.

Entry	% IPP (w/w)	Temperature (°C)	Time (h)
1	4	40	3
		50	1
		60	0.25
2	4	35	5
		45	2
		55	0.7
3	3	35	8
		45	4
		55	1.5

The gel formation for monomer composition occurs approximately at 70% residual unsaturation. Rapid gelation was observed at 4% IPP concentration, hence it was decided to perform kinetics of polymerization kinetics using 3% IPP and at 35, 45 and 55°C. (**Table 2.8**; entry 3).

To begin with kinetic study, 0.5 g polymerizing mixture (monomer + 3% IPP) was placed in a series of test tubes and purged with dry nitrogen to remove any dissolved oxygen. Three such sets of test tube series were prepared, tightly closed and placed in temperature-controlled bath. Each test tubes were taken out at regular time intervals as per previous observation in gelation study. Polymerizing mixture was analysed for monomer conversion as percentage of residual unsaturation and initiator decomposition as residual peroxide estimations using iodometric titration. The analysis results at three different temperatures are summarized in table below.

Table 2.9 Residual peroxide & unsaturation amount at different time interval at 35°C.

Entry	Time (h)	Unsaturation (%)	Peroxide (%)
1	0	100	2.96
2	0.83	95.56	2.86

3	1.67	91.34	2.77
4	2.5	89.05	2.74
5	3.33	88.10	2.72
6	4.17	85.18	2.68
7	5	83.03	2.65
8	5.83	81.35	2.63
9	6.67	79.32	2.57

Table 2.10 Residual peroxide & unsaturation amount at different time interval at 45°C.

Entry	Time (h)	Unsaturation (%)	Peroxide (%)
1	0	100	2.95
2	0.42	93.26	2.76
3	0.83	87.50	2.69
4	1.25	84.78	2.63
5	1.67	81.25	2.53
6	2.08	79.49	2.45
7	2.5	74.45	2.35
8	2.91	68.51	2.26
9	3.33	62.23	2.17

Table 2.11 Residual peroxide & unsaturation amount at different time interval at 55°C.

Entry	Time (h)	Unsaturation (%)	Peroxide (%)
1	0	100	2.95
2	0.17	92.73	2.712
3	0.33	83.25	2.49
4	0.50	80.48	2.38
5	0.67	77.06	2.27
6	0.83	73.37	2.14
7	1.00	69.23	2.02
8	1.17	64.34	1.96
9	1.33	59.13	1.89

Thus, based on the above analysis data, progress of the polymerization is represented graphical as shown in **Figure 2.37**.

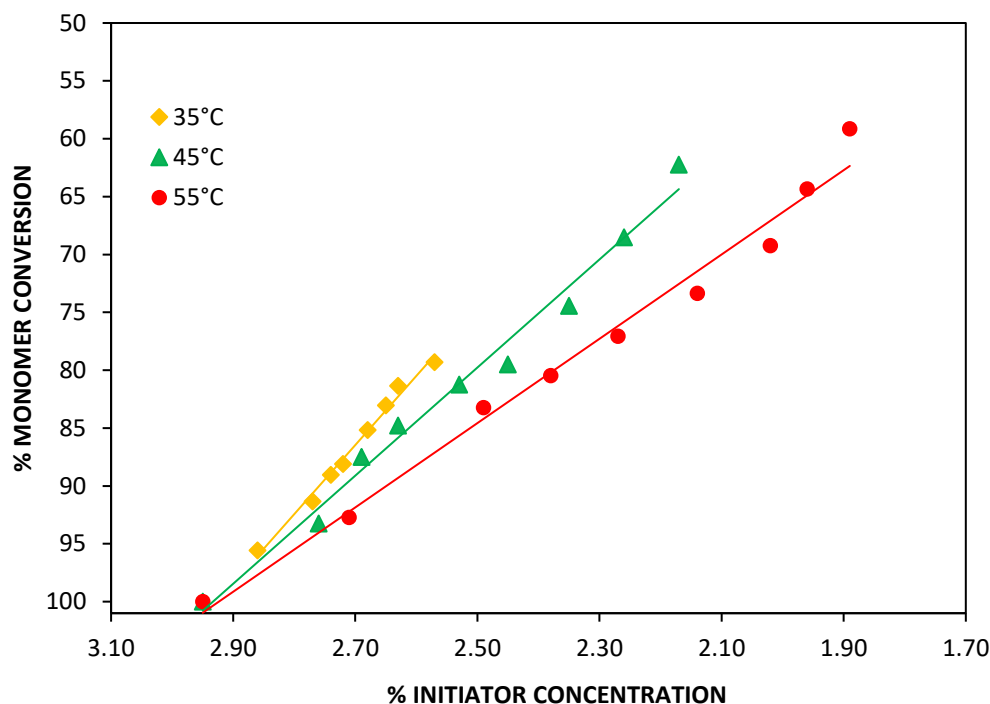


Figure 2.37 Plot of percent monomer conversion to percent initiator decomposition as a function of time at different temperature.

Form the above analysis data it is clear that, rate of polymerization increases with increase in curing temperature. At 55°C, estimations were performed at shorter time duration mainly due to early gelation of the polymerization mixture. Gelation of the polymerization mixture took place between 65-70 % of residual unsaturation.

The slopes obtained for above three lines were

At, 35 °C, $K_1 = 55.80$

45 °C, $K_1 = 46.71$

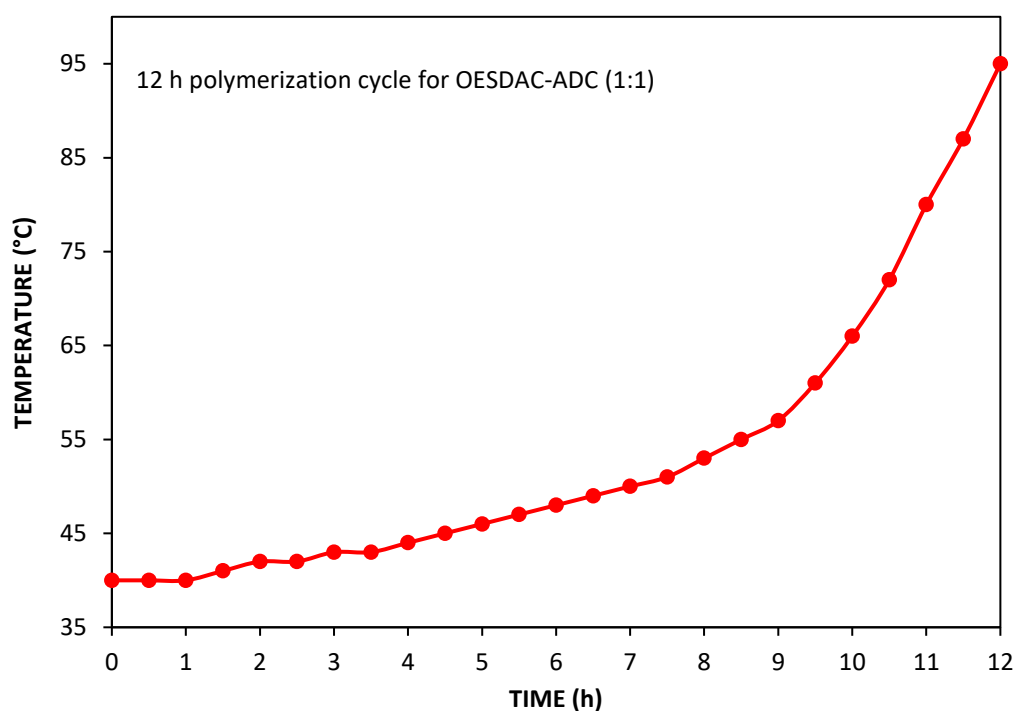
55 °C, $K_1 = 36.43$

The K_1 values obtained above were in decreasing order and above the limiting values for slope. These values were further used to obtain the kinetic constants E_1 , Z_1 , E_3 , and Z_3 . The values are shown in **Table 2.12**.

Table 2.12 Values of constants calculated using Dials kinetic equation.

Entry	Constant	Value
1	E_1	-4259.900
2	E_3	23179.27
3	Z_1	5.26E-02
4	Z_3	7.98E+14
5	K_4	8.33

Further, using a FORTRAN computer program^[43], Dial's kinetic equations were solved and a temperature-time heating profile was generated. It was noted that at the end of profile i.e., beyond 10.5 h, roots of Dial's equations became imaginary, thus program fails to calculate values further. Moreover, smooth extrapolation of the profile was possible to generate profile up to 95°C at the end of 12 h. The constant rate heating profile obtained for OESDAC-ADC (1:1) polymerization is shown in **Figure 2.38**.

**Figure 2.38** 12 h constant rate heating profile for OESDAC-ADC (1:1) using 3% IPP.

Furthermore, to check the effectiveness of newly generated polymerization profile, correlation study was performed, in which series of 12 test tubes containing polymerization mixture was heated in a programmable bath using above heating profile. Residual unsaturation was obtained after every 1 h to determine the percent polymerization over a

period of 12 h. The obtained results are represented graphical as shown in **Figure 2.39**. Results revealed constant rate of polymerization and a linear correlation was observed between the yields of polymer as a function of time.

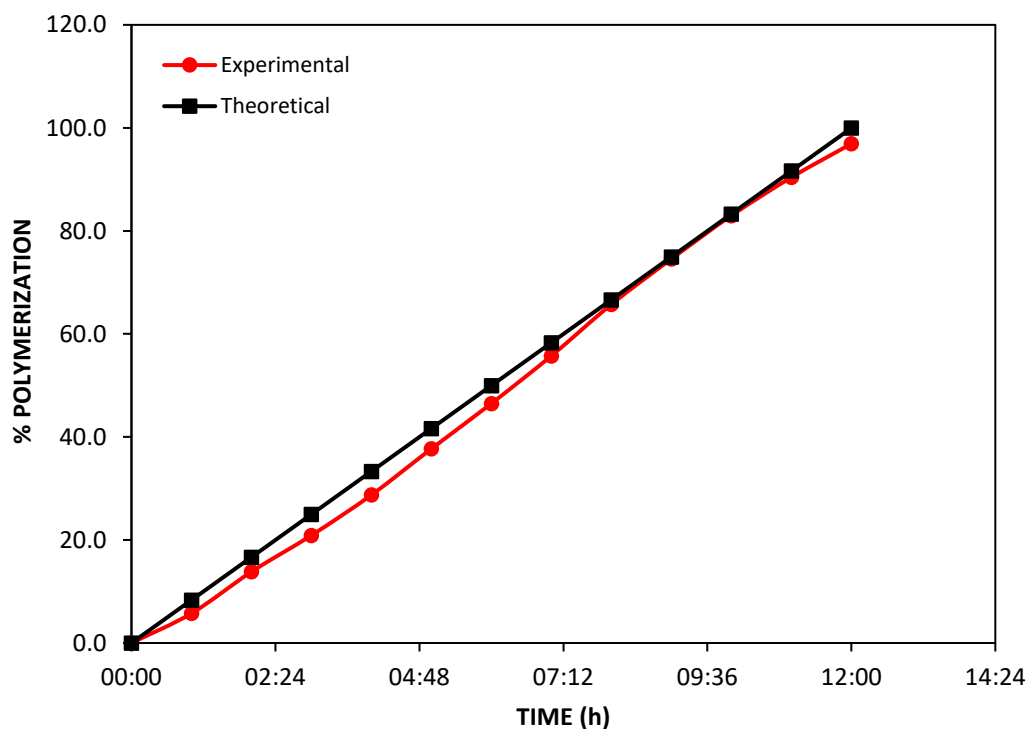


Figure 2.39 Verification of 12 h constant rate polymerization profile for OEDDAC: ADC using 3% IPP.

These experimental results were well supported by linear correlation coefficient (R^2) of 0.9989, obtained from calculated yields at given time. Thus, newly developed polymerization profile showed a good agreement with the kinetic models derived by Dial et al. and can be further used effectively for fabrication of OEDDAC: ADC copolymer films using cast polymerization process.

2.4.3 Attempt towards preparation of thermoplastic films of newly developed linear poly (2,2'-sulfonyl diethylene carbonate) (PSOC)

In the present study, we attempted preparation of composite thin film from newly synthesized sulfone-carbonate polymer, namely poly (2,2'-sulfonyl diethylene carbonate) (PSOC) using technique of spin coating and film application. Also, few trials were made in preparing polymer films by compression molding technique.

I. Preparation of PSOC homopolymer film

i. Choice of solvent

Solubility study was conducted in various polar protic and polar aprotic solvents. Studies showed that synthesized polymer was only soluble in polar aprotic solvents such as DMSO, DMF and DMA. Among this DMSO was chosen as solvent for preparing viscous polymer solution, due to high solubility of polymer.

ii. PSOC polymer solution in DMSO

Polymer was dissolved in portion with constant heating and stirring at 60°C to obtain viscous solution. Necessary additives were added. This viscous solution was cooled and filtered through nylon cloth to afford clear viscous solution.

iii. Polymer film casting

Following techniques were employed for preparation of thin polymer films:

1) Technique of spin coating

Polyester film was fixed on metal plate and attached to magnetic spinning disc. Polymer solution was poured over it and the disc was spun at specific constant RPM. The thickness of the film varies depends on the RPM. Initially when we had set RPM of 200, resultant polymer film formed was very thick and spread within a small area over polyester sheet. At RPM of 500, we observed uniform spreading of film over polyester support with few gaps between the polymer coat. The gaps enlarge further upon slow heating at 50°C in oven. After drying for 3 days, we observed random deposition of polymer film in small portion over spread area (**Figure 2.40**). Deposited film was dry, clear, transparent, irregular in shape and adhered well to the polyester support (**Table 2.13**).

2) Technique of automatic wet film application

Polyester or glass solid support was clamped to the surface of motorized film applicator machine. A wet film thickness of 100 μm was set manually over a graduated metallic film applicator bar of 5 cm width. Also, horizontal gliding length and carriage speed for film application was pre-set on automated machine. The applicator bar was placed on the solid support and held at fix position by side clamping. Polymer viscous solution was poured slowly across the horizontal width of rod and a transparent polymer coat was produced by motorized gliding process. Few air gaps were generated in between the polymer coat. Films were immediately transferred inside an oven to avoid blushing due hygroscopic solvent. After drying for 2-3 days at 50°C, it was observed that gaps enlarged substantially and

polymer film deposited randomly in small portion over a spread area. Comparatively more gaps were seen in this technique. Deposited film area was dry, clear, transparent, irregular in shape and adhered well to polyester and glass support. (**Table 2.13**).

Table 2.13 Results of overall film casting process for PSOC polymer.

Sr. No.	Conc. in DMSO (w/v)	Additives conc. w.r.t polymer	Casting Technique	Solid support	Film appearance and thickness ^a
1	100	-	Spin coating @ 500 rpm	Polyester sheets	Transparent film with T= 35 μ m
2	100	2% Triphenyl phosphate	Spin coating @ 500 rpm	Polyester sheets	Transparent film with T= 35 μ m
3	100	-	Film application @ 4 cm/s	Polyester sheets	Transparent film with T= 35 μ m
4	100	2% Triphenyl phosphate	Film application @ 4 cm/s	Polyester sheets	Transparent film with T= 35 μ m
5	100	-	Film application @ 4 cm/s	Scott pyran glass plates	Dry, transparent, elastic, soft films were peeled off slowly and applied on 2x2cm microscopic glass slide. T= 20 μ m

^afilm thickness were calculated using ELCOMETER thickness gauge.

II. Preparation of PSOC blend with cellulose acetate (CA) and nitrocellulose (CN)

CA and CN are well established polymers as track detectors. Particularly, they can furnish very transparent and uniform polymer film on polyester surface. Our group at Goa University have already established a protocol to cast (CN+CA) thin films on polyester solid support^[88]. Therefore, considering the previous difficulties in casting PSOC homopolymer

films and following these protocols, we tried here to examine the possibility of preparing PSOC blend with CA and CN.

i. Blend preparation

CN and CA are soluble in various low to medium volatile solvents but due to insolubility of PSOC polymer in such solvents, we had no option but to choose DMSO as solvent for preparation of respective polymer blends.

Initially, CA or CN polymer was dissolved in solvent with constant heating and stirring. After its complete dissolution, PSOC powder was added in portion to get a homogenous clear blend. It was cooled and filtered through nylon cloth to afford clear solution.

It was observed that during addition of PSOC to CA solution, CA lumps precipitate out of solution, leading to heterogeneous and turbid blend. Hence, we were unable to prepare clear blend with CA. In case of CN, no such observation was seen.

ii. Polymer film casting

Casting process were performed on similar lines as discussed earlier and following results are summarized in **Table 2.14** below. For both techniques, we observed uniform spreading of polymer film over polyester with no gaps over polyester surface. Upon drying for 50°C in oven for 3 days, film turned opaque, rough, whitish with no gaps in between. For some films, wrinkles were observed along with cracks (**Figure 2.41** and **Figure 2.42**).

Table 2.14 Results on film casting techniques for (PSOC+CN) blend.

Sr. No.	Conc. in DMSO (w/v)		Additive conc. w.r.t polymer	Casting Technique	Solid support	Film appearance and thickness ^a
	PSOC	CN				
1	75	10	-	Spin coating @ 500 rpm	Polyester sheets	Rough, whitish with T= 25 μm
2	75	10	-	Film application @50 μm and 4 cm/s	Polyester sheets	Rough, opaque with T= 15 μm
3	45	35	2% Triphenyl phosphate 2% camphor	Spin coating @ 500 rpm.	Polyester sheets	Rough, whitish, wrinkled with T= 25 μm

4	45	35	2% Triphenyl phosphate 2% camphor	Film application @ 100 μm and 4cm/s	Polyester sheets	Rough, whitish, T= 40 μm .
---	----	----	--	--	---------------------	--

^afilm thickness were calculated using ELCOMETER thickness gauge.

The reason behind the surface roughening and irregular film formation for CN + PSOC polymer blend was its heterogenous mixing. This was noticed upon equilibrating for 2 days as formation of two layers immiscible layer in viscous solution.

III. Attempts to prepare PSOC polymer films by compression molding

Various trials were made to cast polymer film with technique of compression molding. The casting process was performed using polymer press assembly under control temperature and pressure conditions.

i. Polymer film casting using a polymer press

Polymer powder was filled uniformly within a steel O-ring (500 μm) of circular steel mold. The mold arrangement is such that compound remain sandwich within mold die to afford thick film. The mold with polymer was placed between two metal blocks in a polymer press assembly. Pressure and temperature were applied as per requirement. Usually, compression process was stopped when molten polymer leaks out of steel mold. Initially, we set temperature to 110°C just 10°C below the temperature (120°C) at which polymer show melting behaviour in DSC and subsequently pressure to 2 ton. The result of polymer film casting was noted in table below.

Table 2.15 Results of PSOC film casting by technique of compression molding.

Sr. No.	Temperature (°C)	Pressure in tons	Observation
1	110	2	No melt was seen even after 45 min. On cooling powder seen intact at r.t.
2	110	4	No melt was seen even after 45 min. On releasing pressure, sizzling sound appeared followed by flowing melt out of mold. Sticky mass recovered on cooling to r.t. which solidifies after 2 days.

Note: Considering above observation, in next attempts we released the applied pressure upon cooling the pressing assembly at room temperature. Also, temperature was lowered and pressure was raised to 8 tons.

3	80	6	On cooling at r.t. powder was recovered
4	80	8	On cooling at r.t. powder was recovered
5	90	6	On cooling at r.t. waxy mass was recovered
6	90	8	On cooling at r.t. waxy mass was recovered
7	100	6	On cooling at r.t. sticky mass was recovered which solidifies after 2 days.

Thus, under several attempts we could not cast a transparent film out of PSOC polymer using compression molding technique, instead waxy and sticky mass was recovered (**Figure 2.43** and **Figure 2.44**).

IV. Photographs of PSOC homo and (PSOC+CN) blend film prepared using technique of spin coating and film application.



Figure 2.40 PSOC (100% w/v; 2% TPP w/w) film on polyester support by spin coating technique

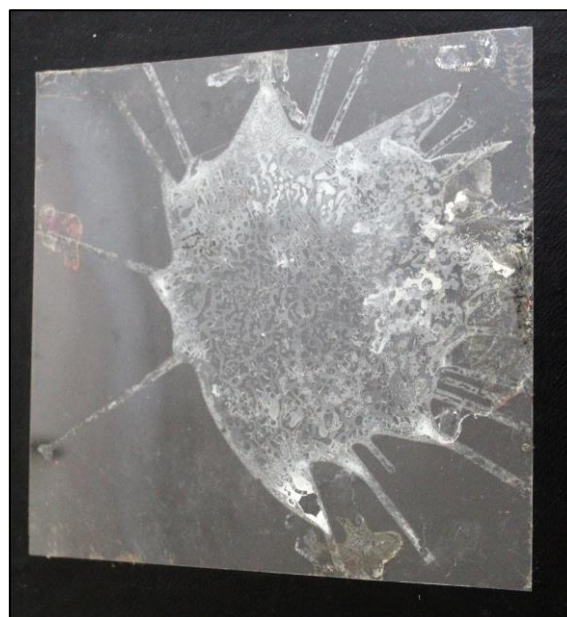


Figure 2.41 PSOC + CN (1:1 w/w; 2% TPP w/w) film on polyester support by spin coating technique.



Figure 2.42 PSOC + CN (1:1 w/w; 2% TPP w/w) film on polyester support by film application technique

V. Photographs of PSOC film processing by technique of compression molding



Figure 2.43 PSOC waxy mass seen after heating at 80°C under 6-ton pressure



Figure 2.44 PSOC sticky mass seen after heating at 100°C under 6-ton pressure.

Thus, our efforts to get a clean and transparent thin film from PSOC were not successful. As a result, we could not study its possible use for nuclear track detection.

2.4.4 Biodegradation studies of sulfur functionalized APCs

Biodegradation^[87] is the degradation process by which the organic substances are broken down into their constituent units by the action of micro-organism such as bacteria, fungi, etc. One of the popularly known organic material studied for the purpose of biodegradation is the polymer/plastics. The biodegradation of polymers can be performed either aerobically with oxygen or anaerobically, in the absence of oxygen. Under aerobic biodegradation, micro-organisms (aerobic microbes) consume oxygen and oxidizes the organic carbon of a material to inorganic carbon i.e., CO₂. During the process small metabolites such as water, biomass and residual carbon is produced. On the other hand, in anaerobic biodegradation process polymer is converted into methane, carbon dioxide, biomass and residual carbon by the action of anaerobic micro-organism.

Biodegradation is governed by various factors that include polymer properties, type of micro-organism, and nature of pre-treatment. The polymer properties such as its molecular weight, crystallinity, tacticity, mobility, the type of functionalities and substituents present in its structure, and plasticizers or additives associated with the polymer, all these features play an important role in its degradation^[88].

The microbial degradation^[89] has been studied for both natural as well as synthetic polymers. Such biotic degradation mainly can take place through the action of enzymes or by products (i.e., acids and peroxides) secreted by microorganisms (bacteria, fungi, yeasts, etc). At least two types of enzymes are actively involved in biotic degradation of polymers i.e., extracellular and intracellular depolymerase. Macromolecular size of the polymer, restrict the microorganism transporting the material directly into the cellular membrane where most biochemical processes are carried out by cellular enzymes. Contrary, monomers, oligomers are much easily degraded. Thus, in order to facilitates the microbial polymer degradation, two important steps occur: 1) depolymerisation or chain cleavage and 2) mineralization.

In the first step, microorganism excretes the extracellular enzymes onto surface of the polymers, which give rise to the formation of “enzyme-polymer complex”. The extracellular enzyme acts either endo (random cleavage of internal polymer links) or exo (sequential cleavage on terminals moieties). Under both this process, long polymer chains disintegrate into small monomer chains, allowing them to transport though the outer bacterial membranes. The process of disintegration is called depolymerization. In a second step, cellular enzyme utilizes these small fragments as carbon source, thereby producing CO₂, H₂O or CH₄. This step is known as biomineralization. It is important to understand here

that biodegradation of polymer substrate can rarely reach 100% mineralization and the reason being small portion of the polymer will be incorporated into microbial biomass and other natural products.

The commonly identified microbial strains^[90] associated with polymer degradation are bacteria in the genera *Streptococcus*, *Staphylococcus*, *Pseudomonas*, *Micrococcus*, *Enterobacter*, *Moraxella*, and *Bacillus* and the fungi such as *Fusarium solani*, *Aureobasidium pullulans*, *Curvularia senegalensis*, and *Actinomyces* sp. The common enzymes responsible for biodegradation include esterases, amylases, serine hydrolases, and lipases. Additionally, it was observed that lipases can further increase the polymer degradation^[76,87].

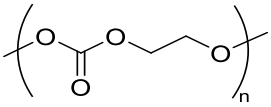
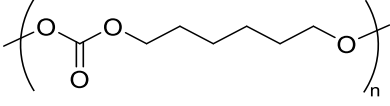
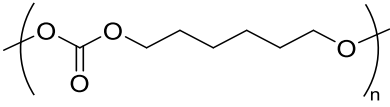
Aliphatic polycarbonates (APCs)^[8] are well known biodegradable material, with potential *in-vivo* application such as biomedical implants and targeted drug delivery carriers. The advantage associated with APCs are their predictable surface erosion properties and release of non-toxic degradation products such as alcohols and CO₂. Additionally, APCs are flexible and carbonate ester linkages in APCs are easily accessible to extracellular enzymes. The first report on biodegradable aliphatic polycarbonate^[91] was investigated for biomedical application, where poly (ethylene carbonate) (PEC) implants were first time studied for dog tissue repair and suggested that the enzyme pronase might be effective in degrading the PEC mass. In literature, most of the biodegradation studies on APCs are based on *in-vitro* enzymatic degradation (mostly lipase and esterase)^[92] and *in-vivo* degradation^[8].

In-vitro bacterial degradation of APCs have been rarely explored. Nishida and Tokiwa^[93], first reported microbial degradation of APCs using various soil inoculum. Here emulsified PEC and Poly (propylene carbonate) (PPC) (of $M_n=50,000$ Da) were tested for *in-vitro* biodegradability using the clear-zone technique on an agar. It was found that, out of total microbial colonies only 0.2 to 5.7% were active in degrading PEC. For PPC no colony with a clear zone was observed. Degradation activity was also supported by decreasing the turbidity of the suspended PEC. However, detailed characterization of microbial strains was not reported.

Comprehensive studies on polycarbonate degrading bacteria (PDB) have been carried on poly(hexamethylene carbonate) (PHC) and poly(tetramethylene carbonate) (PTC). Suyama et al.^[94] identified and isolated several PHC degrading bacterial strains from river water and soil sediments using clear zone test. All these strains were phylogenetically diverse and subclasses of the *Proteo-bacteria*^[95] (**Table 2.16**). Among this, *Roseateles depolymerans* 61A generates adipic acid and di(6-hydroxyhexyl) carbonate from PHC (M_n

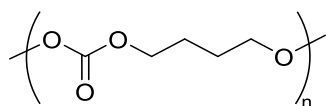
= 2,000 Da), whereas succinic acid and di(4-hydroxybutyl)-carbonate were degradation products from PTC ($M_n = 2,000$ Da)^[96]. Pranamuda et al. found that Actinomycete bacterial strain degraded high molecular-weight (PTC, $M_n = 37,000$ Da)^[97].

Table 2.16 Different types bacterial strains reported to degrade linear APCs.

S.n.	Aliphatic polycarbonates	Bacterial strains	Source
1	Poly (ethylene carbonate) ($M_n = 50$ KDa) 	07 microbial strains were isolated and uncharacterized	Soil
2	Poly(hexamethylene carbonate)  ($M_n = 2,000$ Da)	<ul style="list-style-type: none"> • Beta subclass of the <i>Proteobacteria</i> a) <i>Comamonas</i> group <i>Roseateles depolymerans</i> 61A & 61B2 <i>Variovorax paradoxus</i> WFF52 b) <i>Pseudomonas</i> group <i>Pseudomonas veronii</i> 35L 	River water
3	Poly(hexamethylene carbonate)  ($M_n = 2,000$ Da)	<ul style="list-style-type: none"> • Beta subclass of the <i>Proteobacteria</i> i) <i>Burkholderia</i> group <i>Duganella zoogloeoides</i> MC-9 <i>Pseudomonas lemoignei</i> MC-2, MC-10 <i>Ralstonia pickettii</i> MC-5 ii) <i>Comamonas</i> group 	Soil sediments

Roseateles depolymerans, MC-11,
MC-12.

- | | | | |
|---|--------------------------------|--|-------------|
| 4 | Poly(tetramethylene carbonate) | <ul style="list-style-type: none"> • Sub class of <i>Actinomycete</i> bacterial | Ground soil |
|---|--------------------------------|--|-------------|



Amycolatopsis sp. HT-6

($M_n = 37,000\text{Da}$)

Aliphatic polycarbonates with sulfur functionalities have been mainly synthesized for *in-vivo* application i.e., biomedical application^[98]. In a literature, linear sulfur-based APCs and their PEG copolymers have been known to be biocompatible and projected to be biodegradable^[60]. However, *in-vivo* and *in-vitro* biodegradation studies have not yet reported for any of this sulfur-based APCs.

The objective of present study:

- To isolate poly(sulfur-carbonate) degrading micro-organism from garden soil and sewage sludge using selective enrichment-culture technique under *in-vitro* mesophilic conditions.
- To understand the biodegradation activity of individual strains using cross-streak plate technique.
- To qualitative analyse morphological changes occurring in APCs samples for isolated strain, using agar plate observation followed by SEM studies.
- To identify and characterized the APC degrading micro-organism by Molecular identification and phylogenetic analysis.

Based on this *in-vitro* study, we will be first time reporting the biodegradation characteristics of sulfur based linear as well as crosslinked APCs. Additionally, depending on identification of microbial species and its subsequent activity, will be the first to report isolation of poly(sulfur-carbonate) degrading microbial strains either previously known or completely new type.

I. Isolation of APC degrading micro-organism

In order to isolate the APC degrading microbial strain from an inoculum source, we employed selective enrichment culture technique using MSM (Mineral salt medium) broth supplemented with the polymer.

The basic principle involved in this technique is enrichment^[99] and isolation of xenobiotic (in this study the polymers) degrading microbes. Often, it is desired to isolate microbial strains that are relatively scarce, or are in fact in very low numbers. Normally, bacteria are isolated by the streak plate technique or spread or pour plate technique on standard microbial culture media like nutrient agar and potato dextrose agar. But, if the desired microbial strain is a minority in a given sample, say 0.1% of the total, possibility of visualizing and isolating such strain will be difficult task. One should have at least a thousand isolated colonies on a plate to have a chance of seeing just one of the desired microbial species.

Enrichment culture technique solves this problem. The essence of this technique is to provide growth conditions that are very favorable for the micro-organism of interest, and as unfavorable as possible for competing organisms. Enrichment can also be carried out by modifying the nutrient content of the culture medium. For isolating xenobiotic degrading microbial strains, the desired xenobiotic is the only sole carbon source for microbial growth and only those microbial strains which can utilize the xenobiotic compound for their growth and multiplication will grow appreciably, while others get inhibited. Eventually, the inoculum will contain a sufficiently high proportion of xenobiotic-degraders, which would be easy to isolate them using the spread plate technique.

The enrichment technique has been used often for the isolation of polycarbonate degrading micro-organism. Suyama et al.^[94] utilized the same technique for the isolation of PHC degrading bacterial strains based clear zones of inhibition. Arefian et al.^[75] used this technique for isolation of PC degrading fungal strains based on visual identification growth pattern. Similarly, *Bacillus* strains from soil source were isolated using enrichment-culture technique for aromatic PCs^[76].

Here in our case, we used sulphur functionalized APCs as the sole carbon and energy source for selective enrichment of PC degrading micro-organisms. We used garden soil and sewage sludge as inoculum source.

i. Enrichment culture technique for isolation and primary screening of APC degrading micro-organism

For each APC samples we prepared three MSM broth assemblies, **1) control-** consisting of MSM broth medium and polymer; **2) Garden soil (GS)-** consisting of sterile MSM broth, supplemented with 1% polymer and inoculated with garden soil (GS) and; **3) Sewage sludge (SS)-** consisting of sterile MSM broth, supplemented with 1% polymer and inoculated with sewage sludge sample (**Figure 2.45**). These culture flasks were subjected to incubation at

30°C for 21 days and later utilized as inoculum source for agar plate test for clear zone formation technique.



Figure 2.45 MSM broth culture flasks for isolation of microbial isolates for degradation of PSOC linear APC (control with MSM broth+1% PSOC polymer; MSM broth+1% PSOC polymer + 1% sewage sludge sample; MSM broth+1% PSOC polymer+ 1% garden soil sample).

ii. Primary Screening of APC degrading microbial strains by clear zone formation technique

To identify the number of microbial colonies actively involved in degrading the APCs polymers, we performed MSM agar plate test, wherein APCs polymer was the only carbon source. The prominent strains were isolated based on their ability to show clear zones of inhibitions. Clear zone test has been widely employed for screening polymer degrading micro-organism^[87]. Especially, it is a one of the semi-quantitative tests used to check biodegradability of polymers^[99]. Suyama et al.^[95] isolated 39 different polyester degrading bacterial strains from different soil samples using clear zone test. Nearly, 200 to 300 bacterial colonies appeared in 100 μ L of soil suspension (10^{-4} g/ml) on each agar plate supplemented with polymer. The percentages of PHC degrading colonies that identified from the three soil samples were 1 to 7%. Similarly, in another study, 10 PHC-degrading strains with discrete colony types were isolated from the water samples^[94].

In our study, sterile MSM agar plates supplemented with APC polymer sample were prepared and inoculated with MSM broth culture solution. Each APC agar plate were incubated at 30°C, and observed for microbial growth as well as zones of inhibitions after 24 h and after 72 h.

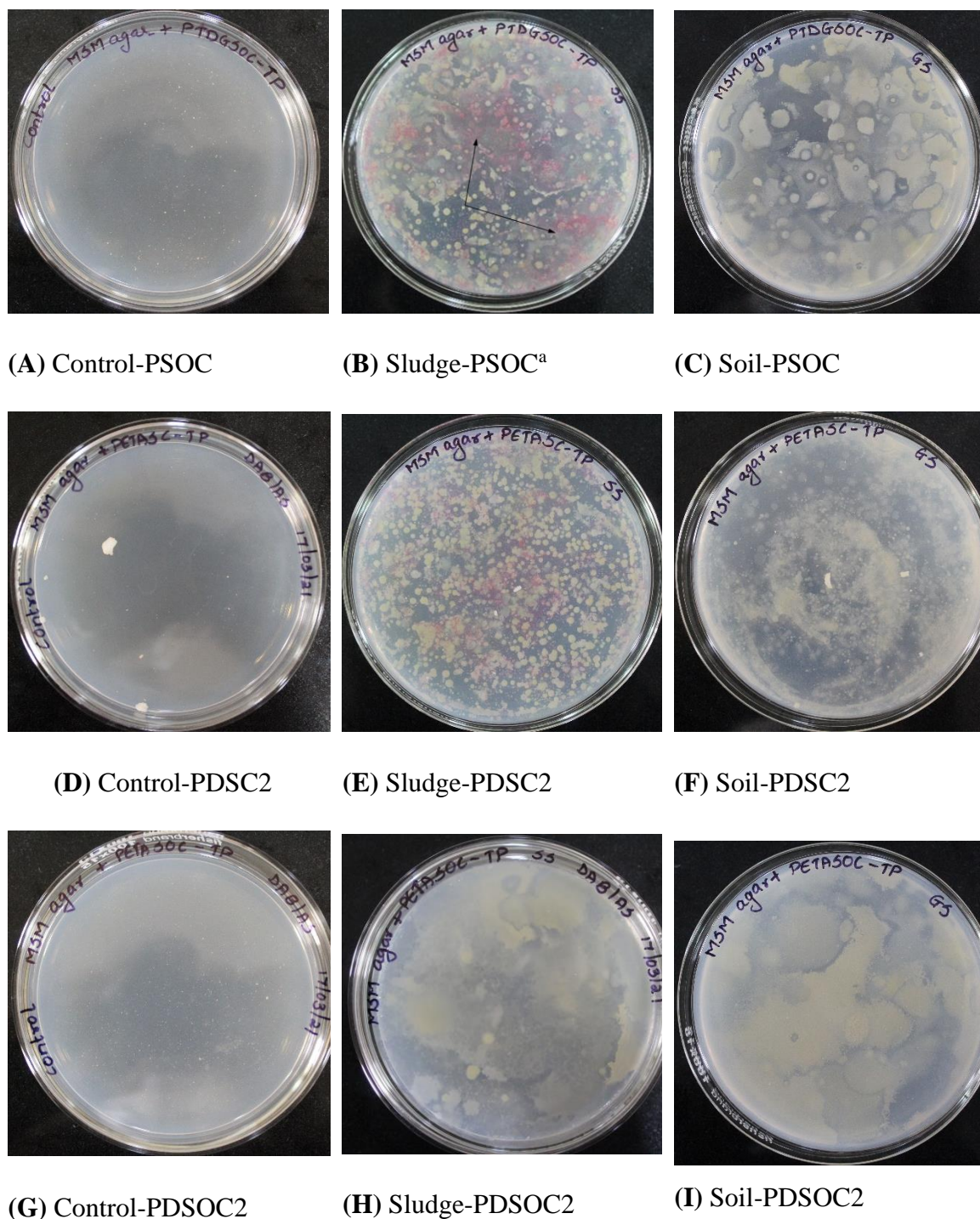
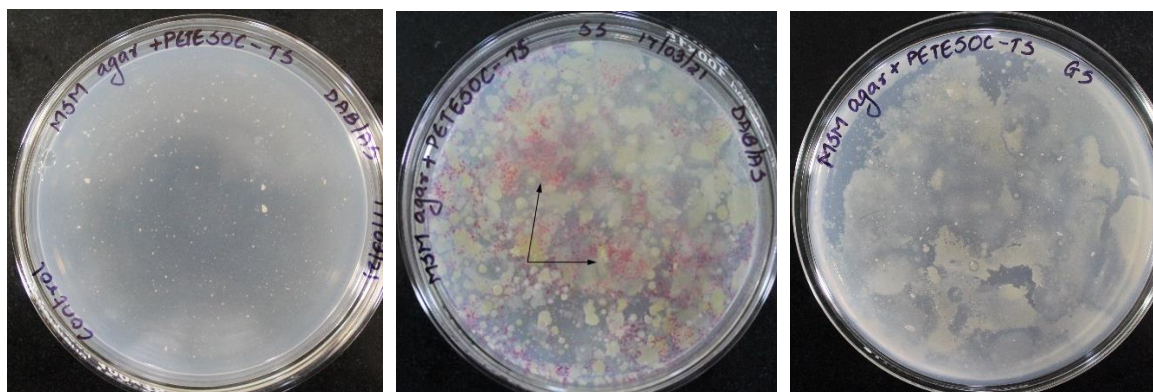


Figure 2.46 Primary screening of microbial strains for linear sulfur containing APCs by clear zone formation technique (images were recorded after 72h of incubation period). ^ablack arrow indication pink pigmentation.

Interestingly, we could observe growth of several microbial colonies for most of the sulphur functionalized APCs within 24 h of incubation period. For sludge culture plates, we could observe densely populated growth of microbial colonies in comparison with that of garden

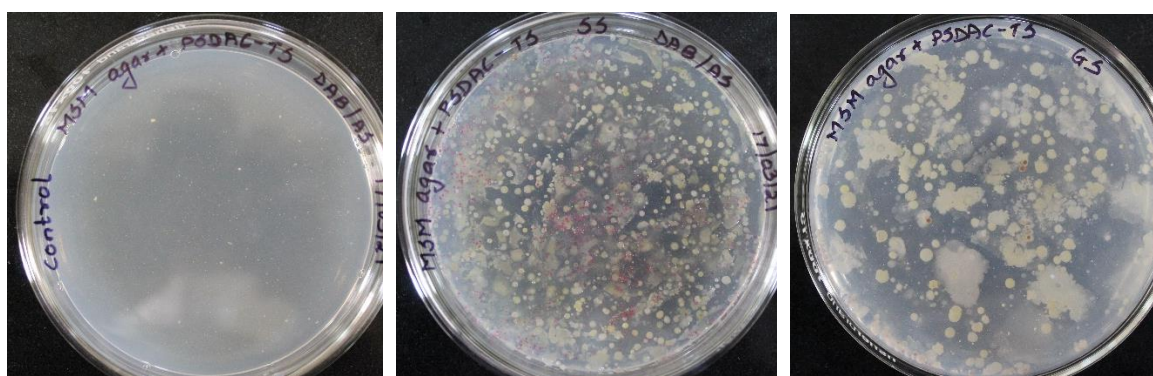
soil cultures (**Figure 2.46** and **Figure 2.47**). This was obvious because sewage sludge is much more enriched in micro-organism especially xenobiotic degraders as compared to garden soil sample. Also, it was interesting to note that even a thermoset APCs showed the growth of considerable number of microbial colonies (**Figure 2.47**).



(A) Control-POESDAC

(B) Sludge-POESDAC^a

(C) Soil-POESDAC



(D) Control-PSDAC

(E) Sludge-PSDAC

(F) Soil-PSDAC

Figure 2.47 Primary screening of microbial strains for cross-linked sulfur containing APCs by clear zone formation technique (images were recorded after 72h of incubation period). ^ablack arrow indicating pink pigmentation.

Among all, sulfone-based APCs showed higher microbial colonies. Especially, sulfone-based APC (PSOC and PSDAC) showed the maximum number of halos or clear zone of inhibitions around the microbial colonies, indicating utilization of the xenobiotic (sulfone-based APCs) for their growth and survival which depicts their ability to degrade the polymer. Best visuals for halos were observed for linear PSOC in garden soil sample and cross-linked PSDAC polycarbonate in sewage sludge (**Figure 2.48**). Additionally, pink pigmented

microbial colonies (**Figure 2.46B** and **Figure 2.47B**; indicated by *black arrow*) were seen for most of the sludge samples. This can be due to stress conditions for microbial growth.

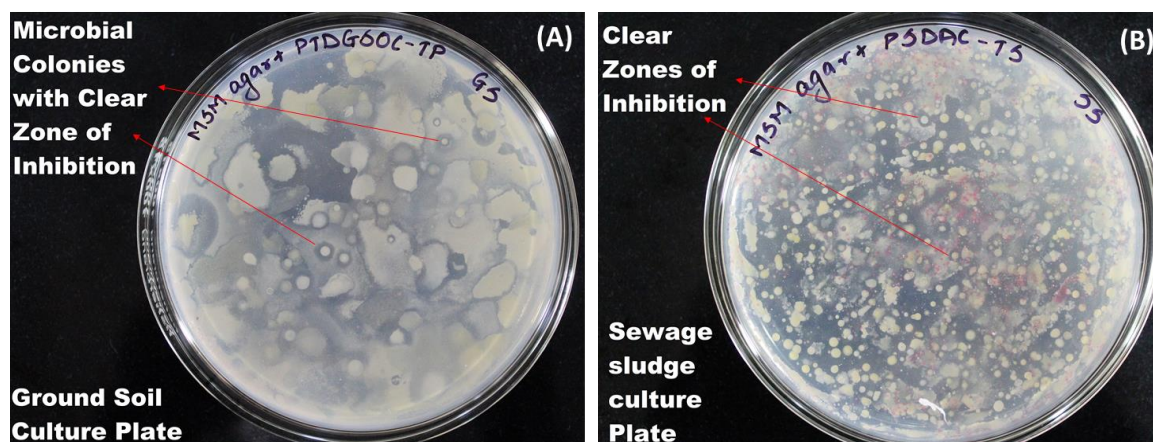


Figure 2.48 Halos or clear zones of inhibition in (A) linear PSOC and (B) cross-linked PSDAC.

Based on this preliminary screening observations, few microbial colonies showing prominent zones of inhibition for every polymer were selected, numbered, isolated, and maintained for further studies (**Table 2.17**).

Table 2.17 Selection of prominent microbial colonies for each sulfur-based PC samples.

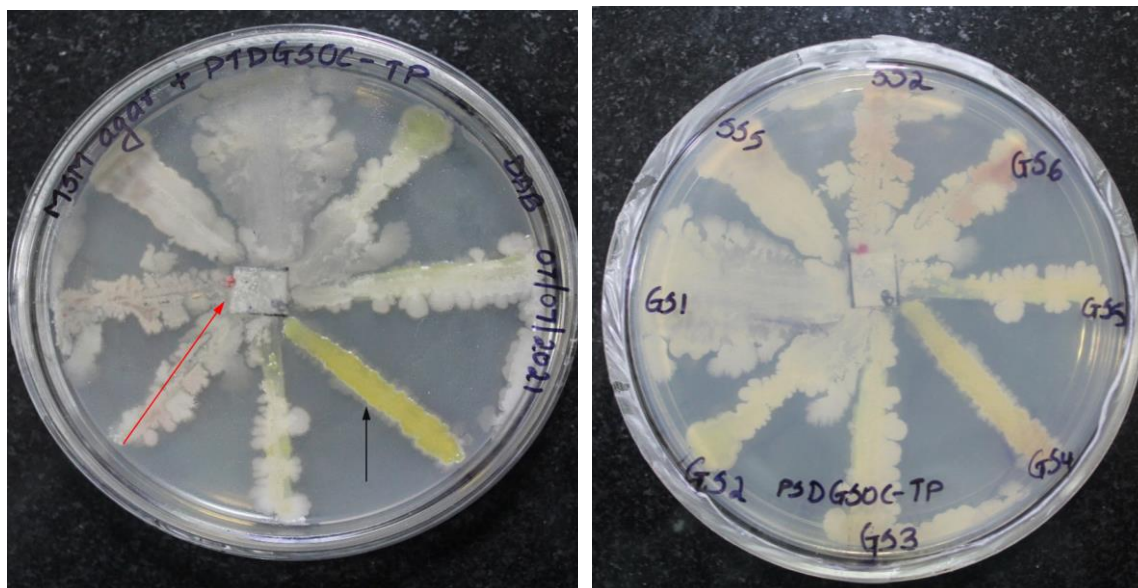
Polycarbonate type	No. of microbial colonies identified and numbered
PSOC, linear	08 (SS2, SS5, GS1, GS2, GS3, GS4, GS5, GS6)
PDSC-2, linear	06 (SS1, SS3, SS6, SS7, GS1, GS2)
PDSOC-2, linear	06 (SS2, SS3, SS5, GS2, GS3, GS5)
POESDAC, crosslinked	06 (SS2, SS3, SS4, GS1, GS2, GS3)
PSDAC, crosslinked	06 (SS2, SS4, SS5, GS4, GS7, GS8)

II. Secondary screening of APC degrading micro-organism

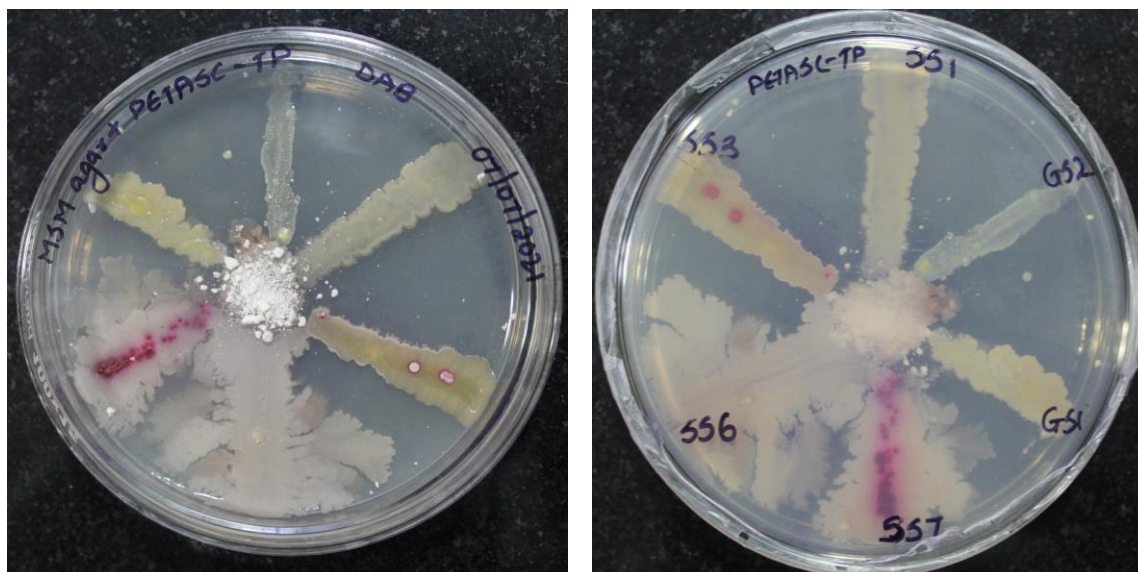
Generally cross-streak plate method is widely practiced to isolate the pure strains (especially bacteria) from the mixed microbial culture. In our study, we employed modified cross-streak plate technique, wherein isolated strains from primary screening method were streaked perpendicular to the polymer sample at the centre in radian pattern. The purpose behind this study was to examine the growth competency of microbial strains towards polymer and isolate its purest form for further studies. Additionally, this study also confirms the biodegradation of polymer by individual strains.

In search to identify PCs degrading microbial strains, several research groups have utilized the traditional streak plate method. Artham and Doble^[100] used streak plate method to isolate PC degrading bacterial strain i.e., *Pseudomonas* sp. from seawater source. Recently, Arefian et al.^[76] employed the streaking technique to isolate two potent BPA-PC degrading bacterial strains i.e., *Bacillus cereus* and *Bacillus megaterium* from landfill soil. However, no one employed this radial or modified cross-streak plate technique to isolate the polycarbonate degrading purest microbial strains.

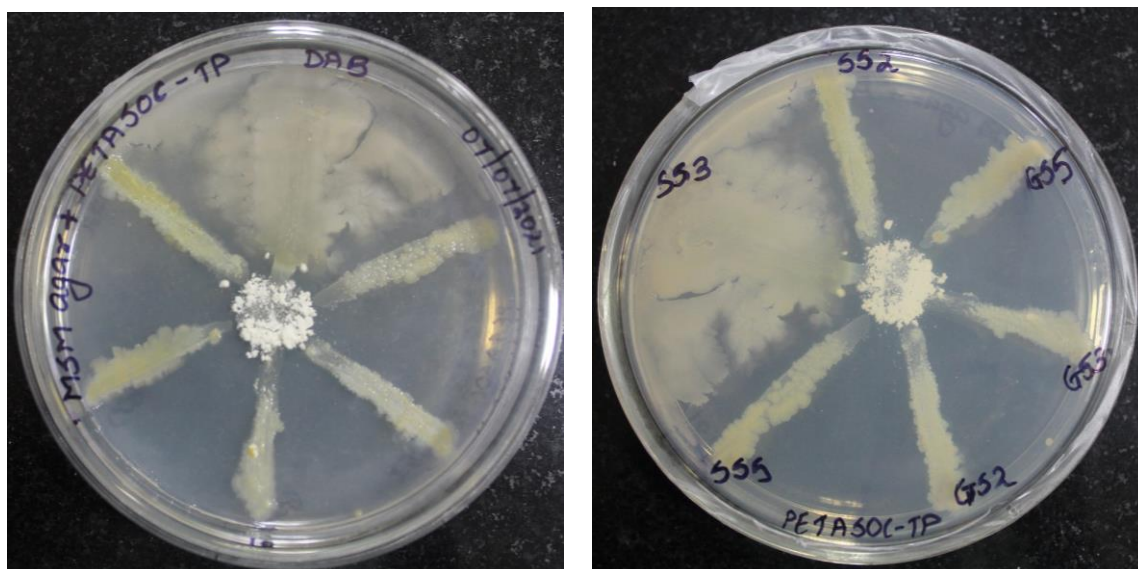
In our study, MSM agar plates were prepared, carrying the polymer sample (film/powder) at the centre of the MSM agar plate as the only carbon source. Inoculations was performed using modified cross-streaking protocol and incubated at 30°C for a period of 2 weeks with constant periodic monitoring. Further microbial growth was observed based on qualitative analysis. The isolates showing prominent growth towards the polymer were further selected for tertiary screening and those isolates that did not show growth towards the polymer were neglected.



(A) PSOC polycarbonate^a



(B) PDSC-2 polycarbonate



(C) PDSOC-2 polycarbonate

Figure 2.49 Secondary screening of microbial strains for linear sulfur containing APCs using cross-streak plate technique (left side obverse view and right side reverse view). *“red arrow indicating microbial growth towards APC film and black indicated pigmentation.*

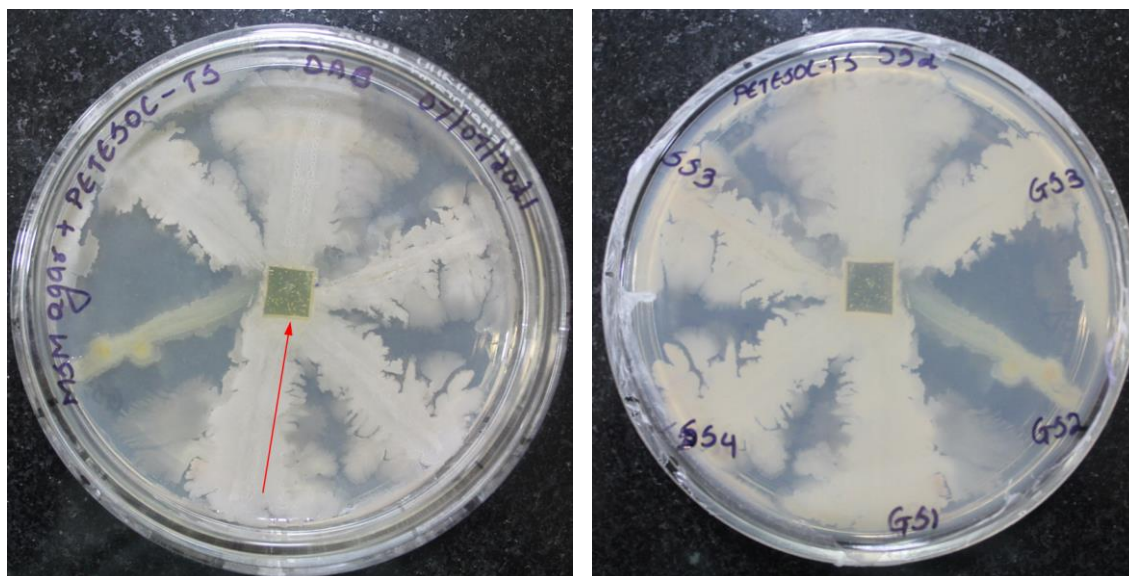
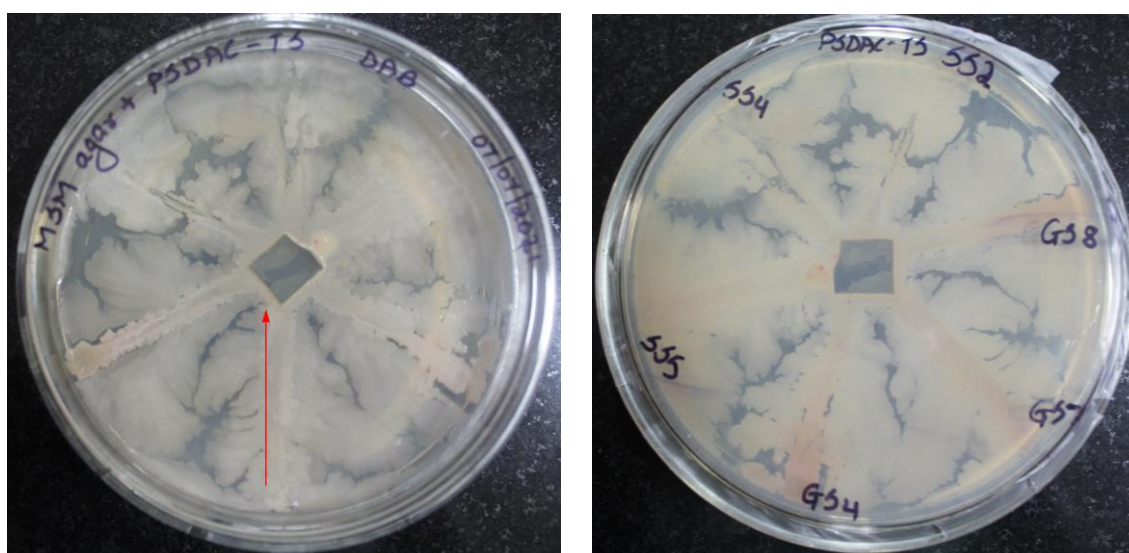
(D) POESDAC polycarbonate^a(E) PSDAC polycarbonate^a

Figure 2.50 Secondary screening of microbial isolates for crosslinked sulfur containing APCs using cross-streak plate technique. (left side obverse view and right side reverse view). *red arrow indicating microbial growth towards APC film and black indicated pigmentation.*

From cross-streak plate test, we could observe active growth of microbial strains towards the polycarbonate samples. Except for powered samples, microbial growth surrounding the polymer sample was more prominent in film-based samples. (**Figure 2.49A** and **Figure 2.50D, E**). For linear polycarbonate i.e., PSOC-linear, microbial activity was clearly indicated by surface deterioration and opacity of transparent film. Among the 08 microbial

isolates selected for secondary screening, 06 isolates (SS2, GS1, GS2, GS3, GS5, GS6) showed promising growth towards the polymer. Additionally, we could also see strong yellow pigmentation for a microbial strain (**Figure 2.49A red arrow**, GS4 strain) isolated from garden soil source. Thus, based on the above results, the purest and potent strains were isolated and further tested for biodegradation of respective PC samples under tertiary screening plate test.

In case of PSDAC-cross linked polymer, out of 6 isolates, 3 isolates (SS2, GS7 and GS8) showed promising result and for POESDAC-cross linked, out of 6 isolates, 2 (SS2, GS1) showed potential growth towards the polymers. However, for the powdered polymer samples PDSOC-2 linear and PDSC-2 linear, there was negligible growth of selected isolates around the polymer, and hence were not selected for tertiary screening.

III. Biodegradability test of APC films by potent and pure isolates

The potent microbial isolates from the secondary screening test were further tested for confirming biodegradability of APCs in this tertiary screening method.

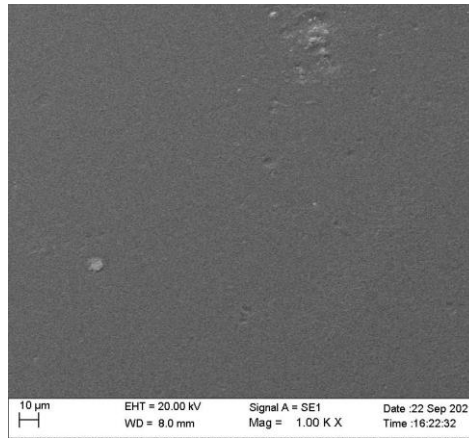
For this purpose, agar plate test was performed using standard protocols, keeping APC polymer film at the centre of the agar plate. Any microbial activity and resulting physical damage to polymer film were examined, by observing growth of microbial isolates on the polymer film, roughening or changes on the surface of the polymer film. Further, to confirm the degradation of PCs by the isolated strains, we performed the scanning electron microscopy (SEM) of polymer samples (**Table 2.18** and **Table 2.19**). Morphological changes to film surface including microbial biofilm formation, holes and cracks on the surface of the polymer were examined using SEM microscopic images.

Table 2.18 Visual observation of microbial colonies grown around and on the PSOC linear polymer film using scanning electron microscopy.

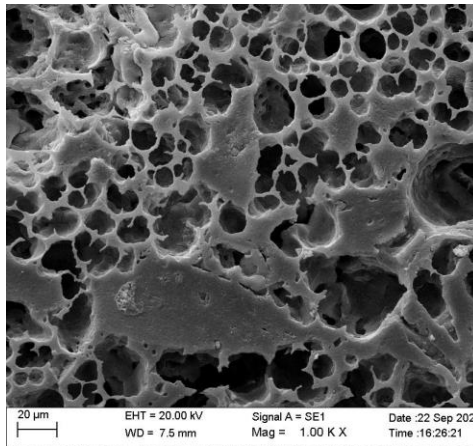
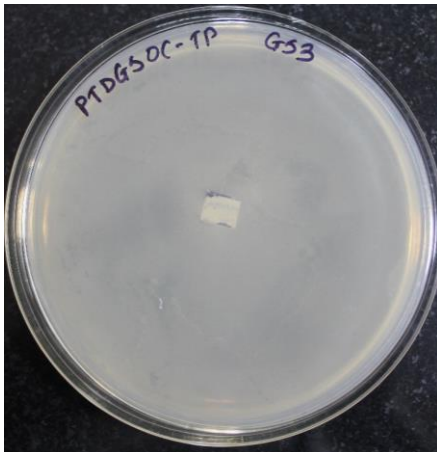
Sn.	Agar plate for microbial isolates ^a	Microscopic images ^a	Source & isolate no. ^b
-----	--	---------------------------------	---

1

Control →

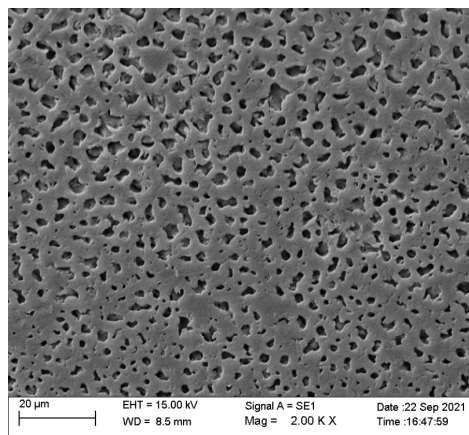
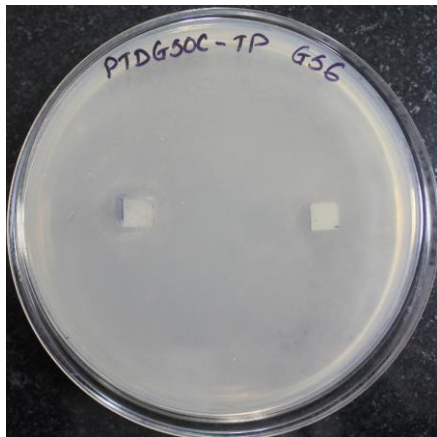


2



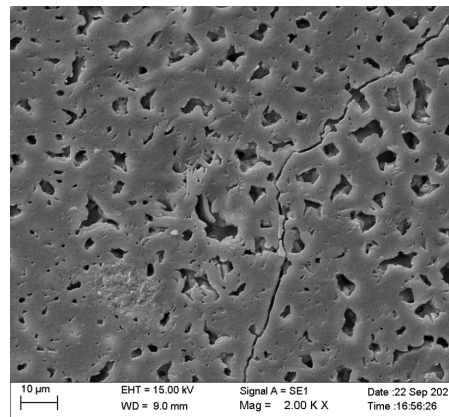
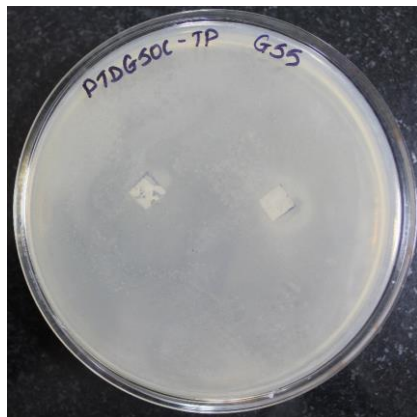
GS3

3



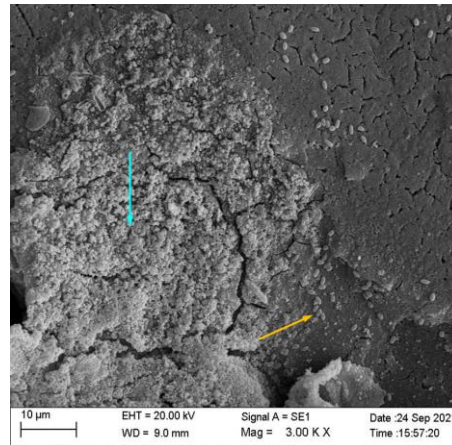
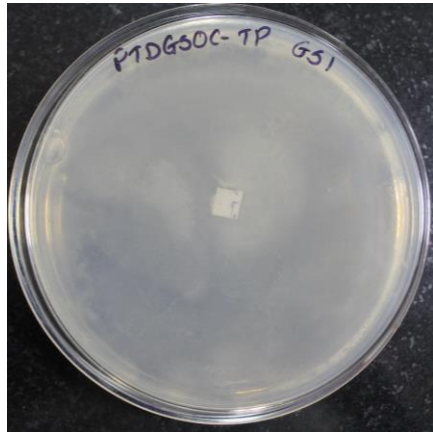
GS6

4



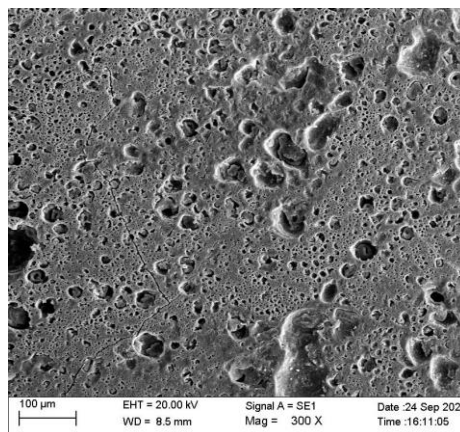
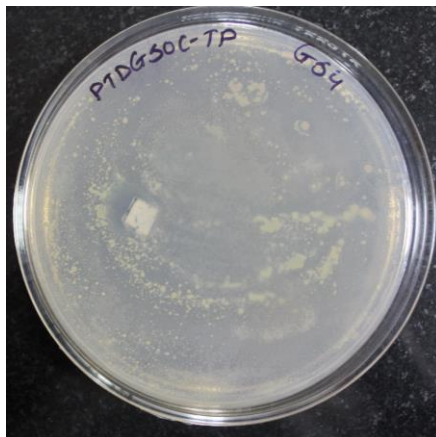
GS5

5^b



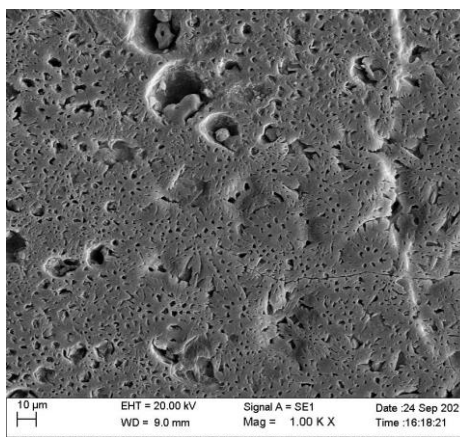
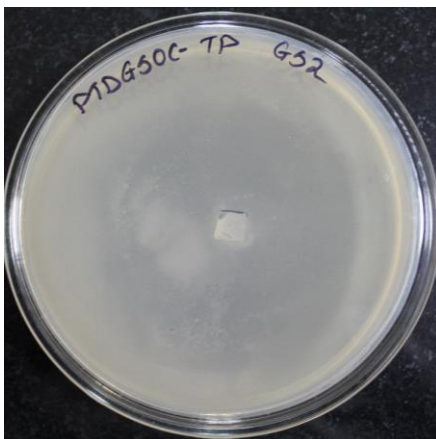
GS1

6



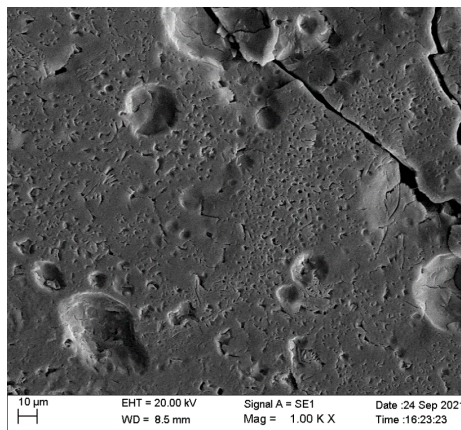
GS4

7

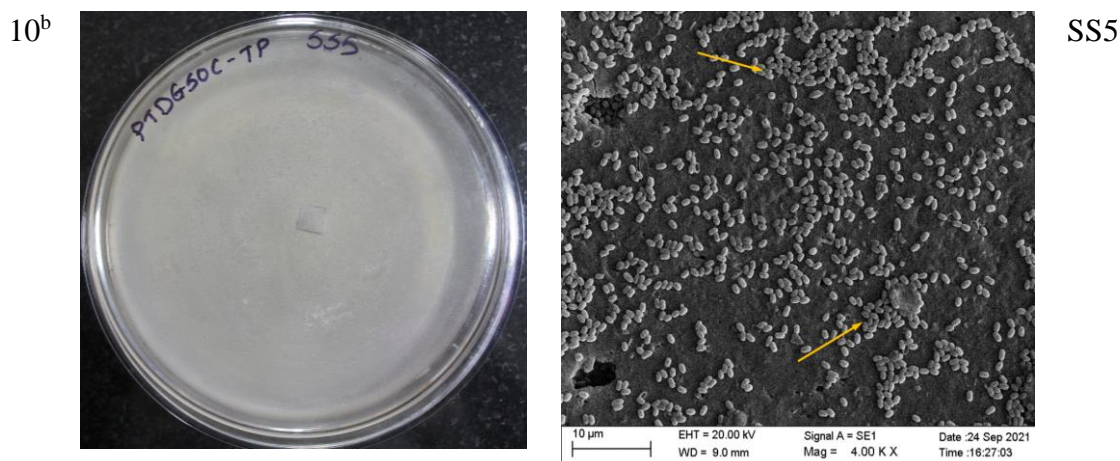


GS2

9



SS2



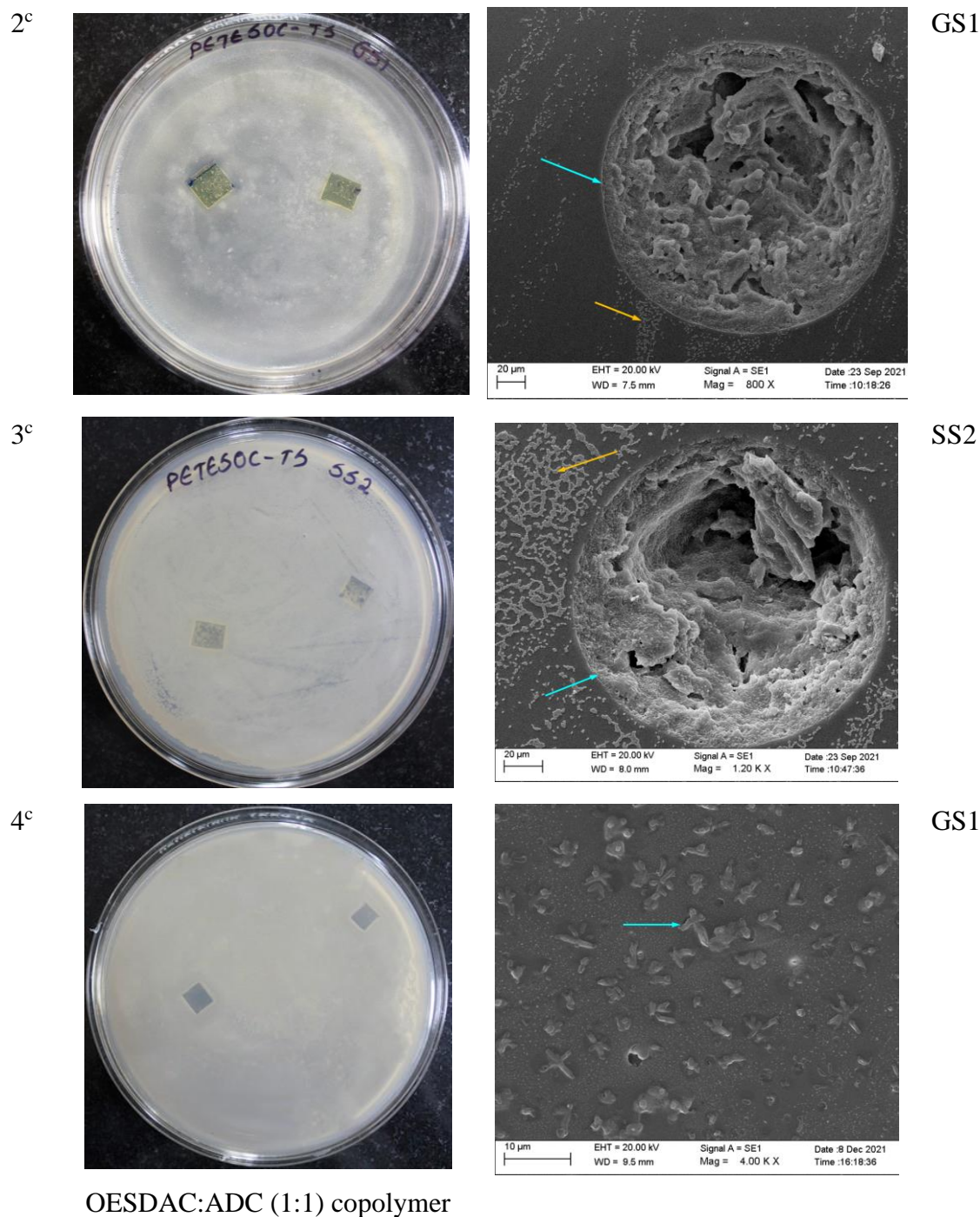
^a Images were recorded after 3 week period of incubation; ^bGS=garden soil, SS=sewage sludge; ^byellow arrow pointing the bacterial colonies and blue arrow indicating biofilm.

The degradation of PSOC polycarbonate by the microbial strains resulted in heterogenous and microporous surface (**Table 2.18, Sn.2-10**). Also, opacity and surface disintegration were clearly visible to naked eye. Kim et al.^[80] reported similar porous morphology with physical holes of approx. 18 μm in height and 23 μm in width for poly (lactic acid) (PLA) film, mainly caused by *Pseudomonas* sp. and *Bacillus* sp.

On the other hand, PSOC film with the uninoculated control showed uniform surface with no morphological changes even after incubation under the identical conditions (**Table 2.18, Sn.1**). Bacterial growth was clearly identified from two culture’s plates, in the form of microbial biofilm/agglomerates’ (blue arrow) (**Table 2.18, Sn.5**) or bacterial colonies (yellow arrow) (**Table 2.18, Sn.10**).

Table 2.19 Visual observation of microbial colonies grown around and on the POESDAC crosslinked polymer film using scanning electron microscopy.

Sn.	Agar plate for microbial isolates ^a	Microscopic images ^a	Source & isolate no. ^b
1	Control →		

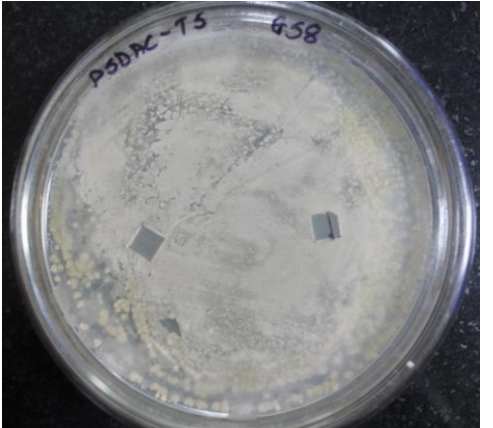
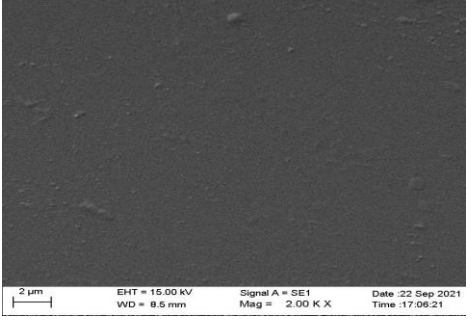
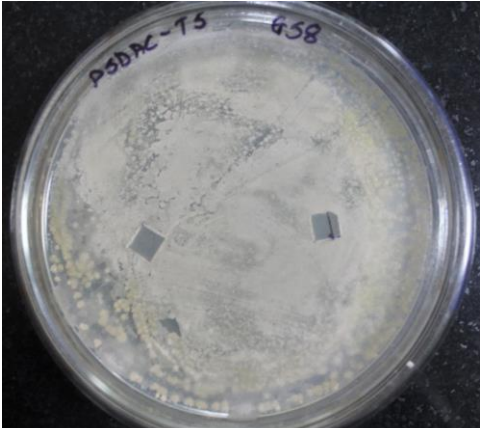
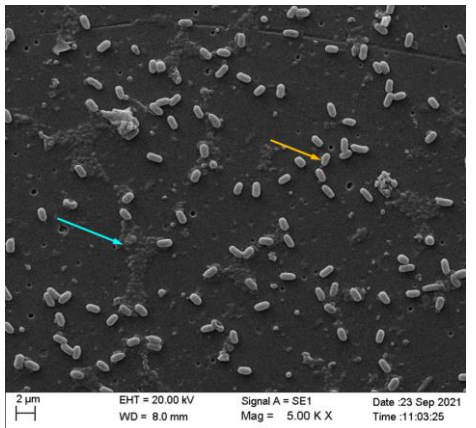
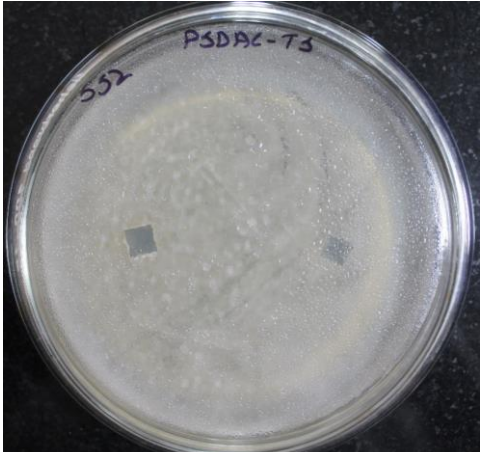
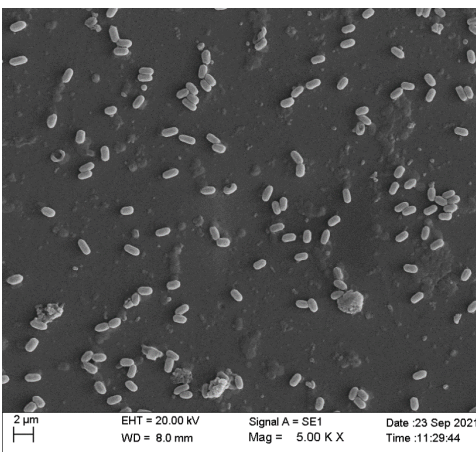


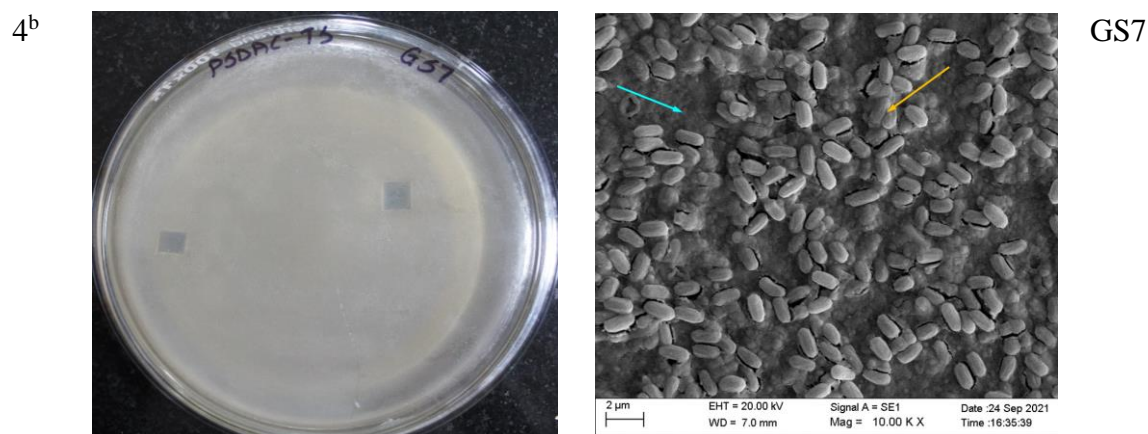
^a Images were recorded after 3 week period of incubation; ^b Src and isolate no. =source and isolate number, GS=garden soil, SS=sewage sludge; ^cyellow arrow pointing the bacterial colonies and blue arrow indicating surface craters and biofilm.

In POESDAC crosslinked homopolymer, microbial degradation was clearly indicated by formation surface craters (*blue arrow*) surrounded by cluster of bacterial colonies (*yellow arrow*) (**Table 2.19, Sn.2-3**). The bacterial isolate GS1 from the sample PSOC linear polycarbonate was used to test the biodegradability of OESDAC:ADC (1:1) polymer

sample. OESDAC:ADC (1:1) polymer is hard crosslinked polymer and thus very slow to undergo degradation. Nevertheless, we could observe surface leaching caused by microbial colonization (**Table 2.19, Sn.4**). On the other hand, uninoculated control showed no such physical damages (**Table 2.19, Sn.1**). This shows the potential activity of bacterial stains in degrading the crosslinked PCs.

Table 2.20 Visual observation of microbial colonies grown around and on the PSDAC crosslinked polymer film using scanning electron microscopy.

Sn.	Agar plate for microbial isolates ^a	Microscopic images ^a	Source & isolate no. ^b
1	<p style="text-align: center;">Control →</p> 		
2 ^b			GS8
3			SS2



^a Images were recorded after 3 week period of incubation; ^b GS=garden soil, SS=sewage sludge; ^b yellow arrow pointing the bacterial colonies and blue arrow indicating biofilm.

In comparison with POESDAC polycarbonate, PSDAC showed less surface damage especially surface craters. Nonetheless, few physical holes and large amount of bacterial (*yellow arrow*) growth was seen on surface along with bacterial biofilm (*blue arrow*) (**Table 2.20, Sn.2-4**). This result indicates, degradation is in the initial stage and need more incubation time for greater damage to polymer film. Also, it was important here to note that, the PSDAC film were a harder thermoset resin as compared to flexible POESDAC film. Thus, we could see slow bacterial degradation process in PSDAC films.

Overall result indicates that, isolated bacterial strains were actively involved in degradation of linear as well as crosslinked PCs by metabolizing polymers as the sole carbon source. Most importantly, biodegradable ability of APCs assists this microbial degradation process. Furthermore, most potent strains, were selected for phylogenetic identification of bacteria.

IV. Identification of potent bacterial isolates

Table 2.21 Molecular identification of potent bacterial isolates with accession numbers assigned by NCBI GenBank.

Sr. No.	Strain number	Source/ isolate	Similarity	Species	Accession number
1	DBVNAS1	POESDAC crosslinked GS1	88.06%	<i>Achromobacter insolitus</i>	OL707631
2	DBVNAS2	PSDAC crosslinked GS7	99.80%	<i>Bacillus subtilis</i>	OL708413

3	DBVNAS3	PSOC linear GS1	99.59%	<i>Bacillus subtilis</i> subsp. <i>spizizenii</i>	OL797969
4	DBVNAS4	PSDAC crosslinked GS3	99.74%	<i>Bacillus subtilis</i>	OL827058

Molecular identification of the most potent isolated bacterial strains (4 isolates) was carried out using bacterial 16s rRNA gene sequencing. 27F and 1492R primers were used for amplification of the 16s rDNA gene and BLAST analysis was carried out for the nucleotide sequencing results. The phylogenetic tree was constructed using the neighbor-joining method using MEGA version 7.0. The 16S rDNA gene sequence of the bacterial strains identified in this study have been deposited in National Centre for Biotechnology Information (NCBI) GenBank under the accession number as given in **Table 2.21** .

Based on above 16s rRNA gene sequencing and phylogenetic analysis, bacterial strains for potent biodegradation of sulfur functionalized aliphatic polycarbonates were identified, such as *Achromobacter insolitus* and *Bacillus subtilis*. Although *Bacillus* spp. have known to degrade bis-phenol based aromatic polycarbonates^[101], yet it is not reported for aliphatic polycarbonates. . Kowalczyk et al.^[102] has reported the biodegradation of a high-density polyethylene by *Achromobacter xylosoxidans*. Similarly, Dey et al.^[103] has reported *Achromobacter* sp. isolated from waste dumpyard with biodegradability of Low-density polythene. However, biodegradation by *Achromobacter* spp. has not been reported for APCs Hence, we report first time these bacterial species for biodegradation of APCs

2.5 Conclusions

1. We have successfully synthesised poly (sulfone-*co*-carbonate) linear polymers using step growth polycondensation process. Among all polymers, thioglycol based APCs shows high conversion rate of 98% and obtained in high yields.
2. Structural characterization of linear APC's has been successfully performed using NMR, IR spectroscopy and MALDI-TOF mass spectrometry.
3. Average molecular weight analysis has been successfully performed using NMR, GPC and hydroxyl value estimation methods. PDI is determined using GPC technique.
4. Further, powder XRD studies has been successfully employed to understand the structural morphology of polymers, thereby confirming the semicrystalline natures of linear PC.
5. Sulfone based APCs have more rigid structure as compared to their sulfide derivatives, which is indicated by high values of glass transition temperature in DSC thermogram.
6. We have successfully synthesized and purified the disulfone diallyl carbonate monomers on large scale (50 g) and subsequently characterization by spectroscopic techniques.
7. Further, disulfone diallyl carbonate monomers has been successfully polymerised using casting process via radical polymerization method.
8. Newly designed monomers were successfully polymerised in a free radical process to afford Poly (sulfone-*co*-carbonate) crosslinked polymeric film.
9. We have successfully extended Dials kinetic model to study polymerization kinetics of disulfone diallyl carbonate monomer and generated constant rate heating profile for OESDAC:ADC (1:1) monomer composition.
10. Using a newly generated profile, we have successfully prepared clear and hard crosslinked polycarbonates films for SSNTD applications.
11. We have successful carried out enrichment and isolation of poly(sulfur-carbonate) degrading bacteria from garden soil and sewage sludge source using selective enrichment-culture technique followed by cross-streaking plate method.
12. We have been successful in observing the morphological changes occurring on sulfur containing linear and crosslinked APC films, caused by biodegradation of bacterial strains under *in-vitro* mesophilic laboratory conditions.
13. We have been successful in identifying new APCs degrading bacterial strains *Achromobacter insolitus* and *Bacillus subtilis* using 16s rRNA gene sequencing and

phylogenetic analysis. Hence, we report first time their isolation, identification and biodegradable activities *in-vitro*.

14. The bacterial strains identified in this study as *Achromobacter insolitus* and *Bacillus subtilis* need to be further tested for the biodegradability of polymers in natural environments especially in polymer contaminated areas including solid plastic wastes that will help in protecting the environment from the harmful effects of polymer/plastic wastes.

2.6 References

- [1] A. Singh, in *Encyclopedia of Polymeric Nanomaterials*, Springer Berlin Heidelberg, Berlin, Heidelberg, **2015**, pp. 1–5.
- [2] K. Takeuchi, in *Polymer Science: A Comprehensive Reference*, Elsevier, **2012**, pp. 363–376.
- [3] D. J. Brunelle, P. M. Smigelski, E. P. Boden, in *Advances in Polycarbonates* (Eds.: D.J. Brunelle, M.R. Korn), American Chemical Society, **2005**, pp. 8–21.
- [4] S. Ye, S. Wang, L. Lin, M. Xiao, Y. Meng, *Advanced Industrial and Engineering Polymer Research* **2019**, 2, 143–160.
- [5] G. Rokicki, P. G. Parzuchowski, in *Polymer Science: A Comprehensive Reference*, Elsevier, **2012**, pp. 247–308.
- [6] D. J. Brunelle, in *Encyclopedia of Polymer Science and Technology*, John Wiley & Sons, Inc., Hoboken, NJ, USA, **2006**.
- [7] D. J. Brunelle, M. R. Korn, *Advances in Polycarbonates*, American Chemical Society, Washington, DC, **2005**.
- [8] W. Yu, E. Maynard, V. Chiaradia, M. C. Arno, A. P. Dove, *Chemical Reviews* **2021**, acs.chemrev.0c00883.
- [9] A. J. Kamphuis, F. Picchioni, P. P. Pescarmona, *Green Chemistry* **2019**, 21, 406–448.
- [10] P. Moulinié, in *Handbook of Thermoplastics* (Eds.: O. Olabisi, K. Adewale), **2016**, pp. 347–368.
- [11] J. Xu, E. Feng, J. Song, *Journal of Applied Polymer Science* **2014**, 131, n/a-n/a.
- [12] A. S. More, D. v. Palaskar, E. Cloutet, B. Gadenne, C. Alfos, H. Cramail, *Polymer Chemistry* **2011**, 2, 2796.
- [13] K. Birnbaum, G. Lurie, *Berichte der deutschen chemischen Gesellschaft* **1881**, 14, 1753–1755.
- [14] A. Einhorn, *Justus Liebig's Annalen der Chemie* **1898**, 300, 135–155.
- [15] C. A. Bischoff, A. von Hedenström, *Berichte der deutschen chemischen Gesellschaft* **1902**, 35, 3431–3437.
- [16] E. W. Spanagel, W. H. Carothers, *Journal of the American Chemical Society* **1935**, 57, 929–934.
- [17] W. H. Carothers, F. J. van Natta, *Journal of the American Chemical Society* **1930**, 52, 314–326.
- [18] R. W. Peterson, *Superpolycarbonate*, **1940**, US2210817A.

-
- [19] L. J. Bruneni, *CR-39: More than Meets the Eye-The Stories behind the Development of Plastic Lenses*, PPG Industries, Inc., Pittsburgh, USA, **1997**.
- [20] L. R. Wakeman, *The Chemistry of Commercial Plastics*, Reinhold Publishing Corp., New York, **1947**.
- [21] Hermann. Schnell, *Industrial & Engineering Chemistry* **1959**, *51*, 157–160.
- [22] H. Schnell, *Angewandte Chemie* **1956**, *68*, 633–640.
- [23] K. Heinrich, H. Schnell, B. Ludwig, *Thermoplastic Aromatic Polycarbonates and Their Manufacture*, **1962**, US3028365A.
- [24] W. D. Fox, *Aromatic Carbonate Resins and Preparation Thereof*, **1964**, US3153008A.
- [25] T. Sakashita, S. Tomoaki, *Catalytic Process for Preparing Polycarbonates from Carbonic Acid*, **1991**, US5026817A.
- [26] T. Sakashita, S. Tomoaki, *Polycarbonate Containing Terminal Hydroxy Groups, Low Sodium and Chlorine Content*, **1994**, US5276129A.
- [27] S. Inoue, H. Koinuma, T. Tsuruta, *Journal of Polymer Science Part B: Polymer Letters* **1969**, *7*, 287–292.
- [28] S. Inoue, H. Koinuma, T. Tsuruta, *Die Makromolekulare Chemie* **1969**, *130*, 210–220.
- [29] Y. H. Choi, M.-Y. Lyu, *Macromolecular Research* **2020**, *28*, 299–309.
- [30] D. J. Saxon, A. M. Luke, H. Sajjad, W. B. Tolman, T. M. Reineke, *Progress in Polymer Science* **2020**, *101*, 101196.
- [31] A. E. Acar, D. J. Brunelle, in *Advances in Polycarbonates*, **2005**, pp. 216–228.
- [32] G. Tondi, A. Kandelbauer, S. H. Goodman, in *Handbook of Thermoset Plastics*, Elsevier, **2014**, pp. 173–189.
- [33] H. T. Pham, S. Munjal, C. P. Bosnyak, in *Handbook of Thermoplastics* (Eds.: O. Olabisi, K. Adewale), Taylor & Francis, **1997**, pp. 609–640.
- [34] J. H. Park, J. Y. Jeon, J. J. Lee, Y. Jang, J. K. Varghese, B. Y. Lee, *Macromolecules* **2013**, *46*, 3301–3308.
- [35] Z. Wang, X. Yang, S. Liu, J. Hu, H. Zhang, G. Wang, *RSC Advances* **2015**, *5*, 87311–87319.
- [36] J. Sun, D. Kuckling, *Polymer Chemistry* **2016**, *7*, 1642–1649.
- [37] P. Hodge, *Chemical Reviews* **2014**, *114*, 2278–2312.
- [38] A. Ben-Haida, L. Conzatti, P. Hodge, B. Manzini, P. Stagnaro, *Macromolecular Symposia* **2010**, *297*, 6–17.

-
- [39] D. J. Brunelle, in *Cyclic Polymers* (Ed.: J.A. Semlyen), Springer Netherlands, Dordrecht, **2002**, pp. 185–228.
- [40] D. J. Brunelle, *Journal of Polymer Science Part A: Polymer Chemistry* **2008**, *46*, 1151–1164.
- [41] J. Feng, R.-X. Zhuo, X.-Z. Zhang, *Progress in Polymer Science* **2012**, *37*, 211–236.
- [42] A. A. A. Mascarenhas, *Development of Plastic Materials for Nuclear Track Detection*, **2007**.
- [43] V. K. Mandrekar, *Novel Polymeric Materials for Nuclear Track Detection*, **2010**.
- [44] T. Şucu, M. P. Shaver, *Polymer Chemistry* **2020**, *11*, 6397–6412.
- [45] L.-Q. Yang, B. He, S. Meng, J.-Z. Zhang, M. Li, J. Guo, Y.-M. Guan, J.-X. Li, Z.-W. Gu, *Polymer* **2013**, *54*, 2668–2675.
- [46] R. L. Snyder, D. J. Fortman, G. X. de Hoe, M. A. Hillmyer, W. R. Dichtel, *Macromolecules* **2018**, *51*, 389–397.
- [47] D. W. Grijpma, E. Kroeze, A. J. Nijenhuis, A. J. Pennings, *Polymer* **1993**, *34*, 1496–1503.
- [48] E. Bat, B. H. M. Kothman, G. A. Higuera, C. A. van Blitterswijk, J. Feijen, D. W. Grijpma, *Biomaterials* **2010**, *31*, 8696–8705.
- [49] Y. Dai, X. Zhang, *Polymer Chemistry* **2017**, *8*, 7429–7437.
- [50] G. Becker, F. R. Wurm, *Chemical Society Reviews* **2018**, *47*, 7739–7782.
- [51] S. Tempelaar, L. Mespouille, O. Coulembier, P. Dubois, A. P. Dove, *Chem. Soc. Rev.* **2013**, *42*, 1312–1336.
- [52] M. Luo, Y. Li, Y.-Y. Zhang, X.-H. Zhang, *Polymer* **2016**, *82*, 406–431.
- [53] R. Wang, W. Chen, F. Meng, R. Cheng, C. Deng, J. Feijen, Z. Zhong, *Macromolecules* **2011**, *44*, 6009–6016.
- [54] L. Yu, Z. Zheng, Y. Liu, Z. Li, X. Wang, *RSC Advances* **2015**, *5*, 64832–64840.
- [55] S. Tempelaar, L. Mespouille, P. Dubois, A. P. Dove, *Macromolecules* **2011**, *44*, 2084–2091.
- [56] A. W. Thomas, P. K. Kuroishi, M. M. Pérez-Madrigal, A. K. Whittaker, A. P. Dove, *Polymer Chemistry* **2017**, *8*, 5082–5090.
- [57] J.-F. Zhang, W.-M. Ren, X.-K. Sun, Y. Meng, B.-Y. Du, X.-H. Zhang, *Macromolecules* **2011**, *44*, 9882–9886.
- [58] J. M. Sarapas, G. N. Tew, *Angewandte Chemie International Edition* **2016**, *55*, 15860–15863.

- [59] C. Wei, Y. Zhang, B. Yan, Z. Du, M. Lang, *Chemistry - A European Journal* **2018**, *24*, 789–792.
- [60] B. Yan, Y. Zhang, C. Wei, Y. Xu, *Polymer Chemistry* **2018**, *9*, 904–911.
- [61] B. Yan, J. Hou, C. Wei, Y. Xiao, M. Lang, F. Huang, *Polymer Chemistry* **2019**, *10*, 5191–5199.
- [62] B. Yan, B. Liang, J. Hou, C. Wei, Y. Xiao, M. Lang, F. Huang, *European Polymer Journal* **2020**, *123*, 109452.
- [63] A. D. Smith, A. G. Tennyson, R. C. Smith, *Sustainable Chemistry* **2020**, *1*, 209–237.
- [64] D. G. Naik, Synthesis of Allylic Monomers and Polymers Containing Sulphur and Phosphorus Functionalities for Solid State Nuclear Track Detection, **2017**.
- [65] M. Fujii, R. Yokota, Y. Atarashi, *International Journal of Radiation Applications and Instrumentation. Part D. Nuclear Tracks and Radiation Measurements* **1988**, *15*, 107–110.
- [66] V. K. Mandrekar, S. G. Tilve, V. S. Nadkarni, *Radiation Physics and Chemistry* **2008**, *77*, 1027–1033.
- [67] D. G. Naik, V. S. Nadkarni, *Radiation Physics and Chemistry* **2019**, *160*, 68–74.
- [68] T. S. Kristufek, S. L. Kristufek, L. A. Link, A. C. Weems, S. Khan, S.-M. Lim, A. T. Lonnecker, J. E. Raymond, D. J. Maitland, K. L. Wooley, *Polymer Chemistry* **2016**, *7*, 2639–2644.
- [69] L. A. Link, A. T. Lonnecker, K. Hearon, C. A. Maher, J. E. Raymond, K. L. Wooley, *ACS Applied Materials & Interfaces* **2014**, *6*, 17370–17375.
- [70] K. Nozaki, *Industrial & Engineering Chemistry Analytical Edition* **1946**, *18*, 583–583.
- [71] A. MASUI, *Analytical Sciences* **1997**, *13*, 1037–1038.
- [72] S.-M. Kim, S.-A. Park, S. Hwang, E. Kim, J. Jegal, C. Im, H. Jeon, D. Oh, J. Park, *Polymers* **2017**, *9*, 663.
- [73] D. G. Naik, V. S. Nadkarni, *Designed Monomers and Polymers* **2016**, *19*, 643–649.
- [74] W. Yue, C.-F. Yin, L. Sun, J. Zhang, Y. Xu, N.-Y. Zhou, *Journal of Hazardous Materials* **2021**, *416*, 125775.
- [75] M. Arefian, M. Zia, A. Tahmourespour, M. Bayat, *International Journal of Environmental Science and Technology* **2013**, *10*, 1319–1324.
- [76] M. Arefian, A. Tahmourespour, M. Zia, *Archives of Environmental Protection DOI - 10.24425/aep.2020.132521* **2020**, *46*, 14–20.
- [77] N. Kamat, S. Velho-Pereira, *Indian Journal of Pharmaceutical Sciences* **2011**, *73*, 223.

- [78] A. L. Leber, *Clinical Microbiology Procedures Handbook*, ASM Press, Washington, DC, USA, **2016**.
- [79] M. Y. Kim, C. Kim, J. Moon, J. Heo, S. P. Jung, J. R. Kim, *Journal of Microbiology and Biotechnology* **2017**, *27*, 342–349.
- [80] E. M. Faber, G. E. Miller, *Organic Syntheses* **1932**, *12*, 68.
- [81] C. M. Timperley, R. M. Black, M. Bird, I. Holden, J. L. Mundy, R. W. Read, *Phosphorus, Sulfur, and Silicon and the Related Elements* **2003**, *178*, 2027–2046.
- [82] F. Strain, W. E. Bissinger, W. R. Dial, H. Rudoff, B. J. DeWitt, H. C. Stevens, J. H. Langston, *Journal of the American Chemical Society* **1950**, *72*, 1254–1263.
- [83] R. v Kupwade, S. S. Khot, U. P. Lad, U. v Desai, P. P. Wadgaonkar, *Research on Chemical Intermediates* **2017**, *43*, 6875–6888.
- [84] S. Choi, J.-D. Yang, M. Ji, H. Choi, M. Kee, K.-H. Ahn, S.-H. Byeon, W. Baik, S. Koo, *The Journal of Organic Chemistry* **2001**, *66*, 8192–8198.
- [85] W. R. Dial, W. E. Bissinger, B. J. DeWitt, F. Strain, *Industrial & Engineering Chemistry* **1955**, *47*, 2447–2451.
- [86] V. S. Nadkarni, *Indian Journal of Physics* **2009**, *83*, 805–811.
- [87] M. van der Zee, in *Handbook of Biodegradable Polymers*, De Gruyter, **2020**, pp. 1–22.
- [88] A. A. Shah, F. Hasan, A. Hameed, S. Ahmed, *Biotechnology Advances* **2008**, *26*, 246–265.
- [89] T. Artham, M. Doble, *Macromolecular Bioscience* **2008**, *8*, 14–24.
- [90] J. Zhang, J. Chen, R. Jia, Z. Dun, B. Wang, X. Hu, Y. Wang, *3 Biotech* **2018**, *8*, 308.
- [91] Y. IMAI, K. KOJIMA, E. MASUHARA, *Jinko Zoki* **1979**, *8*, 246–249.
- [92] T. Suyama, Y. Tokiwa, *Enzyme and Microbial Technology* **1997**, *20*, 122–126.
- [93] H. Nishida, Y. Tokiwa, *Chemistry Letters* **1994**, *23*, 421–422.
- [94] T. Suyama, H. Hosoya, Y. Tokiwa, *FEMS Microbiology Letters* **1998**, *161*, 255–261.
- [95] S. Tetsushi, T. Yutaka, O. Pornpimol, K. Takahiro, K. Yoichi, *Applied and Environmental Microbiology* **1998**, *64*, 5008–5011.
- [96] Y. Tokiwa, B. Calabia, C. Ugwu, S. Aiba, *International Journal of Molecular Sciences* **2009**, *10*, 3722–3742.
- [97] P. Hardaning, C. Rungsima, T. Yutaka, *Applied and Environmental Microbiology* **1999**, *65*, 4220–4222.
- [98] M. Geven, R. D’Arcy, Z. Y. Turhan, F. El-Mohtadi, A. Alshamsan, N. Tirelli, *European Polymer Journal* **2021**, *149*, 110387.

-
- [99] J. Augusta, R.-J. Müller, H. Widdecke, *Applied Microbiology and Biotechnology* **1993**, *39*, 673–678.
- [100] T. Artham, M. Doble, *Journal of Polymers and the Environment* **2009**, *17*, 170–180.
- [101] W. Zhang, K. Yin, L. Chen, *Applied Microbiology and Biotechnology* **2013**, *97*, 5681–5689.
- [102] A. Kowalczyk, M. Chyc, P. Ryszka, D. Latowski, *Environmental Science and Pollution Research* **2016**, *23*, 11349–11356.
- [103] A. S. Dey, H. Bose, B. Mohapatra, P. Sar, *Frontiers in Microbiology* **2020**, *11*, 1-15.

Chapter 3

*Application of polymers in Solid State
Nuclear Track detection*

3.1 Introduction

Solid State Nuclear Track Detection (SSNTD) is a radiation detection technique which deals with permanently recording the trajectory of energetic/charge particles passing through the dielectric insulating solids (minerals, glasses, and polymers). Such materials are known as particle track detectors or dielectric track detectors (DTD's) or solid-state nuclear track detectors (SSNTDs or NTDs).

Technique of SSNTD marked its beginning in the year 1958, when D. A. Young^[1] at Atomic Energy Research Establishment, Harwell discovered etch pits in LiF crystals. As per his observations, when LiF crystal was exposed to fission fragments from U₃O₈, a uranium source at 1mm from LiF crystal, a number shallow etch pits were detected upon chemical treatment with HF+CH₃COOH saturated with FeF₃. These pits were nothing but the path of fission fragments traversing through transparent crystal, observed as dark needle shaped fine channels under optical microscope. They were later named as “etch tracks”. Similar findings were reported by E.C.H. Silk and R.S. Barnes^[2], who observed damage trails in mica sheets caused by heavy charged particles under transmission electron microscope. The technique of ‘Track etching’ and new field of ‘Trackology’^[3] was established by R. L. Fleischer, P. B. Price and R. M. Walker^[4-8] while working extensively on different types of dielectric solids such as glasses, minerals, mica sheets and also synthetic plastics. They also observed similar latent tracks in crystal lattice of minerals, due to naturally occurring phenomenon of spontaneous fission of the small quantity of uranium present in rocks^[9].

The extreme simplicity of the technique in merely counting the number of tracks (recorded on a dielectric detector) of charged particles emitted from a nuclear reaction, one can perform experiments in nuclear physics and chemistry, particle dosimetry and microanalysis^[10]. Many reviews especially by Fleischer et al. help in understanding basic knowledge and technological application of Trackology^[11,12] based on ionographic registration in SSNTDs. Currently, there is hardly any branch of science and technology where SSNTD technique does not have potential application^[13,14].

Solid state nuclear track detectors are special kind of radiation detectors, which records tracks of variety range of charged particles ($Z \geq 1$) in its solid medium. Nearly all types of transparent insulating solids can be used as SSNTDs. These solids are primarily classified into natural and man-made solids. Further, based on chemical composition

SSNTDs are broadly categorized into three major classes: Inorganic crystals, Inorganic glasses and synthetic organic plastics as shown in **Figure 3.1**.

Usually, man-made solids can be made widely available for use as track detectors, especially in examining rare events such as cosmic ray particles. Typical SSNTDs such as crystals, glasses and thermoset polymers are densely ordered (regular or random) materials, thus energized particles passing through it will release all their kinetic energy ionizing the atoms in the path, thereby allowing identification of the incident charge particle. Identification^[15,16] of particle is based on the method measuring residual range and the etch rate along the trajectory. This feature made SSNTDs a versatile radiation detector ever discovered.

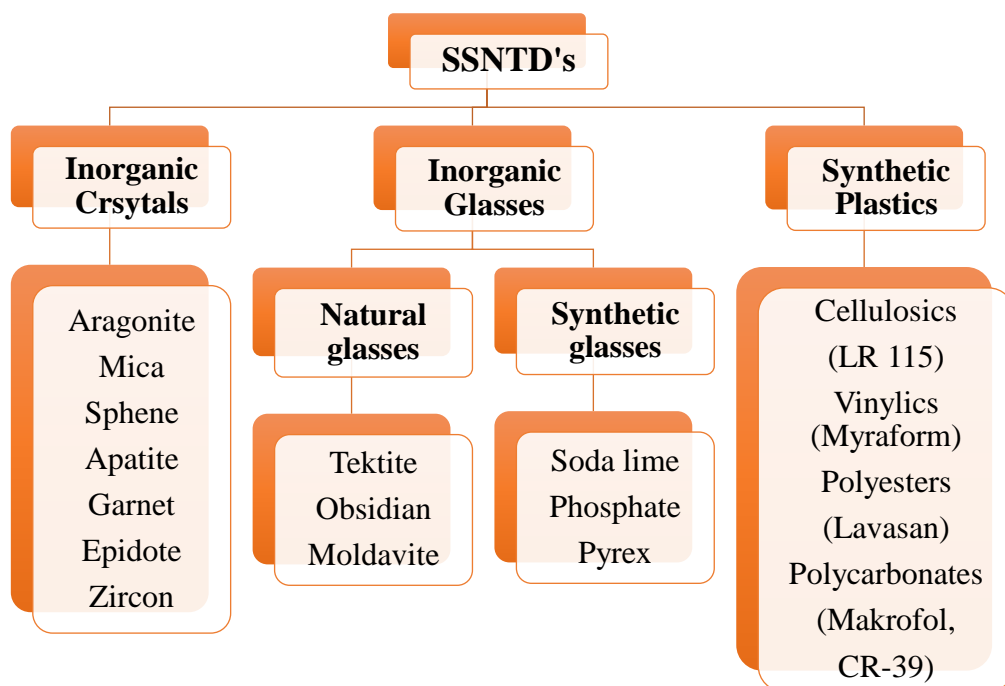


Figure 3.1 Classification of SSNTDs

Among all SSNTD plastics are found to be most effective and globally available under various trade names such as LR-115, PM-500(CR-39), Makrofol etc.

3.1.1 Track formation in SSNTDs

Principle^[3,17,18]: When heavily ionizing particle enters the dielectric medium, it ionizes the atoms along its path thereby leaving the intense narrow trails of 30-100Å diameter. These trails/tracks are nothing but the ruptured region of inter-atomic displacement (in mineral and glasses) or ionized molecular chains and free radicals (in plastics) caused by ionization process. Such narrow trails enriched in ions and free radicals generated by primary ionization are known as “latent tracks”. E.g., in case of cellulose nitrate polymer, alpha

particle travelling with 6 MeV energy produces approx. 150, 000 ion pairs in material with penetration up to 40 μm . This nano scaled passages can be observed only under Transmission Electron Microscope (TEM). Further, using suitable method of electrochemical or chemical etching, tracks can be enlarged and viewed under optical microscope as conical pits of micron size. The diameter of this etch pits can be further enlarged by varying concentration and temperature of chemicals etchants such as alkali metal hydroxides or acid. Here, degradation at damaged region is much faster than at undamaged region. This track effect^[11] is well studied in dielectric insulator materials (crystalline, glassy, and polymeric) but in conductive and semiconductors material track effect is unseen due to recombination process. The track formation and development process in polymeric NTDs is depicted in **Figure 3.2**.

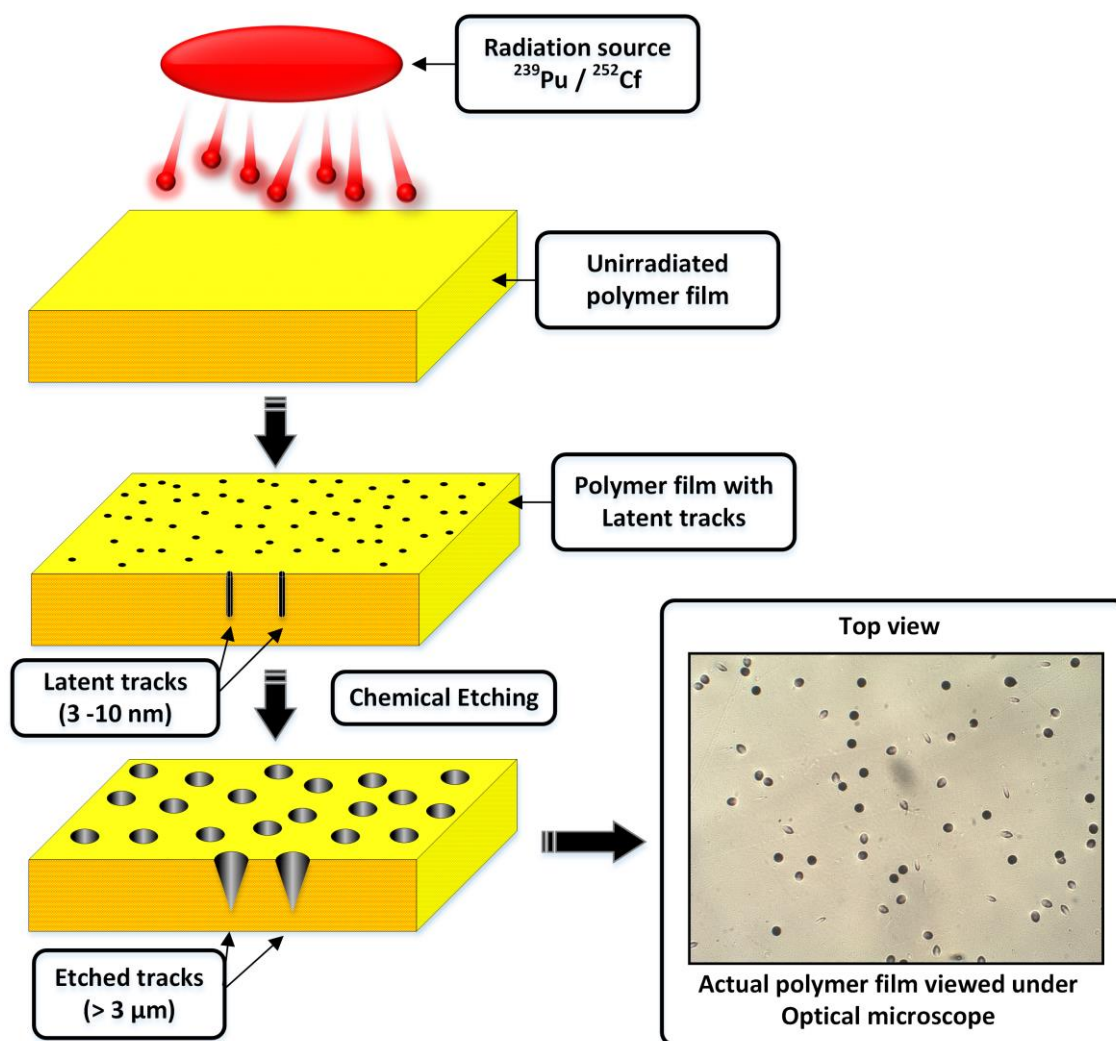


Figure 3.2 Overall process of solid-state nuclear track detection in polymeric NTDs.

3.1.2 Highlighting the features of nuclear tracks

- Latent tracks^[19,20] are narrow damaged region of unstable ionized centres along path of passing projectile.
- Narrow region is continuous along the passage of particle with diameter < 10 nm.
- The damaged track length is equal to range of particle entering the material.
- Unstable ion centres have highly reactive towards chemical reagents.
- Tracks can be viewed using suitable microscopic technique whenever needed.
- Track formation is dependent on resistivity of material used i.e., track formed only when electrical resistivity is > **2000 Ω**, as shown in **Table 3.1** below. Materials with high electrical resistance can retain the tracks with maximum efficiency

Table 3.1 Electrical resistivity of different track forming and non-forming materials.

Material	Resistivity range (ohm.cm)
Track forming	
Insulators: Silicate minerals, Alkali halides, Insulating glasses, polymers	10^6 - 10^{20}
Poor insulators: MoS ₂	3000-25000
Semiconductors: V ₂ O ₅ glass	2000-20000
Non-track forming	
Semiconductors: Germanium, silicon	10-2000
Metals: Cu, Al, Au, Pt, W, Z	10^{-6} to 10^{-4}

3.1.3 Theory and mechanisms of latent track formation

As we understand that latent track formation is an ionization and excitation process^[20] caused by drop in energy of particle entering the solid along its trajectory. This loss corresponds to transfer of energy to surrounding atoms by particle, generating free electrons, ions and radicals. Depending on detector materials, critical rates of energy loss for track formation varies. Organic polymers can record particles at energy loss rates < 4×10^7 MeV m²g⁻¹ enabling detection of proton recoil tracks whereas inorganic materials can record particles with energy loss rates > 15×10^7 MeV m²g⁻¹.

Hence, different theories and models^[21-23] have been proposed to understand the track effect. Among this, we considered few models for explaining the mechanism of track formation in two types of detector material i.e., inorganic crystal and organic polymers. A pictorial representation is shown in **Figure 3.3**.

A. Ion explosion spike model for inorganic solids^[20,24]: A semi-quantitative model was proposed by Fleischer et al. which satisfactorily explains the track formation mechanism in dielectric solids and is widely accepted mechanism for track formation in the inorganic solids. This includes five stages:

- 1. Electron stripping of the charged particle:** When a charge particle enters in a atomic array of detector material, particle loses some or entire electrons by interacting with the electrons of the detector material. E.g., A 280 MeV ^{56}Fe particle entering the mica detector loses its entire electrons interacting with material thereby producing Fe^{2+} , the iron nucleus.
- 2. Penetration at velocity to leave the etchable track:** After entering the material matrix, charge nuclei move with velocity which is sufficient enough to cause the continuous damage along the path, resulting in permanent etchable tracks. Damage should be such that at least one atom must be ionized per atomic plane crossed by the nuclei.
- 3. Actual damage region:** At this stage, particle moves at velocity creating enough damage density along its path. In the process, heavily charge nucleus collides with atoms in path thereby imparting energy to them. Here electron excitation occurs, forcing them to expel out of atom into the surrounding network. This emitted colonies of electrons are known as delta rays or bremsstrahlung electrons. Further, the electron deficient group of atoms will recoil from each other due to columbic repulsion. It is this linear concertation of damage caused by "ion explosion" which give rise to etchable tracks. Stage terminates when penetrating electron slows down the path and start gaining electrons to such an extent that, it is no longer potent enough to create the damage density require for etchable tracks.
- 4. Un-etchable Particle tracks:** In order to generate good track, particle must move with minimum velocity which is insufficient to produce an etchable tracks. Such velocity will be larger for less sensitive detector material. The distance covered with this velocity is called as range deficit, moving particle leaves no track further.
- 5. Termination of the track:** In this stage, the particle comes to complete rest possibly with complete electrons gain, thereby termination the process of traversing.

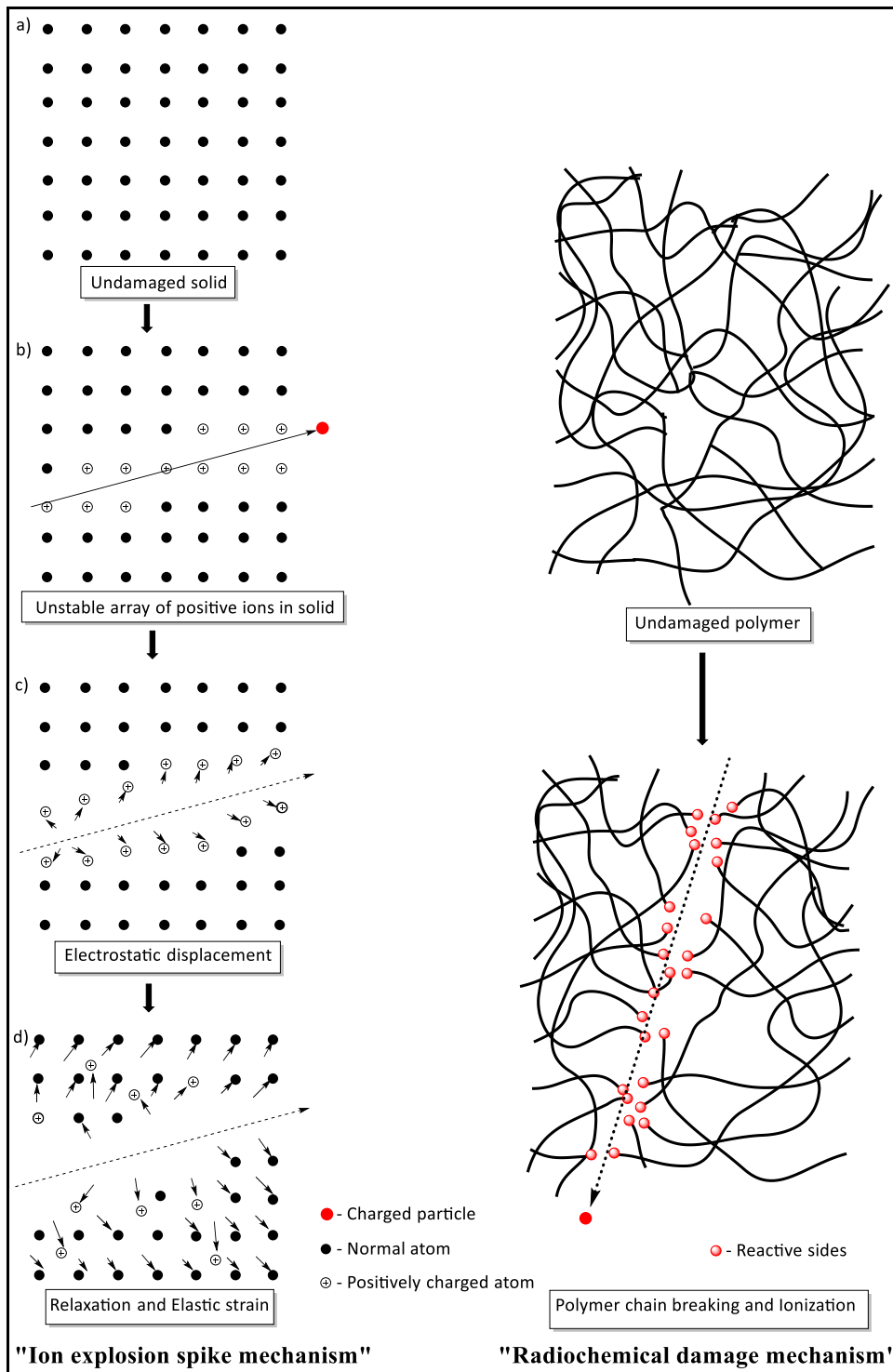


Figure 3.3 Graphical representation of models explaining track formation mechanisms in inorganic solids and organic polymers.

B. Radiochemical damage mechanism in organic polymers^[19,25]: This model helps in understanding track formation in organic polymers. When an energetic charge particle penetrates the polymeric matrix, it collides with the radiation sensitive functionalities in polymeric chains, which results in atomic excitation and emission of electrons into

surrounding. As a consequence, covalent bonds are cleaved in polymer chains forming low molecular weight fragments and array of free radicals^[26] along the trajectory of particle. This process is known as radiolytic scission or radiation degradation of polymer. Also, secondary electrons^[27] ejected during process (delta rays) further enhance the degradation process. Hence, low energy dose is required for degradation (~100 KGy) as compare to ionization (~10 GGy) in inorganic solids. Overall effect, give rise to permanent etchable track region known as latent track, which consist of collection ions, reactive species and low molecular weight intermittent cross links. Chemical etchants like alkalis are capable of predominantly degrading or dissolving these latent track regions as compared to the undamaged part of detector material.

3.1.4 Track etching geometry and etched-track parameters

The chemical etching process helps in understanding growing shape and size of the etched track in micrometer dimensions. It mainly includes two types of chemical reactions: (1) etchant with damaged region and (2) etchant with bulk region of the detector. Both these reactions are examined by two significant etching parameters, namely the **track etch rate** (V_T) and the **bulk etch rate** (V_B)^[25]. Hence, overall etching process is a combined reaction of V_T and V_B .

A) Track etch rate (V_T)

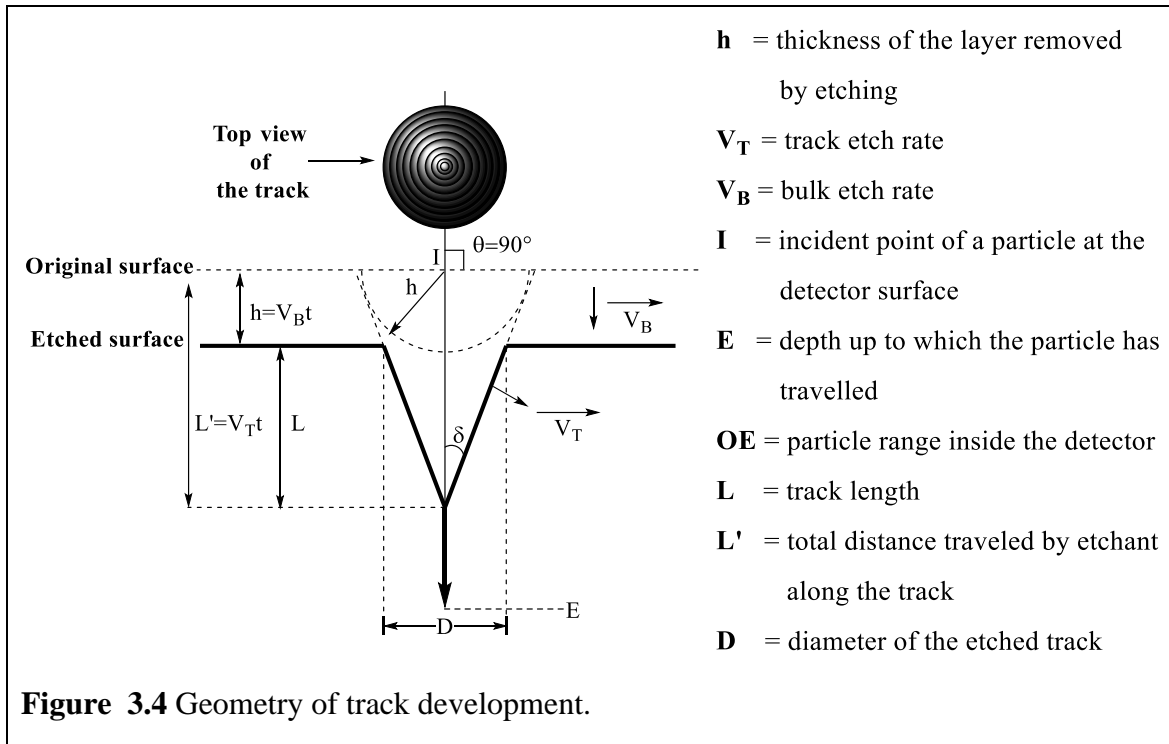
The rate at which the etchant penetrates along the longitudinal path of latent track is called as track etch rate.

B) Bulk etch rate (V_B)^[28]

The rate at which the undamaged portion of the detector material is being removed is called as bulk etch rate. The removal of the detector material is caused by interaction of etchant with detector surface. The material is removed horizontally in layer-by-layer fashion, reducing the thickness of detector. It is the frequently used parameter to find the stability of detector material.

The track etch rate and bulk etch rate is mainly depends upon the chemical constitutions of detector material and etching condition used i.e. normality and temperature of etchant. Beside this, track etch rate is also depends on ion's energy loss properties i.e., $d_E/d_X(Z, \alpha)$. Further, geometry of the etch track^[29] is influence by charge (Z), mass (M) and energy (E) of nuclear particles entering the detector surface. Hence by knowing the change in track length, diameter, track and bulk etch rate, one can characterize the incident particle. **Figure 3.4** shows track etch geometry of particle incident perpendicularly to the detector.

In three dimensions, the track is a conical in shape with the local track developing angle (δ), which is obtained by rotation of the track wall around the particle trajectory.



In a given case of particle entering the detector at angle of incidence ($\theta = 90^\circ$) normal to detector surface and at a constant track etch rate, following etched-track parameters can be calculated using equation below^[16]:

$$L = (V_T - V_B) t \quad (3.1)$$

$$D = 2V_B t \sqrt{\frac{V-1}{V+1}} \quad \text{where } V = \frac{V_T}{V_B} \quad (3.2)$$

Development of nuclear track and etching sensitivity is governed by the “Track etch ratio” i.e., $V = V_T/V_B$. If V is less than or equal to 1, no etch tracks are observed. From the equation 1 and 2, one can envisage that L and D decreases as V_T/V_B decreases. At $V_T = V_B$, both L and D vanishes. Hence, track etch rate should be greater than bulk etch rate for efficient etch track formation. In other words, condition $V_T/V_B > 1$ must be fulfilled to form a track.

C) Critical angle of etching (θ_c)^[25]

Latent track and subsequent etch tracks will have different shapes depending upon the angle at which charged particle enters the surface of the detector. For different detector material,

there exists a critical angle of etching (θ_c), below which no etchable track will be detected after chemical etching. It is a result of the competition of V_B with V_T , which is shown **Figure 3.5**.

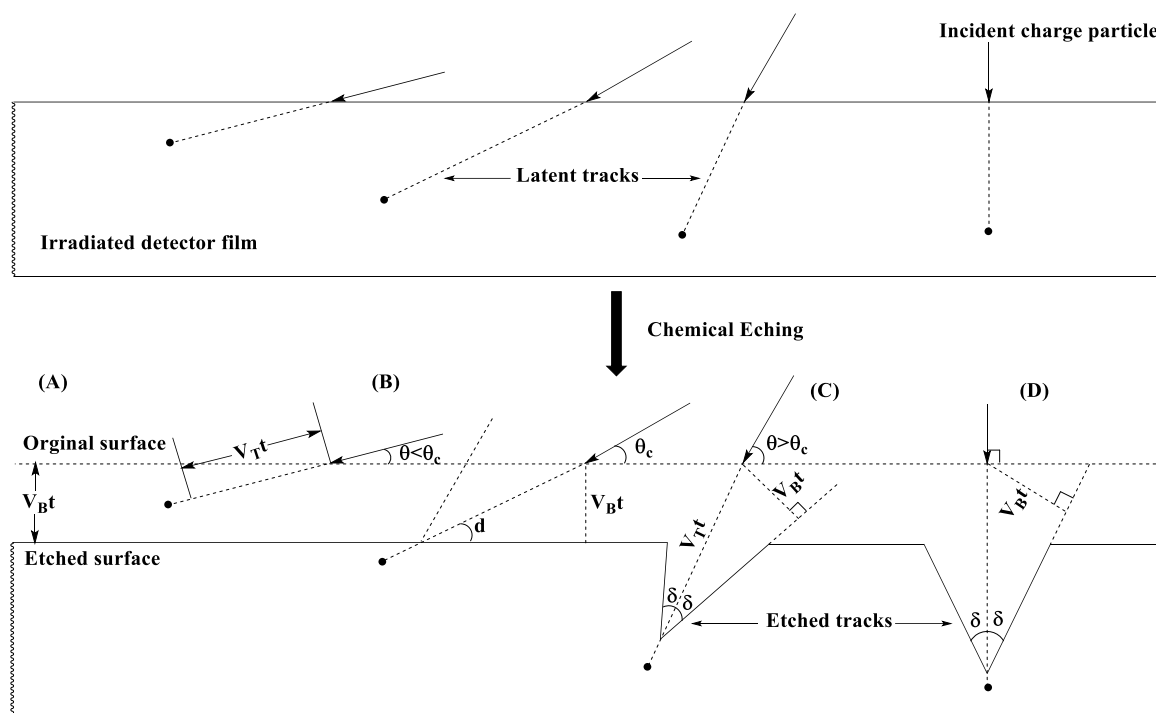


Figure 3.5 Existence of critical angle of etching for track formation.

With given angle of incidence (θ), if $(V_T t \sin \theta < V_B t)$, the track will be removed away by the etchant, leaving no etched track in the detector (**Figure 3.5; part A**). If $(V_T t \sin \theta > V_B t)$, a track cone will be left after etching (**parts C and D**). If $(V_T t \sin \theta = V_B t)$, it is the critical situation for formation of an etched track (**part B**). In this situation, the incident angle is denoted as (θ_c) i.e., it's a critical angle of etching given in equation below,

$$\theta_c = \sin^{-1} \left(\frac{V_B}{V_T} \right) \text{ here } \delta = \theta_c \quad (3.3)$$

Hence it is one of the geometrical limitations for the revelation of the etched tracks in NTDs.

Table 3.2 Track detectors with θ_c values for full energy fission fragments.

Sr. No.	Detector material	Critical angle of etching (θ_c in deg.)
1	Minerals	0-7
2	Glasses	
	Soda, borosilicate, flint, Obsidian etc.	20-70

	Phosphate glass	1-5
	Silica glass	13-19
3	<u>Plastics</u>	
	Nitrocellulose	>2
	Lexan	2.5
	Makrofol	3

As per the given θ_c value for different detector material^[20] in **Table 3.2** it can be noted that the plastics are certainly going to be more efficient in recording etch tracks, due to its lower value of θ_c . In most glasses the θ_c is so large that they are ineffective for most applications as solid state nuclear track detectors.

D) Track etching sensitivity (S)

Detector's track etching sensitivity^[28-30] is a characteristic function of detector material properties, particle charge, energy and direction of the incident charge particle. It is also known as detector response i.e., $V(R)$ to incident charge particle. Traditionally sensitivity is calculated ratio of etch track diameters and removed layer thickness given by equation below

$$S = V = \frac{V_T}{V_B} = \frac{4 V_B^2 t^2 + D^2}{4 V_B^2 t^2 - D^2} = \frac{h^2 + D^2}{h^2 - D^2}, \text{ where } h = V_B t \quad (3.4)$$

Where h is the removed layer thickness and D is diameter of charge particle track.

From the above equation we could see that it is measure of track etch rate (V_T) too. Alternatively,^[31,32] it also calculated by taking ratio of alpha track diameter to fission fragment track diameter as computed by equation below.

$$S = V = \frac{V_T}{V_B} = \frac{1 + x^2}{1 - x^2} \quad (3.5)$$

where, $x = \frac{D^\alpha}{D^\beta}$ the ratio of the diameter of alpha particle tracks to fission is tracks.

E) Track detection efficiency or track etching efficiency^[25,30,33] (η)

The detector etching efficiency (η) is known as the number of particle tracks recorded to the number of incident particles. Hence it is measure of fraction of particles actually incident on the detector surface, determined equation below.

$$\eta = 1 - \sin \theta_c \quad \text{OR} \quad \eta = 1 - \left(\frac{V_B}{V_T}\right) \quad (3.6)$$

3.1.5 Determination of bulk etch rate (V_B)

1) Change in detector mass/weight loss method^[33,34]

In this method, change in weight of the test detector is determined by recording its weight before and after etching. This method is also sometimes called as “gravimetric” method. Bulk etch rate is calculated using following equation

$$V_B = \frac{(M_1 - M_2)T_i}{2M_2t} \quad (3.7)$$

where M_1 and M_2 are the initial and final weight of the test detector, T_i is the initial thickness and t is the time of etching. However, this method lacks in accuracy of measuring the exact weight.

OR

$$V_B = \frac{\Delta m}{2A\rho t} \quad (3.8)$$

where Δm is mass difference^[28,35], A is the etched surface area, ρ is the density of the detector and t is the etching time.

2) Change in detector thickness method^[31,36]

It is an alternative method, where in bulk etch rate for given detector is determined by calculating reduction in detector thickness after a regular etching time, which could be expressed as

$$V_B = \frac{(T_1 - T_2)}{2t} \quad (3.9)$$

where T_1 and T_2 are the initial and final thickness of the test detector and t is the time of etching

3) Fission fragment track diameter method^[29]

This is the most conventional and widely used method for determination of V_B . The rate of variation in fission track diameter in test detector (previously exposed to ^{252}Cf source) is calculated after regular time intervals of etching. Hence relation between bulk etch rate and fission track diameter is given by,

$$V_B = \frac{D_f}{2t} \quad (3.10)$$

Where, D_f is the fission track diameter and t is the etching time.

3.1.6 Track revelation and visualization technique

As discussed earlier, latent track formed by a charge particle of certain threshold energy, are very fine in dimension (3- 10 nm) and can be visualized only under microscopic techniques (TEM, SEM, STM and AFM) and scattering techniques (x-ray and neutron scattering). However, this technique has some serious limitations^[19]: 1) require very thin films of detectors i.e., <300 nm; 2) as observation window is too small, high track density of order $\sim 10^5$ tracks/ cm^2 is required; 3) expensive techniques and availability is restricted. The most successful and widely used techniques of track revelation are chemical and electrochemical etching. This technique helps in visualizing the nuclear tracks under an optical microscope, which is much easy to setup at ordinary laboratory conditions.

1. Chemical etching (CE)^[14,25]

Chemical etching is the basic technique used to reveal charge particle tracks in solids. It is heterogeneous process involving a solid-liquid interface. The essential requirements for CE are two, namely, etchant and etching device.

a) Etchant

An etchant is a specifically a chemical formulation (mostly alkali or acid), which preferentially reacts with the damaged area in the particle track resulting from the passage of a charged particle in NTDs. Degradation of latent track occurs rapidly than the undamaged bulk. This process leads to enlargement of track, making it visible under optical microscope using visible light. This process is known as chemical etching. Before visualization under microscope, detector is washed thoroughly with water and dried under an IR lamp. The etchant is specific for each type of detector material; selection of the wrong etchant composition will never reveal tracks (**Table 3.3**)

For plastics, aq. KOH /NaOH are commonly used. Sometime promoters such as ethanol, propanol, and methanol are used to increase the dissolution rate of the degraded fragments in track region of organic polymer. Also, some oxidizing agents like $\text{K}_2\text{Cr}_2\text{O}_7$, KMnO_4 , and NaClO_4 have been used for plastics. For minerals and glasses, acids such as H_2SO_4 , H_3PO_4 , HF, etc. are used as etchants.

Table 3.3 List of etching condition used for chemical etching of different NTDs^[29]

Category	Detector material	Etchant
Crystals	Feldspar	1 g NaOH + 2 g H ₂ O under reflux.
	Olivine	KOH solution, 160°C, 6 min.
	Mica	48 % HF at 20-25°C, ~40 min.
	Quartz	KOH solution, 210°C, 10 min.
Glasses	Soda-lime glass	48 % HF, at 20 - 25°C, 3 sec.
	Phosphate glass	48 % HF, at 20 - 25°C, 3 sec.
	CR-39 TM	1-12 N NaOH at 40-70°C, 1-4 h.
Polymers	Polycarbonate	6 N NaOH at 50°C, 60 min.
	Cellulose nitrate	3-6 N NaOH at 50°C, 40 min.

b) Etching devices^[19]

An assembly to hold etchants and maintaining the etching conditions. The etchant must be held in a closed system to prevent exchange of substances from inside or outside, in order to retain the concentration and temperature of etchant (refer section 3.3.3 for setup).

2. Electrochemical etching [ECE]^[38,39]

Electrochemical etching was first proposed by Tommasino in 1970. To enhance the process of track revelation, high voltage electric field is applied to chemical etching medium. In a given etching method, etchant diffusing into latent tracks forms a conducting path for current under applied alternating voltage across the detector film. The energy produced in the medium dissipates in the track region resulting in strong local heating which increases the tracks etch rate. Further, the applied voltage concentrates at the tip of the conducting paths of tracks, giving rise to electrical breakdown with tree morphology, hence named as 'treering process'^[40].

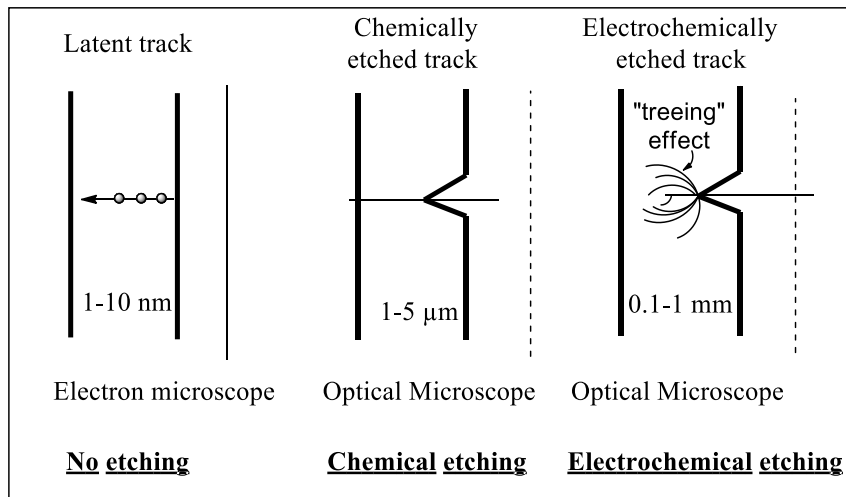


Figure 3.6 Nuclear Track morphologies and treeing effect in ECE.

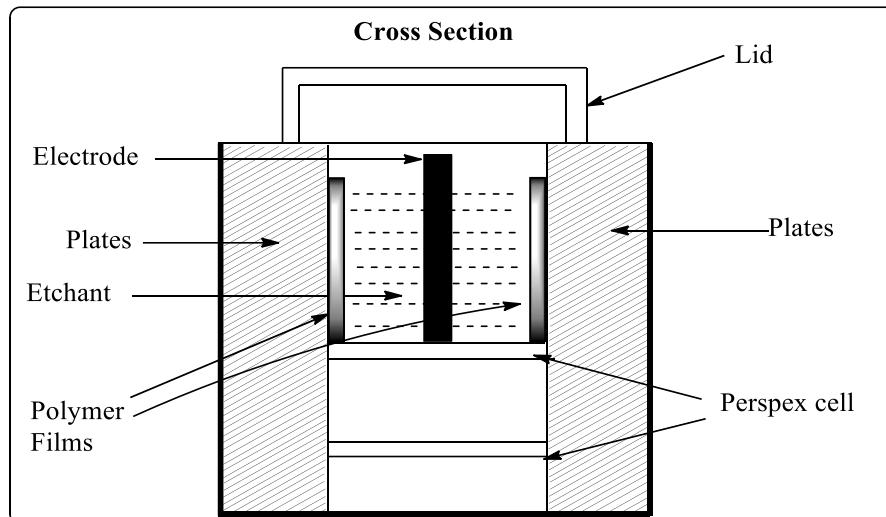


Figure 3.7 Electrochemical etching assembly^[41].

The high temperature generated at tip of the conducting paths leads to thermal degradation of material, thereby forming continuous growth of the track. Further, total degradation causes enlarged tracks to carbonize. Hence, in ECE tracks are seen as black spots under a microscope. Both the bulk etch rate and the track etch rate of dielectric material increases as result of rise in temperature in entire material. This technique allows a large-scale amplification of tracks for visualization by naked eyes. This technique has found to work conveniently with polymers having general properties like good electrical properties, low value of dissipation factor or dielectric loss factor, low water absorptivity and polar nature of the materials.

Beside from its quicker track evaluation, ECE suffers from few disadvantages such as intersection of track geometries at high track density ($>10^3/\text{cm}^2$) and loss of track information upon electro chemical etching.

3.1.7 Microscopic track counting techniques

Most widely used technique for determination of exact amount of dose and density of track generated by charge particle flux. Track analysis were carried out after etching of track in specified etchant.

- i. **Visual track counting using optical microscope**^[42]: Simplest and conventional technique to record the track density less than $10^5/\text{cm}^2$. Although method is time consuming, its effectiveness has been improved by using image projection techniques and image analyzing systems.
- ii. **Optical densometry**^[43,44]: Method to determine high track density from 10^5 to $10^7/\text{cm}^2$. The technique involves measuring the amount of scattered light proportionally between etched and unetched surfaces. A red dye is used to accentuate the material.
- iii. **Confocal microscopy**^[45]: This technique includes 3D re-construction of a nuclear track after etching. The method has strong potential in accurate determination of particle parameters charge, energy and mass number.
- iv. **Atomic force microscopy**^[46-48]: It is a unique tool to examine the etched track structure and track etch kinetics. Studies related to early stages of the etch track formation and post etch surfaces can be performed using AFM.

3.1.8 Merits and demerits of SSNTDs

Beside simplicity, SSNTDs have several advantages over conventional nuclear track detectors such as cloud chamber, ionization chamber, spark chamber, bubble chamber, Geiger Muller counter, scintillation counter, proportional counter, semiconductor detectors, nuclear emulsion, etc.^[19,20]. Some characteristic advantages of SSNTDs along with few demerits are enlisted in **Table 3.4**.

Table 3.4 Merits and demerits of SSNTDs over conventional particle detectors.

Sr. No.	Merits	Demerits
1	Simple in construction and use, rugged, durable. Available in variety	Etching process in SSNTDs, only gives total etched track length with

-
- | | |
|--|---|
| of composition and convenient to use in different sizes as per requirement. | no recovery of etched off part of material. |
| 2 Highly economical as minimum costly electronics are involved in development and detection purpose. | Although resolution of particles in terms of charge and mass is feasible but understanding its precise energy resolution is still subject of study. |
| 3 Portable to use in remote conditions where other techniques fail. | Technique still relies on blank readings of unexposed detectors for comparison purpose. |
| 4 SSNTDs material record particle tracks permanently and stored for longer duration at room temperature and pressure. Also remain unaffected by other environmental conditions. | |
| 5 Property of being threshold type detector helps in detection of heavily charged particles. Effective in recording and differentiating, fission fragments/heavy charged particles in the presence of excessive background of lighter charged particles. | |
| 6 Presence of substantial amount of geometric flexibility promotes in measurement of angular distribution. | |
| 7 Quicker and simpler etching process in revealing nuclear tracks in comparison to nuclear emulsions. | |
| 8 Comprehensively employed detectors for low as well as high energy ionography. Superior motion for high Z-particles is achieved with plastic | |
-

detectors compared to nuclear emulsions.

- 9 Nuclear track detection properties of some naturally occurring minerals and surface materials of celestial bodies, helps in understanding natural geological and cosmological events.

3.1.9 Applications of solid-state nuclear track detection technique

Looking at the widespread applicability of SSNTD technique in various disciplines of science and technology, there is barely any scientific field that left unexplored by this technique. Popular broad area of studies includes nuclear chemistry and physics, dosimetry, medical and astrophysics, archaeology, cosmological and biomedical studies. Currently, most of the NTD researchers are focused towards working in the area of environmental science and health effects. Some of these key applications are elaborated below.

1) Nuclear physics and technology^[19,25,49]:

- a) **Heavy-ion reactions:** The NTDs are used to investigate the ternary and quaternary nuclear fission promoted by heavy ions (low and high energy). Key information such as mean free path of ion fragments and projectile charges are obtained.
- b) **Fission track dating^[13,50]:** This method helps in archaeological dating of minerals containing small quantity of uranium. Process involves recording and analysing tracks of fission fragments emitted by spontaneous fission reaction using etching technique.
- c) **Uranium and thorium exploration:** Finding alpha particle track density using SSNTD technique one can obtain concentration of radon in the soil, which is the alpha decay product of uranium and thorium series.
- d) **Estimation of alpha activity in waste water fields:** Variation of alpha activity (acceptable value is <0.037 Bq/ml) in the radioactive water waste can be evaluated using plastic NTDs.
- e) **Astrophysics and cosmic rays^[16]:** Nuclear track detectors are utilised in finding primary galactic cosmic rays based on its constituent elements and isotopes. Information obtained is processed to construct fluxes of cosmic ray protons and heavy nuclei.

-
- 2) **Environmental and health physics**^[19,25]: The areas of interest related to personnel protection dosimetry include-
- a) **Radon and neutron dosimetry**^[51]: Radioactive pollution in home and work places can be accounted using NTDs by measuring the radon level in environment. Also, evaluation neutron levels at nuclear reactor sites could be revealed. Monitoring of sudden increase of radon level in underground water bodies can help in prediction of earthquakes activities.
 - b) **Exposure at spacecraft**^[16]: The dose level of outer space radiation such as cosmic, ultra-heavy rays, interplanetary dust particles and solar flare particles at global space station and astral landings, can be measured using handy NTDs.
- 3) **iii) Bio-medical science**^[52]:
- a) **Cancer and diagnostic therapy**: Boron neutron capture therapy (BNCT) is used to examine and eradicate malignant brain tumours. In principle, boron delivery agents are targeted towards tumour site, absorbed and irradiated with thermal neutrons. This process emits high energy alpha particles which destroy the tumour cells.
 - b) **Alpha activity in blood and aerosols**: NTDs are used to find out the alpha content of blood samples of workers exposed to radiations at uranium mines and nuclear power plants by immersing detector in frozen blood sample. Also, misdistribution of alpha active aerosols in human lungs can be studied.
 - c) **Lead content in the bones**: Concentration of lead accumulated in bones and teeth can be examined using SSNTD technique.
- 4) **Technological Sciences**^[53]:
- a) **Nucleopore filters**: SSNTDs technique is employed to manufacture microfilters of controlled cylindrical porous geometry by irradiating material with collimated beam of particles followed by etching to desired pore size. These engineered filters are used to study microscopic organisms^[54], treatment of blood cancer, microelectronic and reaction device.
 - b) **Magnetic nanowires**: Magnetic nanowires utilized as miniature pickup sensors for magnetic hard-disk memories and as non-volatile magnetic bit memories

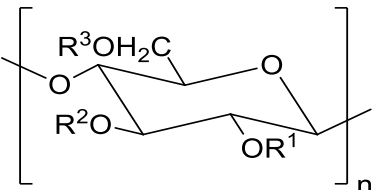
3.2 Literature survey

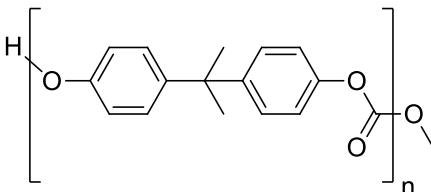
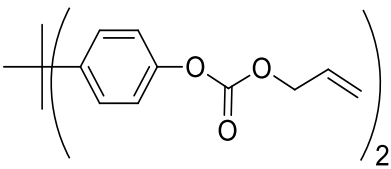
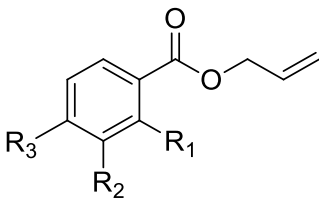
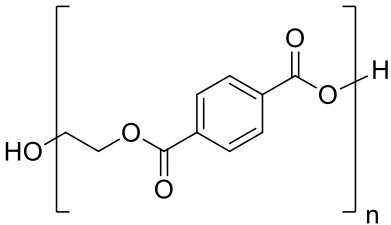
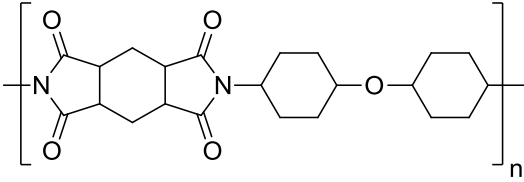
3.2.1 Polymeric nuclear track detectors (PNTDs)

After the discovery of SSNTD technique by D. A. Young in 1958, wide work has been carried to study nuclear tracks using insulating materials such as minerals, glasses, and polymers. This technique has been well established over the past six decades and is useful for the qualitative and quantitative analysis of the charged particles such as alpha, protons, neutrons and heavy ions.

After the introduction of plastics as SSNTDs in 1963^[72], a number of plastic materials, such as cellulose, polycarbonates, polyvinyls and acrylates, have been extensively studied as track detectors. Plastics NTDs gained popularity over the rest dielectric detector materials, significantly due to its high sensitivity towards charged particles (recordable charge $Z \geq 1$) and potential ease in track development, evaluation and long-term registration. The most commonly used plastic NTDs^[25] are the cellulose nitrate (LR-115)TM, poly allyl diglycol carbonate (PADC, CR-39TM), Bisphenol-A polycarbonate (Lexan, MakrofolTM), Polyethylene terephthalate (Mylar)TM and Polyimide (Upilex). Amongst this CR-39TM most widely used and is on the forefront because of its unique sensitivity, high-charge resolution capability, homogeneity and superior optical properties. The minimum recordable ionizing particle for CR-39 detector was found to be 20 keV proton by etching with NaOH solution^[73]. PADC or CR-39 polymer has been extensively used in dosimetry studies of neutrons, heavy ions and cosmic radiations. in the field of neutron dosimetry, environmental dosimetry and other thrust areas of nuclear research and technology. Till date, more than 30 different types of plastic detectors are known in the literature and are summarized in **Table 3.5** below.

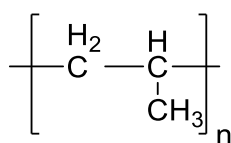
Table 3.5 Some monomers/polymers that have been tested as nuclear track detectors.

Sr. No.	Chemical/Trade names [CAS registry number]	Monomer/CRU	Ref.
1	Cellulosic		[57–59]

- 2 Bisphenol-A Polycarbonate** (Lexan, Makrofol, Tuffak) [9002-88-4]  [60,61]
- 3 Bisphenol-A- bis (allyl carbonate)** (CR-73) [84000-75-9]  [62]
- 4 Polymers of Allylic Phthalates**
- a) Diallyl isophthalate [1087-21-4]  $R_3 = R_1 = H$ $R_2 = \text{diallyl ester}$ [63,64]
- b) Diallyl phthalate [131-17-9] $R_3 = R_2 = H$ $R_1 = \text{diallyl ester}$
- c) Diallyl terephthalate (AW-15) [1026-92-2] $R_1 = R_2 = H$ $R_3 = \text{diallyl ester}$
- 5 Polyethylene terephthalate** (Lavsan, Mylar, Chronar Melinex, Terphane) [25038-59-9]  [65,66]
- 6 Poly(imide)** (PI, Kapton, Upilex)  [67,68]

7 Poly(propylene)

[9003-07-0]

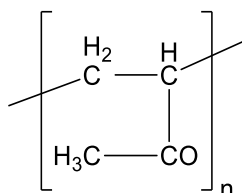


[69]

8 Vinylic polymers

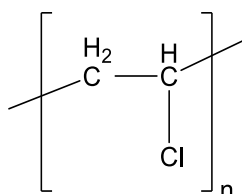
- a) Poly (vinyl acetate)/
Poly(1-acetoxyethylene)

[9003-20-7]



- b) Poly (vinyl chloride)/
Poly(1-chloroethylene)

[9002-86-2]



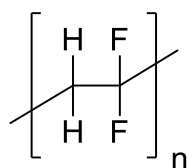
[70-72]

- c) Poly(vinylidene fluoride)/
Poly(1,1-

difluoroethylene)

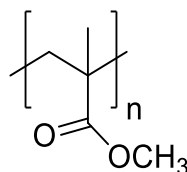
(PVDF)

[24937-79-9]

**9 Poly (methyl methacrylate)**

(PMMA, Perspex)

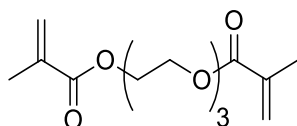
[9011-14-7]



[73]

10 Triethylene glycol bis (methacrylate)

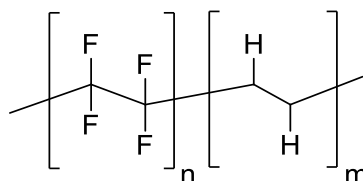
[109-16-0]



[74]

11 Poly(tetrafluoroethylene-co-ethylene)

(PTFE-E)

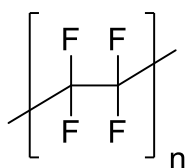


[75]

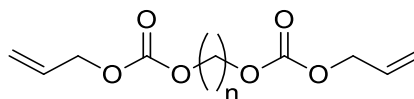
12 Poly(tetrafluoroethylene)

(Teflon)

[9002-84-0]



[76]

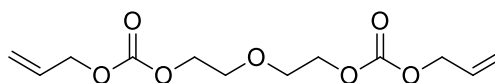
13 Alkanediol bis allyl**Carbonate**

[77]

n= 3 to 5**14 Allyl diglycol****carbonate/ADC**

(PADC, CR-39, PM-500)

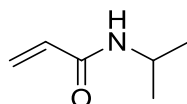
[142-22-3]



[78]

15 N-isopropyl acrylamide

[2210-25-5]



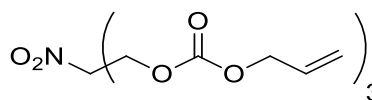
[79]

(copolymer with ADC)

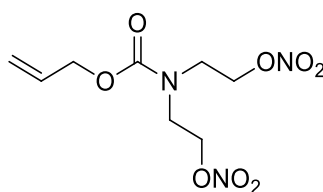
16 Tris-(2,4-dioxa-3-**oxohept-6-1-yl)****nitromethane**

(TDONM)

[119845-30-6]



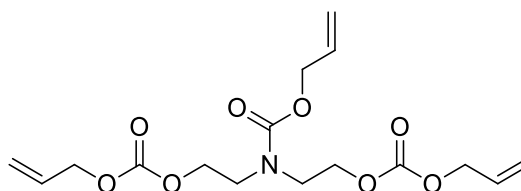
[80]

17 Allyl bis-(2-nitroxy-ethyl)**carbamate (ABNEC)**

[81]

18 N-Allyloxycarbonyloxy-**diethanolaminebis-(allyl****carbonate) (NADAC)**

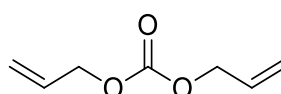
[869885-52-9]



[82]

19 Diallyl carbonate

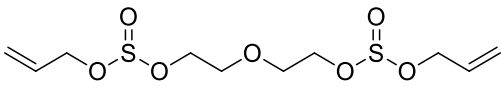
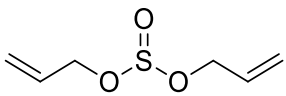
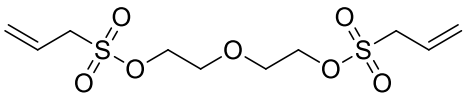
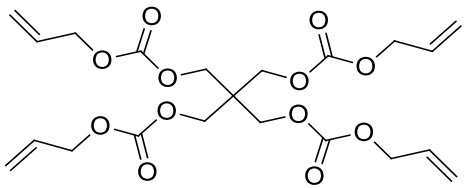
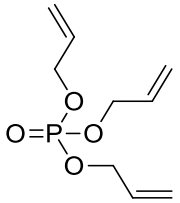
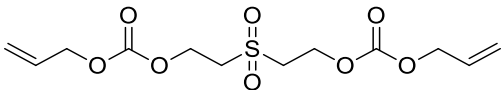
(DAC)



[83]

20 Poly (ADC-co-SO₂)(copolymer of ADC with SO₂)

[84]

- | | | |
|---|--|----------|
| <p>21 Allyl diglycol sulfite
(ADS)
[121752-04-3]</p> |  | [83] |
| <p>22 Diallyl sulfite
(DAS)</p> |  | [83] |
| <p>23 Diethylene glycol bis(allyl sulfonate)
(DEAS) SR-86, SR-90</p> |  | [85-88] |
| <p>24 Pentaerythritol tetrakis (allyl carbonate)
(PETAC)</p> |  | [89] |
| <p>25 Triallyl Phosphate
(TAP)</p> |  | [90, 91] |
| <p>26 2,2'-sulfonyldiethanol bis(allyl carbonate)
(SDAC)</p> |  | [92] |

Literature survey report suggested that, most of the efforts have been directed towards testing the commercially available plastic materials for various SSNTD applications, rather than systematic designing of the novel monomers and polymers materials as NTDs. With exception, primary focus of most of the track worker is enhancing the process of CR-39, LR-115 and Makrofol material for improved track detection efficiency. As a reason, no other better polymeric materials are commercially available to track workers.

CR-39 or PADC: In 1978, Cartwright^[78] and his colleagues first time introduced CR-39 as a polymeric nuclear track detector and since then it remained as plastic of choice for various SSNTD applications. It is discovered in 1940 as Columbia Resin 39th sample. It is an amorphous thermoset polymeric resin with three-dimensional covalent carbon

networks containing carbonates linkages bridged by diethylene ether chain^[93]. The CR-39 detector satisfies most of the need of an ideal NTD and is very sensitive for α -particle detection as well as for tracing the radon daughters in the energy range of around 1–60 MeV. Tsuruta et al. recorded its detection threshold in water as 2KeV/ μm ^[94]. It is preferred choice for personnel neutron monitoring due to its larger cross-section for (n, p) scattering, higher ranges of recoil protons, greater possibility of neutron energy transfer to protons, excellent optical properties that simplifies the analysis and suitably high shelf life. In CR-39 track development can be done using both chemical as well as electrochemical etching. Currently, CR-39 films are procured only through import procedure as it is not manufactured in India.

3.2.2 Criteria for developing polymeric NTDs

Based on the early research work on designing and developing new polymeric track detectors, following important structural parameters should be considered before devising a synthetic scheme for new radiation sensitive plastic material.

- 1) Effect of radiation sensitive groups:** Radiation sensitivity of plastic detectors is highly influenced by the bond dissociation energy of functional groups present in polymer matrix. Table shows the bond energy (KJ/mol) of different chemical bonds and ease of bond scission in descending order.

S=O > P=O > N=O > C=O				C-P > C-S > C-N > C-O > C-C					P-O > S-O	
522	544	607	799	264	272	305	346	358	335	364

Lower the bond energy of functional groups in polymer network, easier will be the bond scission and better will be the overall radiation sensitivity of material. Similar results were also observed in various literature reports^[87]. Among acyclic esters, carbonate esters show high sensitivity. Polymer of butanediol bis (allyl carbonate) has alpha sensitivity 10 times higher than that of diallyl adipate. Polymers having sulfonate, sulfone, nitrate groups are highly sensitive as compared to that with esters and amides moiety.

In such radiation sensitive polymers, lone pairs on hetero atom accelerate the ionization process by forming larger number of unstable sites in the latent tracks region, resulting in faster etching rates and increase in sensitivity of polymeric material is high.

- 2) Effect of chain bridging the radiation sensitive groups^[83,87,95]:** Studies also revealed that, the functionalities in chain, bridging the radiation sensitive groups, have

substantial impact on overall sensitivity of material. CR-39 or PADC and its analogue poly [pentanediol bis (allyl carbonate)] (PPeAC) were analyzed for this purpose. It was found that PADC showed alpha sensitivity 4 times higher than PPeAC. This is owed to presence of sensitive C-O bond in the diethylene glycol chain in case of PADC whereas PPeAC possessed C-C pentane hydrocarbon chain. Also, polymer with lower hydrocarbon chain between the carbonate groups are more sensitive than its higher homologues. Thus poly (propanediol bis (allyl carbonate)) shows better sensitivity than PPeAC.

In 1993 Fuji et al.^[86] reported derivatives of CR-39 by varying the average chain length of diethylene glycol dicarbonate linkage. Among this, material with optimum chain length 1.6 times larger than CR-39 resulted in sensitivity nearly 3 times higher than commercial CR-39 material. This material was named as SR-90. Studies also revealed that radiation sensitivity decrease for a polymer whose chain length value are greater than 1.6.

- 3) **Effect of density of crosslinking in polymer network**^[82,83,89]: When a polymer possesses compact and dense 3D cross-linked structure, the charged particles are likely to interact more frequently with surrounding network causing higher damage/ energy loss thereby creating a greater number of latent tracks. This is the reason why higher density of crosslinking of thermoset resin enhances the alpha sensitivity of material. Crosslinking density is highly influenced by polyfunctional monomers, concentration of initiator and curing temperature.

At higher initiator concentration^[96], density of crosslinking will be lower due to increase in the number of propagating chains. Also, crosslinking density can be increased by carrying out the curing at higher temperature utilizing optimal amount of initiator with high decomposition temperature.

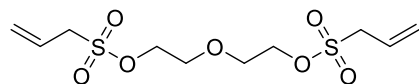
- 4) **Effect of aromatics in polymer matrix**^[95]: All polymeric material possessing aromatic ring such as BAEP, DAIP, CR-73 have low sensitivity as compared to CR-39. Also, addition of aromatic plasticizers such as dibutyl phthalate, dioctyl phthalate, di-(2-ethylhexyl) phthalate into polymer network, reduces the alpha sensitivity. But in order maintain the clarity of post etched polymer surface, addition of plasticizer is must^[100]. Presence of benzene rings in the aromatic plasticizers absorb the electrons/ delta rays owing to lesser interaction with surrounding network.

From above generalization, we can understand that, to have an effective and durable radiation sensitive polymeric NTDs, one should use combined approach of including high

density of cross-links in polymer matrix along with increasing number of radiation sensitive groups in a dense C-C network.

3.2.3 Sulfur containing allyl monomers and their polymers as highly potential polymeric NTDs

Fuji et. al.1990; Mandrekar et. al. 2008



2,2'-(oxybis(ethane-2,1-diyl)) bis (ally sulfonate)
OR

Diethyleneglycol bis(allyl sulfonate) (**DEAS**)

Charge particle detection characteristics

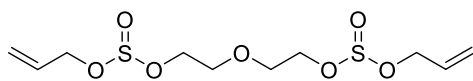
Detector - DEAS-ADC Copolymer
(**SR-86** polymer)

Alpha particle - 60 min

Fission fragment - 30 min

Sensitivity (S) - 2.38-3.1

Mandrekar et. al. 2010



2,2'-(oxybis(ethane-2,1-diyl)) bis(allyl sulfite)
OR

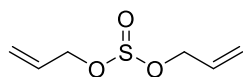
Allyl diglycol sulphite (**ADS**)

Detector - ADS-ADC Copolymer

Alpha particle - 15 min

Fission fragment - 5 min

Sensitivity (S) - N/A



Diallyl sulphite
(**DAS**)

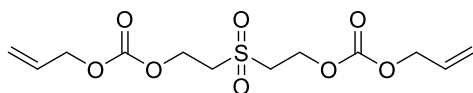
Detector - DAS-ADC Copolymer

Alpha particle - 20 min

Fission fragment - 10 min

Sensitivity (S) - N/A

Naik et al.2019



diallyl (sulfonylbis(ethane-2,1-diyl)) dicarbonate
OR

2,2'-sulfonyldiethanol bis (allyl carbonate) (**SDAC**)

Detector - SDAC-ADC Copolymer

Alpha particle - 1 min

Fission fragment - 30 sec

Sensitivity (S) - 2.75

Note: Above track development and sensitivity studies were performed in **6 N NaOH at 70°C**

Figure 3.8 Different sulfur containing allyl carbonate monomers and charge particle detection characteristics of their ADC copolymers.

In an attempt to prepare rapid and sensitive nuclear track detector, Stejny and portwood^[84] in 1986, first prepared poly(sulfone-*co*-carbonate) polymeric material by bulk co-polymerization of allyl diglycol carbonate (ADC) with liquid sulfur dioxide under UV initiation conditions. Although material could detect the alpha track in one minute with comparable radiation sensitivity as CR-39, it was found to undergo rapid depolymerization and susceptible to aqueous sodium carbonate etchant. This is due weakly held sulfone linkages in polymer network. Later in 1990, Fujii et al.^[85,87], prepared poly(sulfonate-*co*-

carbonate) polymers by co-polymerization of diethylene glycol bis (allyl sulfonate) (DEAS) with ADC using peroxide as initiator. Two compositions of ADC: DEAS namely, SR-86(10) i.e. (90:10 wt%) and SR-86(20) i.e. (80:20 wt%) were prepared, which were showing high sensitivity than CR-39. Also, as per their report due to limited solubility of DEAS (up to 20%) in ADC, they could not prepare other copolymer with higher concentration of DEAS. However, these polymeric detectors were unstable and undergo air degradation within a week's time^[86]. Reason for its short shelf life is presence of labile sulfonate linkages in polymer network.

In 2008, Mandrekar et al.^[88] at Goa university, extended the Fujii's work of developing SR-86 detectors by preparing DEAS homopolymer and several copolymers with ADC using benzoyl peroxide (BP) as initiator. All copolymers showed good track detection properties especially, ADC: DEAS (70:30 wt %) prepared using 4% IPP initiator concentration showed very high sensitivity two times higher than CR-39. DEAS homopolymer was also prepared by melt polymerization with BP. It is relatively unstable and susceptible to alkali etching condition.

Our group at Goa university also developed some poly(sulfite-carbonate)^[83] polymeric materials for detection of charge particles. This includes copolymers of allyl diglycol sulfite (ADS) and Diallyl sulfite (DAS) with ADC. Their homopolymers are soft and unstable, whereas copolymers such as ADC: DAS (80:20 wt %) and ADC: ADS (80:20 wt %) could detect alpha and fission within 20 min. Higher concentration of ADS and DAS (>20%) leads to softening and degradation of films. For both the copolymers, individual track could not be examined for diameter measurements and counting purpose due to opaque nature of polymer film. Although, this sulfur functionalized polymeric NTDs could detect nuclear track relatively quicker with excellent track sensitivity, it still suffers from air degradation over a period of one week at room temperature.

This stability issue of sulfur containing polymeric detectors was addressed by Naik and Nadkarni^[92] at Goa university with their pioneered work on developing novel poly(sulfone-carbonate) polymeric NTDs for rapid revelation of etched track by technique of chemical etching. For this purpose, they designed and synthesized novel sulfur functionalized monomer namely 2,2'-sulfonyldiethanol bis (allyl carbonate) (SDAC). Various homo and copolymers^[41] were prepared with ADC using IPP initiator. All polymers could reveal alpha tracks within 2 min with good alpha sensitivity. Among this, Poly (SDAC-co-ADC; 40:60% w/w) and PSDAC homopolymer showed very high sensitivity and improved track etching efficiency as compared to CR-39. This are the first ever sulfur

functionalized polymeric NTDs showing good optical and post etch clarity, better stability and longer shelf life at ambient temperature. Also, it is important to note that, this is the first report showing sulfur homopolymer having excellent track detection properties and longer stability. According to authors, this material has a potential ability to replace commercial CR-39 detector and expecting remarkable changes in the field of SSNTD.

3.2.4 General protocol for development of thermoset polymers as NTDs

Based on the research expertise in the area of SSNTD, our laboratory has proposed a protocol on systematic preparation of thermoset polymeric material based on allylic monomers and it's testing as nuclear track detector^[41,83,97].

Monomers with two or more allylic functionalities are chosen for the preparation of cross-linked polymers via process of free radical polymerization. Further, 3D cross-linked polymer matrix is achieved from monomer with more than two allyl functional groups. Also, considering the synthesis, purification and stability aspects, designing allylic monomers are easier as compared to vinylic once. Furthermore, if functionalities containing hetero atoms such as N, O, S, and P are introduced in between the allyl end groups, the resulting polymer material shows enhanced radiation sensitivity. Also, in order to increase the crosslink density of 3D polymer network, branched monomers could be utilized. For past more than two decades, our group has reported novel monomers and polymers containing one of the functional connectivity's like -O-CO-O-, -ONO₂ -, -N-CO-O-, O-SO-O-, -O-SO₂-, -SO₂- or materials with more than one type of functionalities within structural unit.

Following is the brief description on the protocol^[97] and the same has been extended for all the monomers and polymers cited in the thesis.

Step 1: Synthesis and initial studies on monomers/polymer:

a) *Design, syntheses and structural characterization of the monomers*

Monomers are designed based on radiation sensitive group effect, chain bridging the two functionalities and the extent of crosslinks. Various organic transformations are utilized to build the target monomers, purified and the same was characterized using NMR, IR spectroscopy and Mass spectrometry.

b) *Thermal stability of monomers*

A thermal study of the monomer is performed using TG/DTA techniques wherever required. By knowing decomposition temperature of monomer, polymerization experiments are performed at temperature lower than its decomposition temperature.

Generally, carbonate monomers are stable up to 150°C but introduction of functionalities varies its decomposition temperature. Monomer with lower decomposition temperature faces heating issues during polymerization.

c) Casting of a test polymer and its characterization

Both homo and copolymer films with ADC are prepared via free radical cast polymerization process under suitable heating profile. Resultant test polymer films are evaluated with respect to its physical properties such as appearance, softness, average thickness, percent unsaturation, and spectral properties.

d) Exposure to radiation source & etching in alkali solution

Polymer films are cut into small pieces of 1×1 cm² size and exposed to ²³⁹Pu source for alpha particles and to ²⁵²Cf source for fission fragments. The exposed and control films are then etched in 6 N NaOH at 70°C to reveal nuclear tracks. Depending on post etching results such as polymer degradation or opacity, above etching condition is varied with respect to temperature or alkali concentration.

e) Determination of bulk etch rate (V_B)

Bulk etch rate is the rate at which the surface of the test polymer film is degraded.

For plastic NTDs, the bulk etch rate per hour of the polymer should remain constant over the entire etching duration.

Step 2: Kinetics of free radical allylic polymerization

Allylic polymerization generates the exotherm which leads to defects in polymer films and loses in its bulk properties. Hence, in order to obtain thermoset polymer film with uniform surface and bulk properties and at the same time to minimize the batch variations, it is important to study polymerization kinetics.

Kinetics parameters are obtained using titrimetric method by plotting percent monomer conversion with respect to percent initiator decomposition as function of time. Further, by extending the Dial's kinetic model, a constant rate polymerization profile for a given pure allylic monomer or a mixture of allylic monomers is generated. Resulting in constant rate of exothermic heat evolution and effective polymerization process.

Step 3: Optimization of initiator concentration

Finding optimum initiator concentration is essential because it determines the amount of crosslinking in given polymer matrix, which in turn defines radiation sensitivity of plastic detector. Crosslinking density increases rapidly with increase in concentration of the initiator up to the certain maximum value and then decreases.

Following are the steps to determine optimum initiator concentration:

- (a) Casting film using varying concentration of initiator/using different types of initiators.
- (b) Exposure to ^{252}Cf source at 4 or 5 cm in vacuum and etch in suitable alkaline condition.
- (c) Finding the sensitivity (**S**) by measuring the diameters of alpha/ fission tracks.
- (d) Repeating steps (a) and (b) for all the films prepared with different initiator concentrations.
- (e) The initiator concentration where the sensitivity reaches a maximum value is the optimum initiator concentration for the given detector material.

Step 4: Optimization of etching conditions

The posts etch surface clarity of a film and its bulk etch (V_B) rate is highly influenced by varying the etchant conditions. Hence in order to achieve good track detection properties along with improved surface clarity, it is important to find optimum etching condition for given detector material.

Following are the steps to determine optimum etching condition:

- (a) Prepare enough polymer films at optimized initiator concentration and expose to fission as well as alpha source.
- (b) Exposed films are etched, keeping temperature of etchant constant but varying normality and vice versa.
- (c) Calculate V_B at every etching interval along with track appearance time.
- (d) Select that etchant condition (normality and temperature) where surface of the film remains clear with moderate V_B and a reasonable track development time.

Step 5: Determination of alpha sensitivity (S) at optimized etching conditions:

Newly prepared polymer films prepared under optimized initiator concentration where exposed to fission source under vacuum at specified height and etched in selected optimum etching condition. Observe the variation in bulk etch rate and alpha sensitivity (**S**) as a function of time to reveal optimum etching time where **S** is maximum. Use this optimized etching condition for further studies.

Step 6: Additional studies:

Following are the various spectral, thermal and nuclear studies that can be performed as per requirements. Some of them require sophisticated instrumental facility.

-
- (a) Determination of track detection efficiency, threshold energy and alpha to fission branching ratio.
 - (b) TG/DTA and XRD studies for films prepared using different initiator concentrations.
 - (c) Study of these films for neutron and gamma dosimetry.
 - (d) Effect of electrochemical etching on as prepared films.

3.2.5 Broad objective

Based on the available literature on polymeric NTDs and our experience in developing novel and sensitive polymers for SSNTD application, we aim for the following with respect to the polymers described in the earlier chapters:

- 1) To study the combined effect of increasing number of sulfone groups and chain bridging the sulfone moieties on track detection properties of newly synthesized poly(sulfone-carbonate) thermoset polymers. Also, to conduct comparative studies with previously reported Poly (SDAC-*co*-ADC) an efficient, sulfone-based polycarbonate NTDs. (For synthetic aspects on monomers and polymers reader is requested to refer Chapter 2, section **2.4.2I** and **2.4.2II**).
- 2) To study combine effect of increasing carbamate functionality and polymeric crosslinking on track detection properties of newly developed poly (EGBDC-*co*-ADC) thermoset co-polymer based on [G-0.5]-bis diallyl carbamate octa-functional dendritic monomer. Also, to conduct comparative studies with previously reported poly (NADAC-*co*-ADC) carbamate containing polycarbonate thermoset NTDs.

3.3 Experimental

3.3.1 Instrumental methods

1) Digital thickness gauge

The thickness of the polymer films was measured using Elcometer 456 F Model S DFT electronic thickness gauge (Made in GB), having a range of 0-1500 μm and least count of 1 μm .

2) Optical microscope

The etch tracks were analyzed using Optical microscope, Axiostar-1122-100, Carl Zeiss, Germany with optical magnifications of 5x, 10x, 40x and 100x. Photomicrographs were recorded using Tucsen ISH500 camera pre-fitted to microscope and track diameter measurements were carried out with Tucsen- IS capture software.

3.3.2 Irradiation methods

Various methods and metallic assemblies used to perform irradiation of newly prepared polymer films are given below.

1) Alpha and fission track revelation at 2π and 4π geometry

Low energy alpha tracks were recorded in polymer films by irradiating film with ^{239}Pu alpha source at various distances, whereas fission fragments were recorded by exposing polymer film to ^{252}Cf fission source at 2mm distance.

The exposure assembly consist of three parts as shown in figure below:

- a) **Source:** To place radioactive source emitting charge particles in upright direction.
- b) **Exposure distance adjuster:** To vary the film exposure distance as per requirement.
- c) **Sample holder:** To place polymer film undisturbed towards vertical approaching radiations.

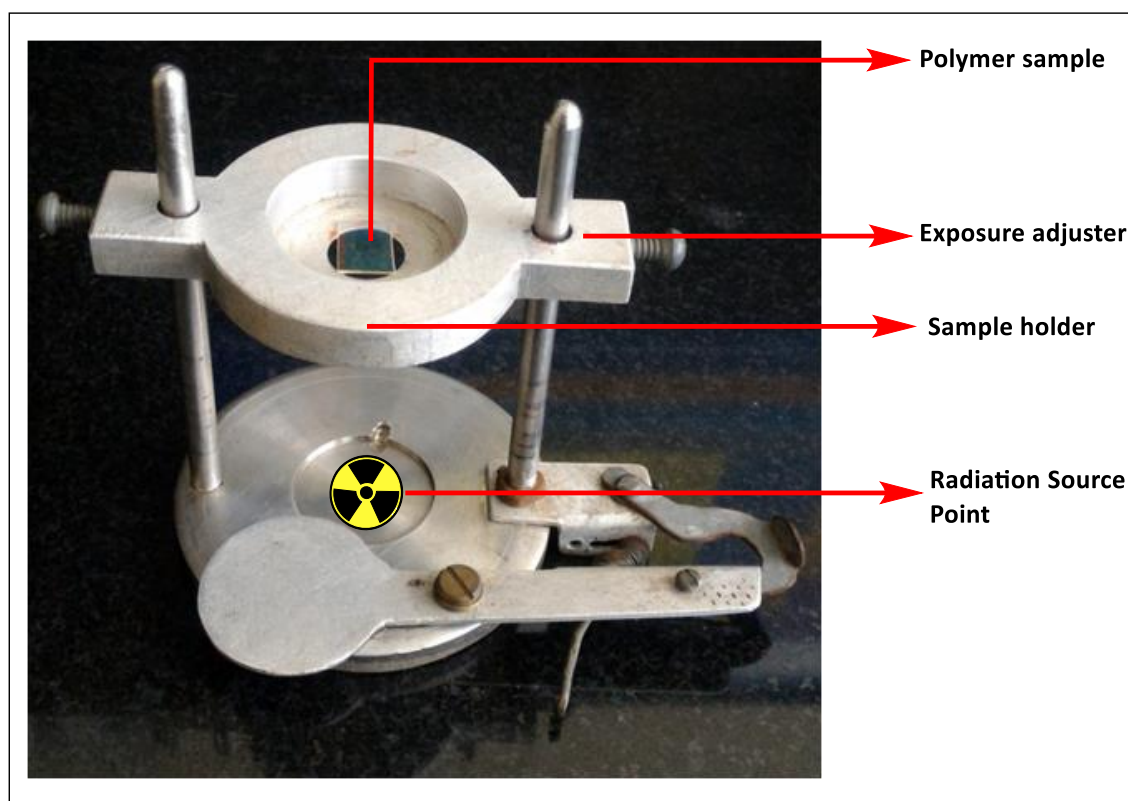


Figure 3.9 Exposure assembly to record alpha and fission tracks.

2) Sensitivity (S) study under normal incidence condition

This particular method is valid for a polymeric detector which can detect alpha as well as fission fragments. Here, polymer films are exposed to ^{252}Cf source at certain distance (3 cm or 5 cm) under highly reduced pressure of 0.5 mbar for 12-24 h. After exposure film were etched and track etching sensitivity (S) was determined by measuring change in alpha and fission diameter at regular time interval under optical microscope. Sensitivity was calculated using equation below.

$$S = V = \frac{V_T}{V_B} = \frac{1 + x^2}{1 - x^2} \quad \text{where,} \quad x = \frac{D^\alpha}{D^\beta} \quad (3.5)$$

A typical setup consists of hemispherical aluminum frame having an arrangement for placing radiation source and polymer film at distance of 3 to 5 cm. The exposure assembly is kept in a vacuum desiccator to generate high reduced pressure of 0.5 mbar. The complete setup I shown in figure below.

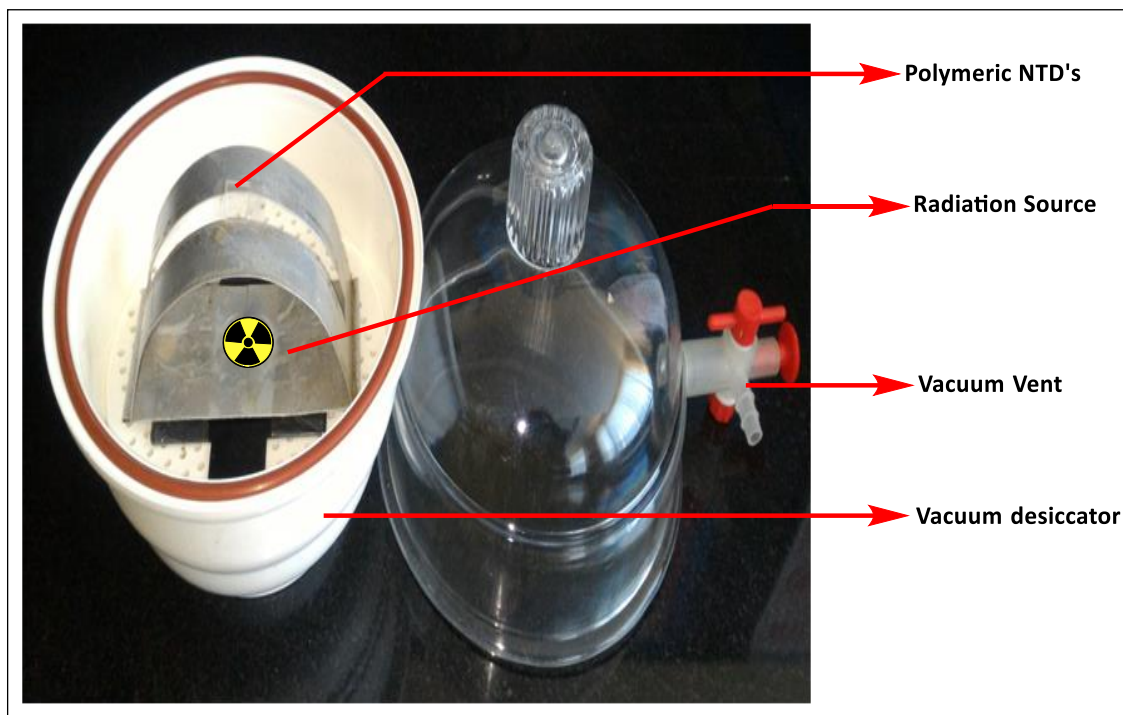


Figure 3.10 Exposure setup to conduct alpha sensitivity study.

3.3.3 Chemical etching method

Chemical etching method has been used to etch the irradiated polymer films. This etching process was conducted in chemical etching glass bath as shown in figure. A typical glass assembly containing alkali etchant (aq. NaOH solution), stainless steel holder and magnetic stirring bar is used. The temperature of the etchant is varied by hot water jacket externally designed to the glass assembly. This jacket is connected to temperature control external water circulator. Once the internal etching temperature is attained, steel holder containing polymer samples was dipped into etchant. The etchant is stirred with the help of external magnetic stirrer.

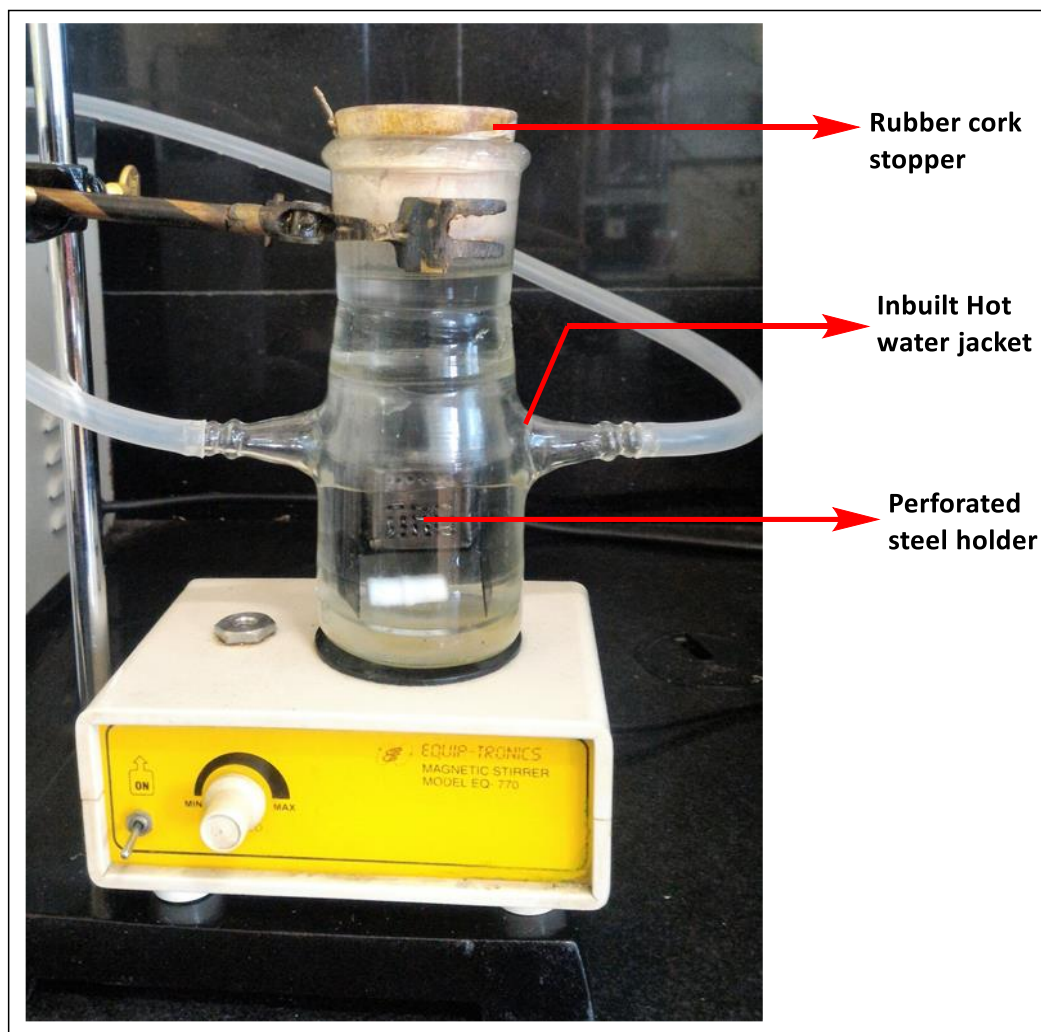


Figure 3.11 Glass assembly for chemical etching of polymeric detector samples.

3.3.4 Etched track counting method

In a typical track density measuring experiment, irradiated and chemically etched polymer detectors were washed thoroughly with tap water and dried under an IR lamp. The dry films are mounted on glass slide and placed on the microscope stage. The polymer film was focused manually under optical microscope to observe etch tracks at required magnification (40x, 10x and 5x). The tracks per view were counted manually for approx. 100-120 view with the help of X-Y scale. The area of the view for the given magnification was determined using the stage micrometer and the track density (tracks /cm²) was calculated using formula given below

$$\text{Track density} = \frac{\text{Total no. of tracks counted}}{(\text{Total no. of view} \times \text{Area of the view})} \text{ per cm}^2 \quad (3.11)$$

3.4 Result and discussion

3.4.1 Investigating newly synthesized poly(disulfonyl-carbonate) thermoset polymers for SSNTD applications

Recent, remarkable finding in our group on poly(sulfone-carbonate) rapid PNTDs, inspired us to further improvise and develop two new class of sulfonyl-carbonate polymeric materials for SSNTD application. Each monomeric unit consist of di-sulfonyl functionalities bridged by diethylene glycol and ether linkages shown in **Figure 3.12**. Following our protocol (refer 3.3.1), we have already described synthesis, purification, polymerization technique and kinetic studies in chapter 2. In this chapter, we will focus on optimizing this polymeric material for charge particle dosimetry and investigating their track recording and etching properties.

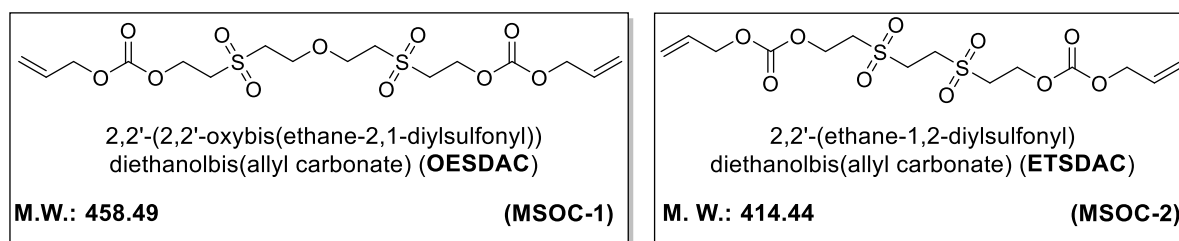


Figure 3.12 Molecular structures of bis-sulfone functionalized allyl carbonate monomers.

I. Track detection characteristics and chemical etching parameters of newly designed test polymeric track detectors

The objective behind the preparation of test polymers is to know whether it is suitable to be used as track detector as such or require some modifications. All this test polymers of a designed monomers were prepared by technique of radical cast polymerization and were examined for their physical properties (refer chapter 2; section **2.4.2II.i**)

Further, these polymer films were cut into small squares of 1 x1 cm² size, exposed to ²³⁹Pu source for alpha particle detection and to ²⁵²Cf for fission fragments in close contact to the source. For determination of alpha sensitivity (S) of test detectors at given track development time, films were exposed to ²⁵²Cf at 3 cm height from the radiation source for 24 h under vacuum followed by chemical etching and measurement of alpha and fission etch track diameter. All irradiated polymeric films were etched in 6 N NaOH at 70°C (standard etching condition for polycarbonate NTDs) and analyzed under optical microscope. **Table 3.6** summarizes, track recording characteristics and chemical etching parameters for all test polymers.

Table 3.6 Track recording properties and chemical etching parameters for different sulfonyl-carbonate test polymers.

Sr. No.	Polymer composition (w/w)	Time to reveal developed tracks (seconds) in 6 N NaOH at 70°C		Sensitivity (S) ^c	Bulk etch rate V _B (μ/min.) ^d	Post etch polymer surface
		Alpha ^a	Fission ^b			
		particle	fragment			
1	6:4 OESDAC:ADC	15	6	1.78	24.25	hazy & hard
2	1:1 OESDAC:ADC	25	12	2.12	22.30	hazy & hard
3	4:6 OESDAC:ADC	30	12	1.93	21.15	slight hazy & hard
4	3:7 OESDAC:ADC	50	25	1.77	9.97	clear & hard
5	1:9 ETSDAC:ADC	10 min	4 min	1.59	0.32	clear & hard
6	PSDAC homo polymer	30	10	1.61	29.34	clear & hard
7	4:6 SDAC:ADC	50	30	1.73	9.52	clear & hard
8	PADC Indigenous	180 min	60 min	1.24	1.15 μm/h	clear & hard

^a film exposed to ²³⁹Pu source at 1 mm for 2 minutes; ^b films exposed to ²⁵²Cf source at 1 mm for 8 h; ^c films exposed to ²⁵²Cf source at height of 4 mm for 24 hours; ^d bulk etch rates were determined using weight loss method.

All the poly (OESDAC-*co*-ADC) co-polymer test films could reveal alpha as well as fission tracks within 2 min with clear post etch surface. Since POESDAC homopolymer was obtained as soft, flexible and brown film, it was not suitable as track detector. Bulk etch rates of co-polymers with higher concentration of OESDAC monomer (>40% w/w) are similar to PSDAC homopolymer and nearly two times higher than as reported for poly (SDAC-*co*-ADC) copolymers^[92]. Also, post etch surface turns hazy after 1 min of etching. On the other

hand, lower concentration of OESDAC monomer (<40% w/w) had low bulk etch rate and clear post etch surface.

In the case of poly (ETSDAC-*co*-ADC) co-polymers, as mention earlier in chapter 2, due to the lesser solubility of ETSDAC monomer in ADC, we were not able to prepare its high concentration copolymer. Also, solid nature of this monomer with m. p. 90-92°C, limited us in obtaining its homopolymer. Poly (ETSDAC-*co*-ADC; 0.5:9.5% w/w) copolymer could reveal tracks much quicker than PADC with low bulk etch rate and clear post etch surface clarity.

Preliminary sensitivity studies showed that all disulfone based copolymers had high sensitivity as compared to PADC detector. Particularly, monomer composition 1:1 and 4:6 of poly (OESDAC-*co*-ADC) copolymer showed sensitivity value nearly 2 times higher than PADC. Further, this value of alpha sensitivity can be increased by optimization of polymerization, initiator and etching conditions.

From the initial track detection studies, it was clear that, poly (ETSDAC-*co*-ADC) polymeric films could detect the nuclear track much quicker than poly (SDAC-*co*-ADC) with relatively higher bulk etch rates and loss of post etch surface clarity. Hence, in order to fix this issue and to identify the best performing detector composition in this series, we performed various optimization protocols as cited further in this chapter. Optimization with respect to polymerization conditions is performed by kinetics study described in chapter 2, section 2.4.2IV.

II. Optimization of initiator concentration as a function of sensitivity (S)

It is well known that performance of polycarbonate thermoset resin (e.g., CR-39) as NTD is highly influence by the curing conditions such as temperature and initiator concentration^[96]. As these conditions are mainly responsible for governing structure of polymer matrix through its density of cross-linking and hence enhances the radiation sensitivity (S) of given thermoset polymer.

For a given polycarbonate NTD^[83], radiation sensitivity increases with the concentration of initiator. At a certain concentration is attains the maximum value and then decreases further with increasing initiator concentration. Also, the bulk etch rate decreases accordingly to a minimum and then increases as the concentration increases further. Sensitivity is low at high initiator concentration probably due to poor 3D crosslinking network. Hence, it is essential to understand the optimum concentration of initiator, which can be determined as function of (S). For this purpose, series of polymer films were prepared

with increasing concentration of initiator and subjected to sensitivity analysis under common etching conditions. Initiator concentration where sensitivity is maximum is considered as optimum condition.

Here, for initiator optimization study we chose (OESDAC: ADC; 1:1 w/w) copolymer composition due to its high sensitivity as indicated in test polymer series. Further, we prepared series of poly (OESDAC-co-ADC; 1:1% w/w) copolymer films with 2, 3, 4, 5, 6% w/w IPP initiator concentration and 0.5% DOP as plasticizer. For every initiator concentration separate heating profile was generated using previously generated kinetic constant and was utilized in the film preparation. The obtained physical properties of the copolymer films are noted in **Table 3.7**.

Table 3.7 Physical and track detection properties of OESDAC: ADC 1:1 w/w copolymers prepared using different IPP initiator concentration.

Sr. No.	IPP concentration (%)	Avg. thickness (μm)	Hardness and Optical clarity	Percent unsaturation	Charge particle detection ^{a,b}
1	2	495.3 \pm 10	Hard and transparent	8.64	Alpha and fission
2	3	601.8 \pm 10	Hard and transparent	6.37	Alpha and fission
3	4	541.1 \pm 10	Hard and transparent	6.12	Alpha and fission
4	5	495.9 \pm 10	Hard and transparent	4.29	Alpha and fission
5	6	600 \pm 10	Hard and transparent	3.95	Alpha and fission

^a films exposed to ²³⁹Pu source at 1 mm for 2 minutes; ^b films exposed to ²⁵²Cf source at 1 mm for 8 h

The polymers prepared using 2 - 6 % w/w initiator concentrations are hard, transparent and are suitable as track detectors. Unsaturation analyses indicated that at higher initiator concentration extent of polymerization is nearly 96 %. All above copolymers showed good physical properties, hence were further subjected to sensitivity studies.

i. Determination of maximum sensitivity by examining variation in fission and alpha etch-track diameters (D_α and D_β) at given etching conditions

For this purpose, the acquired polymer films were cut into the small pieces of 1 x 1 cm² size and were exposed to ²⁵²Cf fission source at a distance of 3 cm under high vacuum conditions. Subsequent chemical etching of latent tracks was performed in mild alkali condition i.e., 3 N NaOH at 60°C, which is the optimized etching condition reported for SDAC homo and copolymer^[92]. Another reason for selecting such mild condition is the higher etch rates in concentrated alkali conditions i.e., 6 N NaOH at 70 °C followed by reduction in post etch clarity as noted in test polymer studies.

Further, sensitivity (S) values and bulk etch rates were calculated at regular time intervals by measuring the alpha and fission track diameters. Based on this values, sensitivity maximum (S_{max}) was revealed for co-polymers under this study. The initiator concentration with high value of S_{max} is considered as optimum initiator concentration for polymer.

The variation of alpha and fission track diameters in the series of polymers prepared using different initiator concentrations is graphically presented in the **Figure 3.13** and **Figure 3.14** respectively. Here, etched-track diameters and sensitivity were measured after every one minute of chemical etching. From the **Figure 3.13** and **Figure 3.14** it is observed that there is linear increase in alpha as well as fission track diameter with etching time indicating uniformity in polymer structure.

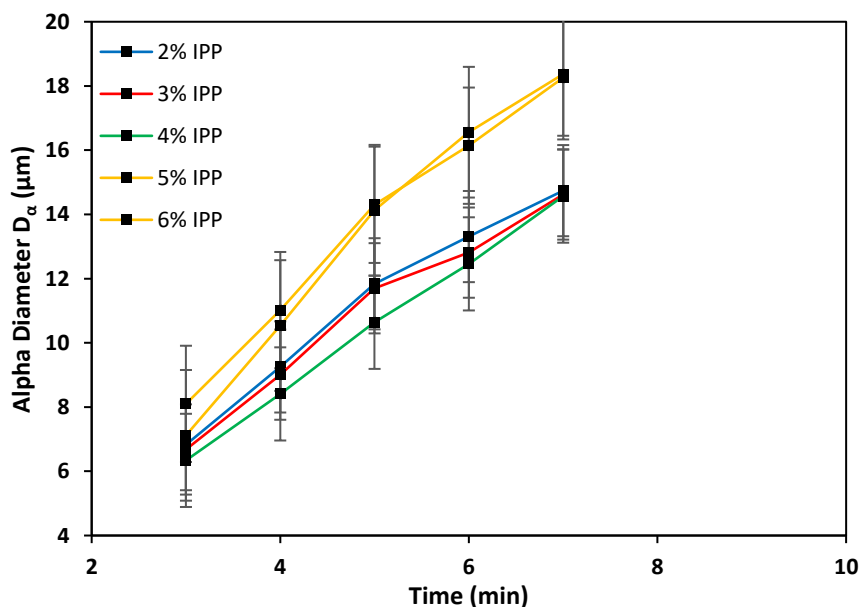


Figure 3.13 Variation of alpha track diameter in Poly (OESDAC-co-ADC; 1:1 w/w) copolymers prepared using different initiator concentration.

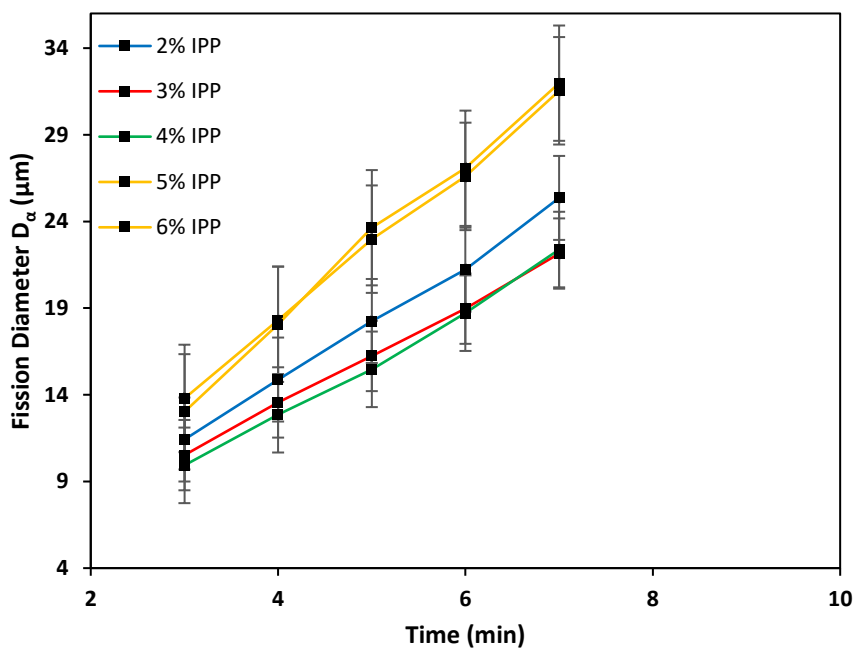


Figure 3.14 Variation of fission track diameter in Poly (OESDAC-co-ADC; 1:1 w/w) copolymers prepared using different initiator concentration.

Using the above variation of the track diameters, values of alpha sensitivities (S) were calculated at regular time intervals for given series of polymers prepared with different initiator concentration as shown in **Figure 3.15**.

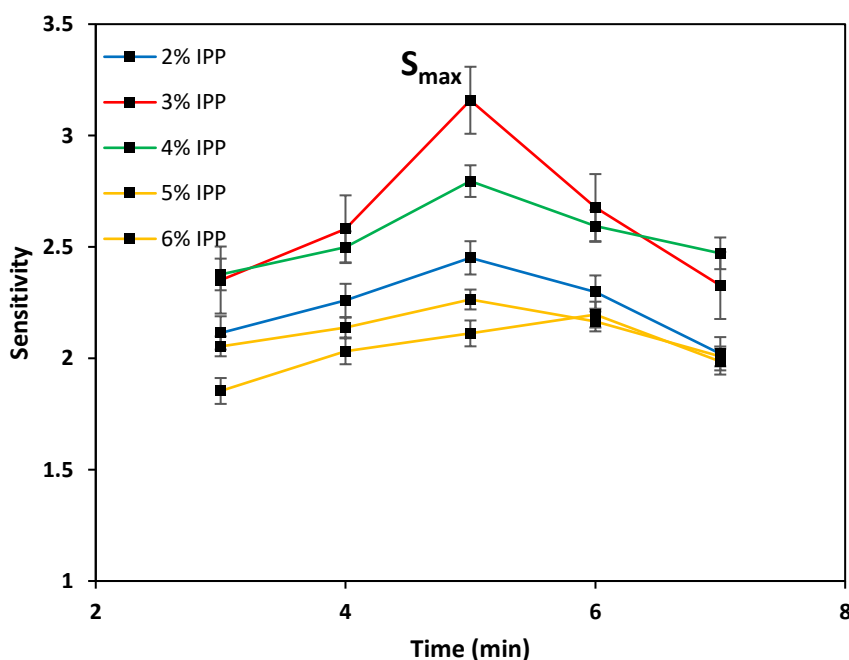


Figure 3.15 Variation of alpha sensitivity in polymers at different initiator concentration.

A notable variation was observed in the values of sensitivity for given set of polymers prepared using different initiator concentration. Polymers films with 3% and 4% w/w IPP concentration showed high values of sensitivity whereas films with 2%, 5% and 6% w/w IPP had a low sensitivity value. Among all, polymer film with 3% IPP initiator concentration showed a highest sensitivity value with $S_{\max} = 3.16$ and was the most sensitive copolymer (**Figure 3.15**). All copolymer films showed sensitivity maximum at 5 min except for 6% w/w polymer.

Also, it was observed that, sensitivity decreases after 7 min of chemical etching in 3 N NaOH at 60°C. This could be attributed to increasing bulk etch rate values. Bulk etch rates (V_B) were calculated at regular time interval using fission track diameter (**Figure 3.16**) as well as weight loss method (**Figure 3.17**).

Post etched surface of all films was clear till 15 minutes, but after etching for 15-20 minutes, films turn dense hazy in appearance and becomes relatively softer.

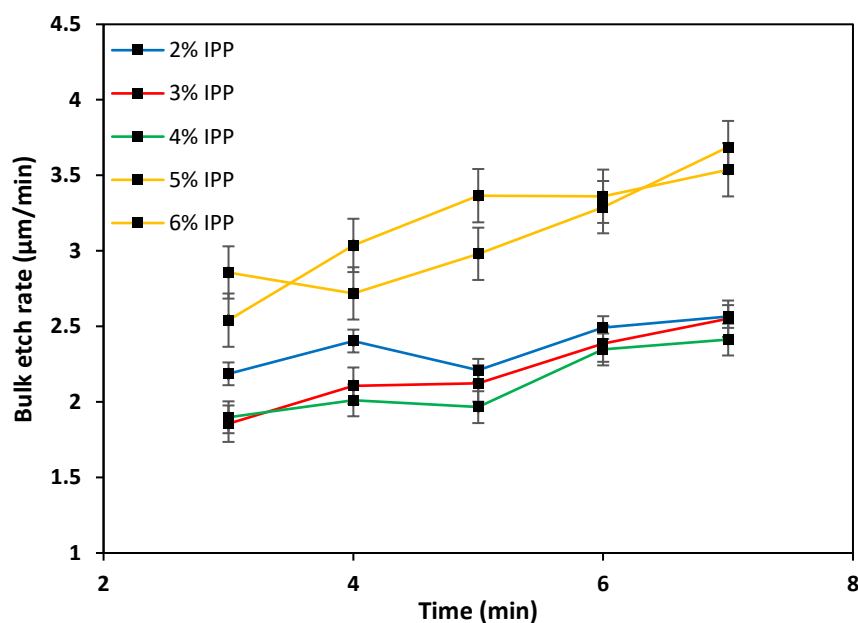


Figure 3.16 Variation of bulk etch rates in Poly (OESDAC-co-ADC; 1:1 w/w) polymers at different initiator concentration calculated using weight loss method.

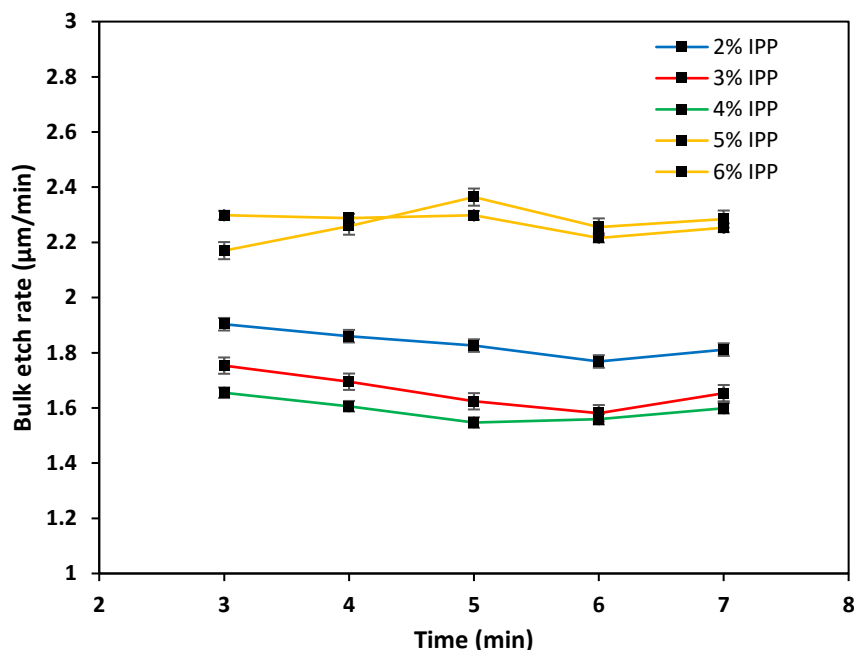


Figure 3.17 Variation of bulk etch rates in Poly (OESDAC-co-ADC; 1:1 w/w) polymers at different initiator concentration calculated using fission track diameter method.

III. Optimization of OESDAC-ADC copolymer concentration

From the initiator optimization studies it was clear that OESDAC copolymers with ADC are highly sensitive detectors owing to its rapid charge particle track detection with high etching sensitivity and moderate etching rates in 3 N NaOH at 60°C. Also, it is well known fact that, copolymers of ADC are more sensitive^[64,95] as compared to their respective homopolymers. This is due to introduction of radiation sensitive ethylene glycol link and more carbonate groups in polymer matrix along with increasing cross link density.

Since we have already obtained an excellent radiation sensitivity for (OESDAC: ADC, 1:1) copolymer composition with $S_{max}=3.16$, this particular study was conducted to identify another best performing detector composition prepared using optimized initiator and polymerization conditions. For this purpose, series of OESDAC copolymers with ADC were prepared in different w/w ratio's such as OESDAC: ADC w/w =1:9, 2:8, 3:7, 4:6, 6:4, 7:3 and 8:2 using 3 to 3.3% w/w IPP concentration (optimized conditions) and 0.5% w/w DOP as plasticizer. For a monomer concentration with OESDAC $\geq 30\%$ w/w, a newly developed OESDAC-ADC, 12 h polymerization profile was utilized whereas for high concentration of ADC i.e., $\geq 80\%$ w/w, polymerization was conducted using previously derived ADC heating profile. For comparison purpose, poly (SDAC-co-ADC;4:6 w/w) and PSDAC polymer were freshly prepare using their respective reported polymerization

profiles. Prepared polymer films were analysed for physical properties and residual unsaturation was estimated in polymer matrix as noted in **Table 3.8**.

Table 3.8 Physical properties and unsaturation analysis of OESDAC-ADC copolymers.

Sr. No.	Polymer composition OESDAC: ADC (w/w)	Thickness of Sample film (μm) ^a	% Residual Unsaturation in polymers ^b	% Polymerization
1	1:9	564.3 \pm 10	5.68	94.32
2	2:8	487 \pm 10	5.35	94.65
3	3:7	522.1 \pm 10	6.47	93.53
4	4:6	555 \pm 10	6.44	93.56
5	1:1	614.7 \pm 10	6.21	93.79
6	6:4	535.3 \pm 10	7.63	92.37
7	7:3	589.9 \pm 10	6:56	93.44
8	8:2	521.4 \pm 10	8.11	91.89
9	9:1	488.1 \pm 10	7.31	92.69
10	SDAC: ADC, 4:6	602 \pm 10	5.41	94.59
11	PSDAC	584.4 \pm 10	6.56	93.44

^a film thickness was calculated using ELCOMETER thickness gauge; ^b unsaturation analysis was performed using Wij's method.

All freshly prepared polymeric films were intact, optically transparent and hard except (OESDAC: ADC, 9:1) which was pale brown and soft. Further, in a search of radiation sensitive copolymer composition (except 1:1), we performed a track revelation and sensitivity study to find out S_{max} for each polymer. Track etching was carried out in 3 N NaOH at 60°C. Resultant track detection parameters were compared with poly (SDAC-co-ADC; 4:6 w/w) and PSDAC as noted in **Table 3.9**.

From the data it can be seen that, time to observe developed track decreases as the concentration of OESDAC monomer increases and the corresponding bulk etch rates increases rapidly. For OESDAC concentration $\geq 50\%$ w/w, track could be revealed in a time scale of seconds. Post etch surface appearance for most of the polymers is clear and hard except for OESDAC: ADC w/w ratios from 7:3 to 9:1.

Table 3.9 Track development time, sensitivity and chemical etching parameters for different Poly (sulfone-carbonate) polymers.

Sr. No.	Polymer composition	Time to observe developed tracks (minutes)		Sensitivity maximum (S_{max}) ^c	Bulk etch rate V_B ($\mu/min.$) ^e	Post etch polymer surface
		Alpha ^a	Fission ^b			
		particle	fragment			
1	OESDAC: ADC (w/w) 1:9	20	10	1.37	0.21	clear & hard
2	2:8	12	5	1.41	0.58	clear & hard
3	3:7	8	3	1.85	0.93	clear & hard
4	4:6	3	1	2.78	1.64	clear & hard
5	1:1	90 sec	40 sec	3.12 ^d	2.89	clear & hard
6	6:4	60 sec	30 sec	2.24	4.67	clear & hard
7	7:3	30 sec	15 sec	1.78	8.51	hazy & hard
8	8:2	20 sec	15 sec	1.72	10.11	hazy & hard
9	9:1	20 sec	10 sec	1.55	12.76	hazy & soft
10	SDAC: ADC, 4:6	10	7	2.23	1.12	clear & hard
11	PSDAC	8	5	1.84	7.37	clear & hard

^a film exposed to ²³⁹Pu source at 1 mm for 2 minutes; ^b films exposed to ²⁵²Cf source at 1 mm for 8 h; ^c films exposed to ²⁵²Cf source at height of 3 cm under 2 mm of Hg vacuum for 24 hours; ^d S_{max} bulk etch rate is calculated using weight loss method; ^e S_{max} was recorded for new batch of polymer.

The sensitivity values of the polymeric films were measured based on variation of alpha and fission track diameters shown in **Figure 3.18** and **Figure 3.19**. Here, alpha as well as fission track growth rate was linear and rapidly increases as concentration of OESDAC increases. Similar trend was observed for bulk etch rate. Variation in bulk etch rate was calculated using fission diameter method as presented graphically in **Figure 3.20**. From the results it is quite clear that the increase in the OESDAC concentration increases the bulk etch rate as well as the track etch rate of the detector. This is due to increasing number of radiation sensitive sulfonyl groups in polymer matrix, which upon ionization rapidly undergo hydrolysis in alkaline etching condition. Also, for copolymers with OESDAC concentration $\geq 70\%$, post etch surfaces were foggy in appearance.

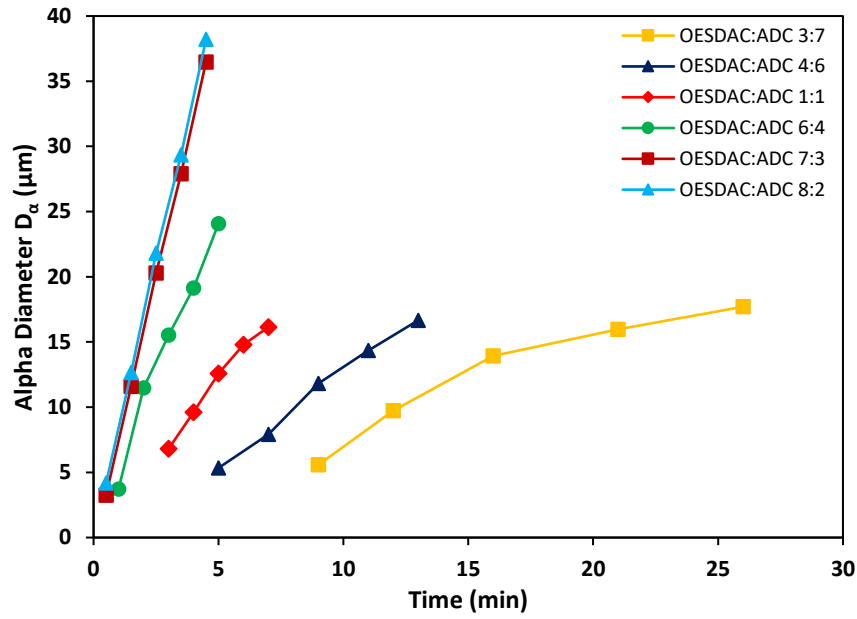


Figure 3.18 Variation in alpha diameter for OESDAC: ADC copolymers.

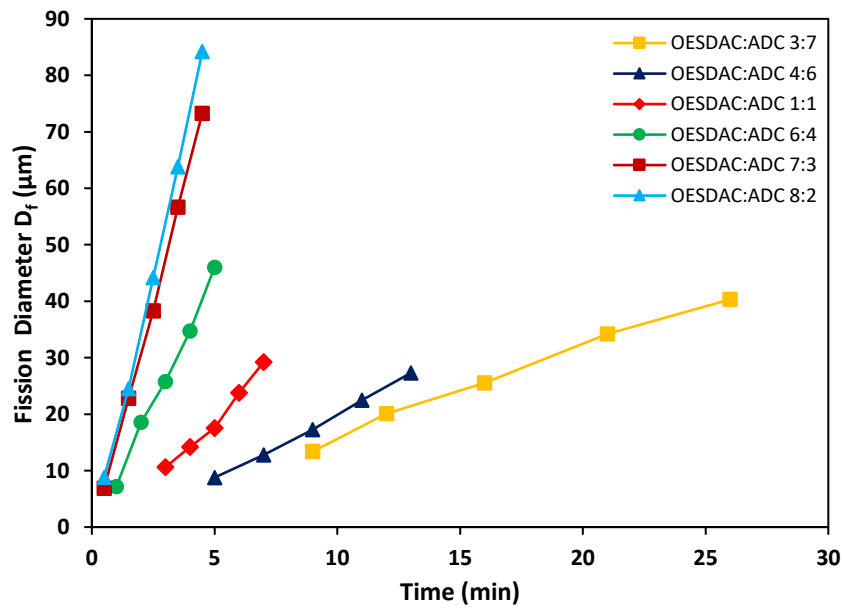


Figure 3.19 Variation in fission diameter for OESDAC: DAC copolymers.

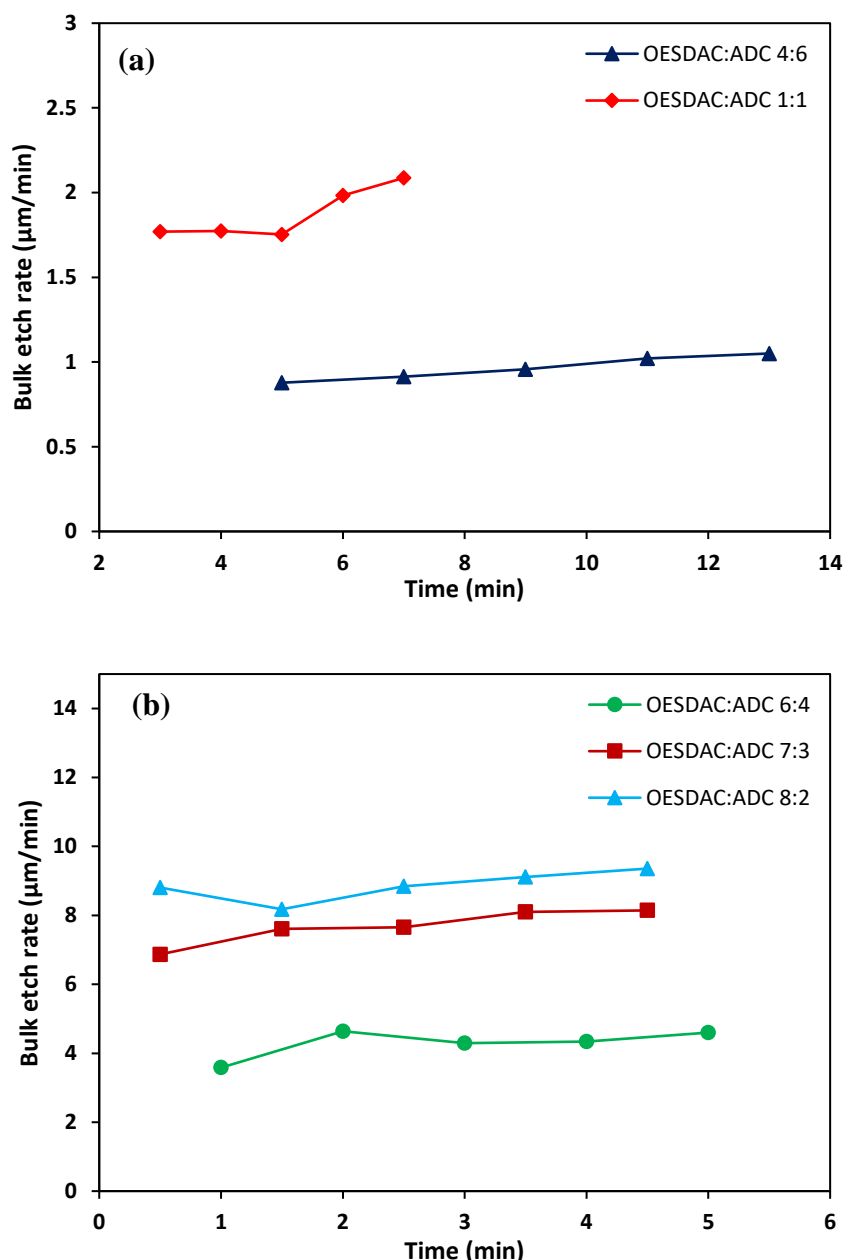


Figure 3.20 Variation in bulk etch rate calculated using fission diameter method for OESDAC: ADC w/w ratios from (a) 4:6 and 1:1; (b) 6:4, 7:3, and 8:2 copolymers.

Sensitivity studies revealed that, all OESDAC: ADC copolymers has higher S_{max} values as compared to those reported for SDAC: ADC copolymers^[92]. For OESDAC: ADC copolymers with w/w ratios from 3:7 to 6:4, showed high S_{max} values close to 2. This value decreases as the concentration of OESDAC increases. This was mainly due to rapid increase in the bulk etch rate values. Among all, poly (OESDAC-co-ADC) with 1:1 and 4:6 w/w ratio had maximum sensitivity in a series. Hence, we considered this monomer composition as optimum and were further optimized for etchant concentration.

IV. Optimization of Etching conditions for polymeric NTDs

We have already observed from the above track detection and optimization studies that alkali concentration affects the etching rates and post etch surface of the given polymer NTDs. Hence, it is essential to optimize the given track detector with respect to chemical etching condition. Following are the detector parameters which are highly affected by etching conditions:

- 1) **Track etch ratio** (V_T/V_B) or **Sensitivity**: It is one of the characteristic properties of any NTD material. Also, we have previously understood that track development in any NTDs is governed by condition $V_T/V_B > 1$. Any change in etching conditions highly affect the etching rates and sensitivity of material. Hence, it is necessary to follow the bulk as well as track etch rates.
- 2) **Track development/ revelation time**: It is one of the important quantities that measures the track development process and helps differentiating between tracks and background track like features. Hence along with type of detector material, etching condition equally contributes in altering the track development time. Now a days quick track detection analysis is need of the hour.
- 3) **Post etch surface**: It is a surface characteristic of the detector films. Etching conditions has great impact on post etch surface clarity. Elevated temperatures and concentrated alkali conditions sometimes lead to loss of surface clarity and more opaqueness. Hence, it is important to maintain the post etch clarity in order to carry out the track analysis under optical microscope.

For polymeric NTDs most commonly employed etchants are aqueous solutions of KOH and NaOH. It is also established that they do not show much difference in etching process^[98]. Hence, optimization study can be performed using one of the etchants. In this particular optimization studies, protocol such as varying temperature at a constant etchant concentration and vice versa are followed in order to monitor etch rates, track development time, post etch surface and sensitivity of polymer under observation. The bulk etch rate, post etched surface appearance and track development time will determine the optimum etching condition for given polymer. In other words, the post etch surface of the detector should be clear with a moderate bulk etch rate and track development time.

i. Optimization of etching conditions for poly (OESDAC-co-ADC) co-polymeric films

We performed here optimization studies on copolymer compositions: **poly (OESDAC-co-ADC, 1:1 w/w)** and **poly (OESDAC-co-ADC, 4:6 w/w)**, due to their high alpha sensitivities observed in initiator optimization studies under etching condition of 3 N NaOH at 60°C (optimized etching condition reported for PSDAC polymers). Although this etching condition showed very good result as compared to stringent condition i.e., 6 N NaOH at 60°C, we still performed optimization studies at much milder conditions in order to understand effect of slow etching rate on track development time, post etch surface clarity and sensitivity.

For this purpose, three pieces of films of size 1 x 1 cm² for each copolymer composition were taken and exposed to ²⁵²Cf source for fission fragments and alpha particles under close contact i.e., 1mm. This were etched at three different set of temperature i.e., 40°C, 50°C and 60°C with varying initiator concentration from 0.5 N to 3 N NaOH. Later, track development time, bulk etch rates and sensitivity at optimized condition was compared with PSDAC polymers. The results on track development time and post etch surface appearance under different etching conditions are noted in **Table 3.10** and **Table 3.11**.

Table 3.10 Time required for alpha and fission track development in the Poly (OESDAC-co-ADC; 1:1 w/w) films by increasing temperature and concentration of etchant medium.

Sr. No.	Normality of NaOH (N)	Temperature °C	Time (min) to observe developed ^a		Observations and Remark on post etch surface appearance
			Fission fragments	Alpha tracks	
1	0.5	40	80	160	Clear and transparent
		50	30	70	Clear and slight hazy
		60	10	20	Film turns hazy after 60 min
2	1	40	30	60	Film turns hazy after 120 min
		50	10	20	Hazy film after 60 min and whitish at 125 min
		60	5	10	White film after 40 min

3	1.5	40	25	50	Film turns hazy at 60 min and white after 120 min
		50	7	10	Hazy film after 20 min and white at 55 min
		60	3	5	White film after 20 min
4	2	40	15	30	Film turns hazy after 70 min of etching
		50	5	8	Film turns dense hazy after 25 min
		60	2	5	Film turned opaque white at 15 min
5	2.5	40	10	20	Foggy film after 60 min
		50	4	6	Whitish film after 30 min of etching
		60	1	3	Film turns white at 7 min
6	3	40	8	20	Foggy film after 50 min
		50	2	5	White film after 20 min
		60	1	2	Film turned hazy after 10 min and opaque white after 15 min

^afilms exposed to ²⁵²Cf source for fission tracks at 1 mm for 12 hours.

Table 3.11 Time required for alpha and fission track development in the Poly (OESDAC-co-ADC; 4:6 w/w) films by increasing temperature and concentration of etchant medium.

Sr. No.	Normality of NaOH (N)	Temperature °C	Time (min) required to observe developed		Observations and Remark on post etch surface appearance
			Fission fragments ^b	Alpha tracks ^a	
1	0.5	40	100	220	Clear and transparent
		50	50	110	Clear and slight hazy
		60	20	50	Film turns hazy after 70 min

2	1	40	50	110	Film turns hazy after 130 min
		50	15	30	Hazy film after 100 min
		60	7	15	Hazy film after 40 min
3	1.5	40	20	65	Film turns hazy at after 100 min
		50	10	20	Hazy film after 30 min and whitish at 110 min
		60	4	9	White film after 25 min
4	2	40	30	50	Film turns hazy after 80 min of etching
		50	8	15	Film turns hazy after 25 min
		60	3	6	Film turned whitish after 20 min
5	2.5	40	20	40	Foggy film after 80 min
		50	5	10	Film turns hazy after 25 min of etching
		60	2	4	Film turn white at 12 min
6	3	40	15	25	Foggy film after 50 min
		50	5	10	White film after 30 min
		60	3	6	Film turned hazy after 15 min and white after 25 min

^afilms exposed to ²³⁹Pu source for alpha tracks at 1 mm for 5 minutes.

^bfilms exposed to ²⁵²Cf source for fission tracks at 1 mm for 8 hours.

From the results it is noted that track development time and loss in post etch surface clarity was delayed by utilizing milder etching conditions. Post etched surface for both copolymers were clear at the time of observation of tracks when they were etched in 0.5 N–3 N NaOH at 40–60°C temperature. At 40°C with alkali concentration less than 2 N, the etching process is very sluggish showing the longer track development time (1 h to 5 h) whereas at high temperature i.e., at 60°C etching process was quickest with much short track development

time (2-20 min). Also, loss of post surface clarity is delayed to period of hours at low temperature whereas for high temperature this loss is observed in few minutes. Further, it is important to note here that, polymer film becomes softer, when it is etched to opaqueness at 60°C for an alkali concentration greater than 1 N. In case of 50°C temperature condition, overall track etching process is intermediate between 40 and 60°C. Track development time was within 30 min except for 0.5 N NaOH etchant and also loss in post etch clarity is delayed to 30-60 min. Another important factor to optimize the etching condition is the bulk etch rate of the polymer. Thus, we studied the variation in the bulk etch rate for poly (OESDAC-co-ADC) copolymer detectors with respect to track development time and etchant concentration. Here in the studies the bulk etch rate for the polymers was determined using the weight loss method.

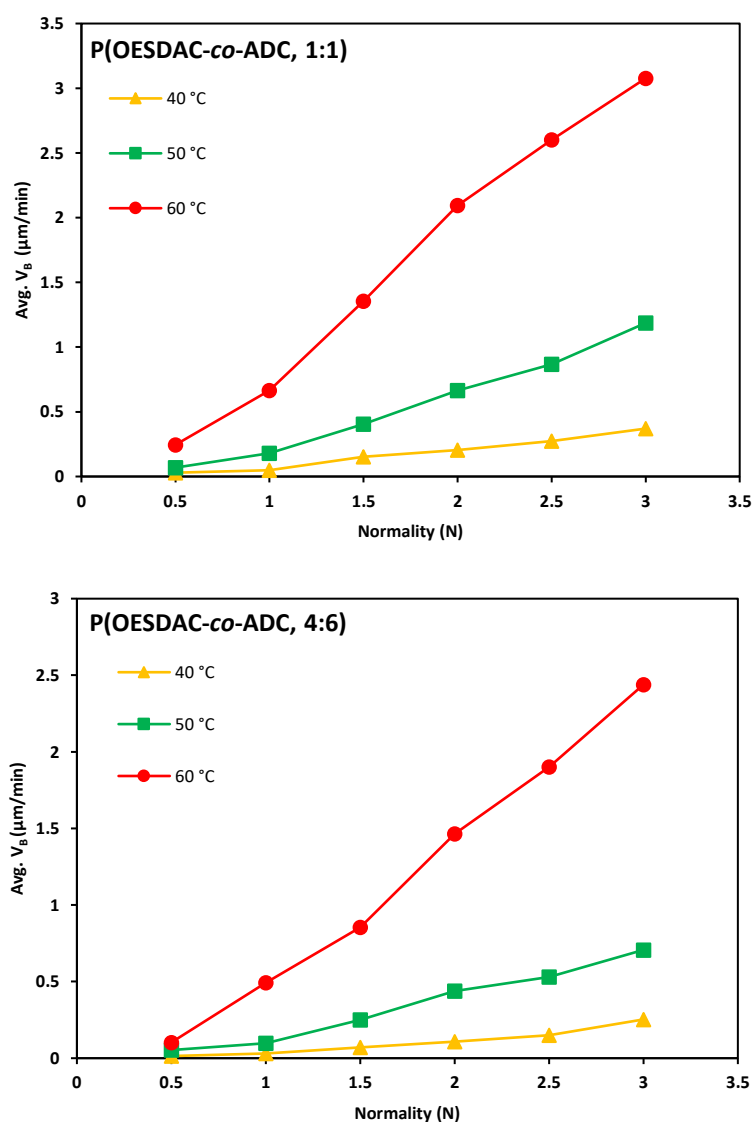


Figure 3.21 The variation of bulk etch rate in poly (OESDAC-co-ADC) copolymer detectors with increasing etchant concentration at constant temperature.

From the **Figure 3.21** one can observe that bulk etch rate at high temperature i.e., at 60°C increases rapidly as compare to other temperature conditions. This was the reason why the loss in post etch clarity observed at lesser time and also polymer films become softer. Bulk etch rate for etching condition at 40°C is relatively very low (<0.5 $\mu\text{m}/\text{min}$) while at 50°C it is moderate from 0.5 to 1.14 $\mu\text{m}/\text{min}$).

Thus, examining the overall etching process, we considered alkali etching condition at 50°C. For Poly (OESDAC-*co*-ADC; 1:1w/w) detector, we chose 1N NaOH at 50°C as an optimized etching condition while for Poly (OESDAC-*co*-ADC; 1:1w/w) etching condition of 1.5 N NaOH at 50°C was selected. At this condition both detectors could develop tracks in 30-40 min with bulk etch rates close to 0.2 $\mu\text{m}/\text{min}$.

V. Sensitivity studies of poly (OESDAC-*co*-ADC; 1:1w/w) and poly (OESDAC-*co*-ADC; 4:6w/w) detectors under optimized etching conditions

In this study, first a new batch of Poly (OESDAC-*co*-ADC) copolymers of 1:1 and 4:6 composition was prepared using previously optimized initiator and polymerization conditions. For comparative purpose, Poly (SDAC-*co*-ADC; 4:6) and PSDAC were freshly prepared using reported optimized conditions i.e., 4% IPP initiator with 0.5% DOP as plasticizer under respective constant rate polymerization heating profile. Secondly, as mentioned earlier the films were exposed to ^{252}Cf radioactive fission source at height of 3 cm under 2 mm of Hg reduced pressure for a period of 24 hours.

Finally, these exposed films were etched under optimized etchant conditions and their sensitivity values and etching rates were determined at increasing track etching time. Results on a comparative study between Poly (OESDAC-*co*-ADC), Poly (SDAC-*co*-ADC; 4:6 w/w) and PSDAC sulfone-based polycarbonate detectors with respect to their track development time, bulk etch rates and alpha sensitivity under optimized etching conditions i.e., 1 N NaOH and 1.5 N NaOH at 50°C were note in **Table 3.12**.

Table 3.12 Comparative study between Poly(sulphone-carbonate) NTDs with respect to its track detection properties at optimized etching conditions

Sr. No.	Poly(sulfone-carbonate) detectors	Time required to observe (minutes) developed		Etching Time (minutes)	Bulk etch rate ($\mu\text{m}/\text{min}$) ^a	Sensitivity (S) ^b
		alpha tracks	fission fragments			
		1	Poly(OESDAC- <i>co</i> -ADC; 1:1 w/w) Etching condition: 1N NaOH at 50°C			
2	Poly(OESDAC- <i>co</i> -ADC; 4:6 w/w) Etching condition: 1.5 N NaOH at 50°C	20	10	30 45 60 75 90	0.2216 0.2380 0.2290 0.2365 0.2460	1.86 2.08 S_{max} = 2.23 1.84 1.71
3	Poly(SDAC- <i>co</i> -ADC; 4:6 w/w) Etching condition: 1.5 N NaOH at 50°C	30	40	45 60 75 90 105	0.0877 0.0803 0.0865 0.0911 0.125	1.66 1.79 S_{max} = 1.84 1.81 1.72
4	PSDAC Etching condition: 1.5N NaOH at 50°C	20	30	50 70 90 110 140	0.3346 0.3457 0.3379 0.3487 0.3545	1.68 1.72 1.71 S_{max} = 1.75 1.55

^a bulk etch rate is calculated using weight loss method; ^b films exposed to ²⁵²Cf source at height of 3 cm under 2 mm of Hg vacuum for 24 hours.

From the tabulated results it is clear that, disulfone based polycarbonate detectors i.e., Poly (OESDAC-*co*-ADC; 1:1 w/w) and Poly (OESDAC-*co*-ADC; 4:6 w/w) showed high values of sensitivity with **S_{max} = 2.51** and **2.23** as compared to Poly (SDAC-*co*-ADC; 4:6 w/w) and

PSDAC detectors, which showed $S_{\max} < 2$. Also, this disulfone base detectors showed quicker track development time.

All the polymeric detectors attained S_{\max} at 75 min of chemical etching and bulk etch rates varies from 0.15 to 0.25 $\mu\text{m}/\text{min}$ calculated using weight loss method. The post etch surface appearance is clear till 90 min. Under this mild etching condition, we find the sensitivity values are lower as compared to 3 N NaOH at 60 $^{\circ}\text{C}$, which showed $S_{\max} \geq 3$. This could be attributed to the slower etching rates in 1 N and 1.5 N NaOH at 50 $^{\circ}\text{C}$ etchant condition.

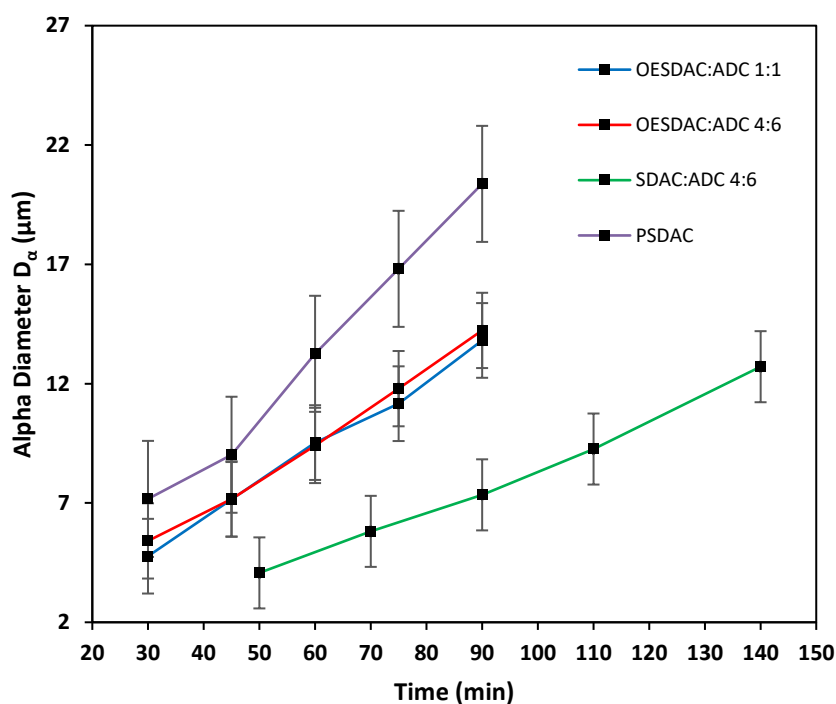


Figure 3.22 Variation of alpha track diameter in poly (OESDAC-co-ADC), Poly (SDAC-co-ADC) and PSDAC detectors under optimized etching condition.

The track size growth for almost all poly(sulfone-carbonate) detectors was linear and nearly same in comparable to etch. The variation in the fission track diameter for different polymers prepared and etched under optimum polymerization and etching conditions is shown in **Figure 3.22** and **Figure 3.23**.

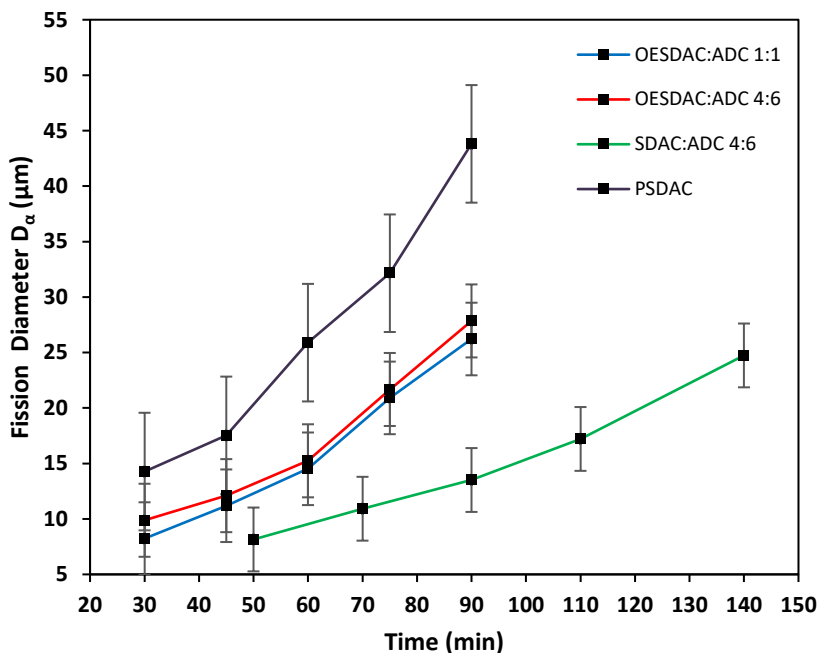


Figure 3.23 Variation of fission track diameter in poly (OESDAC-co-ADC), Poly (SDAC-co-ADC) and PSDAC detectors under optimized etching condition.

Base on above alpha and fission track diameter data we calculated the variation in the sensitivity of the polymers as function track etching time which is represented in **Figure 3.24**.

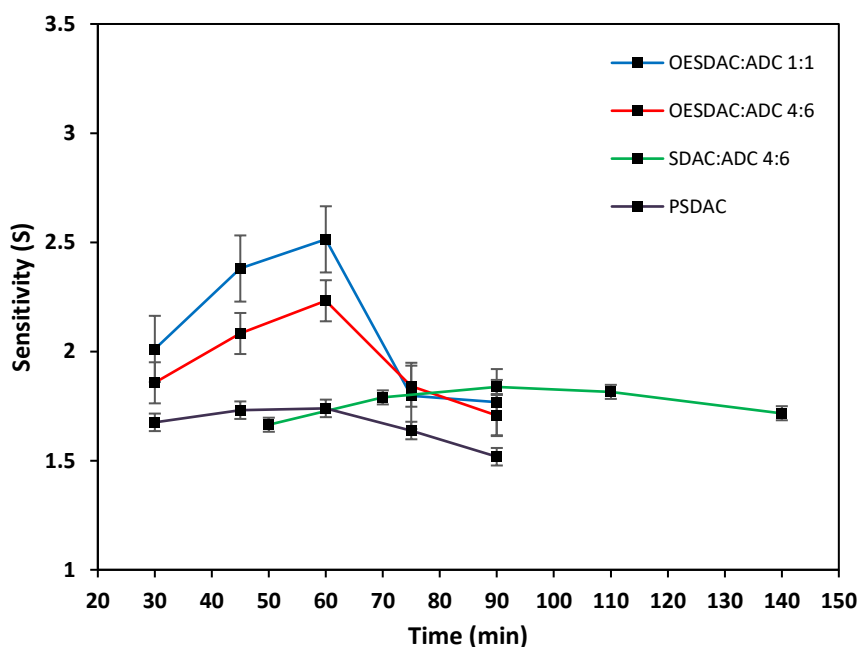


Figure 3.24 Variation in the alpha sensitivity for poly(sulfone-carbonate) detectors etched under etching conditions.

VI. Sensitivity study of poly (ETSDAC-co-ADC, 1:9 w/w) under standard etching condition

As previously mentioned in test polymer study, solid ETSDAC monomer (m. p. 90-92°C) had a limited solubility in ADC monomer. We attempted to dissolve the monomer by various processes such as heating at 90°C with N₂ purging and ultrasonication. But upon cooling, solid slowly got regenerated in the mixture. Sonification and heating process was effective for dissolving ETSDAC monomer concentration $\leq 10\%$ w/w. Above this, solid remained suspended or as suspension in mixture even upon heating to 90°C. Also, heating above 90°C resulted in vitrified gel. Hence, we could prepare only one copolymer composition with ADC i.e., ETSDAC: ADC, 1:9 w/w.

Free radical cast polymerization was performed in the presence of 3.3% IPP as initiator and 0.5% DOP as plasticizer under constant rate heating profile previously calculated for ADC monomer. Polymerization results in obtaining optically clear and hard film, which was used further as nuclear track detector. Polymer film were cut into 1 x 1cm² sizes and exposed to standard irradiation condition in order to determined its track recording characteristics. Films were etched in standard etching condition i.e., 6 N NaOH at 70°C employed for PADC detector. The results were finally compared with the indigenously prepared PADC.

Table 3.13 Comparative study between with respect to its track detection properties at optimized etching conditions.

Sr. No.	Polymeric NTDs	Avg. thickness (μm) ^a	Time required to observe (minutes) developed		Etching Time (minutes)	Sensitivity (S) ^b
			alpha tracks	fission fragments		
1	Poly (ETSDAC-co-ADC; 1:9 w/w)	529	8	3	10	1.76
					20	1.79
					30	1.59
					40	S_{max} = 1.83
					60	1.33
2	PADC (indigenous)	541	180	60	3h	1.06
					4h	1.13
					5h	S_{max} = 1.25

	6h	1.18
	7h	1.2

^a film thickness was calculated using ELCOMETER thickness gauge; ^b films exposed to ²⁵²Cf source at height of 3 cm under 2 mm of Hg vacuum for 24 hours.

From the result noted in **Table 3.13** we could see that, poly (ETSDAC-co-ADC; 1:9 w/w) shows high sensitivity in comparison to indigenous PADC and CR-39 polycarbonate NTDs. It attains maximum sensitivity of **1.83** at 40 min of etching time. Also, the corresponding etching time reduces drastically, nearly eighth times lower than that observed for CR-39 detector. The variation in alpha track diameter and fission track diameter as a function of etching time is shown in **Figure 3.25** below. Both alpha and fission track diameter increases linearly with etching time.

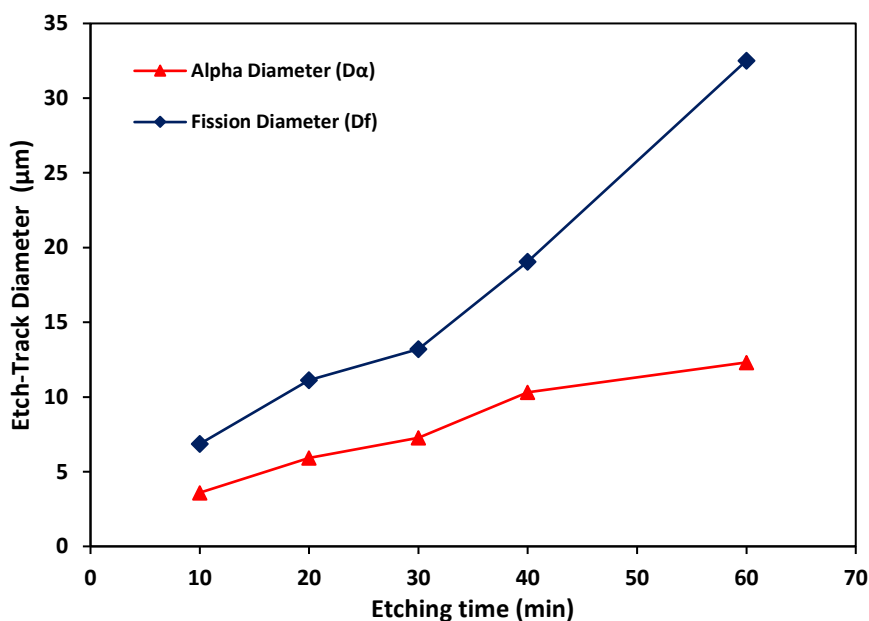


Figure 3.25 Variation of alpha and fission diameter in poly (ETSDAC-co-ADC; 1:9 w/w) detector.

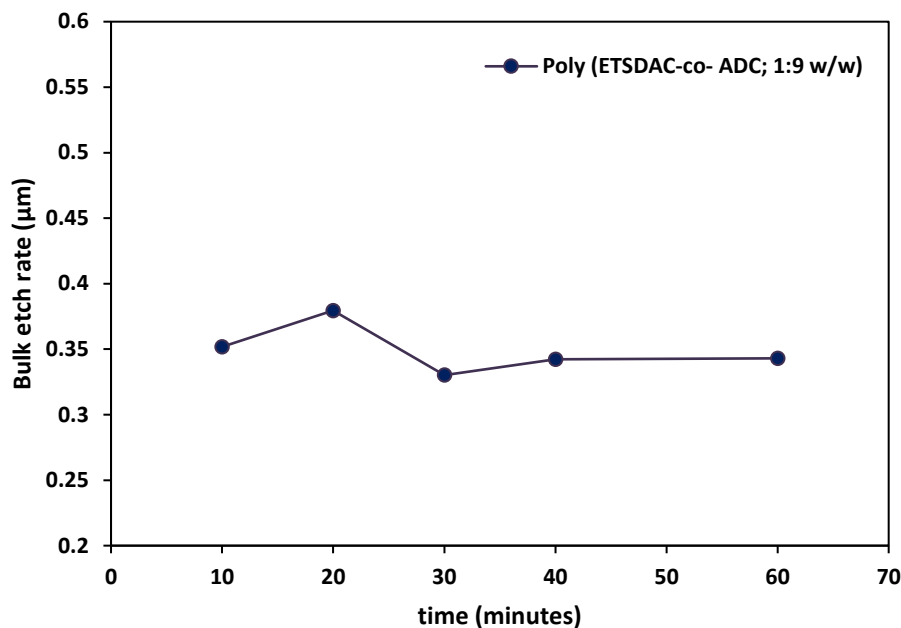


Figure 3.26 Variation of bulk etch rate with etching time for poly (ETSDAC-co-ADC; 1:9 w/w) detector.

Variation in bulk etch rate was calculated using weight loss method (**Figure 3.26**). Indigenous PSDAC and CR-39 attains standard bulk etch rates from 1 to 1.5 $\mu\text{m}/\text{h}$. Post etch surface was clear for all the detector under studies.

VII. Alpha track detection efficiency for newly developed poly (SDAC-co-ADC; 1:1 w/w) and poly (SDAC-co-ADC; 4:6 w/w) NTDs

Alpha track detection efficiency was determined as measure of variation of net alpha track density under given etching condition at 4π exposure condition. For this purpose, newly developed detector film was cut into size of $1 \times 1 \text{ cm}^2$ were expose to alpha particles from ^{239}Pu source for 1.5 minutes at a height of 2 cm. Films were then etched in optimized etching condition. Here, 3 N NaOH at 60°C was selected as etchant condition since we obtained highest sensitivity value at this condition and also it was an optimized etching condition reported for PSDAC detectors. Further, the etched tracks were counted after every regular interval under the optical microscope. Tracks were counted manually for 100 views and net track density was calculated at every etching interval using Equation (3.11) (**section 3.3.4**).

The tracks were counted till a constant or a decreasing value of track density was obtained. Also, time to observe maximum track density was noted and could be considered as optimum etching time for the detector under given etchant condition. An unirradiated films were used as control, which were etched under identical conditions to note the

background tracks. This background tracks were subtracted from alpha track to obtain net track density. For comparative study, PSDAC and poly (SDAC-co-ADC; 4:6 w/w) films were also studied for variation in track density under identical etching condition.

The comparative results on track density, bulk etch rate and S/N ratio of all the poly(sulfone-carbonate) NTDs are shown in **Table 3.14**. Here, the track density for the irradiated and unirradiated detector was calculated and final net track density was obtained by subtracting the control track density from the exposed track density.

Table 3.14 Details on alpha track density, bulk etch rate and signal to noise ratios for poly (sulfone-carbonate) NTDs.

Sr. No.	Polymer NTDs	Time of etching (min)	Bulk etch rate ($\mu\text{m}/\text{min}$)	Control track density ($\text{tracks}/\text{cm}^2$)	Exposed track density ^a ($\text{tracks}/\text{cm}^2$)	Net track density ($\text{tracks}/\text{cm}^2$)	S/N ratio
1	Poly (OESDAC-co-ADC; 1:1 w/w)	3	2.12	276 \pm 10	15722 \pm 172	15446 \pm 175	56 \pm 22
		5	2.19	341 \pm 8	16905 \pm 161	16563 \pm 146	48 \pm 18
		7	2.09	453 \pm 7	18560 \pm 109	18107 \pm 115	40 \pm 8
		9	2.18	486 \pm 10	17976 \pm 149	17489 \pm 155	36 \pm 9
		11	2.26	348 \pm 7	17706 \pm 144	17358 \pm 142	50 \pm 9
2	Poly (OESDAC-co-ADC; 4:6 w/w)	4	1.88	296 \pm 12	13284 \pm 307	12989 \pm 307	44 \pm 60
		6	1.87	361 \pm 10	15985 \pm 120	15623 \pm 116	43 \pm 14
		8	2.06	420 \pm 16	17588 \pm 99	17167 \pm 100	41 \pm 22
		12	2.16	453 \pm 10	17016 \pm 74	16563 \pm 74	36 \pm 11
		16	2.32	447 \pm 11	15912 \pm 156	15564 \pm 158	45 \pm 12
3	PSDAC	2	7.27	434 \pm 14	12246 \pm 214	11813 \pm 204	27 \pm 12
		3	6.75	493 \pm 10	13909 \pm 213	13416 \pm 212	27 \pm 7
		4	6.76	532 \pm 10	15689 \pm 207	15157 \pm 211	28 \pm 8

		6	7.00	519±9	14231±217	13712±220	26±7
		10	7.64	486±9	13028±211	12680±208	36±7
4	Poly	7	0.98	361±13	15374±220	15012±226	42±31
	(SDAC-co-	14	0.88	401±6	16708±187	16307±187	41±9
	ADC; 4:6	21	0.94	473±8	18015±166	17542±165	37±8
	w/w)	28	1.02	512±7	16655±160	16142±162	32±8
		38	0.96	493±10	15807±133	15315±132	31±6

^a Exposed to ²³⁹Pu source at a distance of 2 cm for 90 s, etched using in 3 N NaOH at 60 °C.

From the tabulated data (**Table 3.14**), it is clear that net alpha track densities for different sulfone-based polycarbonate detectors varies substantially. PSDAC homopolymer had relatively lower number of alpha tracks compared to rest sulfone-based ADC copolymers. This confirms that sulfone-based ADC copolymers shows enhanced track detection efficiency. Particularly, newly developed disulfone based polycarbonate detector attains high values for alpha track density due to the added advantage of presence of radiation sensitive ether link between sulfone functionalities.

Hence, confirming the enhanced track detection efficiency of ADC copolymers with newly developed functional monomers. **Figure 3.27** represents trend of net alpha track density as a function of etching time in Poly (OESDAC-co-ADC), PSDAC and Poly (SDAC-co-ADC) nuclear track detectors.

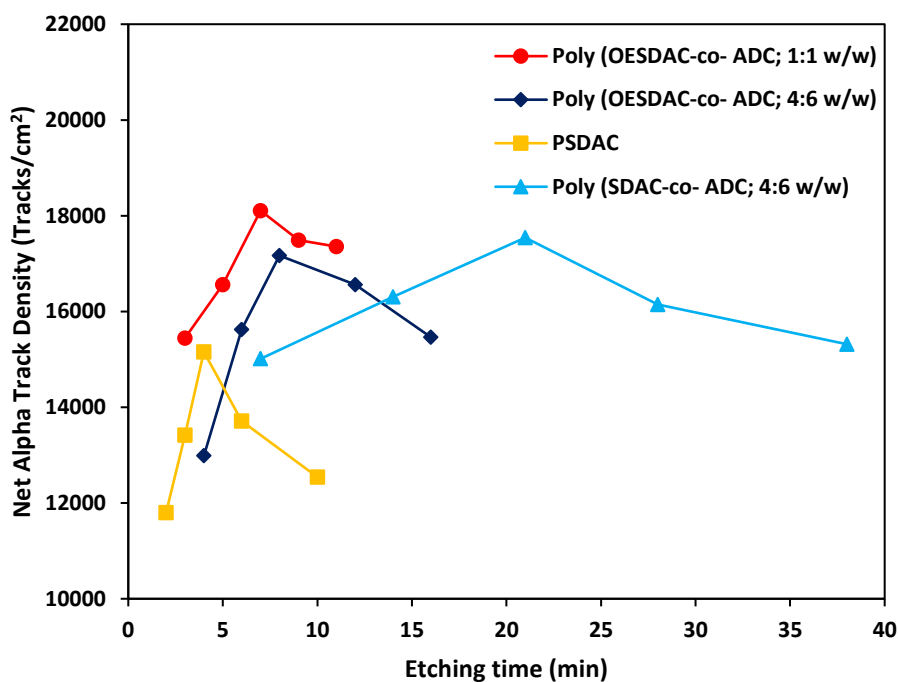


Figure 3.27 Variation of net Alpha Track Density with etching time in different Poly(sulfone-carbonate) NTDs

Figure 3.27 clearly indicates that, although alpha track density values for different NTDs are in close proximity to each other, there is considerable difference in the etching time for different detectors. The etching time where the net track density appeared at maximum peak was considered as optimum etching time for the detector material under given etching condition. Poly (OESDAC-co-ADC; 1:1w/w) detector showed relatively higher value of track density maximum amongst all materials. Also, signal to noise ratio is higher, indicating lower background track density and better track detection efficiency of material. In comparison to all detector materials, PSDAC homo polymer showed higher values background track density (lower S/N ratio) due to more background rack like features.

Background tracks appears^[99] due to the presence of radons or other ions that might exist in the surrounding, which enters the detector material in a process of film cutting and transfer. Hence, maximum care should be taken to pack the plastic material by wrapping it with aluminum foil and then transfer to air-tight pouches to prevent radon entry. Also, some background track like features appears in the polymer matrix due to presence of micro-voids/microbubbles during the polymerization stage. During polymerization, IPP initiator decomposes into isopropyl free radical and evolution of carbon dioxide which could be trapped in the matrix as microbubbles resulting in increasing background like tracks. Although we filter the monomer through microfilters, the overall polymerization process

from mold preparation to monomer filling is not conducted in totally dust free environment. Hence, it is unavoidable to restrict the entry of micro sized dust particles inside the polymer or over the surface under present laboratory preparation conditions.

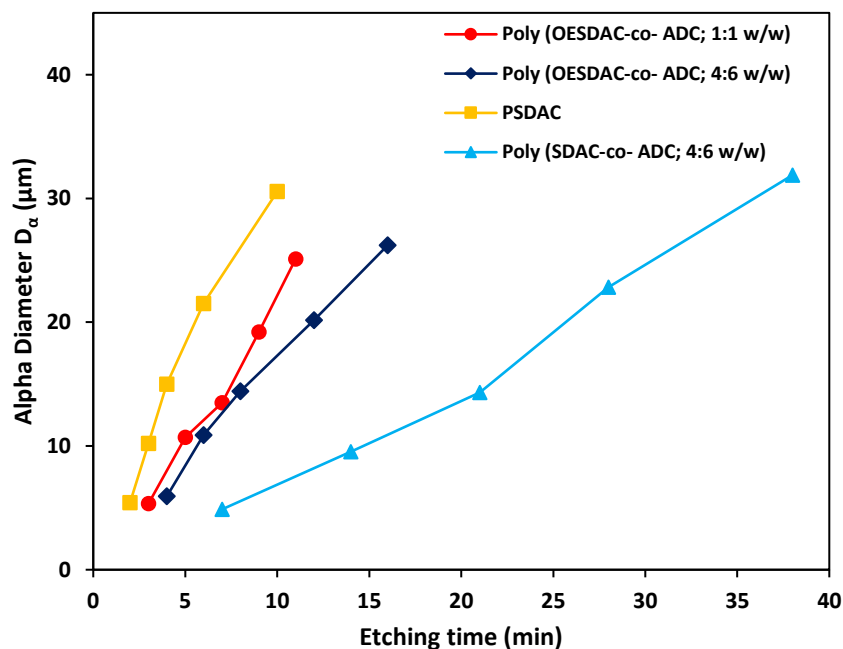


Figure 3.28 Variation in alpha track diameter with etching time for different Poly(sulfone-carbonate) NTDs, pre-exposed to ^{239}Pu alpha source at distance of 2cm for 90s.

From the trends obtained in alpha track diameter for different poly(sulfone-carbonate) detectors (**Figure 3.28**), it is clear that the track diameter increases linearly with etching time and at a certain etching time, tracks tend to merge with each other or get wiped out due to bulk etching thus resulting in decreasing track density. Hence, we see a drop in net track density after a certain maximum value.

VIII. Photomicrograph of newly developed poly(disulfone-co-carbonate) detectors

All photographs of the etched tracks were recorded by using Tucsen ISH500 Camera and corresponding track diameters were measured by using its own imaging software i.e., IS Capture. **Figure 3.29** depicts the fission fragments developed in the poly (OESDAC-co-ADC; 1:1w/w) detector when exposed to ^{252}Cf source at 1mm for 24 hour and subsequent etching for 1 min. **Figure 3.30** depicts the alpha tracks developed in the poly (OESDAC-co-ADC; 1:1w/w) detector when exposed to ^{239}Pu source at 1 mm for 2 minutes and subsequent etching for 5 min.



Figure 3.29 Fission fragments (black, 7-9 μm elongated trails) observed in poly (OESDAC-co-ADC; 1:1w/w) detector when etched for 1 minute in 3 N NaOH at 60°C (40x magnification).

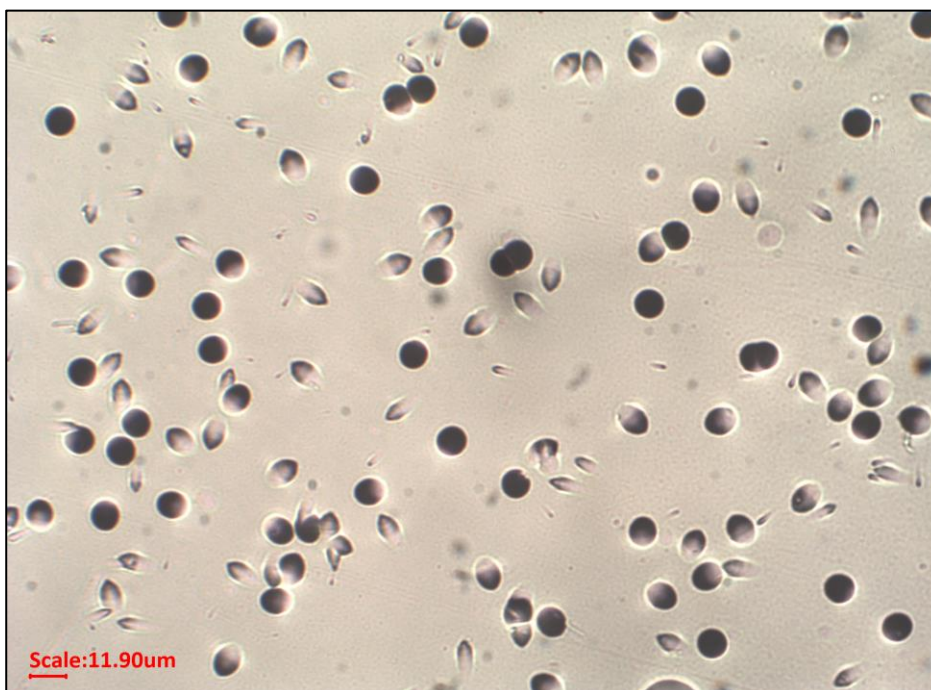


Figure 3.30 Alpha tracks observed in poly (OESDAC-co-ADC; 1:1w/w) detector when etched for 5 minutes in 3 N NaOH at 60°C (40x magnification).



Figure 3.31 An alpha and fission tracks observed in poly (OESDAC-co-ADC; 1:1w/w) detector after 5 minutes of etching in 3 N NaOH at 60°C (magnification: 40X), pre-exposed to ^{252}Cf source at 3 cm height in vacuum for 24 hours.

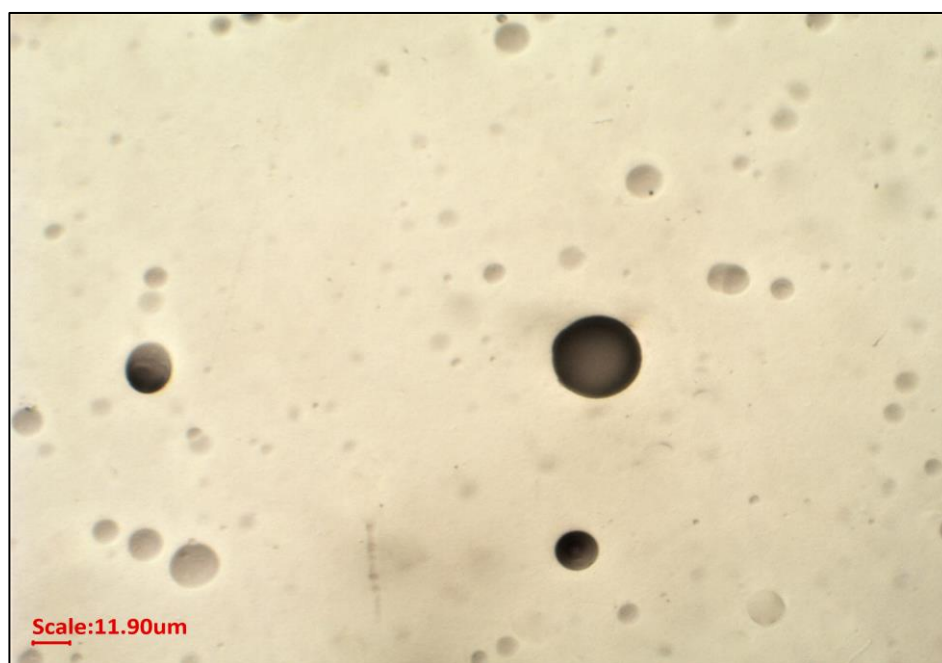


Figure 3.32 An alpha and fission tracks observed in poly (OESDAC-co-ADC; 1:1w/w) detector after 7 minutes of etching in 3 N NaOH at 60°C (magnification: 40X), pre-exposed to ^{252}Cf source at 3 cm height in vacuum for 24 hours

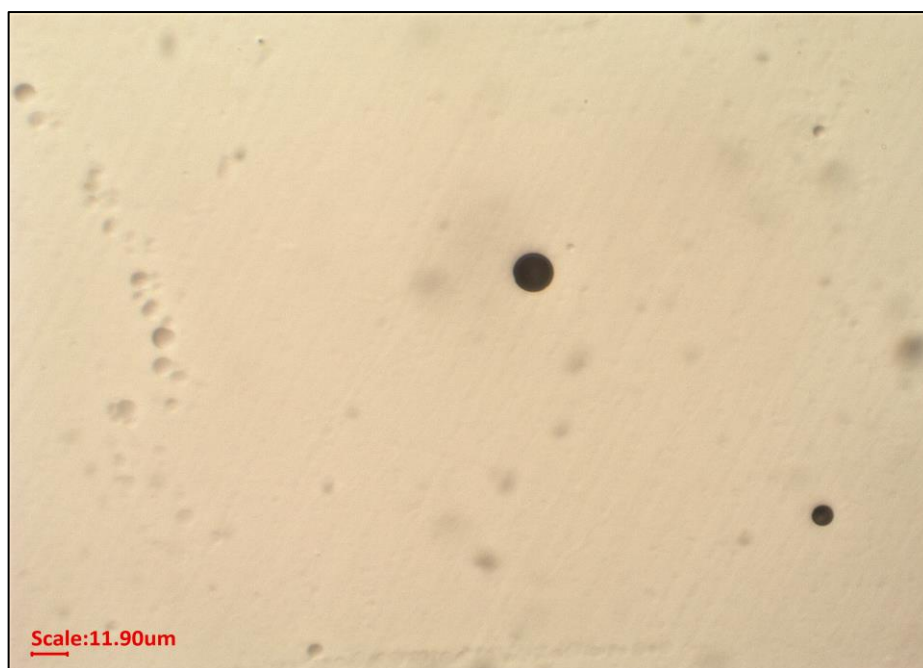


Figure 3.33 An alpha and fission tracks observed in poly (ETSDAC-co-ADC; 1:9w/w) detector after 30 minutes of etching in 6N NaOH at 70°C (magnification: 40X), pre-exposed to ^{252}Cf source at 3cm height in vacuum for 24 hours.

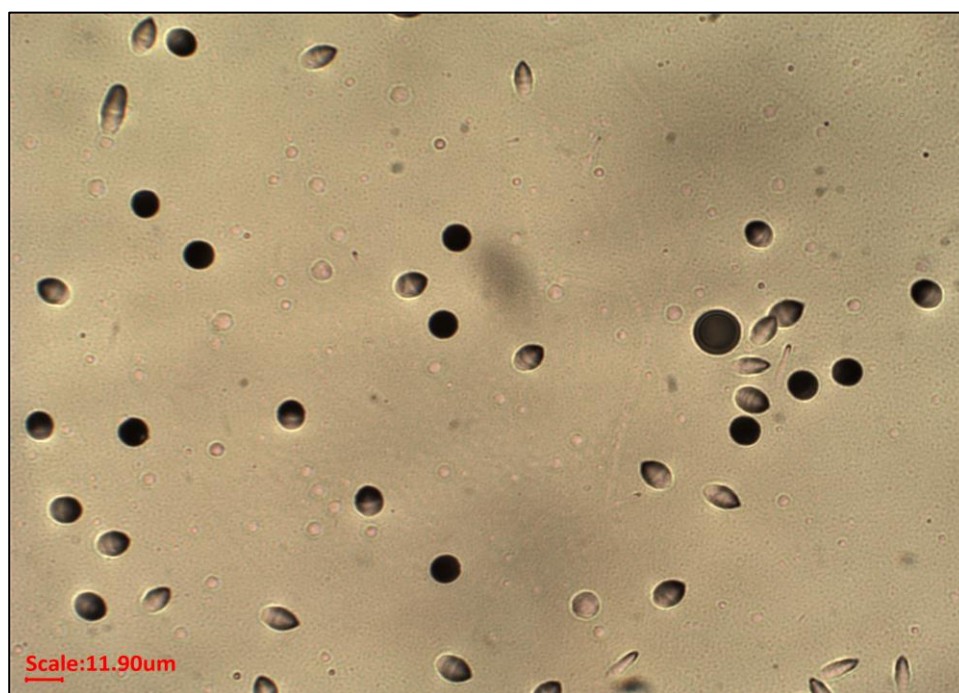


Figure 3.34 An alpha and fission tracks observed in poly (OESDAC-co-ADC; 4:6w/w) detector after 9 minutes of etching in 3 N NaOH at 60°C (magnification: 40X), pre-exposed to ^{252}Cf source at 4 mm height for 24 hours.

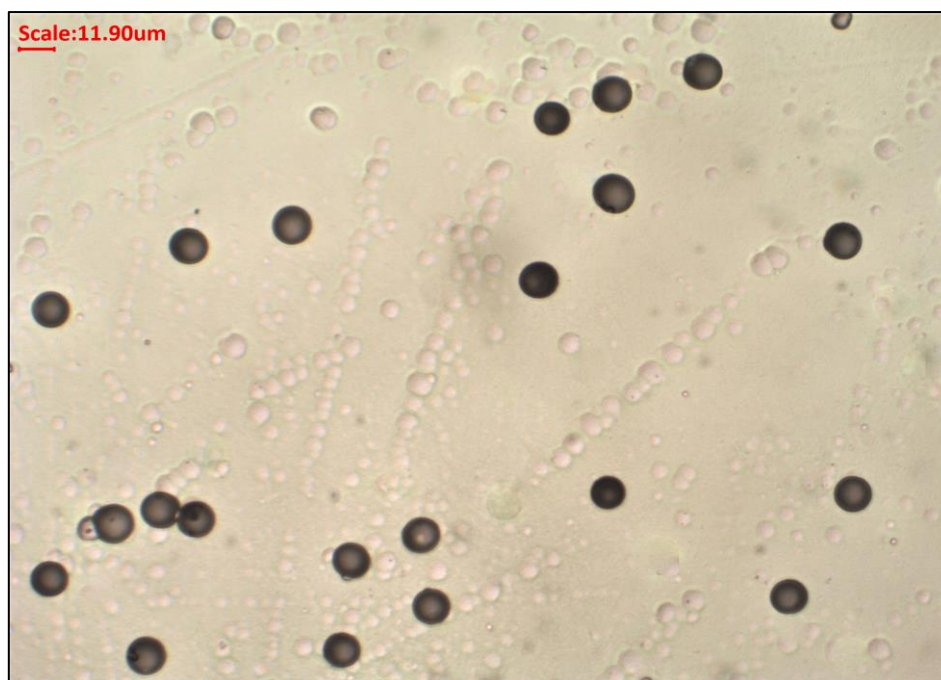


Figure 3.35 Alpha tracks observed in poly (OESDAC-*co*-ADC; 1:1w/w) detector after 7 minutes of etching in 3 N NaOH at 60°C (magnification: 40X), pre-exposed to ^{239}Pu source at 2 cm height for 90 seconds.

3.4.2 Investigating newly synthesized poly(urethane-carbonate) highly crosslinked thermoset polymers for SSNTD applications

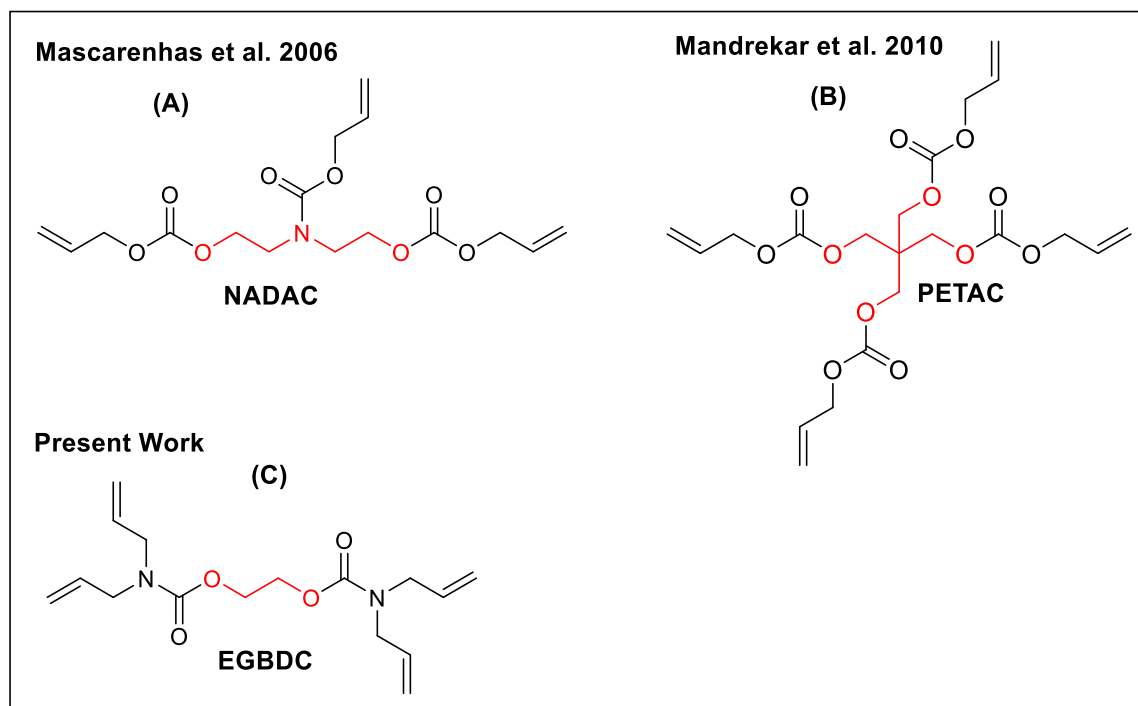


Figure 3.36 Urethane and carbonate containing multifunctional monomers for preparing highly crosslinked polymers as NTDs

We understand that the presence of hetero atoms in the organic monomer enhances the radiation sensitivity of the polymeric detector derived from it. Few of the well-studied radiation sensitive functionality includes organic carbonates (-O-CO-O-), esters(-O-CO-) nitrate (O-NO₂), organic sulfonate (O-SO₂-) and its sensitivity varies in following order ester < carbonate < nitrate esters < sulfonate. Thus, by altering the functionalities in monomer unit one can improvise radiation sensitivity of polymeric detector. Also, presence of such functionalities in highly cross-linked, 3D polymer network would further improve the sensitivity of material. While working on similar line of protocols, in 2005 Mascarenhas et al.^[100] first time introduced a new radiation sensitive functionality commonly known as **carbamate or urethane** into crosslinked polymeric network. For this purpose, a novel hexafunctional monomer (i.e., having three C=C bonds), namely *N*-allyloxycarbonyl diethanolamine bis (allyl carbonate) (NADAC) was designed (**Figure 3.36A**). Its structural unit includes one carbamate and two carbonate moieties. The idea was to introduce different types of functionalities in a dense crosslinked polymer network. NADAC monomer was homopolymerized and copolymerized with allyl diglycol carbonate (ADC). Its copolymer, i.e. (NADAC-*co*-ADC, 1:1w/w)^[82] detector showed high sensitivity value of 1.6 with 3% IPP concentration under 6 N NaOH 75 °C etching condition, which proved to be more sensitive as compared to CR-39 track detector.

In 2010 Mandrekar et al.^[89], designed and developed another highly crosslinked thermoset material as NTDs, derived from octa-functional allyl monomer, namely pentaerythritol tetrakis (allyl carbonate) (PETAC) (**Figure 3.36B**). This octa-functional monomer generated much denser 3-D polymer network and also source of multiple radiation sensitive functionalities i.e., carbonate groups. Here, authors prepared homopolymer as well as series of copolymer thermoset films with ADC using 4% IPP initiator concentration, in order to examine their track detection capabilities. Among all, 4:6; PETAC: ADC copolymer detector showed highest sensitivity value of 2.13, nearly double the value for CR-39 under identical etching conditions. Also, this copolymer could reveal the alpha tracks at half the time taken by CR-29 detector.

In continuation with similar efforts to obtain better radiation sensitive detectors with dense 3D crosslinked network, we designed and synthesized a branched, octa-functional monomer, namely ethylene glycol bis (diallyl carbamate) (EGBDC) (**Figure 3.36C**). Purpose in designing this monomer was to understand the combine effect of increasing carbamate functionalities and polymeric crosslinking on radiation sensitivity of material.

EGBDC synthesis and characterization aspect are described briefly in Chapter 1; section 1.4.3II.ii. In this chapter, we will be focusing on the track detection properties of the designed monomer and its copolymer with ADC.

I. Preparation of test polymers to understand nuclear track detection ability of polymeric materials

Newly designed monomer EGBDC was homopolymerized as well as copolymerized with ADC using constant rate heating profile precalculated for ADC^[80]. In this process, homopolymer forms gel like material whereas copolymers with low EGBDC concentration results in a clear and hard film. During initial attempt, we conducted test polymerization using IPP as initiator. Unfortunately, we could only recover gel polymers, even at high concentration of IPP. Further, we tried test polymerization with benzoyl peroxide (B.P.), yet again similar results were observed at 3-8% (w/w) concentration of BP. Finally, at 9% w/w concentration, we were able to obtain hard polymer and thus decided to cast film using 9% BP concentration.

Poly (EGBDC-co-ADC) copolymer films of thickness ranging from 500-600 μm and ~size 4 x 4 cm^2 were prepared using EGBDC: ADC monomer ration of 1:9, 2:8, 3:7, 1:1, 6:4 (w/w) in the presence of 9% (w/w) BP as initiator and 0.5% DOP as plasticizer. Further it is observed that, as the concentration of EGBDC in monomer mixture increases, the softening of films occurred. Copolymer films prepared from 30% (w/w) and above concentration of EGBDC are found to be very soft in nature. Thus, such copolymer could not be used as a track detector. Physical properties of EGBDC-ADC copolymers are listed in the table below.

Table 3.15 Curing conditions used for polymerization and physical properties of poly (EGBDC-co-ADC) test polymers.

Sr. No.	Polymer composition (w /w) EGBDC: ADC	Heating profile (Temperature range)	Avg. thickness (μm) ^a	Colour and hardness
1	1:9	PADC polymerization profile (45-95°C)	547±10	Colourless and hard film
2	2:8	PADC polymerization profile (45-95°C)	602±10	Pale yellow and hard film

3	3:7	PADC polymerization profile (45-95°C)	490±10	Yellow, soft and flexible film
---	-----	---------------------------------------	--------	--------------------------------

^afilm thickness were calculated using ELCOMETER thickness gauge.

Further, acquired polymer films including poly (EGBDC-*co*-ADC), PADC (indigenously prepared at Goa University) and commercial CR-39™ were cut into pieces of 1 x 1 cm² size and exposed to alpha particles from ²³⁹Pu source at a distance of 2 mm for 5 min. and fission fragments from ²⁵²Cf source at height of 2 mm for 24 h. Subsequently, the exposed films were chemically etched using of 6 N NaOH at 70°C. Track recording characteristics for all test polymers are noted in table below.

Table 3.16 Track recording properties and chemical etching parameters for poly (EGBDC-*co*-ADC) test polymers.

Sr. No.	Polymer composition (w/w)	Time to reveal developed tracks (hours) in 6N NaOH at 70°C		Bulk etch rate V _B (µm/h) ^a	Post etch polymer surface
		Alpha particle	Fission fragment		
1	1:9 EGBDC: ADC	4	1.5	0.92	hard and clear
2	2:8 EGBDC: ADC	4	1.5	0.87	hard and clear

^abulk etch rates were determined using weight loss method.

From the test studies, we observed that copolymers of newly designed monomer can successfully detect the tracks of charge particles at low etch rates. During the etching process we could observe few undeveloped tracks after 2 hours of etching but after 4 hours, well developed etch tracks were seen. The PADC (indigenous) and CR-39 could reveal developed alpha track in 3h with etching rate of 1.26 µm/h. Longer track development time observed for poly (EGBDC-*co*-ADC) polymers is probably due to lower electrophilicity of carbonyl carbon of carbamate compared to that of carbonate thus resulting in a slower initial attack by hydroxide.

II. Sensitivity studies of poly (EGBDC-*co*-ADC) polymers and comparison with NADAC-ADC copolymer

For comparison purpose, we prepared poly(carbamate-carbonate) detector, namely poly (NADAC-*co*-ADC, 1:1w/w) using 3% (w/w) IPP initiator and 1% DOP as plasticizer. This copolymeric detector is an optimized composition showing maximum sensitivity of 1.6 in 6N NaOH at 75 °C. Its track detection properties are already reported in the literature^[82].

Further, to understand the sensitivity of newly developed material, we followed our standard irradiation protocols i.e., prepared polymer films were cut into 1 x 1cm² size and exposed to ²⁵²Cf source at height of 3 cm under 2 mm of Hg vacuum for 24 hours. The irradiated films were etched in 6N NaOH at 75 °C condition for comparative study. The obtained results are noted in **Table 3.17** below.

Table 3.17 Track etching parameters of poly (EGBDC-*co*-ADC; 1:9 w/w).

Sr. No.	Polymeric NTDs	Etching Time (h)	Sensitivity (S)	Bulk etch rate (μm/h) ^a
1	Poly (EGBDC- <i>co</i> -ADC; 1:9 w/w)	3	1.31	1.74
		4	1.32	1.71
		5	1.32	1.73
		6	S_{max} = 1.36	1.73
		7	1.31	1.76
2	Poly (EGBDC- <i>co</i> -ADC; 2:8 w/w)	3	1.25	1.55
		4	1.25	1.56
		5	S_{max} = 1.27	1.55
		6	1.26	1.60
		7	1.22	1.61
3	Poly (NADAC- <i>co</i> -ADC; 1:1 w/w)	5	1.37	1
		6	1.38	1.04
		7	S_{max} = 1.67	1.07
		8	1.53	1.09
		9	1.51	1.11
4	CR-39	3	1.21	2.04
		4	1.26	1.88
		5	S_{max} = 1.29	1.92

6	1.28	1.94
7	1.24	1.98

^abulk etch rate is calculated using fission track diameter method.

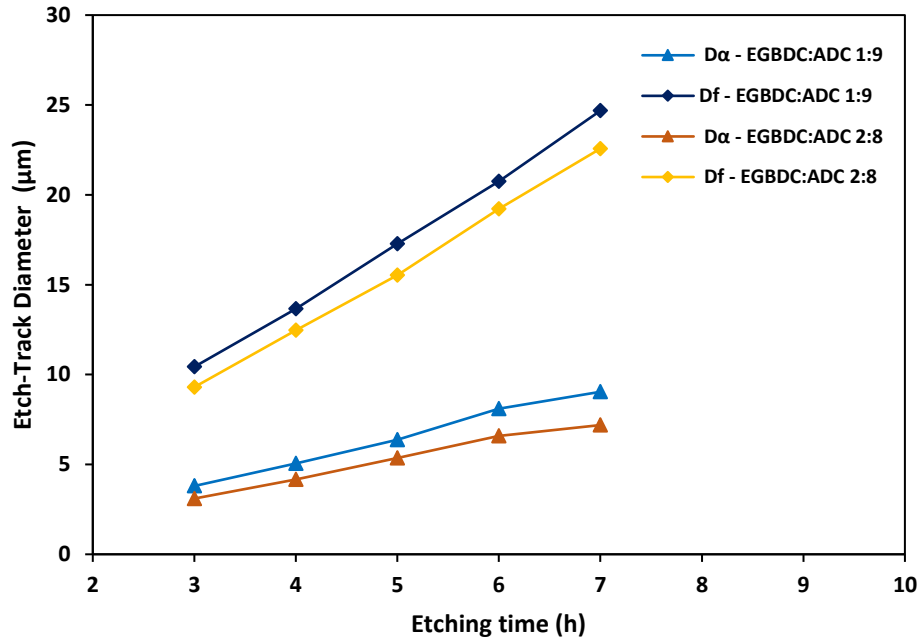


Figure 3.37 Variation of alpha and fission etch track diameters in poly (EGBDC-co-ADC) detectors.

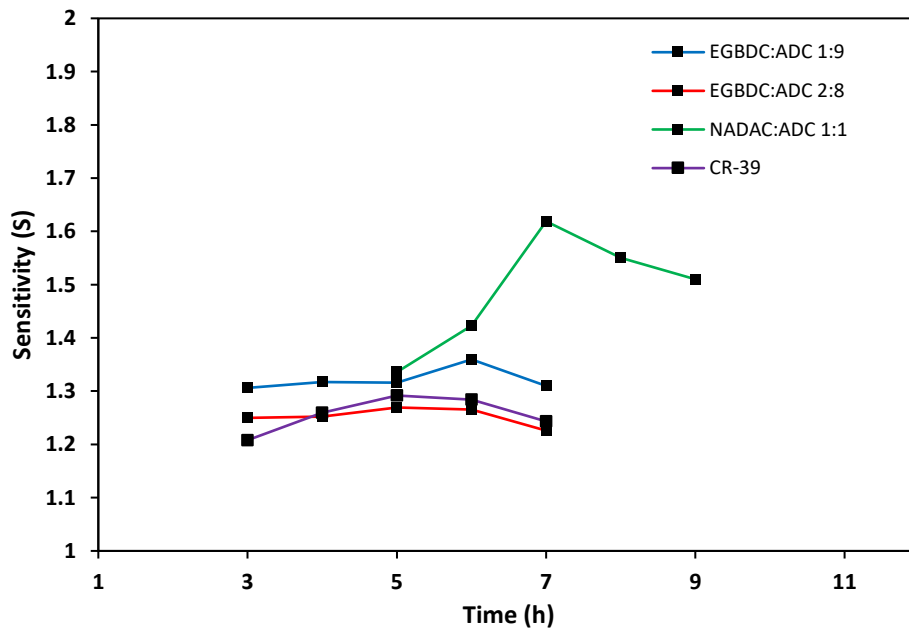


Figure 3.38 Variation of alpha sensitivities in poly(carbamate-carbonate) as compared to CR-39 detector

Track growth for all detectors were linear as shown in **Figure 3.37** and bulk etch rates varies from 1-2 $\mu\text{m/h}$. Also, post etch surface remain clear for all detectors. Among newly developed poly(urethane-carbonate) detectors, we could record highest alpha sensitivity for EGBDC: ADC,1:9 copolymer (**Table 3.17 and Figure 3.38**), which was found to be superior than that of CR-39 detector. However, NADAC-ADC copolymer detector still remained the most sensitive among all above polymer under study. The possible reason for lowering of alpha sensitivity in EGBDC-ADC copolymers could be use of excessive amount benzoyl peroxide as initiator for polymer preparation.

Additionally, if we compare all polymer detectors based on branched monomers, PETAC-ADC detector^[89] is found to be most sensitive among all. Possible reason could be tetra-carbonate arrangement within a compact crosslinked network, which mainly arises due to branching over single carbon atom. In case of NADAC-ADC detector, presence of two carbonate functionalities along with urethane linkages in monomer structure, possibly could help in increasing the radiation sensitivity of detector. However, in case of EGBDC-ADC, absence of carbonate linkages in monomer structure would possibly affect sensitivity of copolymer. Also, (-NCOOCH₂CH₂OCON-) linkage can act as a spacer in a crosslinked network which can further affect detector sensitivity. Overall, it is important to note that presence of carbonate functionality in monomer design is essential requirement in order to enhance the radiation sensitivity.

III. Photomicrograph of newly developed poly (EGBDC-co-ADC) detectors

Figure 3.39 depicts the alpha tracks developed in the poly (EGBDC-co-ADC; 2:8 w/w) detector when exposed to when exposed to ²³⁹Pu source at 2 mm for 5 minutes and subsequent etching for 4 hours. **Figure 3.40** depicts the fission fragments developed in the

poly (EGBDC-*co*-ADC; 1:9 w/w) detector when exposed ^{252}Cf source at 2 mm for 10 hour and subsequent etching for 3 h.

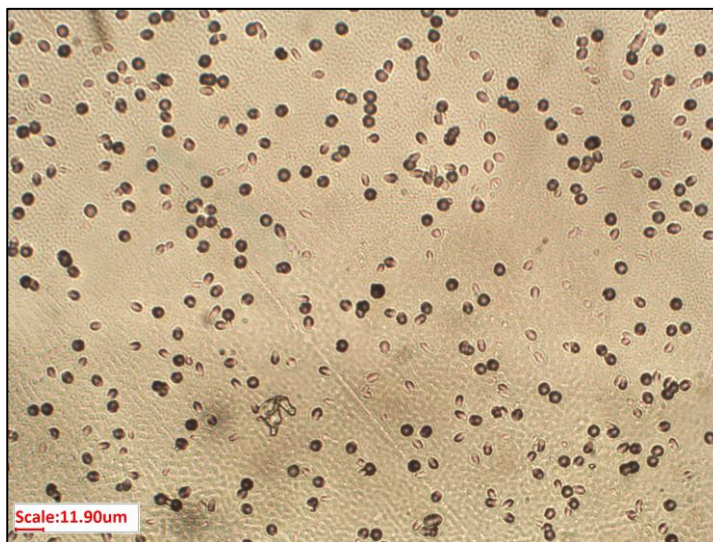


Figure 3.39 Alpha tracks observed in poly (EGBDC-*co*-ADC; 1:9 w/w) detector when etched for 4 h in 6 N NaOH at 70°C (40x magnification).

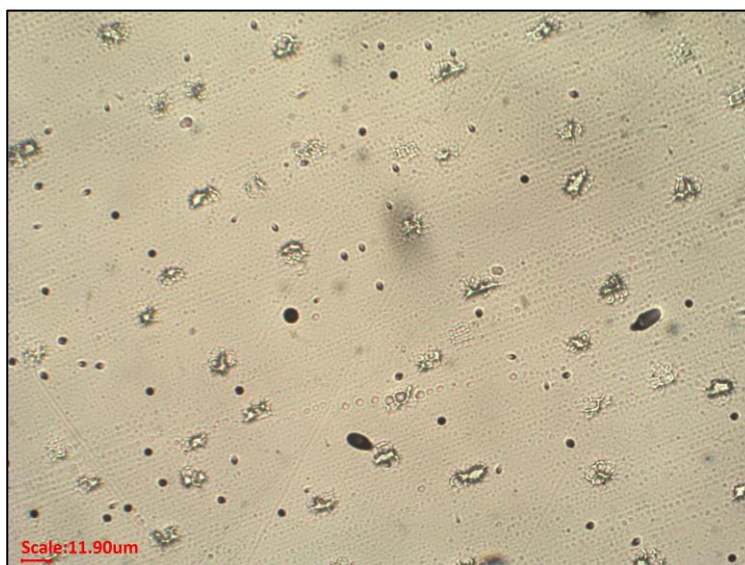


Figure 3.40 Fission fragment (bigger circles and elongated ellipsoid) observed in poly (EGBDC-*co*-ADC; 2:8 w/w) detector when etched for 3 h in 6 N NaOH at 70°C (40x magnification).

3.5 Conclusions

1. We have successfully tested the newly developed thermoset poly(disulfone-carbonate) copolymers for rapid detection of alpha particles and fission fragments.

Based on results we wish to highlight following key points:

- a) Poly (OESDAC-*co*-ADC) copolymers shows much quicker etching rates in 6 N NaOH at 70°C as compare to poly (SDAC-*co*-ADC) rapid detector, which results in reduction of optical clarity of polymer films after chemical etching.
- b) Limited solubility of ETSDAC monomer in ADC restrict us to test only poly (ETSDAC-*co*-ADC; 1:9 w/w) composition track detection. Still the copolymer is more sensitive than indigenous PADAC with shorter track development time of 8 min for alpha and 3 min for fission fragment.
- c) In a copolymer series, poly (OESDAC-*co*-ADC; 1:1 w/w) and poly (OESDAC-*co*-ADC; 4:6 w/w) shows high sensitivity with S_{\max} value of 3.16 and 2.78 under 3% IPP optimized initiator concentration and mild etching condition i.e., 3 N NaOH at 60°C.
- d) Under 3 N NaOH at 60°C conditions, both the poly (OESDAC-*co*-ADC) polymers can reveal alpha tracks within 2-3 min and fission fragments tracks within 30-60 sec.
- e) For optimized poly (OESDAC-*co*-ADC) copolymers composition, S_{\max} values decreases as we lower the etchant concentration to 1 N NaOH at 50°C, indicating slow track growth rates. Nevertheless, the sensitivity values are still higher than poly (SDAC-*co*-ADC) rapid detector.
- f) Poly (OESDAC-*co*-ADC; 1:1 w/w) shows better track detection efficiency as compare to other sulfone-based polycarbonate detectors.

Overall result shows the effectiveness of increasing radiation sensitive parameters such as sulfonyl groups and ether chain through monomer design on track detection properties of newly developed Poly (OESDAC-*co*-ADC) detector. We have therefore succeeded in developing a more efficient sulfone-based polycarbonate NTD having rapid track detection property and sensitivity nearly 3 times higher than PADAC.

2. We have successfully tested newly developed poly(urethane-carbonate) thermoset copolymers for detection of charge particles. Based on results we wish to highlight following key points:

-
- a) EGBDC-ADC copolymers up to 20% w/w EGBDC concentration are tested for track detection purpose due to synthetic limitation in preparing higher versions.
 - b) EGBDC-ADC, 1:9 & 2:8 (w/w) copolymers can develop alpha tracks at 4 h and fission track at 1.5 h after chemical etching in 6 N NaOH at 75°C.
 - c) In comparative study with NADAC-ADC and CR-39 detector, EGBDC-ADC, 1:9 and 2:8 (w/w) copolymers, shows maximum sensitivity values of 1.36 and 1.27.

Overall result shows the newly developed material can successfully detect the tracks of charge particles and found to be more sensitivity than CR-39 detector. However, NADAC-ADC detector still remains as most sensitive urethane containing polymeric detector.

3.6 References

- [1] D. A. Young, *Nature* **1958**, *182*, 375–377.
- [2] E. C. H. Silk, R. S. Barnes, *Philosophical Magazine* **1959**, *4*, 970–972.
- [3] R. L. Fleischer, P. B. Price, R. M. Walker, R. M. Walker, *Nuclear Tracks in Solids: Principles and Applications*, University Of California Press, Berkeley, **1975**.
- [4] P. B. Price, R. M. Walker, *Physics Letters* **1962**, *3*, 113–115.
- [5] P. B. Price, R. M. Walker, *Journal of Applied Physics* **1962**, *33*, 3400–3406.
- [6] P. B. Price, R. M. Walker, *Physical Review Letters* **1962**, *8*, 217–219.
- [7] P. B. Price, R. M. Walker, *Journal of Applied Physics* **1962**, *33*, 2625–2628.
- [8] P. B. Price, R. M. Walker, *Journal of Applied Physics* **1962**, *33*, 3407–3412.
- [9] P. B. Price, R. M. Walker, *Applied Physics Letters* **1963**, *2*, 23–25.
- [10] R. L. Fleischer, H. W. Alter, S. C. Furman, P. B. Price, R. M. Walker, *Science* **1972**, *178*, 255–263.
- [11] R. L. Fleischer, P. B. Price, R. M. Walker, *Science* **1965**, *149*, 383–393.
- [12] R. L. Fleischer, P. B. Price, R. M. Walker, *Annual Review of Nuclear Science* **1965**, *15*, 1–28.
- [13] R. H. Iyer, *Journal of Earth System Science* **1981**, *90*, 437–460.
- [14] S. A. Durrani, R. K. Bull, *Solid State Nuclear Track Detection: Principles, Methods, and Applications*, Elsevier Science Limited, **1987**.
- [15] P. B. Price, R. L. Fleischer, D. D. Peterson, C. O’Ceallaigh, D. O’Sullivan, A. Thompson, *Physical Review* **1967**, *164*, 1618–1620.
- [16] P. B. Price, R. L. Fleischer, *Annual Review of Nuclear Science* **1971**, *21*, 295–334.
- [17] R. M. Walker, *Radiation Effects* **1982**, *65*, 131–132.
- [18] S. A. Durrani, R. K. Bull, in *Solid State Nuclear Track Detection*, Elsevier, **1987**, pp. 1–12.
- [19] A. M. Bhagwat, *Solid State Nuclear Track Detection: Theory and Applications*, India, **1993**.
- [20] C. Hepburn, A. H. Windle, *Journal of Materials Science* **1980**, *15*, 279–301.
- [21] A. N. Goland, *Annual Review of Nuclear Science* **1962**, *12*, 243–284.
- [22] F. Seitz, *Discussions of the Faraday Society* **1949**, *5*, 271.
- [23] S. A. Durrani, R. K. Bull, in *Solid State Nuclear Track Detection*, Elsevier, **1987**, pp. 23–47.

-
- [24] R. L. Fleischer, P. B. Price, R. M. Walker, *Journal of Applied Physics* **1965**, *36*, 3645–3652.
- [25] S.-L. Guo, B.-L. Chen, S. A. Durrani, in *Handbook of Radioactivity Analysis*, Elsevier, **2020**, pp. 307–407.
- [26] R. H. Boyett, D. R. Johnson, K. Becker, *Radiation Research* **1970**, *42*, 1.
- [27] H. G. Paretzke, *Radiation Effects* **1977**, *34*, 3–8.
- [28] D. Nikezic, K. Yu, *Materials Science and Engineering: R: Reports* **2004**, *46*, 51–123.
- [29] S. A. Durrani, R. K. Bull, in *Solid State Nuclear Track Detection*, Elsevier, **1987**, pp. 48–95.
- [30] Y. S. Rammah, O. Ashraf, A. M. Abdalla, M. Eisa, A. H. Ashry, T. Tsuruta, *Radiation Physics and Chemistry* **2015**, *107*, 183–188.
- [31] D. Hermsdorf, *Radiation Measurements* **2012**, *47*, 518–529.
- [32] S. Manzoor, H. A. Khan, Matiullah, M. Tufail, A. A. Qureshi, F. Ansari, R. Shoaib, L. Lembo, *International Journal of Radiation Applications and Instrumentation. Part D. Nuclear Tracks and Radiation Measurements* **1988**, *15*, 207–210.
- [33] V. Chavan, P. C. Kalsi, S.-W. Hong, V. K. Manchanda, *Nuclear Instruments and Methods in Physics Research Section B: Beam Interactions with Materials and Atoms* **2020**, *462*, 82–89.
- [34] S. L. Sharma, T. Pal, V. V. Rao, W. Enge, *International Journal of Radiation Applications and Instrumentation. Part D. Nuclear Tracks and Radiation Measurements* **1991**, *18*, 385–389.
- [35] Zs. Kocsis, K. K. Dwivedi, R. Brandt, *Radiation Measurements* **1997**, *28*, 177–180.
- [36] N. M. Hassan, M. S. Hanafy, A. Naguib, A. A. El-Saftawy, *Nuclear Instruments and Methods in Physics Research Section B: Beam Interactions with Materials and Atoms* **2017**, *407*, 230–235.
- [37] V. M. Pawar, *Polymeric Track Detectors for Neutron and Other Dosimetric Applications*, **2020**.
- [38] L. Tommasino, C. Armellini, *Radiation Effects* **1973**, *20*, 253–255.
- [39] G. Espinosa, F. Fernández, V. M. Castaño, *International Journal of Radiation Applications and Instrumentation. Part D. Nuclear Tracks and Radiation Measurements* **1992**, *20*, 383–387.
- [40] S. A. R. Al-Najjar, R. K. Bull, S. A. Durrani, *Nuclear Tracks* **1979**, *3*, 169–183.
- [41] D. G. Naik, *Synthesis of Allylic Monomers and Polymers Containing Sulphur and Phosphorus Functionalities for Solid State Nuclear Track Detection*, **2017**.

-
- [42] M. M. Monnin, *Nuclear Instruments and Methods* **1980**, *173*, 63–72.
- [43] H. A. Khan, *Radiation Effects* **1971**, *8*, 135–138.
- [44] G. M. Hassib, *Nuclear Instruments and Methods* **1975**, *131*, 125–128.
- [45] G. Meesen, A. Poffijn, *Radiation Measurements* **2001**, *34*, 161–165.
- [46] N. Yasuda, M. Yamamoto, N. Miyahara, N. Ishigure, T. Kanai, K. Ogura, *Nuclear Instruments and Methods in Physics Research Section B: Beam Interactions with Materials and Atoms* **1998**, *142*, 111–116.
- [47] J. P. Y. Ho, C. W. Y. Yip, V. S. Y. Koo, D. Nikezic, K. N. Yu, *Radiation Measurements* **2002**, *35*, 571–573.
- [48] K. N. Yu, J. P. Y. Ho, D. Nikezic, C. W. Y. Yip, in *Recent Advances in Multidisciplinary Applied Physics*, Elsevier, **2005**, pp. 29–34.
- [49] P. B. Price, *Radiation Measurements* **2008**, *43*, S13–S25.
- [50] S. A. Durrani, R. K. Bull, in *Solid State Nuclear Track Detection*, Elsevier, **1987**, pp. 199–244.
- [51] S. A. Durrani, R. K. Bull, in *Solid State Nuclear Track Detection*, Elsevier, **1987**, pp. 144–198.
- [52] S. A. Durrani, R. K. Bull, in *Solid State Nuclear Track Detection*, Elsevier, **1987**, pp. 245–273.
- [53] P. Buford Price, *Radiation Measurements* **2005**, *40*, 146–159.
- [54] K. Ogura, T. Doke, H. Ichinose, K. Kuwahara, H. Tawara, S. Nakamura, S. Orito, *International Journal of Radiation Applications and Instrumentation. Part D. Nuclear Tracks and Radiation Measurements* **1988**, *15*, 315–318.
- [55] R. L. Fleischer, P. B. Price, *Science* **1963**, *140*, 1221–1222.
- [56] D. Xiaojiao, L. Xiaofei, T. Zhixin, H. Yongsheng, G. Shilun, Y. Dawei, W. Naiyan, *Nuclear Instruments and Methods in Physics Research Section A: Accelerators, Spectrometers, Detectors and Associated Equipment* **2009**, *609*, 190–193.
- [57] H. Hasegawa, M. Matsuo, K. Yamakoshi, K. Yamawaki, *Radioisotopes* **1968**, *17*, 419–422.
- [58] I. Nonaka, *Journal of the Physical Society of Japan* **1975**, *38*, 1570–1576.
- [59] J. C. Vareille, J. L. Teyssier, *Radioprotection* **1972**, *7*, 215–228.
- [60] Ž. Todorović, *International Journal of Radiation Applications and Instrumentation. Part D. Nuclear Tracks and Radiation Measurements* **1990**, *17*, 23–26.
- [61] D. O’Sullivan, A. Thompson, in *Solid State Nuclear Track Detectors*, Elsevier, **1982**, pp. 85–88.

-
- [62] P. B. Price, G. Tarlé, *Nuclear Instruments and Methods in Physics Research Section B: Beam Interactions with Materials and Atoms* **1985**, 6, 513–516.
- [63] T. Tsuruta, *Radiation Measurements* **1999**, 31, 99–102.
- [64] T. Tsuruta, *Radiation Measurements* **2000**, 32, 289–297.
- [65] B. Basu, S. Dey, B. Fischer, A. Maulik, A. Mazumdar, S. Raha, S. Saha, S. K. Saha, D. Syam, *Radiation Measurements* **2008**, 43, S95–S97.
- [66] S. M. Farid, A. P. Sharma, *Radiation Effects* **1984**, 83, 77–89.
- [67] T. Yamauchi, S. Kaifu, Y. Mori, M. Kanasaki, K. Oda, S. Kodaira, T. Konishi, N. Yasuda, R. Barillon, *Radiation Measurements* **2013**, 50, 16–21.
- [68] P. Apel, *Radiation Measurements* **2001**, 34, 559–566.
- [69] K. Awasthi, V. Kulshrestha, N. K. Acharya, M. Singh, Y. K. Vijay, *European Polymer Journal* **2006**, 42, 883–887.
- [70] A. Khodai-Joopary, M. A. Sial, H. A. Khan, P. Vater, R. Brandt, *International Journal of Radiation Applications and Instrumentation. Part D. Nuclear Tracks and Radiation Measurements* **1988**, 15, 167–170.
- [71] H. Bessbousse, N. Zran, J. Fauléau, B. Godin, V. Lemée, T. Wade, M.-C. Clochard, *Radiation Physics and Chemistry* **2016**, 118, 48–54.
- [72] G. Somogyi, *Radiation Effects* **1972**, 16, 233–243.
- [73] A. Chambaudet, A. Bernas, J. Roncin, *Radiation Effects* **1977**, 34, 57–59.
- [74] M. Yoshinori, S. Kazuo, *Solid State Track Detector Composed Of Copolymer Of Alkylene Glycol, Bisallyl Carbonate And Minor Amount Of Higher Alkyl Acrylate Or Methacrylate*, **1986**, US4563416A.
- [75] V. V. Shirkova, S. P. Tretyakova, *Radiation Measurements* **2001**, 34, 177–180.
- [76] P. C. Maybury, W. F. Libby, *Nature* **1975**, 254, 209–209.
- [77] M. Fujii, R. Yokota, *International Journal of Radiation Applications and Instrumentation. Part D. Nuclear Tracks and Radiation Measurements* **1986**, 12, 55–58.
- [78] B. G. Cartwright, E. K. Shirk, P. B. Price, *Nuclear Instruments and Methods* **1978**, 153, 457–460.
- [79] K. Ogura, T. Hattori, M. Hirata, M. Asano, M. Yoshida, M. Tamada, H. Omichi, N. Nagaoka, H. Kubota, R. Katakai, *Radiation Measurements* **1995**, 25, 159–162.
- [80] A. A. A. Mascarenhas, Development of Plastic Materials for Nuclear Track Detection, **2007**.

-
- [81] A. A. A. Mascarenhas, V. K. Mandrekar, P. C. Kalsi, S. G. Tilve, V. S. Nadkarni, *Radiation Measurements* **2009**, *44*, 50–56.
- [82] A. A. A. Mascarenhas, R. V. Kolekar, P. C. Kalsi, A. Ramaswami, V. B. Joshi, S. G. Tilve, V. S. Nadkarni, *Radiation Measurements* **2006**, *41*, 23–30.
- [83] V. K. Mandrekar, *Novel Polymeric Materials for Nuclear Track Detection*, **2010**.
- [84] J. Stejny, T. Portwood, *International Journal of Radiation Applications and Instrumentation. Part D. Nuclear Tracks and Radiation Measurements* **1986**, *12*, 59–62.
- [85] M. Fujii, R. Yokota, Y. Atarashi, *International Journal of Radiation Applications and Instrumentation. Part D. Nuclear Tracks and Radiation Measurements* **1988**, *15*, 107–110.
- [86] M. Fujii, T. Asari, R. Yokota, T. Kobayashi, H. Hasegawa, *Nuclear Tracks and Radiation Measurements* **1993**, *22*, 199–204.
- [87] M. Fujii, R. Yokota, Y. Atarashi, *International Journal of Radiation Applications and Instrumentation. Part D. Nuclear Tracks and Radiation Measurements* **1990**, *17*, 19–21.
- [88] V. K. Mandrekar, S. G. Tilve, V. S. Nadkarni, *Radiation Physics and Chemistry* **2008**, *77*, 1027–1033.
- [89] V. K. Mandrekar, G. Chourasiya, P. C. Kalsi, S. G. Tilve, V. S. Nadkarni, *Nuclear Instruments and Methods in Physics Research Section B: Beam Interactions with Materials and Atoms* **2010**, *268*, 537–542.
- [90] D. G. Naik, V. S. Nadkarni, *Designed Monomers and Polymers* **2016**, *19*, 643–649.
- [91] D. G. Naik, V. S. Nadkarni, *Radiation Physics and Chemistry* **2019**, *156*, 259–265.
- [92] D. G. Naik, V. S. Nadkarni, *Radiation Physics and Chemistry* **2019**, *160*, 68–74.
- [93] S. Singh, S. Prasher, *Nuclear Instruments and Methods in Physics Research Section B: Beam Interactions with Materials and Atoms* **2004**, *222*, 518–524.
- [94] T. Tsuruta, Y. Koguchi, N. Yasuda, *Radiation Measurements* **2008**, *43*, S48–S51.
- [95] M. Fujii, *Nuclear Instruments and Methods in Physics Research Section A: Accelerators, Spectrometers, Detectors and Associated Equipment* **1985**, *236*, 183–186.
- [96] S. Ahmad, J. Stejny, *International Journal of Radiation Applications and Instrumentation. Part D. Nuclear Tracks and Radiation Measurements* **1991**, *19*, 11–16.
- [97] V. S. Nadkarni, *Indian Journal of Physics* **2009**, *83*, 805–811.

-
- [98] J. Charvát, F. Spurný, *International Journal of Radiation Applications and Instrumentation. Part D. Nuclear Tracks and Radiation Measurements* **1988**, *14*, 447–449.
- [99] V. M. Pawar, M. Beck, A. D. Shetgaonkar, R. Pal, A. K. Bakshi, V. S. Nadkarni, *Nuclear Instruments and Methods in Physics Research, Section B: Beam Interactions with Materials and Atoms* **2020**, *462*, DOI 10.1016/j.nimb.2019.11.011.
- [100] A. A. A. Mascarenhas, S. G. Tilve, V. S. Nadkarni, *Designed Monomers and Polymers* **2005**, *8*, 176–185.

❑ List of Journal Publications

Appended to thesis

- ❖ **A. D. Shetgaonkar**, V. S. Nadkarni, Synthetically Induced 1→4 C Branching Motif - An Access Towards Dense Urethane Connecting Dendritic Scaffolds and Application in Nuclear Track Detection. *ChemistrySelect* **2019**, 4, 12210-12215. <https://doi.org/10.1002/slct.201903243>.
- ❖ **A. D. Shetgaonkar**, D. G. Naik, V. S. Nadkarni, Poly(disulfonyl-co-carbonate) thermoset resin: A rapid and highly sensitive polymeric nuclear track detector. *Manuscript under preparation*.
- ❖ **A. D. Shetgaonkar**, D.A. Barretto, V. S. Nadkarni, Synthesis and *in-vitro* biodegradation studies of sulfur functionalized linear APCs. *Manuscript under preparation*.

Other Publications

- ❖ V. M. Pawar, M. Beck, **A. D. Shetgaonkar**, R. Pal, A. K. Bakshi, V. S. Nadkarni, Synthesis and Application of Boron Polymers for Enhanced Thermal Neutron Dosimetry. *Nuclear Inst. and Methods in Physics Research B* **2020**, 462, 169–176170. <https://doi.org/10.1016/j.nimb.2019.11.011>.

❑ List of conferences, symposia and workshops

Appended to thesis:

- ❖ **A. D. Shetgaonkar**, V. S. Nadkarni: Rapid Detection of Charge Particle Tracks using Novel Poly(sulfone-co-carbonate) Thermoset Polymers. **Oral**. *National Symposium on Solid State Nuclear Track Detection and Application (SSNTD-19)*. Khalsa College, Amritsar, Punjab, India. Oct. 18-20th, **2019**.
- ❖ **A. D. Shetgaonkar**, V. S. Nadkarni: Synthesis of Novel Water Soluble Polycarbamate Dendrimer. **Poster**. *Int. Conf. on Polymer Science and Technology (SPSI-MACRO-2018)*. IISER-Pune, Maharashtra, India. Dec. 19-22th, **2018**.
- ❖ **A. D. Shetgaonkar**, V. S. Nadkarni: Designing multifunctional carbamate monomeric cores. **Poster (received 2nd best poster award)**. *Int. Conf. on Polymer Processing and Characterization (ICPPC-2016)*. MG University, Kottayam, Kerala, India. Dec. 9-11th, **2016**.

Other conferences/symposia/workshops

- ❖ V. M. Pawar, **A. D. Shetgaonkar**, V. S. Nadkarni: Designing polymers for various solid state nuclear track detection applications. **Poster**. *Two-day work shop on Material Science between Goa University, University of Porto and University of Coimbra*. Goa University, Goa, India. Nov. 18-19th, **2019**.
- ❖ Participated in the two-day capacity building programme on “*Intellectual Property Rights (IPRs)*” organized by Goa State Council for Science and Technology in association with TIFAC, New Delhi, DST New Delhi and IPR cell, Goa University, Goa, India. Sep. 26-27th, **2019**.
- ❖ Participated in two-days skill development workshop on “*Chemical Analysis of Biomolecules and Computation*” organized by Dept. of Biotechnology, Goa University, Goa, India. Nov. 23-24th **2017**.
- ❖ V. M. Pawar, **A. D. Shetgaonkar**, R. Pal, A. K. Bakshi, M. Beck, V. S. Nadkarni: Synthesis of novel polymer called poly(APCC-co-ADC) for Neutron Dosimetry. **Oral**. *Nuclear and Radiochemistry Symposium (NUCAR-2017)*. KIIT University, Odisha, India. Feb. 6-10th, **2017**.
- ❖ Participated in the Symposium “*Emerging Trends in AgroSciences Chemistry and Technology*” organized by Syngenta Biosciences Pvt. Ltd., Goa, Nov. 22-23rd, **2016**.
- ❖ Attended the “*International Conference on Green chemistry, Catalysis, Energy and Environment*” (ICGC-2015) held at Dept. of Chemistry, Goa University, Goa, India. Jan. 22-24th, **2015**.
- ❖ Participated as a facilitator at “*The Salters’ Chemistry Camp*” organized by Royal Society of Chemistry at Goa University, Nov. 22-24th, **2018**.
- ❖ Participated as an exhibitor at the “*Noble Exhibition (Science Impacts Lives)*” as a part of the Nobel Media Prize series, India 2018 events organised by Nobel Media AB, Department of Biotechnology, Govt. of India and DST, Govt. of Goa at Kala Academy, Panaji, Goa from Feb. 1-28th, **2018**.